Effect of Ingredient Interactions and Heat Treatment on the Structure and Stability of Dairy based Oil-in-Water Emulsions

A thesis presented in partial fulfillment
of the requirements for the degree of

Doctor of Philosophy in Food Technology
at Massey University, Palmerston North, New Zealand

By

Yichao Liang

BSc. (Hons)

March 2014

Abstract

Oil-in-water emulsions are an important basis of many pharmaceutical, nutraceutical and food products such as mayonnaise, dressings, coffee creamers, chocolate, infant formulae, parenteral emulsions and enteral medical beverages. The effects of protein adsorption, addition of other food components (i.e. polysaccharides, carbohydrates and minerals), processing conditions (i.e. high pressure, heat and shear) and environmental conditions (i.e. pH, ionic strength and solvent quality) on the physicochemical properties of protein-stabilized oil-in-water emulsions (i.e. heat stability, creaming stability, viscosity and flow behavior) have been covered in past studies. In addition, there is increasing information on the heat stability and the viscosity of emulsions containing high concentrations of protein. However, there is very limited understanding of the inter-particle interactions in high solids emulsion systems containing high amounts of protein, oil or carbohydrate. A lack of studies that have investigated the types of interfacial proteins and non-adsorbed proteins, the aggregation state of the proteins, the particle size distributions of protein particles and oil droplets and the presence of a third component, especially under high temperature heating (i.e. 120−140 °C) conditions, has limited the understanding of how processing and ingredients influence the properties of proteins and, in turn, the physical stability and the rheological properties of protein-stabilized emulsions.

To address this issue, the research described here was aimed at determining the importance of the mechanisms of instability, such as depletion flocculation, bridging flocculation, aggregation, creaming and coalescence, in high solids emulsion systems and at understanding the colloidal forces that drive specific material/rheological properties and the storage stability of complex high solids systems. Five main techniques were used to characterize the structure-material properties of protein-stabilized emulsions: light scattering particle sizing, Turbiscan, rheology, polyacrylamide gel electrophoresis and confocal microscopy. The behaviors of interfacial proteins, non-adsorbed proteins and protein-coated oil droplets before and after heat treatment, in the presence of a third food

ingredient (polysaccharides or sugars) and with pre-homogenization protein preheat treatment were investigated.

As a prelude to addressing the mechanisms of instability of emulsions containing high concentrations of protein, before and after heat treatment (120 °C for 10 min), a stability map approach was developed. The model emulsions were successfully categorized into four model systems based on droplet−protein, protein−protein and droplet−droplet interactions with respect to the roles of the types of adsorbed and non-adsorbed proteins. Emulsions stabilized by whey proteins or containing high whey protein concentrations were shown to be highly sensitive to calcium content and heat treatment. Non-adsorbed whey proteins were involved not only in the heat-induced destabilization of whey-protein-stabilized emulsions but also when the interfacial layer was replaced by sodium caseinate (NaCas). In this case, NaCas-stabilized droplets were incorporated in the gel network, probably through heat-exchanged interfacial interaction. Gels were formed after heat treatment when NaCas was added to whey protein emulsions; this gel formation was dependent on the casein to whey protein ratio. Replacement of the continuous phase intact whey proteins with hydrolyzed whey proteins improved the heat stability of the emulsions. With one notable exception, surface-active fractions from hydrolyzed whey proteins were seen to promote droplet coalescence in Tween-20-stabilized emulsions at high heating temperatures. Model emulsions containing relatively high concentrations of micellar or non-micellar caseins were found to be heat stable. However, rapid enhanced creaming, which was associated with the depletion flocculation, occurred in these emulsions. The non-adsorbed protein concentration, the aggregation state and the polydispersity of the protein determined the extent of depletion flocculation.

Other studies on the effect of the depletion interaction potential and the continuous phase viscosity on the creaming stability of weakly flocculated NaCas-stabilized emulsions showed that an increase in the non-adsorbed protein concentration promoted a stronger depletion interaction potential, which could change emulsion destabilization to restabilization because of the formation of a space-filling droplet network. At higher NaCas concentrations (≥ 6% w/w), there was a significant delay in the formation of the space-filling droplet network, which was attributed to the particularly small diffusive

motion of flocculated droplet clusters and their inability to redisperse under a strong depletion interaction potential. Although the addition of maltodextrin or xanthan gum influenced the creaming behavior, neither additive could be considered to be an inert thickening agent. The reduced network formation caused by the addition of maltodextrin was not an effect of viscosity, but rather a breakdown of the caseinate nano-particles that induced the formation of the network. Once the maltodextrin concentration exceeded 15% w/w, the droplets were entirely non-interacting and would presumably cream at a rate predicted by modified Stokes' law for concentrated emulsion ($\emptyset$ > 0.2) (Tadros, 2004). Adding xanthan gum to the NaCas-stabilized emulsions resulted in local domains that were rich in either xanthan gum or NaCas and emulsion. The effect of these local domains was that the droplets experienced a stronger depletion interaction potential and the high viscosity of the combined xanthan gum and emulsion phases resulted in uniform phase separation across the emulsion rather than gravimetric separation.

Depending on the heating duration, heat treatment (120 °C) of NaCas-stabilized emulsions (2−8% w/w, protein) resulted in a weakened depletion interaction potential and a more rapid formation of the space-filling droplet network. Heat treatment of NaCas-stabilized oil droplets had relatively limited influence on the phase separation kinetics. Heat-induced degradation of non-adsorbed NaCas molecules was the dominant factor determining the creaming stability of NaCas-stabilized emulsions. The particle size, viscosity and molecular weight of continuous phase NaCas decreased as the heating time increased. A deviation of the size of the NaCas nano-particles from the optimum value (~ 20 nm in diameter) resulted in changes in the strength of the depletion interaction potential and the range of attraction. A decrease in the continuous phase viscosity also contributed to rapid formation of the droplet network at higher NaCas concentrations (> 6% w/w).

The droplet break-up and the heat stability of milk protein concentrate (MPC)-stabilized emulsions were determined to understand the impact of carbohydrate type and concentration during emulsification and subsequent heat treatment. The addition of different carbohydrates (up to 30% w/w) slightly increased the droplet diameter to similar extents. However, the addition of 30% w/w maltodextrin significantly decreased the

droplet diameter, which was attributed to the marked decrease in the dispersed/continuous phase viscosity ratio. Generally, added carbohydrates reduced the heat stability maximum in heat coagulation time–pH profiles of MPC-stabilized emulsions. The pH at the heat stability maximum was shifted towards more acidic values by an increased concentration of glucose, maltose, sucrose or trehalose but towards more alkaline values by an increased concentration of maltodextrin. The extent of destabilization also varied between carbohydrates, with trehalose being particularly effective in retaining the original heat stability of the MPC-stabilized emulsion. Reducing carbohydrates (glucose, maltose and maltodextrin) decreased the heat stability maximum more considerably than non-reducing carbohydrates (sucrose and trehalose).

Studies on the effect of pre-homogenization heat treatment on the physicochemical, microstructural and rheological properties of protein-stabilized emulsions showed that preheating the MPC and the whey protein concentrate denatured the whey proteins, leading to a reduction in subsequent heat-induced interactions between adsorbed proteins, between non-adsorbed proteins and between adsorbed and non-adsorbed proteins. This was attributed to fewer reactive groups being available for secondary heat-induced interactions after pre-homogenization heating. Extensive heat-induced aggregation during post-homogenization heat treatment resulted in delayed creaming because of the high viscosity at low shear rates. The presence of non-micellar caseins, the homogenization pressure and the order of heat treatment of the proteins were shown to significantly influence the physical stability and the rheological properties of protein-stabilized emulsions.

Overall, the results of this research have advanced our understanding of how the protein concentration, the aggregation state of caseins, the heat-induced physicochemical changes of proteins and the attractive force impact on the physical stability, rheological properties and microstructures of model protein-stabilized emulsions. This information may have important implications for developing tailor-made milk protein ingredients that allow controlled functionalities in the processing and storage of dairy emulsions and for making strategic plans to control/manipulate the properties of high solids colloid systems.

Acknowledgements

First and foremost, I would like to sincerely thank my chief supervisor Assoc Prof. Matt Golding at Massey for his inspiration, passion, guidance and encouragement, which he gave me during my doctoral study. His appreciation of my effort in each stage during the study including preparation of manuscripts for publication, conference presentations and preparation of thesis and his confidence and determination on the final goals positively drive me to keep up the good work.

I would like to express my sincerely gratitude to my co-supervisor Asst. Prof. Hasmukh Patel (South Dakota State University, Brookings, USA) for his encouragement, enthusiasm and freedom during my first one and half year doctoral study, for his constant support in the preparation of conference presentations. His deep thinking and understanding in the end applications of milk protein ingredients has advanced and influenced my way of thinking in both fundamental science and commercial applications.

I would like to thank Dr. Graeme Gillies (Fonterra Research & Development Centre). Thanks to him for kindly accepting the Fonterra supervisor role after Asst. Prof. Hasmukh left during the last one and half year of doctoral study. His knowledge and expertise on the subject and his thorough supervision, constant support even when I didn't ask for help, guidance for experiments, constructive suggestions on physic and mathematical equations and his enormous help in the preparation of manuscript and thesis reviewing. He always motivates me to produce the best possible results in preparing publication materials based on the findings of the caseinate emulsion systems. I am indeed thankful to my co-supervisor Dr. Lara Matia-Merino (Massey University) for her valuable scientific inputs and advice on experimental plans, coordination of using equipment in Food Science Characterization Laboratory and preparation of publications through the entire doctoral study period and her advices on job seeking. I am also truly thankful to Dr. Aiqian Ye (Riddet Institute) for his constant supervision, advice on the experimental methods and critical review of my publications throughout the whole doctoral study.

Acknowledgements

I would like to express my deep sense of gratitude to Dr. Ran Gao, Dr. Skelte Anema, MD. Sergey Ukraintsev and Dr. Abraham Chawanji for their friendly encouragements, kindly supports, helpful technical discussions and good advices during my studying and living in Palmerston North. I would like to thank Dr. Julita van Oosten-Manski (now FrieslandCampina Ltd) and Dr. Edeline Wong (Fonterra Research & Development Centre) for their assistance and advices on the rheological methods' set up and analysis in my initial stage of doctoral study. I am thankful to Mr. Michael Loh, Dr. Abraham Chawanji (Fonterra Research & Development Centre), Dr. Dimtry, Dr. Jianyu Chen and Mr. Doug Hopcroft (Manawatu Microscopy & Imaging Centre) for their training and assistance of confocal scanning laser microscopy and transmission electron microscopy. I would like to thank Dr. Kerianne Higgs for her assistance and guidance for RP-HPLC experiments. I am sincerely thankful to Dr. Claire Woodhall, Dr. Sheelagh Hewitt, Dr. Thérese Considine, Dr. Nick Robinson and Dr. Steve Taylor for being proof-reader of my publications and conference abstracts. I am thankful to Ms. Christine Ramsay for her administrative assistance with conference registrations.

I am grateful to all technicians, assistants and staff members of Fonterra Research & Development Centre especially to Dr. Dave Elgar, Dr. Jos Schalk, Dr. Jonathan Depree, Dr. Nilesh Saija, Dr. Emmanuelle Riou, Dr. Esra Cakir-Fuller, Dr. Aurelie Cucheval, Ms. Ping Gao, Ms. Yvonne van der Does, Ms. Sue Adam, Ms. Nguyen, Ms. Christina Streicher, Ms. Lucile Tercinier, Ms. Jing Luo, Ms. Carolina Saavedra-Melo, Mr. Ivan Simpson, Mr. Bert Fong, Mr. Rob Hunter, Mr. Kevin Ma, Mr. Thomas Fuller and Mr. Hemang Bhatt for their company and support. I would to thank the members of the Food Science Laboratory for providing a fun and active working atmosphere.

I would like to thank the Ministry of Science and Innovation (MSI) and Fonterra Co-operative Group Limited for funding this work. I am sincerely thankful to Mr. Kevin Palfreyman for his help in preparing this project contract with MSI and Ms. Liz Ricketts and Ms. Maret Sinclair for their help in administrative assistance with technical reports.

Acknowledgements

Last but not least, I would like to thank my partner Chia-Eng Chong, who enjoyed discussions and chats on everything in the hours when the lights in the lab were off, and for providing moral support throughout my study. I would like to express my deepest sense of gratitude to my parents, for their endless encouragement, motivations and blessings. I would like to say without the help from all those aforementioned people, it would have been impossible for me to achieve the good work in my PhD study.

Dedication

The author wishes to dedicate this dissertation to my parents and my girlfriend.

Table of Contents

List of Publications

This work has been published in part in the following papers:

1. Y.C. Liang, H. Patel, L. Matia-Merino, A.Q. Ye and M. Golding (2013). Structure and stability of heat-treated concentrated dairy-protein-stabilized oil-in-water emulsions: a stability map characterization approach, *Food Hydrocolloids*, *33*, 297−308.

2. Y.C. Liang, H. Patel, L. Matia-Merino, A.Q. Ye and M. Golding (2013). Effect of pre- and post-heat treatments on the physicochemical, microstructural and rheological properties of milk-protein-concentrate-stabilized oil-in-water emulsions, *International Dairy Journal*, *32,* 184−191.

3. Y.C. Liang, G. Gillies, H. Patel, L. Matia-Merino, A.Q. Ye, and M. Golding (2014). Physical stability, microstructure and rheology of sodium-caseinate-stabilized emulsions as influenced by protein concentration and non-adsorbing polysaccharides, *Food Hydrocolloids*, *36*, 245−255.

4. Y.C. Liang, L. Matia-Merino, H. Patel, A.Q. Ye, G. Gillies and M. Golding. Effect of sugar type and concentration on the heat-induced behavior of milk-protein-concentrate-stabilized oil-in-water emulsions. *Food Hydrocolloids*, *41*. 332−342.

5. Y.C. Liang, G. Gillies, H. Patel, L. Matia-Merino, A.Q. Ye, and M. Golding. Phase separation behavior of sodium-caseinate-stabilized emulsions as influenced by heat treatment. *Draft intended for Food Hydrocolloids*.

6. Y.C. Liang, G. Gillies, H. Patel, L. Matia-Merino, A.Q. Ye, and M. Golding. Modulation of the heat stability, creaming stability and rheological properties of high protein oil-in-water emulsions. A review. *Submitted for editorial review*.

List of Presentations

This work has been presented in part in the following presentations at scientific conferences:

1. Y.C. Liang, H. Patel, L. Matia-Merino, A.Q. Ye and M. Golding. Physicochemical properties of model milk protein emulsions as influenced by the dispersed and continuous phases, 7th NIZO conference: Flavour and Texture: Innovations in Dairy, Papendal, The Netherlands, September 21-23, 2011. Finalist of student oral competitions.

2. Y.C. Liang, H. Patel, L. Matia-Merino, A.Q. Ye and M. Golding. The physicochemical properties of milk-protein-concentrate-stabilized emulsion as influenced by pre- and post-processing treatments, 7th NIZO conference: Flavour and Texture: Innovations in Dairy, Papendal, The Netherlands, September 21-23, 2011.

3. Y.C. Liang, H. Patel, L. Matia-Merino, A.Q. Ye and M. Golding. Effect of heat treatment on the properties of milk-protein-concentrate-stabilized oil-in-water emulsions prepared with a preheated protein continuous phase, 2011 IDF Annual Meeting, Parma, Italy, October 15-19, 2011.

4. Y.C. Liang, H. Patel, M. Golding, L. Matia-Merino, A.Q. Ye. Physical stability of milk-protein-concentrate based dispersions and emulsions as influenced by heating pH and presence of small molecule components, 2012. NZIFST Annual Conference: Let's Talk, Hamilton, New Zealand, June 26-28, 2012.

5. Y.C. Liang, H. Patel, L. Matia-Merino, A.Q. Ye and M. Golding. Development of a model system to understand the mechanisms of instability and to predict the shelf-life of oil-in-water emulsions, 2012 ADSA®-ASAS Joint Annual Meeting, Phoenix, USA, July 15-19, 2012. Finalist of graduate student oral competitions.

6. Y.C. Liang, G. Gillies, H. Patel, L. Matia-Merino, A.Q. Ye and M. Golding. Structural properties of milk protein concentrate (MPC) dispersions and emulsions as influenced by presence of small molecule components, 2012 ADSA®-ASAS Joint Annual Meeting, Phoenix, USA, July 15-19, 2012. Finalist of graduate student poster competitions.

7. Y.C. Liang, H. Patel, M. Golding, L. Matia-Merino, A.Q. Ye. Particle-particle system characterization of model milk-protein-stabilised emulsions, 2012. NZIFST Annual Conference: Let's Talk, Hamilton, New Zealand, June 26-28, 2012. Finalist of graduate student oral competitions.

8. Y.C. Liang, G. Gillies, H. Patel, L. Matia-Merino, A.Q. Ye and M. Golding. Microstructure, physical stability and rheological properties of concentrated-milk-protein-stabilized oil-in-water emulsions, 2013 NZIFST Annual Meeting: Time For Action, Hawke's Bay, New Zealand, July 2-4, 2013. Finalist of graduate student oral competitions.

9. Y.C. Liang, G. Gillies, L. Matia-Merino, A.Q. Ye, H. Patel and M. Golding. Influence of depletion flocculation and continuous phase viscosity on the stability of sodium-caseinate-stabilized emulsions, 2013 ADSA®-ASAS Joint Annual Meeting, Indianapolis, USA, July 8-12, 2013. Selected finalist of graduate student oral competitions.

10. Y.C. Liang, G. Gillies, H. Patel, L. Matia-Merino, A.Q. Ye, G. Gillies and M. Golding. Impact of processing and storage temperatures on the physical stability of sodium-caseinate-stabilized emulsions, 2013 ADSA®-ASAS Joint Annual Meeting, Indianapolis, USA, July 8-12, 2013.

11. Y.C. Liang, H. Patel, L. Matia-Merino, A.Q. Ye and M. Golding. Influence of the properties of interfacial proteins and heat treatment on the stability and structure of oil-in-water emulsions, 2013 IFT Annual Meeting, Chicago, USA, July 13-16, 2013. Selected finalist of student oral competitions.

12. Y.C. Liang, H. Patel, L. Matia-Merino, A.Q. Ye and M. Golding. Influence of sonication on droplet size and physicochemical properties of milk-protein-concentrate-stabilized oil-in-water emulsions, 2013 IFT Annual Meeting, Chicago, USA, July 13-16, 2013. 2nd place in final graduate poster competition.

List of Tables

Number *Page*

List of Figures

Number *Page*

List of Abbreviations

α-lac:	α-lactalbumin
β-lg:	β-lactoglobulin
BSA:	Bovine serum albumin
BS:	Backscattering
CaCas:	Calcium caseinate
CCP:	Colloidal calcium phosphate
CLSM:	Confocal laser scanning microscopy
CM:	Casein micelle
CMC:	Critical micelle concentration
$d_{3,2}$:	Surface area moment mean diameter
$d_{4,3}$:	Volume-weighted average mean diameter
DLS:	Dynamic light scattering
EDTA:	Ethylene diamine tetra acetic acid
MPC:	Milk protein concentrate
MD:	Maltodextrin
NaCas:	Sodium caseinate
RP-HPLC:	Reverse phase high performance liquid chromatography
SDS-PAGE:	Sodium dodecyl sulfate-poly acrylamide electrophoresis

SLS:	Static light scattering
SMP:	Skim milk powder
TEM:	Transmission electron microscopy
Tris:	Tris(hydroxymethyl)aminomethane
TS:	Transmission
UF:	Ultrafiltration
UHT:	Ultra high heat treatment
WPC:	Whey protein concentrate
WPH:	Whey protein hydrolyzate
WPI:	Whey protein isolate
w/w:	Weight/weight
w/v:	Weight/volume
Γ:	Surface coverage

Chapter 1: Introduction

1.1 Introduction

Oil-in-water emulsions are an important basis of many pharmaceutical, nutraceutical and food products such as mayonnaise, dressings, coffee creamers, chocolate, infant formulae, parenteral emulsions and enteral medical beverages (Dalgleish, 1997; Dickinson, 1992; Kramers, 1940; McClements, 2005). There is growing interest in understanding how liquid foods can regulate calorie intake and enhance increased satiety responses in elderly persons or patients are associated with weight loss and malnutrition (Campbell & Leidy, 2007; Grandjean, Reimers, & Buyckx, 2003; Margetts, Thompson, Elia, & Jackson, 2003; Weaver, 2010). Factors such as palatability, high energy density, low volume and liquid format have important impact on the medical beverages product design. A recent review suggested that nutrient and energy dense oral nutritional supplements serve in a small volume could effectively enhance nutritional intake for elder persons (Nieuwenhuizen, Weenen, Rigby, & Hetherington, 2010).

Medical beverages are commonly protein-based oil-in-water emulsion formulations consisting of emulsion droplets and different aqueous phase components-biopolymers, carbohydrates, minerals and vitamins, with different sizes and concentrations and their interactions determine the heat stability, creaming stability, rheology and microstructure of the emulsions (Dalgleish, 2006; McClements, 2004). However, it is challenging to produce high protein emulsions that have good sensory profile and physical stability. Good physical stability means the physicochemical properties of emulsions are retained during heat treatment and storage.

Beverage emulsions prepared at neutral pH (~ 6.8) are often heat sterilized (i.e., retort or ultrahigh-temperature processes) for long term shelf-life stability (Keowmaneechai & McClements, 2006; Srinivasan, Singh, & Munro, 2002). Milk proteins undergo aggregation and/or proteolysis at high temperatures in absence or presence of minerals or carbohydrates, and sometimes resulting in increased viscosity or gelation. It was well illustrated that increasing the volume fraction of particles increases the overall viscosity

of dispersions (Bouchoux et al., 2009; Dahbi, Alexander, Trappe, Dhont, & Schurtenberger, 2010; Genovese, 2012). To achieve the same viscosity upon concentration of solid content and to retain the heat stability is another major challenge.

Recently, a few studies have been carried out to understand the heat-induced protein−mineral, protein−protein and oil droplet−droplet interactions in dispersion and emulsion systems containing high protein content (> 6%) (de Kort, Minor, Snoeren, van Hooijdonk, & van der Linden, 2011; Huck-Iriart, Álvarez-Cerimedo, Candal, & Herrera, 2011; Sağlam, Venema, de Vries, Shi, & van der Linden, 2013; Sauer & Moraru, 2012). Generally, the colloidal behaviors of oil-in-water emulsions are determined by the mean droplet size, droplet size distribution, the physicochemical properties of the interfacial layer and the continuous phase proteins. Depending on the emulsifier type, emulsification method, heating temperature and duration, pH, ionic strength, presence of small-molecular-weight molecules and other biopolymers (i.e. xanthan gum, maltodextrin), emulsion instabilities such as bridging and depletion flocculation, competitive adsorption and exchange of interfacial materials, coalescence and different degrees of aggregation/coagulation have been shown to occur (Cruijsen, 1996; Dalgleish, 2006; Dickinson, 2013; McClements, 2004; Nikiforidis & Kiosseoglou, 2008).

However, the emulsion stability and instability mechanisms have not been fully understood in high solids systems (i.e. high concentration of protein, carbohydrate and mineral). The extents of heat-induced inter- and intra- protein−protein interactions may vary considerably in high solids systems. Additionally, the droplet−droplet interactions driven by depletion effects may change from destabilization to restabilization, as the increasing non-adsorbed protein increases the depletion energy which determines the extent of droplet flocculation and formation of droplet network. Clearly, more understanding is needed about protein−protein interactions and droplet−droplet interactions in high protein emulsion systems. For this purpose, simple oil-in-water emulsions were used to build a stability map containing heat-sensitive and heat-stable milk proteins and the complexity of ingredient interactions is gradually increased to simulate those occur in the real formulation.

1.2 Aim and thesis structure overview

The overall aim of the PhD work was to enhance the understanding of protein−protein interactions at oil/water interface, in the continuous phase and between the two phases and droplet−droplet interactions on the heat stability, creaming stability and rheological properties of protein-stabilized oil-in-water emulsions in the presence of small-molecular-weight molecules, biopolymers and carbohydrates and at different processing conditions. The specific aims of this thesis were as follow:

- To build and validate model emulsion systems which are suitably complex as the real application and to characterize the physicochemical properties in respect to the inter-particle interactions occurring in the dispersed and continuous phases under heating condition.
- To understand the mechanism(s) that modulates the emulsion stability and rheological properties in a model weakly attractive colloid system containing non-adsorbed protein.
- To investigate the influence of aggregation size of caseins on the droplet size formation, creaming stability, heat stability, microstructure and rheological properties of the model emulsion system.
- To investigate the influence of carbohydrate on the droplet size formation, heat stability, microstructure and rheological properties of the model emulsion system.
- To evaluate the heating regime and the choice of protein ingredients on the emulsion stability and rheological properties of the model emulsion system.
- To develop strategies to control/manipulate the emulsion stability and rheological properties of a sterilized high protein (> 6 g/100 g protein) oil-in-water emulsion stimulant.

To meet those purposes, oil-in-water emulsions prepared with 10−30% w/w oil and 1−10% w/w protein were investigated. Emulsions with high oil content (30% w/w) have been well studied and considered good systems for investigating the adsorption behaviors and rheological properties. The selection of low oil content (10% w/w) was to simulate the oil concentration in real formulations. Milk proteins in their commercial form such as

MPC, NaCas and WPI, acting as either emulsifier or form the protein-rich continuous phase, were included in all studies as they are used commonly in protein-based emulsion formulations. In addition, the non-food grade emulsifier, Tween 20 was included as a non-protein emulsifier control for non-interacting oil droplets.

The main body of PhD work is organized into 10 chapters and tests the following hypotheses:

- Following the general introduction in Chapter 1. Chapter 2 provides general background on the aspects of protein-stabilized oil-in-water emulsions and literature review with some insight from the published materials of our group (to be submitted, 2014).
- The type of milk protein used as emulsifier or used to form the protein-rich continuous phase affects the heat stability, creaming stability, microstructure and rheological properties of simple oil-in-water emulsions due to different particle size, aggregation state of protein, interfacial configuration, amino acid compositions and mineral content. Chapter 4 describes the potential inter- and intra- protein−protein interactions, droplet−droplet interactions and categorizes them into four stability models using food-grade ingredients [published as (Liang, Patel, Matia-Merino, Ye, & Golding, 2013b)].
- Protein-rich oil-in-water emulsions tending to phase separate into two discrete phases (cream phase and serum phase) due to depletion effect have been observed in a number of model emulsions obtained in Chapter 4. An increase in non-adsorbed protein concentration promotes stronger depletion interaction potential that may change emulsion destabilization to restabilization due to the formation of space-filling droplet network. Chapter 5 describes and illustrates the impact of depletion attractive force and continuous phase viscosity on the phase separation behaviors of oil-in-water emulsions formed with sodium caseinate (NaCas). Xanthan gum and maltodextrin were used for comparison for the increased continuous phase viscosity effect governed from the addition of increased NaCas [published as (Liang, Graeme, Patel, Matia-Merino, Ye & Golding, 2014)].

- High temperature heating (i.e. at 120 °C) causes degradation or polymerization of sodium caseinate; subsequently it results in decrease or increase in the particle size and the amount of intact sodium caseinate which influence the depletion interaction potential and therefore the phase separation behavior of caseinate-stabilized oil-in-water emulsions. Chapter 6 extends the knowledge obtained from Chapter 5 and describes the influence of heat treatment on the depletion interaction potential and its impact on the subsequent formation of the space-filling droplet network (to be submitted, 2014).
- Heat-induced inter-particle interactions may derivate significantly if the continuous phase containing high carbohydrate content. Chapter 7 investigates the addition of mono-, di- and polysaccharides (up to 30% w/w) on the heat stability and rheology of oil-in-water emulsions formed with milk protein concentrate (MPC) which have been demonstrated as a promising emulsion system that has good heat stability and low creaming rate in Chapter 4 [published as (Liang, Matia-Merino, Patel, Ye, Graeme & Golding, 2014)].
- Pre-homogenization conditions and different interfacial structure will affect the heat stability, creaming stability and rheological properties by influencing the surface load, denaturation of milk proteins, partitioning of proteins between the oil/water interface and the continuous phase and the protein conformation at oil/water interface. Chapters 8 and 9 describe the effect of interfacial compositions and aggregation state of proteins on the physicochemical properties of protein-stabilized oil-in-water emulsions [Chapter 8 published as (Liang, Patel, Matia-Merino, Ye, & Golding, 2013a)].
- Chapter 10 provides an overall conclusion and recommendations for future research. Industrial significance is described as to how the findings obtained in this thesis may be applied in commercial food/dairy applications.

Chapter 2: Literature Review

The objective of this chapter is to review and discuss the structure, physical stability and rheological properties of milk-protein-based oil-in-water emulsions. The impacts of mechanical and physicochemical factors such as heat treatment temperature, homogenization conditions, pH, ionic strength, droplet size, droplet size distribution and volume fraction on emulsion stability and emulsion rheology are summarized. In addition, emerging approaches and technologies for manipulating heat-induced behavior and the steric repulsive forces of proteins and emulsion droplets are discussed.

2.1 Introduction

Oil-in-water emulsions are an important basis of many pharmaceutical, nutraceutical and food products such as mayonnaise, dressings, coffee creamers, chocolate, whipped cream, infant formulae and meal replacement beverages (Dalgleish, 1997; Dickinson, 1992; McClements, 2005). Oil-in-water type food emulsions are complex colloidal systems consisting of emulsion droplets and different aqueous phase components − biopolymers, carbohydrates, salts, etc. − with different sizes and concentrations; their interactions determine the heat stability, creaming stability, viscosity and texture of emulsions (Dalgleish, 2006; McClements, 2004). Table 2.1 lists various ingredients and their roles in a typical high protein meal replacement beverage. There is strong interest in food industries in developing novel protein-based emulsions, especially at high protein content and with improved stability against environmental stresses (i.e. gravity, heat treatment, ionic strength) while maintaining acceptable viscosity for processing, storage and consumption purposes (de Kort et al., 2011; Huck-Iriart et al., 2011; Nikiforidis & Kiosseoglou, 2008; Sağlam et al., 2013; Sauer et al., 2012).

Colloidal interactions between emulsion droplets are governed by the properties of the interfacial layer and the surrounding environmental conditions such as pH, ionic strength and temperature (McClements, 2005). When emulsion droplet diameters are much larger

than those of solvent molecules and other non-adsorbed materials, the rheology of oil-in-water emulsions is determined solely by droplet−droplet interactions. Other interactions, such as protein−protein, protein−carbohydrate and protein−mineral interactions, cannot be ruled out and should be considered in terms of the droplet−droplet interactions. Hence, it is very important to have a good understanding of the interfacial properties and bulk physicochemical properties of food emulsions to be able to control their functionalities.

Table 2.1. Ingredients and their roles in a typical high protein beverage formulation (Grygorczyk, 2009).

Ingredients	Quantity in w/w basis	Functions
Various protein blends (i.e. MPC, MPI & WPC)	8.5−10%	Nutrition, potentially has a role in emulsifying activity
Vegetable oil (e.g. sunflower oil, corn oil)	10%	Energy source
Carbohydrates (e.g. sucrose, maltodextrin)	30%	Energy source, sweetener
Minerals (e.g. trisodium citrate, tripotassium citrate, sodium chloride)	0.5−1.0%	Stabilizer, mouthfeel enhancer
Emulsifier (i.e. lecithin, DATEM)	0.10%	Emulsifying agent
Water	48.9−50.9%	Solvent

In the following, emphasis is placed on recent advances in the formation, structure and physical stability of oil-in-water emulsions prepared with milk proteins. The behaviors of emulsion droplets in the presence of non-food-grade components are critically summarized in terms of specific stabilizing or destabilizing mechanisms, particularly upon heat treatment. Studies on emulsions prepared with other proteins (i.e. soybean, pea, rice, wheat and egg) also provide important information on droplet formation and physical stability (Euston, Al-Bakkush, & Campbell, 2009; Keerati-u-rai & Corredig, 2009; Kimura et al., 2008; Nikiforidis & Kiosseoglou, 2007). Only results relating to heat stability and creaming behavior are included in this review.

2.2 Protein-stabilized oil-in-water emulsions

Milk is a natural oil-in-water emulsion, in which the oil droplets, so-called milk fat globules (from 0.2 to 20 μm in diameter), are coated by a milk fat globule membrane (MFGM). Along with proteins, they are dispersed in an aqueous phase containing lactose, vitamins and other low molecular weight components (Walstra, Wouters, & Geurts, 2006c). The MFGM consists of proteins, glycoproteins, phospholipids and triacylglycerols (Keenan & Dylewski, 1995). The interfacial materials protect the milk fat globules from aggregation, coalescence and lipolysis (Lopez, 2005). The size and the polydispersity of milk fat globules can be controlled by homogenization. Increasing the interfacial area will allow additional surface-active materials such as casein micelles, casein fragments and whey proteins to adsorb (Darling & Butcher, 1978; Michalski & Januel, 2006; Ye, 2003).

Milk-derived proteins have been used extensively in the preparation of food emulsions because of their amphiphilic nature, which allows them to adsorb and spread around the oil/water interface during homogenization (Dalgleish, 1996; Dickinson, 2001; Leman & Kinsella, 1989). Droplet size, interfacial composition, adsorbed protein conformation and emulsion stability have been found to be influenced by the type of protein (Dalgleish, 2006; Damodaran, 2004; Euston & Hirst, 1999; Qian & McClements, 2011; Surh, 2009; Ye, 2008). Food emulsions prepared with milk proteins are generally divided into two classes according to differences in the protein structure: caseins which show flexible disordered conformations with little secondary structure (Dickinson, 1998; Leman & Kinsella, 1989); and whey proteins which have a considerably ordered secondary structure with a compact tertiary structure that is linked by intramolecular disulfide bonds (Dickinson, 1998; Leman & Kinsella, 1989). The droplet formation, interfacial composition, adsorbed protein conformation and emulsion stability of oil-in-water emulsions prepared with purified milk proteins (i.e. β-casein, β-lactoglobulin) as well as commercial milk protein ingredients (i.e. skim milk powder, sodium caseinate, whey protein isolate) have been studied extensively (Agboola, Singh, Munro, Dalgleish, & Singh, 1998b; Dickinson, 1999b; Euston & Hirst, 1999; Hunt & Dalgleish, 1994;

Neirynck, Dewettinck, & van der Meeren, 2009; Srinivasan, Singh, & Munro, 1996; Surh, Ward, & McClements, 2006b; Ye, 2008) and a brief summary of milk-protein-stabilized oil-in-water emulsions according to protein type is presented below.

2.2.1 Caseins and casein micelles

2.2.1.1 Individual caseins

Casein molecules are amphiphilic, have moderately high charge and contain a large number of proline residues and few cysteine residues. The molecular weight of caseins ranges from about 19 to 25 kDa (Swaisgood, 2003). Although caseins can be distinguished by their primary structures, each varies in different ways. α_{s1}-, α_{s2}- and β-Caseins share similar traits, in that they are precipitated by calcium binding to their phosphoserine residues and can be categorized as calcium-sensitive caseins. In contrast, κ-casein is not only a soluble casein at the concentrations of calcium found in most milks but also a glycosylated casein that interacts with calcium-sensitive caseins and protects them from precipitation (Horne, 2002; Walstra, Wouters, & Geurts, 2006b). At high casein concentration, the individual caseins resemble block copolymers with hydrophobic and hydrophilic domains. Caseins may exhibit ordered structures at sufficiently high casein concentration (Horne, 2002). Caseins have remarkable heat stability comparing to whey proteins. Sodium caseinate is found stable agaist high tempeartuere heat treatment 140 °C, pH 6.5−7.0 for more than 1 h before any visible changes (Fox & McSweeney, 1998).

α_{s1}-Casein

α_{s1}-Casein is composed of 199 amino acid residues and has a molecular weight of ~ 24 kDa. The locations of the amino acid residues on α_{s1}-casein, based on their degree of hydrophobicity and the nature of their charge, are shown in Figure 2.1.

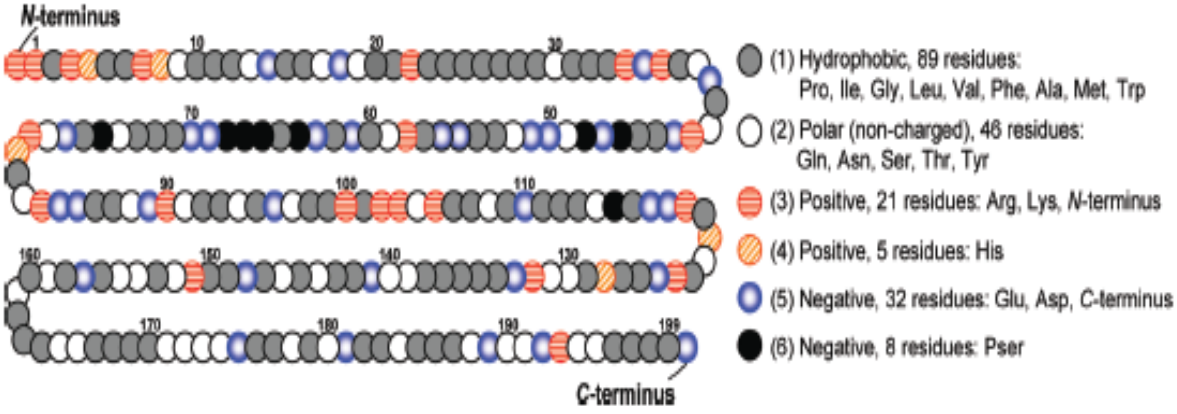

Figure 2.1. Schematic illustration of the linear α_{s1}-casein structure, as simulated by self-consistent field (SCF) calculations; adapted from Akinshina, Ettelaie, Dickinson, & Smyth (2008).

α_{s1}-Casein can be considered to be a tri-block copolymer (Euston, 2004), as its long sequence does not have an even distribution of hydrophobic and charged residues (Huppertz, 2013; Swaisgood, 2003). The evident hydrophobic regions are near residues 20−25, 90−110 and 140−190 and close to the C-terminus. The polar domain of α_{s1}-casein (41−80) has a net charge of −20.6 at pH 6.6 and splits the protein into a polar hydrophilic domain and a neutral hydrophobic domain close to the N-terminus (Huppertz, 2013; Swaisgood, 2003). It has been proposed that α_{s1}-casein may form worm-like micelles under certain ionic conditions (Thurn, Burchard, & Niki, 1987b) (see **Figure 2.2**). The self-association of α_{s1}-casein into dimers, tetramers and hexamers is dependent on pH and ionic strength. Interactions other than hydrophobic interactions, such as hydrogen bonding, are suggested to participate in the associative behavior between α_{s1}-casein molecules because there is no dissociation at low temperatures (Huppertz, 2013; Swaisgood, 2003). Notably, telechelic polymers containing two hydrophobic ends associate in water as "flower-like" micelles. Reversible gelation of telechelic polymers results from molecules bridging across micelles. At a fixed concenration before jamming, telechelics have a higher viscosity than di-block polymers, where in this case β-casein is thought to be a di-block copolymer (Chassenieux, Nicolai, & Benyahia, 2011). α_{s1}-Casein molecule fulfills the characteristics of telechelic polymers that have been desccribed in the associative polymer model.

α_{s2}-Casein

α_{s2}-Casein constitutes about 10% of the total casein in milk. The monomer molecular weight of *α_{s2}-casein* is 25.2 kDa (Huppertz, 2013). *α_{s2}-Casein* shows different degree of phosphorylation and intermolecular disulfide bonding. With amphoteric structure, *α_{s2}-casein* has negative charged residues near N-terminal region and positive charged residues near C-terminal region. *α_{s2}-Casein* is also a calcium sensitive casein and it precipitate with the presence of calcium in the solution. In addition, among the individual caseins, *α_{s2}-casein* is generally considered as the most hydrophilic of caseins as it consists of 3 clusters of anionic groups composed of phosphoseryl and glutamyl residues (Farrell, Jimenez-Flores, Bleck, Brown, Butler, Creamer, Hicks, Hollar, Ng-Kwai-Hang & Swaisgood, 2004).

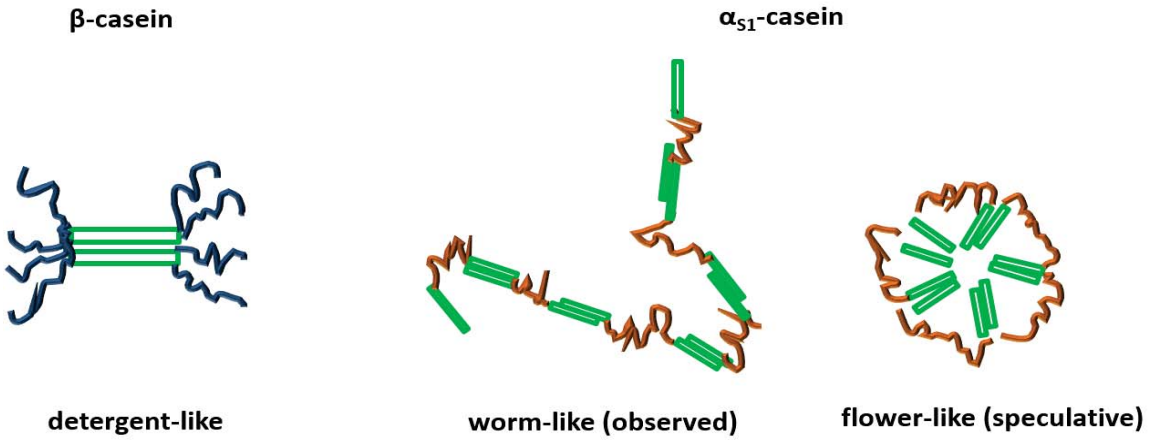

Figure 2.2. Schematic illustration of observed and speculative structures of self-associated individual caseins. Redrawn from Horne (2002).

β-Casein

β-Casein has a net charge of −13.3 at pH 6.6 and a molecular weight of ~ 24 kDa. *β*-Casein is the most hydrophobic of the caseins, with a hydrophobicity of 5.6. The large hydrophobic groups are within residues 51−90 and 130−209 (Huppertz, 2013;

Swaisgood, 2003). The distribution of the amino acid residues on *β*-casein, based on their degree of hydrophobicity and the nature of their charge, is shown in Figure 2.3.

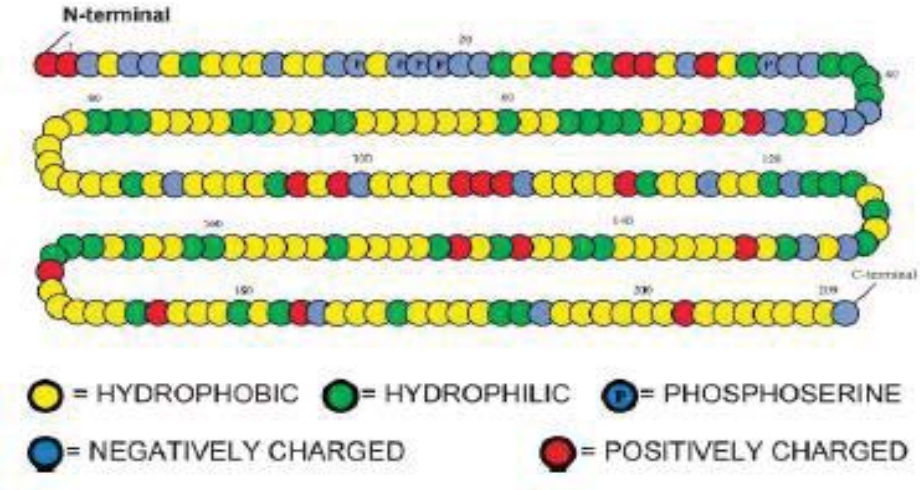

Figure 2.3. Schematic illustration of the primary sequence of *β*-casein, as simulated by self-consistent field (SCF) calculations; adapted from Dickinson (2006).

β-Casein has a very acidic N-terminal region of 24 amino acids, which constitute the anionic phosphoserine cluster (Huppertz, 2013; Swaisgood, 2003). The two domains give *β*-casein an amphiphilic nature, indicating that it can be described as a di-block copolymer (Euston, 2004). It has been predicted that *β*-casein self-associates to form detergent-like micelles with defined critical micelle concentration (CMC) (Horne, 2002; Thurn, Burchard, & Niki, 1987a) (see Figure 2.2). Temperature, ionic strength and protein concentration are the factors that determine the self-assembly behavior of *β*-casein. At low temperature (0−4°C), *β*-casein exists as monomers that exhibit a random-coil-like hydrodynamic behavior. At temperatures above 4°C, *β*-casein self-associates rapidly through hydrophobic interactions, resulting in large micelles in solution (Huppertz, 2013; Swaisgood, 2003). It has been suggested that *β*-casein can interact with other caseins through its hydrophobic domain while concurrently associating with colloidal calcium phosphate (CCP) through its phosphoserine core (de Kruif & Holt, 2003; McMahon & Oommen, 2008).

κ-Casein

κ-Casein is composed of 169 amino acid residues and has a molecular weight of 19 kDa. The lack of phosphoserine clusters gives *κ*-casein a number of positively charged groups and a low net negative charge of −2.0 at pH 6.6 (Huppertz, 2013; Swaisgood, 2003). In a typical cheese making process, chymosin, an enzyme from the bovine abomasum, can further hydrolyze *κ*-casein; the insoluble portion that remains on the micelle surface after chymosin treatment is referred to as para-*κ*-casein and the soluble large peptide present in the serum is glycomacropeptide (Creamer, Plowman, Liddell, Smith, & Hill, 1998). *κ*-Casein is also considered to be a di-block copolymer (Euston, 2004). Similar to *β*-casein, *κ*-casein undergoes self-association into a detergent-like micelle (Horne, 2002). The distribution of amino acid residues on *κ*-casein, based on their degree of hydrophobicity and the nature of their charge, is shown in Figure 2.4. The C-terminal (residues 106~169) region of *κ*-casein is very hydrophilic because of the glycosylation of the threonine residues whereas the N terminus of the protein (residues 1~105) is strongly hydrophobic. This amphipathic property enables *κ*-casein to play an important role in stabilizing casein micelles (Fox & McSweeney, 1998; Swaisgood, 2003). *κ*-Casein contains a pair of cysteine residues, which cross link into disulfide-bonded polymers intermolecularly (Creamer et al., 1998).

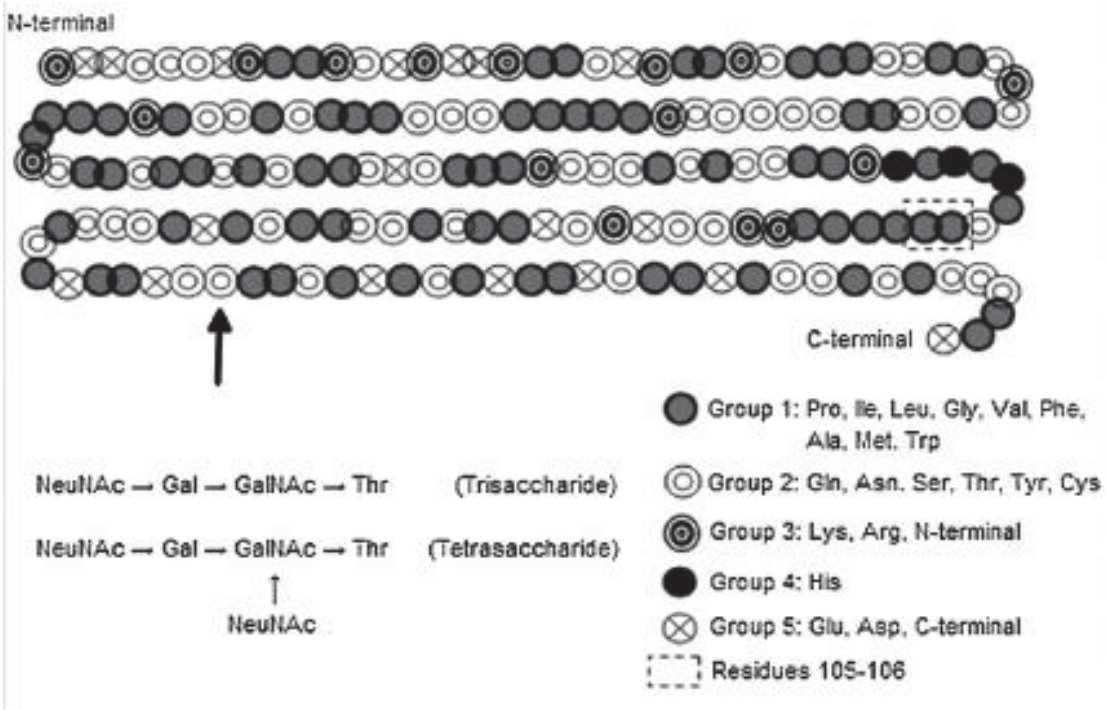

Figure 2.4. Schematic illustration of the primary sequence of κ-casein, as simulated by self-consistent field (SCF) calculations; adapted from Ettelaie, Khandelwal, & Wilkinson (2014).

Interfacial properties of individual caseins

α_{s1}- and β-Caseins adsorb rapidly at the oil/water interface, forming extended layers that protrude towards the continuous phase because of their flexible structures (Dickinson, 1997, 1999b). They tend to form a thick surface layer with the long hydrophilic patches (polar residues) protruding into the continuous phase and the hydrophobic patches (non-polar residues) located at the oil/water interface (Figure 2.5). α_{s1}-Casein exhibits a loop-like conformation whereas β-casein shows a tail-like phenomenon at the oil/water interface. β-Casein has a highly charged tail extending away from the surface for up to about 11 nm; α_{s1}- and α_{s2}-caseins dangle from the surface with thicknesses of about 5.4 and 8.5 nm respectively; the interfacial layer thickness provided by κ-casein is about 8.3 nm (Dalgleish, 1993, 1996a; Dickinson, 1999b). Despite α_{s1}-casein conferring more electrostatic charge than β-casein at neutral pH, β-casein-stabilized emulsion droplets are

less susceptible to flocculation at equivalent ionic strength because of the conformational differences at the oil/water interface (Dickinson, Semenova, & Antipova, 1998). It has been suggested that adsorbed *β*-casein has a rather tenuous, extended layer at the oil/water interface, and that this extended layer inhibits sequential adsorption of the caseins (Nylander & Wahlgren, 1994). A multi-layered interfacial film may be formed at high surface coverage (i.e. 3 mg/m^2) (Britten & Giroux, 1993; Srinivasan et al., 1996). A conformation for *κ*-casein at the oil/water interface has been proposed more recently, based on SCF theory (Ettelaie et al., 2014). The uncharged hydrophobic domains show a rather flat conformation at the oil/water interface, whereas the domains around the carbohydrate moieties of *κ*-casein stick out from the interface, providing some degree of steric repulsive force. It appears that *κ*-casein shows a rather loop−train conformation and its lack of a tail end protruding towards the continuous phase is due to the uneven distribution of charge. It has been suggested that *κ*-casein is far from the predicted di-block copolymer (Ettelaie et al., 2014).

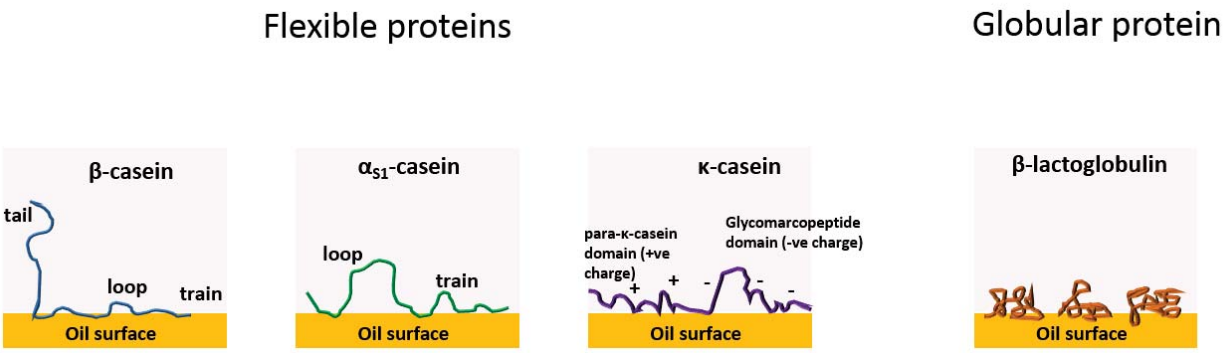

Figure 2.5. Schematic illustration of the conformation of the interfacial layer formed by flexible and globular proteins. Redrawn based on Dickinson (1998b), Ettelaie et al. (2014) and McClements (2005).

Sodium caseinate (NaCas), a commercial casein protein ingredient, consists of α_{s1}-, α_{s2}-, *β*- and *κ*-caseins in the same ratio as found in the casein micelle but is lacking colloidal calcium phosphate (CCP), whey proteins and lactose. NaCas has been widely used as an emulsifier in food formulations (Hunt & Dalgleish, 1994; Mulvihill & Murphy, 1991). The CCP, which is responsible for the integrity of the native casein micelle, has been

removed during processing, allowing NaCas to self-assemble into predominantly small aggregates (~ 10 nm in radius) along with a low volume fraction of large particles with a hydrodynamic radius of ~ 65 nm (HadjSadok, Pitkowski, Nicolai, Benyahia, & Moulai-Mostefa, 2008; Lucey, Srinivasan, Singh, & Munro, 2000). The adsorption behavior of NaCas is different from that of pure caseins because competitive adsorption between α_{s1}- and β- caseins occurs in NaCas-stabilized emulsions. The adsorption behavior is dependent on the total protein concentration and/or the NaCas-to-oil ratio (Srinivasan et al., 1996; Srinivasan, Singh, & Munro, 1999). It has been found that β-casein adsorbs more than α_{s1}-casein at the oil/water interface at low protein-to-oil ratios (< 0.15), whereas α_{s1}-casein adsorbs at the interface in preference to β-casein at high protein-to-oil ratios. The reduced β-casein adsorption has been attributed to the formation of casein nano-particle in concentrated solutions, which reduces its adsorption (Srinivasan et al., 1996).

Calcium caseinate (CaCas) is another commercial casein ingredient that has been studied for its adsorption behavior and emulsion stability (Srinivasan et al., 1999). CaCas consists of approximately 25% aggregated caseins (mainly cross linked via calcium bridges) and the aggregated caseins contain high proportions of α_s-caseins. CaCas spreads poorly at the oil/water interface with aggregates adsorbing intact and has higher surface protein loads (5−20 mg/m^2) than other milk proteins. These dense layers impart better creaming stability than NaCas layers (Srinivasan, Singh, & Munro, 2001).

2.2.1.2 Casein micelles

In bovine milk, casein molecules exist in forms of colloidal aggregates, so-called supramolecules (McMahon & Oommen, 2008). Four main caseins (α_{s1}, α_{s2}, β and κ-caseins) make up the components of casein micelles, in weight ratios of 4:1:4:1 respectively (de Kruif & Holt, 2003). Casein micelle models have been proposed and extensively discussed over the last few decades; two modified nanocluster models proposed by Dalgleish (2011) and de Kruif, Huppertz, Urban, & Petukhov (2012) appear to successfully describe how casein micelles respond to changes in environmental

stresses such as changes in pH, addition of proteolytic enzymes, temperature, pressure, presence of urea and removal of CCP.

The stability of the internal structure of casein micelles is maintained by a balance of hydrophobic and electrostatic forces and the assembly of calcium phosphate nanoclusters (Dalgleish, 2011; de Kruif et al., 2012). In terms of heat stability, the surface properties of casein micelles play important roles in preventing casein micelles from aggregating in aqueous media. The macropeptide region of κ-caseins on the surface of the casein micelle protrudes into the milk serum and forms a brush-like layer, the so-called hairy layer, which is considered to prevent the aggregation of casein micelles. κ-Casein contains 63 amino acids locating outside of the casein micelles which have a high concentration of charged sialic acid residues contributing to the thickness of the hairy layer of casein micelles and hence the steric stability (Tuinier & de Kruif, 2002). Because κ-caseins carry charges, the repulsion of casein micelles can be referred to as electrosteric repulsion (Horne, 2002; Tuinier & de Kruif, 2002). In addition, recent studies have also investigated the effect of water channels in the inner core of the casein micelles on the integrity of the casein micelle (Bouchoux, Gésan-Guiziou, Pérez, & Cabane, 2010; Dalgleish, 2011; Trejo, Dokland, Jurat-Fuentes, & Harte, 2011).

The emulsifying ability and the emulsion stability of casein micelles have been studied using commercial milk protein ingredients [i.e. milk protein concentrate/isolate (MPC/MPI), micellar casein] (Euston & Hirst, 1999; San Martin-González, Roach, & Harte, 2009; Vega, Goff, & Roos, 2007). MPC is a spray-dried powder product that is manufactured by concentrating pasteurized skim milk using ultrafiltration, which is sometimes followed by diafiltration process. Standard MPC is a high protein and low lactose powder in which the casein is in its micellar form, similar to that found in milk, and the whey proteins are also mainly in their native form. Protein-bound minerals are retained (Guinee, O'Kennedy, & Kelly, 2006; Kelly et al., 2000; O'Regan, Ennis, & Mulvihill, 2009). MPC is a cost-effective ingredient and its functional properties has been studied in a number of food systems including ice cream, high protein bars, cheese and dairy beverages (Crowley, Megemont, Gazi, Kelly, Huppertz & O'Mahony, 2014). The compositions and functionalities of different MPCs will vary and will be further affected

by modifications during processing. It has been reported that the ethanol and heat stability of casein micelles increase upon the reduction of colloidal calcium content. Those changes are closely related to the aggregation state of the casein micelles and the calcium ion activity (Grimley, Grandison, & Lewis, 2010).

Casein micelles adsorb at the oil/water interface during emulsification as they do in homogenized milk. However, much higher concentrations of casein micelles are required to achieve a similar droplet size under the same homogenization conditions (Euston & Hirst, 1999). Casein micelles adsorb in thick dense layers that enhance the long term stability of emulsions (Dalgleish, 2006; Euston & Hirst, 1999; Singh, Fox, & Cuddigan, 1993). Increasing the proportion of non-micellar casein increases the amount of protein that can form thin protein layers. Consequently, the surface loading and the average layer thickness decrease, as illustrated in Figure 2.6 (Ye, 2011).

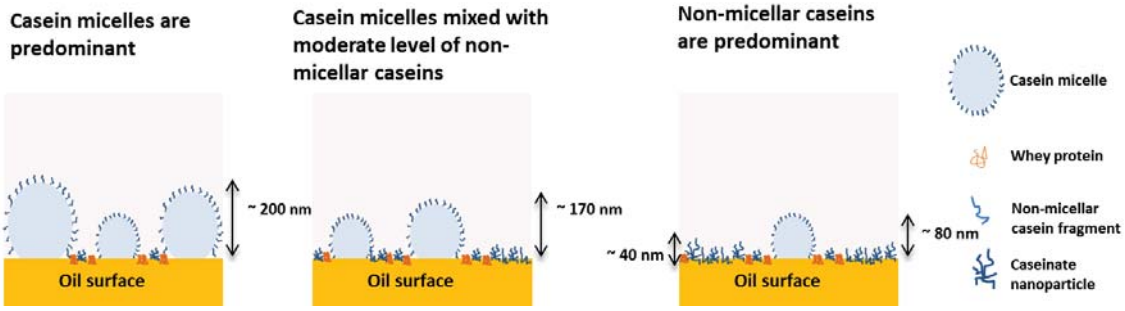

Figure 2.6. Schematic illustration of interfacial structures with different proportions of casein micelles and non-micellar caseins, based on a study of oil-in-water emulsions prepared using milk protein concentrate (MPC) (Ye, 2011).

2.2.2 Whey proteins

Whey proteins constitute the remaining 20% of the protein when bovine milk is acidified to its isoelectric point of pH 4.6 and the precipitated casein is removed (Fox & McSweeney, 1998). The properties of whey proteins are predominantly represented by α-lactalbumin (α-lac) and β-lactoglobulin (β-lg).

α-Lactalbumin

α-Lac is a small, compact, globular protein representing 20% of the total whey protein in bovine milk (Fox et al., 1998). It consists of 123 amino acids and has a molecular weight of 14,146 Da (Boye, Alli, & Ismail, 1997; Fox & McSweeney, 1998). α-Lac has a lower denaturation temperature than β-lg, 65.2 °C at pH 6.7. However, it is the only whey protein that has a thermoreversible profile (> 90% denaturation), especially when it binds Ca^{2+} ions. As the pH is lowered, the Ca^{2+} ion content is substantially reduced and the protein loses its renaturation ability. A reduction in protein stability also occurs when the intramolecular disulfide bridges undergo thiol-disulfide interchange interactions with other proteins (Fox & McSweeney, 1998; Zhang & Brew, 2002).

β-Lactoglobulin

β-Lg is the main whey protein, and plays a dominant role in the properties of whey protein preparations, particularly the reactions that take place during thermal processing (Walstra et al., 2006b). β-Lg comprises approximately 50−58% of the whey protein in milk (Fox & McSweeney, 1998). It contains 162 amino acid residues, has a molecular weight of ~ 18.3 kDa and has an isoelectric point of 5.2 (Kilara & Vaghela, 2004). β-Lg appears as a dimer (molecular weight = 36.6 kDa) at the neutral pH of milk. The molecules are linked strongly together primarily by hydrophobic interactions (Creamer & Sawyer, 2003; Walstra et al., 2006b). Native β-lg has two disulfide bonds and a free thiol group that are located within the protein structure, as illustrated in Figure 2.7 (Edwards, Creamer, & Jameson, 2008).

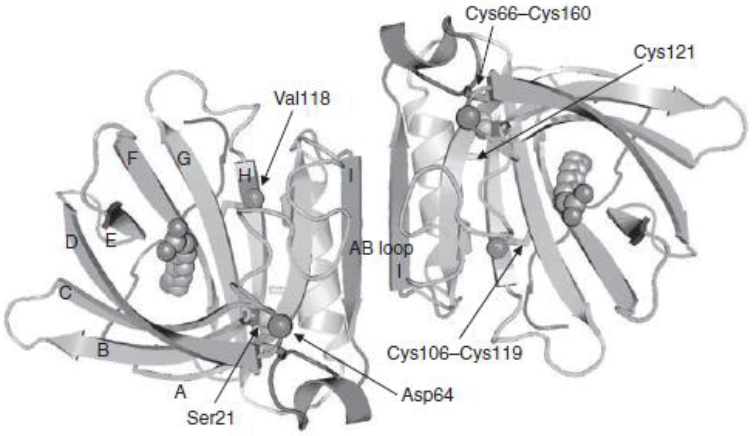

Figure 2.7. Schematic illustration of the three-dimensional structure of *β*-lg, showing the relative positions of the five Cys residues. Adapted from Edwards et al. (2008).

The heat-induced denaturation of *β*-lg has been studied extensively. One thiol group per *β*-lg molecule will be exposed by heat treatment at near-neutral pH (Creamer & Sawyer, 2003). Exposure of the Cys^{121} residue will initiate a series of reactions involving sulfhydryl−disulfide interchange reactions and this has been shown to influence the structural and functional properties of whey proteins during processing (Creamer et al., 2003; Dalgleish & Corredig, 2012; Havea, Watkinson, & Kuhn-Sherlock, 2009). The heat stability of *β*-lg is greatest at acidic pH (pH 3.0), with a denaturation temperature of 85 °C. Raising the pH significantly decreases the denaturation temperature to 78 °C (neutral pH) and 64.6 °C (pH 8.0) (Ju, Hettiarachchy, & Kilara, 1999; Liu, Relkin, & Launay, 1994).

Bovine serum albumin

Bovine serum albumin (BSA) constitutes about 5~10% of the whey protein. BSA contains 582 amino acids, has a molecular weight of 66,443 Da in a single chain and contains 17 disulfide bridges and one free thiol group. The disulfide bonds help to stabilize the primary structure, which consists of nine loops. The tertiary structure of BSA divides into three regular sized globular domains, each consisting of three disulfide-

stabilized loops. Thus, it has an elongated shape (~ 3 nm x 12 nm in size) (Fox & McSweeney, 1998; Haggarty, 2003; Walstra et al., 2006b). BSA has been suggested to be the second most heat-tolerant whey protein behind *β*-lg; it has a small denaturation temperature range (72−74°C) with a wide pH range from 3.5 to 6.5 (Bernal & Jelen, 1985).

Interfacial properties of whey proteins

β-Lg and *α*-lac are the main protein components that contribute to the emulsifying properties of the total whey proteins (Dickinson, 2001; Leman & Kinsella, 1989). *β*-Lg, the most studied whey protein fraction, exhibits slow conformational changes after adsorption. It partially unfolds and slowly forms a two-dimensional solid-like layer (~ 2 nm) through non-bonded intermolecular interactions and thiol−disulfide interchange interactions (Dickinson & Matsumura, 1991; Lefèvre & Subirade, 2003; Tcholakova, Denkov, Ivanov, & Campbell, 2006a). There is a loss of the native tertiary structure as some unfolded hydrophobic side-chains are exposed to the lipid side of the interface (Dickinson, 1998; Leman & Kinsella, 1989). The adsorbed globular protein structure is regarded as being somewhere intermediate between the native state and the fully denatured state. Thus, some globular proteins exist in a so-called molten globule state (Creamer & MacGibbon, 1996; Dalgleish, 1996). Limited denaturation has been shown to improve the emulsifying properties of whey proteins, because unfolding of the protein molecules exposes hydrophobic groups that contribute to the more flexible orientation at the oil/water interface (Leman & Kinsella, 1989). In addition, when they adsorb at the oil/water interface, the globular proteins change their *β*-sheet-rich structure into an open flat structure consisting predominantly of non-native *α*-helix. This structural change has been stated to be responsible for good heat stability at high temperatures (Zhai et al., 2011a; Zhai et al., 2011b). The commercial forms of whey proteins are whey protein isolate (WPI) and whey protein concentrate (WPC). The latter contains lactose, fat and various amounts of calcium salts in addition to crude whey proteins. In general, the physical stabilities of WPI-stabilized emulsions are qualitatively similar to those of

emulsions stabilized by β-lg (Demetriades, Coupland, & McClements, 1997). It is well known that all globular proteins will undergo unfolding, denaturation and subsequent aggregation when heated at above 70 °C (Euston, Finnigan, & Hirst, 2000; Sliwinski, Roubos, Zoet, van Boekel, & Wouters, 2003). The final structure of whey-protein-stabilized emulsions can be tuned between liquid-like and solid-like by changing the conditions of heat treatment, pH and ionic strength (Dickinson, 2012).

Whey protein ingredients can be modified by hydrolysis for specific functional and nutritional uses (Agboola et al., 1998b). Whey protein hydrolyzate (WPH) is a product from the enzymatic hydrolysis of whey proteins and has been extensively used in hypoallergenic infant formulae and enteral formulations (Ryan, Benson, & Flammang, 2000). The functionalities of WPH are affected by its degree of hydrolysis. Lower degrees of hydrolysis (1~10%) have been found to improve the emulsion stability and heat stability of WPH-stabilized oil-in-water emulsions (Euston, Finnigan, & Hirst, 2001b; Singh & Dalgleish, 1998) because the hydrolyzed peptides are less likely to aggregate during heating (Foegeding, Luck, & Vardhanabhuti, 2011). Extensive hydrolysis (10~30%) of the whey proteins can cause rapid creaming and heat-induced coalescence, which results in complete phase separation between the aqueous phase and the oil layer because of a reduced interfacial layer thickness and reduced interfacial viscosity (Agboola et al., 1998b; Euston et al., 2001b; Singh et al., 1998). More extensive hydrolysis will cause a marked decrease in gelling ability of the whey protein peptides because the hydrophobicity of peptides decreases and the electrostatic repulsion increases.

2.2.3 Mixed proteins

Commercial food/dairy formulations are often fortified with mixtures of caseins, casein micelles and whey proteins in order to achieve desired sensory, nutritional and physical profiles. Some competitive adsorption phenomena occur when mixed milk proteins are used for emulsifying the oil droplets (Damodaran, 2004). Some competitive adsorption behaviors of the milk proteins at the interfaces during emulsification have been reported

in emulsion models using commercial milk proteins (i.e. WPC, WPI, NaCas, and MPC) (Brun & Dalgleish, 1999; Dalgleish, Goff, Brun, & Luan, 2002a; Ye, 2008). Ye (2008) reported that, when emulsions stabilized by a combination of NaCas and WPC (1:1 by protein weight) at protein concentrations < 3%, the whey proteins showed greater adsorption than the caseins. In contrast, caseins adsorbed at interfaces in preference to whey proteins at protein concentrations > 3%. After emulsion is made, it was found that the displacement or exchange reaction of caseins by whey proteins occurred at temperatures above 40 °C (Dalgleish et al., 2002a). In emulsions stabilized by WPI and NaCas in a 1:1 ratio, whey proteins were found adsorbed to the interface and displaced α_{s1}- and β-caseins after heating at 80 °C (Brun & Dalgleish, 1999).

2.3 Mechanisms of emulsion stability

2.3.1 Attraction in colloidal interactions

Most emulsions are analogous to atomic and molecular fluids (gases and liquids). Droplets diffuse with an average energy of about k_BT (Mezzenga, Schurtenberger, Burbidge, & Michel, 2005; Trappe, Prasad, Cipelletti, Segre, & Weitz, 2001). Diffusion becomes hindered as the concentration of droplets increases. As the oil droplet concentration increases, the interparticle distances of oil droplets become relatively small comparing to the droplet radius. At sufficiently high concentrations of oil droplets, the spacing between the droplets is very small, and the droplets can only undergo vibration with an amplitude smaller than the droplet radius. At this situation, a suspension will behave like a "solid" exhibiting elastic character. This highly concentrated suspension is often referred to as "solid suspension" (Tadros, 2011).

In the presence of an attraction of 1−1.5 k_BT, droplets fluctuate in and out of the attractive zone but generally phase separate into a condensed phase and a dilute phase, analogous to a gas−liquid condensation. When the attractions are much stronger, the droplets collide but are unable to separate and aggregates are formed. Aggregates will typically cream due to density difference between disperse and continuous phases but, in a sufficiently

concentrated system, aggregation will result in a gel − a network of droplets held together with sufficient strength that the structure is elastic (Aben, Holtze, Tadros, & Schurtenberger, 2012; Dickinson & Golding, 1997c; Hemar, Tamehana, Munro, & Singh, 2001; Lu et al., 2008; Moschakis, Murray, & Dickinson, 2005; Starrs, Poon, Hibberd, & Robins, 2002; Teece, Faers, & Bartlett, 2011). Aggregation can be prevented by a steric barrier that is larger than the energy of the droplets. A biopolymer such as sodium caseinate or gum arabic would be a good candidate as steric stabilizer for preventing aggregation.

In an open gel network, the gel can evolve dynamically by slowly compacting (Dickinson & Golding, 1997a; Moschakis et al., 2005). The actual rate at which this structural evolution occurs should depend on the time for a droplet to escape from the attractive zone of neighboring particles. The concept of the escape time was put forward by Kramers (1940) and, although an analytical solution to the escape time for depletion interactions was not known to the authors, the escape time for triangle-shaped interaction–distance profiles suggested that the following form could apply (Buscall, Choudury, Faers, Goodwin, Luckham & Partridge, 2009):

$$\tau \approx \tau_0 / e^{\frac{-zW}{kT}} = \frac{\pi \eta_s a \Delta^2}{k_B t} e^{\frac{zW}{k_B T}} \qquad (2.1)$$

Here τ is a time that should scale with the escape time, τ_0 is the time required for droplets to freely diffuse across $<\Delta^2>$, where Δ is the range of the attraction. η_s is the continuous phase viscosity (unit in Pa.s). The triangle brackets remind the reader that displacement by diffusion is always the mean-squared displacement. W is the interaction potential (unit in k_BT), z is the number of neighbors to which the particle is attached and k_BT is the thermal energy. Examination of Equation (2.1) reveals that judicious choice of three key parameters − the range of the interaction, the viscosity of the continuous phase and the interaction potential − can change the shelf life of a product from hours to months.

2.3.1.1 van der Waals' forces

The van der Waals' interactions that act between all types of molecule in dispersions, suspensions and emulsions can be calculated based on two mathematical approaches (Hunter, 1986; McClements, 2005). Molecules with a permanent dipole will attract similar molecules when the dipoles approach closely. Alignment of the dipoles induces an attraction because of the addition of a dipole in the nearest neutral atom or molecule (Eastman, 2005). In the presence of a fluctuating electromagnetic field, the neutral atoms have a fluctuating dipole because of the motion of the electrons around the nucleus. Colloidal particles are essentially large assemblies of atoms and therefore the van der Waals' forces from the London dispersion interaction operate between particles to induce attraction (Eastman, 2005).

The van der Waals' interaction between two colloidal particles can be calculated by two approaches. The microscopic approach simply summarizes all the interaction potentials from the nearest neighbors with polarizabilities, dipole moments and electronic energy levels taken into account (Hunter, 1986). The macroscopic approach takes the physicochemical properties of the continuous phase such as dielectric constants, refractive indices and adsorption frequencies into account (Hunter, 1986). Generally, the macroscopic mathematical approach is the most appropriate for describing van der Waals' interactions between emulsion droplets (Hunter, 1986). The van der Waals' inter-droplet potential energy of two emulsion droplets of the same radius, r, separated by a surface-to-surface distance, h, is expressed by the following equation (Eastman, 2005; McClements, 2005):

$$W_{van\ der\ Waals}(h) = -\frac{A_{212}}{6}\left[\left(\frac{2r^2}{h^2+4rh}\right) + \left(\frac{2r^2}{h^2+4rh+4r^2}\right) + \ln\left(\frac{h^2+4rh}{h^2+4rh+4r^2}\right)\right] \quad (2.2)$$

where A_{212} is the Hamaker constant for emulsion droplets (medium 2) separated by the continuous phase (medium 1).

At close separations (h << 2r), this equation reduces to the form:

$$W_{van\ der\ Waals}(h) = -\frac{A_{212}r}{12h} \quad (2.3)$$

In real formulations, with emulsion droplets stabilized by an adsorbed layer of emulsifier molecules, the molecules at the closest proximity to the surface of a colloidal particle influence the total van der Waals' interaction markedly. Taking the contribution of the interfacial layer into account, the van der Waals' potential energy between emulsion droplets can be expressed in the form:

$$W_{van\ der\ Waals}(h) = -\frac{1}{12}\left[A_{131}H\left(\frac{h}{2(r+\delta)}, 1\right) + A_{232}H\left(\frac{h+2\delta}{2r}, 1\right) + 2A_{132}H\left(\frac{h+\delta}{2r}, \frac{r+\delta}{r}\right)\right] \quad (2.4)$$

where the subscripts 1, 2 and 3 represent the continuous phase, the droplet and the interfacial layer respectively and δ is the thickness of the adsorbed layer (Vold, 1961).

2.3.1.2 Hydrophobic interactions

Hydrophobic interactions often occur in two situations. (1) When insufficient or no emulsifier is adsorbed at the oil/water interface, the exposure of non-polar oil molecules is significant (Tcholakova, Denkov, Ivanov, & Campbell, 2002). (2) The adsorbed interfacial material, proteins or sterically stabilizing polymers, contains some exposed non-polar patches and is akin to a "negative" steric stability where the entropy of the macromolecule is outweighed by the exclusion of water from the contact zone (Kim, Decker, & McClements, 2002b; Knudsen, Ogendal, & Skibsted, 2008). In the first situation, the water molecules at one or two layers from the interface have a high free energy, mostly attributed to the lack of entropy. Water molecules align at the interface with hydrogen atoms pointing to the bulk water. The hydrophobic interaction is observed when two of these "structured" layers overlap; the attraction occurs as a result of the reduced number of water molecules with restricted entropy. It should be noted that hydrophobic interaction occurs over a small range, two or three water layers or less than 1 nm. In terms of aggregation in an emulsion system, increasing the capture radius by the length of a water molecule will not increase the capture efficiency of colliding droplets; neither can the non-polar region of a droplet outweigh a repulsive force unless it is

equally short ranged. Aggregation rates are limited by the collision frequency or the height of the repulsive barrier, and not by the depth of the attraction. The depth of attraction will only influence the ability of aggregated droplets to separate and re-disperse. In food emulsions, the strength of the hydrophobic interactions has been illustrated well in emulsions formed with whey proteins. The hydrophobicity of the emulsion droplets has been found to increase on adsorption and particularly under heating conditions (Kim, Decker, & McClements, 2002a; Kim et al., 2002b; Knudsen et al., 2008).

2.3.1.3 Depletion interaction

Many hydrocolloids are used to stabilize the structure of food emulsions; their thickening/gelling abilities mean that they will form weak gel-like entangled biopolymer networks at low concentrations (Dickinson, 2009). Polysaccharides such as xanthan gum and maltodextrin are frequently used in emulsions to inhibit gravity-induced creaming and/or phase separation by increasing the low shear viscosity. Unfortunately, above a certain critical polysaccharide concentration, phase separation occurs because of a depletion effect (Dickinson, Semenova, Antipova, & Pelan, 1998; Hemar, Tamehana, Munro, & Singh, 2001; McClements, 2000; Parker, Gunning, Ng, & Robins, 1995; Sosa-Herrera, Berli, & Martínez-Padilla, 2008; Sun, Gunasekaran, & Richards, 2007; Tuinier & de Kruif, 1999).

Depletion flocculation tends to occur in droplet/polymer mixtures with a marked size difference between the populations and at above a critical non-adsorbed polymer concentration. The smaller population is typically a non-adsorbing polymer, and the larger population is oil droplets. Depletion interaction between two oil droplets occurs when the gap between the two surfaces becomes smaller than the diameter of the biopolymers; the biopolymers are sterically excluded from the interstitial space, increasing the concentration of smaller particles in the bulk solution. This imbalance in osmotic pressure results in an effective attraction between larger particles (Asakura & Oosawa, 1958; Vrij, 1976). At sufficiently high concentrations of oil, the depletion

attraction will create a droplet network that spans the entire sample volume; this gelation can result in partial restabilization of the emulsion (Aben, Holtze, Tadros, & Schurtenberger, 2012; Dickinson, 1999). When the strength of the depletion interaction is comparable with the thermal energy, the position of the droplets fluctuates, and the microstructural network rearranges (Starrs, Poon, Hibberd, & Robins, 2002) and eventually collapses under the influence of gravity (Aben et al., 2012; Dickinson & Golding, 1997b; Lu et al., 2008; Moschakis, Murray, & Dickinson, 2005; Teece, Faers, & Bartlett, 2011). When the depletion interaction potential is relatively strong compared with the thermal energy, the droplets in the network are kinetically trapped and microstructural ageing is said to be arrested (Tanaka, Nishikawa, & Koyama, 2005).

2.3.2 Repulsion in colloidal interactions

2.3.2.1 Steric stability

Steric stability of colloidal particles is established by the anchoring of macromolecules (i.e. polymers) to the surface of the particles. In protein-stabilized emulsions, steric stabilization refers to the stability conferred by the adsorbed protein layers on the oil droplet (Dalgleish, 2006; Dickinson, 1992; McClements, 2005). Steric repulsion occurs when two colloidal particles approach each other at a distance at which undisturbed layers would overlap (Claesson, Blomberg, & Poptoshev, 2004). In a well-known entropic stabilization theory, it is assumed that the adsorbed layer is impenetrable by other large molecules. When the surfaces are brought close together, the polymer segment density increases, leading to an increased number of segment−segment contacts in the approaching zone. As a result, the polymer segments lose conformational entropy, and this reduction in entropy produces a net repulsive force between the colloidal particles, unless water acts as a poor solvent for the segment, in that case an attraction is observed (Claesson et al., 2004).

It has been stated that amphiphilic di-block or graft copolymers are effective steric stabilizers, because they have some polymer chains that have high affinity for the surface

of colloidal particles and other polymer chains that are more compatible with the dispersion medium and extend into the dispersion medium to a significant distance, which prevents the colloidal particles from coming close together (Napper, 1983). The steric stabilization properties of the di-block copolymer, *β*-casein, have been studied in food emulsion systems. It has been suggested that the steric repulsive force will decrease when the adsorbed polymer is desorbed from the particle surface and a complete surface coverage is not established (Claesson et al., 2004; Dickinson, 1992; McClements, 2005; Moro, Gatti, & Delorenzi, 2001; Napper, 1983). Steric stabilization is also affected by the solvent quality of the continuous phase, i.e. by changing the temperature or by adding a miscible component such as ethanol to the aqueous dispersion medium. Under such conditions, the steric layer shrinks (Dickinson, 1992), and droplets may become attractive.

Steric stabilization confers several distinct beneficial effects on colloid stability, in contrast to electrostatic stabilization. They include: (1) relatively insensitive to pH and electrolytes; (2) effective in both aqueous and non-aqueous dispersion media; (3) reversible flocculation; (4) good freeze−thaw stability; (5) less prone to coalescence (Moro et al., 2001; Napper, 1983). It must be stressed that the properties listed above are highly dependent on the properties of the brush layer and do not spontaneously apply to caseins.

2.3.2.2 Electrical double layer repulsion

In most food emulsions, the oil droplets and molecules in the dispersion medium carry an electrical charge. The electrical charge comes from two main sources (Dickinson, 1992): 1. Ionization of carboxylic (−COOH → COO^- + H^+) and amines groups (NH_2 + H^+ → NH_3^+) of the adsorbed materials and 2. Adsorption of small ions from the continuous phase. Preferential adsorption of OH^- and/or Cl^- can occur on emulsion droplets coated by non-ionic surfactants; as a result, the emulsion droplets carry net negative charge (Dickinson, 1992). In case of casein-stabilized emulsions prepared at neutral pH, the negative charges of droplets mainly come from two sources: (1) ionization of the

carboxylic groups (Dickinson, 1992) and (2) the phosphoserine groups (Tuinier & de Kruif, 2002).

The electrostatic interactions between emulsion droplets are determined by the electrical properties of the droplet surfaces and the distribution of ions at interface. A layer of ions adsorbs strongly at the interface and this layer is neutralized electrically by another layer of ions (counter-ions) in the continuous phase. The inner immobile region of the adsorbed ions is referred to as the Stern plane while the outer mobile region where the ions diffuse according to a balance between electrical forces and Brownian motion is referred to as the diffuse layer (Dickinson & Stainsby, 1982; Israelachvili & Wennerström, 1996). The combination of the charged surface and the neutralization of ions by counter-ions in its immediate vicinity is known as the electrical double layer. Electrostatic repulsion occurs when two oil droplets with the same net charge are brought close together and their electrostatic double layers overlap. The counter-ions between the droplets occupy a smaller volume, for instance, the entropy decreases leads to a strong repulsive force between two droplets (Dickinson et al., 1982; McClements, 2005). It has been experimentally illustrated that the electrical potential at the Stern plane is closely related to the electrical potential at the shear plane (also known as zeta potential) (see Figure 2.8). The strength of the electrostatic interaction is closely related to the Debye screening length (κ^{-1}) which corresponds to the distance at which the electrical potential has decayed to a fraction $1/e$ of its surface value (Hiemenz & Rajagopalan, 1997).

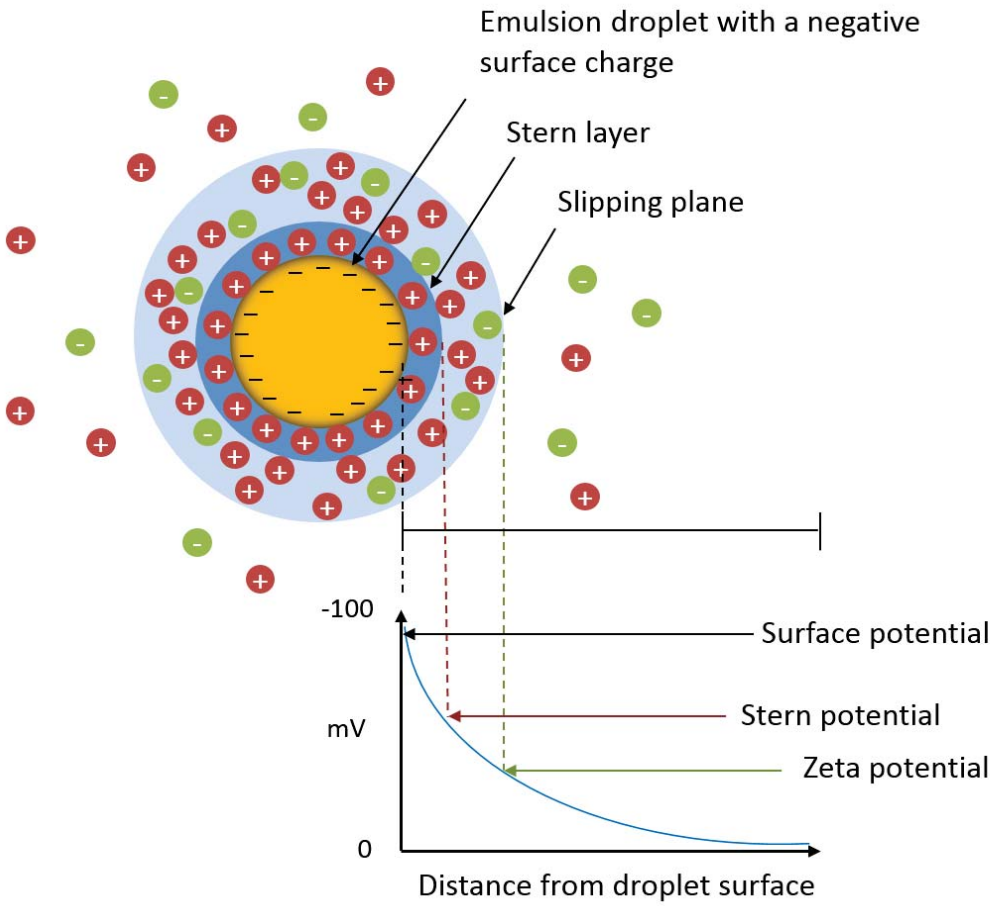

Figure 2.8. Schematic illustration of the electrical double layer at the surface of protein-stabilized emulsion droplet with negative surface charge (Malvern Instruments Ltd, 2004).

The thickness of the electrical double layer is related to the characteristics of the electrolyte solution can be calculated by the following equation:

$$\kappa^{-1} = \sqrt{\frac{\varepsilon_0 \varepsilon_R kT}{e^2 \sum n_{oi} z_i^2}} \tag{2.5}$$

where ε_0 is the dielectric constant of a vacuum, ε_R is the relative dielectric constant of the solution, e is the electrical charge of a single proton, n_{oi} is the concentration of ionic species of type I in the bulk electrolyte solution (in molecules per cubic meter), z_i is their valency (McClements, 2005). The effect is not a Coulomb effect but rather an osmotic

pressure effect from the concentration of ions in the overlapping layers. The electrostatic interaction can be calculated using Poisson-Boltzman theory:

$$W_{electrostatic} = 2\pi\varepsilon\psi_0^2\, a\, \ln\{1 + \exp[-\kappa(h - 2a)]\} \quad (2.6)$$

where ψ_0 is the electrical potential at the surface of the charged droplet and the parameters which have been defined previously in Eq. 2.5. The strength of electrostatic interactions between oil droplets depends on the electrical properties of the adsorbed layer of a droplet, the size of the oil droplets, the ionic strength and the presence of polyvalent ions in the continuous phase (McClements, 2005; Napper, 1983).

Electrostatically stabilized dispersions/emulsions can be said to be kinetically stable but are very sensitive to the presence of electrolytes, while sterically stabilized dispersions/emulsions are thermodynamically stable and show much less dependency on electrolytes (Napper, 1983). In protein-stabilized emulsions, to enhance the long-term stabilization of oil droplets has been attempted by combining electrostatic and steric stabilization. This combined mechanism is referred to as electrosteric stabilization (Dickinson, 1997, 1999b). In dispersions stabilized by proteins, it has been challenging to distinguish whether steric or electrical double layer repulsion is the dominating one. The electrosteric stabilization may arise in food emulsions under three different situations. (1) When polyelectrolytes adsorb in dense layers at interface, not all charge is neutralized within the adsorbed layer and an electrical double layer extends from the surface of the adsorbed layer. The dense layer therefore confers an electrical double layer force and a short ranged steric force from the elastic compression of the adsorbed layer. Under these circumstances the zeta-potential provides a good estimate of the electrical double layer force (Biggs & Healy, 1994; Ortega-Vinuesa, Martín-Rodríguez, & Hidalgo-Álvarez, 1996; Popa, Gillies, Papastavrou, & Borkovec, 2009, 2010; Seebergh & Berg, 1994). (2) The electrostatic force plays an important role in controlling the solubility and flexibility of the polyelectrolyte brush and steric repulsion. When polyelectrolytes adapt an open conformation of loops and tails or are grafted to form a brush layer, the vast majority, if not all of the charge, is usually neutralized within the layer, and the electrical double layer emanating from the surface can be neglected. The charge expands the conformation

of adsorbed layer and keeps it open (Fritz, Schädler, Willenbacher, & Wagner, 2002). Here, the adsorbed layer has a steric stabilizing effect with the thickness of the layer regulated by the layer's charge and electrolytes in the continuous phase (Balastre et al., 2002; Block & Helm, 2008). The κ-casein "hairy" layer on casein micelles (de Kruif & Zhulina, 1996) and the adsorbed layer of β-casein (Blomberg, Claesson, & Fröberg, 1998; Claesson, Blomberg, Fröberg, Nylander, & Arnebrant, 1995; Nylander & Wahlgren, 1997) are good examples of this electrosteric based interaction. (3) An exception occurs at vanishingly small electrolyte concentrations whereby the charge of the polyelectrolyte is not neutralized within the layer. This last example is sometimes referred to as a "Pincus" brush (Pincus, 1991), but is not generally observed in food systems as the ionic strength is generally too high. Particles and droplets covered with an open layer will exhibit an electrophoretic mobility but the apparent zeta potential is meaningless.

2.3.3 Destabilization mechanisms of protein-stabilized oil-in-water emulsions

Oil-in-water emulsions are thermodynamically unstable and their long term stability is influenced by a number of physical and chemical processes (McClements, 2005). The emulsion may undergo gravitational separation (creaming and sedimentation), flocculation, coalescence and phase separation, as illustrated in Figure 2.9, which could result in poor visual attractiveness and reduced mouthfeel of the emulsion product (Dickinson, 1992; McClements, 2005; Tan, 2004; Tcholakova et al., 2006a).

2.3.3.1 Creaming

In oil-in-water emulsions, the upward movement of oil droplets under gravity is referred to as creaming (Dickinson, 1992; McClements, 2005). The gravity-induced upward force needs to exceed Brownian diffusion (Equation 2.7) (k_BT, where k is the Boltzmann constant, T is the absolute temperature, r is the hydrodynamic radius of the oil droplet and L is the height of the container) (Tadros, 2004).

$$\frac{4}{3}\pi r^3 \Delta\rho g L \gg kT \tag{2.7}$$

Creaming generally occurs when, first, the particle radius r is larger than a few hundred nanometers; second, the density difference between the dispersed phase and the continuous phase exceed 0.1. Creaming of an emulsion is undesirable, because an opaque droplet-rich layer is a sign of a heterogeneous appearance that reduces the visual attractiveness. Nevertheless, creaming is a reversible phenomenon when the droplets are repulsive or only weakly attractive. The droplets from the cream layer can return to their original homogeneous distribution with gentle mixing (Dickinson, 1992). In addition, the perception of the droplet-rich phase will affect the mouthfeel of the emulsion (McClements, 2005; Tan, 2004). In the absence of flocculation, the rate of creaming of an oil droplet in a dilute emulsion ($\emptyset < 0.01$) can be estimated by equating the gravity force with the opposing hydrodynamic force, following Stokes' Law (Equation 2.8), where ρ_p and ρ_s are the dispersed phase density and the continuous phase density respectively and η_s is the continuous phase viscosity.

$$V_{stokes} = \frac{2gr^2(\rho_p - \rho_s)}{9\eta_s} \tag{2.8}$$

For more concentrated emulsions ($0.1 < \emptyset < 0.2$), the creaming velocity of the droplets decreases because, as the number of particles increases, the particle crowding produces hydrodynamic interactions as well as an increasing probability of collisions between particles. Then the creaming rate follows Equation 2.9 (McClements, 2005).

$$V = V_{stokes}(1 - 6.55\emptyset) \tag{2.9}$$

When $\emptyset > 0.2$, the volume fraction of droplets plays a dominant role in determining the creaming velocity, and a semi-empirical equation (Equation 2.10) can be used to predict the creaming rate. $\emptyset_c$ is the maximum packing fraction, at which the creaming velocity approaches zero. k is a semiempirical quantity and its determination depends on the nature of the emulsion (McClements, 2005).

$$V = V_{stokes}\left(1 - \frac{\emptyset}{\emptyset_c}\right)^{k\emptyset_c} \tag{2.10}$$

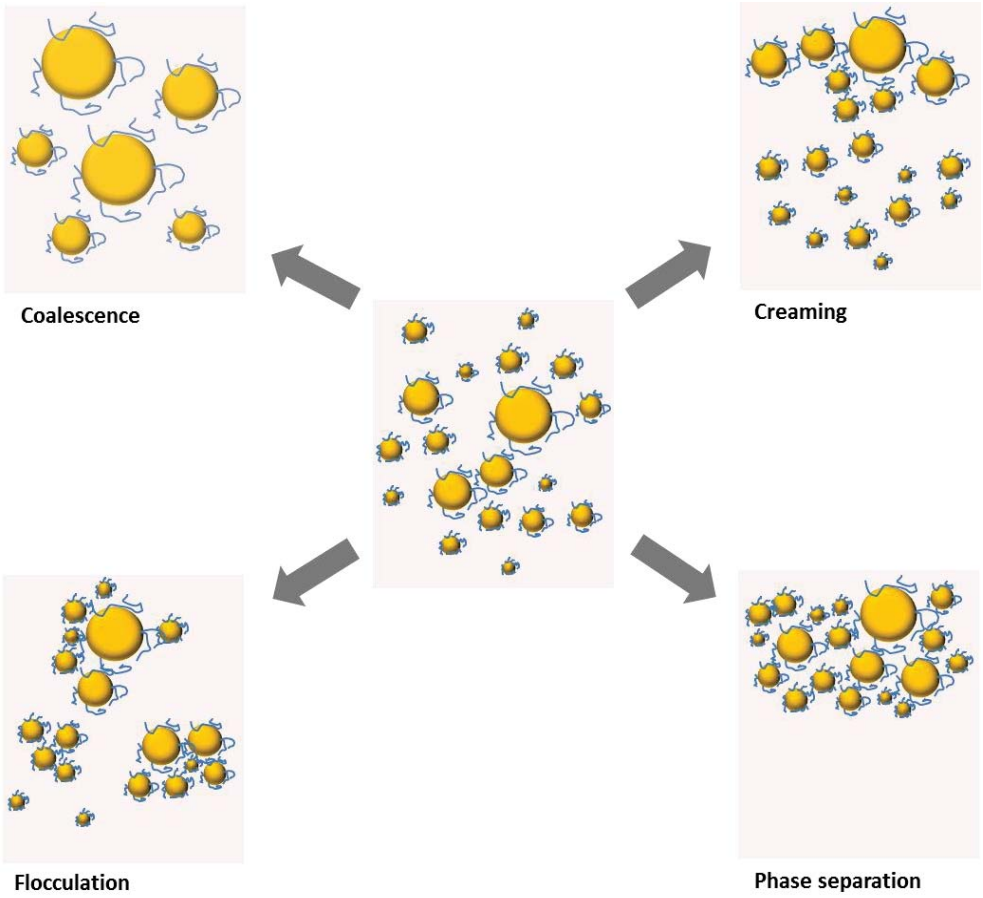

Figure 2.9. Schematic illustration of emulsion instability in oil-in-water emulsions (redrawn from McClements, 2005).

2.3.3.2 Coalescence

Coalescence is the irreversible merging of two or more emulsion droplets into a larger single droplet. Coalescence leads to accelerated creaming (not as fast as flocculation-induced creaming) and can eventually result in a layer of oil on top of the product (oiling-off) (Dickinson, 1992; McClements, 2005) (see Equation 2.7, as r increases). This phenomenon occurs only when the droplets are in close proximity under the influence of van der Waals' forces and the thin film (lamellae) between the droplets bursts (Dickinson, 1992; McClements, 2005). The oil droplets may be deformed as they encounter each other if the interaction force or applied force (gravitational or hydrodynamic) outweighs the effect of the interfacial tension (Walstra, 2003, 2005). The

balance between external forces and the Laplace pressure is indicated by the Weber number:

$$We = \frac{\Delta\sigma_{ext}}{P_L} = \frac{a^2\sigma_{ext}}{2\gamma h} \quad (2.11)$$

For $We \ll 1$, it is expected that the droplets will show stability against coalescence. At $We = 1$, droplet deformation becomes steadily stronger and a flat film is expected to form on both sides. For $We \gg 1$, a larger flat film is formed and increases the rate of coalescence (Walstra, 2005). It has been found that the coalescence rate is affected by the intensity of agitation, the rigidity of the interface, the surfactant type and concentration, the surface shear viscosity, the droplet size and the volume fraction (Walstra, 2005). It is important to note that, if the oil droplets are stabilized by polymers, steric stabilization can keep the droplets apart and prevent the film from rupturing even for $We \gg 1$ (Walstra, 2005).

2.3.3.3 Partial coalescence

Coalescence can also be originated and arrested prior to the formation of a single spherical droplet, and this phenomenon is referred to partial coalescence (Fredrick, Walstra, & Dewettinck, 2010; Walstra, 2003). Partial coalescence is required to achieve the desired structure and physicochemical properties of food emulsions such as ice cream, toppings, whipped creams, and so on (Goff, 1997; Walstra, 2003). Partial coalescence occurs only when the droplets/globules contain solid particles and the oil phase is partly crystalline (Walstra, 2003). Before partial coalescence is initiated, the fat crystals exhibit a strong tendency to move towards the oil/water interface because this is thermodynamically more favorable. An internal fat crystal network is formed within the droplet/globule as it is induced by van de Waals attraction during undercooling. Upon collision, two partly crystalline droplets/globules will initiate partial coalescence when the distance between the two droplets/globules is smaller than the extended section of the fat crystal; the extending crystals will penetrate the thin film between the two droplets/globules into the liquid oil portion of the neighboring droplet. If there is sufficient liquid oil within the droplets/globules, the oil preferably wets the fat crystals

enhancing the structure of the aggregated droplets/globules (Fredrick et al., 2010; Walstra, 2003). Not only is the dynamic balance between the forces driving shape relaxation but also an opposing force desired for the partial coalescence structures. The droplet elasticity at the droplet surface or within its volume has been shown to regulate the resistance of droplets to complete coalescence (Pawar, Caggioni, Ergun, Hartel, & Spicer, 2011; Pawar, Caggioni, Hartel, & Spicer, 2012). Other factors that influence the rate of partial coalescence have been reviewed recently (Fredrick et al., 2010).

2.3.3.4 Flocculation and aggregation

The terms flocculation and aggregation/coagulation are often used interchangeably. In the present review, flocculation implies the process of the formation of a loosely connected protein or droplet network in which the particles retain their individual integrity. The flocculated network may be disrupted by force and can be re-dispersed. Aggregation/coagulation refers to the formation of large aggregates which may precipitate out from solution, float or sediment and strong forces are usually required to dissociate aggregates (Dickinson, 1992; Walstra, 2005; Walstra, Wouters, & Geurts, 2006a).

Of all emulsion destabilization mechanisms, droplet flocculation appears to be the most complicated to manipulate because it is affected by a number of parameters such as type of emulsifier, mean droplet size, oil volume fraction, protein-to-oil ratio, pH, ionic strength and ionic calcium content (Dickinson, 2010; Piorkowski & McClements, 2014). Droplet flocculation also directly influence creaming and coalescence. Two types of droplet flocculation are noteworthy: bridging flocculation and depletion flocculation.

Bridging flocculation arises when the emulsifier (high molecular weight)-to-oil ratio is too low and the amount of emulsifier is not sufficient to completely coat the entire surface of the oil droplets. As a result, the coating is able to adsorb on to two or more oil droplets (Dalgleish, 1997; Dickinson, 2009). This irreversible droplet−droplet interaction exhibits shear-thinning behavior because of the presence of a strongly aggregated droplet

network and is often followed by coalescence (Surh, Decker, & McClements, 2006a). Other types of bridging flocculation can form by reactions between specific groups of adsorbed emulsifiers. The steric repulsion provided by emulsifiers does not prevent temporary partial overlap of the adsorbed layers. For example, emulsion droplets will flocculate in the presence of Ca^{2+} ions and this is referred to as calcium bridging (Walstra, 2005). The binding of Ca^{2+} ions to α_{s1}-, β-casein or κ-casein results in decreasing electrostatic repulsion (Horne, 2002; Jeurnink & de Kruif, 1995). Another example of bridging flocculation is the formation of covalent −S−S− linkages between proteins from different droplets (Havea et al., 2009; Walstra, 2005). It is also important to note that Ca^{2+} ions induce the formation of small aggregates of Ca^{2+}−protein complexes that have reduced emulsifying properties (Ye & Singh, 2000, 2001).

Different classes of polymer (depletant) − milk proteins (Dickinson & Golding, 1997a; Rosa, Sala, van Vliet, & van de Velde, 2006; ten Grotenhuis, Tuinier, & de Kruif, 2003; Ye, 2011), polysaccharides (Blijdenstein, Veerman, & van der Linden, 2004; Chanamai & McClements, 2001; Moschakis et al., 2005; Parker, Gunning, Ng, & Robins, 1995; Tuinier & de Kruif, 1999) and surfactant micelles (Dickinson & Ritzoulis, 2000; Dickinson, Ritzoulis, & Povey, 1999) − have been found to cause depletion flocculation in oil-in-water emulsions. Depletion flocculation arises when the gap between the surfaces of two large spheres becomes smaller than the hydrodynamic diameter of the non-adsorbed polymers as the two large spheres move close together. If the non-adsorbed polymers are flexible, they are excluded because of the reduction in configurational entropy. Subsequently, an osmotic pressure gradient between the interstitial space and the continuous phase is generated because the concentration of non-adsorbed polymers outside the interstitial space increases. The neighboring large spheres are eventually pushed into contact to form larger flocculates (see Figure 2.10). The large sphere is surrounded by a depletion layer that is induced by the non-adsorbed polymers. The characteristic thickness is dependent on the hydrodynamic radius of the non-adsorbed polymers and is a measure of the range of the depletion interaction potential (Asakura & Oosawa, 1954; Radford & Dickinson, 2004; Vrij, 1976).

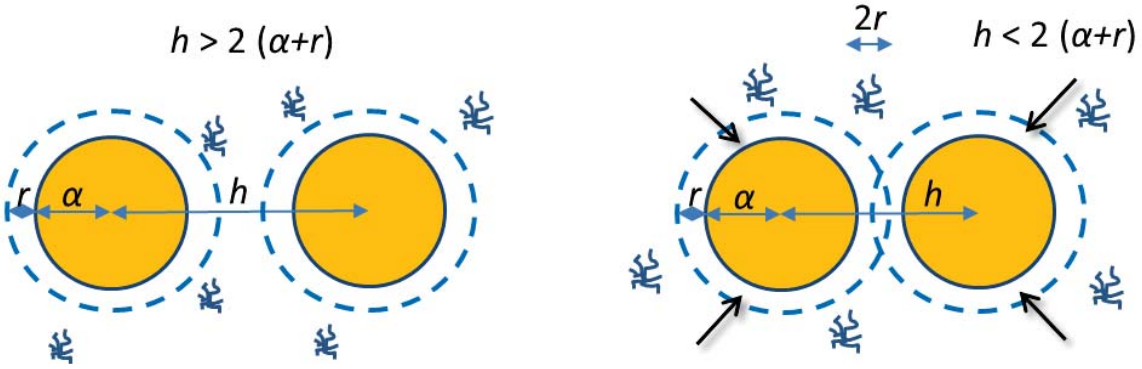

Figure 2.10. Schematic illustration of depletion-induced weakly attractive spheres. α is the radius of the large sphere, h is the surface−surface distance and r is the hydrodynamic radius of the non-adsorbed polymers, based on Asakura & Oosawa (1954).

The stability of depletion-flocculated emulsions is influenced by the depletion interaction potential, which in turn is affected by the polymer-to-droplet ratio, the applied stress and the volume fraction of droplets and non-adsorbed polymers (Asakura & Oosawa, 1954; Lu et al., 2008; Radford & Dickinson, 2004; Trappe et al., 2001; Vrij, 1976). The depletion interaction potential can be calculated as follows:

$$W_{depletion} = -\frac{4\pi}{3}(a+r)^3\left[1-\frac{3h}{4(a+r)}+\frac{h^3}{16(a+r)^3}\right]nk_BT\left(1+\frac{2C_{non-adsorbed}}{\rho_{sm}}\right) \quad (2.12)$$

$h < 2(a+r)$

Under some specific conditions, i.e. high concentrations of oil (Parker, 2009) or high depletion interaction potential (Berli, Quemada, & Parker, 2002; Dickinson & Golding, 1997c), the depletion-attraction-induced droplet network occupies the entire sample volume. In this way, the depletion-flocculated network is said to provide partial restabilization (Aben et al., 2012; Dickinson, 1999b). It has been confirmed that the restabilization induced by depletion is thermodynamic in origin because of the lack of a sufficiently large attractive force (Vincent, 1990). The position of the droplets fluctuates and the droplet network rearranges when the strength of the depletion interaction is comparable with the thermal energy (Starrs et al., 2002). The droplet network eventually coarsens and collapses under the influence of gravity (Aben et al., 2012; Dickinson & Golding, 1997c; Lu et al., 2008; Moschakis et al., 2005; Teece et al., 2011). If the depletion interaction potential is relatively strong compared with the thermal energy, the

droplets in the network can be kinetically trapped and the microstructural aging is said to be arrested (Tanaka, Nishikawa, & Koyama, 2005).

2.3.4 Impact of heat treatment on protein-stabilized oil-in-water emulsions

Liquid food/dairy emulsions at neutral pH (6.5−7.0) are often subjected to heat treatment (i.e. retort, ultra-high temperature processes) to achieve consumer acceptability across the shelf life of the products (Cruijsen, 1996; Keowmaneechai & McClements, 2002; Livney, Corredig, & Dalgleish, 2003; McSweeney, Mulvihill, & O'Callaghan, 2004). In the dairy industry, the heat stability of milk refers to the ability of milk to withstand high heating temperatures (i.e. 120−140 °C) without gelation or the formation of visible coagulants (Singh, 2004; Walstra et al., 2006a). Heat coagulation is referred to as the time at which the protein dispersion becomes visible, when large dense aggregates have precipitated or when a gel-like texture has emerged. The time required for coagulation is the so-called heat coagulation time (HCT) (Davies & White, 1966; McSweeney, Healy, & Mulvihill, 2008; McSweeney et al., 2004). The heat stability of milk protein dispersions has been investigated in the temperature range 60−140 °C. The use of heating temperatures between 120 and 140 °C in a silicone oil bath does not perfectly simulate the actual sterilization conditions, as in a pilot-scale retort or UHT sterilizer, but is sufficient to indicate the ability of a protein-fortified product to withstand prolonged heating at these temperatures (de Kort, Minor, Snoeren, van Hooijdonk, & van der Linden, 2012; Rattray & Jelen, 1997; Singh, 2004).

In some cases, heat-induced emulsion destabilization is desirable, such as in the formation of a whey protein emulsion gel matrix (Dickinson, 2012); in others, e.g. liquid emulsion-type products, heat-induced droplet−droplet, protein−droplet and protein−protein interactions, especially those that eventually result in accelerated creaming, coalescence or increased viscosity, are undesirable (Dickinson & Parkinson, 2004; McClements, 2005; Nikiforidis & Kiosseoglou, 2008). A number of experimental studies have shown that the protein molecular structures of both the adsorbed proteins and the non-adsorbed proteins determine the extent and the type of the heat-induced

destabilization of oil droplets (Euston et al., 2000; Hunt & Dalgleish, 1995; Nikiforidis & Kiosseoglou, 2007; Sliwinski et al., 2003). Nevertheless, some studies have emphasized the effect of pre-homogenization heat treatment of protein solutions on droplet size formation and creaming stability (Dybowska, 2007, 2008, 2011). Here, the recent advances on the effects of pre- and post-homogenization heat treatments on the physical stability of protein-stabilized oil-in-water emulsions will be captured.

2.3.4.1 Impact of pre- and post-homogenization heat treatment on interfacial proteins

Heat-induced effects on casein adsorption and inter-particle interactions

Caseins and one of their most used commercial form, NaCas, have a disordered structure, contain small amount of cysteine residues (mainly from α_{s2}- and κ-casein) and are particularly stable to heat coagulation. Nevertheless, dephosphorylation, hydrolysis and polymerization of NaCas solutions can occur at high temperatures (110−140 °C) (Gaucheron, Mollé, & Pannetier, 2001; Guo, Fox, Flynn, & Kindstedt, 1996; Hustinx, Singh, & Fox, 1997; van Boekel, 1999). Several studies have investigated the effect of pre-homogenization heat treatment of caseinates on their emulsifying ability, droplet formation and interfacial structures (Jahaniaval, Kakuda, Abraham, & Marcone, 2000; Srinivasan et al., 2002; Srinivasan, Singh, & Munro, 2003). It was found that, although the surface hydrophobicity of NaCas increased upon heating, the oil droplets stabilized by heated NaCas had slightly larger droplet size (Srinivasan et al., 2002). Similar results were found for CaCas (Srinivasan et al., 2003) and MPC (Dybowska, 2007, 2008) emulsion systems.

It has been observed that NaCas-stabilized oil droplets are more susceptible to heat-induced destabilization than non-adsorbed NaCas particles in solution at high temperatures (i.e. 120 °C) (Srinivasan et al., 2002). A similar change in the heat stability has also been reported in casein-micelle-stabilized emulsion systems (Singh, Sharma, Taylor, & Creamer, 1996; Sweetsur & Muir, 1983). It has been found that, when heated in the pH range 6.3−6.7, the κ-casein from partially disrupted casein micelles at oil/water

interface has a greater tendency to dissociate into the continuous phase than the κ-casein that dissociates from casein micelles in the continuous phase (Singh et al., 1996). Collectively, the heat stability of casein-stabilized oil droplets decreases with increasing volume fraction of oil (Cruijsen, 1996) and follows the order: NaCas > MPC > CaCas (Augustin, Oliver, & Hemar, 2011; Munro, 2002). Not only the effect of casein composition on the heat stability of oil droplets is important, the aggregation state of the casein micelles and calcium activity also play major roles in determining the heat stability. The higher the degree of dissociation of casein micelle, the lower the heat stability of casein micelle solution (de Kort et al., 2012). The lower the calcium activity, the better the heat stability of milk (Faka, Lewis, Grandison, & Deeth, 2009; Sharma & Singh, 1999).

Heat-induced effects on whey protein adsorption and inter-particle interactions

Heat-induced interactions under certain conditions have been used to create controlled whey protein morphologies and structures (Nicolai, Britten, & Schmitt, 2011; Nicolai & Durand, 2013; Spiegel & Huss, 2002). Improved emulsifying properties of heat-treated β-lg and whey proteins in their commercial form (WPC and WPI) have been reported extensively (Bernard, Regnault, Gendreau, Charbonneau, & Relkin, 2011; Dissanayake & Vasiljevic, 2009; Kim, Cornec, & Narsimhan, 2005; Moro, Báez, Ballerini, Busti, & Delorenzi, 2013; Moro et al., 2001). It has been shown that the denaturation of whey proteins (> 70 °C) increases the surface hydrophobicity because of the unfolding of the whey protein molecules and exposure of their thiol groups (Dissanayake & Vasiljevic, 2009; Kim et al., 2005; Relkin, 1996; Tcholakova, Denkov, Sidzhakova, & Campbell, 2006b). Similar heat-induced denaturation of whey proteins has also been observed after high pressure homogenization (Kuhn & Cunha, 2012; Sandra & Dalgleish, 2005) and ultrasonication (Chandrapala, Zisu, Palmer, Kentish, & Ashokkumar, 2011; Nguyen & Anema, 2010). It has been reported that heat-induced whey protein aggregates lose their intermolecular β-sheet structure at the oil/water interface, but can still cover the oil droplet surface efficiently (Audebrand, Ropers, & Riaublanc, 2013). The denaturation of whey proteins results in smaller droplet sizes and narrower droplet size distributions. This

change has been attributed to the complementary effect of native and denatured whey proteins and the small proportion of protein aggregates. The native whey proteins adsorb at the oil/water interface first and the denatured whey protein particles facilitate the formation of a thick layer (Bernard et al., 2011). The thickness of the denatured whey protein aggregates will be enhanced when whey proteins are heated at high ionic strength (Audebrand et al., 2013). Conflicting results for the heat-induced emulsifying properties of whey proteins have also been reported. It has been revealed that the emulsifying ability of whey proteins reduces significantly after heating and that the whey protein aggregates are unable to spread on the oil droplet surface efficiently because of restricted flexibility (Millqvist-Fureby, Elofsson, & Bergenstahl, 2001; Segall & Goff, 2002); this results in a larger droplet size (Dybowska, 2011; Knudsen et al., 2008; Millqvist-Fureby et al., 2001; Moro et al., 2013). The heat treatment and the homogenization conditions may have a synergistic effect on improving the creaming stability (Guggisberg, Chollet, Schreier, Portmann, & Egger, 2012).

Whey-protein-stabilized oil droplets are very heat stable at low ionic strength (<50 mM of NaCl or KCl), with little change in the droplet size on post-homogenization heat treatment up to 121 °C (Hunt & Dalgleish, 1995; Ye, 2010; Ye & Singh, 2006). However, extensive droplet aggregation occurring at high heating temperatures in emulsions formed with WPC has been reported in several studies (Euston et al., 2000; Keowmaneechai et al., 2006; Surh et al., 2006b). It is generally agreed that the adsorbed whey proteins unfold during heating, leading to increased surface hydrophobicity and droplet aggregation associated with the disulfide-mediated interactions between adsorbed and non-adsorbed proteins, which is strengthened in the presence of Ca^{2+} ions (Euston et al., 2000; Monahan, McClements, & German, 1996). However, several heat-induced physicochemical changes that remain unclear include: (1) the change in the amount of adsorbed protein during heating (Ye, 2010); (2) the displacement of α-lac from the interface by β-lg (Ye & Singh, 2006); (3) the pattern of change in droplet size during prolonged heating (Sliwinski et al., 2003). It has been suggested that, if the surface protein coverage of the oil droplets decreases, there will be less aggregation of the particles because fewer interfacial proteins will participate in aggregation (Euston, Finnigan, & Hirst, 2001a).

2.3.4.2 Impact of heat treatment on non-adsorbed proteins

Heat-induced effects on caseins

Heat stability studies on milk proteins in solution can be used to explain the heat-induced mechanisms that are associated with non-adsorbed proteins in emulsion systems. The caseins in the form of NaCas in solution are extremely stable to heat coagulation from 110 to 140 °C at pH ≥ 6.5 at low ionic strength (Guo et al., 1996; Guo, Fox, Flynn, & Mahammad, 1989). However, a number of changes occur at these temperatures including aggregation, dephosphorylation, deamidation, polymerization and hydrolysis (Guo et al., 1996; Guo et al., 1989; van Boekel, 1999). The mechanism of heat-induced dephosphorylation is either hydrolysis of phosphoserine or β-elimination. The former results in formation of phosphate and the latter results in formation of dehydroalanine and phosphate (van Boekel, 1999). Non-disulfide cross-linking of caseins can occur via the formation of dehydroalanine. Dehydroalanine can subsequently react with the amino group of lysine residues yields intra- or intermolecular lysinoalnaine cross-links. Dehydroalanine can also react with histidine or cysteine resulting in histidinoalanine or lanthionine cross-links (Fox & McSweeney, 1998; Holland, Gupta, Deeth & Alewood, 2011). These cross-links will reduce protein solubility, digestibility and nutritional values (Fox & McSweeney, 1998). Heat-induced dephosphorylation has another effect on casein micelle structure as the casein-phosphate groups provide negative charge governing the micelle stability. During heating, the loss of casein-phosphate groups, the casein or casein micelle has less charge which may lead to increased attractive association of the casein molecules (van Boekel, 1999).

It has been shown that α_{s2}-casein is the most susceptible casein to heat-induced degradation (Guo et al., 1989). It has been revealed that κ-casein is able to stabilize α_s-caseins against heat-induced precipitation in the presence of Ca^{2+} ions through the formation of disulfide bonds (Zittle, 1969). Similarly, remarkably good heat stability has been observed in casein micelles because of their rheomorphic structure (Holt & Sawyer, 1993). Recent studies have investigated the heat stability of micellar caseins (the commercial form of intact casein micelles) under sterilization conditions. The kinetics of

casein micelle aggregation and/or coagulation are controlled by the heating conditions and the aqueous phase environment, with the heating temperature, initial pH and aggregation state of the casein micelle being the main factors determining the extent of casein−casein interactions (Beliciu, Sauer, & Moraru, 2012; Sauer & Morara, 2012). In addition, O'Connell & Fox (2000) have suggested that casein micelles of smaller size and narrower micelle size distribution confer better heat stability than large micelles because the proportion of κ-casein content of small casein micelle is higher and the degree of κ-casein glycosylation is lower for smaller micelles.

Heat-induced effects on whey proteins

Although whey proteins are susceptible to heat denaturation − β-lg denatures at ~75−80 °C and α-lac denatures at ~60−65 °C (Relkin, 1996) − under low ionic strength conditions, α-lac has been found to be extremely heat stable at pH values > 6.7 upon heating at 140 °C whereas β-lg is less stable (McSweeney et al., 2004; Rattray & Jelen, 1997). Under high ionic strength conditions, denatured whey proteins form a precipitate or a gel-like texture at neutral pH (Keowmaneechai & McClements, 2006). The heat-induced aggregation behavior of whey proteins in terms of aggregation kinetics, particle size, conformational change, charge density and morphology at different pH, ionic strength and protein concentration has recently been reviewed (Nicolai et al., 2011; Nicolai & Durand, 2013).

Heat-induced effects on mixed proteins

Caseins and whey proteins often coexist in commercial food emulsions, e.g. in recombined milk emulsions (Kasinos, Tran Le, & van der Meeren, 2014) and infant formulae (McSweeney et al., 2004). Recently, a number of studies have found that α_{s1}-, β- and κ-caseins and micellar casein are able to stabilize globular proteins, such as β-lg, against heat-induced aggregation. This stabilization derives from a chaperone-like behavior (Morgan, Treweek, Lindner, Price, & Carver, 2005; Thorn, Ecroyd, & Carver,

2009; Thorn et al., 2005). On heating, α_{s1}- and β- caseins do not change the denaturation of β-lg and the aggregation steps of whey proteins (Kehoe & Foegeding, 2011; Parker, Donato, & Dalgleish, 2005). They probably compete to interact with denatured β-lg through hydrophobic interactions and can refold the denatured β-lg to its native state or protect it from forming large insoluble aggregates (O'Kennedy & Mounsey, 2006; Sakono, Motomura, Maruyama, Kamiya, & Goto, 2011; Thorn et al., 2009; Yong & Foegeding, 2010). In contrast, κ-casein interacts with unfolded whey proteins through disulfide bonds and increases the steric repulsion of the heat-induced whey protein−κ-casein complexes. This mode of action of κ-casein shares some similarities to that for casein micelles, and inhibits the extensive formation of whey protein−κ-casein complexes by repelling other proteins (Guyomarc'h, Nono, Nicolai, & Durand, 2009). In comparison with the protein aggregation inhibition behavior of non-micellar casein, micellar casein promotes denaturation but controls aggregation (O'Kennedy & Mounsey, 2006). When α_{s1}-, β- and κ-caseins are present together in a whey protein solution, the efficiency of the chaperone-like activity of the α_{s1}- and β-caseins is reduced. This occurs probably because α_{s1}- and β-caseins can protect κ-casein from aggregating into fibrils (Thorn et al., 2009) and they may compete with κ-casein for interaction with the denatured whey proteins (Guyomarc'h et al., 2009). At a certain concentration of salt, the chaperone-like activities of the α_{s1}- and β-caseins become significantly less effective (Kehoe & Foegeding, 2011; Treweek, Thorn, Price, & Carver, 2011). In addition, at around the critical gelling concentration (10% w/w) of whey protein, the presence of NaCas does not prevent it from gelling (Picone, Takeuchi, & Cunha, 2011).

When a mixture of casein micelles and whey proteins, similar to the composition of bovine milk, is heated, the heat-induced destabilization is noticeably pH dependent (McSweeney et al., 2004; Rattray & Jelen, 1997; Singh & Fox, 1985; van Boekel, Nieuwenhuijse, & Walstra, 1989a). The HCT maximum−minimum profiles of milk and concentrated milk are well documented (Singh, 2004). The destabilization mechanisms of milk involve a decrease in pH, the precipitation of soluble calcium phosphate and the denaturation of whey proteins (Holt & Sawyer, 1993; van Boekel et al., 1989a; van Boekel, Nieuwenhuijse, & Walstra, 1989b, 1989c). Studies found that when whey proteins were depleted from milk (casein micelles only), the HCT of the protein solution

significantly decreases in the pH range 6.8−7.3 and increases the HCT in the pH range 6.4−6.8 (McSweeney et al., 2004; Rattray & Jelen, 1997). The specific casein−whey protein interactions play an important role in determining the maximum−minimum in the HCT−pH profile of mixed casein micelles and whey proteins. At pH values close to the heat stability maximum (~ pH 6.7), whey proteins, especially *β*-lg, interact with *κ*-casein in the hairy layer of the casein micelle, acting as a steric enhancer. At higher pH values > 6.7, there is increased hydrolysis and dissociation of *κ*-casein from the casein micelles. The dissociation is probably due to the surface charge of *κ*-casein reaches a critical value and the hydrophobic bonds no longer sufficient to link *κ*-casein to the casein micelle surface (Singh, 2004). The denatured *β*-lg preferentially interacts with the serum *κ*-casein dissociated from the micelles rather than the *κ*-casein on the surface. The casein micelles become more sensitive to calcium-induced coagulation because of the reduced *κ*-casein content (Anema, 2008; Singh, 2004). Recent studies have allowed us to illustrate the casein micelle−whey protein interactions in milk: at pH values < 6.6, all denatured whey proteins associate with the casein micelles and the *β*-lg−*κ*-casein complexes formed are inhomogeneous; at pH values > 6.6, some of the denatured whey proteins associate with the casein micelles and some denatured whey proteins self-associate to form soluble aggregates in the serum; at pH 6.55, the distribution of denatured whey proteins on the casein micelles is rather homogeneous (Donato & Dalgleish, 2006; Vasbinder & de Kruif, 2003). The even coverage of denatured whey proteins on the casein micelles at pH 6.55 is consistent with the small change in particle size of the casein micelles compared with at other pHs during heating (Anema & Li, 2003). The calcium equilibrium is also important in determining the heat stability of casein micelle−whey protein mixtures. The detailed mechanisms and kinetics of the heat-induced changes have been well documented elsewhere (van Boekel et al., 1989a, 1989b, 1989c).

2.4 Impact of droplet size and volume fraction on heat stability, creaming stability and rheological properties of protein-stabilized emulsions

2.4.1 Influence of droplet size

2.4.1.1 Formation of emulsion droplet and creaming stability

The production of small emulsion droplets has been of great interest in food and pharmaceutical industries; they not only provide high colloidal stability against creaming and coalescence but also enhance mouthfeel, flavor release and the delivery of oil-soluble bioactive components (Rao & McClements, 2011; Wooster, Golding, & Sanguansri, 2008). The droplet size is affected not only by the emulsifier type and concentration but also by the homogenization conditions (McClements, 2005). Emulsification is the result of an equilibrium between droplet break-up and re-coalescence and is affected by the type and concentration of emulsifier present, the volume fraction of oil, the ratio of the viscosities of the dispersed and continuous phases, energy input, residence time of the emulsion in the emulsification zone and the type of flow (Jafari, Assadpoor, He, & Bhandari, 2008; Lee, Niknafs, Hancocks, & Norton, 2013; Piorkowski et al., 2014). High pressure homogenizers, such as the two-stage valve homogenizer and the microfluidizer, are the most common emulsification equipment for preparing emulsions in institutes and industry (see Figure 2.11) (Dumay et al., 2013; Lee & Norton, 2013). The main difference between the two techniques is that, within the microfluidizer, droplet break-up occurs when the droplets collide at the end of a very small channel in the interaction chamber. The droplets reduce in size because of the collision (Schultz, Wagner, Urban, & Ulrich, 2004).

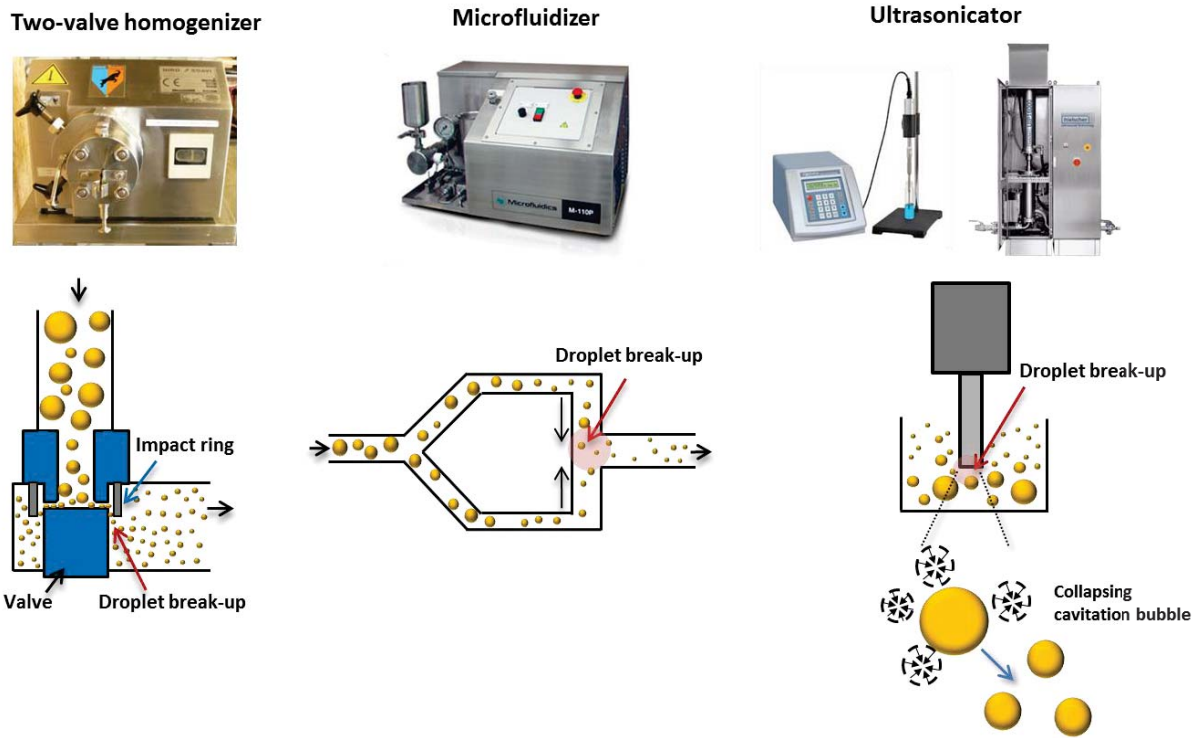

Figure 2.11. Schematic illustration of three types of emulsification equipment that can be used to produce fine emulsion droplets: two-valve high pressure homogenizer; microfluidizer; ultrasonicator (Piorkowski & McClements, 2014).

At an emulsifier concentration above that required to form a monolayer at the oil/water interface, Qian & McClements (2011) found that, using the microfluidizer, the formation of small oil droplets is dependent on the homogenization pressure and the number of passes. Under the same microfluidization conditions, low molecular weight surfactants produced smaller droplets than proteins, with the descending order of minimum droplet diameter achieved being NaCas > β-lg > Tween 20 > sodium dodecyl sulphate (SDS). The discrepancy between surfactant and protein is probably because surfactant diffuses and adsorbs more rapidly at the oil/water interface than protein during the droplet break-up and re-coalescence process (Qian & McClements, 2011). A similar trend in the minimum droplet diameter was observed by (Jafari, He, & Bhandari, 2007a). However, Lee & Norton (2013) found no difference in mean droplet diameter between surfactant (SDS and Tween 20) and protein (NaCas) at the same pressure and number of passes during microfluidization but SDS formed smaller droplets than Tween 20 and NaCas

during two-valve homogenization. It was suggested that the elongational flow at the exit of the microfluidizer provided sufficient time for the newly formed droplets to be coated by emulsifier and hence the droplet diameter was independent of emulsifier type. For two-valve homogenization, the formation of smaller droplets by SDS is attributed to the electrostatic repulsive force provided by the SDS. After droplet break-up, the electrostatic repulsive force between droplets limits the possibility of re-coalescence (Tcholakova, Denkov, & Danner, 2004). Small droplets can also be formed by ultrasonication, in which the disruptive forces generated by cavitation are mainly responsible for droplet break-up. However, its use is limited to low viscosity fluids (Jafari, He, & Bhandari, 2006, 2007b). Although droplet formation has been shown to be dependent on the ratio of the viscosities of the dispersed and continuous phases (Qian & McClements, 2011; Wooster et al., 2008), it has been concluded that the effect of this ratio on droplet formation remains controversial and deserves further research (Lee & Norton, 2013).

2.4.1.2 Influence of droplet size on heat stability

Very few studies emphasized on the impact of droplet size on the heat stability of protein-stabilized emulsions. However, it has been reported that the heat stability in terms of the HCT decreases after the raw milk undergoes homogenization (Sweetsur & Muir, 1983). McCrae & Muir (1991) have found a correlation between surface load and heat stability. The heat stability of homogenized milk decreases with an increased amount of interfacial protein adsorbed at fat globule surface. Singh & Latham (1993) have advanced the understanding of the heat coagulation behavior. It can be assumed that the oil droplets present in milk are predominantly stabilized by intact casein micelles and that large micellar fragments are large casein micelles. At a given protein concentration, the large casein micelles may contain fewer κ-casein molecules per unit area at the oil/water interface because the adsorbed casein micelles may redistribute at the interface upon adsorption and some κ-casein molecules may adsorb directly at the interface. Therefore, the large oil droplets may act as κ-casein-depleted casein micelles and are more susceptible to heat-induced aggregation/coagulation due to the electrosteric stability large

casein micelle decreases (Singh, Fox & Cuddigan, 1993). Although the heat-induced interactions between denatured whey proteins in the serum and the interfacial casein micelles of fat globules in homogenized milk has been studied (Ye, 2003). However, the heat coagulation behavior in a colloidal system containing casein-micelle-stabilized oil droplets is still not fully understood.

2.4.1.3 Influence of droplet size and droplet size distribution on emulsion rheology

In most liquid food emulsions, the viscosity of the dispersed phase makes a smaller contribution to the overall rheology than the viscosity of the continuous phase, which is usually modified by adding thickening agents (Dickinson, 2003; Ford, Borwankar, Pechak, & Schwimmer, 2004; Tadros, 2004). However, the rheological properties of the droplets have a significant effect on concentrated oil-in-water emulsions, such as salad dressings and mayonnaise (Tadros, 2004; Walstra, 2003). Both the volume fraction of the dispersed phase and the nature of the colloidal interactions determine the extent of contribution of the droplet size and droplet size distribution to the rheology of an emulsion. In the absence of appreciable colloidal interactions and at relatively high droplet concentrations ($\emptyset$ > 0.45), the droplet size has a more significant impact (McClements, 2005). For polydisperse oil-in-water emulsions stabilized by adsorbed proteins, the relative viscosity of the emulsion η_r can be calculated from (Howe, Clarke, & Whitesides, 1997):

$$\eta_r = \frac{\eta}{\eta_o} = \left(1 - \frac{\emptyset_e}{\emptyset_m}\right)^{-[\eta]\emptyset_m} \quad (2.13)$$

where η is the measured viscosity (zero-shear Newtonian plateau value), η_o is the measured zero-shear viscosity of the continuous phase, $[\eta]$ is the intrinsic viscosity (2.5 for hard spheres), $\emptyset_e$ is the effective volume fraction of the dispersed phase and $\emptyset_m$ is the maximum packing volume fraction for polydisperse spheres (0.71 is a typical value for randomly packed polydisperse spheres) (Schaertl & Sillescu, 1994). For emulsion droplets stabilized by adsorbed emulsifier molecules, the role of $\emptyset_e$ in the shear modulus of a jammed emulsion can be described as (Mason, Bibette, & Weitz, 1995):

$$G' = \frac{\emptyset_e{}^{1/3}(\emptyset_e - \emptyset_m)\,\sigma}{r} \tag{2.14}$$

where r is the total hydrodynamic radius of the emulsion droplet, σ is the interfacial tension and $\emptyset_m$ is 0.71. Figure 2.12 shows the influence of an adsorbed layer stabilized by milk proteins with different hydrodynamic radii on the predicted zero-shear droplet−droplet interactions. The hydrodynamic radii for casein micelles, NaCas, whey proteins and aggregated whey proteins were obtained from (de Kruif et al., 2012), (Radford & Dickinson, 2004), (Zhai et al., 2011b) and (Schmitt, Bovay, Rouvet, Shojaei-Rami, & Kolodziejczyk, 2007) respectively. It is clear that it takes less volume fraction to achieve the same relative viscosity as the hydrodynamic radius of the emulsion droplets increases. At $\emptyset_e$ close to the $\emptyset_m$, the difference becomes difficult to measure and the relative error increases.

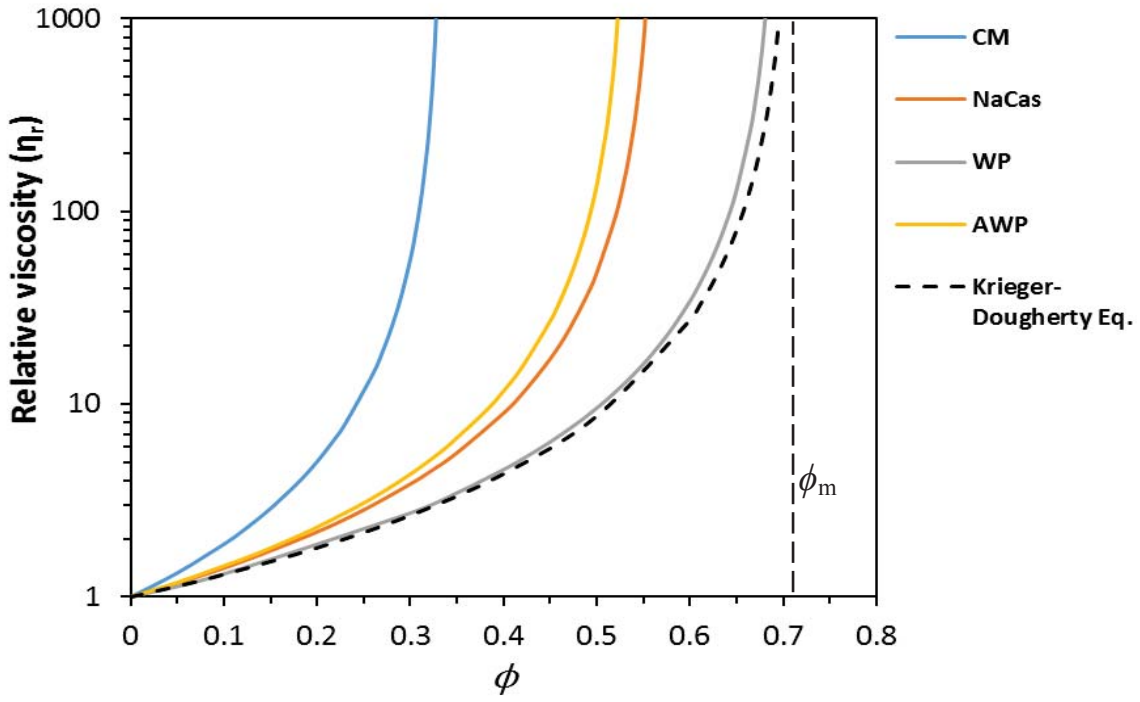

Figure 2.12. Zero-shear relative viscosity of polydisperse oil-in-water emulsions stabilized by casein micelle (CM), NaCas nano-particle (NaCas), whey protein (WP) and aggregated whey protein (AWP), as predicted by Equation 2.13 with $\emptyset_m = 0.71$ (Schaertl & Sillescu, 1994). The R_h of milk proteins used in the calculation is 100 nm for CM (de Kruif et al., 2012), 10 nm for NaCas (Radford & Dickinson, 2004), 2 nm for WP (Zhai et al., 2011b) and 50 nm for aggregated whey protein (Schmitt et al., 2007).

It has been well documented that the maximum packing volume fraction of a polydisperse suspension is higher than that of monodisperse spheres and is controlled by the particle size distribution (PSD) (Farris, 1968; Servais, Jones, & Roberts, 2002). In general, the effective maximum packing volume fraction increases and the relative viscosity decreases with increasing PSD (Farris, 1968; Servais et al., 2002). Figure 2.13 shows the shift in the maximum packing volume fraction in emulsions with different PSDs. The PSD has a greater effect on the maximum packing volume fraction when it changes from monomodal to bimodal. However, there is a less pronounced effect on viscosity reduction if the shape of polydispersity of oil droplets is greater than trimodal, for instance, tetramodal (Servais et al., 2002). Basically, small particles provide a lubrication effect to the flow of large particles and hence decrease the overall viscosity under shear conditions (Servais et al., 2002). In addition to the PSD, the maximum packing volume fraction has also been found to be dependent on the particle size ratio. The particle size ratio, $\lambda = d_L/d_S$, refers to the ratio of the diameter of large particles to that of smaller particles in the next particle class. For a given PSD, the larger the particle size ratio, the greater the maximum packing volume fraction. At infinite diameter ratio, the $\emptyset_m$ reaches a maximum value (Servais et al., 2002).

Moreover, the increase in the volume fraction of oil droplets not only results in increased relative viscosity at low shear rates but also increases the extent of shear-thinning behavior (Pal, 2000). A sharp transition in the shear-thinning effect can be seen in a narrow concentration range when close to the maximum packing volume fraction (Pal, 2000). Emulsions containing finer droplets have much higher relative viscosities and storage moduli at low shear rates than emulsions containing coarse droplets (Pal, 1996). Interestingly, the low shear viscosities of emulsions formed with WPC decrease and the shear flow behavior changes from shear-thinning behavior to Newtonian behavior as the droplet size and the droplet size distribution decrease. However, the exact reason is not known and the change in shear flow behavior cannot simply be attributed to the droplet size distribution effect (Floury, Desrumaux, & Lardières, 2000).

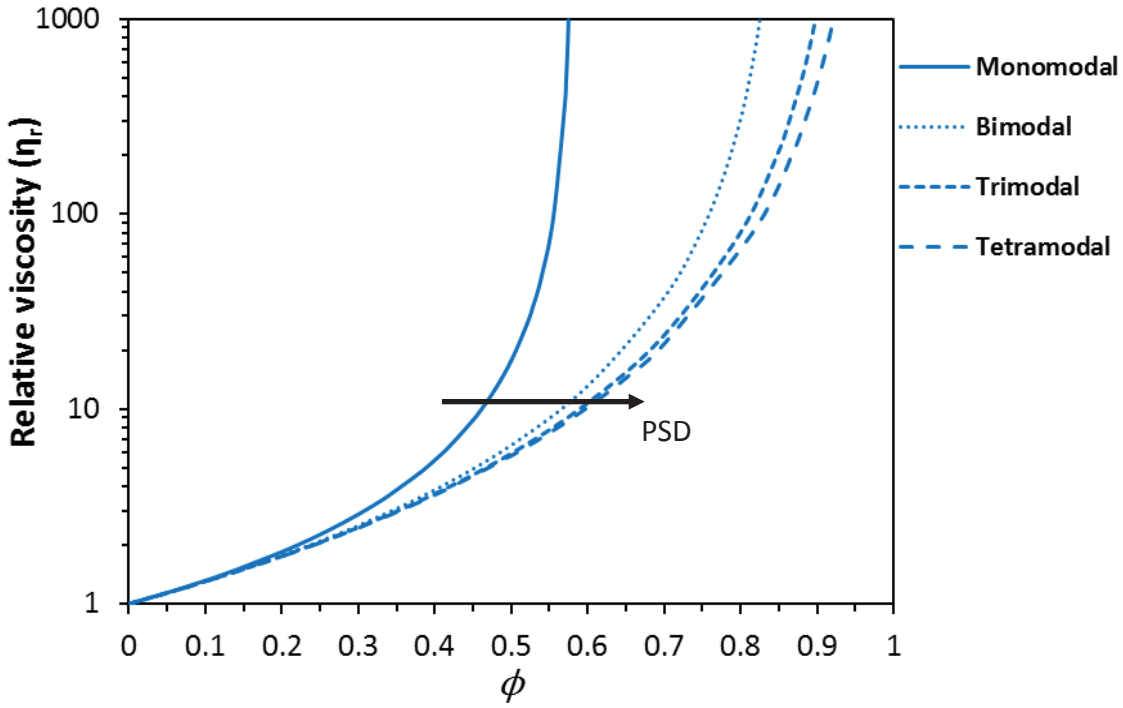

Figure 2.13. Predicted zero-shear relative viscosities of suspensions of polydisperse spheres for different PSDs, with the infinite particle size ratio based on data from Genovese (2012). The arrow indicates that higher solids contents can be packed in a suspension for a given relative viscosity.

2.4.2 Influence of volume fraction

2.4.2.1 Influence of volume fraction on heat stability

The volume fractions of both oil droplets and continuous phase proteins contribute to the heat stability of protein-stabilized oil-in-water emulsions. The presence of NaCas-coated oil droplets has a significant effect on the HCT−pH curve of NaCas-stabilized emulsions (Cruijsen, 1996). Generally, the HCT decreases at all pH values and can be attributed to the increase in the effective volume fraction of caseinate particles. The addition of 25% w/w oil increases the volume fraction from 0.47 to 0.65 in oil-free NaCas dispersions (Cruijsen, 1996). A similar decrease in HCT has also been reported when milks are concentrated (Huppertz & Fox, 2006b; Sievanen, Huppertz, Kelly, & Fox, 2008; Singh,

2004). The concentration effect causes slight decrease in pH and increase Ca^{2+} activity, which also contribute to the decreased HCT. It has been suggested that the coagulation kinetics of casein particles when salt-induced coagulation is the predominant factor can be quantitatively described by fractal aggregation theory (Njeuwenhuijse, van Vliet, & Walstra, 1992). In addition, heating whey protein dispersions at high protein concentration increases the aggregation rate and the formation of large aggregates (Grácia-Juliá et al., 2008). The critical gelation point of whey proteins at low ionic strength is ~10−12% w/w concentration (Purwanti, Moerkens, van der Goot, & Boom, 2012).

2.4.2.2 Influence of volume fraction on emulsion rheology

In a concentrated-protein emulsion system (protein concentration ≥ 8% w/w and oil content ≤ 10% w/w) in which colloidal interactions are absent, the rheology behavior is mostly dominated by the viscosity of the continuous phase protein (Tadros, 2004). Understanding the physicochemical and rheological properties of concentrated protein dispersions helps in an understanding of the rheology of the concentrated-protein emulsion system. In the following, the rheology of the protein-rich phase is described using caseinate nano-particles and casein micelles as the model proteins. The recently reported zero-shear viscosity trend of concentrated casein micelles and caseinate nano-particles is summarized in Figure 2.14. Here, casein nano-particle is referred to small self-assembled reversible aggregate of sodium caseinate. Use of this term intends to avoid any potential confusion with surfactant micelles and to distinguish the term "sub-micelle" from the popular sub-micelle model of the casein micelle (Radford & Dickinson, 2004).

It was well known that the viscosity of non-interacting monodisperse hard spheres increases as the concentration increases and diverges as the critical volume fraction approaches the random close packing volume fraction $\emptyset_m \sim 0.6$ (Meeker, Poon, & Pusey, 1997; van der Werff & de Kruif, 1989). The viscosity of a lactose-free casein micelle dispersion up to a volume fraction of $\emptyset \sim 0.45$ has been well described using the hard

sphere model (Alexander, Rojas-Ochoa, Leser, & Schurtenberger, 2002; de Kruif, 1992, 1998). It has been shown by light scattering that above 7% protein, the casein micelles in milk were no longer free diffusing (Nair, Dalgleish, & Corredig, 2013). The rheology of casein micelle dispersion does not deviate from hard sphere behavior up to $\emptyset \sim 0.25$ (de Kruif, van Iersel, Vrij, & Russel, 1985) but it undergoes jamming at $\emptyset \sim 0.45$ (Dahbi et al., 2010). However, the zero shear viscosity increases steeply at higher volume fractions of casein micelles and deviates from hard sphere behavior at a volume fraction of 0.69 (Bouchoux et al., 2009; Dahbi et al., 2010). At higher packing fractions (~ 0.55−0.61), the deformability of the casein micelle describes the deviation of the viscosity from hard sphere behavior (Bouchoux et al., 2009; Dahbi et al., 2010). At volume fractions above 0.55, casein micelle dispersions can be considered to be microgel particles (Dahbi et al., 2010; Mezzenga et al., 2005; Panouillé, Benyahia, Durand, & Nicolai, 2005). The effective radius of the casein micelles may decrease because of hydrodynamic forces acting on the κ-casein layer (Berli & Quemada, 2000) and correspondingly the casein micelles undergo deformation (Bouchoux et al., 2009; Dahbi et al., 2010). The deformed casein micelles with transiently changed shape can still align with each other at high packing volume fractions (Bouchoux et al., 2009; Dahbi et al., 2010). Nonetheless, in a recent study, Nair et al. (2014) argued that casein micelles behave as incompressible hard spheres up to high critical packing volume fractions ($\emptyset_m \sim 0.8$) under shear conditions (shear rate of 300 s^{-1}), because they found that the voluminosity of the casein micelles was independent of the protein concentration. Colloidal calcium phosphate (CCP) nanocluster (about 2 nm in diameter) plays a critical role in casein micelle integrity by attaching the caseins on the centers of phosphorylation (3−5 nearby phosphorylated amino acid residues) (de Kruif et al., 2012). In addition to a change in viscosity, the release of CCP from the casein micelles at high protein concentrations has been observed (Anema, 2009). However, it has been suggested that the release of CCP has little effect on the integrity of the casein micelles during concentration (Nair et al., 2014).

A similar trend of a protein-concentration-dependent viscosity change has also been reported in NaCas dispersions (Farrer & Lips, 1999; Pitkowski, Durand, & Nicolai, 2008). The steep increase in viscosity in > 8% NaCas dispersions has been attributed to the jamming of soft caseinate particles (Thomar, Durand, Benyahia, & Nicolai, 2012).

The effect of the addition of $CaCl_2$ on the rheology of NaCas dispersions has recently been investigated (Thomar et al., 2012) and the results have also been compared with those obtained in CaCas dispersions (Thomar, Nicolai, Benyahia, & Durand, 2013). It can be concluded that the presence of Ca^{2+} ions results in the formation of dense caseinate domains caused by Ca^{2+}-mediated attractive interactions, which is the main factor determining the shear flow and viscoelastic behavior of casein dispersions. At low protein concentrations (< 16%), the effective volume fraction of CaCas dispersions is lower because of the presence of dense caseinate domains and, as a consequence, results in a lower relative viscosity. Above a critical concentration (> 16%), the relative viscosity increases dramatically and the viscosity change can be attributed to the percolation of the dense domains and the formation of a space-spanning network (Thomar et al., 2013). Interestingly, if eight Ca^{2+} ions per casein molecule are present in an NaCas dispersion, the zero-shear relative viscosity is analogous to that of a CaCas dispersion. At any given concentration up to 30%, the effect of Na^{+} ions on Ca^{2+}-fortified NaCas dispersions is negligible (Thomar et al., 2013).

The rheology of casein micelles in heated milk as a function of protein volume fraction is largely unexplored. Recent study by Nair et al (2013) found that casein micelles in heated milk (90 °C, 10 min) behaved rheologically as unheated milk with similar packing voluminosity despite there were soluble whey protein aggregates present in the continuous phase. However, in heated milk, the voluminosity of casein micelles was found to be smaller at pH 7.0 than that obtained at pH 6.4 and 6.7. Similar to heated milk, the motion of casein micelles was found to be arrested at above 7% protein concentration (Nair et al., 2013).

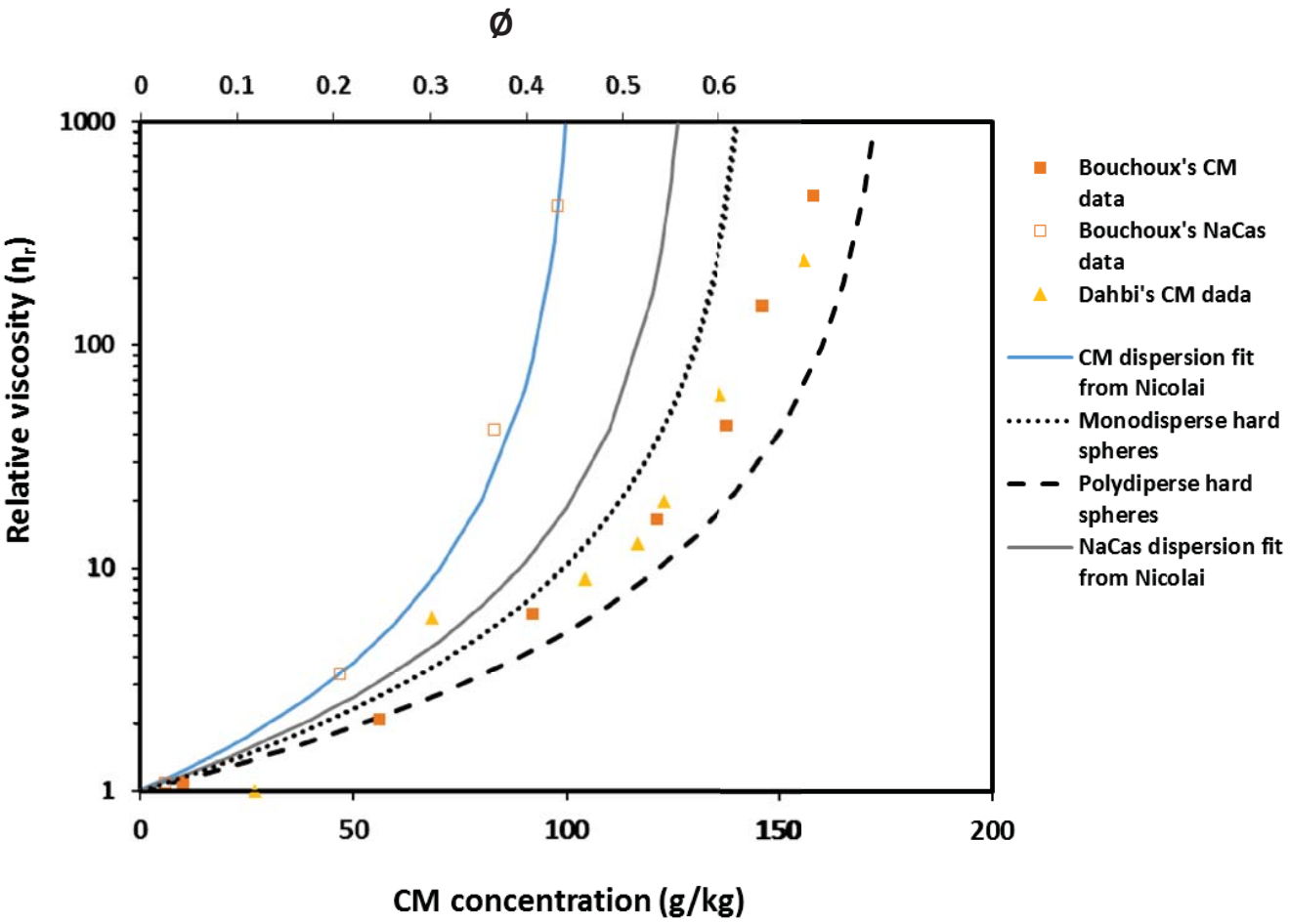

Figure 2.14. Comparison of the relative zero-shear viscosities of casein micelle (CM) and NaCas dispersions as a function of casein concentration with those of a predicted monodisperse hard sphere dispersion with $\emptyset_m \sim 0.64$ (dotted line) and a polydisperse hard sphere dispersion with $\emptyset_m \sim 0.78$ (dashed line), as calculated using the Quemada equation (de Kruif, van Iersel, Vrij, & Russel, 1985). The voluminosity of the casein micelle was estimated to be 4.4 g/cm^3 (de Kruif, 1998).

2.5 Impact of attractive and repulsive forces on the heat stability, creaming stability and rheological properties of protein-stabilized emulsions

2.5.1 Effect of attractive force on heat stability, creaming stability and rheological properties

2.5.1.1 Impact of depletion force on the heat stability of protein-stabilized emulsions

The presence of non-adsorbed biopolymer not only induces emulsion instability, as described in Section 2.3.1.3, but also reduces the heat stability of protein-stabilized emulsions (Euston, Finnigan, & Hirst, 2002; Ye et al., 2006) because of a strong depletion-induced effect (Diftis & Kiosseoglou, 2006; O'Regan & Mulvihill, 2010). The reasons for the destabilization of emulsions containing proteins and polysaccharides include the following. (1) The presence of depletion forces increases the droplet encounter frequency because of the rapid formation of a weakly attracted droplet network (Diftis & Kiosseoglou, 2006). Additionally, it is possible that the rate of droplet flocculation increases at high temperature (i.e. > 100 °C). It has been reported that the viscosity of xanthan gum reduces as a function of heating temperature (60−120 °C). The droplet network rearrangement is influenced by the continuous phase viscosity (Parker, 2009; Vélez, Fernández, Muñoz, Williams, & English, 2003). Therefore, droplet network formation may occur well before heat-induced aggregation. (2) It is possible that heat-induced xanthan gum aggregates may interact with proteins at the oil/water interface and cause destabilization depending on if thermal motion is larger than depletion interaction potential (Euston et al., 2002). (3) Bryant & McClements (2000) have suggested that heat-induced aggregation of whey proteins increases the molecular weight and the size of the aggregate, which results in phase separation in the presence of xanthan gum in the continuous phase because of thermodynamic incompatibility. This in turn increases the aggregation rate of unfolded whey protein molecules. Consequently, the association between non-adsorbed denatured whey proteins and interfacial whey proteins increases. A similar mechanism has been proposed for carrageenan−β-lg mixtures (Capron, Nicolai, & Durand, 1999).

2.5.1.2 Impact of depletion force on the creaming stability and rheology of protein-stabilized emulsions

It has been argued that the "weak gel" properties of biopolymer solutions or the presence of a yield stress at a certain biopolymer concentration is responsible for the permanent stabilizing effect against creaming. However, the exact mechanism for the improved creaming stability is still debatable. Recently, several groups have emphasized the importance of droplet−droplet interactions on the partial restabilization of depletion-flocculated emulsions (Aben et al., 2012; Dickinson & Golding, 1997c; Moschakis et al., 2005). The broad agreement is that, above a certain biopolymer concentration, a colloidal droplet network is formed by the long-lived droplets that span the entire volume and transiently stabilize the emulsion structure.

Dickinson and co-workers (1997a, 1997b) have studied the droplet network formation behaviors as a function of caseinate concentration (1−6%) and the main findings are summarized in Figure 2.15. At 1.5−3% NaCas, the low shear relative viscosities are 100−1000 times greater than expected for non-interacting droplets. Creaming profiles and microscopy further indicate the formation of interconnected droplet networks that coarsen and eventually collapse under gravity. The increase in the concentration of non-adsorbed NaCas up to 6% increases the number of droplets participating in the network, which in turn kinetically stabilizes the emulsion structure against phase separation. It has been suggested that once the emulsion phase separates into two phases, the bound droplets within the network is shown to increase slightly proving that the depletion-flocculated network still contribute to the stability of the emulsion (Aben et al., 2012).

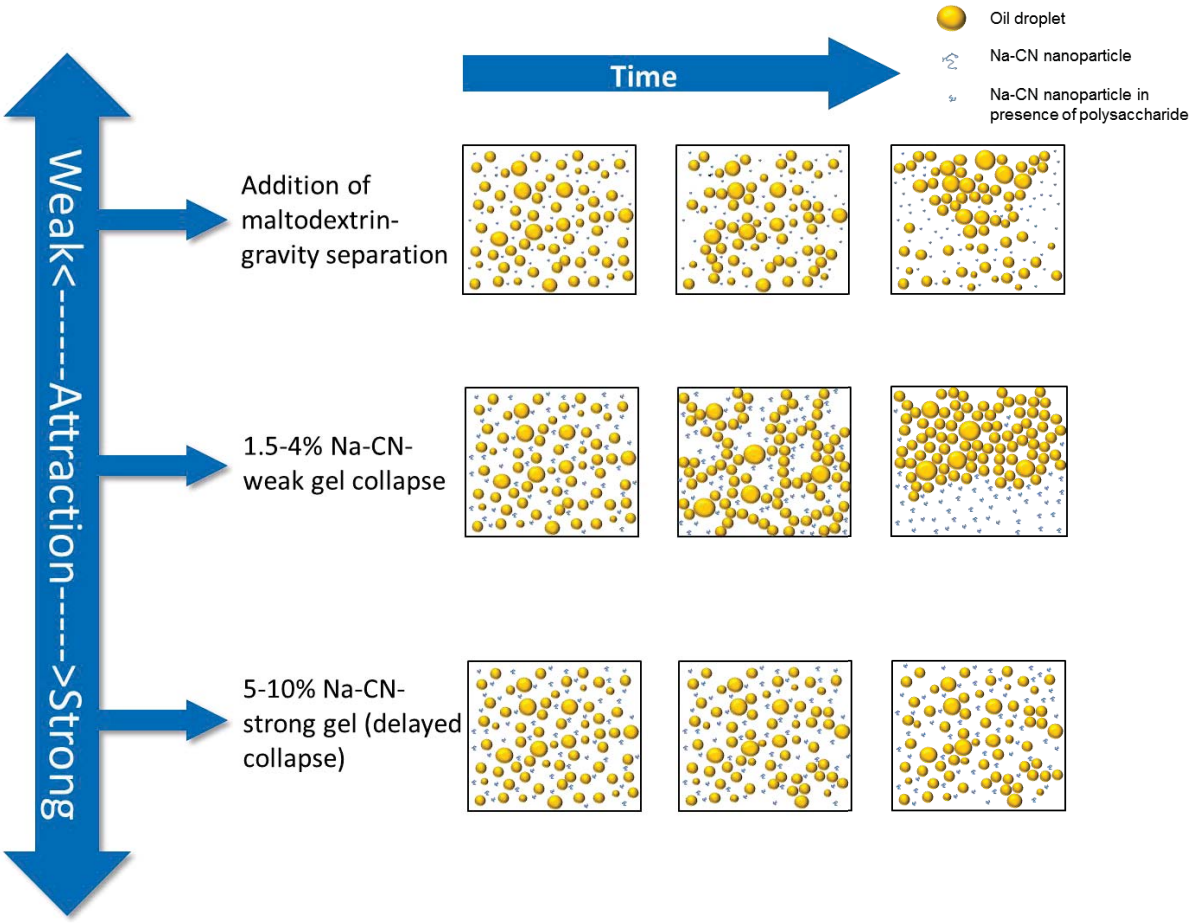

Figure 2.15. Schematic illustration of the structure, stability and depletion force relationship in NaCas emulsions with the addition of non-adsorbed NaCas and non-adsorbed polysaccharide.

In a binary system, the impact of carbohydrate on the creaming behavior of a weakly flocculated protein-stabilized emulsion has also been investigated. However, the addition of carbohydrate could not be considered simply to be an inert thickening agent. The reduced network formation in NaCas-stabilized emulsions caused by adding trehalose was not simply an effect of viscosity, but rather a dissociation of the caseinate nano-particles that induce network formation (Álvarez-Cerimedo, Iriart, Candal, & Herrera, 2010). The addition of xanthan gum to the NaCas emulsions mimics the phase separation behaviors of NaCas emulsions resulting in local domains that were rich in mixtures of xanthan gum and NaCas and rich in emulsion droplets. The effect of these local domains was that the droplets experienced a larger depletion interaction potential and the high viscosity of the combined xanthan gum and emulsion phases resulted in uniform phase

separation across the emulsion rather than gravimetric separation (Hemar et al., 2001; Moschakis et al., 2005).

The restabilization mechanism in weakly flocculated protein-stabilized emulsions facilitates our understanding of the relationship between the delay time and the emulsion structure. It is possible to develop formulation strategies to make the delay time longer than the shelf life of protein-stabilized emulsion products by modulating the depletion force, pH and ionic environment. Nevertheless, in food emulsion formulation, the presence of other components could change the structural and mechanical properties; for instance, caseinate nano-particle size may be affected by the presence of xanthan gum (Long et al., 2013), trehalose (Álvarez-Cerimedo et al., 2010) and sucrose (Belyakova et al., 2003). The effect of self-assembly behavior of casein nano-particle in different solvent environment on the extent of depletion flocculation deserves further research at a wider range of protein concentration.

2.5.2 Effect of repulsive force on the heat stability of protein dispersion

2.5.2.1 Modulation of repulsive force through controlled protein aggregation

There are different approaches to producing soluble whey protein aggregates that have better heat stability. (1) Microparticulated whey proteins prepared by preheating and high shear homogenization to reduce sizes of the whey protein aggregates to less than 3 μm (Onwulata, Konstance & Tomasula, 2002). (2) Denatured whey proteins prepared by drying and milling a whey protein gel (Purwanti et al., 2012). (3) Micro-aggregates prepared in solution by a combination of heating and high intensity shearing (Dissanayake & Vasiljevic, 2009). (4) Whey protein nano-particles/microparticles prepared by heating and recovering whey proteins from those dispersed in a water-in-oil emulsion (Sağlam et al., 2013; Zhang & Zhong, 2010). Most studies have reported that the heat stability of soluble whey protein aggregates is improved (i.e. longer HCT, less viscous, lower turbidity than native whey proteins) after a secondary heat treatment. The possible mechanisms associated with the improved heat stability can be summarized. (1)

Heat-induced whey protein denaturation results in less/no reactive sites such as free thiol groups to initiate further denaturation during a second heat treatment (Dissanayake & Vasiljevic, 2009). (2) The surface of whey protein aggregates has a higher net charge and this increases the electrostatic repulsion (Ryan, Vardhanabhuti, Jaramillo, van Zanten, Coupland & Foegeding, 2012; Zhang & Zhong, 2010). In addition, the smaller size of whey protein aggregates tends to result in a slow aggregation rate (Dissanayake & Vasiljevic, 2009; Zhang & Zhong, 2010). The shape of heat-induced whey protein aggregates is also important in determining the heat stability. It has been proposed that the desired characteristics of soluble whey protein aggregates that are more resistant to heat and lower in viscosity are low surface hydrophobicity, small aggregate size, compact shape, high surface charge and more spherical (Ryan, Zhong, & Foegeding, 2013). Recent studies by Sağlam and her co-workers (2013 & 2014) have suggested that highly dense, irregular, very compact whey protein aggregates prepared at pH 5.5 do not gel after heating at 90 °C for 30 min at protein concentration above 20% w/w. In contrast, whey protein aggregates formed at pH 6.8 show spherical and smoother morphology and have weaker heat stability mainly because of a stronger swelling of the whey protein particles than in aggregates prepared at pH 5.5.

2.5.2.2 Modulation of repulsive force through protein−surfactant, protein−protein and protein−polysaccharide interactions

In a number of food emulsion studies, the improved stability of the oil droplets against creaming, coalescence and heat has been attributed to enhanced steric stabilization. The routes for manipulating steric stabilization through protein−surfactant, protein−protein and protein−polysaccharide interactions are summarized in Figure 2.16. Although the primary emphasis is on the steric stabilization of oil droplets, the role of non-adsorbed surfactant, protein and polysaccharide in the continuous phase is briefly discussed.

Enhanced repulsive force through protein−surfactant interactions

Food grade surfactants such as lecithin and Tween are small molecular weight surface-active agents. They not only stabilize the oil droplets along with proteins during homogenization, but also confer improved heat stability to protein-stabilized oil-in-water emulsions. A number of studies have investigated the influence of lecithin, modified lecithin and Tween on the heat stability of food emulsions, which include milk (McCrae & Muir, 1992), recombined evaporated milk (Kasinos et al., 2014; McCrae, 1999), infant formulae (McSweeney et al., 2008), coffee cream (van der Meeren, El-Bakry, Neirynck, & Noppe, 2005), caseinate-stabilized emulsions (Cruijsen, 1996), globular-protein-stabilized emulsions (Euston et al., 2001a; Jimenez-Flores, Ye, & Singh, 2005; Nikiforidis & Kiosseoglou, 2007) and hydrolyzed-whey-protein-stabilized emulsions (Agboola, Singh, Munro, Dalgleish, & Singh, 1998a). Non-food-grade surfactants (i.e. SDS, Brij 35) have also been studied to understand the stabilizing mechanisms in solution (Hansted, Wejse, Bertelsen, & Otzen, 2011; Tran Le et al., 2007; Tran Le et al., 2011) and emulsion systems (Kelley & McClements, 2003).

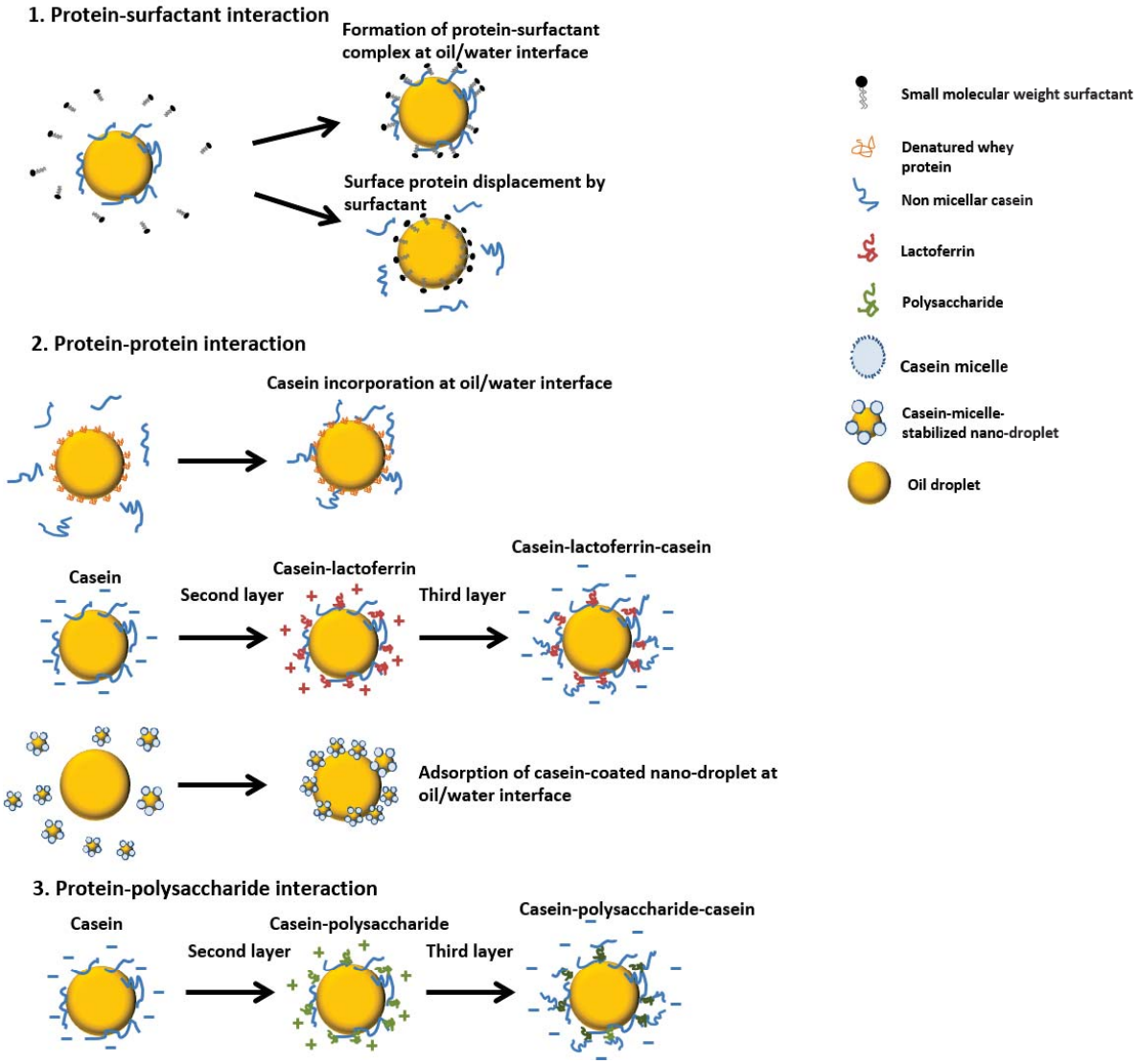

Figure 2.16. Schematic illustration of the modulation of interfacial layer properties at the oil/water interface through protein−surfactant, protein−protein and protein−polysaccharide interactions.

Although the exact stabilizing mechanisms of low molecular weight surfactant are still not clear, the possible modes of action for inhibiting the heat-induced aggregation of oil droplets can be summarized as follows. (1) Displacement of the surface proteins by hydrophilic surfactants (i.e. Tween, SDS, phospholipids) is responsible for the inhibition of the heat-induced destabilization of oil droplets. The improvement can be partially attributed to the increase in surface charge by the ionic or zwitterionic surfactant (Kelley & McClements, 2003; McCrae, 1999) or the enhanced repulsive force (Demetriades &

McClements, 1998). (2) Hydrophilic surfactants may bind competitively to unfolded whey proteins through hydrophobic interactions. In this manner, the reactive sites of the non-adsorbed whey proteins are shielded and not available for further aggregation (Euston et al., 2001a; Nikiforidis & Kiosseoglou, 2007). (3) Hydrophilic surfactants may stabilize the ligand-bound state of *β*-lg and solubilize unfolded protein monomers, restricting protein−protein association for further aggregation (Hansted et al., 2011). (4) It is also possible that surfactant−protein binding results in an increase or decrease in the denaturation temperature of the adsorbed and non-adsorbed whey proteins depending on critical aggregation concentration (CAC) (Giroux & Britten, 2004; Kelley & McClements, 2003; van der Meeren et al., 2005). It is important to note that, in milk-based systems, the presence of lecithin may promote the formation of *β*-lg−*κ*-casein complexes, which are known to play an important role in heat stability/HCT (Singh, Sharma, & Tokley, 1992). The effectiveness of hydrophilic surfactants in inhibiting heat-induced protein aggregation depends on the surfactant-to-protein ratio and the critical aggregation concentration (CAC). At a low surfactant-to-protein ratio, the droplet−droplet interactions are enhanced. This change is probably due to the partial desorption of some hydrophobic proteins (Kim et al., 2002b) or the low surface coverage by surfactant molecules, which leads to a conformational change in the adsorbed proteins (Euston et al., 2001a). Subsequently, the adsorbed proteins have a greater tendency to interact with other adsorbed proteins through the mediation of non-adsorbed proteins (Euston et al., 2001a). Hydroxylated and hydrolyzed lecithin have been found to have higher CACs than native lecithin at the same concentration, and provide a more pronounced stabilizing effect against the heat-induced aggregation of whey-protein-stabilized droplets and whey proteins in the continuous phase (Jimenez-Flores et al., 2005; Tran Le et al., 2011).

Enhanced repulsive force through protein−protein interactions

An enhanced steric repulsive force by the incorporation of a small amount of casein at the oil/water interface has been reported (Dickinson & Parkinson, 2004; Parkinson &

Dickinson, 2004; Parkinson & Dickinson, 2007; Parkinson, Ettelaie, & Dickinson, 2005). β-Casein has a better protecting effect than NaCas and α_{s1}-casein against heat-induced aggregation of β-lg-stabilized droplets. Alternatively, the presence of a small amount of casein at the oil/water interface may enhance the formation of the intralayer −S−S− linkage between the adsorbed whey proteins. Consequently, the reactivity between adsorbed and non-adsorbed β-lg reduces (Parkinson & Dickinson, 2004). The role of a low surface coverage of casein molecules is supported by the self-consistent-field theory of Scheutjens and Fleer. It has been suggested that the dense primary layer of adsorbed whey proteins reinforces the protrusion of casein tails and loops from the surface (Parkinson, et al., 2005). The effectiveness of the protection of β-lg-stabilized droplets is dependent on the Ca^{2+} ion concentration and the type of globular protein. A slightly higher concentration of casein is required to provide the same protecting effect at moderate concentrations of Ca^{2+} ions and for BSA emulsions (Parkinson & Dickinson, 2007).

Alternatively, the adsorption of thick and dense proteins because of the pre-homogenization heat-induced effect results in improved emulsion stability. The stabilizing effects are attributed mainly to the formation of a thicker adsorbed layer at the oil/water interface by heat-induced protein nano-particles when steric repulsion is enhanced (Dybowska, 2011; Kim et al., 2005; Rullier, Novales, & Axelos, 2008; Tcholakova et al., 2006b). A similar effect with respect to the creaming and heat stabilities of protein-stabilized emulsions has been observed following the formation of electrostatic protein−protein complexes at the oil/water interface (Figure 2.16) (Liu & Tang, 2013; McCarthy, Kelly, O'Mahony, & Fenelon, 2014; Schmelz, Lesmes, Weiss, & McClements, 2011). The multi-layer interfaces formed by the layer-by-layer technique show better stability to environmental stresses than conventional emulsions stabilized by single-layer interfaces (Guzey & McClements, 2006). Basically, in the layer-by-layer deposition technique, a “primary” emulsion consisting of small droplets is made with an ionic emulsifier during homogenization, and then an oppositely charged polyelectrolyte is added to the emulsion, when a “secondary” layer containing the new adsorbed particles is formed. Based on this method, many different polymers can be incorporated in individual

multi-layer films and the film structures are entirely determined by the adsorption sequence (Decher, 1997; Guzey & McClements, 2006).

Additionally, a recent study has illustrated that nano-scale emulsion droplets (~ 150 nm in diameter) coated with casein micelles can be used as emulsifying agents to stabilize oil droplets (Ye, Zhu, & Singh, 2013). The adsorption of casein-micelle-coated nanodroplets is dependent on the nanodroplet concentration. Stable emulsions can be formed even when there is no full coverage of nanodroplets at the oil/water interface. Full coverage is established at higher nanodroplet concentration, leading to the formation of a multi-layered interfacial layer consisting of a network of assembled nanodroplets. The adsorbed nanodroplets behave similarly to large casein micelles and change their configuration from a sphere to an ellipse or even a rectangle at the oil/water interface (Ye et al., 2013). Theoretically, the adsorption of casein-micelle-stabilized nanodroplets and the formation of a three-dimensional network at the oil/water interface have great potential to enhance the steric repulsive force under heating conditions and to provide a novel path to improve long term emulsion stability.

Enhanced repulsive force through protein−polysaccharide interactions

Polysaccharides are not only used as thickening agents in food emulsions, but also can be tailored to form an effective steric layer at the oil/water interface. The uses of protein−polysaccharide conjugates and complexes to stabilize oil-in-water emulsions have recently been reviewed (Evans, Ratcliffe, & Williams, 2013). The general concept is to fabricate gum arabic mimetic molecules that consist of a surface-active proteinaceous component that preferentially interacts with the oil phase and a covalently linked carbohydrate block that extends into the continuous phase, providing electrosteric repulsion (Evans et al., 2013). Maillard-type protein−polysaccharide conjugates are prepared by dry heating protein and polysaccharide powders and the end products are used as emulsifiers (Dickinson, 2006; Dickinson, 2008). In contrast, soluble protein−polysaccharide electrostatic complexes are formed by adding polysaccharide with an opposite charge (net positive or net negative) on to the protein-stabilized layer.

Multi-layers can be formed by the subsequent addition of a biopolymer of the opposite surface charge (Guzey & McClements, 2006).

A thicker stabilizing layer at the oil/water interface can be fabricated not only through protein−protein interactions but also via the protein−polysaccharide route (Dickinson, 2008; Guzey & McClements, 2006). It has been shown that a smaller droplet size is obtained during prolonged heat treatment (i.e. ≥ 90 °C) when the oil droplets are stabilized by protein−polysaccharide conjugates (Diftis & Kiosseoglou, 2006; Xu & Yao, 2009) or soluble protein−polysaccharide electrostatic complexes (Bengoechea, Jones, Guerrero, & McClements, 2011; Tokle, Lesmes, & McClements, 2010). The improvement in long term creaming stability and heat stability can be attributed to the increased steric layer thickness, increased hydrophilicity and possibly the increase in zeta potential (Wooster & Augustin, 2006; Xu & Yao, 2009). Tran & Rousseau (2013) have suggested that emulsion droplets stabilized by polysaccharide-coated proteins decrease the tendency for protein−protein interactions. With respect to salt stability, it has been found that an increase in steric layer thickness by only 5 nm gives marked steric stabilization against Ca^{2+}-induced droplet flocculation (Wooster & Augustin, 2006). This phenomenon was observed in emulsions stabilized by protein−protein complexes before and after heat treatment (McCarthy et al., 2014; Schmelz et al., 2011; Ye, Lo, & Singh, 2012).

Little information on heat-induced casein−polysaccharide interactions is available. However, Ibanoglu (2005) has found that adding polysaccharides such as pectin, guar gum and *ι*-carrageenan inhibits whey proteins against heat-induced aggregation because they are able to interact with the unfolded hydrophobic patches of whey proteins during heating (up to 100 °C). Of the three reported polysaccharides, pectin exhibits the best result.

2.5.2.3 Alteration of thermodynamic properties by protein−carbohydrate and carbohydrate−water interactions and their impact on the physicochemical properties of protein-stabilized emulsions

The presence of small polar molecules such as carbohydrates and polyols may directly or indirectly affect the thermodynamic properties of the interfacial proteins and the non-adsorbed proteins in oil-in-water emulsions, including heat stability, preferential hydration, self-assembly, conformation stability, gelation and surface activity (McClements, 2002, 2004; Semenova, Antipova, & Belyakova, 2002). Over the past few years, considerable effort has been spent on understanding the protective effect of carbohydrates against the unfolding of globular proteins in dispersion and emulsion systems. Although the relative importance of the stabilizing mechanisms of carbohydrates on globular protein stability remains unclear, the generally accepted mechanisms for the protective effect of carbohydrates against the unfolding of globular proteins include the following. (1) Steric exclusion effect. The excluded volume effect arises when considerably large sized (compared with water molecules) carbohydrate molecules such as sucrose are present. The carbohydrate molecules are excluded from the region surrounding each protein molecule and only water molecules can enter. The movement of a protein molecule from the pure solvent to a carbohydrate solution is thus thermodynamically unfavorable because free energy is required to withstand the concentration gradient between the carbohydrate-rich aqueous continuous phase and the carbohydrate-depleted zone surrounding the protein molecule (Timasheff, 1993). Concurrently, the hydrodynamic radius of proteins decreases and their compactness and consequently stability increases (Jain & Roy, 2009). (2) Hydrogen bonding interactions. Proteins and carbohydrates directly interact by hydrogen bonding because of additional hydration. The protein hydration occurs when the newly formed multiple hydrogen bonds with carbohydrates cause the formation of an extra hydrophilic layer surrounding the protein molecule. Subsequently, the hydrogen bonding can modify the original intramolecular interactions of protein molecules, changing their unfolding or folding behavior (Semenova et al., 2002). (3) Increased viscosity effect. The increase in the continuous phase viscosity on the addition of carbohydrates decreases the collision rate between protein-stabilized droplets (Kim, Decker, & McClements, 2003). Other

interpretations in terms of molecular interactions have also been proposed. The concentrated carbohydrate molecules compete for hydration, resulting in weaker protein−water interactions and in turn stabilizing the proteins because of diminished water activity (Barone, Del Vecchio, Giancola, & Notaro, 1992). Additionally, the changes in density, dielectric constant, refractive index and osmotic pressure could influence the height of the repulsive energy barrier and alter the aggregation mechanisms (Kim et al., 2003).

In contrast, although it is out of the scope of this subsection of the thesis, it is important to note that the results for globular proteins may not be extrapolated accurately to casein. Under the influence of carbohydrate, the casein molecules may dissociate because of strengthening of protein−protein hydrophobic interactions when the hydrophobic groups of casein molecules are exposed to the continuous phase (Belyakova et al., 2003). Moreover, the κ-casein hairy layer of casein micelles may partial collapse under the influence of sucrose (Schorsch, Jones, & Norton, 2002). Both these physicochemical changes of the caseins result in a decreased particle size, which in turn could alter the kinetics of depletion-induced droplet flocculation (Álvarez-Cerimedo et al., 2010), the gelation of casein micelle dispersions (Schorsch et al., 2002) and possibly the heat stability of concentrated milk dispersions (Huppertz, Tan-Kintia, Arriaga, & Fox, 2012).

2.5.2.4 Manipulation of Ca^{2+} ion activity by addition of polyphosphates

Calcium chelators, such as phosphate, citrate and hexametaphosphate are commonly used in dairy foods processing to increase the heat stability and to prevent protein gelation in condensed milk and UHT sterilized milk during heat treatment and storage (Datta & Deeth, 2001; Kocak & Zadow, 1985). Calcium chelators such as sodium hexametaphosphate and sodium phytate are strongly negatively charged. As they bind Ca^{2+} ions, causing the formation of soluble complexes with Ca^{2+}, calcium-induced protein aggregation will be reduced. Simultaneously, they will alter the casein−mineral equilibrium by binding the positively charged region of the casein residues (Holt, 1992; Lewis, 2011; Mizuno & Lucey, 2005). Other studies have revealed that phosphate salts

can interact with casein micelles, providing more negative charge and making them more water soluble; in this manner, proteins have stronger electrostatic force to repel each other. Concurrently, κ-casein will associate with casein micelles more strongly via ionic interactions, the dissociation of heat-induced β-lg–κ-casein complexes from the casein micelle will be delayed and consequently gelation will be delayed (Kocak & Zadow, 1985). A recent comparison study of the effect of various types of phosphate salts on retorted skim milk showed that the addition of sodium dihydrogen phosphate had the most promising overall performance with respect to heat stability and heat-induced browning, compared with trisodium citrate, disodium hydrogen phosphate and sodium hexametaphosphate (Tsioulpas, Koliandris, Grandison, & Lewis, 2010). The efficacy of polyphosphates in the improvement in heat stability depends on the chain length of the polyphosphates. Polyphosphates with an average of 4.8 phosphorus atoms per chain have been found to be the most effective against heat-induced gelation (Hernandez, 2005). It should be borne in mind that hydrolytic degradation of long chain phosphates can occur during heat treatment (100−120 °C), which may result in poorer calcium chelating activity (Rulliere, Perenes, Senocq, Dodi, & Marchesseau, 2012). Moreover, it has been found that polyphosphates have higher efficacy in solution than in an emulsion system (Hernandez, 2005).

Despite the improved heat stability that can be achieved by the addition of calcium chelators, it should be stressed that, by adding at above a critical concentration, calcium chelators can bind the CCP within the casein micelle and lead to a complete dissociation of the casein micelle into non-micellar caseins (Griffin, Lyster, & Price, 1988) with a slight decrease in the isoelectric point of the caseins (de Kort, 2012). This may decrease the heat stability of milk solutions and cause a considerable change in viscosity. The extent depends on the type and concentration of the calcium chelators (de Kort et al., 2011, 2012). A similar improvement in ethanol stability was observed in skim milk at levels of 10 and 19% calcium removal by ion exchanger; the ethanol stability decreased at higher levels of calcium removal (Grimley, Grandison, & Lewis, 2010). However, this study reported a contradictory change in casein micelle size, which increased rather than decreased on a reduction in the calcium level.

2.6 Concluding remarks

The stabilization of emulsion droplets and protein particles against creaming, phase separation and heating is extremely important in determining the functionalities of protein-based emulsion formulations, especially in the presence of other food components such as low molecular weight surfactants, carbohydrates and minerals. Although interfacial adsorption, interfacial composition, creaming stability, freeze−thaw stability and salt stability under different physical conditions such as heat, pressure and shear have formed the major body of the research on biopolymer (i.e. proteins, polysaccharides)-stabilized emulsions, the behavior of oil-in-water type emulsions with high solids content (i.e. high protein, high carbohydrate) is largely unknown. It is crucial to understand the properties of the emulsion droplets and non-adsorbed proteins in a concentrated form to produce an emulsion that is stable against heat, creaming and phase separation and has better texture perceptions and acceptable flow properties. MPC is an emerging milk protein ingredient that is rapidly gaining wide popularity. MPC is suitable for those liquid protein formulations in which the original structure of the milk proteins is desired in terms of functionality. In addition, micellar calcium phosphate is mostly retained in the casein micelles during the ultrafiltration/diafiltration process. Therefore, the high content of bioavailable calcium makes MPC favorable for specific formulations such as infant formulae and medical nutrition. Recent studies on casein-micelle-concentrated dispersions have shown that the heat stability and viscosity are largely affected by the initial heating pH, the protein concentration, the dissociation of κ-casein from the casein micelles and the aggregation state of the casein micelles at the oil/water interface and in the continuous phase. However, there has been little focus on the physicochemical properties of emulsion systems containing MPC and multiple ingredients under heating conditions.

Additionally, in a ternary system (protein + two ingredients), the presence of a third ingredient is likely to affect the interactions between the two other ingredients. There is to date a lack of studies in this “grey” area. Several other knowledge gaps need to be bridged, including understanding the influence of the depletion force, the droplet size, the

protein size and the continous phase viscosity on changes in the microstructure and stability of emulsions as the protein concentration increases and after heat treatment. It is of great interest to gain more understanding on how the emulsion droplet network induced by depletion effects restabilizes the emulsion against phase separation at high biopolymer concentrations without the presence of a yield stress.

Most of the previous studies on inter-particle interactions in emulsion systems have been conducted under either unheated or heated at relatively low temperature (≤ 90°C) conditions. Only a few studies have investigated the heat-induced inter-particle interactions at temperatures > 100 °C. It is expected that high-temperature-heated protein-based emulsions may have different properties from emulsions that are either unheated or heated at relatively low temperatures. The fundamental knowledge established in concentrated-protein model emulsion studies before and after heat treatment will have potential applications and will help to develop milk protein ingredients with different functionalities for the production and storage of real protein-based emulsion products. Therefore, linkages of the insights obtained from model colloidal systems, combined with future mathematical modelling and in-line determination of the physicochemical properties of colloidal particles will be required to build and develop a robust and predictive colloid model that could be implemented in a vast number of food/dairy formulations.

Chapter 3: Materials and Methods

3.1 Materials

3.1.1 Milk protein ingredients

Whey protein concentrate 392 (WPC), whey protein isolate 895 (WPI), whey protein hydrolyzate 821 (WPH), whey protein concentrate 515 (pre-denatured WPC), sodium caseinate 180 (NaCas), milk protein concentrate 4850 (MPC) and milk protein concentrate 4861 (calcium-depleted-MPC) were obtained from Fonterra Co-operative Group Ltd, Auckland, New Zealand. The extent of denaturation of the pre-denatured WPC was estimated to be > 65% by reverse-phase high-performance liquid chromatography (RP-HPLC). The calcium-depleted MPCs were manufactured utilizing cation exchange technique to replace Ca^{2+} by Na^{+} ions and then undergo ultrafiltration/diafiltration processes. When calculating the amount of protein powder to be added, a conversion for the protein content of the powder was taken into account. The composition of the protein samples is shown in Table. 3.1. The protein content was determined by the Kjeldahl method using a conversion factor of 6.38.

Table 3.1. Composition of milk protein ingredients (in g/100g)

Milk protein ingredient	Protein	Fat	Total carbohydrate	Sodium	Calcium
WPC-80 (WPC I)	80.3	6.2	7	0.34	0.4
pre-denatured WPC (WPC II)	80.3	6.2	7	0.34	0.4
WPI	93.5	0.2	0.6	0.6	0.06
WPH[1]	91.9	0.1	1	0.6	0.06
MPC-85 (MPC I)	82.2	1.6	3.7	0.07	2.23
Calcium-depleted-MPC (MPC II)	82.2	1.6	3.7	1.15	1.34
NaCas	92.7	0.7	0.2	1.12	0.03

[1] The degree of hydrolysis is 18.1%.

3.1.2 Corn oil

Bulk corn oil was purchased from Davis Trading Co., Palmerston North, New Zealand. The density of corn oil is 0.92 kg/m^3 and the corn oil was used without any further purification.

3.1.3 Chemicals

All the chemicals used were of analytical grade, obtained from either BDH Chemicals (BDH Ltd, Poole, England) or Sigma Chemical Co. (St Louis, MO) unless otherwise specified. The different protein solutions, emulsions and buffer solutions were made with double deionised water, so-called Mili-Q water (Milipore Corporation, Massachusetts, USA). 0.02% w/w sodium azide was used as an antimicrobial agent.

3.2 Methods

The standard methods and analytical techniques are applicable to most of the experiments described in this chapter. The modifications or specific techniques to particular experiments have been described in specific chapters separately.

3.2.1 Preparation of protein solutions

Milk protein concentrate (MPC)

MPC solutions were prepared by adding MPC powders to Milli-Q water and then the protein dispersions were at 50 °C for 60 min. This temperature was sufficient enough to ensure complete dissolution of the aggregated protein products while was low enough to prevent whey protein denaturation.

Sodium caseinate (NaCas)

The preparation of dilute NaCas solutions is the same as MPC. For concentrated NaCas solutions (> 10% w/w), the NaCas powders were added to Milli-Q water and mixed at 70 °C for 2 h and then it was stirred at 600 rpm for another 3 h to allow complete dissolution.

Whey protein concentrate (WPC)/isolate (WPI)/ hydrolyzate (WPH)

The WPC/WPI/WPH solutions were prepared at ambient temperature (~20 °C) by dispersing protein powders in Milli-Q water and stirring for 2 h to allow complete dissolution. The pH of all the protein solutions was adjusted to desired pH using 1 M NaOH or 1 M HCl. Sodium azide (0.02% w/w) were added to avoid microbial growth and the protein solutions were stored in the refrigerator (4°C) overnight to fully hydrate.

To investigate the pre-heat treatment of protein dispersion on the functionalities of emulsions, the milk protein dispersions were subjected to a heat treatment in a water bath at 90°C (45−90°C, 6 min) and held at 90°C for 5 min (total heating time is 11 min). Immediately after the heat treatment, the dispersion was rapidly cooled in an ice bath. To determine the effect of initial heating pH on the protein dispersion on the functionalities of emulsions, the milk protein solution was adjusted to different pHs (6.2 ~7.4) using 1 M HCl and 1 M NaOH.

3.2.2 Preparation of milk protein stabilized emulsions

Appropriate quantities of corn oil and Milli-Q water were then mixed with the protein solutions to give 30% oil (w/w) and 3% protein (w/w) in the final emulsion. A coarse emulsion pre-mix was prepared by homogenizing the mixtures for 2 min using Ultra-Turrax T25 (IKA®Werke GmbH & Col.KG, Staufen, Germany). The coarse emulsions were heated to 60°C and homogenized 1−3 times using two-stage homogenizer (type Panda, NIRO SOAVI, Parma, Italy) at the pressure of 20 MPa on the first stage and 4 MPa on the second stage. Emulsions were prepared at least in duplicate.

3.2.3 Particle size measurement of protein solutions and milk protein stabilized emulsions

Particle sizing based on light scattering is one of the most commonly used emulsion characterization techniques. Two main instruments are used to measure particle size and particle size distribution of emulsions, namely Zetasizer and Mastersizer. The Zetasizer is built based on dynamic light scattering (DLS) (McClements, 2005). Dynamic light scattering measures the Brownian motion of particles and relates this to their hydrodynamic size (r). The light scattered from a (dilute) dispersion of particles (no particle−particle interactions) fluctuates with a characteristic time scale inversely proportional to the translational diffusion coefficient (D). The size of particles can be calculated using the Stokes-Einstein equation:

$$r = \frac{k_B T}{6\pi\eta D} \tag{3.1}$$

where k_B is Boltzmann constant, T is temperature, and η is the viscosity of the continuous phase. The particle sizing from DLS produces information about colloidal particles from a few nanometers and several micrometers. It is important to stress that the translation diffusion coefficient not only depends on the size of the particle and viscosity of the aqueous continuous phase but also the surface structure and shape of the particle (McClements, 2005; Tadros, Izquierdo, Esquena, & Solans, 2004). The Mastersizer is built based on static light scattering (SLS) (McClements, 2005). The Mastersizer

measures the intensity of the scattered light in dependence of the scattering angle and obtains information on particle size by fitting the scattering intensity to theoretical models based on Mie theory (McClements, 2005). The sample is generally subjected to extensive dilution and stirring, this leads to the dissociation of weakly attractive flocculates. It is important to notice that any aggregates/flocculates held together weakly are not detected using Mastersizer.

Particle size (z-average hydrodynamic diameter) measurements of protein dispersions were performed at room temperature using the method of Anema (2007). A Malvern Zetasizer Nano ZS (Malvern Instruments Ltd, UK) built in dynamic light scattering is with a He/Ne laser emitting at 633 nm and a 4.0 mW power source. MPC dispersion was diluted at a ratio of 1:100 with Ca-imidazole buffer (20 mM imidazole, 5 mM $CaCl_2 \cdot H_2O$, 30 mM NaCl, pH 7.0) which has been filtered through 0.45 μm membrane. The NaCas dispersion was diluted with Milli-Q water. The average diffusion coefficients of protein particles were calculated from those changes of intensity and were converted to average particle diameters following the Stokes-Einstein correlation for spheres (Anema & Li, 2003). The hydrodynamic diameter was calculated based on an assumption that the diffusing particles were monodisperse spheres and was based on 5 measurements with 10 sub-runs.

A Malvern Mastersizer 2000 (Malvern Instruments Ltd, UK) with an effective diameter range of 0.1−2000 μm was used to determine emulsion particle size distributions and the surface-weighted ($d_{3,2}$) and volume-weighted diameter ($d_{4,3}$) of emulsion droplets. The method was taken from Ye et al. (2000) with some modifications. The droplet size distribution was determined using a set pump speed of 2900 rpm. Optical parameters were: refractive indexes of corn oil and water 1.456 and 1.330, respectively; adsorption: 0.001. The Sauter-average diameter, surface-weighted $d_{3,2}$ (μm) was expressed as following:

$$d_{3,2} = \sum \frac{n_i d_i^3}{n_i d_i^2}$$

And De Brouckere diameter, volume-weighted $d_{4,3}$ (μm) was calculated as following:

$$d_{4,3} = \sum \frac{n_i d_i^4}{n_i d_i^3}$$

In which, n_i is the number of particles with diameter d_i of the emulsion droplets.

The average droplet size and the droplet size distribution were determined under two conditions: (1) measurements were carried out without non-dissociating agents in water at ambient temperature and (2) samples were dispersed in solutions with dissociating agents before measurements. The reasons are: first it aims to dissociate the casein micelles present in MPC powders which interfere with particle size measurement, second it aims to disrupt the strongly flocculated droplets caused by bridging mechanism but it would not breakdown aggregates if the droplets were disulfide bridging and third to replace the adsorbed proteins from oil/water interface as much as possible and to detect the fat globules only. Thereby, prior to particle size measurements, emulsions were carefully mixed with two types of dissociating solutions, one is a solution containing 3.75 g/L disodium ethylenediamine tetra-acetate (EDTA) and 1.25 g/L polysorbate 20 (Tween-20) and another one is a solution containing 1% w/w SDS. The samples mixed gently with the solutions at 1:9 ratio and measured after at least 20 min equilibration time. Mean particle diameters were calculated as the average of duplicate measurements.

3.2.4 Determination of surface protein concentration and composition

The procedure of determination of surface protein concentration and composition in the milk protein stabilized emulsions was taken from Ye (2003). The emulsions were centrifuged at 45,000 g for 40 min at 20 °C in a temperature-controlled centrifuge (Sorvall RC5C, DuPont Co., Wilmington, DE, USA). Three fractions were obtained, namely top (cream) layer, middle layer and sediment. The subnatant (middle fraction) was collected by using a 10 mL syringe and filtered sequentially through 0.45 and 0.22 μm filters (Millipore Corp, Bedferd, MA). The cream layer was re-dispersed in

corresponding MPC-permeates that obtained from ultrafiltration to remove the casein micelles and subsequent filtering through 0.45 µm membrane. The serum composition of the MPC-permeates is the same as skim milk (pH 6.8, acquired from Fonterra pilot plant, Palmerston North, New Zealand) containing the original mineral content as milk and re-centrifuged at 45,000 g for 40 min at 20 °C. The cream layer was dried on a filter paper (Whatman No.42, Whatman International Ltd, Maidstone, Kent, UK) overnight at ambient temperature and Analyzed for total protein following Kjeldahl procedure (1030 Distiller and 1007 Digestor Block, Tecator AB, Hoganas, Sweden) and a nitrogen-to-protein conversion factor $N \times 6.38$ was used to quantitatively calculate the amount of protein. The surface protein concentration (mg m^{-2}) was calculated from the surface area of the oil droplets, determined by Mastersizer, and the adsorbed protein (g) on the cream layer.

Total protein coverage (mg m^{-2}) = total protein adsorbed (mg) / total fat surface area (m^2)

The compositions of the adsorbed protein at the surface of the emulsion droplets were evaluated using sodium dodecyl-sulphate polyacrylamide gel electrophoresis (SDS-PAGE), as described by Havea et al. (1998) and Ye (2003). The SDS-PAGE gels were prepared using the Mini-Protein II dual cell unit (Bio-Rad Laboratories, Hercules, CA, USA). The preparation was described in details as follows:

3.2.4.1 Resolving gel

The resolving gel mixture consisted of 3.75 mL of SDS resolving gel buffer (stock solution prepared by dissolving 18.15 g of Tris (hydroxymethyl) methylamine base in about 60 mL of Milli-Q water, adjusting the pH to 8.8. The total volume is made up to 100 mL with Milli-Q water, i.e. 1.5 M Tris-HCL buffer adjusted to a pH of 8.8), 3.0 mL of water and 7.95 mL of acrylamide solution [30% stock solution of a 37.5:1 (2.6%) mixture of acrylamide and N, N'-methylenebis (acrylamide)] was accurately transferred to a vacuum flask, mixed well and allowed to stand at ambient temperature (20−23 °C) for about 30 min. This mixture was then degassed under vacuum for 20 min with constant

stirring of the mixture using a magnetic stirrer. Meanwhile, the gel setting apparatus was assembled using 0.75 mm spacers, following the standard description in the Bio-Rad manual. Immediately after the degassing step and just prior to the gels being poured, 150 µL of stock 10% w/v SDS solution, 7.5 µL of *N, N, N', N'*-tetramethylethylenediamine (TEMED) and 75 µL of a 10% pre-made solution of ammonium persulfate (APS) were added to the mixture. The remaining steps were same as described for native PAGE resolving gel.

3.2.4.2 Stacking gel

The stacking gel was made from a mixture of 2.50 mL of stacking gel buffer (stock solution prepared by dissolving 6 g of Tris base in about 60 mL of Milli-Q water, adjusting the pH to 6.8 with 6 M HCL and making the final volume up to 100 mL, i.e. 0.5 M Tris-HCl buffer adjusted to pH 6.8), 6.10 mL of water and 1.30 mL of acrylamide solution [30% stock solution of a 37.5:1 (2.6% C) mixture of acrylamide and N, N'-methylenebis (acrylamide)]. This was then degassed as described above and 100 µL of stock 10% w/v SDS solution, 50 µL of 10% APS and 10 µL of TEMED were added. The remaining steps were same as described for native PAGE stacking gel.

3.2.4.3 Electrode buffer

The stock solution of SDS electrode buffer (5X) was prepared by dissolving 15.0 g of Tris base, 72.0 g of glycine and 5 g of SDS powder in about 800 mL Milli-Q water and then finally making the volume up to 1 L. The pH of the stock solution was in the range of 8.6 ± 0.1. In use, this stock solution was diluted 1:4 with Milli-Q water.

3.2.4.4 SDS sample buffer

SDS-PAGE sample buffer consisted of 125 mL of 0.5 M Tris-HCl buffer (pH 6.8), 100 mL of glycerol, 200 mL of 10% w/v SDS, 500 mL of Milli-Q water, and 25 mL of 0.4 % w/v Bromophenol blue solution. Protein to SDS-buffer ratio used in this study followed: milk (25µL/mL), casein or caseinate (0.5 mg/mL), MPC (1.5 mg/mL) and WPC (0.6 mg/mL). For interfacial composition determination, the air-dried cream fraction was reconstituted with SDS sample buffer in a 2.0 mL Eppendorf centrifuge tube to make up the volume fraction similar to that of original emulsion. Small aliquots (250 µL) of emulsions were mixed with 300 µL of SDS buffer. In order to disrupt any disulfide linkages between proteins, a reducing thiol agent, 0.05% β-mercaptoethanol, was added to emulsion−sample buffer mixtures. The mixtures were heated (95−100 °C, 5 min) to allow accelerated dissociation reactions (Dalgleish, Goff, Brun, & Luan, 2002b). After cooling for 15 min, the samples were vortexed and centrifuged in an Eppendorf Centrifuge 5417C (Eppendorf AG, Hamburg, Germany) at 2500 g for 30 min before carrying out SDS gel electrophoresis. Finally, the samples stained with Amindo Black which allowed visually the migration of the proteins.

3.2.5 Characterization of heat stability of emulsion

The heat stability of emulsion was measured as the heat coagulation time (HCT) at temperatures of 96−140°C by the method of Davies and White (1966). A temperature of 140°C was used in the present study, the advantage was that it represents the ability of a milk protein stabilized emulsion to withstand prolonged heating at this temperature. If stable it would give good indication in almost all industrial thermal processing conditions such as in-can sterilization or UHT processing (Rattray & Jelen, 1997). The heat coagulation time (HCT) of emulsions was evaluated by heating at 140 °C and the procedure was followed as described by McSweeney et al. (2004). Aliquots (2.5 mL) of milk protein stabilized emulsion samples were transferred in 8 mL glass tubes with rubber lined cap (Wheaton, Millville, NJ, USA), immersed in a silicone oil bath thermostatically controlled at 140 ± 1°C, with consistent rocking speed of 8 rev/min.

Coagulation time accounted when large aggregates became visible to eyes or visible curd-like structure formed. All HCT values were determined in triplicate from duplicate productions, and mean values obtained from all data.

To evaluate the effect of heat treatment on milk protein stabilized emulsions in laboratory scale, an approach of heating emulsions in a silicone oil bath was adapted. Aliquots (5 mL) of milk protein stabilized emulsion samples were transferred in 8 mL glass tubes with rubber lined cap (Wheaton, Millville, NJ, USA), immersed in a silicone oil bath thermostatically controlled at 120 ± 1°C, with consistent rocking speed (8 rev/min). All the samples removed after 10 min heating time and immediately cooled with running tap water. The treated emulsions were allowed to equilibrate to room temperature and held for at least 1 h before further analysis (i.e. particle size, rheological measurement) was carried out.

3.2.6 Emulsion rheology

Rheological properties of the emulsions were measured with a controlled stress rheometer (Physica MCR301, Anton Paar, Graz, Austria) using the cone and plate geometry (cone-1 diameter = 40 mm, angle = 4.005°, gap = 0.048 mm; cone-2 diameter = 50 mm, angle = 2.009°, gap = 0.047 mm) as shown in Figure 3.1. For cone and plate geometry, all samples were vortexed in the same manner for 1 min prior to the measurements. In every measurement, 1.2 mL of the emulsion was carefully pipetted over the plateau of the rheometer. All emulsion samples were set to rest for 2 min after loading to allow temperature equilibration. Low shear rate 0.01 s^{-1} was applied for another 2 min and steady-state flow measurements were conducted at 20°C ± 0.1°C in the range of shear rate 0.01 s^{-1} to 1000 s^{-1} over the next 2 min. To determine the zero shear viscosity of protein solution/emulsion and to probe the droplet−droplet interactions in concentrated emulsions, concentric cylinder geometry (cup and bob, CC27 with measuring bob radius 13.33 mm, measuring cup radius 14.46 mm) was used for both rotational and oscillatory measurements (Figure 3.1). Rotational measurements were performed to obtain flow behavior and viscosity. Steady-state flow measurements were

conducted at 20°C ± 0.1°C in the range of shear rate 0.01 s^{-1} to 1000 s^{-1}. Zero shear viscosity was referred to the viscosity obtained at the lowest shear rate as possible. Oscillatory measurements were used for determining the viscoelastic properties and tracking the viscosity change of concentrated system at very small deformation. All rheological parameters (shear stress, shear rate, apparent viscosity) were collected from the software. Repeat measurements were carried out twice on each sample and the mean viscosity values obtained.

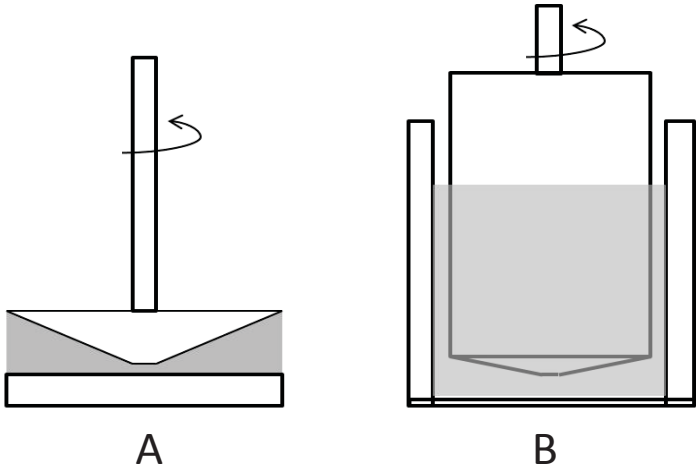

Figure 3.1. Schematic of the cone and plate geometry (A) and cup and bob geometry (B).

The flow behavior can be characterized as Newtonian, non-Newtonian, time independent and time dependent (Rao, 2007b; Steffe & Daubert, 2006).

Newtonian behavior

A Newtonian fluid shows proportional relationship between shear rate and shear stress and the plot begins at the origin. In other words, it is independent on the shear rate and the shear histories. Examples of Newtonian foods include water, sugar syrups, honeys, edible oils, filtered juices and milk (Rao, 2007a).

Non-Newtonian behavior

All other types of fluids are non-Newtonian which indicates either the fluid does not show a linear relationship between shear rate and shear stress and/or the plot does not start at the origin. Non-Newtonian flows can be divided into time independent (flow behavior may depend only on shear rate and on the length of shear) and time dependent (flow behavior may depend on shear rate and length of shear) (Rao, 2007a).

Time independent

Time independent flow behaviors include pseudoplastic, Bingham plastic and dilatant fluids. Pseudoplastic is also termed shear thinning, is a fluid which the viscosity decreases as the shear rate increases. Shear-thinning can be attributed to disruption of structural units in a food due to the shear induced hydrodynamic forces (i.e. pumping). In theory, any kind of interactions between dispersed droplets (attractive or repulsive) will result in non-Newtonian behavior (Dickinson, 1992; Rao, 2007a). A more complex rheological model such as Bingham plastic may be involved when a very thick fluid with a large yield stress (Steffe & Daubert, 2006).Yield stress is a specific shear stress threshold at which the material begins to flow under shearing. The shear rate-shear stress curve shows a straight line with a yield stress. Herschel-Bulkley model can be used to describe Bingham plastic behavior (Rao, 2007a; Steffe & Daubert , 2006). Dilatant is also called shear thickening, which the fluid increases in viscosity with increasing the shear rate. Starch solution and some types of honey are examples on shear thickening fluids.

3.2.7 Emulsion stability (cream layer thickness)

The model emulsions were transferred into flat-bottom screw-top tubes (15 mm × 140 mm). They were stored at room temperature and measured periodically using a vertical scan analyser Turbiscan Classic MA 2000 (Formulaction, Toulouse, France). The transmission (T) and backscattering (BS) profiles as a function of the sample height (total height = 60 mm) were collected at room temperature. Transmission is useful for

analysing non-opaque samples whereas backscattering is useful for analysing opaque samples (see Figure 3.2) (Chauvierre, Labarre, Couvreur, & Vauthier, 2004; Mengual, Meunier, Cayré, Puech, & Snabre, 1999; Wulff-Pérez, Torcello-Gómez, Gálvez-Ruíz, & Martín-Rodríguez, 2009). Measurements were carried out after preparation of the emulsions and at different times for 7 days.

The creaming curves were obtained by subtracting the *BS* profiles measured at 0 h (BS_0) from those measured at time *t* (BS_t), $\Delta BS = BS_t - BS_0$. The shape of the creaming curve gives a good indication of creaming, flocculation and other destabilization processes. *BS* mean values (BS_{av}) in the selected zone of the tube were measured as a function of storage time to determine flocculation kinetics because BS_{av} varies with the change in particle size (Chauvierre et al., 2004). The zone 15−30 mm was chosen for analysis of the model emulsions through the whole storage period and the aim was to avoid the area affected by creaming (Álvarez-Cerimedo et al., 2010). Visual determination of the classified layer thickness in the serum phase of the model emulsions was also carried out. 2% methylene blue staining solution (containing 21% w/v ethanol) was added to selected emulsion samples to aid determination of the phase boundary between cream and serum phases. The dilution ratio of the staining solution to sample is 1:200.

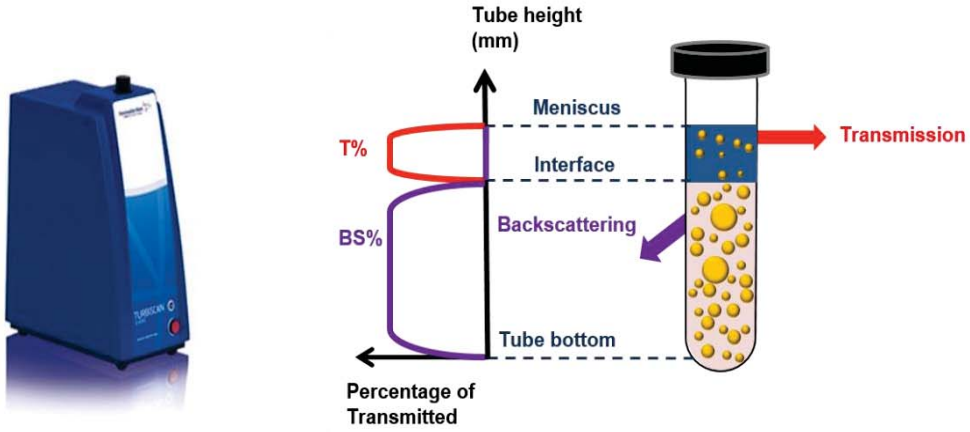

Figure 3.2. Schematic representation of Turbiscan Classic MA 2000.

3.2.8 Microstructure of emulsions

Confocal laser scanning microscopy (CLSM)

A schematic representation of a typical CLSM is given in Figure 3.3. Light from a laser beam (dark blue) is reflected by the dichroic mirror and focused onto a spot on the sample in the x−y plane. This excites fluorescence, and the sample then emits light at a lower wavelength (green), which passes through the objectives, goes through the dichroic mirror, and is focused down to a spot surrounded by a pinhole. The detected light then goes to the detector (Loren, Langton, & Hermansson, 2007; Rossetti, Depieri, & Bentley, 2013).

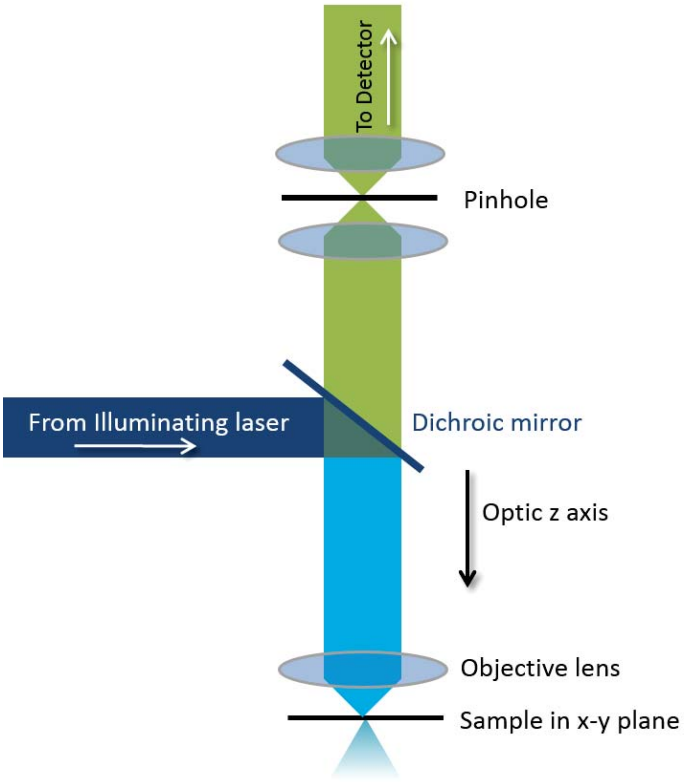

Figure 3.3. Schematic illustration of a confocal laser scanning microscopy (CLSM).

In CLSM, the pinhole blocks all fluorescence light originating from regions above or below the in-focus plane, therefore, only the light from the illumination volume is detected, and this is referred to optical sectioning. Three-dimensional microstructure can

be obtained by gathering optical sections at different depths in the specimen by adjusting the specimen in an axial direction (Loren et al., 2007).

Images of the emulsions were captured using a Leica SP5 DM6000B (Heidelberg, Germany) confocal laser scanning microscope. A 0.5 mL aliquot of each emulsion sample was transferred into a 2 mL centrifuge tube before adding Nile Red and Fast Green (approximately 0.1% w/w). After thorough mixing, a drop of each sample was placed on a microscope slide (Sail, Sailing Medical-Lab Industries Co. Ltd, China). The emulsion samples were imaged using 40x and 63x/1.32-0.6 oil-immersion objective at λ = 543 nm for Nile Red and λ = 488 nm for Fast Green. Images were scanned at a constant 7 μm below the level of the coverslip.

Transmission electron microscopy (TEM)

Emulsion samples were fixed, stained and processed as described by Langton & Hermansson (1996) and the transmission electron microscopy images were recorded electronically. The emulsion sample processing in the present study is described as following:

Fixation: The liquid emulsion sample was filled in an agarose tube and the tube was sealed. In this manner, the sample was embedded in the agarose gel without leakage. The tubes were put into a bijoux bottle containing 6.25% glutaraldehyde in 0.2 M imidazole buffer. This was stored at 4°C for two days. The glutaraldehyde solution was rinsed twice with 0.2 M imidazole buffer over two hours. The buffer was then removed and the sample was immersed in 1% osmium tetroxide prepared in 0.2 M sodium cacodylate overnight. The sample was rinsed with distilled water, placed in 1% uranyl acetate for 30 min and then again rinsed twice with distilled water.

Dehydration: The dehydration was carried out at 4°C in 25% acetone (15 min) and then subsequently in 50, 70, 90% acetone (for 30 min each) followed by 100% acetone (three changes over 90 min).

Embedding: The acetone was carefully pipetted out in fume hood and Procure 812 embedding resin solution was filled in 50%, and the sample was put on rollers for 24 hours. The sample was then fill with100% embedding resin next day and a cube of the sample was placed into a BEEM embedding capsule and put into an incubator at 60°C for 48 hours.

Sectioning: The embedded samples were sectioned to a thickness of 100 nm using a Leica Ultra cut R microtone. These sections were inserted on 3 mm copper/rhodium grids and stained using lead citrate before observation and image capturing on a Philips 201C transmission electron microscope (Philips, Eindhoven, The Netherlands) at an accelerating voltage of 60 kV.

Light microscopy

Selected samples (~15 µL) were placed on a microscope slide, carefully covered with a cover slip and observed under 40x objective using an optical microscope (Olympus BX60, GmBH, Hamburg, Germany) equipped with a digital camera. Representative images were displayed.

Chapter 4: Structure and Stability of Heat-treated High-Protein-Stabilized Oil-in-Water Emulsions: A Stability Map Characterization Approach [1]

4.1 Abstract

Emulsion instabilities such as depletion flocculation, coalescence, aggregation and heat-induced protein aggregation may be detrimental to the production of sterilized food emulsions. The type and the amount of protein present in the continuous phase and at the oil−water interface are crucial in the design of emulsions with appropriate stability, material and organoleptic properties. In this study, four oil-in-water model emulsion systems (pH 6.8−7.0) were formulated, characterized and categorized according to the potential interactions between interfacial layer and non-adsorbed proteins present in the continuous phase. The heat stability, the creaming behavior and the shear flow behavior of the model emulsions were influenced by both the emulsifier type and the type of protein in the continuous phase. The results suggest that this stability map approach of predicting droplet−droplet, droplet−protein and protein−protein interactions will be useful for the future design of heat-stable emulsion-based beverages with good creaming stability at high protein concentrations.

---

[1] Part of the content presented in this chapter has been published as a orginal paper in *Food Hydrocolloids* (2013) *33* 297−308.

Part of the content was also presented as an oral presentation at the 7th NIZO Dairy Conference, Papendal, the Netherlands, 21−23 September 2011.

4.2 Introduction

Caseins and whey proteins are widely used to emulsify and to stabilize oil droplets in emulsion systems (Dickinson, 1997). Food emulsions formulated with high protein content are generally subjected to harsh heat treatment (e.g. retort-, and ultra-high-temperature processes) to avoid long-term microbial growth. A number of studies have investigated on the heat-induced destabilization of whey protein emulsions (Raikos, 2010) and a few studied the effects of mixed proteins and mixed protein and surfactant on heat-induced destabilization of emulsions (McSweeney et al., 2008; McSweeney et al., 2004; Nikiforidis & Kiosseoglou, 2007; Parkinson & Dickinson, 2007). Emulsions with good stability against heating during production and against creaming during storage are an important requisite of many food products, but can be challenging to formulate. In principle, the heat stability of a protein based emulsion is determined by the properties of interfacial layer and the non-adsorbed protein in the continuous phase (Dalgleish, 2006). In addition, non-adsorbed protein could cause instabilities of oil-in-water emulsions regardless of the heat treatment. It has been suggested that in the presence of a considerable excess of non-adsorbed protein in the continuous phase, the emulsion droplets will undergo droplet flocculation, resulting in rapid phase separation (Dickinson & Golding, 1997a; Dickinson, Golding & Povey, 1997).

Few studies have investigated the impact of various milk protein types in the dispersed and continuous phases and the influence of high temperature treatment on the macroscopic and microscopic stabilities of emulsions fortified with high amounts of protein. The objectives of this study were to design a simple model system to understand the emulsion interactions at high temperatures that determine stability or instability, to characterize the roles of the proteins and surfactants present at the interface and/or in solution of an emulsion, to address heat-induced destabilization at high temperatures in mixed protein systems and to predict emulsion stability.

In this study, the heat-treated model emulsions were characterized and categorized into four proposed model systems in terms of their continuous and dispersed phase interactions. A schematic presentation of four model droplet−droplet, droplet−protein and

protein− protein interaction diagrams with respect to the role of the type of adsorbed and non-adsorbed protein is shown in Figure 4.1. In order to achieve the proposed model systems, heat-sensitive proteins (WPC & WPI) and heat-insensitive proteins (MPC I, MPC II, NaCas and WPH) and food-grade surfactant (Tween 20) were used.

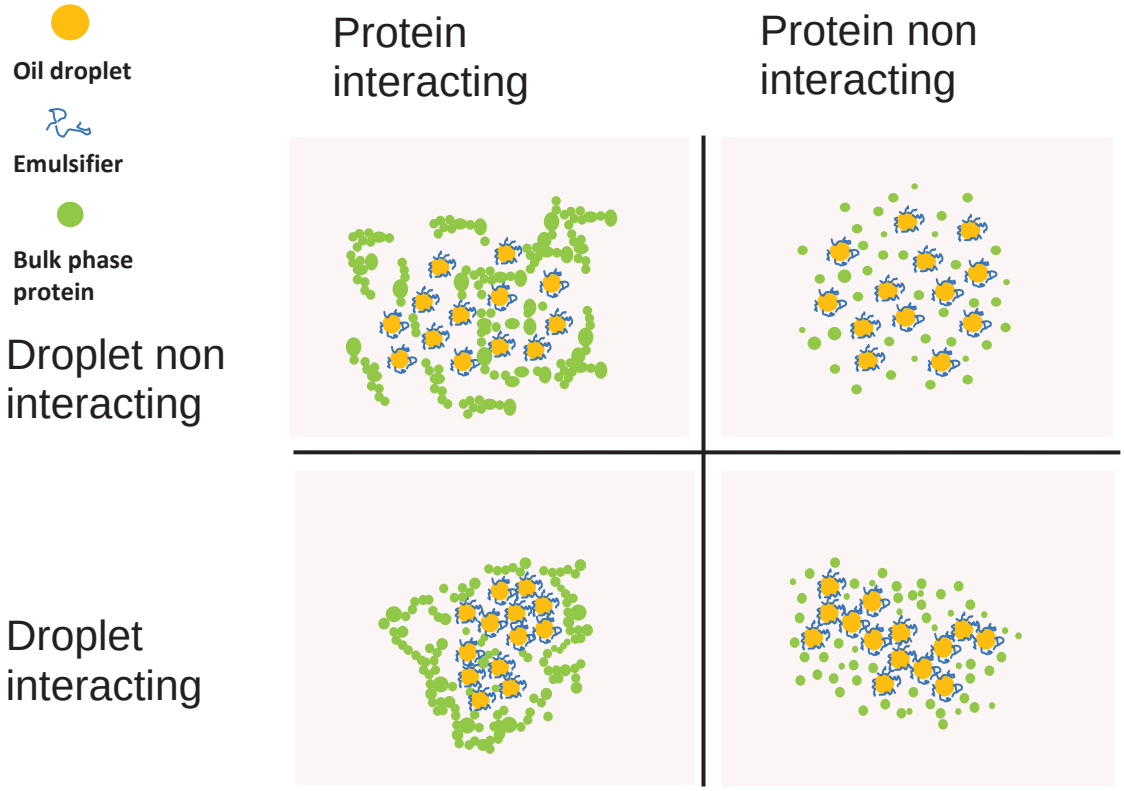

Figure 4.1. Schematic diagrams of the proposed model systems: top left system, no interactions between droplets but non-adsorbed proteins interact with each other (i.e. an unstable system with a partly liquid and a partly gel-like structure); top right system, no droplet−droplet interactions and no protein−protein interactions at the oil−water interface and in the continuous phase (i.e. a stable system with no coagulation and no phase separation); bottom left system, interactions between adsorbed proteins, between non-adsorbed proteins and between adsorbed and non-adsorbed proteins (i.e. a whey protein emulsion gel); bottom right system, interactions between droplets but no protein−protein interactions at the oil−water interface and in the continuous phase (i.e. a phase separation induced by depletion flocculation).

4.3 Materials and methods

4.3.1 Materials

Milk protein concentrate 4850 (MPC I), calcium-depleted-MPC (MPC II), sodium caseinate 180 (NaCas), whey protein concentrate 80 (WPC), whey protein isolate 895 (WPI) and whey protein hydrolyzate 821 (WPH) were obtained from Fonterra Co-operative Group Ltd, Auckland, New Zealand. The compositions of the milk protein powders are shown in Chapter 3 (Table 3.1). All of the chemicals used were of analytical grade, obtained from either BDH Chemicals (BDH Ltd, Poole, England) or Sigma Chemical Co. (St Louis, MO, USA) unless otherwise specified.

4.3.2 Preparation of model emulsion systems

Two primary stock emulsions stabilized with food grade NaCas or Tween 20 were prepared. NaCas was selected as an emulsifier because of its excellent heat stability and good emulsifying properties. From preliminary experiments, an oil-in-water emulsion stabilized with Tween 20 (10% w/w oil) was also found to be very heat stable, with no coagulation being observed on heating at 120 °C for at least 40 min.

The model emulsions were prepared following the procedure described in Fig. 4.2. The stock emulsion (20% w/w oil) stabilized by either 0.5% w/w NaCas or 0.5% w/w Tween 20 was mixed with stock protein solutions – MPC I, MPC II, WPC and WPH respectively in a 1:1 weight ratio to yield final dispersions containing 8.5% w/w protein and 10% w/w oil. Model emulsions (8.5% protein, 10% oil) stabilized by sole protein ingredients were also prepared for comparison. WPC was used as a heat-sensitive control while NaCas and MPC were used as heat-stable controls containing non-micellar casein and micellar casein respectively. The approximate total casein and whey protein contents are shown in Table 4.1. The surface protein coverages for NaCas-stabilized-, whey protein-stabilized- and Tween-20-stabilized droplets are theoretically calculated according to

$C_{non-ad} = \frac{6 \cdot \Gamma \cdot \emptyset}{d_{32}}$ (McClements, 2005).

Here, Γ is the surface load (in kg m^{-2}), $\emptyset$ is the disperse phase volume fraction (0.1 is used in calculation), C_{non-ad} is the concentration of emulsifier in the continuous phase (in kg m^{-3}). The surface load of sodium caseinate (NaCas) and whey protein concentrate (WPC) have been reported to be around 2 mg m^{-2} (Srinivasan et al., 2002; Tcholakova et al., 2006) while the surface load of Tween has been reported to be around 3 mg m^{-2} for a mean droplet size of around 0.5 μm (Yang, Leser, Sher, & McClements, 2013).

Reverse-phase high-performance liquid chromatography (RP-HPLC) was used to determine whey protein composition (Elgar, Norris, Ayers, Pritchard, Otter & Palmano, 2000). Sodium azide (0.02% w/w) was added to the emulsion samples as an anti-microbial agent. All emulsions were stored at 4 °C overnight until further use. Each model emulsion was prepared at least in duplicate.

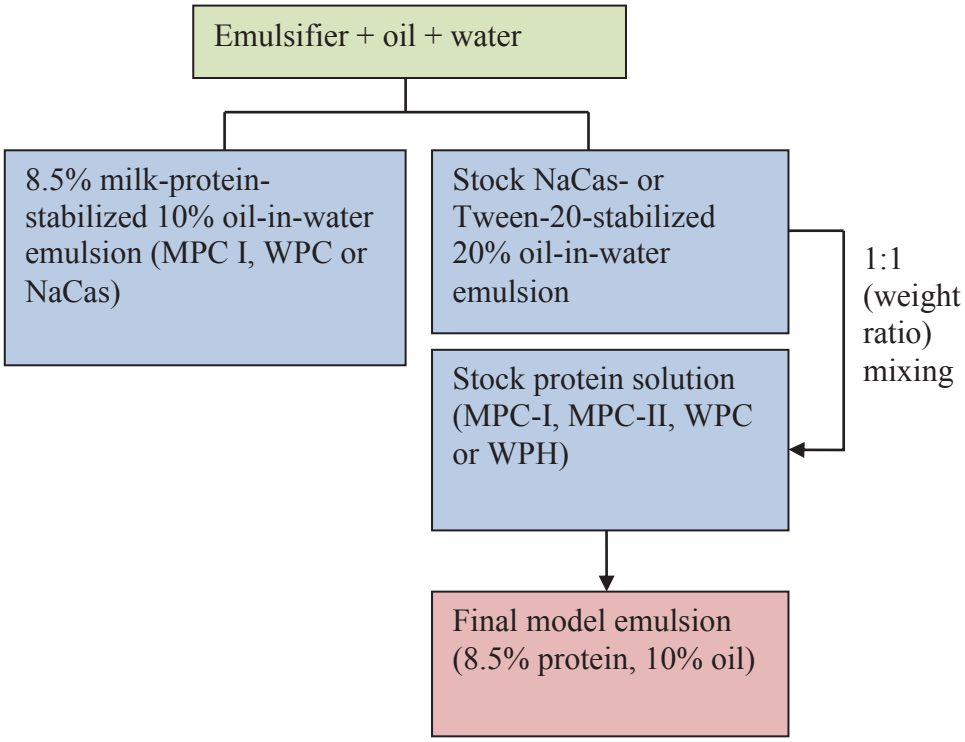

Figure 4.2. Flow chart of the preparation of model emulsions (8.5% w/w protein, 10% w/w oil).

4.3.3 Characterization of heat stability of the model emulsions

The heat stability of the model emulsions was determined as the procedure described in Chapter 3, Section 3.2.5. The gelled or coagulated samples were not included in particle size, creaming stability and rheological measurements.

4.3.4 Determination of surface protein composition

The determination of interfacial protein composition was followed according to the procedure described in Chapter 3, Section 3.2.4.

4.3.5 Particle size determination

The particle size measurements were carried out using procedures described in Chapter 3, Section 3.2.3. The particle size of protein solutions was measured by Zetasizer and the results were reported as Z-average. The particle of protein-stabilized emulsions was determined by Mastersizer. The average droplet size was expressed as the surface-weighted diameter $d_{3,2}$ (μm) and the volume-weighted mean diameter $d_{4,3}$ (μm).

4.3.6 Emulsion stability

The model emulsions were stored at ambient temperature and measured periodically for 7 days using a vertical scan analyser Turbiscan Classic MA 2000 (Formulaction, Toulouse, France). Details of the techniques are described in Chapter 3, Section 3.2.7.

4.3.7 Rheological properties of model emulsions

Details of the rheological measurement of emulsions have been described in Chapter 3, Section 3.2.6. The viscosity of emulsions was measured using cone and plate geometry. Low shear rate 0.01 s^{-1} was applied for another 2 min and steady-state flow measurements were conducted at 20°C ± 0.1°C in the range of shear rate 0.01 s^{-1} to 500 s^{-1} over the next 2 min.

4.3.8 Microsturcture of model emulsions

Details of the confocal scanning laser microscope and transmission electron microscope characterization techniques have been described in Chapter 3, Section 3.2.8.

4.3.9 Statistical analysis

All experiments were carried out at least in triplicate using freshly prepared samples and the results are reported as the mean and standard deviation of these measurements.

Table 4.1. Distributions of casein and whey protein in the protein- and surfactant-stabilized model emulsions (8.5% w/w protein, 10% w/w oil).

Compositions of model emulsions (% w/w)		Micellar casein (% w/w)	Non-micellar casein (% w/w)	Whey protein (% w/w)
Continuous phase	Dispersed phase			
MPC I	MPC I	~ 6.8	trace	~ 1.7
NaCas	NaCas	–	8.5	–
WPC	WPC	–	–	8.5
8.0% MPC I	0.5% NaCas	~ 6.4	0.5	~ 1.6
8.0% MPC II	0.5% NaCas	~ 3.84	~ 3.06	~ 1.6
8.0% WPC	0.5% NaCas	–	0.5	8
8.0% WPH	0.5% NaCas	–	0.5	8
8.5% MPC I	0.5% Tween 20	~ 6.8	trace	~ 1.7
8.5% MPC II	0.5% Tween 20	~ 4.08	~ 2.72	~ 1.7
8.5% WPC	0.5% Tween 20	–	–	8.5
8.5% WPH	0.5% Tween 20	–	–	8.5

4.4 Results and Discussion

4.4.1 Model emulsions with interactions between adsorbed proteins, interactions between non-adsorbed proteins and cross-interactions between adsorbed and non-adsorbed proteins

Table 4.2. Mean effective particle sizes of model emulsions (8.5% w/w protein, 10% w/w oil) before and after heat treatment (120°C for 10 min).

Continuous phase (w/w)	Emulsifiers (w/w)	Effective $d_{4,3}$ (μm)	
		Before heat treatment	After heat treatment
NaCas stock emulsion	0.5% NaCas	1.04 ± 0.26[a]	1.02 ± 0.23[a]
Tween 20 stock emulsion	0.5% Tween 20	0.78 ± 0.01[a]	0.77 ± 0.01[a]
MPC-I	8.5% MPC-I	1.00 ± 0.02[a]	1.02 ± 0.00[a]
NaCas	8.5% NaCas	1.08 ± 0.04[a]	3.06 ± 0.79[b]
WPC [f]	8.5% WPC	1.05 ± 0.03	N/A
8.0% MPC-I	0.5% NaCas	1.18 ± 0.10[a]	1.14 ± 0.14[a]
8.0% MPC-II	0.5% NaCas	1.12 ± 0.02[a]	2.30 ± 0.18[b]
8.0% WPC [f]	0.5% NaCas	1.10 ± 0.18	N/A
8.0% WPH	0.5% NaCas	1.03 ± 0.18[a]	1.11 ± 0.27[a]
8.5% MPC-I	0.5% Tween 20	0.61 ± 0.01[a]	0.58 ± 0.01[a]
8.5% MPC-II	0.5% Tween 20	0.69 ± 0.01[a]	1.07 ± 0.05[b]
8.5% WPC [g]	0.5% Tween 20	0.77 ± 0.01[a]	0.81 ± 0.05[a]
8.5% WPH [f]	0.5% Tween 20	0.80 ± 0.02	N/A

[a,b] Means within the same row having the same superscript are not significantly different with Student's t-test at $p < 0.05$.

N/A Not analyzed due to gelation.

[f] Significant differences between means were not determined due to sample gelation.

[g] The particle size measurement was carried out on the turbid liquid layer after heating.

Table 4.3. Mean primary particle sizes of model emulsions (8.5% w/w protein, 10% w/w oil before and after heat treatment (120°C for 10 min).

Continuous phase (w/w)	Emulsifiers (w/w)	Primary $d_{4,3}$ (μm)	
		Before heat treatment	After heat treatment
NaCas stock emulsion	0.5% NaCas	1.06 ± 0.18 [a]	1.02 ± 0.24 [a]
Tween 20 stock emulsion	0.5% Tween 20	0.81 ± 0.02 [a]	0.77 ± 0.02 [a]
Sole MPC-I	Sole MPC-I	1.35 ± 0.04 [a]	1.35 ± 0.08 [a]
Sole NaCas	Sole NaCas	1.10 ± 0.08 [a]	1.38 ± 0.28 [a]
Sole WPC [f]	Sole WPC	1.09 ± 0.08	N/A
8.0% MPC-I	0.5% NaCas	1.42 ± 0.09 [a]	1.47 ± 0.11 [a]
8.0% MPC-II	0.5% NaCas	1.30 ± 0.03 [a]	1.41 ± 0.07 [a]
8.0% WPC [f]	0.5% NaCas	1.08 ± 0.20	N/A
8.0% WPH	0.5% NaCas	1.01 ± 0.19 [a]	1.04 ± 0.20 [a]
8.5% MPC-I	0.5% Tween 20	0.80 ± 0.00 [a]	0.80 ± 0.01 [a]
8.5% MPC-II	0.5% Tween 20	0.80 ± 0.02 [a]	1.08 ± 0.07 [b]
8.5% WPC [g]	0.5% Tween 20	0.82 ± 0.03 [a]	0.80 ± 0.00 [a]
8.5% WPH [f]	0.5% Tween 20	0.80 ± 0.02	N/A

[a,b] Means within the same row having the same superscript are not significantly different with Student's t-test at $p < 0.05$.

N/A Not analyzed due to gelation.

[f] Significant differences between means were not determined due to sample gelation.

[g] The particle size measurement was carried out on the turbid liquid layer after heating.

The mean effective and primary particle sizes of unheated and heated model emulsions were reported as volume-weighted mean diameter ($d_{4,3}$) in Table 4.2 & 4.3. The particle size of emulsions either gelled or completely destabilized upon heat treatment could not be measured except the turbid liquid layer from the WPC emulsion containing oil droplets stabilized by 0.5% (w/w) Tween 20. There was a little change in the effective particle size ($d_{4,3}$ values) between unheated and heated emulsion samples expect the emulsions containing non-micellar caseins in the continuous phase regardless of the

emulsifier type. The effective particle size ($d_{4,3}$ value) of heated NaCas emulsion, NaCas stabilized MPC-II emulsion and Tween 20 stabilized MPC-II emulsion was significantly greater ($p < 0.05$) than that before heating (Table 4.2). On the other hand, reduced $d_{4,3}$ values of heated NaCas emulsion and NaCas stabilized MPC-II emulsion were seen in the primary particle size measurements (in the presence of dissociating agent) and their means were not significant different ($p > 0.05$) (Table 4.3). This change suggests that the heat-induced protein-protein and/or protein-droplet flocs may be disrupted or solubilized by the dissociating agent.

From visual observations, the 8.5% w/w WPC-stabilized emulsion formed a paste-like texture upon heating indicating a high degree of structure. Confocal micrographs indicated droplet−droplet interactions to form clusters, with the droplet clusters appearing to interact with whey proteins in the continuous phase to form a gel matrix (Figure 4.3A). It was calculated that the interfacial whey protein concentration was approximately 0.4% w/w and that the rest of the whey proteins remained non-adsorbed (~ 8.1% w/w) in the continuous phase. In the case of an emulsion with a high protein-to-oil ratio, the extent of destabilization of the emulsion will be predominantly influenced by the concentration of non-adsorbed protein in the continuous phase (Euston et al., 2000). The extent of heat-induced droplet−droplet and droplet−protein aggregations will be increased if non-adsorbed whey proteins were present (Euston et al., 2000). This is not only due to the ability of the interfacial and serum globular proteins to form covalent cross-links, but may also be influenced by the ionic components present as part of the whey protein (Euston et al., 2000). Previous studies have also shown that calcium ions promote protein aggregation/coagulation in emulsion and solution systems (Buzzaccaro, Rusconi, & Piazza, 2007; Keowmaneechai & McClements, 2006). WPC at 8.5% w/w has a reasonably high calcium content (~ 8.5 mM/L), which may contribute to the extent of heat-induced whey protein aggregation.

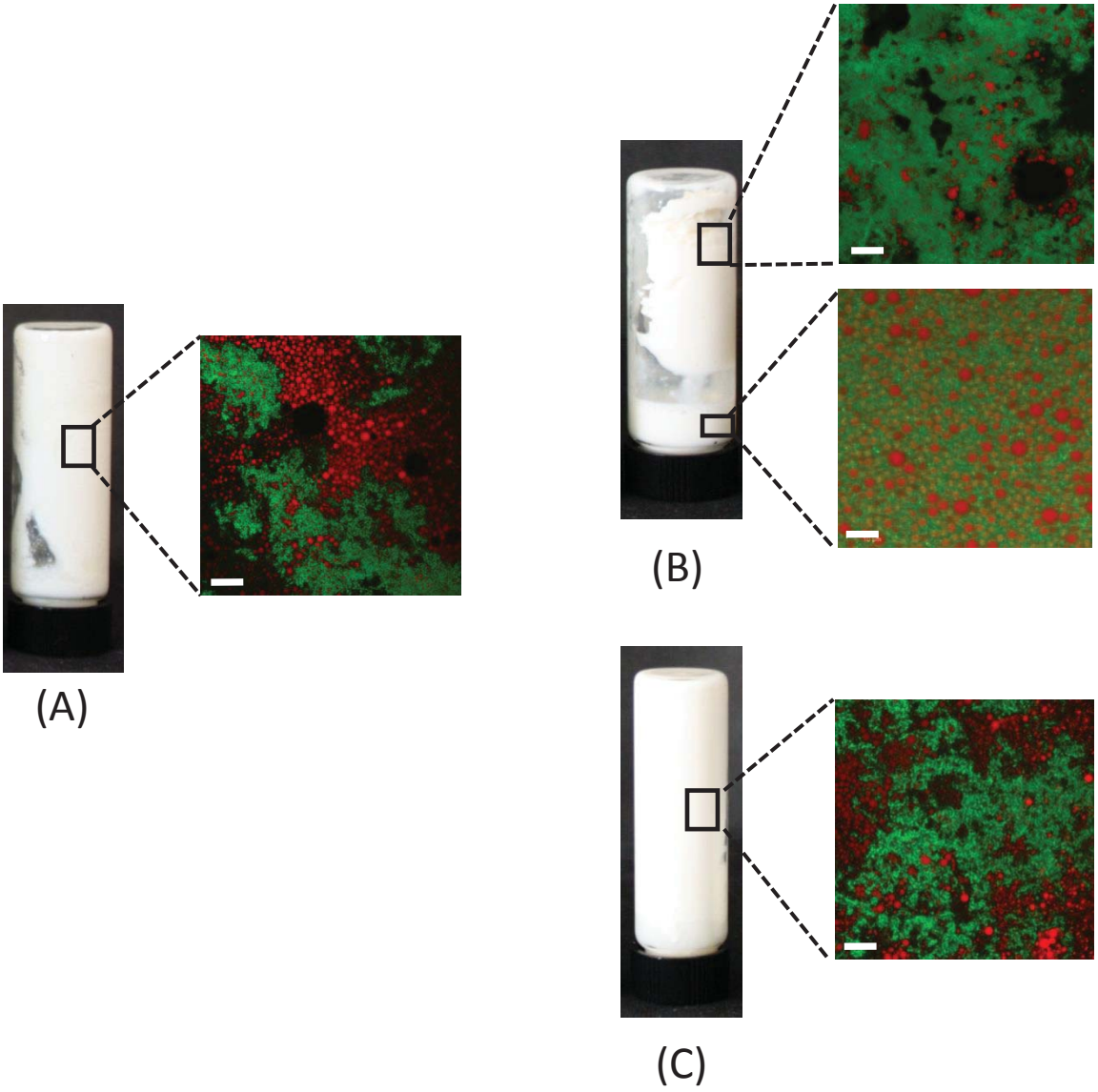

Figure 4.3. Visual appearance and microstructure of heated (120 °C, 10 min) model emulsions (8.5% w/w protein, 10% w/w oil): (A) sole WPC-stabilized emulsion; (B) Tween-20-stabilized emulsion containing WPC, with the top image showing the gelled phase and the bottom image showing the serum layer expelled from the gel; (C) NaCas-stabilized emulsion containing WPC. Red: oil droplet; Green: protein. Scale bar = 10 μm.

To determine the phase transition of whey protein emulsions in the initial heat-induced aggregation/gelation process, a heat stability map (90 °C for 10 min) of whey protein concentration against calcium content in a 10% oil-in-water emulsion was obtained using

WPI as a whey protein source of low ionic strength (Figure 4.4). It was found the WPI emulsions at high protein contents (4.5 and 6.5% w/w) formed a precipitate or a gel-like texture in the presence of 4 and 5 mM $CaCl_2$ respectively during heating. *β*-Lactoglobulin (*β*-lg) is a major component of whey proteins and has two internal disulfide bonds and one free thiol group (Havea, Singh, & Creamer, 2002). The *β*-lg content of WPI can be almost twice that of WPC (Morr & Ha, 1993). RP-HPLC results showed WPI contained about 70.2% *β*-lg while WPC contained about 35.7% *β*-lg. Therefore 4.5% w/w WPI is approximately equivalent to 8.5% w/w WPC in terms of *β*-lg content. Additionally, as the WPC content in the model emulsion is within the range of gelation concentration, it has a strong tendency to gel upon heating (Havea et al., 2002). The results confirmed the role of calcium in the heat stability of whey protein emulsions of high protein content. The gel-like texture observed in the heated 8.5% w/w whey-protein-stabilized emulsion fitted with a model in which interactions occur between all adsorbed and non-adsorbed proteins.

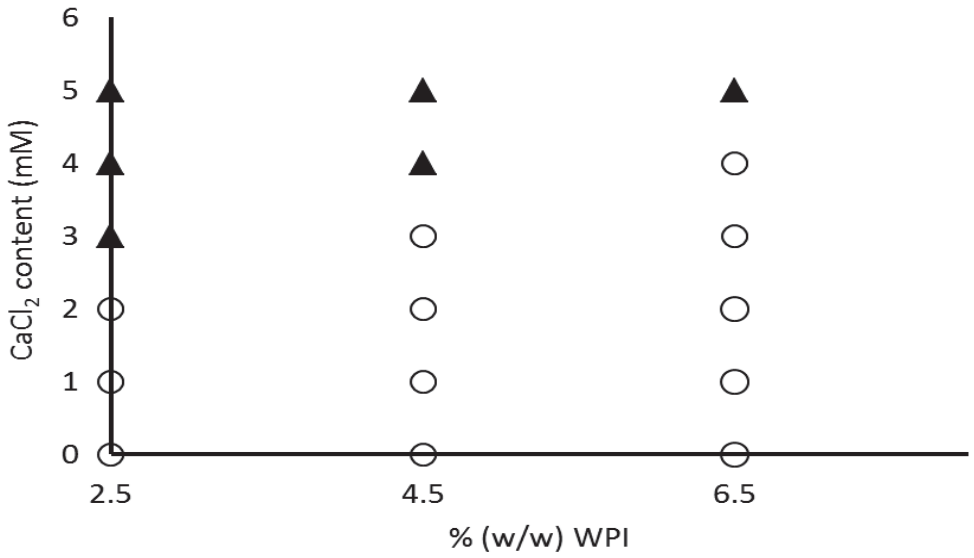

Figure 4.4. Heat stability map of WPI-stabilized 10% w/w oil-in-water emulsions (pH 6.8-7.0) with different $CaCl_2$ contents after heating for 10 min at 90°C. Depending on the visual appearance and measured viscosity after heating, samples may be assigned to different categories: ○, stable against heat (remained liquid); ▲, unstable against heat (formed precipitate or gel-like paste).

4.4.2 Model emulsions with no interactions between adsorbed proteins but with protein−protein interactions between non-adsorbed proteins

NaCas-stabilized and Tween-20-stabilized droplets were considered not to be susceptible to heat treatment. Previously, it has been shown that NaCas-stabilized emulsion droplets are very heat stable (Srinivasan et al., 2002). Furthermore, a number of studies have indicated that caseins, either in their individual form or in their self-assembled form (such as NaCas), have a stabilizing effect, a so-called chaperone-like activity, against heat-induced whey protein aggregation at neutral pH when present in small amounts (Guyomarc'h et al., 2009; O'Kennedy & Moussey, 2006; Yong & Foegeding, 2010). Additionally, it has been shown that a small amount of low molecular weight surfactant (e.g. Tween 20) would effectively shield the hydrophobic areas of heat-induced globular proteins from interactions (Nikiforidis & Kiosseoglou, 2007). For the model emulsions containing NaCas-stabilized or Tween-20-stabilized oil droplets, it was estimated that the non-adsorbed NaCas and Tween 20 were within 0.2−0.3% w/w. It was hypothesized that the interfacial layer would not be expected to form bonds with the continuous phase protein before heating and there would be little heat-induced flocculation between droplets and non-adsorbed proteins upon heating because of the stabilizing ability of casein and the Tween molecule against extensive heat-induced globular protein aggregation.

The Tween-20-stabilized emulsion containing WPC partially coagulated into a paste-like material following heating and retained a reasonable amount of turbid fluid, which was expelled from the paste. A homogeneous emulsion droplet distribution can be clearly seen in the serum layer of the Tween-20-stabilized emulsion containing WPC (Figure 4. 3B). Protein aggregates and the gel network can be clearly seen in the gelled phase; trace amounts of droplets can also be seen because they may have been trapped within the whey protein gel network (Figure 4.3B).The result of homogeneous droplet distribution after heating when droplets were coated with Tween 20 was in agreement with expectation. As hypothesized, the Tween-20-stabilized droplets were not affected either by the electrostatic shielding nor displaced by milk proteins from the oil/water interface, since Tween 20 is both non-ionic and highly surface active (Dickinson, 1992). However,

intensive heat-induced protein−protein aggregation still occurred in presence of Tween 20. It has been reported that Tween 20 can stabilize globular-protein-stabilized oil droplets and globular protein against heat (Nikiforidis & Kiosseoglou, 2007; Tran Le et al., 2011). The high heating temperature or high protein concentration may play a critical role in the aggregation mechanism(s).

The particle size distribution of the turbid liquid layer from the Tween-20-stabilized emulsion containing WPC showed little difference from that of the Tween 20 stock emulsion (Figure 4.5) suggesting no heat-induced droplet-droplet interaction had occurred. The microstructure and particle size results suggest that the proposed phenomenon (an emulsion with no droplet−droplet interactions but with protein−protein interactions in the continuous phase) was evident in the heated Tween-20-stabilized emulsion containing WPC. These results also agree with those of Chen and Dickinson (1998), who found that Tween-20-coated oil droplets neither were trapped within the three-dimensional whey-protein-stabilized emulsion gel matrix nor contributed to the gel strength of the emulsion. The Tween-20-coated droplets can be considered as "inactive" fillers in protein gel network (Corredig, Ion Titapiccolo, Gaygadzhiev, & Alexander, 2011).

The NaCas-stabilized emulsion containing WPC formed a paste-like texture during heating, with the confocal micrographs showing a similar microstructure to that of the sole WPC-stabilized emulsion (Figure 4.3A and 4.3C). This result was contrary to the expectation that the NaCas would have governed the steric-stabilizing effect on heat-induced droplet−droplet and droplet−protein interactions and would not expect covalent crosslinking/aggregation due to low occurrence of cysteine residues at the casein interface. The association of NaCas-stabilized droplets with the gel network may have been due to the high mineral content of the WPC powder, especially the presence of excess free ionic calcium (Ca^{2+}) (~ 8 mM in 8.0% w/w WPC). The binding of Ca^{2+} to caseins will reduce the thickness of the adsorbed casein at the interface and will diminish steric repulsion by causing partial collapse of the casein tails (Hemar & Horne, 1998; Parkinson & Dickinson, 2007). It was shown recently that, after the addition of 10 mM $CaCl_2$ to a β-casein/β-lg dispersion at a 1:5 protein concentration ratio, β-casein lost its

chaperone-like stabilizing effect against whey protein aggregation completely (Kehoe & Foegeding, 2011). Therefore, the NaCas-stabilized droplets may interact with denatured whey proteins in the continuous phase because of the weakened steric repulsion. Alternatively, the *κ*-casein of NaCas can interact chemically with denatured whey proteins via disulfide bonds and formed the gel matrix when whey-protein-to-casein ratio is high (Surel, Foucquier, Perrot, Mackie, Garnier, Riaublanc & Anton, 2014).

Different amounts of EDTA (5, 10, 15 and 20 mM) were added to determine whether gelation still occurred in a NaCas-stabilized emulsion containing WPC. All of the emulsions heated at 120 °C formed paste-like gels within 2 min. This was consistent with Keowmaneechai and McClements's study (2006), which suggested that heat-induced coagulation/gelation occurred in whey protein emulsions regardless of the addition of EDTA at high temperatures.

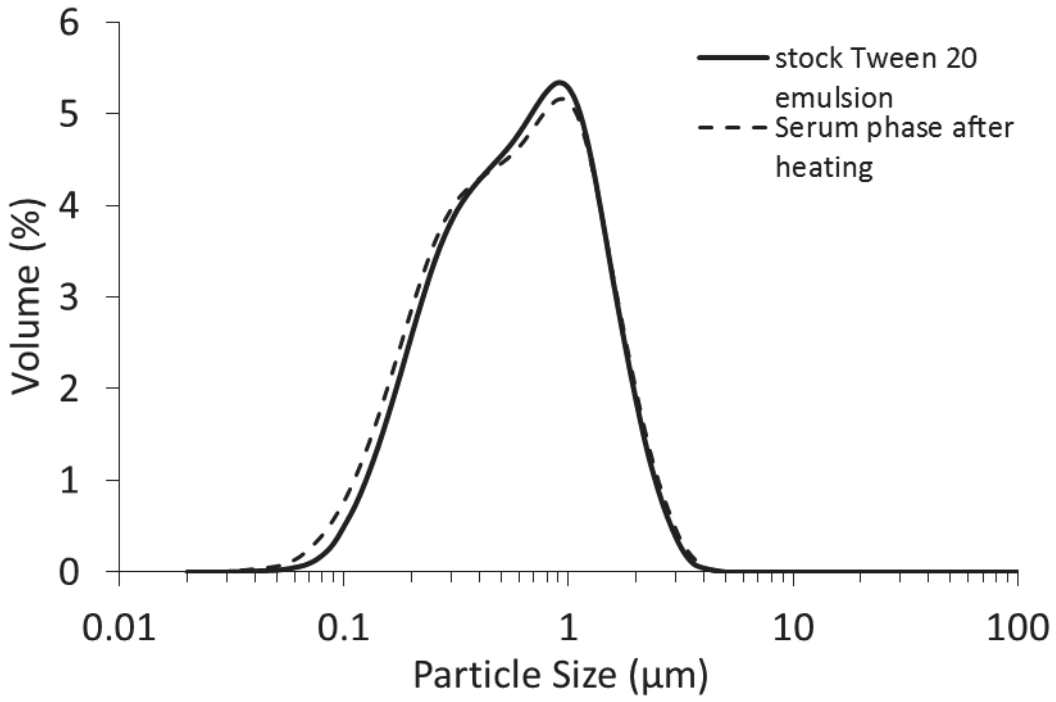

Figure 4.5. Droplet size distribution of the serum phase that was expelled from the gel phase in a heated (120 °C, 10 min) Tween-20-stabilized emulsion containing 8.5% w/w WPC.

Alternatively, competitive adsorption between whey proteins and caseins at the oil−water interface could occur during storage or heating when whey proteins are in excess (Dalgleish, Goff, & Luan, 2002b). β-lg will preferentially displace α_{S1}- and β-caseins from the oil−water interface whereas α-lactalbumin adsorbs to the casein-stabilized droplet surface rather than displacing the other proteins (Dalgleish, Goff, & Luan, 2002b). Any such exchange of casein by whey proteins could increase the tendency for the formation of disulfide-mediated polymers. Figure 4.6 shows the SDS-PAGE patterns of the interfacial proteins of unheated and heated NaCas-stabilized emulsions containing WPC. An increased amount of whey proteins was observed to be at the oil−water interface even before heat treatment. Some disulfide-cross-linked whey proteins formed upon heating as the whey protein bands became denser in the presence of a reducing agent (Figure 4.6B). The emulsion droplets co-adsorbed by caseins and whey proteins may have participated in the formation of gel matrix as interacting particles in the presence of calcium during heating. As interfacial exchange interactions between caseins

and whey proteins become more extensive at higher temperature, the droplets behave more like whey-protein-coated droplets. This may increase the tendency for heat-induced droplet collision and eventually the droplets become involved in the formation of the protein gel matrix (Surel et al., 2014). This result indicates that the exchange interactions between whey proteins and non-micellar caseins and the heating temperature are crucial in the heat-induced coagulation of a NaCas-stabilized emulsion containing WPC.

4.4.3 Model emulsions with no interactions between adsorbed proteins and between non-adsorbed proteins but with droplet−droplet interactions

In previous studies, the creaming stability of NaCas-stabilized emulsions has been found to be sensitive to the oil-to-protein ratio. At low oil-to-protein ratios, the creaming stability reduces because of depletion flocculation of emulsion droplets by the excess non-adsorbed caseinate particles. The creaming stability increases again at very high protein concentration, because the higher initial viscosity governed by a weak gel network helps to reduce the flocculation rate of the oil droplets (Dickinson, 1999a; Dickinson & Golding, 1997a; Surh, 2009).

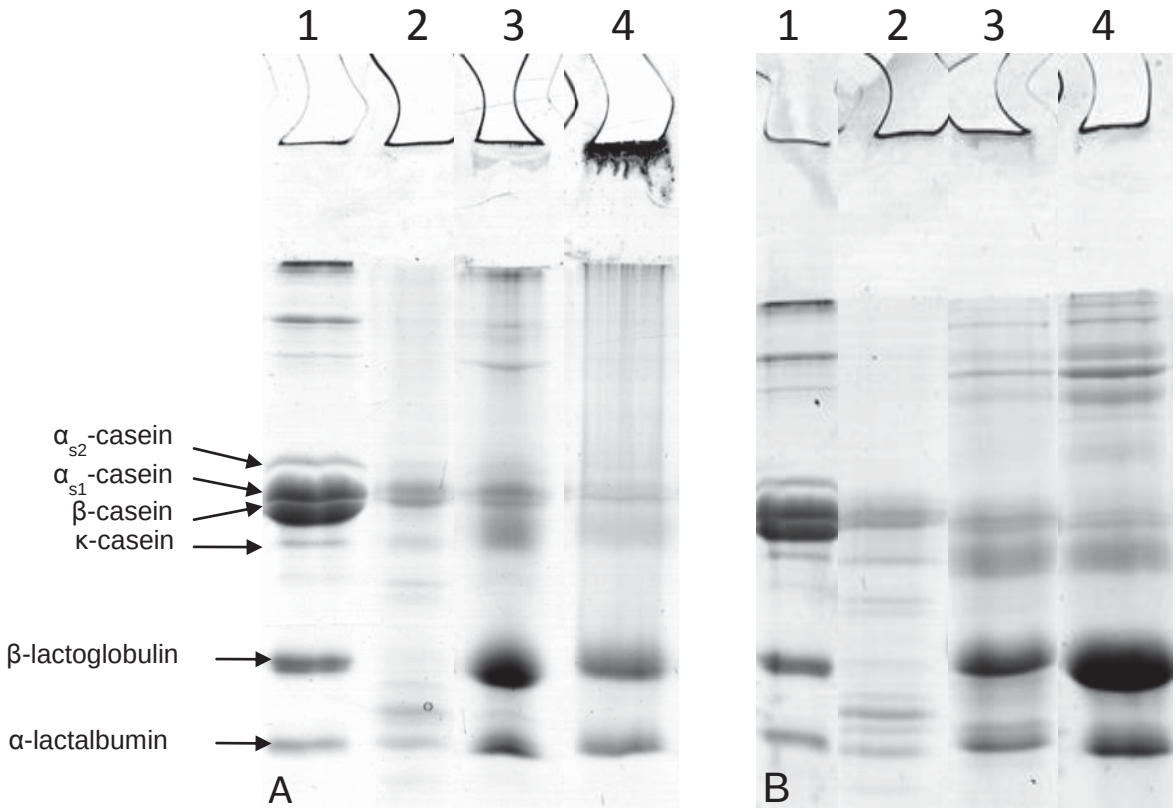

Figure 4.6. SDS-PAGE patterns of the interfacial proteins (A) under non-reducing conditions and (B) under reducing conditions (*β*-mercaptoethanol was added). Lane 1: skim milk standard; lane 2: unheated NaCas stock emulsion; lane 3: unheated NaCas-stabilized emulsion containing WPC; lane 4: heated NaCas-stabilized emulsion containing WPC. The heated emulsion was collected after heating at 90 °C for 10 min.

Emulsion separation was visually observed in the NaCas-stabilized and Tween-20-stabilized emulsions containing MPC I and MPC II, regardless of heat treatment. This was assumed to be caused by depletion flocculation, as there was no change in the droplet size distribution. The depletion phenomenon was confirmed using Turbiscan, rheology and microscopy. With the Turbiscan, the difference between a stable emulsion sample and a creamed or phase-separated emulsion sample can be probed at an early stage to determine the flocculation kinetics. It was shown that there was a dramatic change in *BS* (%) at the bottom of the tube and the shape of the profile at the top of the tube was a consequence of the migration of emulsion droplets contributing to the formation of the

floc network (Figure 4.7). This sharp migration of emulsion droplets was also evident from decreased $d_{3,2}$ and $d_{4,3}$ values obtained from the bottom region of the emulsion sample after 1 day (data not shown) (here, it was hypothesized that the depletion forces present would be insufficient to promote flocculation of the smaller droplets in the particle size distribution).

The ΔBS (%) of the unheated and heated model emulsions over a 6-day period is shown in Figure 4.8. It can be seen that the stock NaCas emulsion showed a small change (< 5%) in *BS* from time zero and displayed gravitational creaming that followed Stokes' law (Figure 4.8A). The sole NaCas-stabilized emulsion and the NaCas-stabilized and Tween-20-stabilized emulsions containing MPC I and MPC II appeared to have large variations (> 10%) in *BS* from time zero. These samples displayed sharp changes in *BS* (%) after 1 day and the values reached a plateau at up to 144 h (Figure 4.8). The emulsions containing MPC II showed a greater extent of separation than those containing MPC I. This large deviation in classified layer is attributed to the presence of non-micellar content in calcium-depleted MPC which causes depletion flocculation (Ye, 2011). The heated emulsions, which also underwent depletion flocculation, showed consistently smaller changes in ΔBS (%) than the unheated emulsions, suggesting that fewer droplets were depleted.

Figure 4.9 shows confocal micrographs of model emulsions before and after heat treatment. The NaCas-stabilized and Tween-20-stabilized emulsions containing MPC I and MPC II showed a certain degree of droplet flocculation regardless of the heat treatment. The visual appearances of NaCas-stabilized and Tween-20-stabilized emulsions containing 1~8% w/w MPC I in the continuous phase are shown in Figure 4.10. Gradual creaming was seen with increased protein concentration in the continuous phase. This indicates that the depletion flocculation is dependent on the bulk protein concentration. It is interesting to note that the casein micelles present in MPC I and MPC II appeared to be different. TEM images provided more detailed microstructure information on the dispersed and continuous phases of the model emulsions (Figure 4.11). Casein micelles with more compact structure were seen in MPC I whereas some casein micelles with more swollen structure were seen in MPC II, suggesting that MPC II

contained more polydisperse casein micelles. This result is consistent with the findings in Ye's study (2011) which suggests that the reduction of Ca ion concentration in MPC results in increased amount of non-micellar caseins.

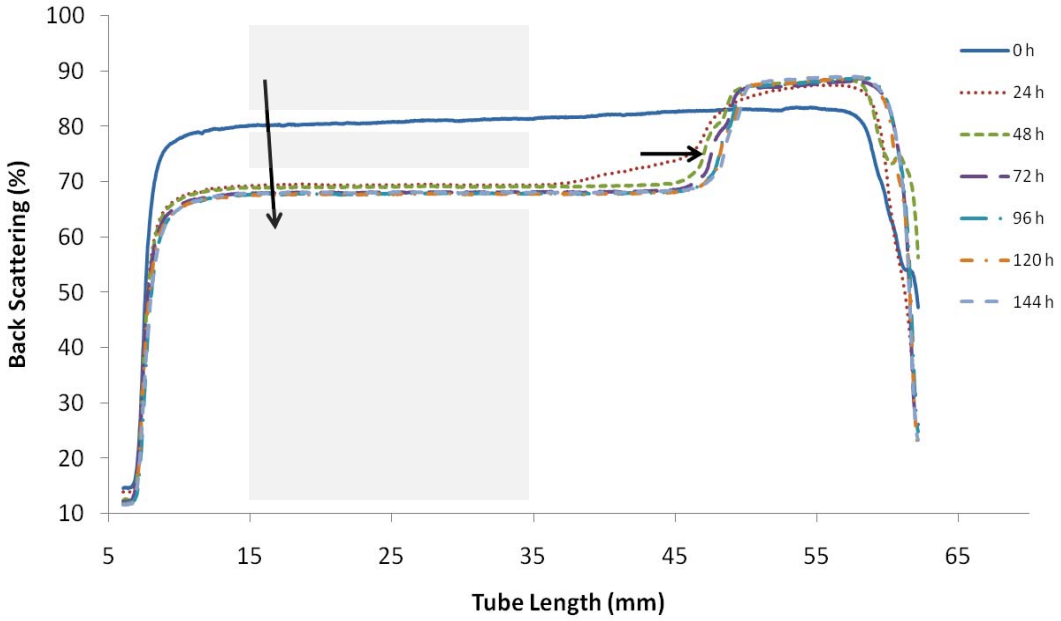

Figure 4.7. Phase separation was detected in the unheated 8.5% w/w NaCas-stabilized 10% w/w oil-in-water model emulsion. Changes in *BS* profile as a function of sample height with storage time at room temperature. The shaded areas indicate the extent of creaming (top), the extent of the change in *BS* (%) between 0 and 144 h (middle) and *BS* (%) after 144 h of storage (bottom).

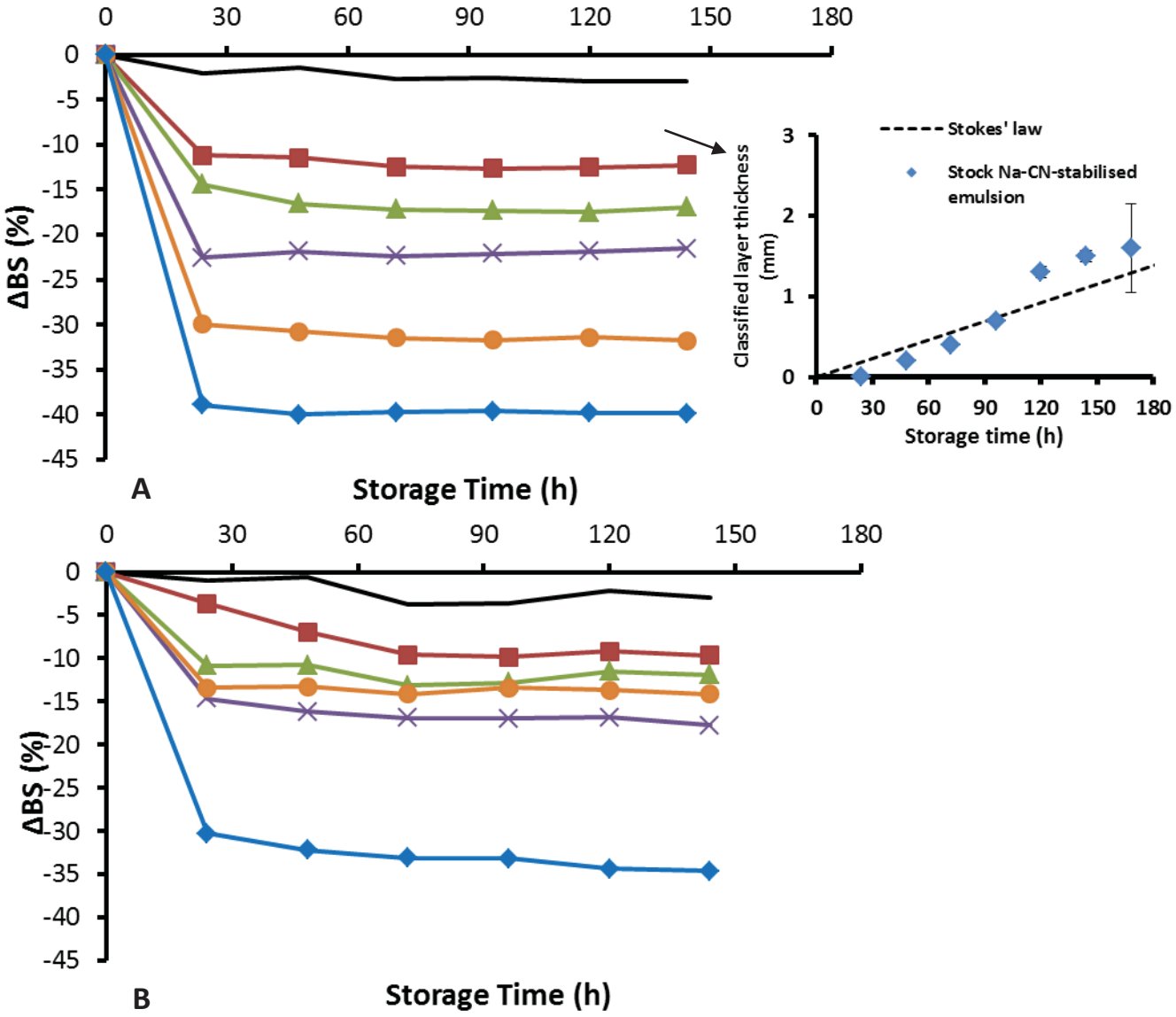

Figure 4.8. Variation in backscattering expressed as ΔBS (%) of (A) unheated model emulsions. In set: variation in classified layer thickness of stock NaCas emulsion during storage. (B) heated (120 °C, 10 min) model emulsions (8.5% w/w protein, 10% w/w oil) monitored over 144 h at 20 °C for: a stock NaCas emulsion (solid line); a sole NaCas-stabilized emulsion (■); an NaCas-stabilized emulsion containing MPC I (▲); an NaCas-stabilized emulsion containing MPC II (×); a Tween-20-stabilized emulsion containing MPC I (●); a Tween-20-stabilized emulsion containing MPC II (♦).

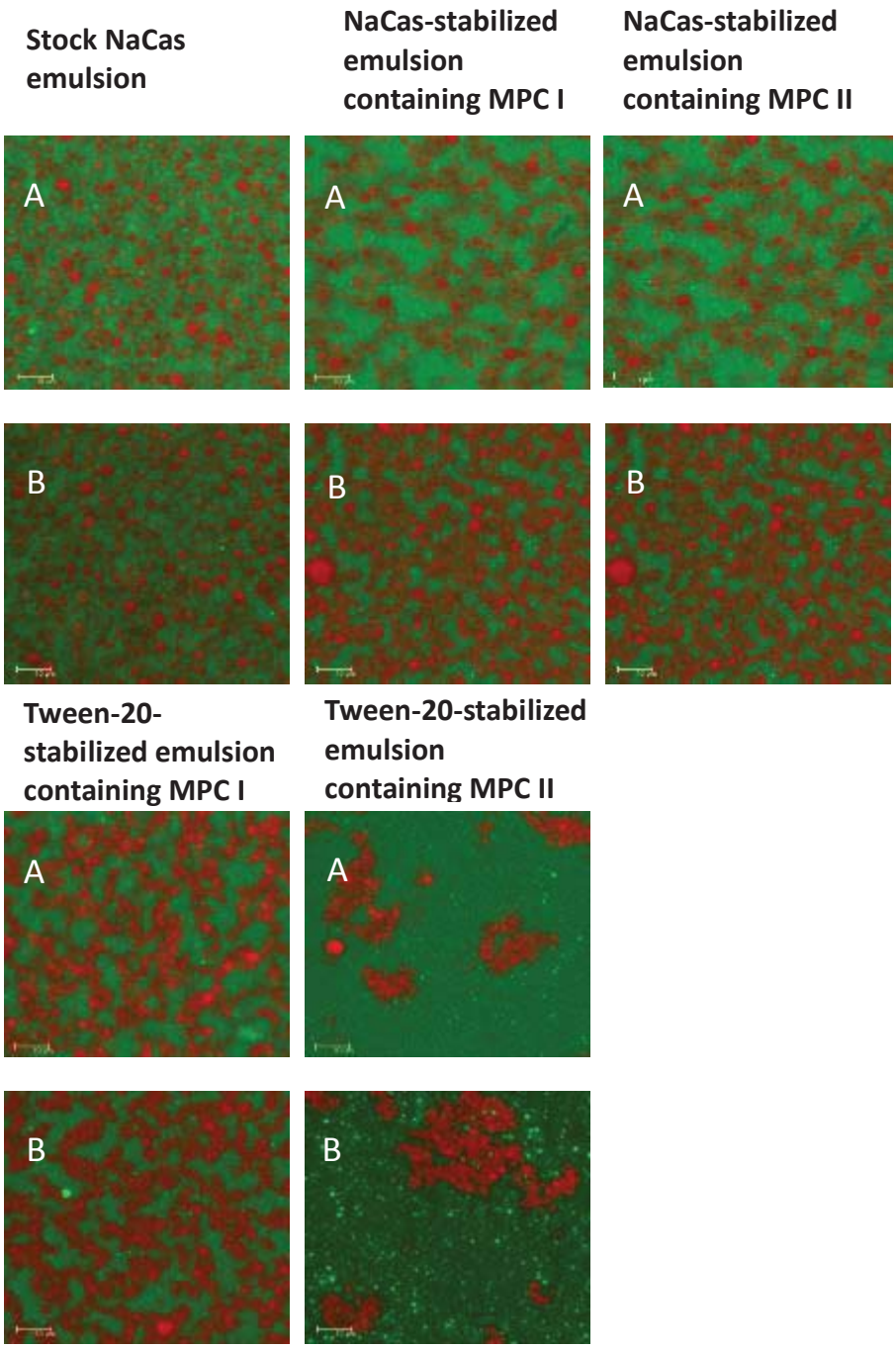

Figure 4.9. Confocal micrographs of model emulsions (8.5% w/w protein, 10% w/w oil): (A) unheated emulsion; (B) heated (120 °C, 10 min) emulsion. Scale bar is 10 μm.

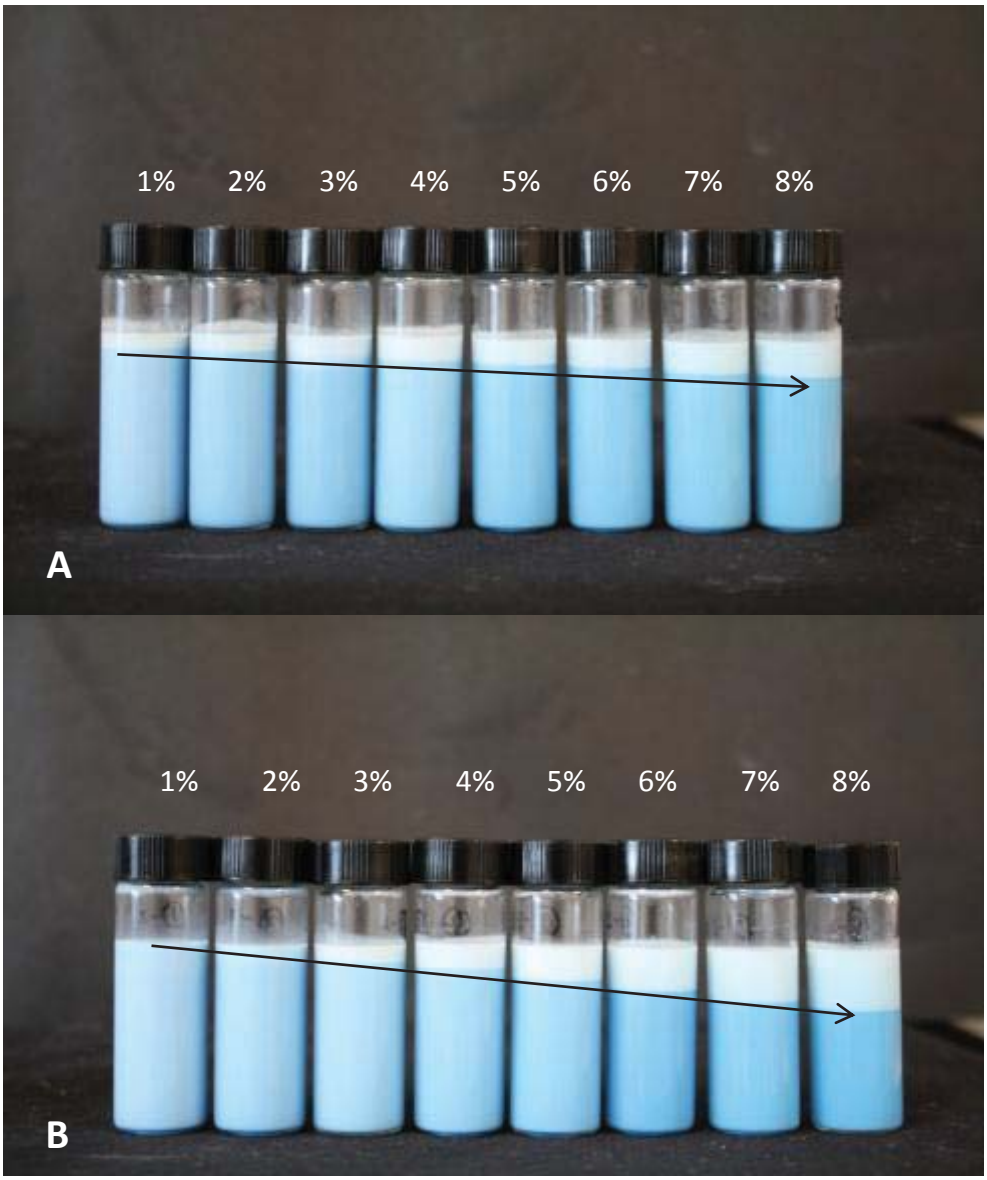

Figure 4.10. Creaming (after 24 h of storage at 20 °C) of unheated 10% w/w oil-in-water model emulsions containing 1~8% w/w MPC I as the continuous phase and (A) NaCas-stabilized oil droplets and (B) Tween-20-stabilized oil droplets. The arrow shows the creaming trend.

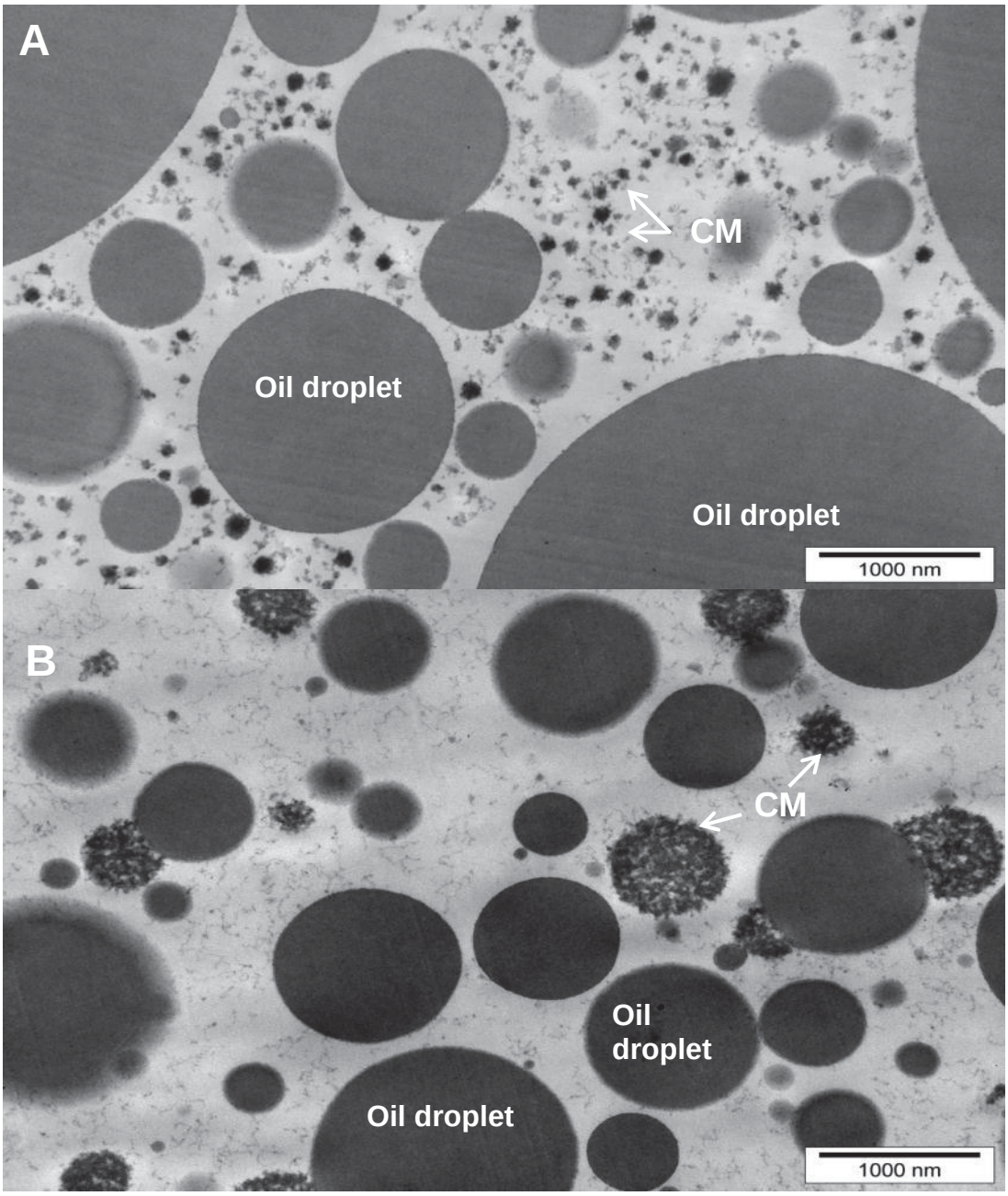

Figure 4.11. TEM images of selected heated (120 °C, 10 min) model emulsions: (A) NaCas-stabilized emulsion containing MPC I; (B) NaCas-stabilized emulsion containing MPC II. The images were captured at 19 000× magnification. Scale bar is 1000 nm. CM = casein micelle.

The shear flow rheology of the unheated model emulsions is shown in Figure 4.12A. The sole NaCas-stabilized emulsion exhibited slight shear-thinning behavior, with *n* values close to 1. The NaCas-stabilized and Tween-20-stabilized emulsions containing MPC I and MPC II also showed shear-thinning flow behavior. The apparent viscosity decreased with increasing shear rate, which was confirmed by the *n* values (< 1). The flocculated droplets would occupy a greater effective volume than the sum of the individual droplet volumes; this would increase the effective volume fraction of the dispersed phase and therefore increase the low shear viscosity. At high shear rates, the breakup of flocculated droplets/clusters and the release of the trapped continuous phase resulted in Newtonian behavior. Figure 4.12B shows the marked effect of droplet−droplet interactions in NaCas-stabilized emulsions in the presence of casein micelles at high volume fractions of oil. The droplet network induced by depletion flocculation contributes to the low shear viscosities (Dickinson & Golding, 1997a). The heat treatment of the depletion-flocculated emulsions had little effect on the viscosity and flow behavior ($p > 0.05$).

The rate of depletion flocculation was expected to be low in an emulsion containing casein micelles, because the casein micelles in MPC and SMP have greater molecular size than NaCas or denatured whey proteins that will induce depletion energy (Euston & Hirst, 1999; Rosa, Sala, van Vliet and van de Welde, 2006). Although the optimum caseinate size to cause depletion flocculation in a casein-stabilized emulsion has been determined to be around 20 nm in radius (Radford & Dickinson, 2004), depletion flocculation could occur in a dairy emulsion system containing NaCas-stabilized emulsion droplets and casein micelles (ten Grotenhuis et al., 2003). The polydispersity of the casein particles needs to be considered because casein nano-particles/micelles have mean diameters in the range 40~200 nm (Lucey et al., 2000). Depletion flocculation occurs if the ratio between the sizes of colloidal and non-adsorbed particles exceeds 3:1 (ten Grotenhuis et al., 2003). In the presence of a high concentration of non-adsorbed casein micelles, it is possibly that oil droplets with diameters in the range 0.4−2 μm are depleted by casein micelles, with increasing contribution predominantly provided by casein micellar fractions at the lower end of the casein particle size range. It is possible that the particle size distribution of MPC II is more polydisperse than MPC I because it

contains more non-micellar casein particles (Ye, 2011); hence more droplets were depleted (Figure 4.8).

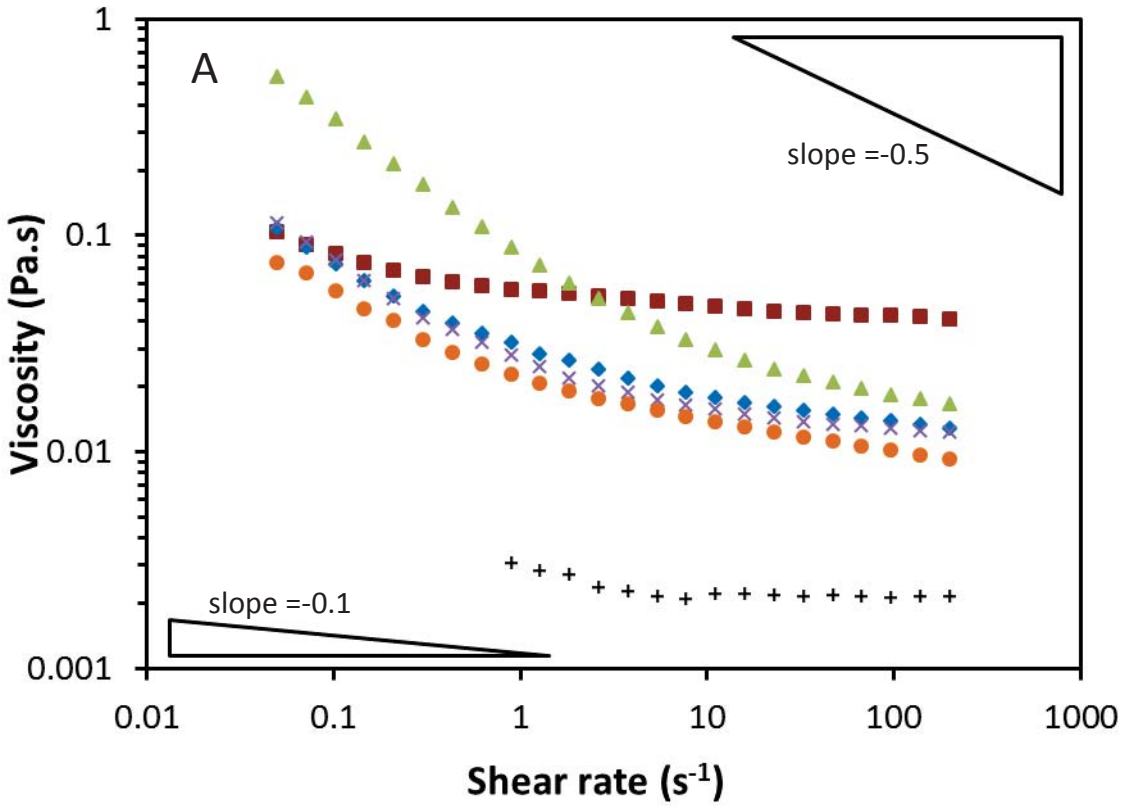

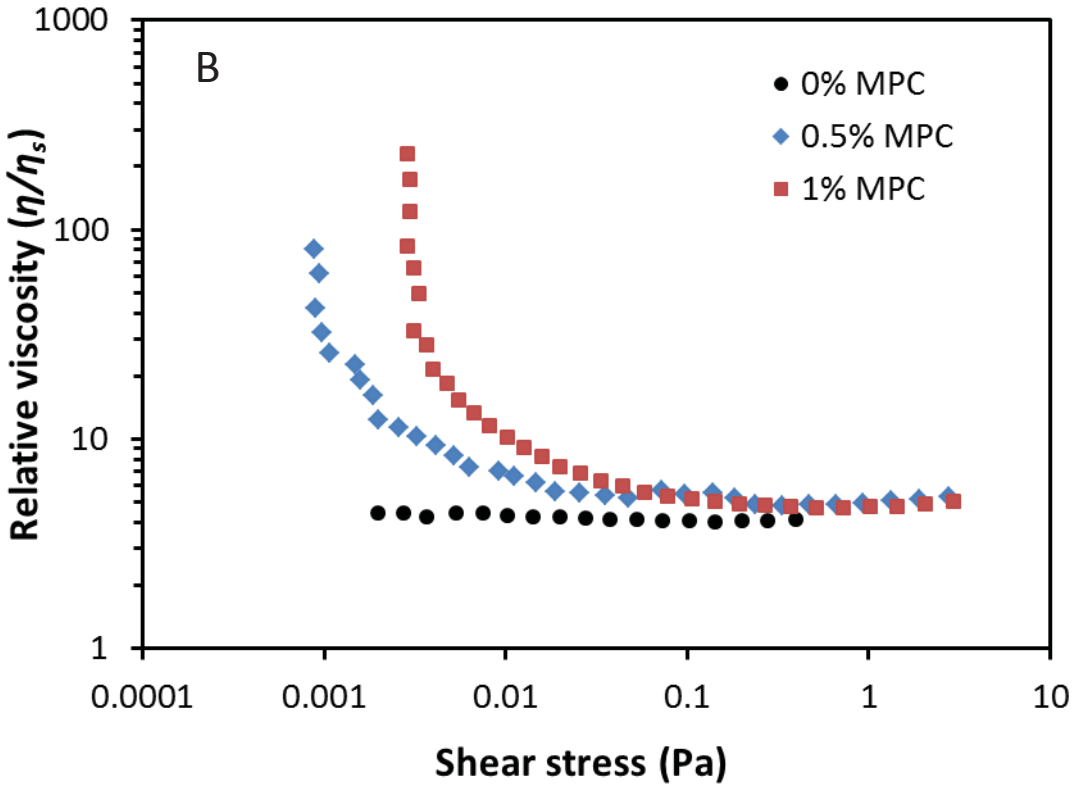

Figure 4.12. (A) Flow behavior of unheated model emulsions: stock NaCas emulsion (+); sole NaCas-stabilized emulsion (■); NaCas-stabilized emulsion containing MPC I (▲); NaCas-stabilized emulsion containing MPC II (×); Tween-20-stabilized emulsion containing MPC I (●); Tween-20-stabilized emulsion containing MPC II (♦). (B) Relative viscosity of unheated NaCas-stabilized 30% w/w oil-in-water emulsions containing 0, 0.5 and 1% w/w MPC as a function of shear stress at 20 °C. η_s is the corresponding viscosity of MPC in the continuous phase.

4.4.4 Model emulsions with no apparent interactions between adsorbed proteins, cross-interactions between adsorbed and non-adsorbed proteins and between non-adsorbed proteins

In our hypothesis, an emulsion with good heat stability and creaming stability can be expected when there are no droplet−droplet and droplet−protein interactions. Oil droplets

formed with MPC I can be treated as "large casein micelles" since the adsorbed materials consist of mainly casein micelles and whey proteins with a similar ratio as those find in milk (Sharma & Singh, 1999; Singh, Fox, & Cuddigan, 1993; Singh, Sharma, Taylor, & Creamer, 1996). When MPC is used in excess (protein-to-oil ratio > 0.3) to stabilize the oil droplets, bridging flocculation is absence, although depletion flocculation is observed at high protein levels (Euston & Hirst, 1999). It was also expected the emulsion containing WPH as the continuous phase protein to be heat stable because the hydrolyzed whey proteins would not be expected to undergo covalent cross-linking at a 18.1% hydrolysis degree (Euston et al., 2001b; Singh et al., 1998). The emulsion containing WPH will not undergo depletion flocculation because hydrolyzed whey proteins are too small to induce depletion interaction (Euston et al., 2001b).

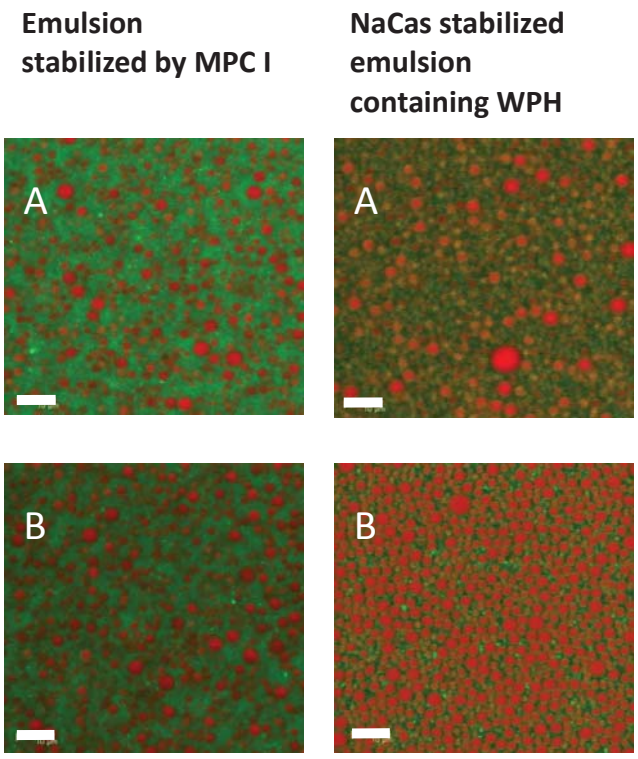

Figure 4.13. Confocal micrographs of model emulsions (8.5% w/w protein, 10% w/w oil): (A) unheated emulsion; (B) heated (120 °C, 10 min) emulsion. Scale bar is 10 μm.

Both the emulsion purely stabilized by MPC I and the NaCas-stabilized emulsion containing WPH showed no sign of heat-induced coagulation and no rapid phase separation during ageing. This result was confirmed by the droplet size distribution,

confocal microscopy, shear-flow rheology and Turbiscan data. There was no change in the primary particle size distribution between unheated and heated emulsions. The confocal micrographs showed that the emulsion droplets were fairly homogeneously distributed in the MPC-I-stabilized emulsion and the NaCas-stabilized emulsion containing WPH with few flocculated droplets appearing (Figure 4.13).

Interestingly, some very small droplets formed clusters in the heated NaCas-stabilized emulsion containing WPH, as shown by TEM (Figure 4.14). However, the droplet clusters appeared to have little effect on the creaming stability, as studied by Turbiscan. The nature of those small droplet aggregates and their corresponding colloidal interactions will be studied in more details in future studies. The flow curves of the heated emulsions showed Newtonian-like flow behavior, which was similar to their corresponding continuous phase viscosity.

It was also expected the Tween-20-stabilized emulsion containing WPH to be heat stable since it was found that Tween-20-stabilized emulsion droplets without addition of any protein were not affected by heat treatment from preliminary experiments described in materials and methods section. Unexpectedly, the emulsion was susceptible to heat-induced droplet coalescence, which eventually led to complete oil and serum separation (Figure. 4.15). An 8% WPH solution was heated at 120 ºC for 10 min to verify the heat-induced physicochemical changes at oil/water interface and in the continuous phase. It was found that the WPH solution was heat stable and it remained transparent (slight yellowish) after heating. Tween-20-stabilized emulsions containing various amount of WPH (1−8% w/w) were also prepared. During heating at 120 ºC, it was found that as little as 1% w/w WPH was able to cause the droplet coalescence. Additionally, this heat-induced droplet coalescence appeared to be temperature dependent. Little change in particle size of Tween-20-stabilized emulsions containing 1% w/w WPH was found after heating for 10 min at 80−110 ºC. However, large droplets were formed as a function of time when the emulsion was heated at 120 ºC, as shown in Figure 4.15. When heated beyond the critical heating time (~2−3 min), the droplet size increased significantly. Prior research has similarly indicated that rapid coalescence and oiling-off in lecithin-stabilized emulsions containing WPH (degree of hydrolysis = 27%); the destabilization was

attributed to interfacial competition between surface active peptides of the WPH and the lecithin (Scherze & Muschiolik, 2001). A recent study also reported destabilization in a Tween-20-stabilized coconut milk oil-in-water emulsion on heating (120 °C, 1 h). The destabilization was attributed to the prolonged autoclave treatment and lack of electrostatic repulsive force of Tween-20-stabilized emulsion droplets (Tangsuphoom & Coupland, 2009). In our case, it is possible that some small protein peptides, formed upon heating, with very high surface hydrophobicity could displace a small molecule surfactant such as Tween 20 from the oil surface; however, they are not able to stabilize the emulsion droplets, probably because of poor steric and electrostatic repulsion governed by low molecular weight peptides, and cause destabilization of the emulsion during heat treatment. This might correspond to the collapse of the Tween-20-stabilized emulsion. A further study of the interaction between WPH and various types of surfactant at the oil−water interface is in progress to probe the destabilization mechanism.

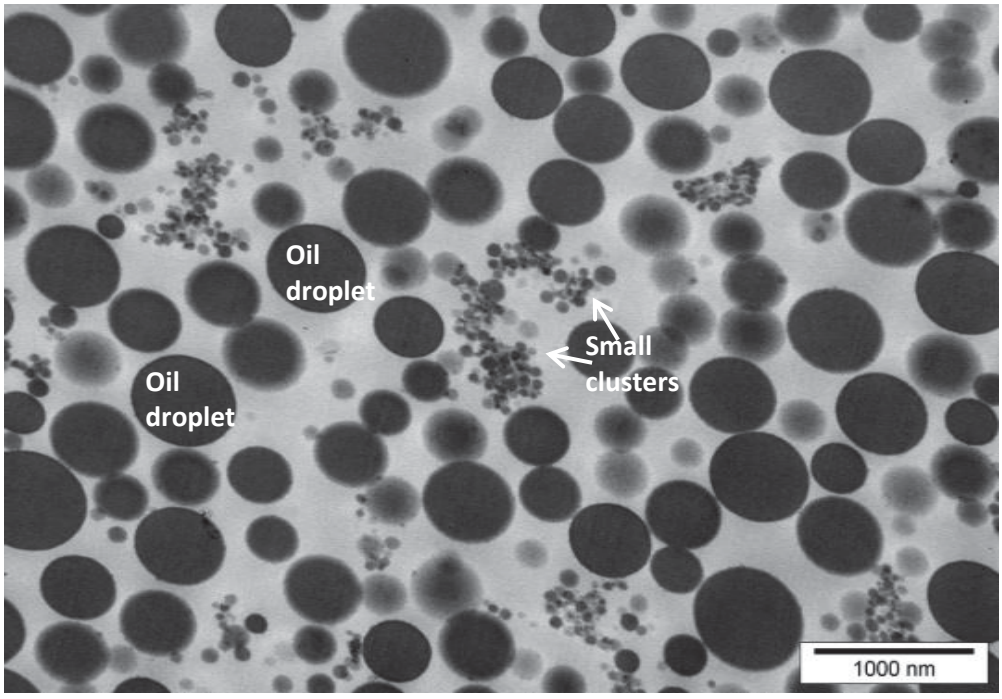

Figure 4.14. TEM image of heated (120 °C, 10 min) NaCas-stabilized emulsion containing WPH. The image was captured at 19 000× magnification. Scale bar is 1000 nm.

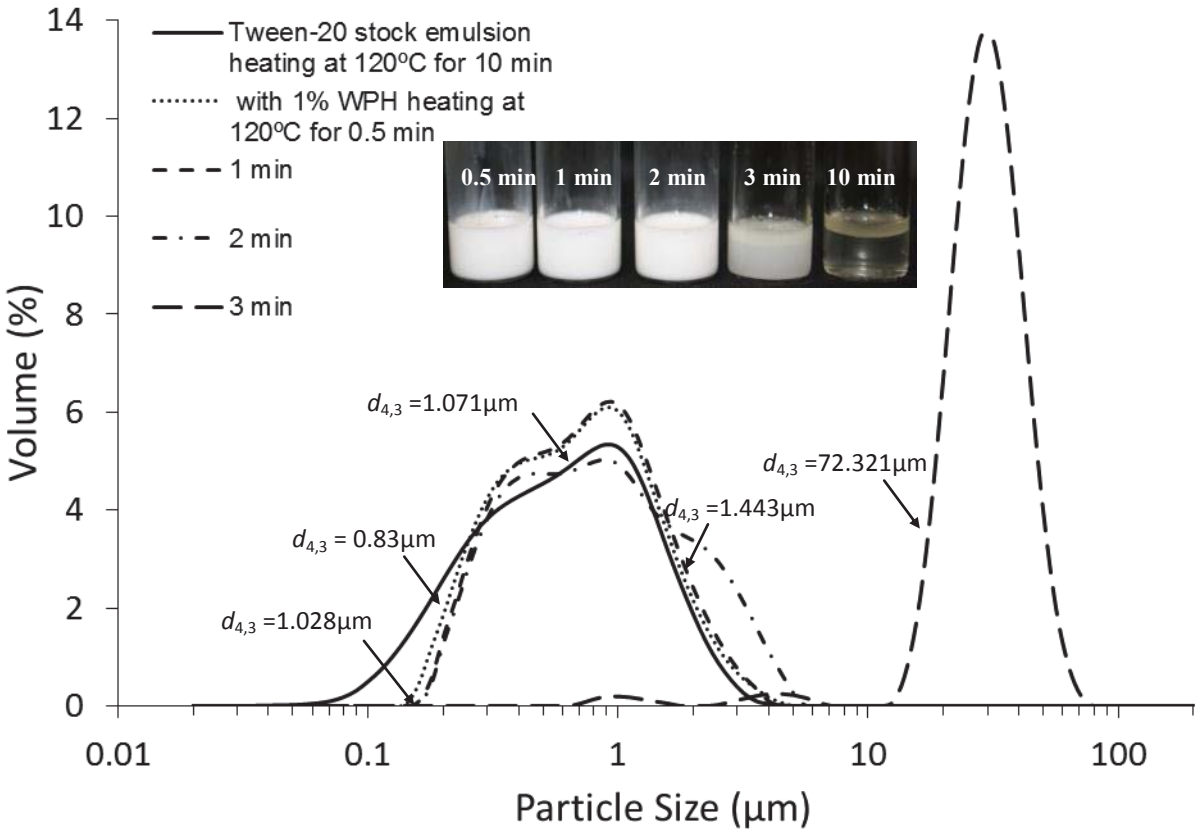

Figure 4.15. Particle size distributions of Tween-20-stabilized emulsions (10% w/w oil); control heated at 120 ºC for 10 min (solid line); containing 1% w/w WPH heated at 120 ºC for 0.5 min (dotted line), for 1 min (dashed line), for 2 min (dashed dotted line) and for 3 min (long dashed line).

4.5 Conclusions

The stability and destabilization of milk-protein-stabilized emulsion systems as a consequence of heating is influenced by both the emulsifier type and the type of protein in the continuous phase. Emulsions stabilized by whey proteins or containing high whey protein concentrations have been shown to be highly sensitive to calcium content and heat treatment. The concentration of non-adsorbed whey proteins is the main destabilization factor in emulsion stabilized by whey proteins, NaCas or Tween-20.

However, the incorporation of NaCas-stabilized droplets in the gel network through heat-exchanged interfacial interaction and the loss of steric repulsion. Replacement of continuous phase whey protein with whey protein hydrolyzates improves the heat stability of emulsions with one notable exception, in which surface active fractions from hydrolyzed whey are seen to promote droplet coalescence at high heating temperatures of Tween 20-stabilized emulsions.

Model emulsions containing relatively high concentrations of micellar or non-micellar caseins were found to be heat stable. However, rapid enhanced creaming, which is associated with the depletion flocculation, arises in these emulsions. The non-adsorbed protein concentration, the aggregation state and the polydispersity of protein determine the extent of depletion flocculation.

The model systems describe the potential droplet−droplet, protein−protein and droplet−protein interactions using food-grade surfactants and commercial milk protein ingredients. It has been successful to produce a stability map based on the potential states of interaction between continuous and dispersed phases. Some systems (i.e. emulsions stabilized by MPC or NaCas) could be formulated to give predictive effects through a hypothetical consideration of the mechanisms of interaction, while some formulations gave unexpected findings (i.e. Tween-20-stabilized emulsion containing WPH), based on mechanisms which were not anticipated as part of the initial hypothesis. To further probe the stabilization mechanism(s) in a weakly attracted dairy colloid system, we used NaCas as model protein and the correlation between the depletion interaction potential and the continuous phase viscosity of NaCas emulsions was studied in the next chapter.

Chapter 5: Physical Stability, Microstructure and Rheological Properties of Sodium-Caseinate-Stabilized Oil-in-Water Emulsions as Influenced by Depletion Interaction Potential and Viscosity [2]

5.1 Abstract

The emulsion stability, microstructure and rheological properties of 30% w/w oil-in-water emulsions (droplet diameter ~0.73 μm, pH 6.8) containing NaCas, 1−10% w/w, were investigated. Small deformation rheology showed that the development of a transient droplet network depended markedly on the caseinate concentration. We distinguished between the contributions of the continuous phase viscosity and the depletion force by investigating the influence of maltodextrin and xanthan gum on the stability and rheology of 1.5% w/w caseinate emulsions. Surprisingly, the droplet−droplet interactions were weakened by the addition of maltodextrin, and the stabilizing mechanism differed from the prediction that high zero shear viscosity is the dominant factor in preventing phase separation of a depletion-flocculated emulsion. Furthermore, the droplet rearrangements within the flocculated network played an important role in the stability of the emulsions, and were influenced by both the strength of the depletion force and the continuous phase viscosity at high caseinate concentrations. Both depletion force and continuous phase viscosity increased with the addition of xanthan gum. The phase separation kinetics and the restabilization mechanisms were analogous to those of the caseinate system.

---

[2] Part of the content presented in this chapter has been published as an original paper in *Food Hydrocolloids* (2014) *36*, 245−255.

Part of the content was also presented as a graduate student oral presentation at ADSA-JAM Meeting, Indianapolis, USA, 8−12 July 2013 and as a graduate student oral presentation at NZIFST, Hastings, NZ, 2−4 July 2013.

5.2 Introduction

The properties of both the dispersed phase and the continuous phase determine the heat stability, creaming stability and rheological properties of milk-protein-stabilized oil-in-water emulsions. Some of the earlier reports suggested that NaCas- and Tween-20-stabilized oil droplets could form heat stable dispersed phase and casein micelles, non-micellar caseins (caseinate nano-particles) or casein micelle/non-micellar casein mixture could form the heat stable continuous phase. However, the mixture of both phases had high tendency to separate into two phases (a cream phase and a serum phase) in a few days due to depletion effect. It has been reported that the droplet-casein size ratio, concentration of non-adsorbed caseins, volume fraction of dispersed phase, aggregation state of caseins, the presence of Ca^{2+} and pH affect the final emulsion stability of casein micelle/caseinate based oil-in-water emulsions (Huck-Iriart et al., 2011; ten Grotenhuis et al., 2003; Ye, 2011). However, the effect of the continuous phase viscosity on the stability of caseinate-stabilized emulsions at higher protein concentration has received little attention.

Immediate depletion flocculation can be prevented by either the apparent yield stress or increasing continuous phase viscosity upon the use of polysaccharide or protein solutions (Blijdenstein, van Vliet, van der Linden, & van Aken, 2003; Sun, Gunasekaran, & Richards, 2007; van Gruijthuijsen, Herle, Tuinier, Schurtenberger, & Stradner, 2012; Vélez et al., 2003; Ye, Hemar, & Singh, 2004). In addition, at sufficiently high concentrations of oil, the depletion attraction will create a droplet network that spans the entire sample volume. This formation of droplet network can result in partial restabilization of the emulsion and will depend on the depletion interaction potential (Aben et al., 2012; Dickinson, 1999b; Lu et al., 2008; Moschakis et al., 2005; Tanaka et al., 2005; Teece et al., 2011).

It is hypothesized that the inhibition of phase separation at elevated caseinate concentrations may be due to either a retardation of the dynamics of droplet−droplet interactions (because of viscous effects) or an increase in the depletion interaction potential, thereby strengthening the droplet network. To test the validity of the hypothesis, two highly contrasting viscosity-controlling hydrocolloids, xanthan gum and maltodextrin, were used to assess the stabilizing mechanisms. 30% w/w oil volume was used in this study to create a sufficiently strong droplet network and to

yield a better rheological response with regards to structural rearrangement and phase separation of emulsions. The interrelations among the extent of depletion flocculation, the formation of the droplet network and its structural rearrangement and the caseinate concentration are discussed. The study will provide better understanding of the change in depletion interaction potential and viscosity on a general phase separation of attractive dairy colloids.

5.3 Materials and methods

5.3.1 Materials

Sodium caseinate 180 (NaCas) was obtained from Fonterra Co-operative Group Ltd, Auckland, New Zealand. Maltodextrin (Glucidex® 2, DE=2) was purchased from Roquette, France. Xanthan gum (Grindsted® Xanthan 80) was obtained from DuPont-Danisco (Vernon, TX, USA).

5.3.2 Preparation of model emsulsions

The model emulsions were prepared following the procedure described in Figure 5.1. Each model emulsion was prepared at least in triplicate. Throughout the color version of this chapter, blue is used to represent caseinate emulsions without polysaccharides, red indicates the addition of xanthan and green indicates the addition of maltodextrin. In this article the concentration of polysaccharide and caseinate is reported on a mass basis relative to the entire emulsion and not the concentration in the aqueous phase. Aqueous concentrations are given in Table 5.1.

5.3.3 Particle size determination

The particle size measurements were carried out using procedures described in Chapter 3, Section 3.2.3. The average droplet size was expressed as the surface-weighted diameter $d_{3,2}$ (μm) and the volume-weighted mean diameter $d_{4,3}$ (μm).

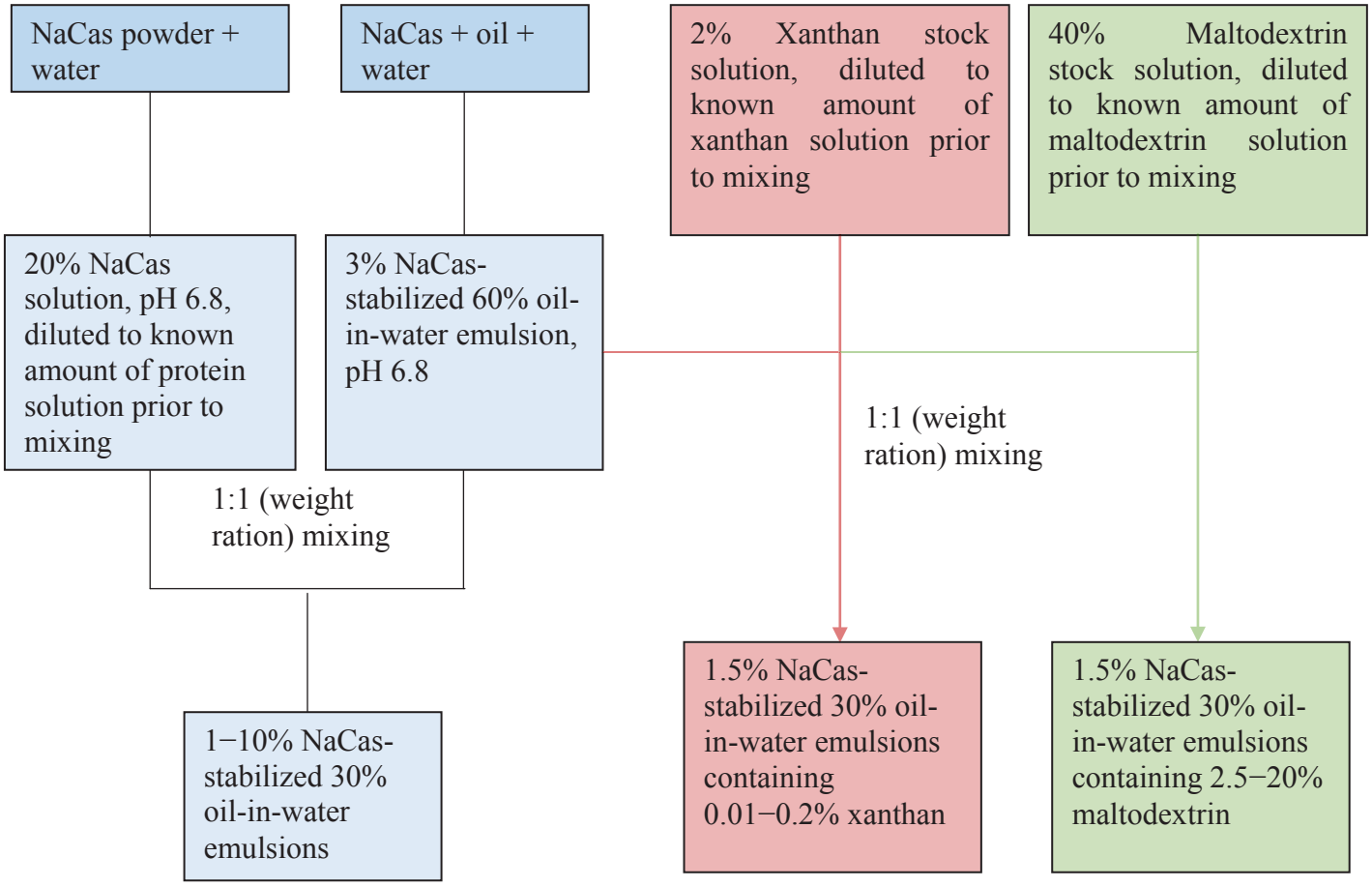

Figure 5.1. Flow chart of the preparation of model emulsions (1−10% w/w protein, 0.025−0.2% w/w xanthan and 2.5−20% w/w maltodextrin respectively).

Table 5.1. The concentration of non-adsorbed caseinate particles, xanthan and maltodextrin as a function of the overall fraction of biopolymer in the entire emulsion.

NaCas				
Overall mass fraction C (g/kg)	Continuous phase concentration[1] $C_{non\text{-}ad}$ (g/kg)	Osmotic pressure (Pa)	Depletion interaction potential $(W_{4,3})/k_BT$	Continuous phase viscosity (mPa s)
15	10.8	10.13	−1.0	1.68
20	17.9	17.06	−1.7	2.09
30	32.2	31.46	−3.2	3.25
40	46.5	46.57	−4.8	5.06
50	60.8	62.4	−6.4	7.87
60	75.1	78.94	−8.1	12.25
80	103.6	114.18	−11.7	60.86
100	132.2	152.27	−15.6	816.84
Xanthan				
0.01	0.014	0.01	-0.1	1.8
0.025	0.036	0.41	-5.6	3.1
0.05	0.071	1.21	-16.4	13.2
0.075	0.107	2.41	-32.5	76.7
0.1	0.143	4.01	-53.9	476.4
0.2	0.286	14.3	-192.2	2420
Maltodextrin				
2.5	3.57	N/A	N/A	1.69
5	7.14	N/A	N/A	3.17
7.5	10.71	N/A	N/A	5.95
10	14.29	N/A	N/A	11.18
15	21.43	N/A	N/A	39.36
20	28.57	N/A	N/A	138.59

[1] The equation for calculating the continuous phase protein concentration is: [the total protein – the adsorbed protein (in this case, the amount of adsorbed caseins is about 0.75 g/100g)]/(1-$\emptyset$). $\emptyset$ is 0.3 in the final emulsion. The calculation of aqueous phase xanthan and maltodextrin content is: the total biopolymer/(1-$\emptyset$).

5.3.4 Calculation and application of depletion interaction potential

It was calculated using a radius-dependent depletion interaction combined with a Boltzmann partition as an ad-hoc estimate for the fraction of freely dispersed droplets with respect to the droplets in the collapsing network. Using data from a histogram of droplet diameters, it was calculated a surface area of 7.45 m^2/mL oil. Then, using an adsorption density of 3 mg/m^2, the concentration of caseinate remaining in the continuous phase, $C_{non\text{-}ad}$, was established (Table 5.1). The depletion interaction, W, was calculated from $W = -\Pi V$, where Π is the osmotic pressure and V is the volume of overlapping depleted layers; this attractive force is conventionally negative. The osmotic pressure was calculated from an expansion of van't Hoff's law, which accounts for the size of the caseinate nano-particle (Radford & Dickinson, 2004).

$$\Pi = \frac{C_{non-ad} N_A}{M} k_B T \left(1 + \frac{C_{non-ad}}{\rho}\right) \tag{5.1}$$

N_A is the Avogadro number, M is the molecular weight of the caseinate nano-particle (300 kDa, was calculated for caseinate particle with a radius of 10 nm according to $M = \frac{4}{3}\pi r^3 \rho N_a$). ρ is the density of caseinate (~ 1050 kg/m^3) and k_BT is the thermal energy (Radford & Dickinson, 2004).

For simplicity, it is convenient to refer to the maximum depletion interaction rather than the dependence of the depletion interaction on droplet separation. The depletion effect between two droplets is greatest when the two droplet surfaces touch. The excluded volume V can be calculated from two sphere caps. Each sphere cap has a radius of $a + r_{cn}$ and a height of r_{cn}, where a is the radius of the droplet ($d_{4,3}/2$ = 617 nm) and r_{cn} = 10 nm is the radius of a caseinate nano-particle. The volume of each sphere cap is

$$V_{sc}(a) = \frac{\pi r_{cn}^2}{3}(3a + 2r_{cn}) = \pi a r_{cn}^2 \left(1 + \frac{2r_{cn}}{3a}\right) \tag{5.2}$$

When $a > 15 r_{cn}$, the approximation $V_{sc}(a) \approx \pi a r_{cn}^2$ has less than 5% error. An average sphere cap volume $\overline{V_{SC}}$ = 5.6 × 10^{-23} m^3 can then be established from the droplet distribution, and the

radius-dependent depletion interaction potential can be calculated without assuming symmetrical interactions via

$$W(a) = -\Pi \times (V_{SC}(a) + \overline{V_{SC}}) \quad (5.3)$$

Similarly, the average depletion interaction potential is $\bar{W} = -2\Pi\overline{V_{SC}}$. It should be noted that these averages are number averages and it was found $\bar{W}$ not much use in this case; rather, it was the distribution of interaction potentials that best described the data. To facilitate the reader's comparisons with previously published data, we present $W_{4,3}$, the interaction potential calculated from $d_{4,3}$ or Sauter diameter which in this article $W_{4,3} = 3.3\bar{W}$

An approximation of the droplet network population can now be established by applying a Boltzmann partition function to the histogram of droplet diameters via:

$$\frac{n_i}{N_i - n_i} = e^{-W(a_i)/k_B T} \quad (5.4)$$

Here, N is the total number of droplets in the sample, n is the number of freely dispersed droplets and $N - n$ is the number of droplets in the collapsing network. The subscript i indicates droplets from a particular histogram bin. When Eq. (5.4) is applied to the entire histogram of droplet diameters, the volumes of freely dispersed and network droplets can be established for a given osmotic pressure. In the case of a collapsing network forming a cream layer and a clarified layer, the osmotic pressure can be fitted to experimental data for the clarified layer and assuming that the concentration of freely dispersed droplets in the cream layer is the same as that in the clarified layer. This approach is only approximate and does not consider complexities such as: multiple droplet interactions, possible re-equilibration of freely dispersed and network droplet populations as the network collapses, or how the collapsing layer may expel freely dispersed droplets with the necessary back flow of serum.

5.3.5 Emulsion stability

The model emulsions were stored at ambient temperature and measured periodically for up to 6 months using a vertical scan analyser Turbiscan Classic MA 2000 (Formulaction, Toulouse,

France). The phase separation data of 7 days was used to plot the creaming curve. Details of the techniques are described in Chapter 3, Section 3.2.7.

5.3.6 Rheology measurements

Shear-rate-dependent flow curves of NaCas, xanthan and maltodextrin were obtained by first pre-shearing at 500 s^{-1} to eliminate any shear history and subsequently decreasing the shear rate from 500 s^{-1} to lower shear rates and then increasing it again to 500 s^{-1}. The flow curves showed no hysteresis within experimental error (5%). The zero shear viscosity of the effective biopolymer concentration in the continuous phase has been shown in Table 5. 1.

The shear flow properties of the model emulsions were determined with a stress-controlled rheometer (Physica MCR301, Anton Paar, Graz, Austria) at 20 °C using a cup and bob geometry. Samples were pre-sheared at shear rate of 300 s^{-1} for 1 min to erase any shear history. Flow curves at shear rates from 0.001 to 500 s^{-1} were obtained. To ensure that wall slip was not significant, a few NaCas concentrations using vane and cone−plate geometries were investigated; the results obtained were essentially the same as those obtained using the cup and bob geometry, suggesting that wall slip was negligible. The dynamic viscoelastic properties of the emulsions were assessed as function of time at 20 °C. Emulsion samples were gently poured into the cup and a layer of mineral oil was applied to prevent water evaporation during the measurement. The emulsions were pre-sheared at 300 s^{-1} for 1 min to disrupt any flocculated or phase-separated regions, and then a constant small strain, 0.5%, which was determined from the linear viscoelastic region, was applied at 1 Hz for 6 h. After 6 h or 12 h, shear flow rheological measurements at shear rates from 0.001 to 500 s^{-1} were made.

In order to elucidate droplet interaction, it is referred to the viscosity of the emulsion relative to the viscosity of the continuous phase viscosity unless otherwise stated. The actual rate at a network evolves should depend on the time for a droplet to escape from the attractive zone of neighboring particles. The concept of the escape time was put forward by Kramers (1940), and while an analytical solution to the escape time for triangle shaped interaction−distance profiles suggest a following form could apply (Buscall et al., 2009):

$$\tau \approx \tau_0 / e^{\frac{-zW}{kT}} = \frac{\pi \eta_s a \Delta^2}{k_B t} e^{\frac{zW}{k_B T}} \quad (5.5)$$

Here τ is a time that should scale with the escape time, τ_0 is the time required for droplets to freely diffuse across (Δ^2), where Δ is the range of the depletion potential. The triangle over the power of 2 in the bracket (Δ^2) reminds the reader that displacement by diffusion is always the mean-squared displacement. *W* is the interaction potential, *z* is the number of neighbours the particle is attached to and k_BT is the thermal energy. Examining equation 5.5 reveals that judicious choice of three key parameters, range of the interaction, viscosity of the continuous phase and interaction potential can change a shelf life of a product from hours to months.

5.3.7 Microstructure of model emulsions

Details of the confocal scanning laser microscope characterization techniques have been described in Chapter 3, Section 3.2.8.

5.3.8 Statistical analysis

All experiments were carried out at least in triplicate using freshly prepared samples and the results are reported as the mean and standard deviation of these measurements.

5.4 Results and discussion

5.4.1 Influence of non-adsorbing biopolymers on the phase separation of caseinate-stabilized emulsions

The size distribution of the stock NaCas-stabilized emulsion droplets is shown in Figure 5.2. The volume/surface weighted average diameter ($d_{3,2}$) of the droplets was 0.73 ± 0.02 μm and the volume-weighted mean diameter ($d_{4,3}$) was 1.23 ± 0.11 μm. NaCas emulsions showed gravimetric separation with a clear meniscus within a few days of preparation (Figure 5.3). The

experimental creaming profile of the 1% w/w NaCas emulsion was well fitted with Stokes' law using a droplet radius of > 1 μm for a concentrated emulsion. At NaCas concentrations between 1.5 and 4% w/w, the height of the meniscus rose faster than the rate predicted from the gravitational force of isolated droplets using Stokes' law. The significant changes in creaming behavior from low to moderate NaCas concentration were in good agreement with previous findings (Dickinson & Golding, 1997b; Huck-Iriart et al., 2011). Fitting the effective droplet radii to these creaming rates resulted in radii of ~18 μm in the 1.5% w/w samples and ~3.5 μm in the 4% w/w sample. Alternatively, using the Boltzmann distribution and the range of droplet sizes, see section 5.3.4, we estimate the volume fraction of droplets bound to another varies from 13.1% at 1% w/w caseinate to 27.7% at 4% w/w caseinate. These volume fractions are sufficient to create a sample spanning network, however, bonds in the network are expected to be short lived. A significant volume of droplets with long lived network junctions only occurs above concentrations of 4% w/w caseinate based on a $4k_BT$ threshold. The life time of network bonds is naturally further compounded by the continuous phase viscosity as droplets are less able to diffuse out of the attractive well.

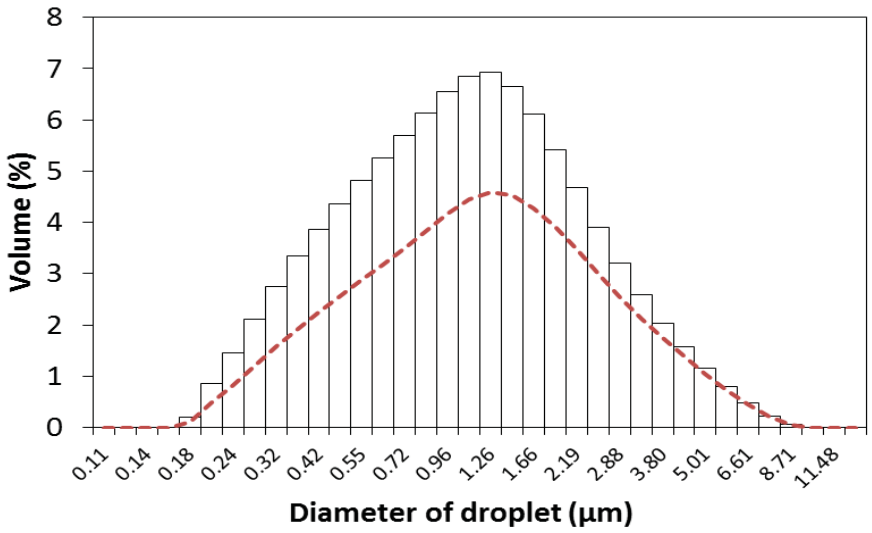

Figure 5.2. Droplet size distribution in a 60% w/w oil-in-water stock emulsion stabilized by 3% w/w NaCas. Dashed line represents the droplet population in a network based on the calculation from Section 5.3.4 using an osmotic pressure of 5 Pa, note below diameters of 0.5 μm only ≈ 50% of the droplets participate in the network above diameters of 3 μm ≈ 80% of the droplets participate in the network.

Further increasing the NaCas concentration reduced the creaming rate, with 6% w/w NaCas emulsions showing no visible creaming after a week. Nonetheless, 5 and 6% w/w NaCas emulsions eventually phase separated, with a visible clarified layer at the bottom of the tube, after 2 months of storage. At concentrations above 8% w/w NaCas, there was no sign of phase separation even after 6 months. A "delay" in the first appearance of a clarified layer has been observed in collapsing attractive networks (Buscall, 1994; Manley, Skotheim, Mahadevan, & Weitz, 2005; Moschakis et al., 2005; Parker et al., 1995; Vélez et al., 2003). The meniscus height profile during ageing has a form that can be fitted by a model reported for collapsing particle networks, in which phase separation is driven by compaction of the network and its subsequent viscous compression is due to gravity rather than the rapid creaming of larger aggregates (Manley et al., 2005).

Emulsions containing less than 4% w/w NaCas showed some residual turbidity below the rising meniscus. This turbidity was particularly noticeable in emulsions containing 1.5 and 2% w/w NaCas and the classified layer became more translucent as increased NaCas concentration. The fitting of calculated volume fraction of unbound droplets to experimental determined value by Turbiscan is shown in Figure 5.4. At these low concentrations, our calculations predict the volume fraction of freely dispersed is 11% and 8% which compares well with the experimental values of 4.7 and 1.2% given that three or more body interactions have been ignored. It is important to note that the delay time for the phase separation of a weakly flocculated emulsion not only depends on the depletion force but also depends on the volume fraction of bound droplets. Higher volume fraction of flocculated droplets associates with the droplet network, the longer it takes the emulsion to separate into two discrete layers (Parker et al., 1995). Better fits could be achieved by adjusting the size and non-spherical conformations of the casein nano-particles, which we have not attempted.

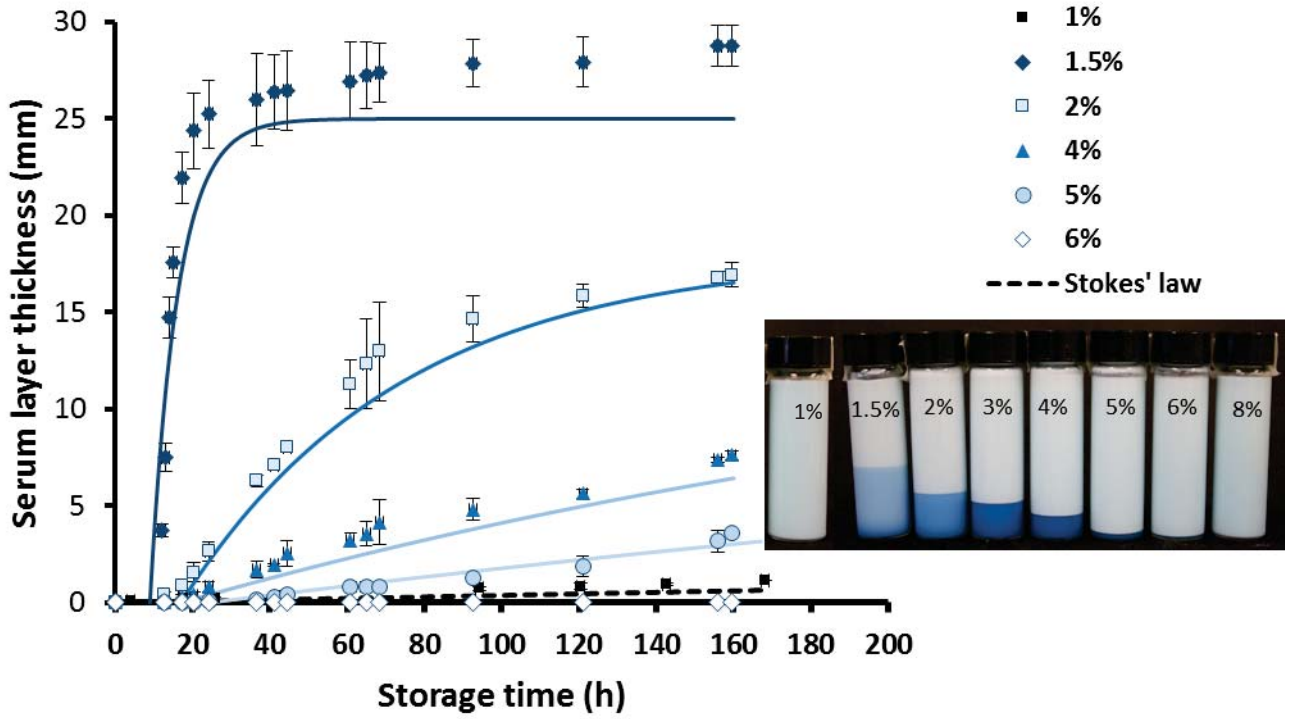

Figure 5.3. Variation in clarified layer thickness as monitored by Turbiscan over 160 h at 20 °C for 30% w/w oil-in-water emulsions containing 1, 1.5, 2, 4, 5 and 6% w/w NaCas. The black dashed line shows a prediction for the creaming of concentrated emulsions with non-interacting droplets (McClements, 2005). Inset: visual appearance of NaCas-stabilized oil-in-water emulsions after storage for 2 weeks at 20 °C. A small amount of 2% methylene blue stain was added for better observation of the movement of the creaming boundaries. The solid lines are theoretical fits, as predicted by Manley, Skotheim, Mahadevan, & Weitz (2005), giving $h_0 - h(t) = \Delta h(1 - e^{\frac{-t}{\tau}})$, where h_0 is the initial height, Δh is the total change in height and τ is the time scale for the collapse.

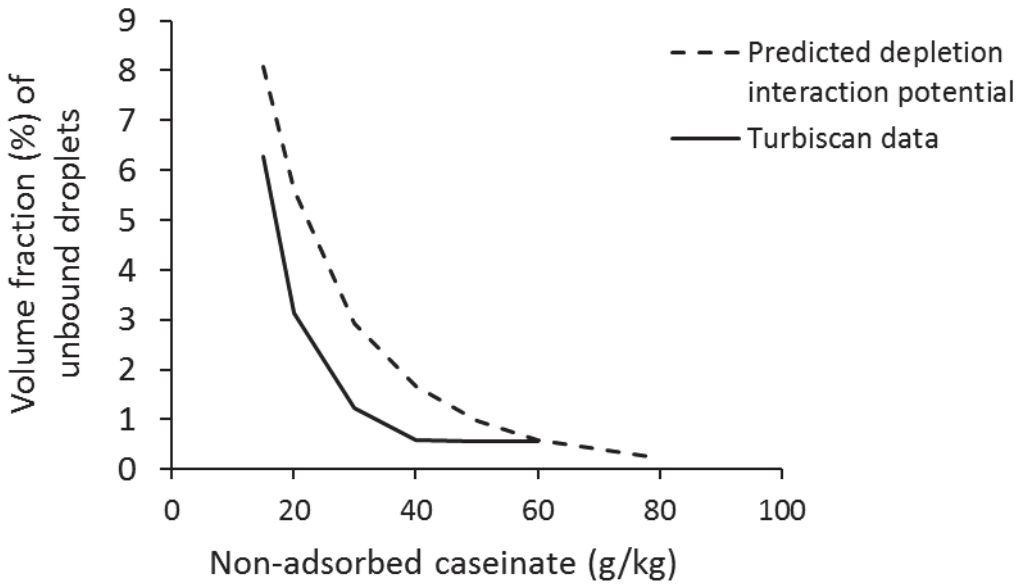

Figure 5.4. The predicted and experimental determined depletion interaction potential of NaCas-stabilized 30% w/w oil-in-water emulsions as a function of protein concentration.

The addition of xanthan to 1.5% w/w NaCas-stabilized emulsions resulted in a distinct meniscus that rose with time and could be observed in samples with 0.01−0.075% w/w xanthan (Figure 5.5). Although the theoretical fit for the creaming profiles of NaCas emulsions with xanthan was different (data not shown), the creaming behavior was qualitatively similar to that observed in NaCas emulsions without added polysaccharides. At concentrations above 0.075% w/w xanthan, phase separation was delayed beyond 2 weeks and even the 1.5% w/w NaCas-stabilized emulsion containing 0.1% w/w xanthan creamed and a clear clarified layer could be seen after 2 months (data not shown). At a concentration of 0.2% w/w xanthan, no visible separation was observed over 6 months. The addition of 0.025 and 0.05% w/w xanthan resulted in transparent cracks throughout the sample. These cracks were tentatively attributed to a local fracture driven by phase separation; round holes would be expected when phase separation deforms the network without fracture.

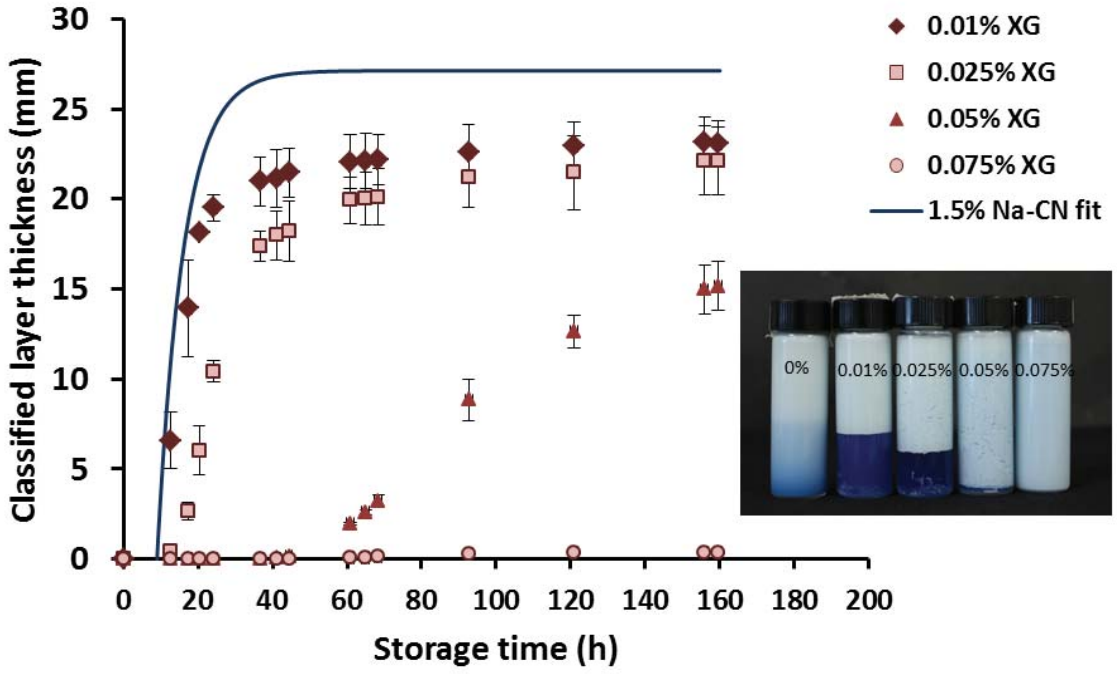

Figure 5.5. Variation in clarified layer thickness as determined by Turbiscan over 160 h at 20 °C for 1.5% w/w NaCas-stabilized 30% w/w oil-in-water emulsions containing 0.01, 0.025, 0.05 and 0.075% w/w xanthan. Inset: visual appearance of 1.5% NaCas-stabilized emulsions containing xanthan after 2 weeks of storage at 20 °C.

The addition of maltodextrin to the 1.5% w/w NaCas-stabilized emulsions inhibited gravity separation (Figure 5.6). Rapid creaming still occurred at low concentrations of maltodextrin because a rising meniscus was visible; however, compared with the emulsion without maltodextrin, a larger fraction of the emulsion remained stable against creaming. The creaming behavior of NaCas emulsions containing 2.5−7.5% w/w maltodextrin showed good correlation with the calculated creaming rate of the control emulsion (1.5% w/w NaCas). The difference in turbidity between the cream layer and the clarified layer in emulsions with maltodextrin became less noticeable as the maltodextrin concentration increased. The collapsing network phenomenon was not obvious at high concentrations of maltodextrin (10% w/w). The effect of maltodextrin was further investigated using a Turbiscan to monitor the variation in backscattered light with sample height (%) (Figure 5.7). The volume fraction of the freely dispersed droplets was estimated from a calibration curve of the backscattered intensity of the stock emulsion with various dilutions. Volume fraction were of dispersed droplets were 4.3, 7.9, 9.5, 10.3, and 10.7%

for 0, 2.5, 5, 7.5, and 10% w/w maltodextrin respectively. Fitting an osmotic pressure to these values using a 10 nm sphere cap results in a $W_{4,3}$ between ~ 3 k_BT and ~ 1 k_BT which seems too large for the phenomena observed, likely values would be a factor of 3 times smaller. Nonetheless, the predicted trends are plausible. The droplet diameters measured in the cream layer for the emulsions containing 0, 2.5, 5, 7.5, 10 and 15% w/w maltodextrin were 0.78, 0.85, 0.96, 1.102, 0.75 and 0.69 μm respectively, after 7 days of storage. The increasing diameter with up to 7.5% w/w maltodextrin further suggests increasingly weaker attractions. The increase in diameter is a consequence of the radius dependent attraction with the larger droplets more likely bound in the network, equations (5.2−5.4), see Figure 5.2 as an example. At maltodextrin concentrations of 10% w/w and above, the mean diameter returned to the value measured in the stock emulsion; this finding, together with the lack of a collapsing network, indicated that the attraction was effectively zero.

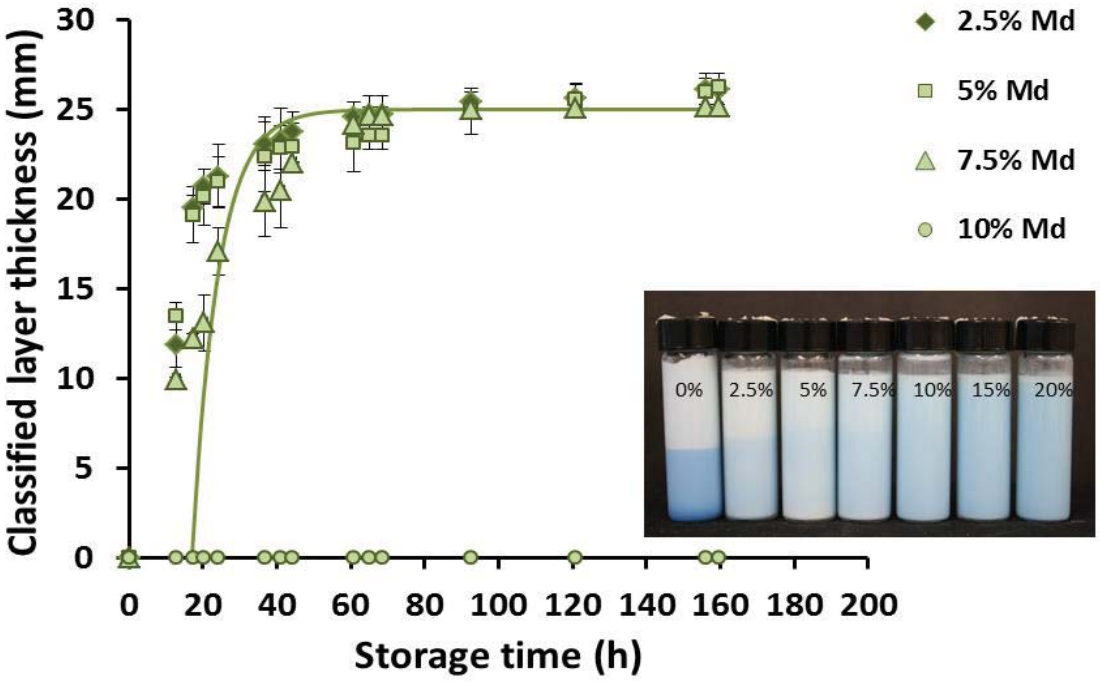

Figure 5.6. Variation in clarified layer thickness as determined by Turbiscan over 160 h at 20 °C for 1.5% w/w NaCas-stabilized 30% w/w oil-in-water emulsions containing 2.5, 5, 7.5 and 10% w/w maltodextrin. Inset: visual appearance of 1.5% NaCas-stabilized emulsions containing maltodextrin after 2 weeks of storage at 20 °C. Arrows indicate the barely visible boundary between the cream phase and the stationary phase.

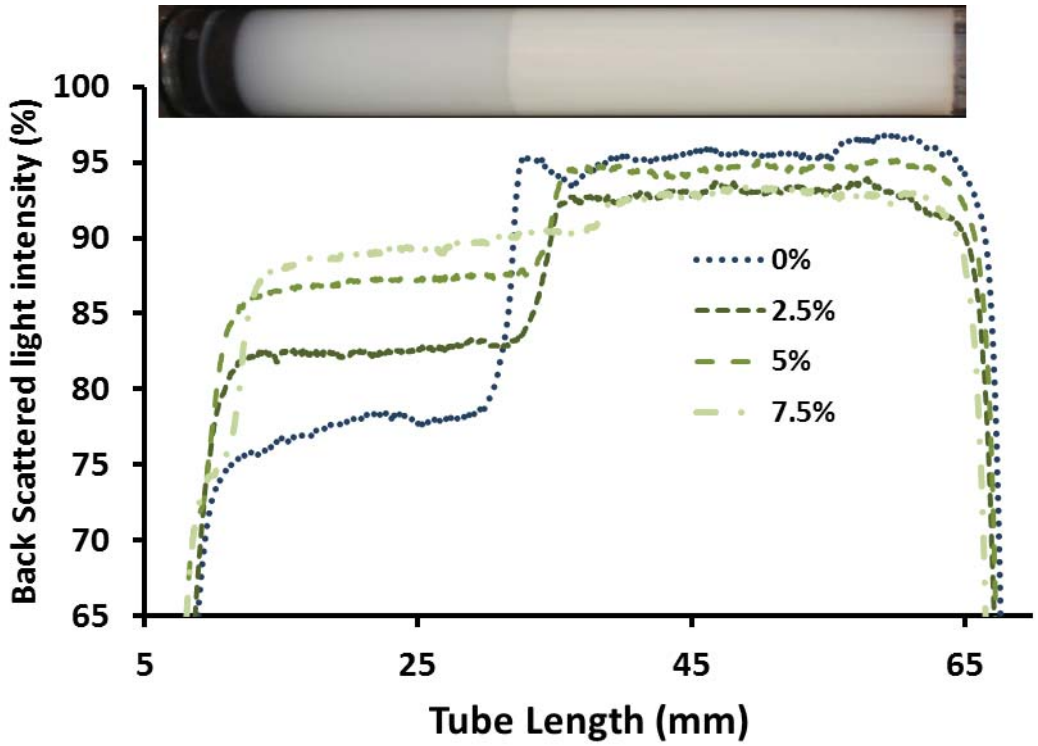

Figure 5.7. Variation in the backscattered light intensity (%) of 1.5% w/w NaCas-stabilized 30% w/w oil-in-water emulsions as a function of maltodextrin concentration after 2 weeks of storage at 20 °C. The visual appearance of the 1.5% NaCas emulsion is added to distinguish the cream layer from the clarified layer.

The decreasing droplet−droplet attraction with increasing maltodextrin concentration has been attributed to the change in caseinate particle size (Huck-Iriart et al., 2011). The depletion energy is sensitive to the polymer-to-droplet size ratio. A small change in caseinate size could have changed the depletion interaction potential moderately (Radford & Dickinson, 2004). Consequently, the change will influence the extent of the associated droplets in the transient droplet network and the creaming behavior. It has been reported that the presence of sucrose dissociates casein particles (Belyakova et al., 2003; Mozersky, Farrell Jr, & Barford, 1991). In our case, it is possible that the casein particles became smaller in the presence of maltodextrin, hence changing the depletion interaction potential.

5.4.2 Influence of non-adsorbing biopolymers on the microstructure of caseinate-stabilized emulsions

The structural evolution of the transient droplet network during ageing of the emulsions as a function of NaCas concentration is shown in Figure 5.8. The 2% and 4% w/w NaCas emulsions are clearly open networks with small voids that compact with time with no sign of the individual 3 to 20 μm aggregates required to fit stokes law to creaming profiles. The 5% w/w NaCas emulsion initially showed a more open network with larger voids than observed at lower concentrations of NaCas. This network also showed compaction during ageing. However, after 6 h, the network formed in the 5% w/w NaCas emulsion seemed to compact at a slower rate and appeared to retain a more open structure than the network formed in the 4% w/w NaCas emulsion. The 6% w/w NaCas emulsion showed some flocculated clusters initially and an open network with large voids became more visible after 4 and 6 h. It was difficult to see structural changes in the 8% w/w NaCas emulsion and there were no signs of the appearance of a macroscopic droplet network during the first 6 h. The large depletion attraction in the 8% w/w NaCas emulsion was expected to lead to substantial dynamically arrested phase separation through a strengthening of the bonds between interconnected clusters; however, the development of a network was compromised by slow viscous rearrangement of these clusters.

Figure 5.9A−5.9D show the microstructures of 1.5% w/w NaCas-stabilized emulsions containing various concentrations of maltodextrin. The emulsion with 5% w/w maltodextrin was qualitatively similar to the analogous emulsion without maltodextrin, but was not similar to NaCas emulsions with high continuous phase viscosity. After 4 h, the 5% w/w maltodextrin emulsion had an open droplet network with voids that eventually compacted. Further increasing the concentration of maltodextrin reduced the network formation as flocculated clusters or network-like structures were not visible after 4 h and even after 1 week. Figure 5.9E−5.9G show the effect of xanthan addition on 1.5% w/w NaCas-stabilized emulsions. It can be seen that the emulsion droplets associated with each other, forming a flocculated microstructure. All NaCas emulsions containing xanthan had a compact structure at 4 h and were clearly different from those containing maltodextrin. The formation of a compact structure was possibly due to the increasing degree of viscoelasticity of the continuous phase provided by the xanthan (Moschakis et al., 2005). The contrast between droplet-rich and xanthan-rich phases on the confocal

micrograph became more distinct after 1 week. It appeared that the excess NaCas in the continuous phase may have formed part of the droplet network, leading to localized depletion effects within the network itself.

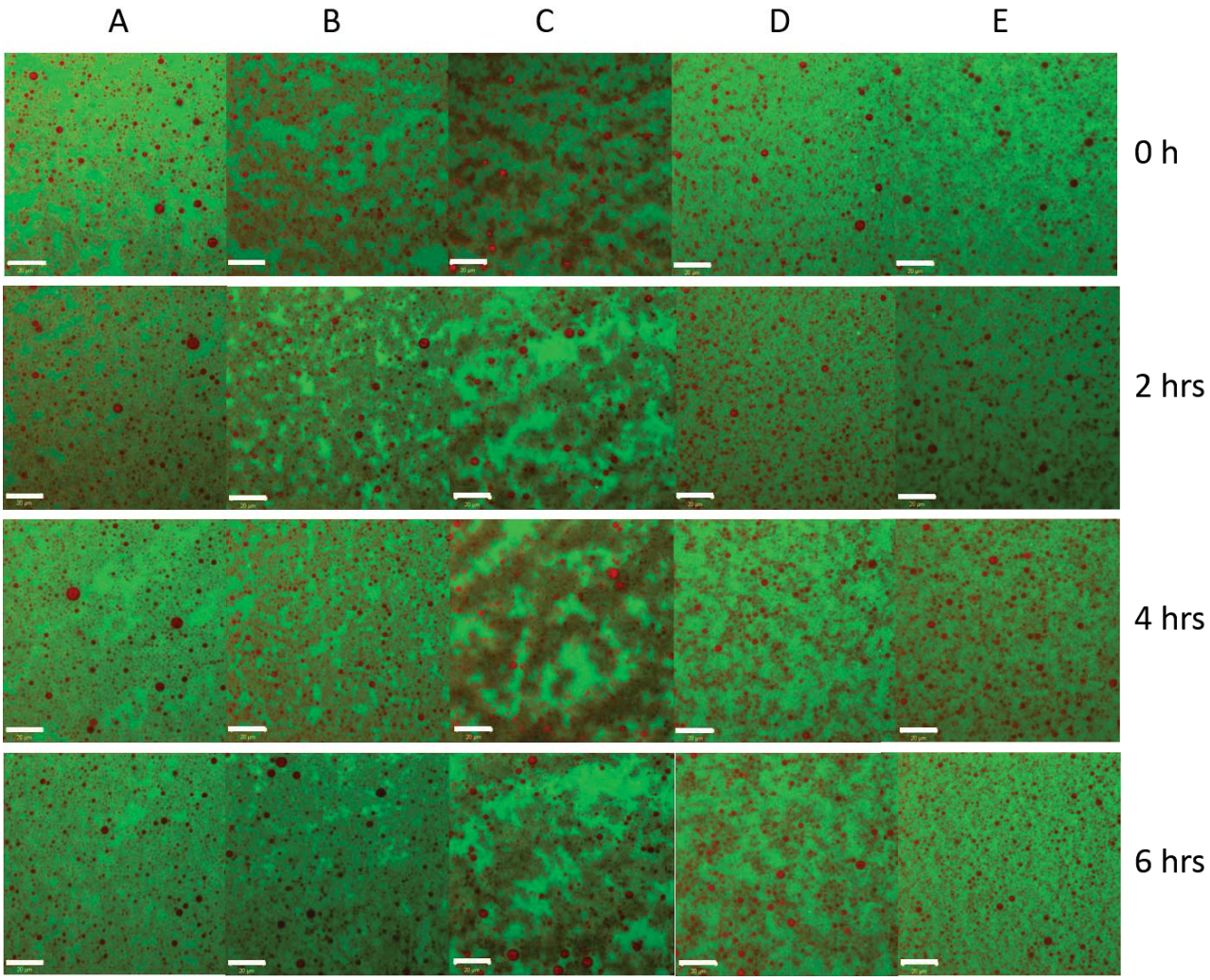

Figure 5.8. Representative confocal micrographs of NaCas-stabilized 30% w/w oil-in-water emulsions containing (A) 2% w/w, (B) 4% w/w, (C) 5% w/w, (D) 6% w/w and (E) 8% w/w NaCas as a function of time. Scale bar = 20 μm.

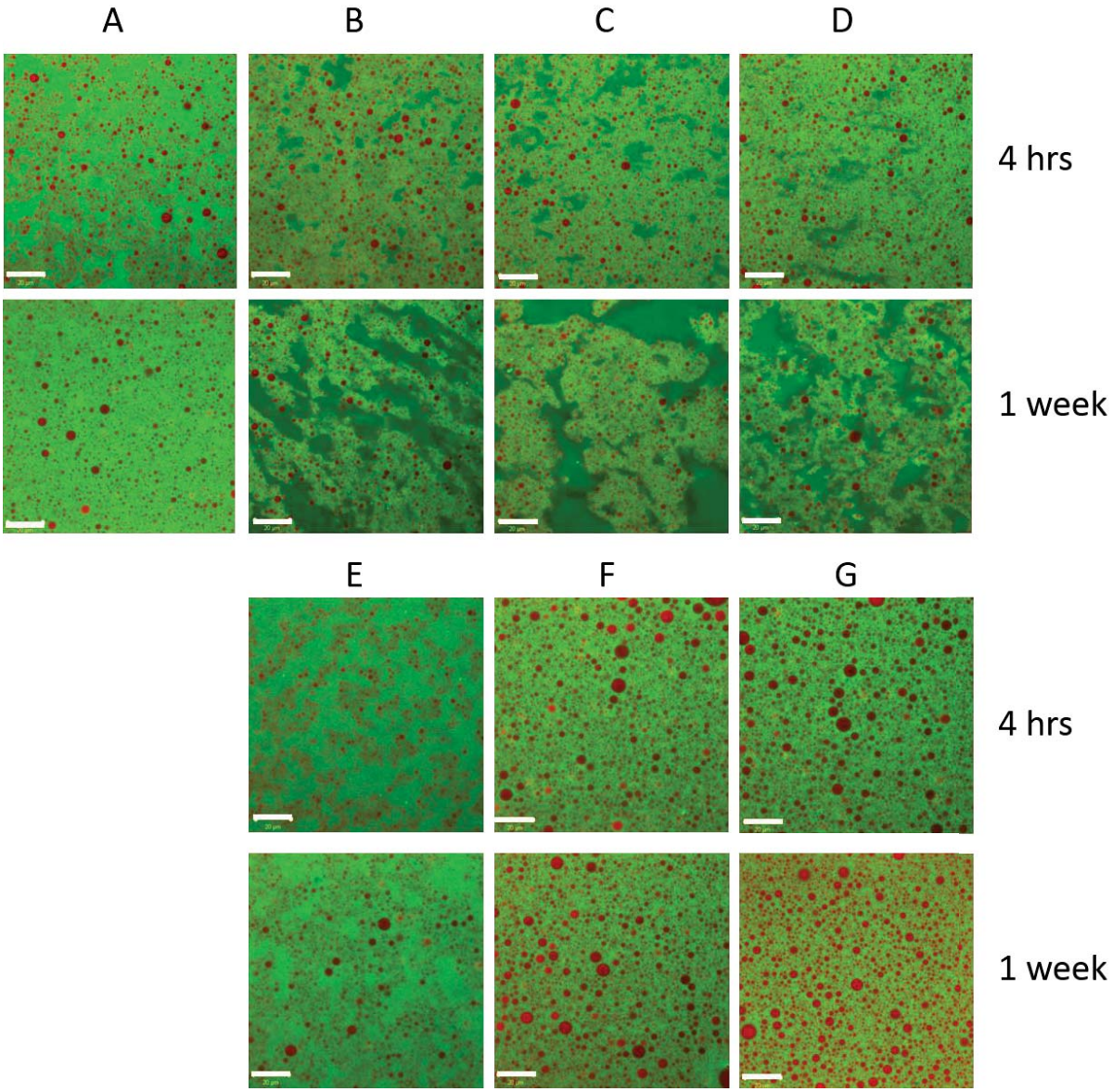

Figure 5.9. Confocal micrographs of 1.5% w/w NaCas stabilized 30% w/w oil-in-water emulsions containing (A) 0% w/w polysaccharide, (B) 5% w/w maltodextrin, (C) 10% w/w maltodextrin, (D) 15% w/w maltodextrin, (E) 0.05% w/w xanthan, (F) 0.075% w/w xanthan and (G) 0.1% w/w xanthan after 4 h and 1 week. Scale bar = 20 μm.

5.4.3 Influence of non-adsorbing biopolymers on the mechanical properties of caseinate-stabilized emulsions

The relative viscosity−shear stress curves for emulsions containing 1−10% w/w NaCas are shown in Figure 5.10. In this section, all viscosity data are reported relative to the continuous phase and differences are interpreted as differences in droplet behavior only. The 1% w/w NaCas emulsion contained a relative low concentration of non-adsorbed protein (< 0.1%) and the viscosity of the emulsion showed a lack of shear rate dependence. The shear flow curve shared the similarity to the prediction from the Krieger-Dougherty equation further suggested that this emulsion was essentially non-interacting. From 1.5 to 4% w/w NaCas, the emulsions showed shear-thinning behavior. At above critical shear stresses, the relative viscosities of the emulsions markedly decreased, indicating the breakdown of a microstructural network. The low shear viscosity increased as the NaCas concentration increased and reflected the stronger and more numerous droplet−droplet interactions in the transient network induced by depletion flocculation (Manoj, Watson, Hibberd, Fillery-Travis, & Robins, 1998). The higher viscosity created by the depletion-induced network has been reported to transiently stabilize the emulsion against phase separation (Aben et al., 2012; Dickinson & Golding, 1997b). The high shear viscosity increased with increasing NaCas concentration, with much larger values than those predicted by the Krieger-Doughty equation, suggesting that some shear-stable aggregates remained and that the emulsion microstructure was still sensitive to the NaCas concentration.

The flow curves for emulsions containing ≥ 5% w/w NaCas exhibited were distinctly different from those for emulsions containing lower NaCas concentrations. Beyond 5% w/w NaCas emulsions exhibited less pronounced shear-thinning behavior as the NaCas concentration increased. Furthermore, these emulsions showed, initially, a smaller low-shear viscosity than their counterparts with lower NaCas concentration. However, the low-shear viscosity of the 6% w/w NaCas emulsion increased more than 6 times to a plateau value after 6 h measured at 20 °C (Figure 5.11), indicating network formation in these emulsions was more gradual. The high-shear viscosities of 5 and 6% w/w NaCas emulsions still increased linearly with NaCas concentration. For 8 and 10% w/w NaCas emulsions, the slight shear-thinning behavior indicated the presence of some flocculated droplets/clusters but again a strong network was not formed. The increased resistance of NaCas emulsions against phase separation at high caseinate

concentrations probably involves the slow aggregate movement in a higher continuous phase viscosity only the emulsion viscosity is so high, creaming rates are particularly small. We estimate from equation (5.6), where the denominator is nine times the viscosity of the emulsion that even droplets as large as ten microns only cream about ten microns per day.

$$V = \frac{2a^2\Delta\rho g}{9\eta_s}\left(1 - \frac{\emptyset}{\emptyset_{max}}\right)^{8\emptyset_{max}} \tag{5.6}$$

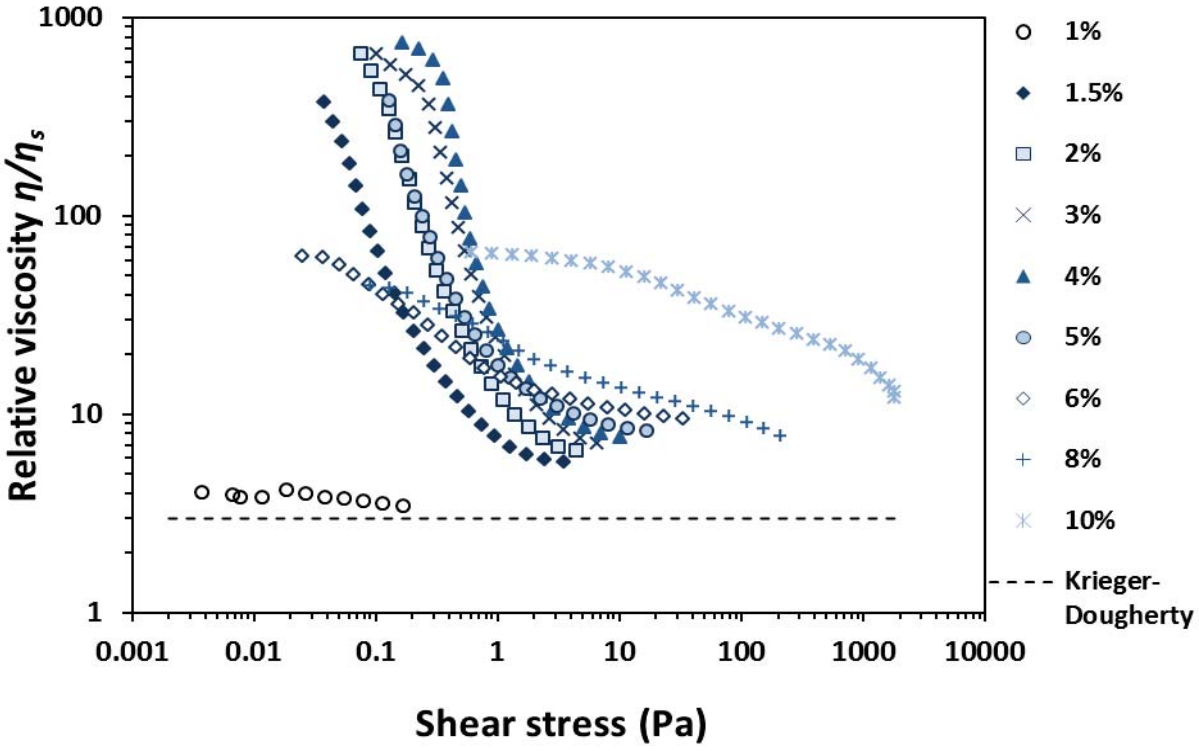

Figure 5.10. Viscosity of 30% w/w oil-in-water emulsions containing increasing concentrations of NaCas relative to their low shear rate viscosities (η_S) in the continuous phase as a function of shear stress at 20 °C. Samples were pre-sheared to eliminate any shear history and there was no equilibration time during measurement. The dashed line is the prediction of the zero shear relative viscosity of a hard sphere dispersion of $\emptyset$ = 0.3, as calculated using the Krieger-Dougherty equation $\frac{\eta}{\eta_o} = (1 - \frac{\emptyset}{\emptyset_m})^{-[\eta]\emptyset_m}$, where $\emptyset$ is the volume concentration of particles and $\emptyset_m$ is the maximum packing (~ 0.71 for a polydisperse system) (Schaertl & Sillescu, 1994).

The relative viscosity−shear stress curves for emulsions containing 0−20% w/w maltodextrin are shown in Figure 5.12. It should be noted that adding maltodextrin to a 1.5% w/w NaCas emulsion resulted in a significant decrease in the low shear viscosity, with almost a tenfold reduction at 5% w/w maltodextrin and a further fourfold decrease at 7.5% w/w maltodextrin. After 6 h, the viscosity of the emulsions containing 5 and 7.5% w/w maltodextrin decreased rather than increased, suggesting that this level of maltodextrin weakened the droplet network rather than delaying network formation. This weakening was further supported by the lower high-shear relative viscosities with increasing maltodextrin concentration. Increasing the maltodextrin concentration above 10% w/w resulted in little change in the low shear behavior but did increase the high shear viscosity.

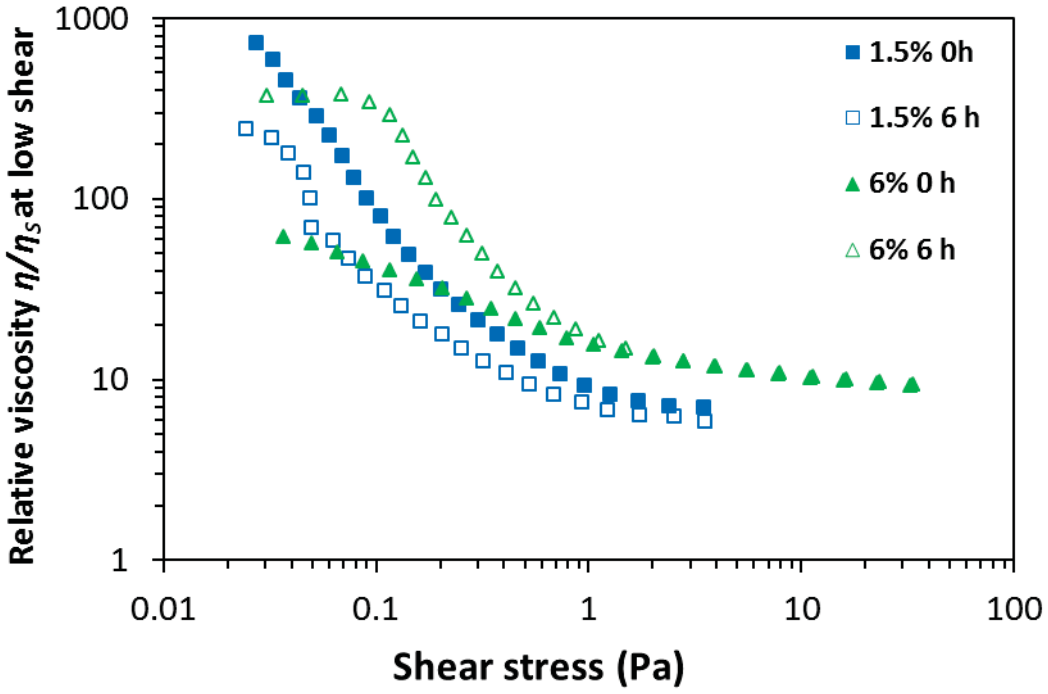

Figure 5.11. Viscosity of 30% w/w oil-in-water emulsions containing 1.5% and 6% w/w NaCas relative to their low shear rate viscosities (η_S) in the continuous phase as a function of shear stress measured at 0 h and 6 h at 20 °C.

To further verify the effect of the continuous phase viscosity on the structural changes during the development of the droplet network, the relative viscosity was monitored over time under a small amplitude oscillatory strain within the linear response region (Figure 5.13A–13C). In each figure,

the time axis is normalized by the continuous phase viscosity to determine whether any differences were merely a result of increased viscosity or were caused by an alternative phenomenon. Figure 5.13A shows the dynamic structural change in emulsions as a function of NaCas concentration. The structural changes were characterized into three distinct time periods. Initially, the increase in relative viscosity reflected the formation of a transient non-equilibrium network structure. Once the relative viscosity reached a peak value, it gradually decreased. This decrease in peak viscosity suggested that the droplet network underwent thermally driven reorganization and restructuring. The transient droplet network became more close packed (Dickinson & Golding, 1997b). Subsequently, the locally trapped continuous phase within the droplet network began to release into the clarified layer. This change led to a decrease in viscosity because the "effective" dispersed phase volume fraction decreased. During this period, the mixture of oil droplets and continuous phase began to form an interface between two different bulk phases (droplet-rich + droplet-poor). Finally, the droplet network collapsed and underwent consolidation of the cream phase once it could not withstand the gravitational stress.

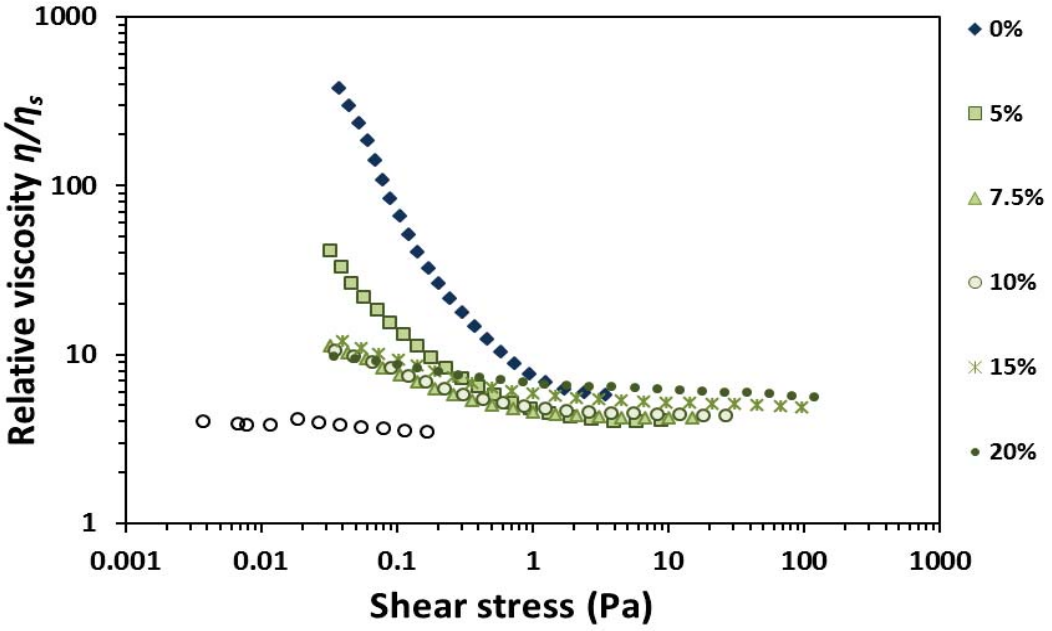

Figure 5.12. Viscosities of 1.5% w/w NaCas-stabilized 30% w/w oil-in-water emulsions containing various concentrations of maltodextrin relative to their low shear viscosities (η_S) in the continuous phase as a function of shear stress at 20 °C. The dash line indicates the viscosity of an emulsion with non-droplet-droplet and/or protein-protein interactions.

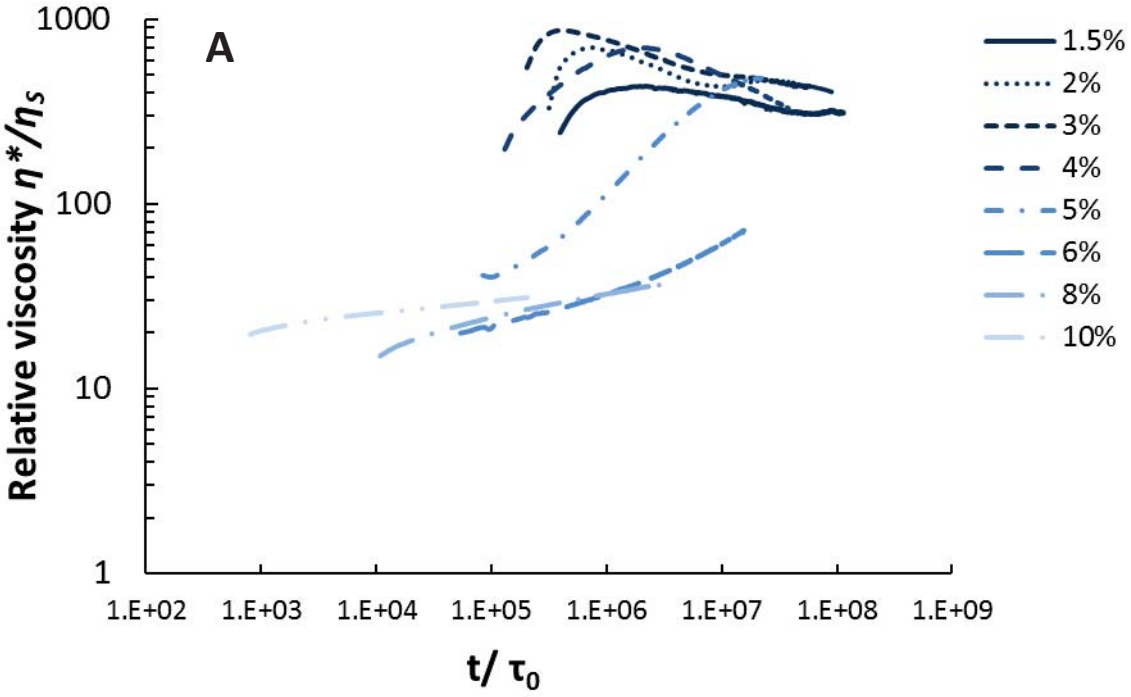
A
1000
100
10
1
Relative viscosity η^*/η_S
1.E+02
1.E+03
1.E+04
1.E+05
1.E+06
1.E+07
1.E+08
1.E+09
t/ τ_0
1.5%
2%
3%
4%
5%
6%
8%
10%

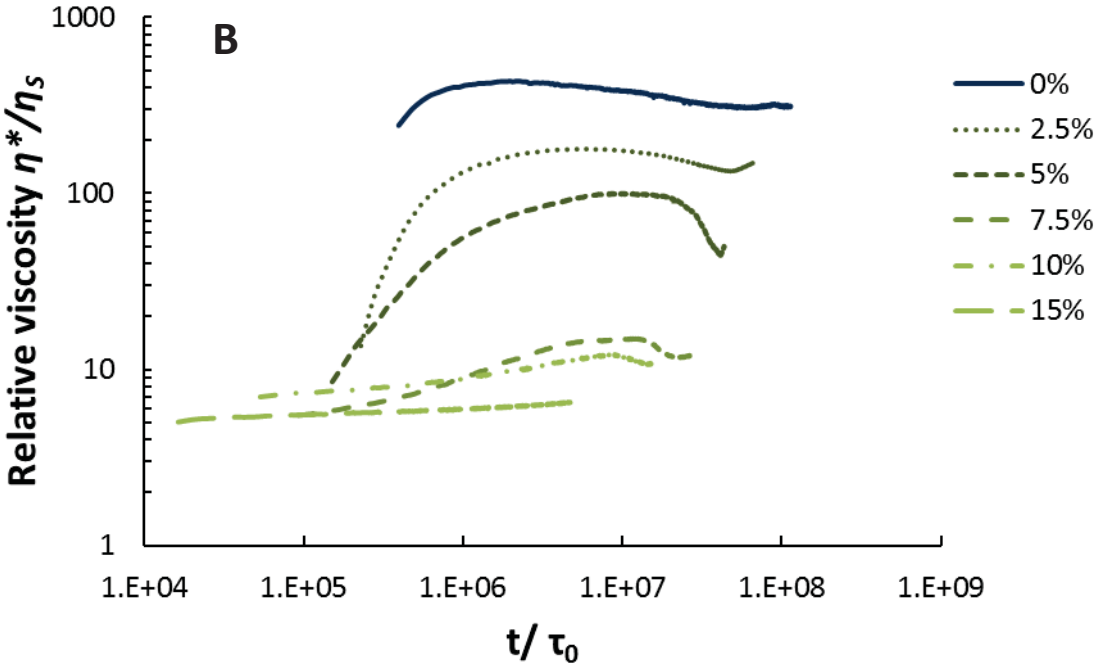
B
1000
100
10
1
Relative viscosity η^*/η_S
1.E+04
1.E+05
1.E+06
1.E+07
1.E+08
1.E+09
t/ τ_0
0%
2.5%
5%
7.5%
10%
15%

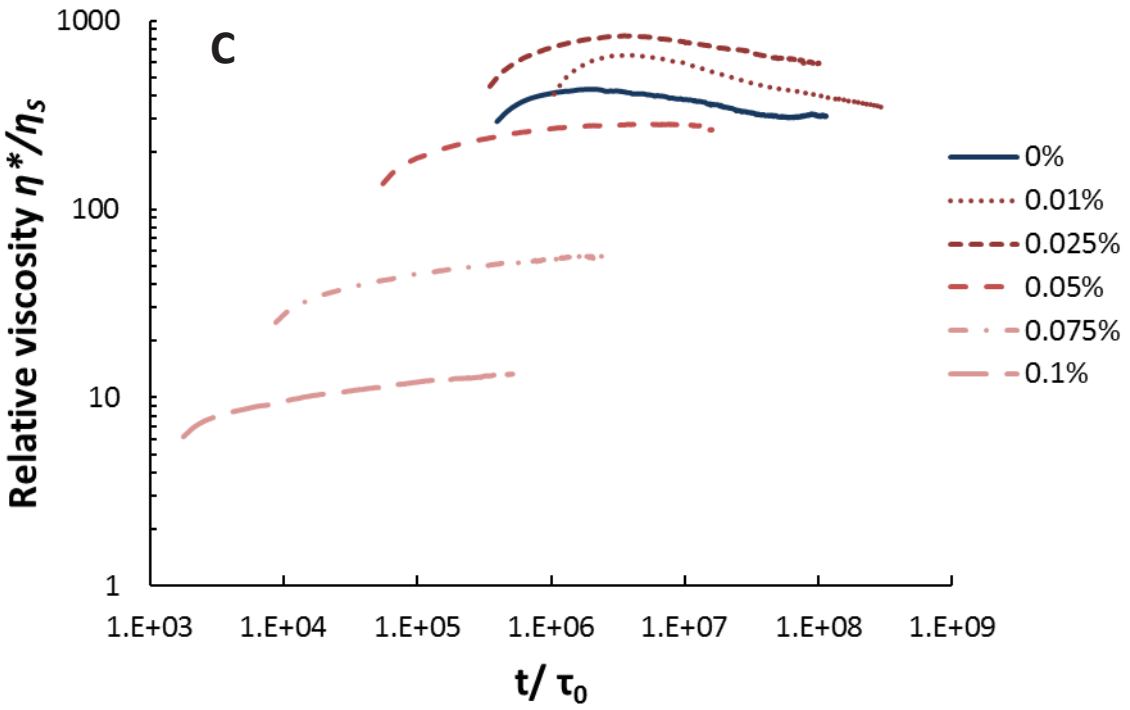

Figure 5.13. (A) Relative viscosity (performed at 1 Hz, 0.5% strain, 20 °C) as a function of time for various emulsions normalized by the time taken for a droplet to diffuse an arbitrary distance, in this case 20 nm was used in equation (5.6). Emulsions stabilized by various concentrations of NaCas: 1.5% w/w (solid line); 2% w/w (round dot); 3% w/w (square dot); 4% w/w (dash); 5% w/w (dash dot); 6% w/w (long dash); 8% w/w (long dash dot); 10% w/w (long dash dot dot). (B) Relative viscosity (performed at 1 Hz, 0.5% strain, 20 °C) as a function of time for 1.5% w/w NaCas-stabilized emulsions containing various concentrations of maltodextrin: 2.5% w/w (round dot); 5% w/w (square dot); 7.5% w/w (dash); 10% w/w (dash dot); 15% w/w (long dash). (C) Relative viscosity (performed at 1 Hz, 0.5% strain, 20 °C) as a function of time for 1.5% NaCas-stabilized emulsions containing various concentrations of xanthan: 0.01% w/w (round dot); 0.025% w/w (square dot); 0.05% w/w (dash); 0.075% w/w (dash dot); 0.1% w/w (long dash).

The peak in relative viscosity observed in all emulsions was markedly dependent on the NaCas concentration. There was a clear rapid increase in the initial viscosity with an increase in the NaCas concentration from 1.5 to 3% w/w. The peak relative viscosity occurred slightly earlier for the 2% and 3% w/w NaCas emulsions than for the 1.5% w/w NaCas emulsion. The reorganization and rearrangement of the droplet network was still detectable within the

measurement timeframe for these emulsions. The slow dynamics of the formation of the droplet network became obvious for the 4% and 5% w/w NaCas emulsions. It was estimated that the formation of the transient droplet network was about 100 times slower for 5% w/w NaCas than for 2% w/w NaCas, despite only a 4 fold change in the continuous phase viscosity. Interestingly, the 5% w/w NaCas emulsion exhibited transient viscoelastic character in a 12 h oscillatory measurement (Figure 5.14). The storage modulus increased as a function of time initially, and there was a cross-over of the storage and loss moduli at about 2.5 h. The emulsion showed elastic character for approximately 4 h, and then the storage modulus started to decrease over time. The loss of elastic character probably relates to the time-dependent structural reorganization and rearrangement processes. Nevertheless, there was no elastic character showed by emulsions < 5% w/w NaCas.

For higher NaCas concentrations (≥ 6% w/w), the dynamics of the formation of a transient droplet network became considerably slower. It was estimated that it took the 6% w/w NaCas emulsion about 420 hours to reach the peak in relative viscosity, based on the convergence of the slopes. This approximation was in fairly good agreement with the creaming behaviors determined by Turbiscan. Some weak polysaccharide gel network could possibly have formed in the continuous phase at the critical polymer concentration (Thomar et al., 2012), which may have strongly hindered the formation of the transient droplet network and its corresponding structural rearrangement; subsequently, the gel network may have prevented creaming by preventing gel collapse.

The effect of maltodextrin concentration on the dynamics of structural change in 1.5% w/w NaCas emulsions is shown in Figure 5.13B. The droplet network developed at a slower rate as the maltodextrin concentration was increased up to 10% w/w. Furthermore, across the maltodextrin concentrations investigated, increasing the concentration also decreased the maximum viscosity by 1–2 orders of magnitude. A slower network formation with increased maltodextrin concentration is consistent with previous findings on the effect of carbohydrate on creaming stability (Blijdenstein, Zoet, van Vliet, van der Linden, & van Aken, 2004; Dokic-Baucal, Dokic, & Jakovljevic, 2004; Thomar et al., 2012; Udomrati, Ikeda, & Gohtani, 2013). The decrease in maximum viscosity suggested that the attractions that supported network formation were weakened with the addition of maltodextrin. It should be noted that, apart from

simply increasing the continuous phase viscosity, a maltodextrin with high molecular weight fractions (i.e. low DE value) forms firmly packed segments or arranges like "fringes" to form a network structure in solution because of self-association as branched molecules are added to amylase (Chronakis, 1998). This structural change cannot be ruled out as an additional factor involved in the slowed dynamic effect.

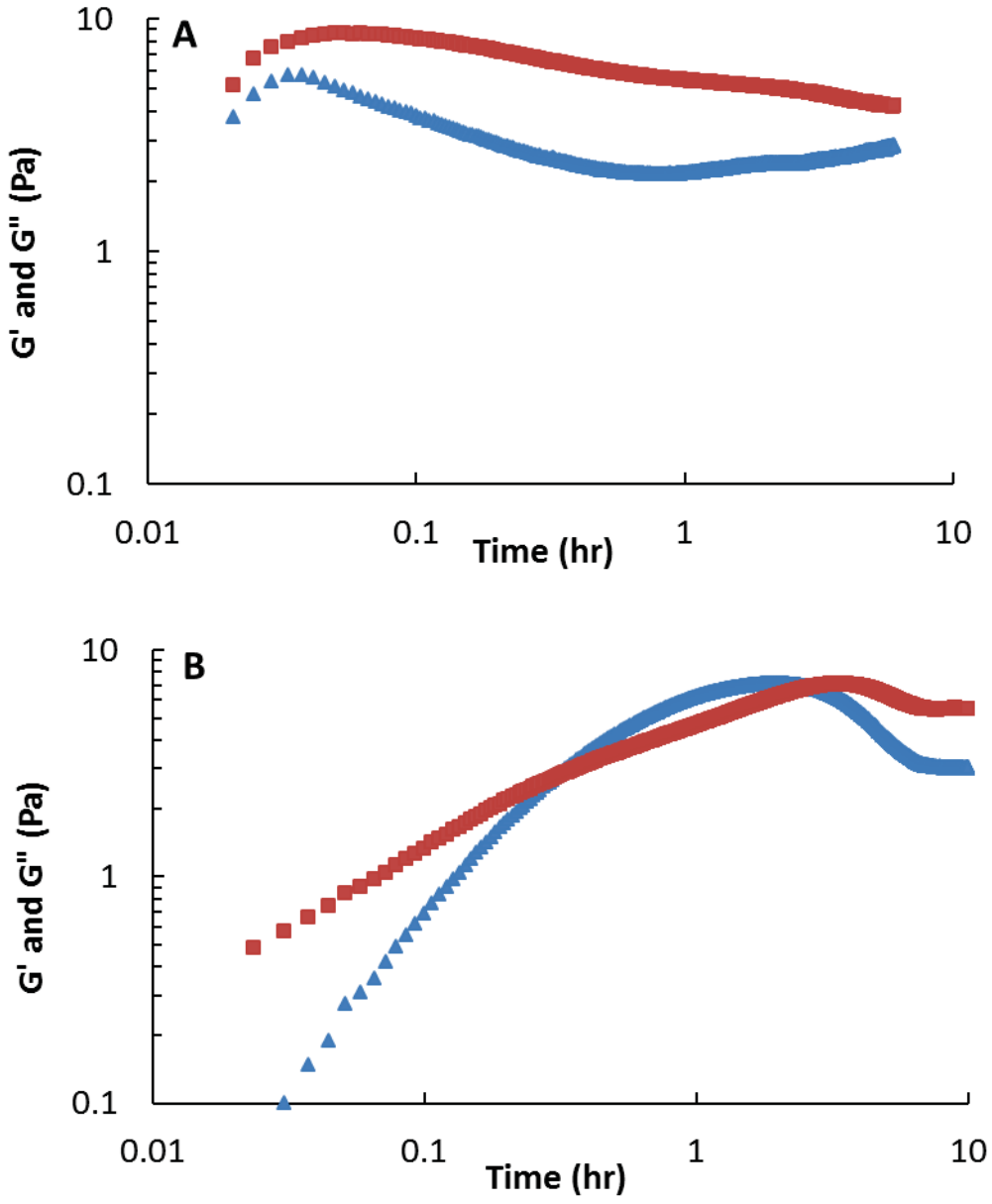

Figure 5.14. Variation of *G'* (▲) and *G"* (■) as a function of time for (A) 3% w/w and (B) 5% w/w NaCas emulsions at 20 °C (performed at 1 Hz, 0.5% strain).

The effect of xanthan concentration on the dynamics of structural change in 1.5% w/w NaCas emulsions is shown in Figure 5.13C. The trend in structural evolution in the xanthan-containing NaCas emulsions was similar to that in the NaCas-stabilized emulsions fortified with different amounts of non-adsorbed NaCas. The addition of xanthan up to 0.025% w/w led to a stronger droplet network as the relative viscosity increased. The emulsions containing 0.01% and 0.025% w/w xanthan displayed a trend such that the relative viscosity increased initially and then there was an onset rearrangement of the droplet network that eventually resulted in a decrease in relative viscosity as the network was no longer self-supporting. Further increasing the xanthan concentration led to a slower network formation as the relative viscosity of the emulsions decreased considerably. This change suggested that the viscosity of the non-adsorbed xanthan slowed down the dynamics of droplet network formation.

5.5 Conclusions

This study provided a better understanding of the creaming behavior of emulsions (30% oil w/w), induced by depletion effects, over a wide range of NaCas concentrations (1−10% w/w). At 1.5−5% w/w NaCas, the low shear relative viscosities were 100−1000 times greater than expected for non-interacting droplets. Creaming profiles and microscopy further indicated the formation of interconnected droplet networks that coarsened and eventually collapsed under gravity. By considering the entire population of droplet sizes, it was able to account for both the weak network formation and the portion of droplets that remained freely dispersed after the network collapse. For intermediate NaCas concentrations (3−5% w/w), the increase in the concentration of non-adsorbed NaCas increased the number of droplets participating in the network, which in turn kinetically stabilized the emulsion structure against creaming. Diffusion limited aggregation is characterized with a rate constant of $8k_BT/3\eta_s$, and suggests that droplets and small aggregates would be consumed into multi-droplet aggregates in an instant, yet at higher NaCas concentrations (≥ 6% w/w), the significant delay in network formation could not be accounted for by simply renormalizing time scales against the rate diffusion of single droplets. It is thought that these emulsions consist of large aggregates in a pre-network state. These large aggregates do not evolve into a network in an accessible time frame due to the particularly small

diffusive motion and their inability to redisperse. Presumably in these systems the rate of creaming in these aggregate samples would begin to resemble that creaming rates determined by aggregate size, gravity and Stokes' law.

Adding maltodextrin or xanthan influenced the creaming behavior, but neither could be considered to be an inert thickening agent. The reduced network formation caused by adding maltodextrin was not an effect of viscosity, but rather a breakdown of the caseinate nano-particles that induce network formation. Once the maltodextrin concentration exceeded 15% w/w, the droplets were entirely non-interacting and would presumably cream at a rate predicted by Stokes' law. Adding xanthan to the NaCas emulsions resulted in local domains rich in either xanthan or NaCas and emulsion. The effect of these local domains was that the droplets experienced a larger depletion interaction potential and the high viscosity of the combined xanthan and emulsion phases resulted in uniform phase separation across the emulsion rather than gravimetric separation. The structure, stability and depletion energy relation can be summarized in Figure 5.15.

Food emulsions are subjected to different heating conditions, i.e. high temperature long time (retort process) or high temperature short time (UHT process). Since high temperature heating can potentially alter the sodium caseinate nano-particle size and the molecular weight of sodium caseinate, hence it will change the depletion interaction potential and the continuous phase viscosity (Guo et al., 1996; Radford & Dickinson, 2004). The structural properties and emulsion stability of heated NaCas-stabilized emulsions were investigated in the next chapter.

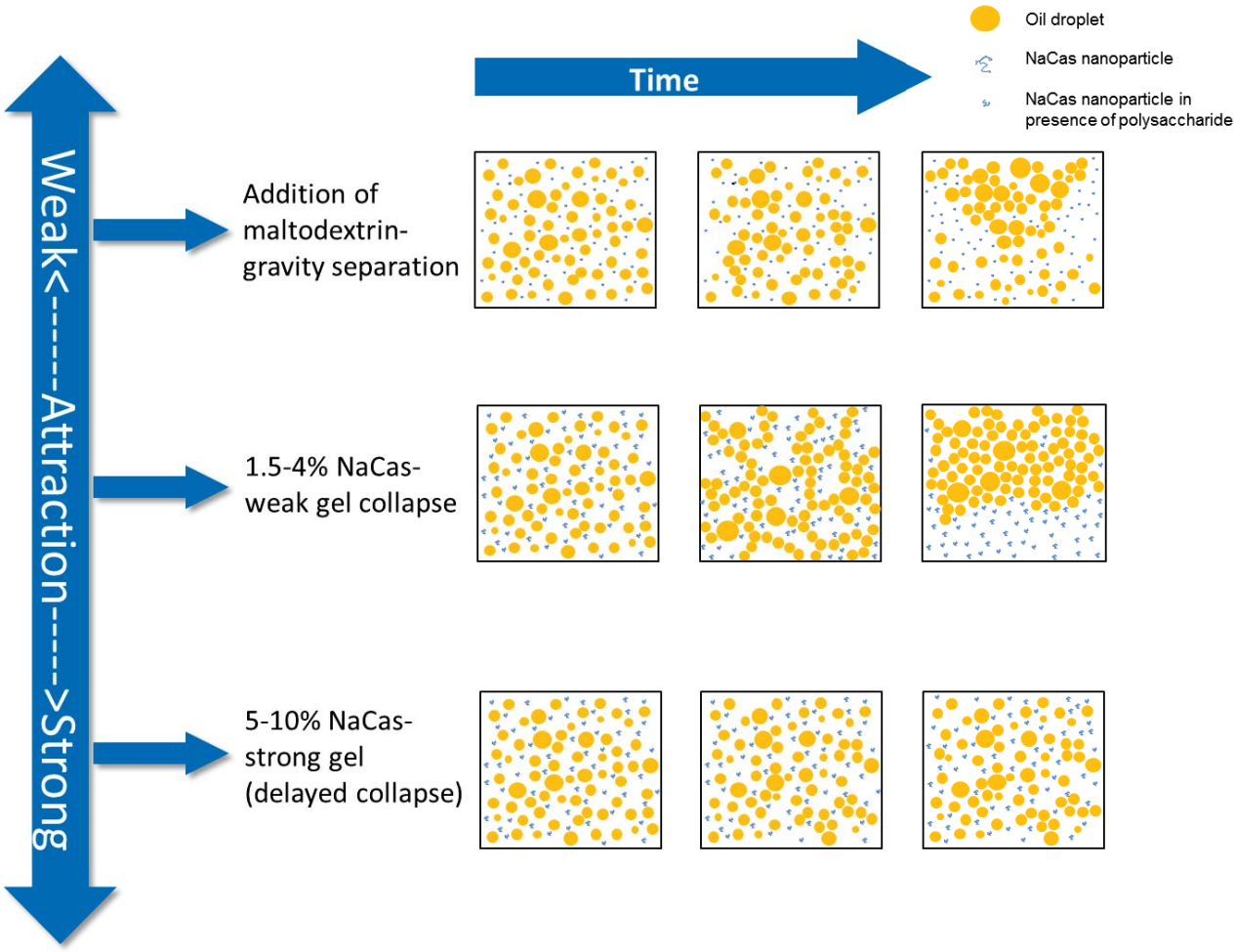

Figure 5.15. Schematic illustration of structure, stability and depletion force relationship in NaCas emulsions with addition of non-adsorbed NaCas and non-adsorbed polysaccharide.

Chapter 6: Effect of Heat Treatment on the Phase Separation Behavior of Sodium-caseinate-stabilized Oil-in-Water Emulsions [3]

6.1 Abstract

The emulsion stability and rheological properties of heated (120 °C, 0−60 min) 30% w/w oil-in-water emulsions (droplet diameter ~ 0.73 μm, pH 6.8) containing sodium caseinate (NaCas), 2−6% w/w, were investigated. The creaming kinetics, determined by Turbiscan, showed that the phase separation of NaCas-stabilized emulsions was markedly dependent on the duration of the heat treatment. The differences between unheated and heated emulsions were attributed to heat-induced physicochemical changes in the NaCas nano-particles. The emulsion structures, with varied extents of depletion flocculation, were well reflected by small and large deformation rheology. The droplet−droplet interactions were weakened at low and moderate NaCas concentrations (2% and 4% w/w) but were strengthened at high NaCas concentration (6% w/w) in the presence of heated NaCas nano-particles. Whereas the former structural change was predominantly due to reduced depletion attraction, both reduced depletion attraction and decreased continuous phase viscosity influenced the latter structural change. The heat-induced physicochemical changes in the NaCas nano-particles played a significant role in the physical stability of the emulsions. The insights from this study can be used to create novel droplet sizes and protein particle sizes to manipulate the droplet/protein size ratio, and therefore the extent of droplet−droplet interactions, and to maintain the desirable shear-thinning flow behavior at high protein concentrations.

---

[3] Part of the content presented in this chapter is to be submitted for publication.

Part of the content was also presented as a graduate student poster presentation at the ADSA−ASAS Joint Annual Meeting, Indianapolis, IN, USA, 8−12 July 2013.

6.2 Introduction

A number of studies have been carried out to understand the onset of the development of the emulsion droplet network, its structural rearrangement and the kinetics of the eventual phase separation (Aben et al., 2012; Blijdenstein et al., 2003; Dickinson & Golding, 1997b; Moschakis et al., 2005). In Chapter 5, the structure−rheology relationship across a wide range of NaCas concentrations was illustrated; both the continuous phase viscosity and the depletion interaction potential made important contributions to the phase separation behaviors of NaCas-stabilized emulsions at high protein conentration. A good relation between the size of the caseinate nano-particle and the depletion interaction energy was established in a recent theoretical study (Radford & Dickinson, 2004). In the presence of a sufficient amount of non-adsorbed NaCas for depletion flocculation, the depletion interaction energy will decrease with any change in the caseinate nano-particle size from its original value (near optimum, radius of ~ 20 nm). It was found that extensive heating of a NaCas solution led to polymerization and degradation of caseinate nano-particle and that the extent depended on the temperature and the heating time (Gaucheron et al., 2001; Guo et al., 1996; Hustinx et al., 1997; van Boekel, 1999). It was suggested that the NaCas-stabilized droplets were more prone to heat-induced degradation than the non-adsorbed NaCas in the continuous phase. However, there is still little understanding of the phase separation behaviors in heated emulsions. The size of the NaCas nano-particle and the contribution of individual caseins to the self-association of NaCas after high temperature heating remain unclear.

Hence, the aims of this study were: (1) to investigate the effect of heat treatment on NaCas-stabilized emulsions with 2−8% w/w protein concentration and the effect of the heating history of NaCas solutions on the phase separation behaviors of the recombined emulsions; (2) to explore the correlation between the depletion interaction potential and the physicochemical change in NaCas nano-particles on heating.

6.3 Materials and methods

6.3.1 Materials

Sodium caseinate 180 (NaCas) was obtained from Fonterra Co-operative Group Ltd, Auckland, New Zealand.

6.3.2 Preparation of model emsulsions

The model emulsions were prepared following the procedure described in Figure 6.1. Each model emulsion was prepared at least in triplicate.

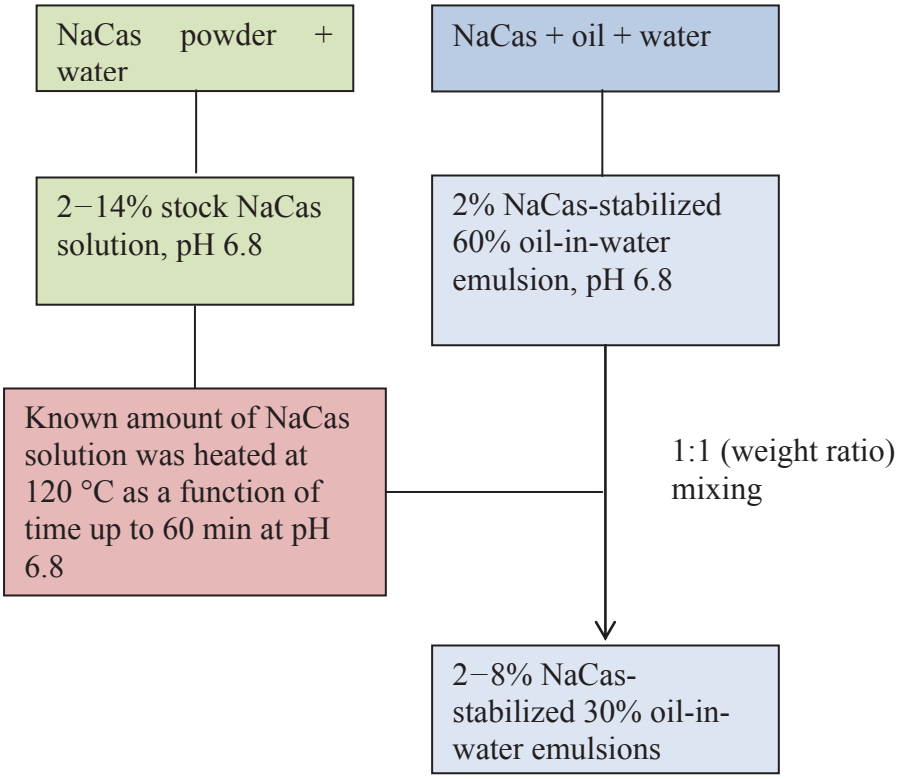

Figure 6.1. Flow chart of the preparation of model emulsions (2−8% w/w protein, 30% w/w oil).

6.3.3 Heat treatment of caseinate-stabilized emulsions and corresponding oil-free phase

All caseinate emulsions and their corresponding oil-free caseinate solutions were heated in 8 mL glass tubes with rubber-lined caps containing 5 ml of sample at pH 6.8 ± 0.04 in a silicone oil bath at 120 ± 1 °C, with a constant rocking speed (8 rev/min). The heating-up time was estimated to be about 2 min and it was not included in the heating time. All samples were removed after a selected time up to 60 min and immediately cooled under running cold water. The heat-treated emulsions were allowed to equilibrate to room temperature and were held at 20 °C for at least 1 h before further analysis (i.e. pH, particle size and rheological measurements) was carried out.

6.3.4 Determination of protein content of heated NaCas solutions and oil-free phase of NaCas stabilized emulsions

A CEM microwave moisture/solids analyzer (Matthews, USA) was used to measure the total solids content of the heated NaCas solutions and the oil-free phase of NaCas-stabilized emulsions. About 2−3 g of sample was used for the determination (Reh & Gerber, 2003). The total nitrogen determination was carried out using the Kjeldahl method described in Chapter 3, Section 3.2.4.

6.3.5 Particle size determination of heated NaCas solution

The particle size measurements were carried out using procedures described in Chapter 3, Section 3.2.3. The NaCas solution was diluted with Milli-Q water to achieve 110−130 kilocounts per second. No attempt was made to measure the absolute particle size of NaCas. The Z-average (intensity-based mean) was used to calculate the relative change in the scattered intensity of the caseinate particle. Measurements were performed in duplicate for each sample.

6.3.6 Particle size determination of NaCas-stabilized droplets

The particle size measurements were carried out using procedures described in Chapter 3, Section 3.2.3.

6.3.7 Quantification of total native caseins in NaCas solutions after heating

The sodium dodecyl sulphate polyacrylamide gel electrophoresis (SDS-PAGE) technique is described in Chapter 3, Section 3.2.4. The NaCas samples were diluted with SDS sample buffer to achieve a 0.5 mg/g sample buffer for casein determination. The SDS gels were scanned using an Image Scanner III (GE Healthcare Bio-Sciences AB, Uppsala, Sweden). The intensities of the protein bands were obtained using Molecular Dynamics ImageQuant software (GE Healthcare Bio-Sciences AB).

6.3.8 Emulsion stability

The phase separation data at 7 days were used to plot the creaming curves. The techniques are described in detail in Chapter 3, Section 3.2.7.

6.3.9 Rheology measurements

The details of the rheology measurement conditions are given in Chapter 5, Section 5.3.6.

6.3.10 Calculation of depletion interaction potential

The details of the calculation of the depletion interaction potential are given in Chapter 5, Section 5.3.4.

6.3.11 Statistical analysis

All experiments were carried out at least in duplicate using freshly prepared samples and the results are reported as the mean and standard deviation of these measurements.

6.4 Results and discussion

6.4.1 Impact of heat treatment at 120 °C on the phase separation behavior of NaCas-stabilized emulsions

A preliminary trial was performed to determine whether a heat treatment at 120 °C improves the creaming stability of NaCas-stabilized emulsions, as reported by Srinivasan et al. (2002). Emulsions containing 1, 2, 4 and 6% w/w NaCas were heated for 10, 20 and 30 min. Figure 6.2 shows the development of the classified layer as determined by Turbiscan over 7 days. In general, emulsions stabilized by 1% w/w NaCas followed natural creaming kinetics, and heating had little effect on their creaming behaviors (Figure 6.2A). The migration of droplets followed Stokes' Law of a concentrated emulsion without flocculation ($\emptyset_{oil}$ = 0.3) quite well. Above a certain concentration of non-adsorbed NaCas, the main destabilization mechanism is depletion flocculation; as a consequence, the emulsion phase separates into a creaming layer and a classified layer (Dickinson & Golding, 1997b). At 2 and 4% w/w NaCas, pronounced phase separation occurred, and the development of the classified layer was rapid (Figures 6.2B and 6.2C). At these concentrations, the creaming was slowed down by the addition of non-adsorbed NaCas.

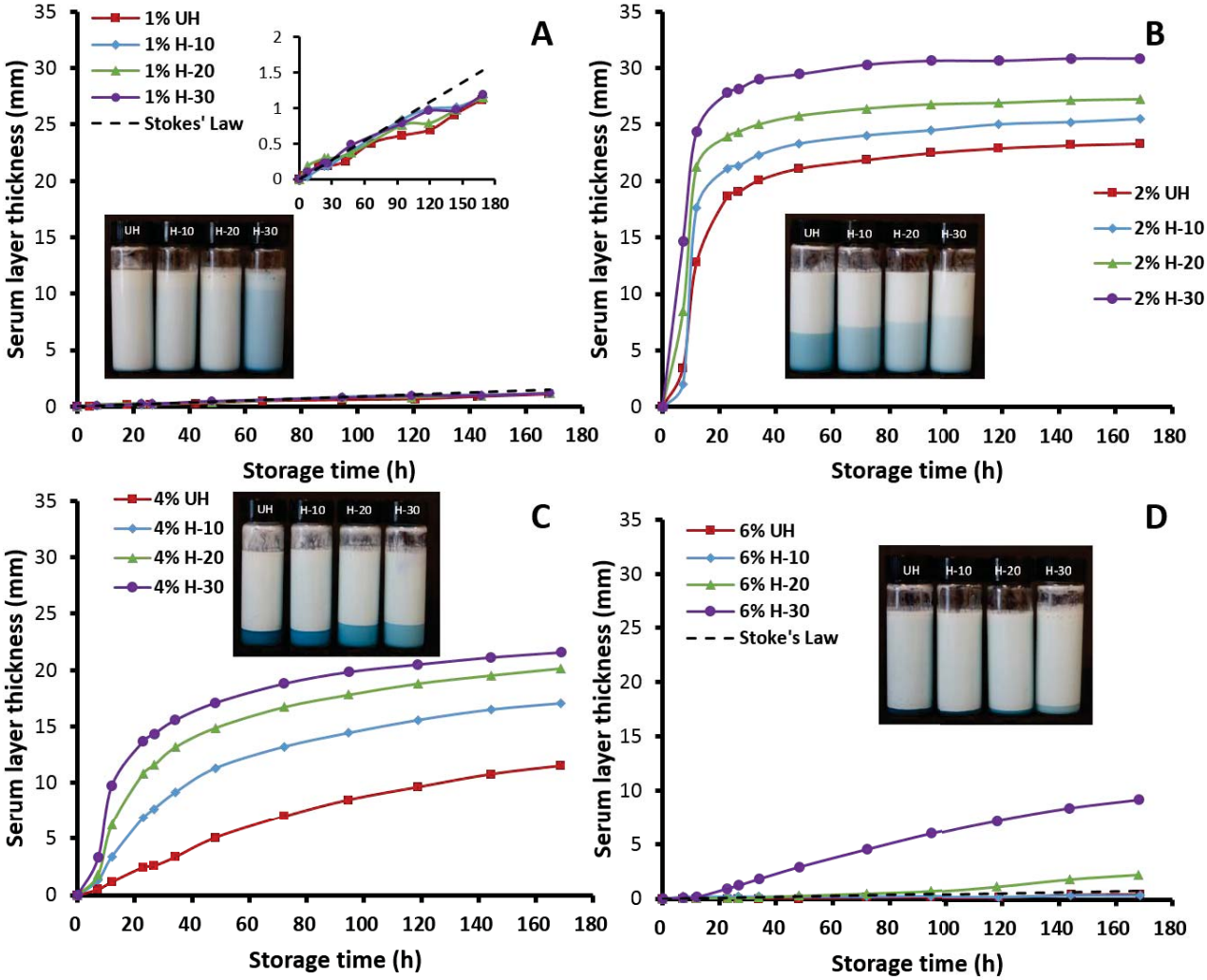

Figure 6.2. Variation in classified layer thickness as determined by Turbiscan over 168 h at 20 °C for heated NaCas-stabilized 30% w/w oil-in-water emulsions containing 1% w/w (A), 2% w/w (B), 4% w/w (C) and 6% w/w (D) NaCas. Inset: visual appearance of NaCas-stabilized emulsions after 1 week of storage at 20 °C.

Interestingly, the heated NaCas-stabilized emulsions phase separated at a faster rate as a function of heating time for 2−6% w/w NaCas. Although the phase separation became more pronounced, the bottom of the tubes became more turbid. At 6% w/w NaCas, the unheated emulsions showed a delay time for the initial phase separation (~ 72 h). As the emulsions were heated, the delay time shortened and the emulsions phase separated more rapidly. The creaming behavior of the

emulsion heated for 30 min was markedly different from that of the unheated emulsion (Figure 6.2D). It has been illustrated that the creaming behavior and the turbidity of the separated serum phase are strongly associated with the depletion interaction potential. A smaller depletion interaction potential is often associated with increased turbidity of the classified layer and results in a weaker droplet network that collapses rapidly and displays faster separation (Liang, Gillies, Patel, Matia-Merino, Ye & Golding, 2014). The creaming behavior demonstrated that a reduced depletion interaction potential was very probably the reason for the fast phase separation observed in the heated NaCas-stabilized emulsions.

Alternatively, the emulsion stability of NaCas-stabilized emulsions has been found to be pH dependent (Perrechil & Cunha, 2010). After the 2% and 6% w/w NaCas-stabilized emulsions were heated for 30 min, the pH of the samples decreased by only 0.2 and 0.1 pH units respectively. The effect of pH on emulsion stability was considered to be very small, as it has been suggested that the extent of depletion flocculation decreases because of a high viscosity that is governed by a gel network or protein aggregation when the pH of NaCas-stabilized emulsions shifts by 1 pH unit towards to a more acidic value (Perrechil & Cunha, 2010).

It has been suggested that the improved creaming stability in heated emulsions is due to the combined effect of increased surface protein coverage, higher continuous phase viscosity and more aggregates present in the continuous phase (Srinivasan et al., 2002). The effects of the latter two on creaming stability are discussed in Section 6.4.2. The total nitrogen and total solids contents of the continuous phases of NaCas-stabilized emulsions heated for up to 60 min were measured (Table 6.1). It was found that there was no change in the total nitrogen and total solids contents of the continuous phases regardless of the initial NaCas concentration in the emulsions, suggesting that the serum caseinate nano-particles did not interact with the interfacial caseins to form a thicker layer.

Table 6.1. The total solids content (by CEM microwave solids analyzer) and the total nitrogen content (by the Kjeldahl method) as a function of heating time of 30% w/w oil-in-water emulsions formed with 2−6% w/w NaCas.

Continuous phase concentration $C_{non\text{-}ad}$ (g/kg)[1]	Total solids of serum phase (g/kg) after heat treatment at 120 °C (min)				Total nitrogen of serum phase (% m/m) after heat treatment at 120 °C (min)			
	UH	10	30	60	UH	10	30	60
17.9	21.0 ± 0.3	22.0 ± 0.4	22.0 ± 0.2	21.0 ± 0.3	0.33 ± 0.02	0.32 ± 0.01	0.32 ± 0.01	0.32 ± 0.01
32.2	37.3 ± 0.4	35.8 ± 0.5	35.6 ± 0.4	36.1 ± 0.3	N/A			
46.5	52.0 ± 0.4	55.0 ± 0.4	53.8 ± 0.5	54.8 ± 0.4	0.76 ± 0.03	0.76 ± 0.03	0.79 ± 0.04	0.75 ± 0.02
60.8	68.1 ± 0.6	66.7 ± 0.7	67.6 ± 0.5	67.5 ± 0.6	N/A			
75.1	N/A				1.23 ± 0.05	1.22 ± 0.04	1.21 ± 0.04	1.20 ± 0.03

[1] The equation for calculating the continuous phase protein concentration is: [the total protein – the adsorbed protein (in this case, the amount of adsorbed caseins is about 0.75 g/100g)]/(1-Ø). Ø is 0.3 in the final emulsion. The calculation of aqueous phase xanthan and maltodextrin content is: the total biopolymer/(1-Ø).

6.4.2 Impact of heat treatment at 120 °C on the physicochemical properties of NaCas in the continuous phase

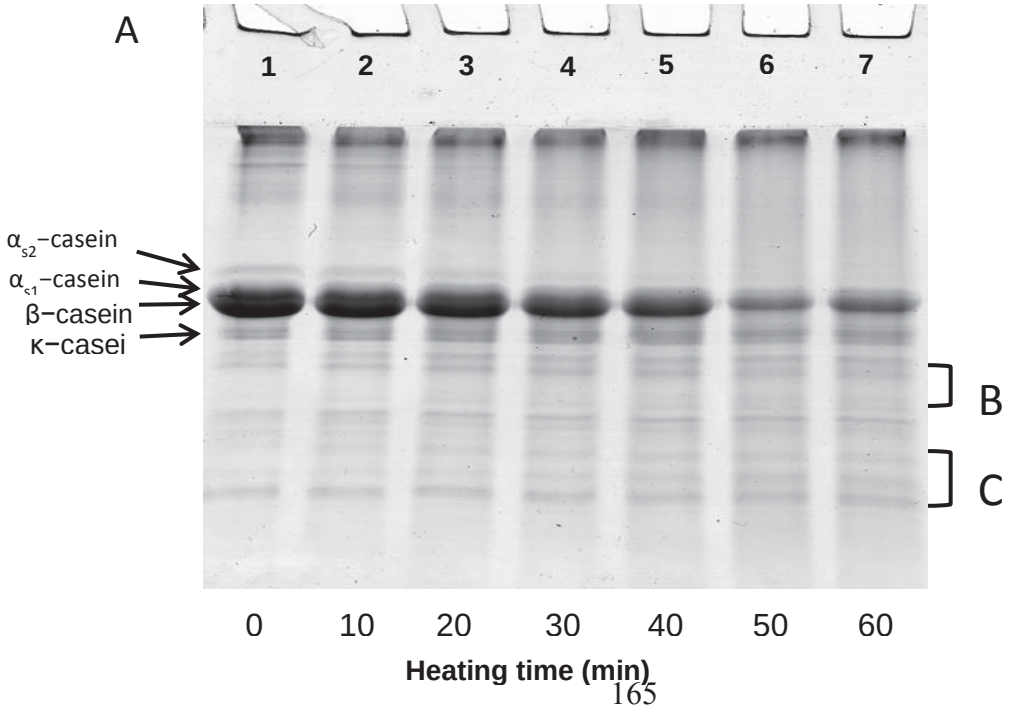

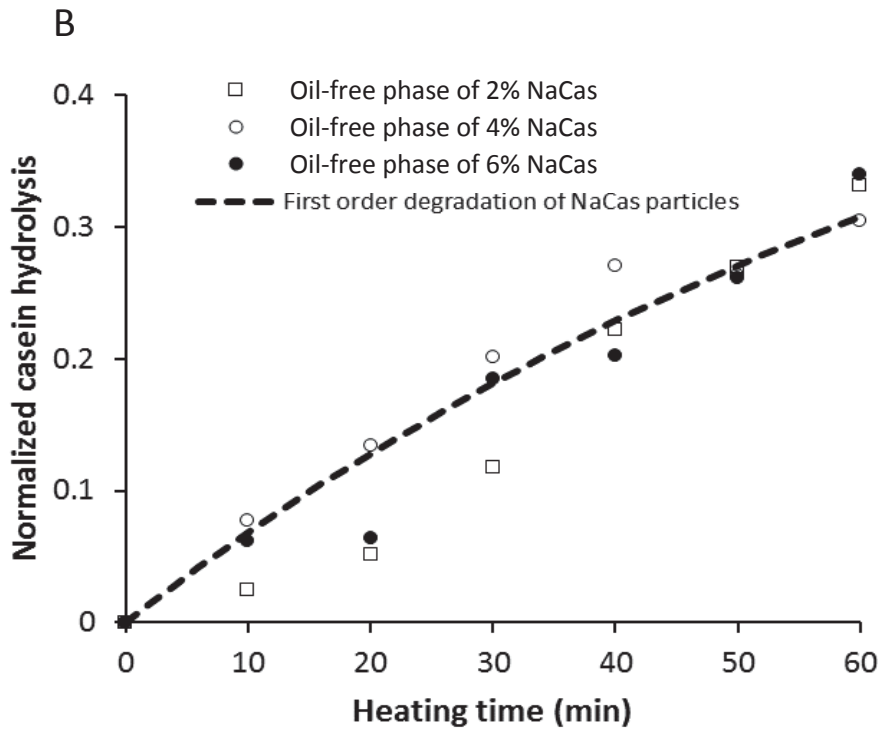

Figure 6.3. (A) Representative SDS-PAGE patterns of unheated (lane 1) and heated NaCas in the continuous phase of 6% w/w NaCas-stabilized 30% w/w oil-in-water emulsions (lanes 2−7). Each lane was loaded with approximately 25 μg of protein. The major casein proteins are α_{s2}-casein, α_{s1}-casein, β-casein and κ-casein. Some degradation products were indicated in the zones marked B and C. (B) Normalized casein hydrolysis (determined by SDS-PAGE) in NaCas after heating at 120 °C as a function of time. NaCas at different concentrations that corresponded to the continuous phases of 3% w/w (□), 4% w/w (○) and 6% w/w (●) NaCas-stabilized 30% w/w oil-in-water emulsions was heated.

The results described in Section 6.4.1 indicated that there was no heat-induced deposition of non-adsorbed NaCas at the oil/water interface. To investigate the heat-induced physicochemical changes in NaCas on the phase separation behaviors of heated NaCas-stabilized emulsions, the molar mass, particle size and viscosity of NaCas were determined. It has been reported that heating NaCas solutions at high temperatures (120−140 °C) will result in the formation of degradation products of NaCas as well as polymerized casein molecules, depending on the heating conditions (Guo et al., 1996; Hustinx et al., 1997). The degree of heat-induced hydrolysis

of NaCas after heating at 120 °C was analyzed using SDS-PAGE (Figure 6.3). The SDS-PAGE patterns of NaCas in the continuous phase of 6% w/w NaCas-stabilized emulsions showed pronounced changes were caused by the heat treatments. The intensities of the major casein bands, especially the α_{s1}- and β- casein bands, reduced markedly and the degraded casein peptides became more visible (Figure 6.3A). In this manner, the densitometric area of intact caseins can be used to calculate the degree of casein hydrolysis (the amount of intact casein after heating relative to the original amount of total casein). It is clearly shown that the extent of casein hydrolysis increases linearly with the heating time regardless of protein concentration (Figure 6.3B). This result was in good agreement with the literature (Guo et al., 1996; Hustinx et al., 1997). It was determined that the heat degradation of NaCas followed first-order kinetics, which agreed with previous studies (Metwalli & van Boekel, 1998). Based on the SDS-PAGE determination, approximately 65~70% intact casein remained in the NaCas solutions that were heated for 60 min.

The relative changes in particle size and viscosity of unheated and heated NaCas solutions are shown in Figure 6.4. Both the particle size and the zero-shear viscosity of NaCas solutions decreased as a function of heating time and followed a linear relationship. It has been well established that the decreased viscosity that is caused by hydrolysis of NaCas is proportional to the decrease in molecular weight (Guo et al., 1996; Swaisgood, 2003). α_{s1}-casein molecule fulfils the characteristics of a polymer containing two associative groups, as described in the associative polymer model, which giving a high zero-shear viscosity than a copolymer with a single associative group (like β-casein) at the same polymer concentration (Chassenieux et al., 2011). Hence, the degree of α_{s1}-casein hydrolysis during heating may play a very important role in determining the viscosity of the NaCas solution.

In general, our data suggested that protein degradation has a major impact on the physicochemical properties of the heated non-adsorbed NaCas. Thus, the effective concentration of NaCas for inducing depletion flocculation decreased after heating, which would have effectively changed the depletion interaction potential and the kinetics of the formation and rearrangement of the droplet network.

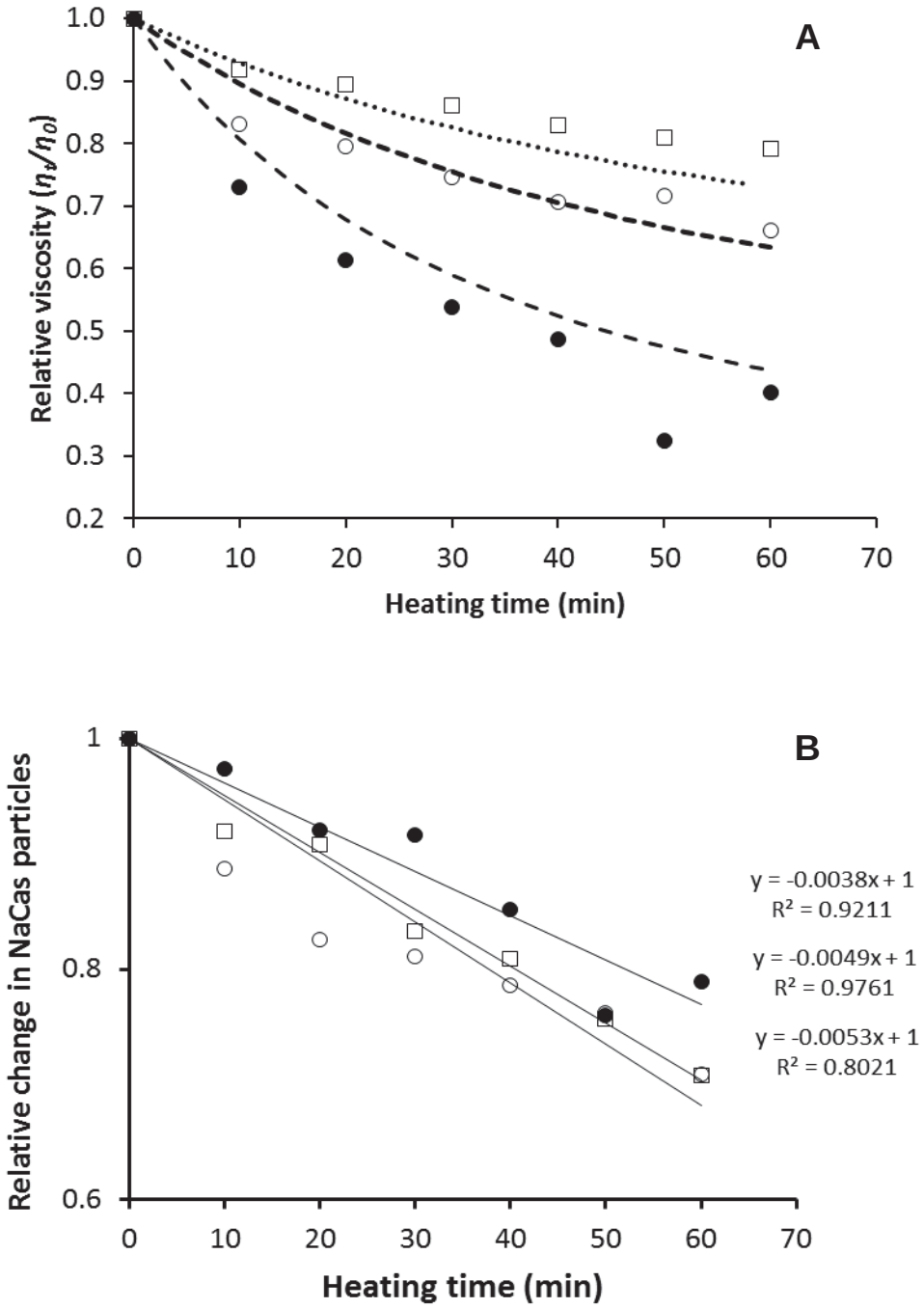

Figure 6.4. (A) Relative viscosity (η_t/η_0) and (B) Relative change in hydrodynamic diameter (D_t/D_0) of NaCas heated at 120 °C as a function of time. NaCas at different concentrations that corresponded to the continuous phases of 3% w/w (□), 4% w/w (○) and 6% w/w (●) NaCas-stabilized 30% w/w oil-in-water emulsions was heated.

6.4.3 Prediction of the phase separation behavior of heated NaCas-stabilized emulsions

To study the impact of the heat-induced degradation of NaCas on the phase separation behavior in more detail, the creaming profiles over time of heated (up to 60 min) 4% and 6% w/w NaCas-stabilized emulsions containing non-adsorbed NaCas were obtained (Figure 6.5). The rate of the emulsions separating into two phases increased as the heating time increased. The turbidity of the serum phase changed from translucent to opaque with increasing heating time. In the 4% w/w NaCas-stabilized emulsions, the creaming rate changed rapidly when the non-adsorbed NaCas was subjected to 10 and 20 min of heating and then more gradually at heating times > 20 min. The trend in the change in creaming rate appeared to be slightly different in the 6% w/w NaCas-stabilized emulsions. The creaming rate increased moderately when the non-adsorbed NaCas was heated for 10 and 20 min, increased gradually up to 40 min, with a greater increase at 50 min and then decreased slightly at 60 min. The observed changes were in line with the results in Section 6.4.1. The weaker the depletion interaction potential, the more rapid the droplet network formation, rearrangement and reorganization, and the faster the separation of the emulsion into two distinct layers. The continuous phase viscosity also plays an important role in the structural rearrangement of the droplet network. For a given NaCas concentration, the phase separation behavior depends on the balance of the effect between depletion interaction potential and continuous phase viscosity. The creaming behavior and the visual appearance of the emulsions containing non-adsorbed NaCas that was heated up to 60 min were totally expected.

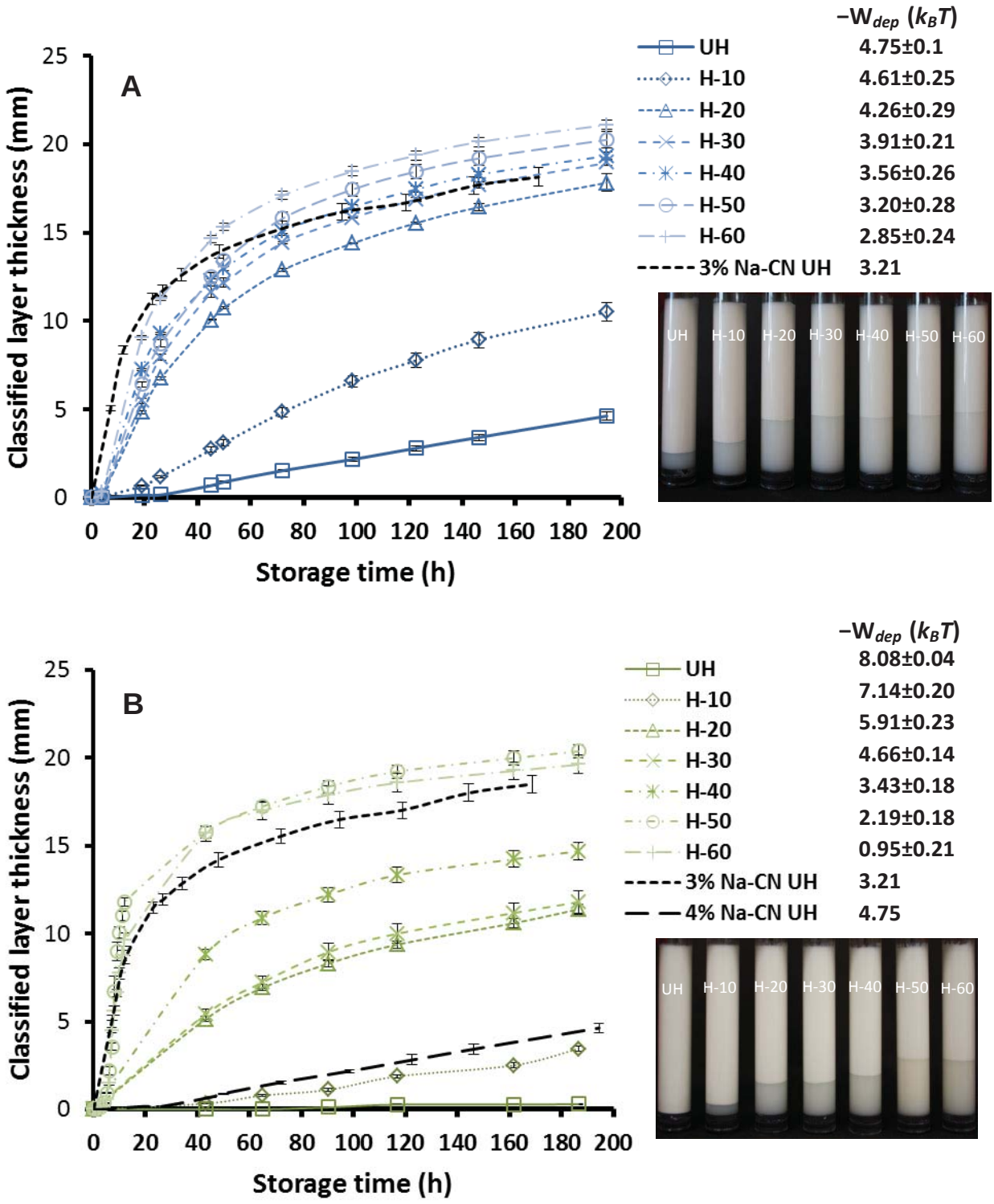

Figure 6.5. Variation in classified layer thickness, as determined by Turbiscan over 196 h at 20 °C, for 4% w/w NaCas-stabilized 30% w/w oil-in-water emulsions (A) and 6% w/w NaCas-stabilized 30% w/w oil-in-water emulsions (B) containing unheated NaCas and NaCas heated at 120 °C as a function of time. The dashed lines indicate the predicted creaming rates.

It was of interest to determine if the creaming trend of heated NaCas-stabilized emulsions could be estimated based on the change in the amount of intact NaCas. The estimations of the non-adsorbed NaCas concentrations of 4% and 6% w/w NaCas-stabilized emulsions at different heating times based on SDS-PAGE and rheology determinations are shown in Figure 6.6. Kinetics of protein hydrolysis was determined following the general rate law (van Boekel, 1999):

$$Rate = -\frac{dc}{dt} = kc^n \tag{6.1}$$

in which c is concentration, t time, k the reaction rate constant and n the order of the reaction. It was found that the protein proteolysis data from SDS-PAGE and viscosity had a better fit with zero-order kinetic, except the SDS-PAGE data of the non-adsorbed NaCas concentrations of 3% w/w NaCas-stabilized emulsions fitted any order between 0 and 2 almost equally well. The non-adsorbed intact NaCas content was calculated by using the slopes that are obtained in Sections 6.4.2 and 6.4.3. The estimated depletion interaction potentials in 4% w/w NaCas-stabilized emulsions based on SDS-PAGE determination were very similar to those obtained by rheological measurement. It was reasonable to expect that the creaming rate of the 4% w/w NaCas-stabilized emulsion containing non-adsorbed NaCas and heated for 50 min would be similar to that of the unheated 3% w/w NaCas-stabilized emulsion because their depletion interaction potentials were very similar, ~ −3.2−3.45 k_BT for the former and −3.2 k_BT for the latter. The creaming profile of the unheated 3% w/w NaCas-stabilized emulsion had a faster rate of phase separation initially (up to about 40 h) and then fell between the creaming profiles of the 4% w/w NaCas-stabilized emulsion at heating times of 30 and 40 min (Figure 6.5A). For the 6% w/w NaCas-stabilized emulsions, there was a marked difference in the estimations of the depletion interaction potential.

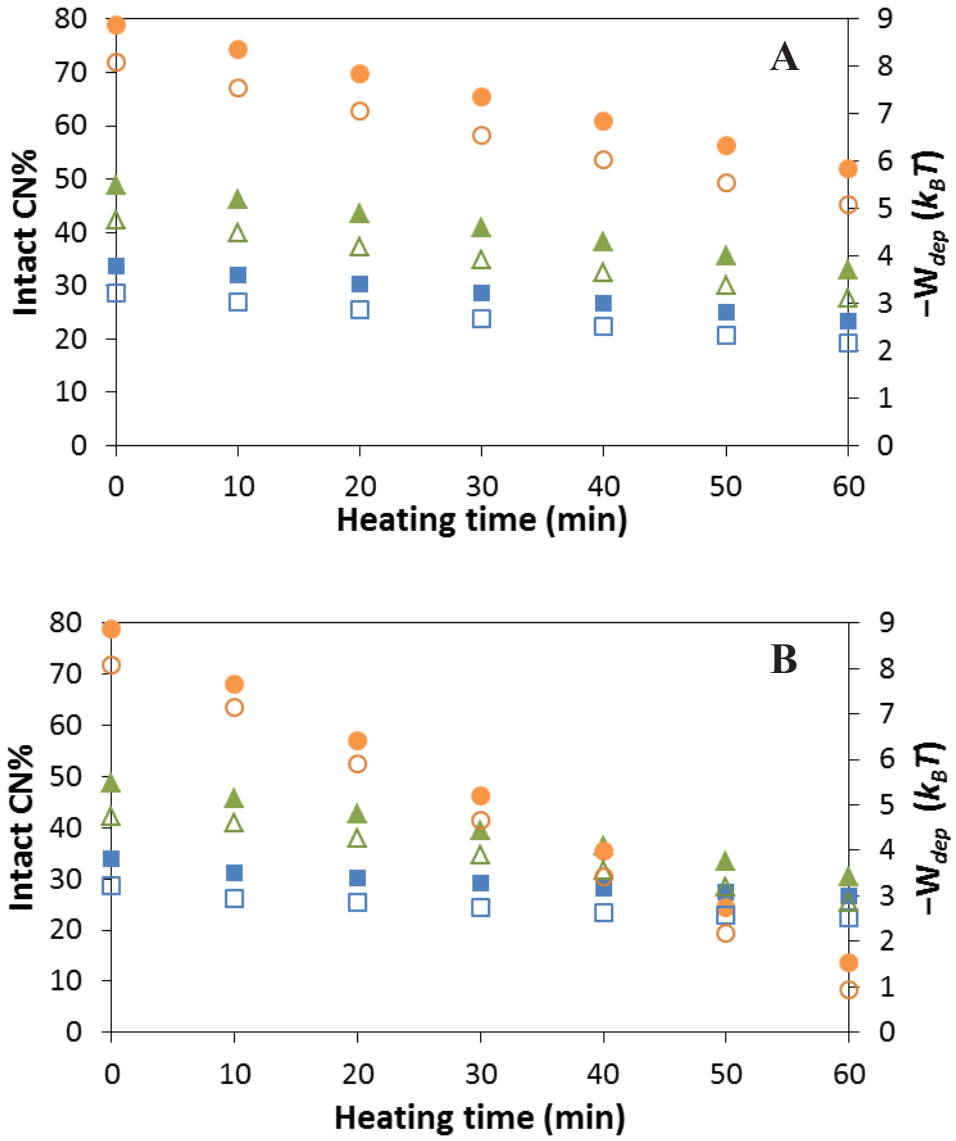

Figure 6.6. Estimation of non-adsorbed NaCas concentrations (close symbols) and the corresponding depletion interaction potentials (open symbols) based on SDS-PAGE (A) and viscosity (B) for 3% w/w (■, □), 4% w/w (▲, Δ) and 6% w/w (●, ○) NaCas-stabilized 30% w/w oil-in-water emulsions after heat treatment at 120 °C as a function of time (min).

The depletion interaction potential calculated based on rheology was consistently lower than that obtained based on SDS-PAGE determination. The calculated depletion interaction potential value based on SDS-PAGE determination did not appear to be sensible. However, when using the calculated depletion interaction potential based on rheology, the creaming profiles of the heated 6% w/w NaCas-stabilized emulsions still showed marked differences from the creaming

profiles of the unheated 3% and 4% w/w NaCas-stabilized emulsions, which had similar depletion interaction potentials but showed marked differences in their creaming profiles (Figure 6.5B).

It has been suggested that the continuous phase viscosity also plays a role in the formation of the depletion-induced droplet network and its subsequent rearrangement (Liang et al., 2014). The classified layer thickness was normalized by the corresponding continuous phase viscosity of the emulsion (Figure 6.7). The continuous phase viscosity had little impact on the shape of the creaming profiles of the 4% w/w NaCas-stabilized emulsions (Figure 6.7A), but had a greater effect on the normalized classified layer thickness of the 6% w/w NaCas-stabilized emulsions containing NaCas and heated for 50 and 60 min because the normalized classified layer thickness increased by about fourfold (Figure 6.7B). After taking the continuous phase viscosity into account, the creaming kinetics of the heated NaCas-stabilized emulsions still did not fit with the creaming profiles of the unheated NaCas-stabilized emulsions at similar depletion interaction potentials. The calculated depletion interaction potential seemed to be higher than the effective depletion interaction potential. It should be noted that not only the intact protein concentration and the continuous phase viscosity influence the depletion interaction potential level at higher NaCas concentration, but also the particle size, the attraction range and the spherical shape of the caseinate nano-particle affect its estimation (Radford & Dickinson, 2004). The smaller is the caseinate nano-particle (deviating from the optimum radius for a caseinate nano-particle, in this case 20 nm), the smaller is the depletion interaction potential but the range of attraction becomes shorter (Radford & Dickinson, 2004). Additionally, a polymer with a rod-like shape confers the maximum depletion interaction potential (Asakura & Oosawa, 1954). It has been postulated that the NaCas nano-particle adopts a rod-like shape at high protein concentration (Farrer & Lips, 1999). The heat-induced degradation apparently affects the self-association behavior of NaCas nano-particles. In future attempts to calculate the depletion interaction potential, all these factors need to be taken into account.

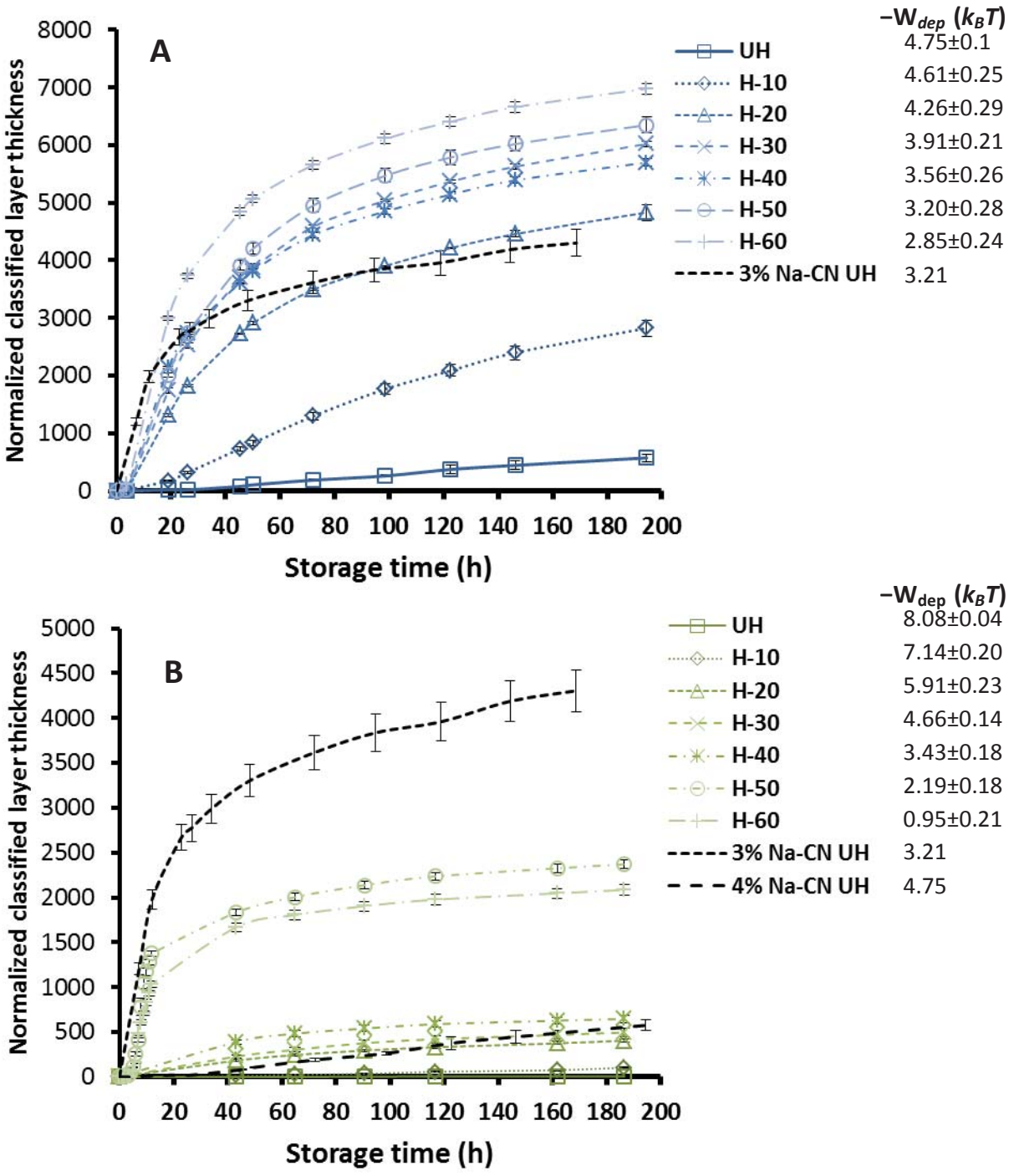

Figure 6.7. Normalized classified layer thickness of 4% w/w NaCas-stabilized 30% w/w oil-in-water emulsions (A) and 6% w/w NaCas-stabilized 30% w/w oil-in-water emulsions (B) containing unheated NaCas and NaCas heated at 120 °C as a function of storage time at 20 °C. The classified layer thickness was normalized by the corresponding continuous phase viscosity of the emulsion.

6.4.4 Rheological properties of heated NaCas-stabilized emulsions

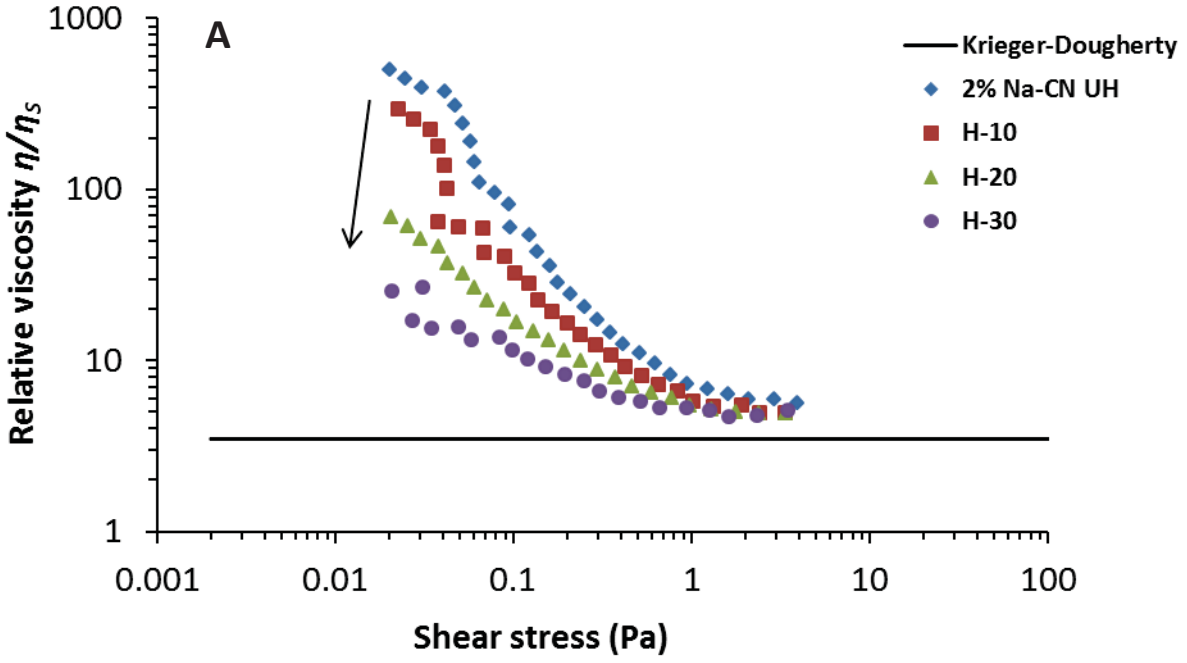

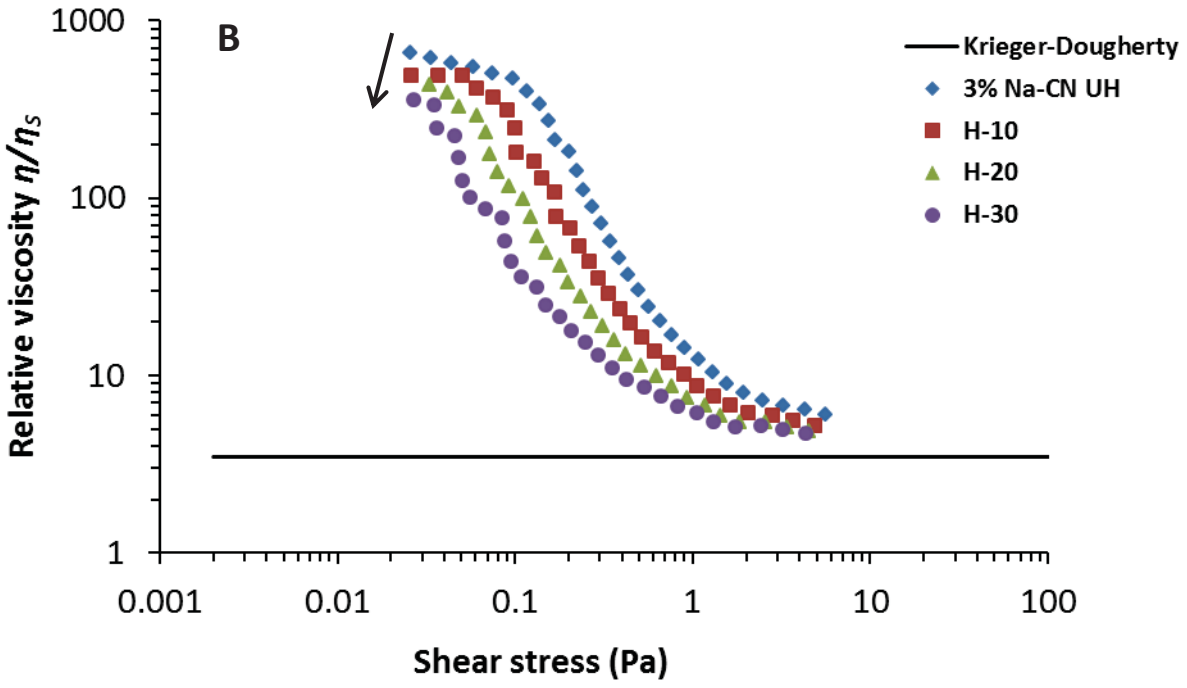

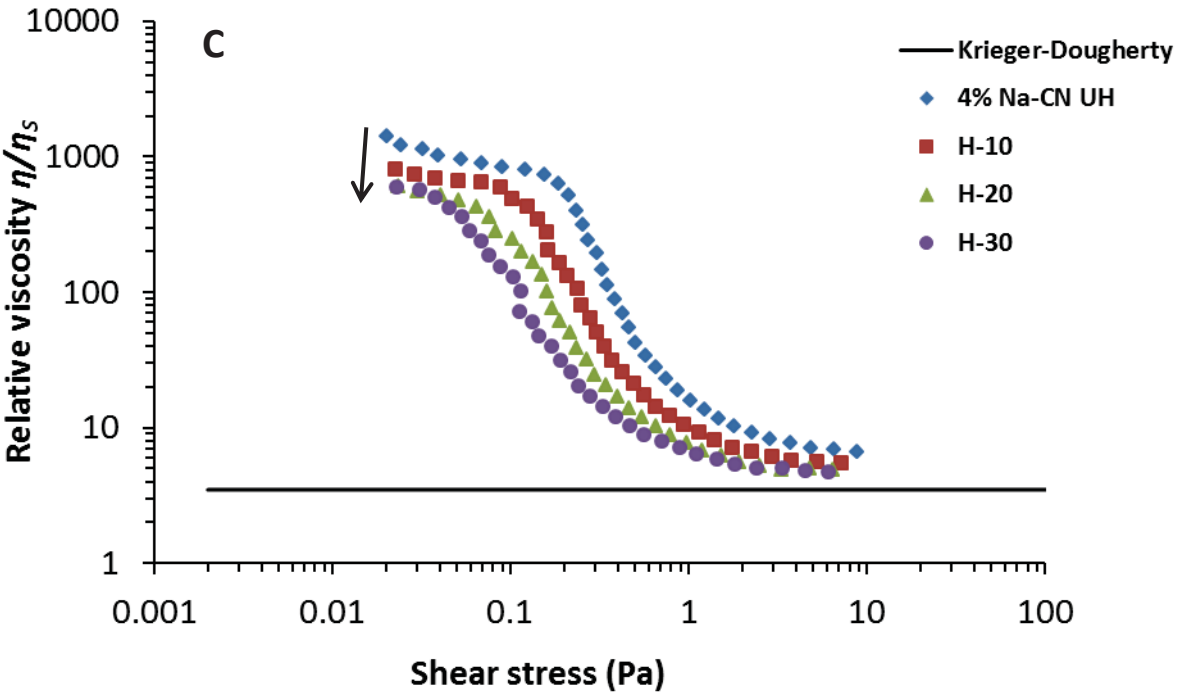
C
Krieger-Dougherty
4% Na-CN UH
H-10
H-20
H-30
Relative viscosity η/η_s
10000
1000
100
10
1
0.001
0.01
0.1
1
10
100
Shear stress (Pa)

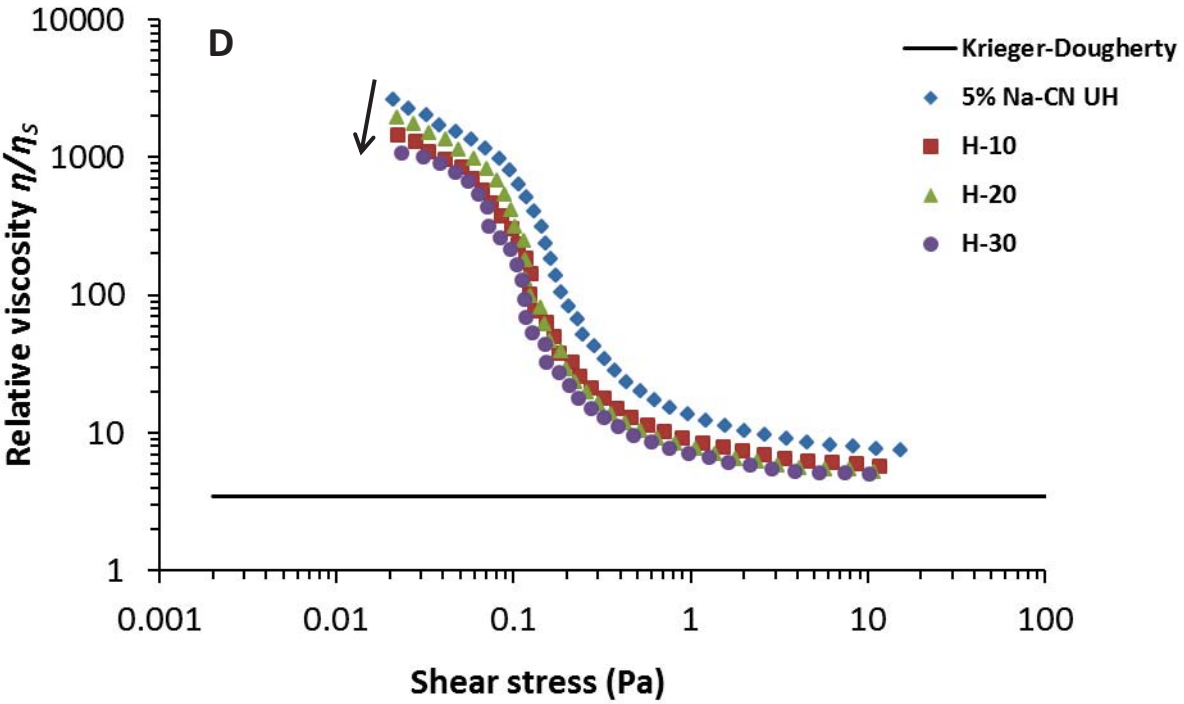
D
Krieger-Dougherty
5% Na-CN UH
H-10
H-20
H-30
Relative viscosity η/η_s
10000
1000
100
10
1
0.001
0.01
0.1
1
10
100
Shear stress (Pa)

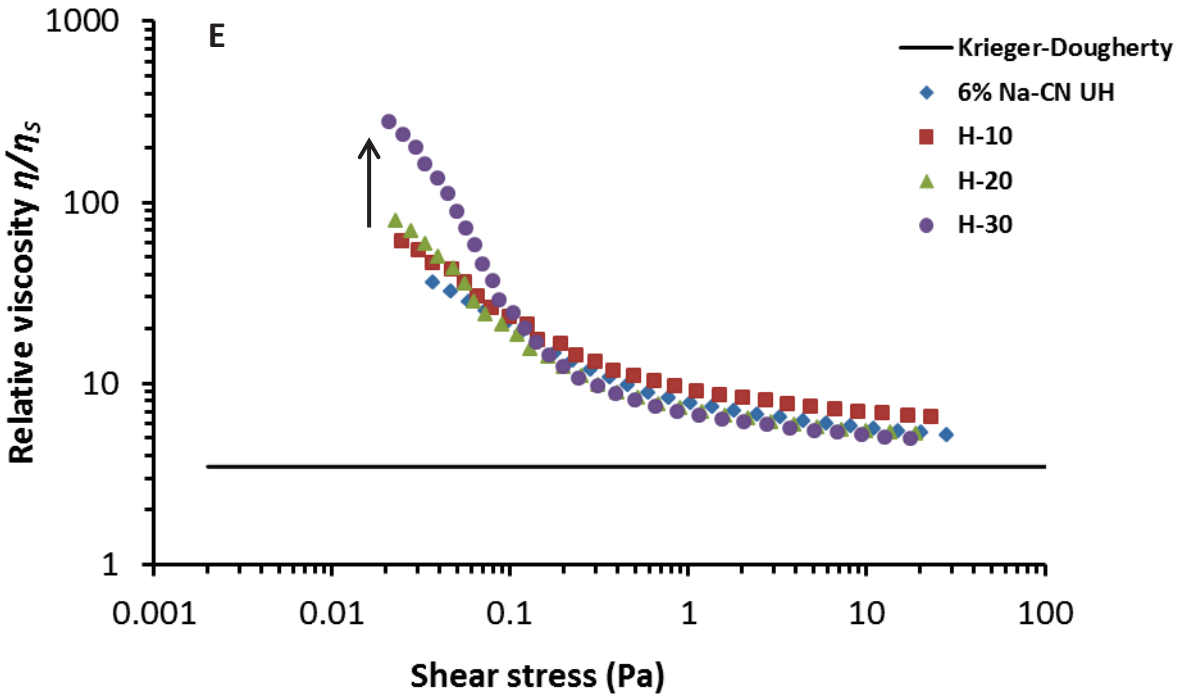

Figure 6.8. Relative viscosities of unheated and heated (120 °C, up to 30 min) (A) 2% w/w, (B) 3% w/w, (C) 4% w/w, (D) 5% w/w and (E) 6% w/w NaCas-stabilized 30% w/w oil-in-water emulsions as a function of shear stress at 20 °C. Samples were pre-sheared to eliminate any shear history and there was no equilibration time during measurement. The solid line is the prediction of the zero-shear relative viscosity of a polydisperse hard sphere dispersion of $\emptyset$ = 0.3, as calculated using the Krieger–Dougherty equation $\frac{\eta}{\eta_0} = (1 - \frac{\emptyset}{\emptyset_m})^{-[\eta]\emptyset_m}$.

The relative viscosity–shear stress curves for unheated and heated oil-in-water emulsions containing 2–6% w/w NaCas are shown in Figure 6.8. In general, all the unheated and heated NaCas-stabilized emulsions showed shear-thinning behavior. At low shear rates, the relative viscosities were high; at above critical shear stresses, the relative viscosities of the emulsions markedly decreased. This indicated the breakdown of a microstructural network. The low shear viscosities decreased as the heating time increased and reflected the weaker and less frequent droplet–droplet interactions in the space-filling droplet network induced by depletion attraction.

At high shear rates, the relative viscosities also decreased as a function of heating time, suggesting that the extent of depletion-induced droplet−droplet interactions decreased.

It can be seen that the relative viscosity of the 2% w/w NaCas-stabilized emulsion after heating for 30 min changed from shear-thinning behavior to more Newtonian-like behavior, which was similar to that for the non-interacting emulsion (1% w/w NaCas) reported in a previous study (Liang et al., 2014). For 6% w/w NaCas-stabilized emulsions, the low shear viscosity decreased after heating for 10 min and then increased after heating above 20 min. This possibly occurred because the depletion interaction potential decreases upon heat treatment and the subsequent formation of the depletion-induced droplet network becomes faster as, at above 5% w/w NaCas, the formation and the rearrangement of the space-filling droplet network have been shown to be influenced by the depletion interaction potential and the continuous phase viscosity (Liang et al., 2014). The fast droplet network formation of 6% w/w NaCas-stabilized emulsions after heating above 20 min was resolved by rheometer within the measurement timeframe; therefore the shear viscosity increased. The high shear rate viscosities of 6% w/w NaCas-stabilized emulsions showed a decreasing trend, indicating that the emulsion microstructure was sensitive to the depletion interaction potential.

It has been shown that the impact of the depletion interaction potential and the continuous phase viscosity on the structural changes during the development, rearrangement and reorganization of the droplet network can be monitored using oscillatory rheology. Figure 6.9 shows the dynamic structural change in 2%, 4% and 6% w/w NaCas-stabilized emulsions as a function of heating time at 120 °C. Depletion-flocculated emulsions initially undergo rapid space-filling droplet network formation, which results in an increase in relative viscosity; subsequently, the network rearranges and reorganizes to accommodate the gravitational stress (consolidation), which leads to a slight decrease in relative viscosity. The transient droplet network continues to coarsen and the trapped continuous phase within the droplet network eventually starts to diffuse to form the serum phase and the relative viscosity gradually increases (Liang et al., 2014; Moschakis et al., 2005). For the 2% w/w NaCas-stabilized emulsions, the peak in the relative viscosity was clearly observed in the unheated emulsion, then became less obvious and eventually disappeared after heating for 30 min. It was speculated that the structural change of very weakly attracted droplet clusters could not be resolved by the rheometer used in this study; the macroscopic phase

separation into two phases was observed as increased tailings only after 6 h of monitoring (Figure 6.9A). The peak in the relative viscosity in the 4% w/w NaCas-stabilized emulsions was markedly dependent on the heating time, and decreased as the heating time increased. After 12 h, the relative viscosity was higher for emulsions containing NaCas heated for ≥ 30 min, as shown by a threefold increase in droplet−droplet interactions (Figure 6.9B).

The decrease in relative viscosity correlated well with the shear flow curves and previous results presented in Chapter 5, suggesting that a weaker space-filling network formed after heating. Also, a weaker depletion-induced droplet network contained less volume fraction of unbound droplets and rearranged and reorganized more rapidly (Liang et al., 2014). As a result, the trapped continuous phase within the droplet network was released more rapidly to form the bulk serum phase, resulting in a higher relative viscosity. It was mentioned in Chapter 5 that τ depends on the depletion interaction potential and the continuous phase viscosity; the larger are these two parameters, the larger τ will be. The dynamic evolution of the microstructure of 4% w/w NaCas-stabilized emulsions shifted from left to right as a function of heating time, indicating that the extent of depletion flocculation diminished.

For 6% w/w NaCas-stabilized emulsions, the unheated emulsion showed considerably slower dynamics of the formation of a space-filling network and a peak in the relative viscosity was not observed (Figure 6.9C). As the heating time increased, the droplet−droplet interactions increased (~ fourfold increase in relative viscosity after heating for 60 min) and a peak in the relative viscosity became obvious after heating for > 30 min. It is known that NaCas-stabilized emulsions undergo slow dynamics of droplet network formation at NaCas concentrations of > 5% w/w; the heat-induced degradation of NaCas effectively switched the slow dynamics to fast dynamics of droplet network formation. In addition, in contrast to the 4% w/w NaCas-stabilized emulsions, the 6% w/w NaCas-stabilized emulsions containing NaCas heated from 20 to 40 min did not show a noticeable τ dependence and the dynamic evolution of the microstructure (a shift towards the right) was more obvious after 60 min of heating.

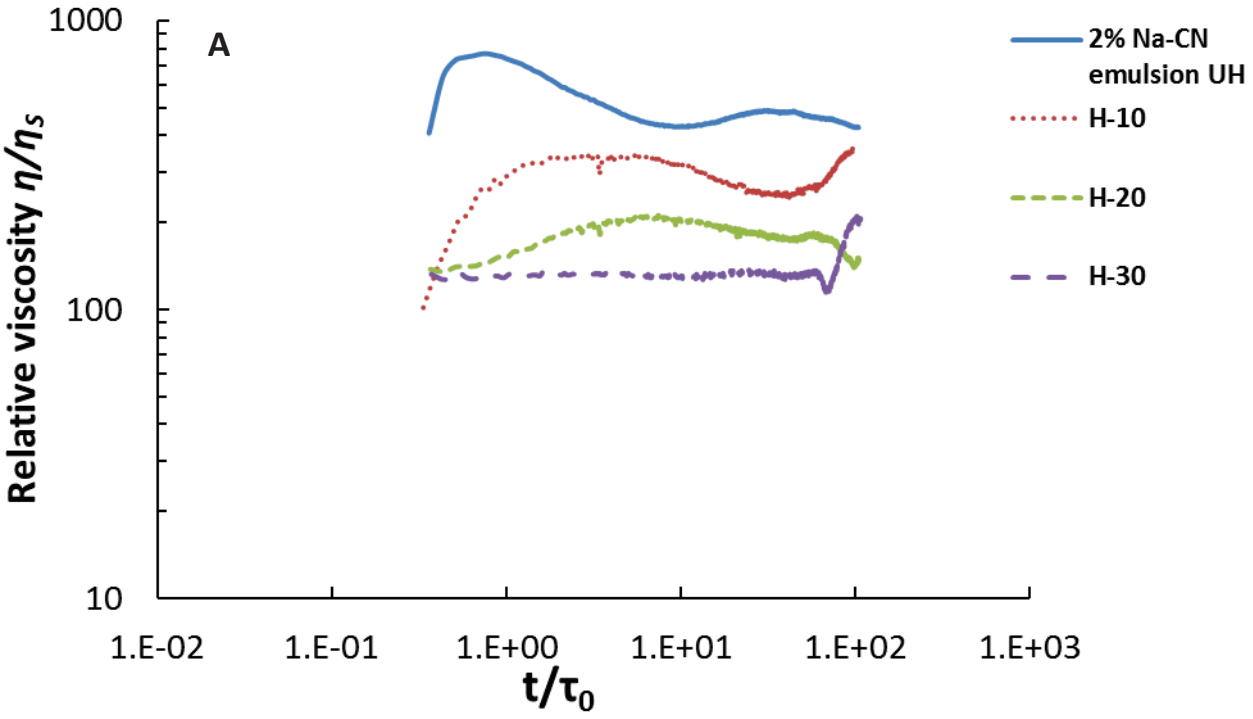
A
1000
100
10
Relative viscosity η/η_S
1.E-02
1.E-01
1.E+00
1.E+01
1.E+02
1.E+03
t/τ_0
2% Na-CN emulsion UH
H-10
H-20
H-30

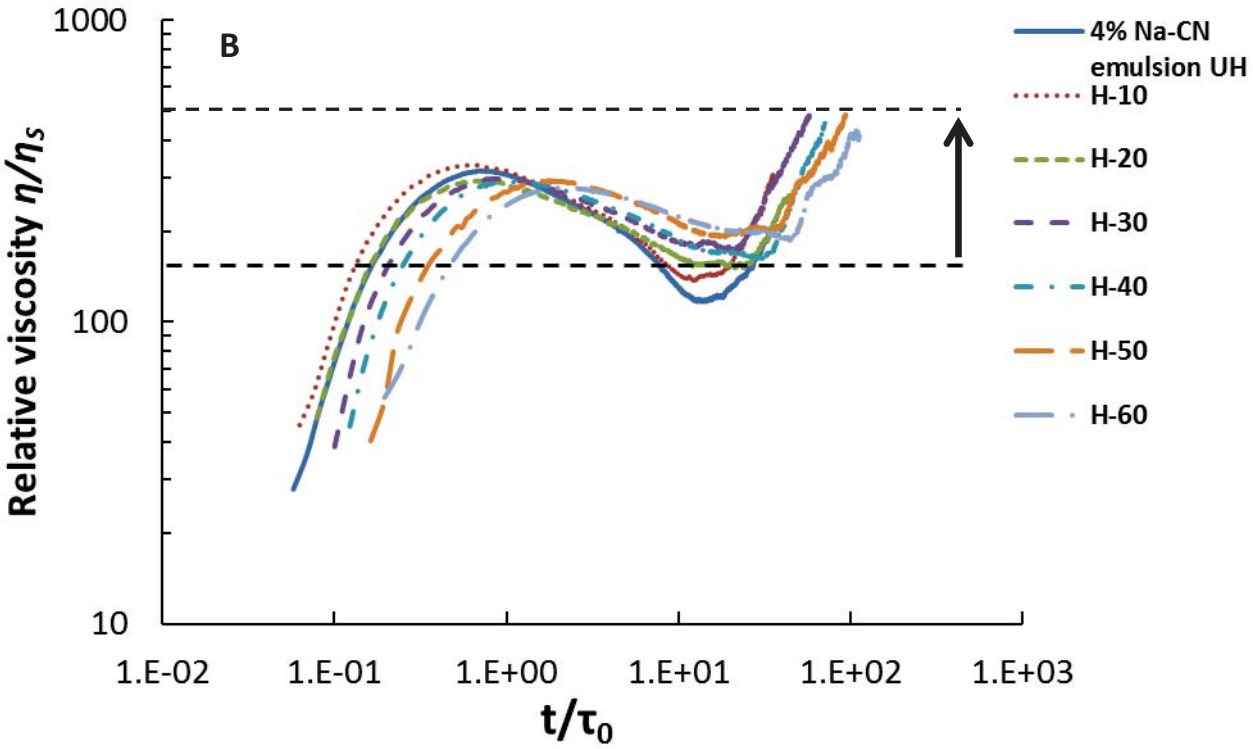
B
1000
100
10
Relative viscosity η/η_S
1.E-02
1.E-01
1.E+00
1.E+01
1.E+02
1.E+03
t/τ_0
4% Na-CN emulsion UH
H-10
H-20
H-30
H-40
H-50
H-60

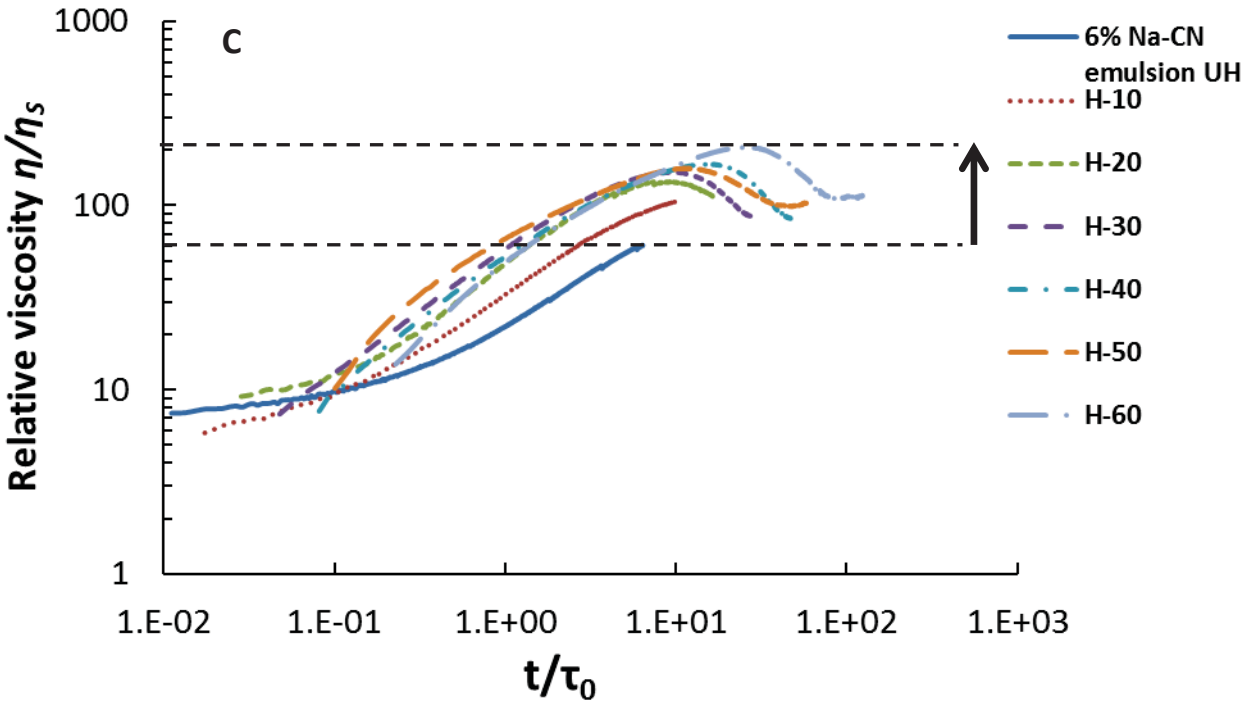

Figure 6.9. Relative viscosity (performed at 1 Hz, 0.5% strain, 20 °C) as a function of time for 2% w/w (A), 4% w/w (B) and 6% w/w (C) NaCas-stabilized emulsions containing unheated NaCas (solid line), and NaCas heated at 120 °C for 10 min (round dot), 20 min (square dot), 30 min (dash), 40 min (dash dot), 50 min (long dash) and 60 min (long dash dot).

6.5 Conclusions

This study investigated the impact of heat treatment on the phase separation behavior of NaCas-stabilized emulsions. Generally, the heat-induced degradation of NaCas modified the creaming kinetics and the rheological properties. It was found that the total solids content of the continuous phase had little effect on the extent of depletion flocculation. Heating NaCas at 120 °C effectively reduced the intact NaCas content, which was reflected in its reduced amount of intact caseins, particle size and viscosity. During heating, the reduction in the concentration of non-adsorbed NaCas that was caused by proteolysis diminished the depletion interaction potential and decreased the continuous phase viscosity. As a consequence, the volume fraction of bound droplets within the droplet network decreased and this caused rapid development of the space-

filling droplet network and subsequent structural rearrangement and reorganization, resulting in rapid phase separation. The small and large deformation rheology further showed the transition between slow and fast dynamics of the formation of space-filling networks. In future work, the attraction range and the contribution of α_{s1}-casein to the depletion interaction potential should be considered because the attraction range changes as the NaCas nano-particle size moves away from the optimum and the conformations of NaCas nano-particles can vary from non-spherical (rod-like, induced by α_{s1}-casein) to spherical (induced by α_{s1}-, β- and κ-casein). In future experimental work, the role of α_{s1}-casein in the depletion interaction potential could be studied in more detail.

Long term physical stability of depletion-induced weakly attractive emulsions can be tuned by making the "delay time" longer than the shelf life or by completely eliminating the depletion interaction potential. The results presented are useful for extending our understanding of the behavior of NaCas-stabilized emulsions under conditions that are close to commercial thermal processing environments. Such insights can be used to create novel droplet sizes and protein particle sizes to manipulate the droplet/protein size ratio and to maintain the desirable shear-thinning flow behavior at high protein concentrations.

Chapter 7: Effect of Carbohydrate Type and Concentration on the Heat-induced Behavior of Milk-Protein-Concentrate-Stabilized Oil-in-Water Emulsions [4]

7.1 Abstract

The influence of various carbohydrates, on the heat stability of a milk-protein-concentrate (MPC)-stabilized emulsion (10% w/w protein, 10% w/w oil) which has been identified as a stable emulsion to work with from Chapter 4 was studied. Regardless of carbohydrate type, the addition of carbohydrates during emulsification slightly increased the droplet diameter except the addition of 20−30% w/w maltodextrin significantly ($p < 0.05$) decreased the droplet diameter and was attributed to the larger change in disperse/continuous phase viscosity ratio. Generally, the addition of carbohydrate reduced the heat coagulation time (HCT) determined at 140 °C. The increased concentration of glucose, maltose, sucrose, and trehalose shifted the pH at heat stability maximum towards more acidic values whereas the increased concentration of maltodextrin shifted the pH at heat stability maximum towards more alkaline values. The extent of destabilization also varied between carbohydrates, with trehalose being particularly effective in retaining the original heat stability of the MPC-stabilized emulsion. Reducing carbohydrates (glucose, maltose, and maltodextrin) decreased the heat stability maximum more significantly than non-reducing carbohydrates (sucrose and trehalose). Particle size distribution, microstructure, and rheological measurements showed very good correlations with the heat stability.

[4] Part of the content presented in this chapter has been submitted as a original paper to *Food Hydrocolloids,41,* 332−342.

Part of the content was also presented as a graduate student poster presentation at ADSA-JAM Meeting, Phonenix, USA, 15−19 July 2012 and as a graduate student poster presentation at NZIFST, Hamilton, NZ, 26−28 June 2012.

7.2 Introduction

The interfacial protein type and the continuous phase protein type on emulsion stability and the potential protein−protein, droplet−droplet and droplet−protein interactions have been described in Chapter 4. Emulsion destabilization due to depletion effects seemed to be a common phenomenon in protein concentrated systems; the non-adsorbed protein concentration-dependent destabilization and restabilization behaviors were studied in more details using NaCas as the model protein in Chapters 5 and 6. It has been found that the size and concentrations of NaCas modulated the emulsion stability in a weakly flocculated system. The studies described in previous chapters attempted to understand the inter-particle interactions in a sole protein emulsion system. However, how milk proteins interact with other ingredients (i.e. carbohydrates) in a formulated food/dairy emulsion is not clear. The presence of a third ingredient is likely to influence the interactions between two other ingredients. In a heat treated system, the addition of a third ingredient may change the size or the amount of intact milk protein particle. Previously, the sole MPC-stabilized emulsion has been found to be heat stable and not showing any sign of depletion flocculation at 8.5% w/w protein (Chapter 4). Hence, the sole MPC-stabilized emulsion can be used as a model emulsion to study the effect of carbohydrate on the heat-induced protein−protein, droplet−droplet and droplet−protein interactions.

Carbohydrates are commonly used as functional ingredient in a number of food and pharmaceutical formulations. They are used, for instance, (1) to control the heat-induced denaturation and aggregation behavior of globular proteins in solution (Panzica, Emanuele, & Cordone, 2012) and in emulsion (Kim, Decker, & McClements, 2003; Kulmyrzaev, Bryant, & McClements, 2000), (2) to improve heat stability of milk and concentrated milk (Holt, Muir, & Sweetsur, 1978; Tan-Kintia & Fox, 1996), (3) to prevent cold protein denaturation (Xiong, 1997), (4) to improve freeze–thaw stability (Ghosh, Cramp, & Coupland, 2006) or (5) to control the texture and stability of food emulsions (Álvarez-Cerimedo et al, 2010; Chanamai & McClements, 2000; Li, Fu, Luo, & Huang, 2013). Carbohydrate in the form of lactose is present in condensed milk in high concentrations. Condensed milk is converted to Dulce de leche via retort heating. Condensed emulsions are good model systems for studying this process and may open pathways to create caramelized products that fill the pourable to the solid spectrum.

The heat stability of protein solutions or protein-based emulsions is often studied as a function of the initial pH and reported using heat coagulation time (HCT) (McSweeney, Mulvihill, & O'Callaghan, 2004; Rattray & Jelen, 1997; Singh, 2004; van Boekel, Nieuwenhuijse, & Walstra, 1989b, 1989c). The HCT is the time required for a heat-induced coagulum to become visible during heating in an oil bath. It indirectly measures the resistance of milk proteins against heat-induced coagulation (Singh, 2004; Walstra, Wouters, & Geurts, 2006a). The HCT of milk is largely dependent on initial heating pH and protein concentration. As total solid concentration increases in skim milk, there are progressive changes in the nature of the HCT-pH profile. In concentrated milk, the HCT decreases as the protein concentration increases (7.0−9.0% protein) and the heat stability minimum shifts towards more acidic values and the stability remains low at all pH values above about 6.8−7.0 (Fox & McSweeney, 1998; Singh, 2004).

The combination of the mechanism framework of heat-induced changes in the micelles and in the serum phase described in van Boekel, Nieuwenhuijse and Walstra's study (1989a) and that described in Vasbinder and de Kruif's (2003) and Anema and Li's (2003) studies will be used to qualitatively interpret the experimental data on heat-induced destabilization of MPC-stabilized emulsions (Figure 7.1). Anema has reported that a larger extent of dissociation of casein especially κ-casein was detected at lower pH and at higher temperatures (above 80 °C) as the milk was concentrated (1998). In recent studies on the heat stability of concentrated micellar casein solutions (8.0% protein) which contain negligible whey proteins found that casein dissociation occurred even without the presence of whey proteins. The dissociation enhanced as pH increased above 6.9 for all caseins, with larger extent of dissociation for κ-casein and β-casein (Sauer & Moraru, 2012). In this study, the aim is to build upon the knowledge gained in the previous chapters and obtain qualitative information on the heat-induced behavior of oil droplets and continuous phase proteins in high protein and carbohydrate conditions and to elucidate the possible mechanism(s) of the instabilities.

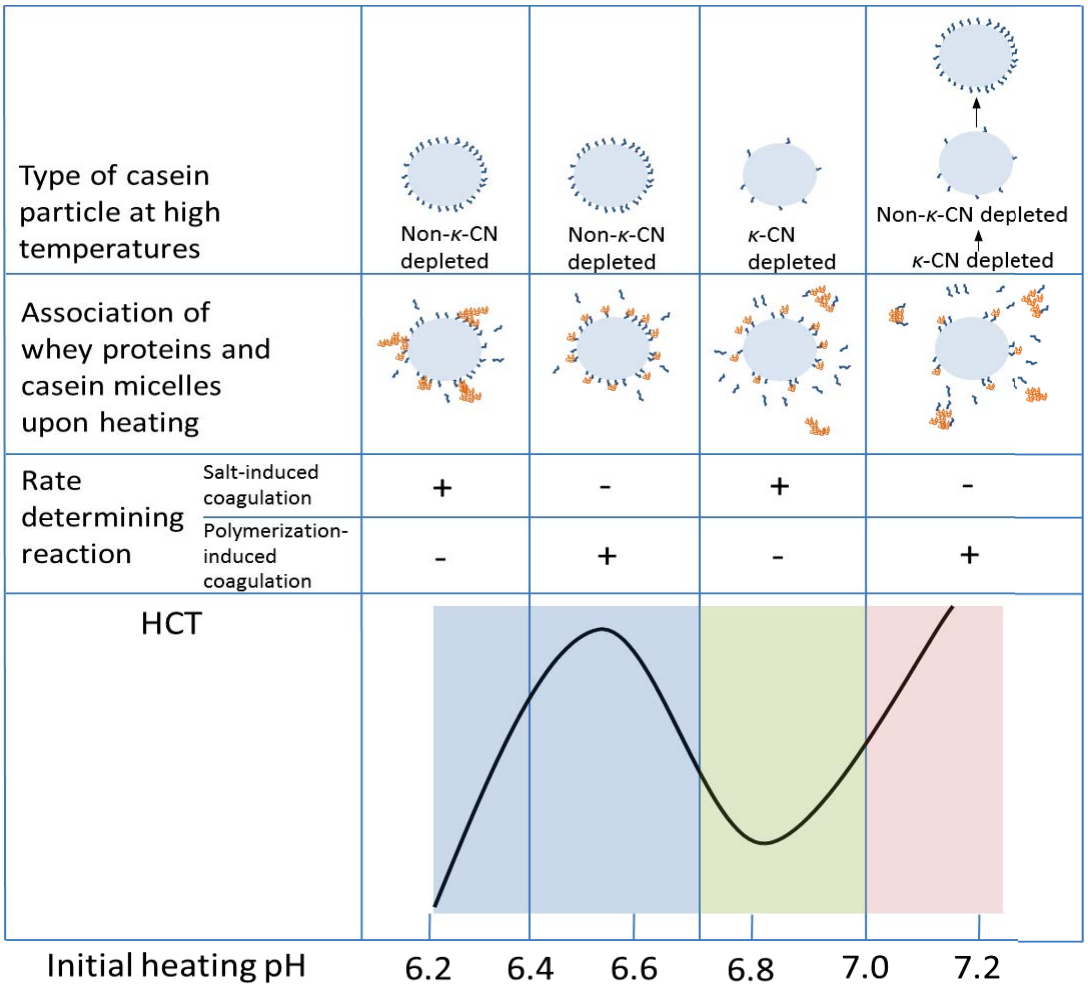

Figure 7.1. Schematic illustration of the effect of initial heating pH on the type of casein particle at high temperature, on the casein−whey protein interactions, on the type of rate determining reaction and on the HCT (Anema & Li, 2003; van Boekel et al., 1989a; Vasbinder & de Kruif, 2003).

7.3 Materials and methods

7.3.1 Materials

MPC 4850 (MPC) was obtained from Fonterra Co-operative Group Ltd, Auckland, New Zealand. Glucose, maltose hydrate, and trehalose dihydrate were obtained from Sigma Chemical

Co. (St Louis, MO, USA). Maltodextrin (Md 180) with a dextrose equivalent (DE) value of 18 was obtained from Grain Processing Corporation (Muscatine, IA, USA).

7.3.2 Prepration of model emulsions

The model emulsions were prepared following the procedure described in Figure 7.2. The molar concentrations of the different carbohydrates are shown Table 7.1. Taking the range of droplet size of model emulsions into account, the amount of adsorbed proteins at oil/water interface was calculated to be 1.35 ± 0.15 g using the experimentally determined surface coverage of MPC 4850, 13.19 ± 1.49 mg/m^3. The non-adsorbed protein concentration was estimated to be ~ 9.62% w/w in a 10% oil-in-water emulsion containing 10% w/w MPC. In this study, a 10% w/w MPC solution was prepared for the evaluation of the heat stability for the corresponding continuous phase of the emulsion. It was also assumed that the casein−whey protein ratio of the adsorbed proteins had negligible effect on the heat stability of the continuous phase. Sodium azide (0.02% w/w) was added to the samples as an antimicrobial agent. All samples were stored at 4 °C for 1−7 days until further use. Each sample was prepared at least in triplicate.

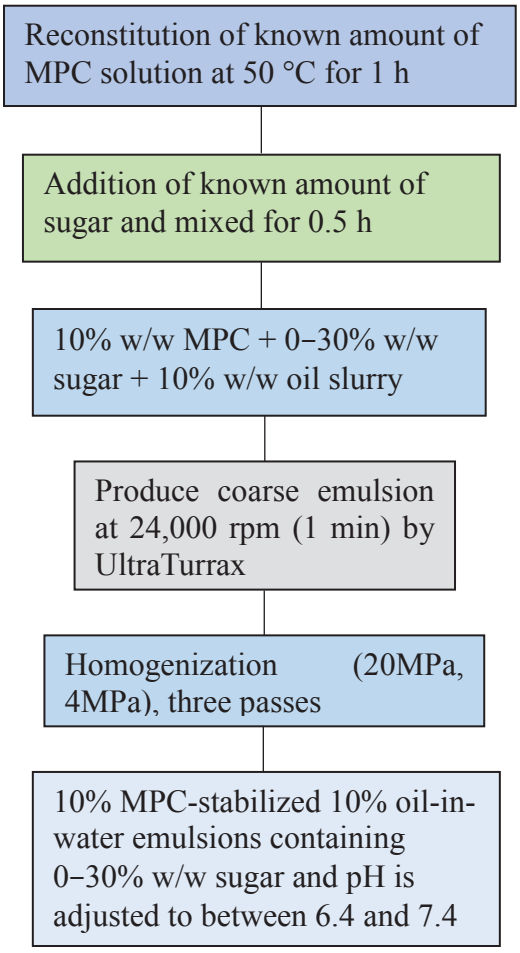

Figure 7.2. Flow chart of the preparation of model emulsions (10% w/w protein, 10% w/w oil and 0−30% w/w carbohydrate).

Table 7.1. Molar concentration for different carbohydrate types at concentrations used in this study.

		Weight (g/kg)		
		100	200	300
Carbohydrate type	Molecular weight (g/mol)	Molar concentration (M)		
Glucose	180.2	0.6	1.1	1.7
Maltose	342.3	0.29	0.58	0.88
Sucrose	342.3	0.29	0.58	0.88
Trehalose	342.3	0.29	0.58	0.88
Maltodextrin (DE 18)	1000	0.10	0.20	0.30

7.3.3 Determination of heat coagulation time (HCT)

The time required for coagulation of the sample or precipitation to become visible throughout the sample was recorded as the heat coagulation time (HCT).The procedure described in Chapter 3, Section 3.2.5).

7.3.4 Determination of heat-induced changes of model emulsions

The heat stability of the model emulsions was determined as the procedure described in Chapter 3, Section 3.2.5). All samples were removed between 1 and 20 min and were immediately cooled under running cold water. The large aggregates that appeared in heated samples were diluted with NaOH (1 M, pH 8.0), a disodium ethylenediamine tetra-acetate (EDTA)/polysorbate 20 (Tween 20) mixture (0.04 mol kg^{-1} and 5 g kg^{-1}), urea (6 mol kg^{-1}) and sodium dodecyl sulphate (SDS) (100 g kg^{-1}). The solubility was checked visually after 24 h.

7.3.5 Determination of particle size distributions of protein solutions and emulsions

The particle size and droplet size measurements were carried out using procedures described in Chapter 3, Section 3.2.3.

7.3.6 Calcium-ion activity measurement

The calcium ion activity of MPC emulsions and MPC solutions was measured with a pH meter (PHM220, Radiometer Pacific Ltd, Auckland, New Zealand) with a mV reading to one decimal place using a calcium ion electrode (ISE25Ca, Radiometer Pacific Ltd) and a double junction reference electrode (REF251, Radiometer Pacific Ltd). Calibration was conducted at 20 °C with standard solutions containing 0.5, 1, 2, 3, 4, 5, and 10 mM calcium/L (as $CaCl_2$) and 8 mM potassium chloride/L. The calcium electrode was held in a stock solution of 1 mM $CaCl_2$/L and

the reference electrode was held in a stock solution of 8 mM potassium chloride/L for at least 60 min before the calibration was performed.

7.3.7 Rheological properties of model emulsions

Details of the rheological measurement of emulsions have been described in Chapter 3, Section 3.2.6. To describe and to compare the extent of aggregation from one sample to another, a viscosity index determined at shear rate (1 s^{-1}) was used to indicate the attractiveness between unheated and heated samples. η_t/η_0 = viscosity determined after a heat treatment/ viscosity before a heat treatment. Oscillatory rheology was performed to track the structural changes in selected heat-induced emulsions in more detail. An aliquot (20 mL) of emulsion sample was gently poured into the cup and a layer of mineral oil was added to prevent water evaporation during the measurement. The sample was subjected to a heating and cooling cycle (20→90→20 °C) at a constant rate of 3 °C/min. The experiment was conducted at a frequency of 1 Hz and at a strain of 0.01. The gelation time was determined to be when G' exceeded 1 Pa (McCarthy, Kelly, O'Mahony, & Fenelon, 2014). Steady-state flow measurements were also conducted after the heating and cooling cycle. All the rheological measurements were performed twice and mean values of viscosity were obtained from duplicate samples.

7.3.8 Microstructure of model emulsions

Details of the confocal scanning laser microscope and transmission electron microscope characterization techniques have been described in Chapter 3, Section 3.2.8.

7.3.9 Statistical analysis

All experiments were carried out at least in triplicate using freshly prepared samples and the results are reported as the mean and standard deviation of these measurements. The experimental data were analyzed by Student's t-tests using Microsoft Excel 2007 (Microsoft Corporation,

Redmond, WA, USA) and significant differences among the means were determined at a 95.0% confidence level.

7.4 Results and discussion

7.4.1 Effect of carbohydrate type and concentration on the droplet size formation of model MPC-stabilized emulsions

The primary droplet diameters of freshly prepared MPC-stabilized emulsions with and without added carbohydrate are shown in Table 7.2. The primary surface-weighted mean diameter ($d_{3,2}$) and the volume-weighted mean diameter ($d_{4,3}$) of the droplets in the control MPC-stabilized emulsion were 0.64 (± 0.02) μm and 1.03 (± 0.03) μm, respectively. Emulsions containing glucose, maltose, sucrose, and trehalose formed slightly larger droplets than the control emulsion regardless of the carbohydrate concentration. Álvarez-Cerimedo and co-workers (2010) found that the addition of trehalose caused a reduction in the droplet diameter of sodium-caseinate-stabilized emulsions at a similar volume fraction of oil, because of strong protein−carbohydrate interactions. In our case, the addition of trehalose did not result in a significant reduction in the mean droplet diameter of the MPC-stabilized emulsion. However, the addition of maltodextrin resulted in a slight increase and then a marked decrease in the mean droplet diameter. At a maltodextrin level of 30% w/w, the $d_{3,2}$ and $d_{4,3}$ values of the emulsion were reduced significantly to 0.37 (± 0.10) μm and 0.58 (± 0.13) μm, respectively.

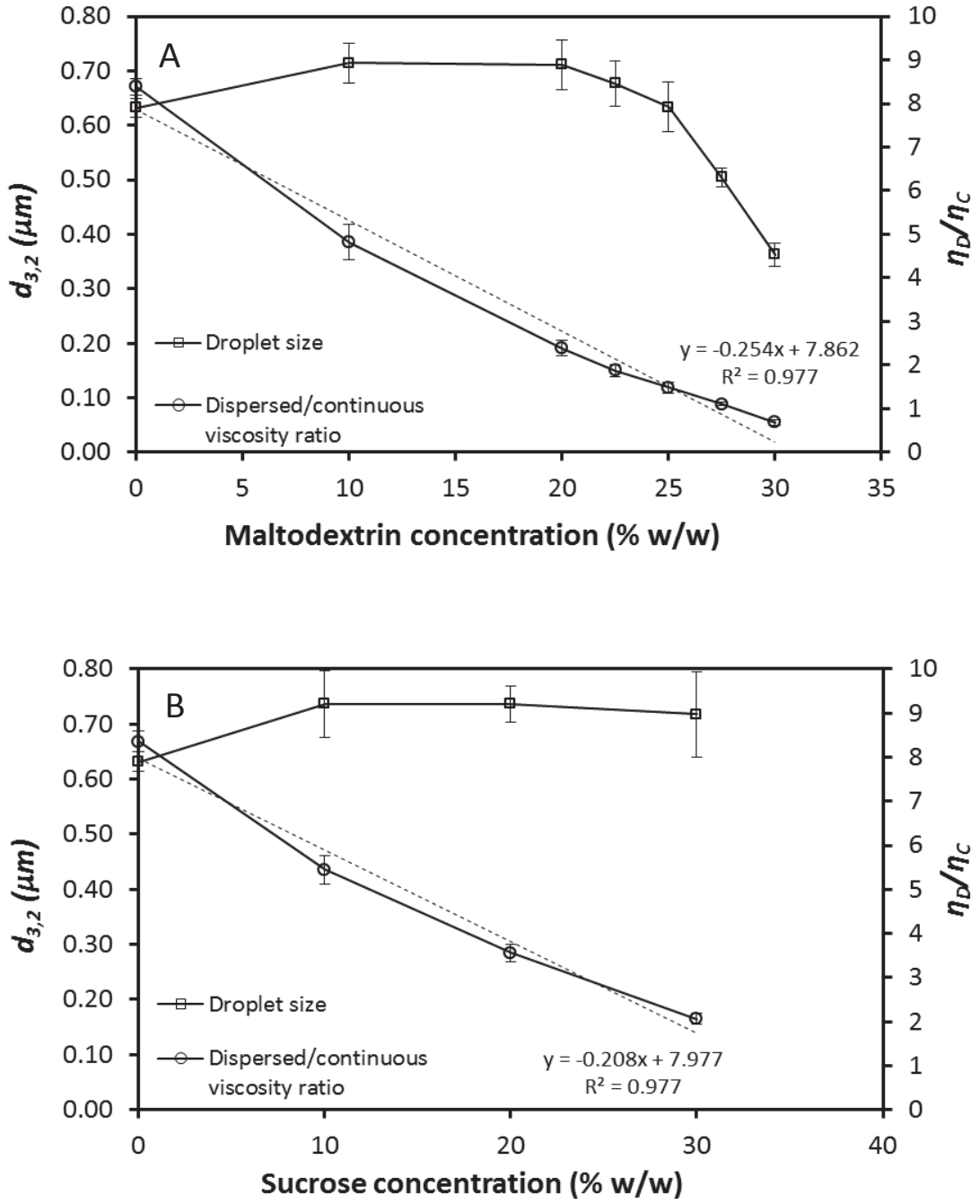

Figure 7.3. Effect of carbohydrate content (A) maltodextrin, (B) sucrose on the volume-weighted droplet size ($d_{4,3}$) (square symbol) and η_D/η_C ratio (viscosity of dispersed phase/viscosity of continuous phase which was determined within the Newtonian region between shear rate 1 to 1000 s^{-1}) (round symbol) of MPC-stabilized oil-in-water emulsions (10% w/w oil).

It has been reported that the viscosity ratio (dispersed/continuous) of an emulsion influences the droplet size from emulsification; the lower the ratio, the smaller the droplet size (Lee & Norton, 2013; Qian & McClements, 2011; Wooster, Golding, & Sanguansri, 2008). In order to test this hypothesis, the influence of the ratio of the viscosities of dispersed and continuous phases (η_D/η_C) on the droplet break-up was tested further by adding maltodextrin in a narrower concentration between 20 and 30% w/w (Figure 7.3A). The continuous phase viscosity was increased through addition of maltodextrin to each emulsion and the η_D/η_C ratio followed a linearly decreasing trend (R^2 = 0.978). However, the change in droplet size did not follow a linear trend. The droplet size was independent of the η_D/η_C ratio from 10 to 20% w/w maltodextrin. The droplet size showed a gradual decreasing trend with addition of maltodextrin between 20 and 25% w/w and it followed a sharp decreasing trend between 25 and 30% w/w maltodextrin. This result was in a good agreement with the literature which observed a minimum droplet size within the optimum viscosity ratio range (η_D/η_C = 0.5−5) for droplet break-up under simple shear flow condition (Lee & Norton, 2013; Wooster, Golding, & Sanguansri , 2008).

The difference between carbohydrate types on the droplet size break-up was also compared using sucrose (See Figure 7.3B). Similar to the effect of maltodextrin, addition of sucrose resulted in a linear relationship (R^2 = 0.977) between carbohydrate content and η_D/η_C ratio. Generally, the effect of sucrose resembled the other carbohydrate types investigated because of the impact on the continuous phase viscosity was similar, with η_D/η_C ratio above 2 at 30% w/w carbohydrate content. The contribution of 30% w/w sucrose on viscosity was roughly equivalent to that of 20% w/w maltodextrin. The η_D/η_C ratio dependency on droplet size break-up upon addition of maltodextrin between 20 and 30% w/w was not shown in emulsions containing sucrose at the same carbohydrate concentration probably because the η_D/η_C ratio did not reach the critical point (< 2). The present results suggest that not only the protein−carbohydrate interactions but also the viscosity ratio (dispersed/continuous) influence the emulsification process.

Table 7.2. Primary droplet diameters, $d_{3,2}$ and $d_{4,3}$ (μm), of MPC-stabilized oil-in-water emulsions (10% w/w protein, 10% oil w/w) with and without the addition of different types of carbohydrate.

Emulsion samples	Droplet size (μm) $d_{3,2}$	$d_{4,3}$
MPC-stabilized emulsion with no added carbohydrate	0.64 ± 0.02[a]	1.03 ± 0.03[a]
Glucose		
10%	0.74 ± 0.04[b]	1.28 ± 0.14[b]
20%	0.72 ± 0.03[b]	1.24 ± 0.16[b]
30%	0.75 ± 0.04[b]	1.19 ± 0.11[b]
Maltose		
10%	0.74 ± 0.05[b]	1.26 ± 0.08[b]
20%	0.74 ± 0.05[b]	1.19 ± 0.12[b]
30%	0.73 ± 0.04[b]	1.17 ± 0.12[b]
Sucrose		
10%	0.75 ± 0.05[b]	1.31 ± 0.13[b]
20%	0.76 ± 0.04[b]	1.30 ± 0.05[b]
30%	0.72 ± 0.06[b]	1.13 ± 0.11[b]
Trehalose		
10%	0.74 ± 0.04[b]	1.23 ± 0.11[b]
20%	0.74 ± 0.06[a]	1.19 ± 0.16[a]
30%	0.69 ± 0.03[a]	1.04 ± 0.06[a]
Maltodextrin		
10%	0.70 ± 0.06[a]	1.12 ± 0.05[a]
20%	0.64 ± 0.04[a]	0.96 ± 0.02[a]
30%	0.37 ± 0.10[c]	0.58 ± 0.13[c]

[a,b,c] Means within the same column and having the same superscript are not significantly different from the control by Student's t-test at $p < 0.05$.

7.4.2 Heat stability of MPC solutions with added carbohydrate

The heat-induced casein micelle/whey protein interactions occurred in milk was expected to take place in a similar manner in a MPC solution since MPC contains similar components to that found in milk, caseins and whey proteins, in their native forms and also colloidal ash, calcium phosphate (O'Regan, Ennis & Mulvihill, 2009). The HCT−pH profile of 10% w/w MPC solution

is different from that of concentrated milk and the heat stability maximum was at pH 7.0 rather than at pH 6.5 for concentrated milk. At the same protein concentration, concentrated milk will contain higher concentration of lactose and mineral (especially free ionic calcium content). Both lactose and mineral content affect the HCT of milk and concentrated milk. It has been shown that the addition of $CaCl_2$ decreases the heat stability of concentrated milk (Huppertz, 2006). It can be postulated that the concentrated MPC solution would have better heat stability due to the reduction of ionic calcium content. Secondly, the heat-induced oxidation of lactose to organic acids accounts for 50% of the pH decrease. The rapid drop of pH causes the decreased heat stability of concentrated milk (Singh, 2004). The addition of reduced sugar like lactose to a model emulsion 2 in McSweeney's study (2004) causes a shift of heat stability maximum towards more acidic pH values. This will explain why the heat stability maximum of 10% w/w MPC solution is around pH 7.0 rather than 6.5 in concentrated milk.

The HCT−pH profiles of 10% w/w MPC solutions containing different types of carbohydrate added at 0−30% w/w are compared in Figure 7.4. They had similar shapes to that of the control 10% w/w MPC solution but different heat stability maximum values. With the addition of 10% w/w carbohydrate, the heat stability maximum of the MPC solution shifted from pH 7.0 to pH 6.8 for glucose, maltose, sucrose, and trehalose but was unaffected for maltodextrin. In the presence of 20% w/w carbohydrate, the shape of the HCT−pH profile and the heat stability maximum of the MPC solution containing trehalose were unaffected whereas the other MPC solutions were affected. In general, the HCT decreased with the increase in carbohydrate concentration. The pH at the heat stability maximum of the MPC solution containing sucrose did not change comparing to 10% addition of carbohydrate. However, the addition of glucose and maltose shifted the maximum to a more acidic value (pH 6.6) whereas the addition of maltodextrin shifted the maximum to a more alkaline value (pH 7.2). When the carbohydrate concentration was further increased to 30% w/w, the HCT decreased for all carbohydrate types, however, some samples seem to have no significant difference compared to those at 20% w/w carbohydrate. The addition of glucose and maltose reduced the heat stability in the region of the maximum and the HCT was less dependent on the initial heating pH in the pH region 6.6−7.4. The heat stability maximum shifted to a more acidic value (from pH 6.8 to 6.6) on the addition of

sucrose. The addition of maltodextrin continued to shift the maximum to a more alkaline value (pH 7.2−7.4), but no clear maximum was observed.

The decrease in the HCT and the shift in the heat stability maximum to more acidic values can be partially explained by the increase in protein concentration in the continuous phase as the carbohydrate concentration was increased. Figure 7.5A shows that the HCT decreased in the region of the heat stability maximum and the heat stability maximum shifted to a more acidic pH value with increasing MPC concentration. The former phenomenon is consistent with previous results (Cruijsen, 1996; Sievanen, Huppertz, Kelly, & Fox, 2008). Figure 7.5B indicates that there is a clear linear decline trend in the heat stability maximum of a MPC solution as protein concentration increases. It was assumed that the weight of the water phase of a MPC solution decreased upon addition of carbohydrate and it will affect the HCT. The addition of carbohydrate regardless of carbohydrate type was shown to decrease the heat stability maximum of MPC solutions (Figure 7.5B).

The extent of change in the HCT varied among the carbohydrate types. A shift in the pH of the heat stability maximum has also been observed in concentrated milk with the addition of sodium chloride (Huppertz & Fox, 2006a, 2006b). Reduced heat-induced dissociation of micellar κ-casein and increased micellar hydration have been attributed to the shift of the heat stability maximum to a more alkaline value and the increase in the maximum HCT at a higher pH value (Huppertz et al., 2006a). Bridging due to the Maillard reaction is often observed when reducing carbohydrate is present during heating, especially at high pH values (Ashoor & Zent, 1984; Cruijsen, 1996). The heated MPC solutions containing 30% w/w maltodextrin showed less browning than those containing 30% w/w glucose at all pH values, see inset in Figure 7.4C (maltose as well, data not shown). The color difference suggested that the Maillard reaction in maltodextrin containing samples has less contribution to the HCT.

The heat-induced particle aggregation in the heated samples with and without added carbohydrate was evaluated by determining the effective particle diameter in the MPC solutions after heat treatment (120 °C) at pH 6.8 (Figure 7.6). The MPC solutions containing 30% w/w maltodextrin were very susceptible to heat treatment. In all cases, aggregation was visible to the naked eye during heating-up period, which made it inappropriate to be measured using dynamic

light scattering. The MPC solutions containing 30% w/w glucose or maltose showed strong aggregation after 10 min of heating, and complete coagulation with noticeable aggregates after 20 min of heating. The heated control samples had an effective diameter of 174.08 ± 6.5 nm, which is very similar to that of the unheated MPC solution reported in Ye's study (2011). After heat treatment at 120 °C for 10 min, the effective particle diameter for casein micelles in MPC solution containing glucose was 427.2 ± 16.7 nm, more than twice the size detected in the control. The effective diameter of heated MPC solution containing sucrose after heating at 120 °C for 20 min was 218.5 ± 3.4 nm, slightly larger than the size measured in the control. For the same heating time, the effective diameter of the MPC solution containing trehalose (183.7 ± 4.1 nm) was very comparable with that of the control. The observed change in the particle size has a good agreement with the HCT data, showing fewer propensities for aggregation of MPC solutions containing non-reducing carbohydrate, particular for trehalose.

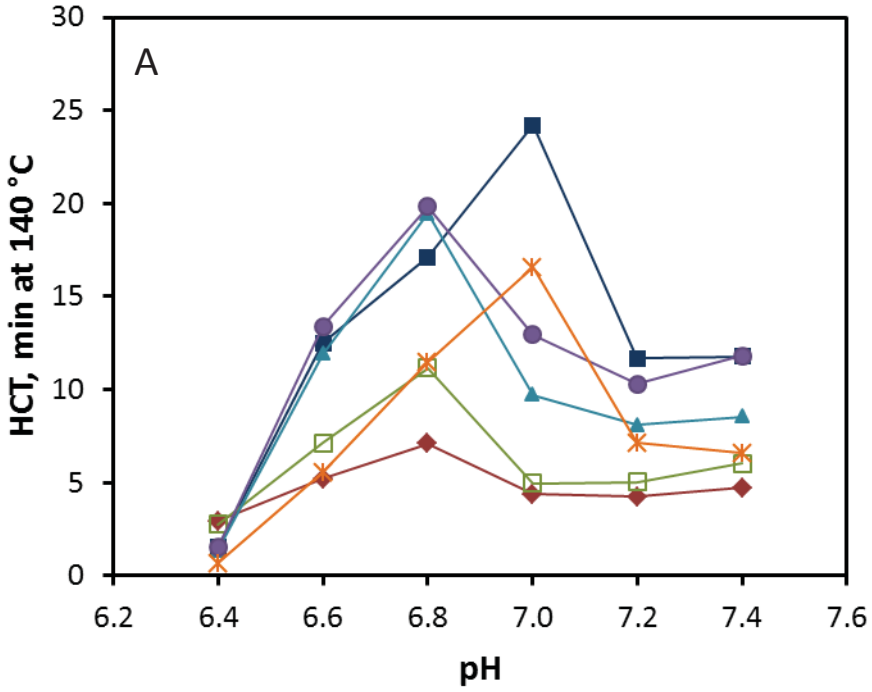

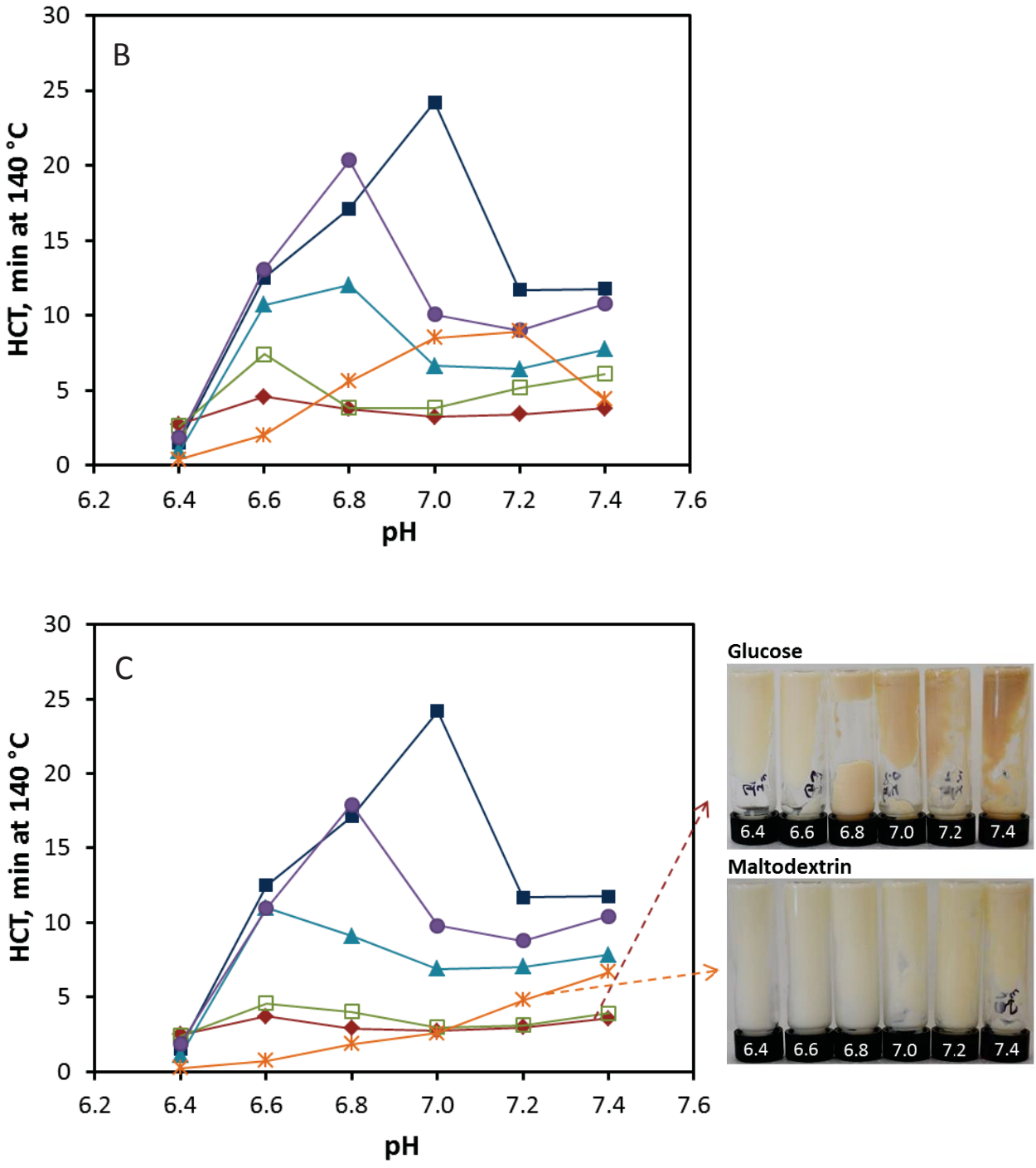

Figure 7.4. HCT−pH profiles of 10% w/w MPC solutions: with no added carbohydrate (■) and with addition of (A) 10% w/w, (B) 20% w/w, (C) 30% w/w glucose (♦), maltose (□), sucrose (▲), trehalose (●), and maltodextrin (✳). Visual images showed the color of the heated MPC solutions containing glucose and maltodextrin as a function of pH, respectively.

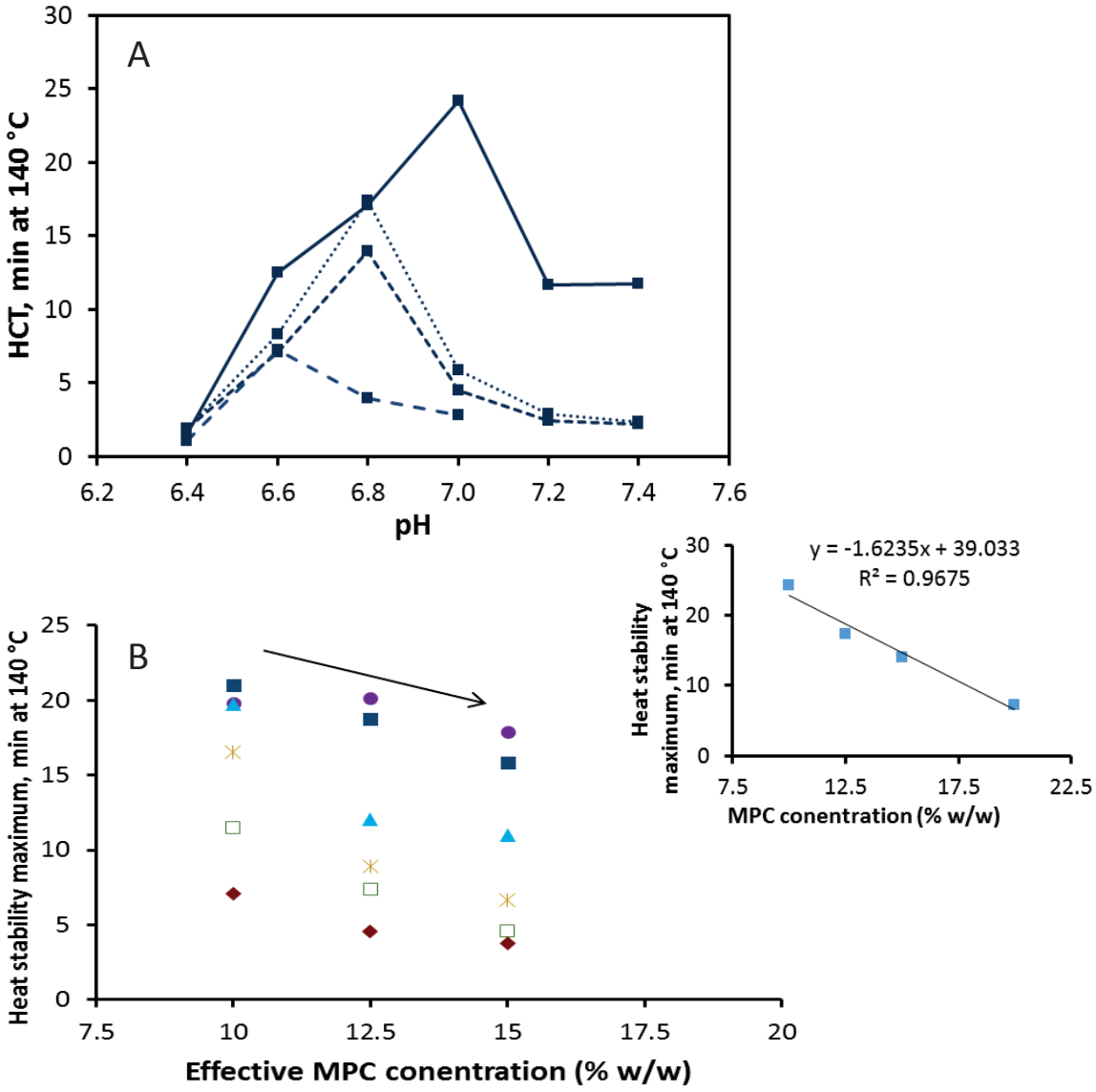

Figure 7.5. (A) HCT−pH profiles of MPC solutions at protein concentrations of 10% w/w (solid line), 12.5% w/w (round dot), 15% w/w (square dot), and 20% w/w (dash dot). (B) The effect of protein concentration on the heat stability maximum of MPC solutions with no added carbohydrate (■) and with the addition of 10−30% of glucose (♦), maltose (□), sucrose (▲), trehalose (●), and maltodextrin (✳). Heat stability maximum was obtained from Figure. 4. The effective protein concentration of MPC solutions was calculated based on the protein concentration in the water phase in which the weight of carbohydrate was excluded. Inset: heat stability maximum obtained from Figure. 5A was plotted as a function of MPC concentration.

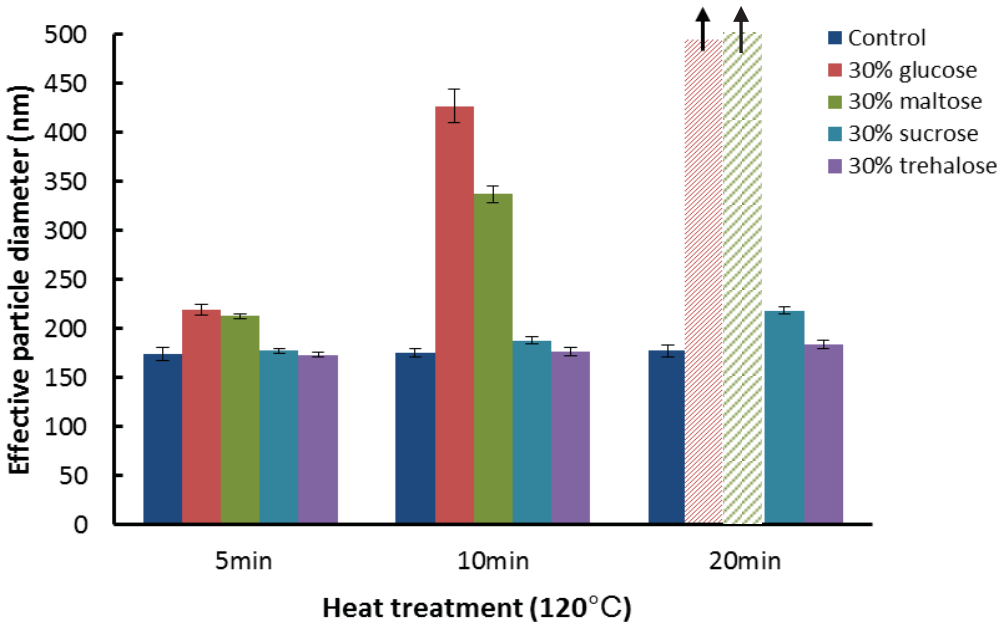

Figure 7.6. Particle size of 10% w/w MPC solutions with and without added carbohydrate after heat treatment (120 °C) at pH 6.8. Plotted are intensity-based effective mean diameters. The patterned filled bars indicate the samples contain large aggregates and the arrows indicate the effective particle diameters of the aggregates are outside the detection limit.

7.4.3 Heat stability of model MPC emulsions with added carbohydrate

The HCT of the control 10% w/w MPC-stabilized emulsion was lower than that of MPC solution over the entire pH range and the heat stability maximum shifted from pH 7.0 to pH 6.8 (Figure 7.7). In general, across the entire pH range, adding carbohydrates decreased the HCT of the 10% w/w MPC-stabilized emulsions. The addition of 10% w/w trehalose and sucrose to the emulsions slightly decreased HCT while 10% w/w added maltodextrin decreased the heat stability further still. The shapes of the HCT−pH profiles of trehalose and sucrose were similar while maltodextrin shifted the heat stability maximum from pH 6.8 to pH 7.0. The addition of 10% w/w glucose and maltose decreased the heat stability markedly and shifted the heat stability maximum from pH 6.8 to pH 6.6 (Figure 7.7). When trehalose and sucrose levels were increased to 20% w/w, the heat stability of the emulsions decreased by ~ 8 min. However, the maximum heat stability occurred over a broader pH range for sucrose. The heat stability generally

decreased slightly with the addition of 20% w/w glucose, maltose, and maltodextrin; the HCTs of the emulsions with added glucose and maltose showed less dependence on the initial heating pH whereas the emulsion with added maltodextrin had a similar shaped HCT−pH profile to the MPC solution containing the same amount of maltodextrin. The addition of 30% w/w carbohydrate decreased the heat stability further. The heat stability maximum of those containing trehalose occurred over a broader pH range (6.8−7.4). The shapes of the HCT−pH profiles in MPC-stabilized emulsions containing glucose, maltose, and maltodextrin were similar to those of the oil-free phase of MPC emulsions.

The reduced HCT in MPC-stabilized emulsions compared with the solution systems resembled the heat stability change between milk and homogenized milk (Sweetsur & Muir, 1983). Upon adsorption, the casein micelles partially spread at the oil/water interface into smaller fragments and may redistribute at the interface. Some *κ*-casein molecules may adsorb directly at the interface. It can be assumed that the oil droplets behave like large casein micelles as they are stabilized by intact casein micelles and some large micellar fragments. The *κ*-casein is still the main component governing the steric stability for the oil droplets, as such, the large oil droplets act as *κ*-casein-depleted casein micelles as they may contain few *κ*-casein molecules per unit area at the oil/water interface (Sharma & Singh, 1999; Singh, Fox, & Cuddigan, 1993; Singh, Sharma, Taylor, & Creamer, 1996). It was observed that the *κ*-casein of adsorbed casein micelles had a greater tendency to dissociate into the continuous phase in the pH range 6.3−6.7 than the *κ*-casein that dissociates from bulk casein micelles upon high temperature heating (i.e., > 130 °C). Even a small reduction of *κ*-casein content from the oil droplets that are already short of *κ*-casein content will have a considerable impact on the heat stability (Singh et al., 1996). Therefore, in addition to the concentration effect which was described in Section 7.4.2, those aforementioned physicochemical changes of adsorbed casein micelles are also attributed to a lower heat stability of emulsions.

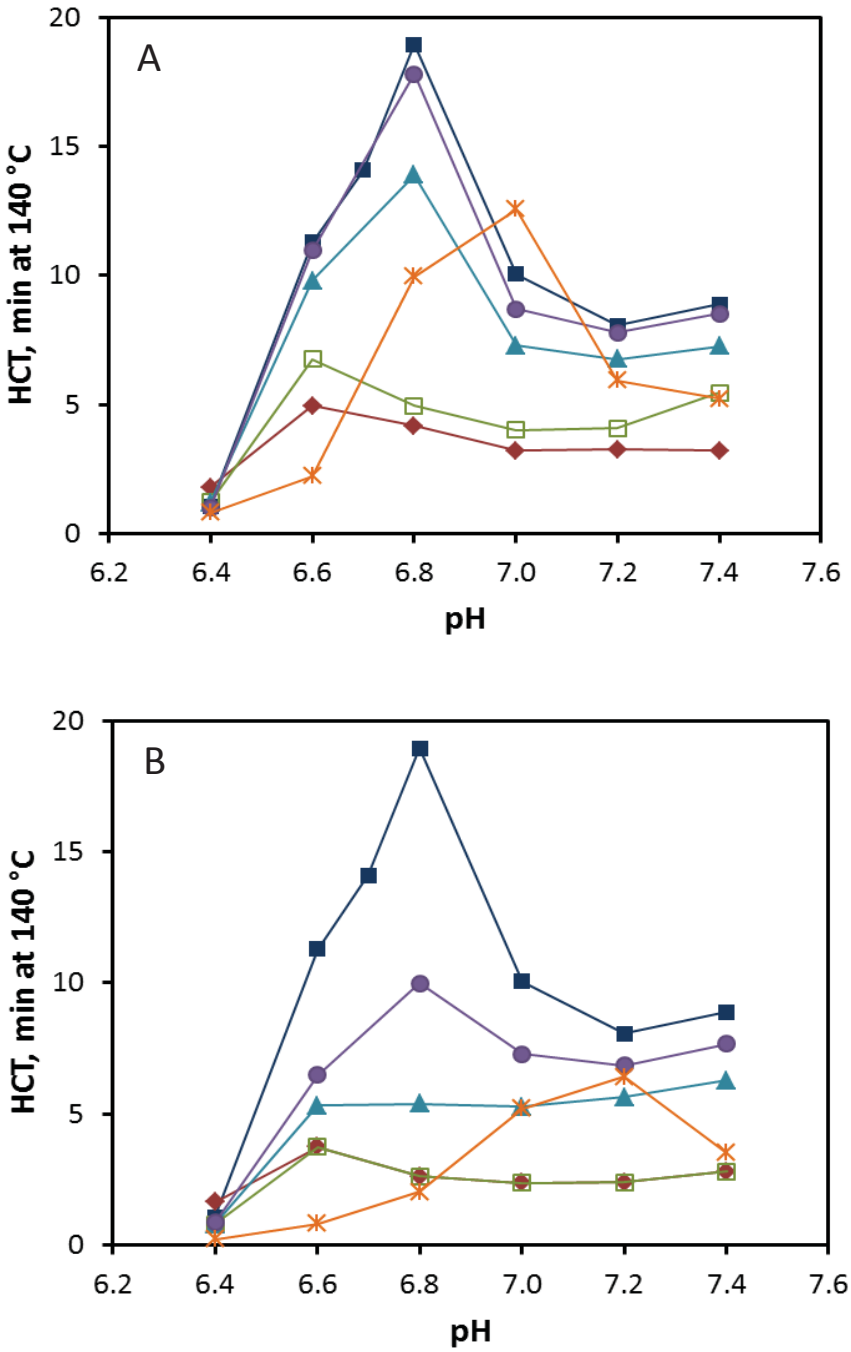
A
HCT, min at 140 °C
pH
20
15
10
5
0
6.2
6.4
6.6
6.8
7.0
7.2
7.4
7.6
B
HCT, min at 140 °C
pH
20
15
10
5
0
6.2
6.4
6.6
6.8
7.0
7.2
7.4
7.6

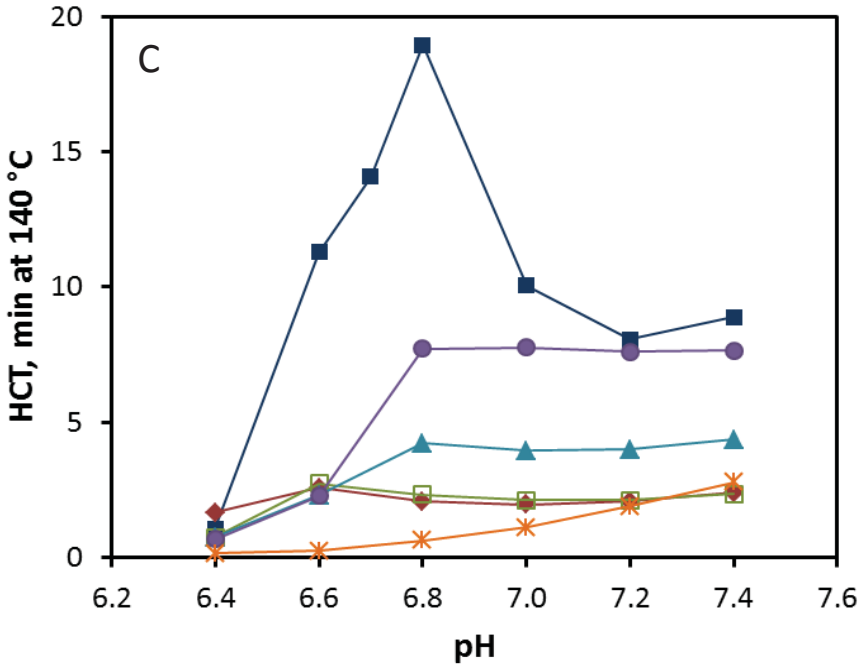

Figure 7.7. HCT−pH profiles of MPC-stabilized oil-in-water emulsions (10% w/w protein, 10% w/w oil): with no added carbohydrate (■) and with the addition of (A) 10% w/w, (B) 20% w/w, (C) 30% w/w glucose (♦), maltose (□), sucrose (▲), trehalose (●), and maltodextrin (✳).

7.4.4 Correlation between particle size, microstructure and rheological properties of heated MPC emulsions with added carbohydrate

The effect of heat treatment at 120 °C on the physicochemical changes of MPC-stabilized emulsions containing 30% w/w carbohydrate was also studied. Figure 7.8 shows an example of particle size distribution of heated MPC-stabilized emulsions containing carbohydrate. All the unheated MPC-stabilized emulsions showed a population of casein micelles and a second population of oil droplets. As the heating time increased, the particle size distribution of the emulsion changed from bimodal to multi-modal. The additional mode showed large particles rather than individual droplets, indicating aggregation of casein micelles, droplets and mixtures of both. The population of those aggregates generally grew in number and diameter and there was a corresponding decrease in the number of casein micelles and droplets. It has been reported that the heat-induced inter-particle interactions of an oil-in-water emulsion include those

between interfacial proteins, between interfacial proteins and non-adsorbed proteins and between non-adsorbed proteins (Dalgleish, 2006; Euston, Finnigan, & Hirst, 2000; Liang et al., 2013b). The non-adsorbed unfolded globular proteins play an important role in the formation of large aggregates during heating (Euston, Al-Bakkush, & Campbell, 2009; Euston et al., 2000; Nikiforidis & Kiosseoglou, 2007). Aggregation of MPC-stabilized emulsions can be understood in three key phenomena: (1) Nucleation; (2) Growth. Clusters form from individual casein micelles and droplets and they increase the diameter of aggregates; (3) Aggregation of aggregates. The aggregation phenomena are explained elsewhere (van Boekel, Nieuwenhuijse, & Walstra, 1989a), but not the focus of this thesis.

In general, the effect of heat treatment on the particle size of MPC-stabilized emulsions without and with added carbohydrate was consistent with the change in microstructure and rheology. Given this consistency, only the essential features of the aggregation are presented. Aggregates are described by their relative volume in the distribution and the peak size and confocal micrographs were presented occasionally to demonstrate similarities and differences. In MPC-stabilized emulsion systems, heat-induced bridging was expected, unlike the colloidal system described in Chapter 5, where aggregates are in equilibrium with single droplets. Aggregates here do not redisperse. The adhesion of protein−protein and droplet−droplet is too strong due to the presence of covalent bonds. The lack of redispersion was evident by the fact that large aggregates were not fully dissolved in the dissociating agent (1 mM of Tween 20 and 12.8 mM of EDTA, pH 10).

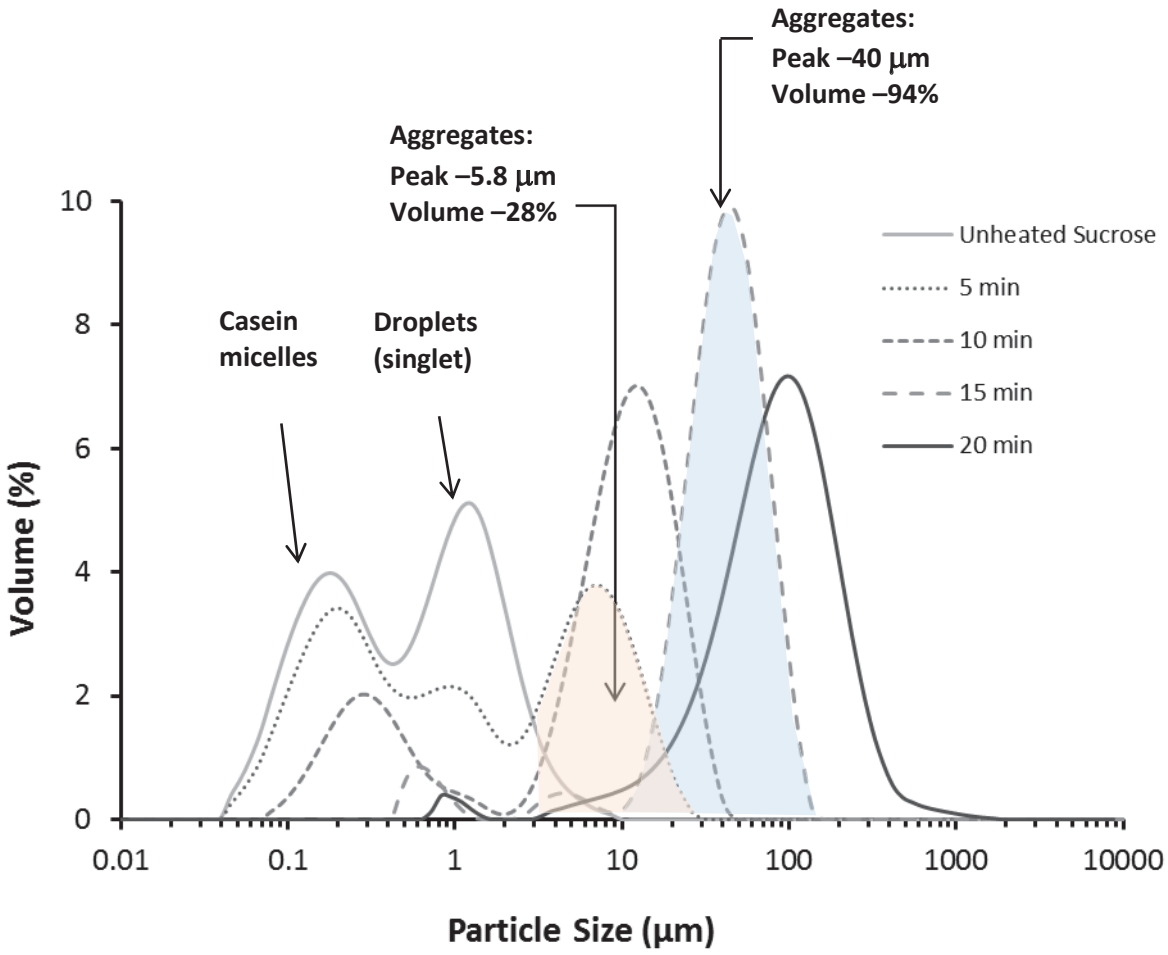

Figure 7.8. Effective particle size distributions of MPC-stabilized oil-in-water emulsions (10% w/w protein, 10% w/w oil) with and without 30% w/w sucrose unheated and heated (at pH 6.8) at 120 °C for the times indicated. Shaded region indicates how aggregates are described in other figures.

Here, the viscosity index (η_t/η_0) is used to indicate the aggregation of the samples. For the MPC emulsions containing glucose and maltose, there was little change in particle size during the initial stage of heating (Figure 7.9A). The peak size of aggregates in maltose samples increased from 5 to 60 µm with a volume that increased from 4 to 91% during heating from 3 to 5 min. The corresponding viscosity index increased steadily with increased heating time. In glucose samples, the peak size of aggregates increased more rapidly from 5 µm at 4 min of heating to 158 µm after 5 min of heating. Correspondingly, the viscosity index increased markedly from 1.7 at 2 min of heating to 961 after 5 min of heating, which is more than 8 times higher than that of a

weakly attractive colloid as calculated from the extracted viscosity data from Liang et al. (2014). The differences between glucose and maltose indicate a significant difference in steric stability with less steric stability in the glucose sample. From 4 to 5 min, the volume of aggregates is similar but a big increase in size occurred due to aggregation of aggregates. During the same time interval, maltose samples showed a steady loss of droplets with increasing aggregation size, no clear indication of a particular aggregation mechanism dominating. As it can be seen from the confocal micrographs, the droplets of glucose containing sample aggregated into clusters and appeared to be associated within a gel-like network. On the other hand, the maltose containing sample had more homogeneous droplet distributions at the same heating intervals than glucose, however, with further heating towards the HCT (~ 6.5 min), the microstructure was essentially similar to that for glucose. The sudden jump in viscosity index with a marked increase in peak size of aggregates and an open gel-like structure with increased amount of void area is a common feature in these systems. A dramatic jump in aggregation indicates steric stability has fallen below a critical level, and perhaps associates with the loss of steric stability with a rate of reaction like the sharp increase in gelation kinetic of casein micelles during acidification (Vasbinder, van de Velde, & de Kruif, 2004).

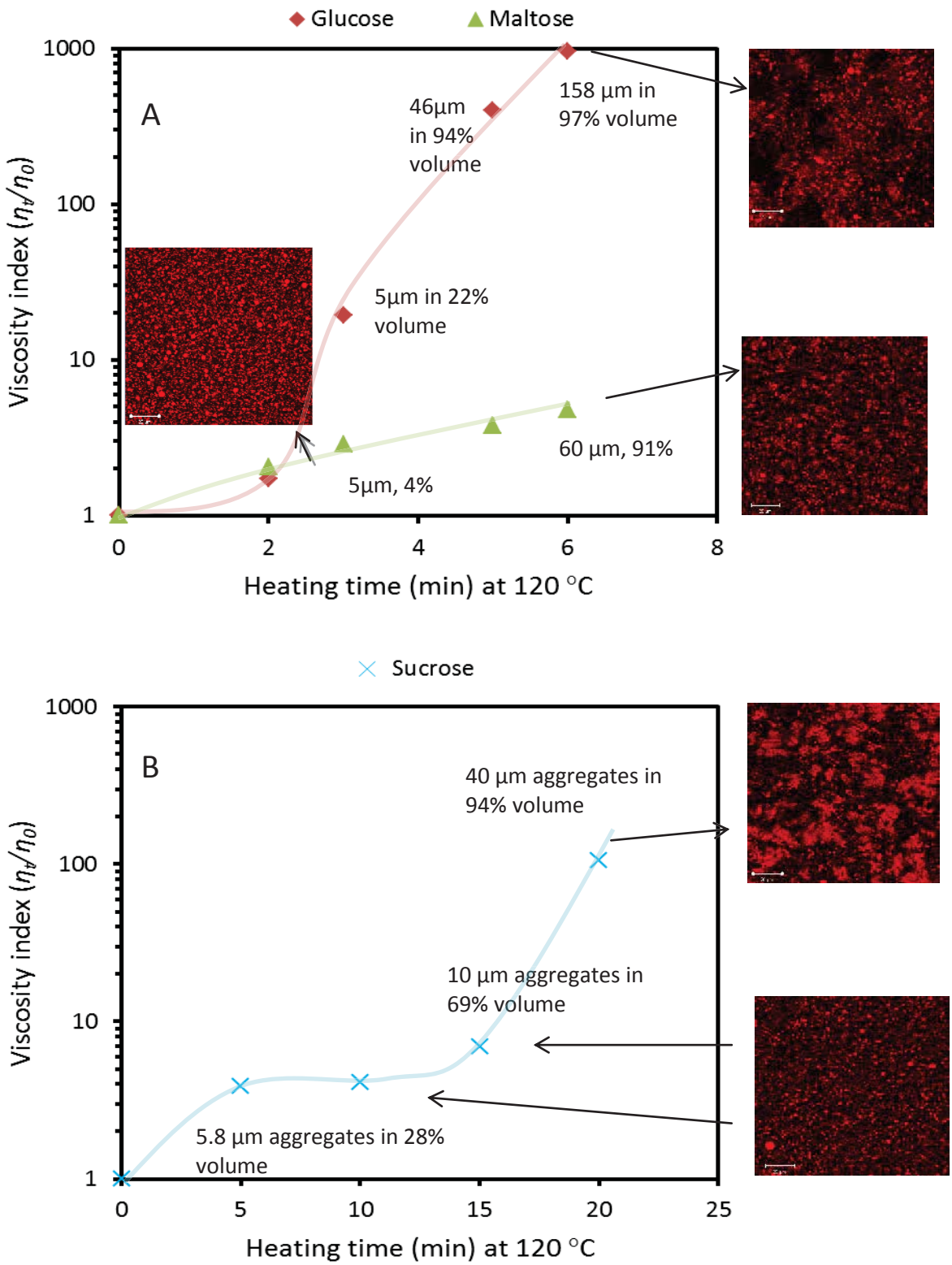
Glucose
Maltose
A
Viscosity index (η_r/η_0)
1000
100
10
1
0
2
4
6
8
Heating time (min) at 120 °C
46µm in 94% volume
158 µm in 97% volume
5µm in 22% volume
5µm, 4%
60 µm, 91%
Sucrose
B
40 µm aggregates in 94% volume
10 µm aggregates in 69% volume
5.8 µm aggregates in 28% volume
0
5
10
15
20
25

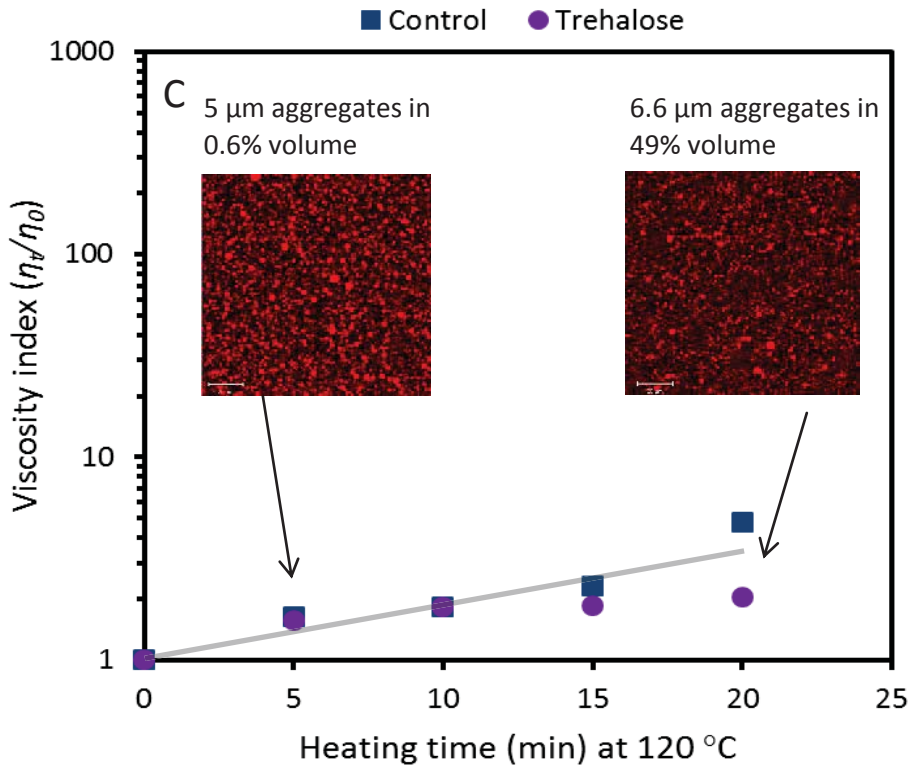

Figure 7.9. Aggregation time lines of the heat-induced physicochemical changes of model MPC emulsions in terms of particle size, microstructure and rheological properties. Viscosity index of unheated and heated (120 °C, pH 6.8) MPC-stabilized oil-in-water emulsions (10% w/w protein, 10% w/w oil) with and without 30% w/w added carbohydrate at 20 °C: (A) glucose (♦) and maltose (■); (B) sucrose (▲); (C) control (■) and trehalose (●). Confocal micrographs show the fat signal only, scale is identical in all images with 20 µm scale bars. Data labels indicate the essential features size and volume taken from particle size distributions of Figure 7.8. The lines are drawn to guide the eye.

For the other reducing carbohydrate, maltodextrin, all samples (2, 4, 6 min) formed a visible coagulum upon heating at 120 °C and no further particle size measurements were performed. It is important to note that the MPC-stabilized emulsion with added maltodextrin had a larger droplet/particle size even before heating. Figure 7.10 shows that the two major peaks shifted towards larger sizes, suggesting that some large aggregates may have formed and that they were not disrupted by dilution and shear. These large aggregates also appeared in MPC-maltodextrin mixed solution (data not shown). However, this phenomenon was not seen with the addition of

10% and 20% w/w maltodextrin. These large aggregates dissociated with the addition of the dissociating agent [a solution containing 3.75 g/L disodium ethylenediamine tetra-acetate (EDTA) and 1.25 g/L polysorbate 20 (Tween-20)], when the primary droplet size was measured (Table 7.2). The particle size result suggests that a bridging-type droplet/protein flocculate has formed and that it is probably linked by non-covalent bonds (Cruijsen, 1996). It has been shown that bridging-type flocculation of droplets are more susceptible to heat-induced destabilization (Liang et al., 2013a).

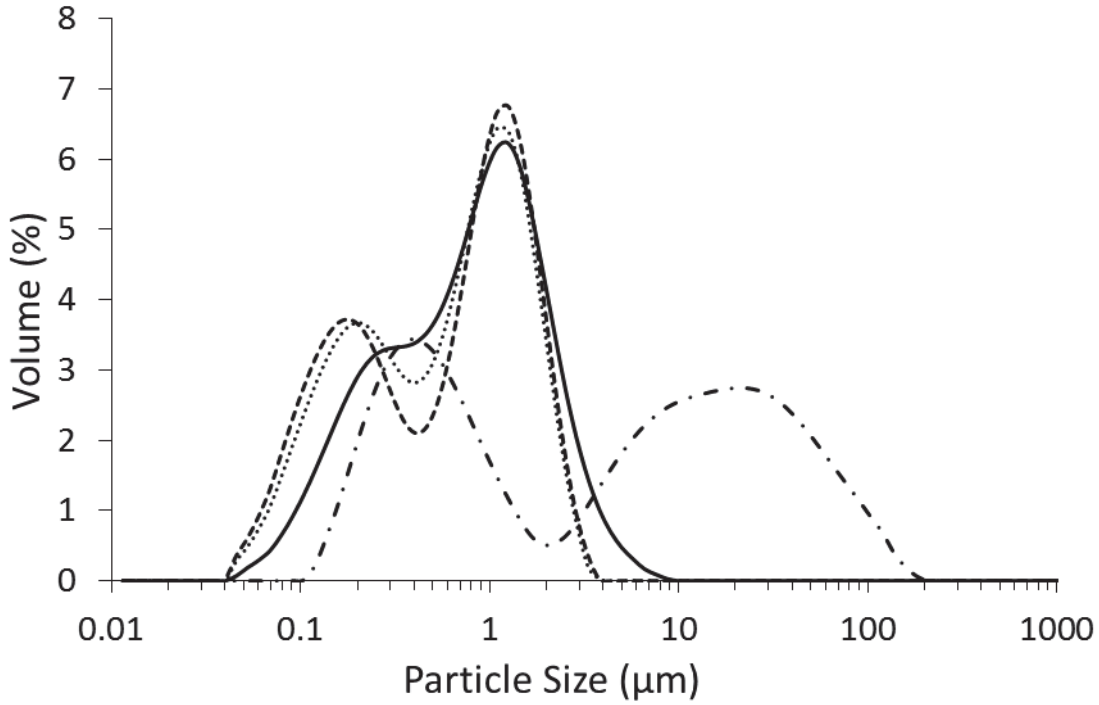

Figure 7.10. Effective particle size distributions of unheated MPC-stabilized oil-in-water emulsions at pH 6.8 (10% w/w protein, 10% w/w oil): control (solid line); containing 10% w/w maltodextrin (dotted line), containing 20% w/w maltodextrin (dashed line), and containing 30% w/w maltodextrin (dashed dotted line).

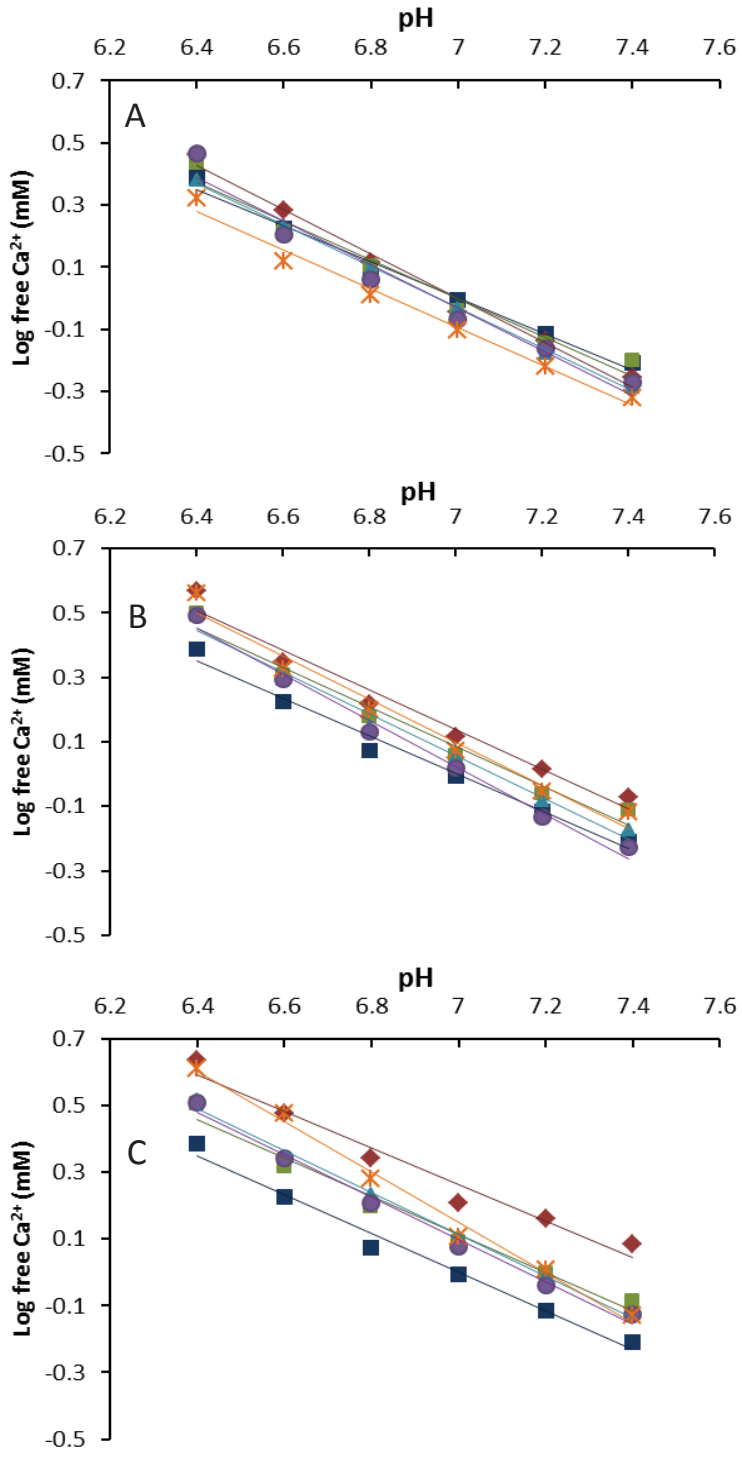

Figure 7.11. Effect of pH on the logarithm of the free calcium ion concentration of MPC-stabilized emulsions with no added carbohydrate (■) and with the addition of (a) 10% w/w, (b) 20%, w/w (c) 30% w/w glucose (♦), maltose (■), sucrose (▲), trehalose (●), and maltodextrin (✳).

The emulsions containing two non-reducing carbohydrates (sucrose and trehalose) showed less susceptibility to heat-induced aggregation than reducing carbohydrates. For the emulsion containing sucrose, the particle size increased moderately from 0 to 15 min of heating with an appearance of 10 μm aggregates after 15 min (Figure 7.9B). Further heating to 20 min, the size of aggregate changed markedly with a shifting to 40 μm and the volume increased from 69% to 94%. The confocal micrographs of sucrose containing sample showed a relatively homogeneous distribution of droplet size after heating for up to 15 min; on heating for 20 min, the droplets tended to form clusters and an interconnected droplet pattern became apparent. The emulsion containing trehalose was more resistant to heat-induced protein/oil droplet aggregation than that containing sucrose and was comparable with the control MPC-stabilized emulsion (Figure 7.9C). The particle size slightly increased after 5 min of heating but there was little change in the growth of particle size between 5 and 10 min. A peak of aggregates of 6.6 μm was apparent only after 20 min of heating and the scattered volume (49%) was nearly half of that of sucrose containing sample.

Cruijsen (1996) concluded that the heat-induced destabilization mechanisms of caseinate-stabilized emulsions containing carbohydrate include: (1) dephosphorylation of the caseins; (2) hydrolysis of the caseins; (3) deposition of insoluble calcium phosphate on casein micelles; (4) the formation of acids, resulting in a decrease in pH to close to the isoelectric point of the caseins; (5) increase in calcium ion activity. As the calcium ion concentration has a direct correlation with the heat stability of milk, concentrated milk, and protein-stabilized emulsion systems (Cruijsen, 1996; Faka, Lewis, Grandison, & Deeth, 2009; Lewis, 2011; Sievanen et al., 2008), the effect of carbohydrate concentration on the free calcium ions in MPC-stabilized emulsions without and with added carbohydrates can be assessed. Figure 7.11 shows the equilibrium relationship between the logarithm of the free calcium ion concentration and the pH. The logarithm of the free calcium ion concentration decreased linearly (the lowest R^2 value was 0.963) as the pH increased, regardless of the addition of carbohydrate. The average slope value was −0.605 and the standard deviation was 0.064. The slopes of the curves were very similar among the carbohydrate types, except for 30% w/w maltodextrin when the slope was −0.72. These results were in very good agreement with previous studies in milk (Tsioulpas, Lewis, & Grandison, 2007). Regardless of concentration, the addition of glucose resulted in slightly higher log free calcium ion values than for the control and the other carbohydrate types. There was no

significant difference in the log free calcium ion values for maltose, sucrose, trehalose, and maltodextrin at up to 20% w/w addition (Figure 7.11A and 7.11B). The addition of 30% w/w carbohydrate resulted in a marked difference in the log free calcium ion values between the control and the emulsions containing carbohydrate. The emulsion containing 30% w/w maltodextrin had a slightly higher log free calcium ion value from pH 6.4 to pH 6.8 than those containing the other carbohydrate types except glucose. It has been suggested that increase in activity coefficient results in an increased Ca^{2+} activity in milk-based system (Gao et al., 2010). An increase in excluded volume effect causes ions to behave far more nonideally in a single concentrated carbohydrate solution regardless of carbohydrate type. The presence of proteins or other type of carbohydrate like lactose will enhance the excluded volume effect. Hence, excluded volume accounts for the change of thermodynamic properties of ions in a carbohydrate-concentrated milk system (Gao et al., 2010).

Several other factors may also explain the better heat stability of MPC-stabilized emulsions with added non-reducing carbohydrates than those with added reducing carbohydrates. Recent studies have revealed that sucrose and trehalose have stabilizing effects against heat-induced globular protein aggregation by increasing the thermal denaturation temperature of the proteins, such as bovine serum albumin (Panzica et al., 2012) and β-lactoglobulin (Tang & Pikal, 2005). Panzica et al. (2012) have indicated that the solvent quality effect governed by sucrose and trehalose is responsible for the initial stages of protein aggregation. It is noteworthy that sucrose and trehalose are more resistant than glucose to hydrolysis of the glycosidic bonds (O'Brien, 1996) and so does maltodextrin (Crowley, Megemont, Gazi, Kelly, Huppertz & O'Mahony, 2014). The less impact on the heat stability by disaccharide and polysaccharide was probably attributed to a slow heat-induced degradation process. First, the maltodextrin must go through degradation from polysaccharide to mono- and di-saccharides, and then further break down into organic acids through Maillaid reactions which are slower than glucose degradation (Crowley et al., 2014).

In addition, the presence of carbohydrate can potentially affect the solvent quality of the water phase and cause partial collapse of the κ-casein on the casein micelles and on the surface of the oil droplets, reducing the steric stabilization during heating. Schorsch, Jones, and Norton (2002) proposed that the addition of sucrose (up to 30% w/w) reduces the solvent quality and causes the collapse of the κ-casein layer of casein micelles when combined with the decreased pH during

acidification based on the fact that a rennet-induced casein gel was weaker and had a longer gelation time. Reduced particle sizes of non-micellar caseins upon the addition of sucrose and trehalose have also been reported (Álvarez-Cerimedo et al., 2010; Belyakova et al., 2003; Dickinson & Matia Merino, 2002).

A low-amplitude oscillatory rheological measurement has been shown to be useful for tracking the evolution of heat-induced aggregation/gelation in protein solution and emulsion systems (McCarthy, Kelly, O'Mahony, & Fenelon, 2014; Tran Le et al., 2011). The changes in storage modulus (*G'*) during a heating and cooling cycle (from 20 to 90 to 20 °C) of MPC-stabilized emulsions with and without added glucose and maltodextrin are displayed in Figure 7.12 The MPC control emulsion showed no change in *G'* (0 value) over the temperature cycle period. The emulsion containing 30% w/w glucose showed a slight increase in storage modulus, but was far from the gelation point (*G'* = 1 Pa). A similar surprisingly small result was obtained with added maltose (data not shown), which may suggest that the heat-induced protein−glucose properties at high temperature are very important in determining the heat stability. The emulsion with 30% w/w added maltodextrin formed a gel after ~ 6 min at a temperature of 90.3 °C, with *G'* increasing over the holding time at 90 °C and on the cooling back to 20 °C (Figure 7.12). This gelation was in good agreement with the HCT results and showed the high susceptibility of an MPC-stabilized emulsion to heat-induced aggregation/coagulation.

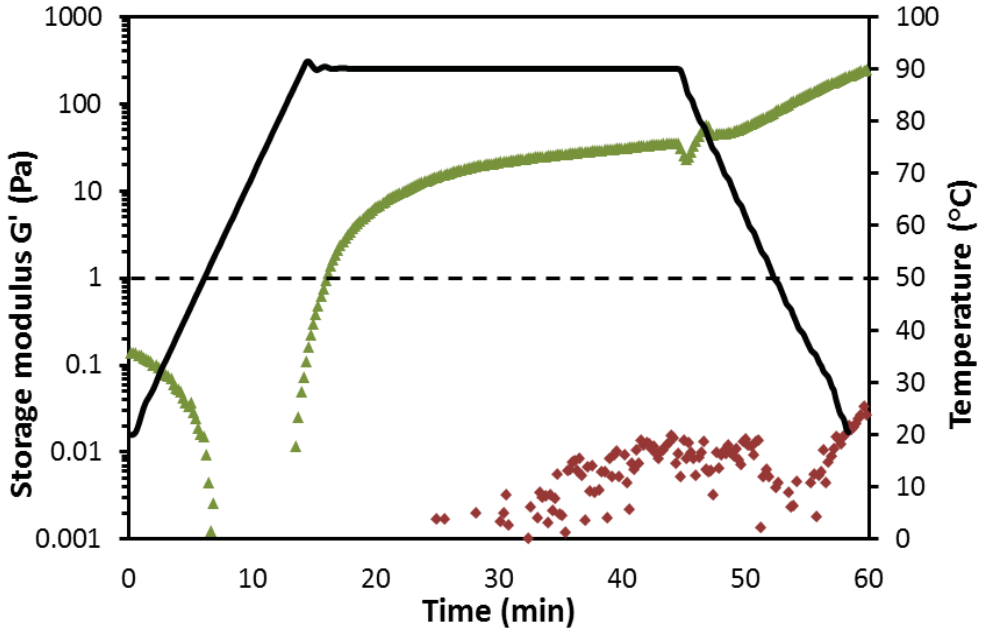

Figure 7.12. Oscillation rheology of MPC-stabilized emulsions (10% w/w protein, 10% w/w oil) with and without added glucose and maltodextrin (30% w/w) as a function of time during a heating and cooling cycle (from 20 to 90 to 20 °C) at pH 6.8: (♦) glucose; (▲) maltodextrin. The solid line indicates the heating and cooling cycle. The dashed line indicates gel formation when $G' > 1$ Pa.

7.5 Conclusions

This study has demonstrated the effect of the addition of carbohydrate on the droplet size and the heat stability of MPC-stabilized emulsions. It was found that, the addition of carbohydrates slightly increased the $d_{3,2}$ to a similar extent (~ 0.1μm) except that the addition of 30% w/w maltodextrin significantly ($p < 0.05$) decreased the droplet diameter. This could be attributed to the large change in disperse/continuous phase viscosity ratio. Close to the HCT, the viscosity index increased sharply corresponding to the aggregation of the aggregates and interconnected droplet clusters. Adding carbohydrate decreases HCT of MPC solutions and emulsions suggests adding carbohydrate generally decreases the repulsive force between protein particles and between droplets. This effect is strongly dependent on the carbohydrate type and concentration.

Heat-induced increases in aggregate size were more extensive with increasing molecular weight of the carbohydrate. Reducing carbohydrates showed faster coagulation and more browning suggesting the Maillard reaction accelerates the destabilization. Non-reducing carbohydrates were more effective, especially trehalose, in retaining the original heat stability of MPC solutions and emulsions. Several factors, including free calcium ion level, volume fraction and solvent quality of the continuous phase protein, will affect the heat stability of MPC-stabilized emulsions with added carbohydrates.

The incorporation of other components in complex food/dairy formulations such as, low molecular weight surfactants, calcium/magnesium salts and sodium polyphosphates is known to have a large impact on the heat coagulation behavior of concentrated milk and micellar casein solutions. The results presented in this study are useful for extending our understanding of the behavior of casein micelles in systems containing high protein and high carbohydrate. Such insights will facilitate the formulation and stability prediction of recombined high protein beverages containing complex ingredients and can be utilized to create desirable droplet sizes and structures to maintain stability against creaming without large compromise with the heat stability.

Chapter 8: Effects of Pre- and Post-heat Treatments on the Physicochemical, Microstructural and Rheological Properties of Milk-Protein-Stabilized Oil-in-Water Emulsions [5]

8.1 Abstract

The effect of heat treatment on the physical stability of milk protein concentrate (MPC) stabilized emulsions was investigated; 3% w/w MPC solutions were preheated at 90 ºC for 5 min at neutral pH prior to emulsification. Heat-treated (120 °C, 10 min) emulsions stabilized by preheated MPC had slightly weaker inter-droplet interactions than those stabilized by unheated MPC. Preheating the MPC denatures the whey proteins leading to a reduction in subsequent heat-induced droplet−droplet and droplet−protein interactions. Emulsions stabilized by calcium-depleted MPC were also investigated. The presence of some non-micellar casein fractions gave better emulsification and may have conferred a stabilizing effect on whey protein aggregation, in both the dispersed phase and the continuous phase during the secondary heat treatment. It was concluded that calcium manipulation and thermal modification of MPC can be utilized to control the functionality in oil-in-water emulsions.

[5] Part of the content presented in this chapter has been published as a original paper in *International Dairy Journal* (2013) *32* 184−191.

Part of the content was also presented as a graduate student poster presentation at 7th NIZO conference, Papendal, the Netherlands, 21−23 September 2011 and as a graduate student oral presentation at IFT, Chicago, USA, 13−16 July 2013.

8.2 Introduction

The behavior of different type of milk proteins and the influence of size and non-adsorbed concentration of milk proteins have been studied and described in unheated and heated oil-in-water emulsions in Chapters 4, 5 and 6. Heat-induced inter-particle interactions in different solvent conditions have been studied in Chapter 7. The functionality of milk proteins can be modified by physical, chemical and enzymatic methods (Augustin, Udabage, & Steve, 2007), with physical modification being the most cost-effective and adaptable way for the dairy industry.

Heating sodium caseinate and calcium caseinate dispersions by retort processing prior to emulsification increased the surface protein coverage and improved the creaming stability of the final emulsions (Srinivasan et al., 2002, 2003). The improvement was attributed to the increased size of the non-adsorbed protein and the increased viscosity of the continuous phase after heating. A preheating treatment of protein dispersions prior to homogenization has also been reported to influence the droplet size distribution, creaming stability and rheological properties of MPC-stabilized emulsions (Dybowska, 2008). The emulsion droplet size increased when the protein solution was heated before emulsification. Moreover, the adsorption of more protein molecules at the oil−water interface increased the density of the interfacial layer, resulting in an overall enhanced stability against creaming (Dybowska, 2008, 2011).

The compositions and functionalities of different MPCs will vary and will be further affected during powder manufacturing process. It has been reported that the ethanol and heat stability of casein micelles increases with decreasing colloidal calcium content. Those changes are closely related to the aggregation state of the casein micelles and the calcium ion activity (Grimley et al., 2010). It is of interest to identify the role of non-micellar protein in emulsion preparation and in subsequent heating process. The aims of this study were to evaluate: (1) the influence of preheating the proteins on the heat stability of oil-in-water emulsions stabilized by standard MPC and calcium-depleted MPC; (2) the rheological and creaming behaviors of the emulsions after heat treatment (120 °C, 10 min).

8.3 Materials and methods

8.3.1 Materials

MPC 4850, calcium-depleted MPC and NaCas were used as model proteins and corn oil was used as oil source for the emulsion preparation (details mentioned in section 3.1.1). In the results and discussion, MPC 4850 is referred to as MPC I and calcium-depleted-MPC is referred to as MPC II.

8.3.2 Preparation of model emulsions

The model emulsions were prepared following the procedure described in Figure 8.1. Each model emulsion was prepared at least in triplicate. The pH of the final dispersions was adjusted to 6.8 with 1 M HCl or 1 M NaOH. The heat treatment consisted of holding the sample at 90 °C for 5 min (the heating-up time was about 6 min), after which the dispersion was immediately cooled rapidly in an ice bath. Reverse-phase high performance liquid chromatography (RP-HPLC) was used to determine the amount of native whey protein after the heat treatment (Elgar et al., 2000). All the MPC solutions were mixed with sodium acetate (0.2% w/v) at a 1:1 weight ratio to reach pH 4.6. The mixtures were then centrifuged at 17,900 g for 6 min, as a result, the solutions separated into supernatant and a pallet of micellar caseins. The supernatant of the protein solution was taken for the determination of the denaturation level of native whey proteins and the injection volume is 50 μL.

8.3.3 Determination of effects of heat treatment on emulsions

The heat stability of the model emulsions was determined as the procedure described in Chapter 3, Section 3.2.5). The large aggregates that appeared in MPC I samples were diluted with NaOH (1 M, pH 8.0), a disodium ethylenediamine tetra-acetate (EDTA)/polysorbate 20 (Tween 20) mixture (0.04 mol kg^{-1} and 5 g kg^{-1}), urea (6 mol kg^{-1}) and sodium dodecyl sulphate (SDS) (100 g kg^{-1}). The solubility was checked visually after 24 h.

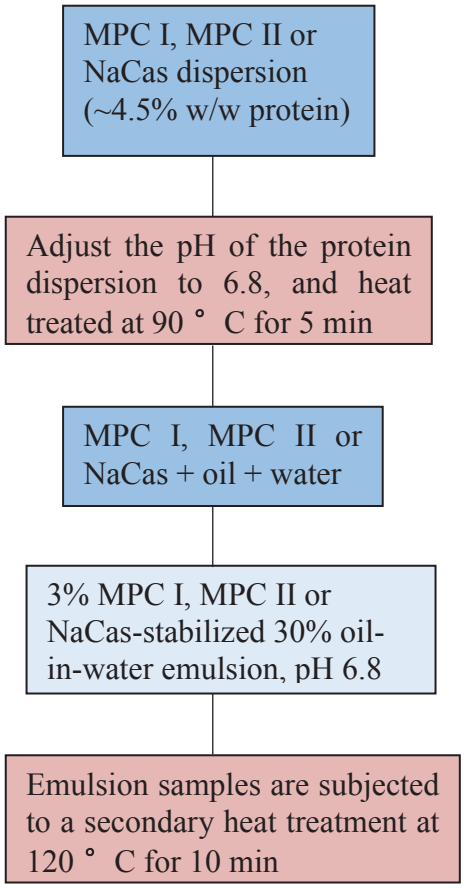

Figure 8.1. Flow chart of the preparation of model emulsions (3% w/w protein, 30% w/w oil).

8.3.4 Determination of heat coagulation time (HCT) of emulsions

The time required for coagulation of the sample or precipitation became visible throughout the sample was recorded as the heat coagulation time (HCT). The procedure described in Chapter 3, Section 3.2.5.

8.3.5 Determination of particle size distributions of protein dispersions and emulsions

The particle size and droplet size measurements were carried out using procedures described in Chapter 3, Section 3.2.3.

8.3.6 Determination of surface protein concentration and composition

The surface protein concentration and composition were measured according to the procedures described in Chapter 3, Section 3.2.4.

8.3.7 Emulsion stability

The model emulsions were stored at ambient temperature and measured periodically for up to 5 days using a vertical scan analyser Turbiscan Classic MA 2000 (Formulaction, Toulouse, France). Details of the techniques are described in Chapter 3, Section 3.2.7.

8.3.8 Rheological properties of model emulsions

Details of the rheological measurement of emulsions have been described in Chapter 3, Section 3.2.6.

8.3.9 Microstructure of model emulsions

Details of the confocal scanning laser microscope and transmission electron microscope characterization techniques have been described in Chapter 3, Section 3.2.8.

8.3.10 Statistical analysis

All experiments were carried out at least in triplicate using freshly prepared samples and the results are reported as the mean and standard deviation of these measurements. The experimental data were analyzed by Student's t-tests using Microsoft Excel 2007 (Microsoft Corporation, Redmond, WA, USA) and significant differences among the means were determined at a 95.0% confidence level.

8.4 Results and discussion

8.4.1 Particle size of milk protein dispersions and whey protein denaturation level of MPC dispersions

The mean primary particle size of each of the MPC I, MPC II and NaCas dispersions did not change significantly ($p > 0.05$) after heat treatment at 90°C for 5 min (Table 8.1). The average particle sizes of the MPC I and MPC II were close to the reported size of casein micelles in milk (~ 200 nm) (Dalgleish, 1998) and in micellar casein solution (Beliciu & Moraru, 2011). For the MPC II dispersion, which contained both micellar and non-micellar casein, the particle size result correlated well with those obtained previously (Ye, 2011). The MPC I dispersion showed a monomodal size distribution (163.9 ± 2.7 nm). In contrast, the particle size distribution of the MPC II dispersion had one peak showing particles in the 20−70 nm size range and a second peak in the 100−600 nm size range (Figure 8.2). Semenova and her co-workers (2009) and Tan (2010) have shown the aggregate formation of NaCas nano-particle can range from the size of ~40 nm to ~1 μm. The extent of whey protein denaturation of the MPC I and MPC II dispersions after the preheat treatment (90 °C, 5 min) is shown in Table 8.1. The total whey protein denaturation levels for MPC I and MPC II were around 90% during preheat treatment. The denaturation level of α-lactalbumin was slightly higher in the MPC II dispersion than in the MPC I dispersion.

Table 8.1. Particle sizes determined by Zetasizer of MPC and NaCas dispersions before and after heating (90 °C, 5 min) and the denaturation level of whey proteins in the oil-free aqueous phase.

Milk protein	Unheated (nm)	Heated (nm)	Total whey protein denaturation (%)	β-Lactoglobulin denaturation (%)	α-Lactalbumin denaturation (%)
MPC I	165.5 ± 2.8 ^{aA}	163.9 ± 2.7 ^{aA}	88.4 ± 1.2	92.8 ± 1.5	66.7 ± 2.3
MPC II	168.5 ± 3.6 ^{aA}	166.1 ± 4.1 ^{aA}	87.2 ± 1.4	89.7 ± 1.7	74.6 ± 2.2
NaCas	94.0 ± 3.5 ^{aB}	99.6 ± 5.0 ^{aB}	N/A	N/A	N/A

Each value represents the mean of two−four measurements from three independently trials.
^{a,b} Means within the same row and having the same superscript are not significantly different ($p > 0.05$).
^{A,B} Means within the same column and having the same superscript are not significantly different ($p > 0.05$).

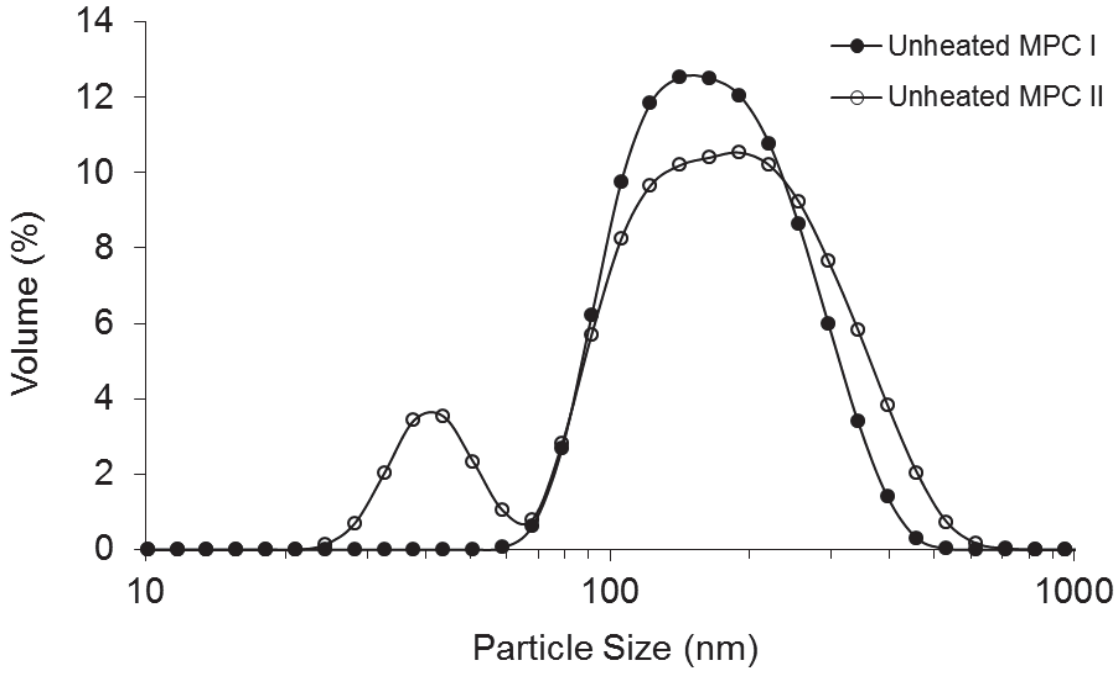

Figure 8.2. Particle size distribution of unheated MPC I and MPC II dispersions (pH 6.8) determined by Zetasizer at 20 °C.

8.4.2 Particle size distribution of emulsions

The primary particle size ($d_{3,2}$ value) of milk-protein-stabilized emulsions is shown in Table 8.2. Under the same homogenization conditions, the $d_{3,2}$ value indicates the emulsifying capability of the emulsifier (Euston & Euston, 1999). Preheating the MPCs resulted in no significant change in the emulsifying properties as determined by $d_{3,2}$ values. Unheated emulsions, stabilized by MPC I were significantly larger than those of stabilized by MPC II and NaCas regardless of any preheat treatment of the protein solution prior to emulsification (Table 8.2).

The $d_{4,3}$ value is known to be more sensitive to oil droplet aggregation (Relkin & Sourdet, 2005). The effective particle sizes ($d_{4,3}$ value) of milk-protein-stabilized emulsions are shown in Table 8.2. Preheating MPC I resulted in significantly smaller droplet size ($p < 0.05$) than emulsions formed from unheated MPC I. Heating MPC I emulsions resulted in even larger droplets. The composition of these aggregates formed by heating MPC I emulsions were investigated for 1, 3

and 10 minutes of heating. Aggregates were diluted with various agents, as described in Section 3.2.3.

Aggregates obtained after heating for 1 min could be dissolved in all dissolving agents after 24 h, whereas those from heating for 3 and 10 min could not be fully dissolved. Insoluble aggregates suggest that some heat-induced droplet clusters have been formed by strong protein−protein interactions, possibly covalent bonds between adsorbed layers.

The $d_{4,3}$ values of MPC II emulsion stabilized by unheated protein were very similar after heat treatment at 120 °C for 10 min and were significantly smaller than MPC I emulsions ($p < 0.05$). Preheating the MPC II before homogenization had little effect on the particle sizes before and after heat treatment at 120 °C for 10 min. The change in the mean particle sizes of NaCas emulsions stabilized by unheated and preheated proteins before or after heat treatment at 120 °C for 10 min resembled those of MPC II emulsions. In an agreement with previous study (Hunt & Dalgleish, 1995), little heat-induced flocculation or coalescence of droplets occurred when oil droplets were stabilized by NaCas when heating in low ionic strength for quite some time.

8.4.3 Protein load and protein composition of emulsions

Preheating the protein solution before emulsification had little effect on the surface protein load of the unheated emulsions (Table 8.2). The MPC II and NaCas emulsions had similar surface protein concentrations at the oil−water interface whereas the MPC I emulsion had a significantly higher ($p < 0.05$) surface protein load. The results for the MPC I and MPC II emulsions were in good agreement with previous studies on MPC emulsions (Euston & Euston, 1999; Ye, 2011) and that for the NaCas emulsion correlated well with the study of Srinivasan, Singh, and Munro (2000). The protein load was not significantly different in emulsions stabilized by MPC II and NaCas regardless of the protein preheat treatment after the subsequent heating. However, the protein load of the MPC I emulsion formed with unheated protein was significantly higher ($p < 0.05$) after the subsequent heating, suggesting heat-induced inter-droplet protein−protein interactions are extensive and coalescence of emulsion droplets may have occurred.

SDS-PAGE patterns of the emulsions stabilized by unheated protein and preheated protein are shown in Figure 8.3A (unheated) and Figure 8.3B (heated). Compared with the skim milk standard (Lane 1, Figure 8.3A), the proportions of the casein fractions at the surface of MPC I emulsion droplets (Lane 2) were similar to those in casein micelles but fewer whey proteins were adsorbed at the interface. For MPC II (Lane 3), more α_{s1}-casein and less β-casein were adsorbed at the oil−water interface, probably because of competitive adsorption when the aggregation state of the caseins is no longer entirely micelles which is consistent with earlier studies (Ye, 2011). The presence of whey protein bands in Figure 8.3B confirmed that β-lactoglobulin/k-casein complexes formed during the preheat treatment.

Table 8.2. Mean primary particle sizes, mean effective particle sizes and surface protein concentration of 30% w/w oil-in-water emulsions formed with 3% w/w MPC and NaCas before and after heat treatment (120 °C, 10 min).

Heat treatment of protein solution	Primary d_{32} (μm)					
	Unheated MPC I	Unheated MPC II	Unheated NaCas	Preheated MPC I	Preheated MPC II	Preheated NaCas
Unheated emulsion	1.36 ± 0.05^{aA}	1.05 ± 0.04^{bA}	1.02 ± 0.05^{bA}	1.46 ± 0.07^{aA}	1.17 ± 0.18^{bA}	1.11 ± 0.02^{bA}
Heated emulsion	4.17 ± 1.48^{aB}	1.06 ± 0.02^{bA}	0.97 ± 0.07^{bA}	1.74 ± 0.22^{cB}	1.16 ± 0.09^{bA}	1.09 ± 0.02^{bA}
	Effective d_{43} (μm)					
Unheated emulsion	13.3 ± 1.31^{aA}	2.33 ± 0.02^{bA}	2.26 ± 0.03^{bA}	10.0 ± 0.78^{cA}	2.42 ± 0.11^{bA}	2.46 ± 0.10^{bA}
Heated emulsion	228.5 ± 36.2^{aB}	2.42 ± 0.06^{bA}	2.29 ± 0.05^{bA}	189.8 ± 37.4^{aB}	2.45 ± 0.02^{bA}	2.53 ± 0.43^{bA}
	Surface protein concentration (mg/m^2)					
Unheated emulsion	13.16 ± 1.29^{aA}	4.12 ± 1.04^{aB}	2.82 ± 0.47^{aB}	13.26 ± 1.24^{aA}	3.84 ± 0.45^{aB}	3.15 ± 0.42^{aB}
Heated emulsion	60.81 ± 3.66^{aC}	4.51 ± 0.49^{aB}	2.90 ± 0.73^{aB}	13.44 ± 1.79^{bA}	4.21 ± 0.08^{aB}	3.03 ± 1.17^{aB}

[a,b,c] Means within the same row and having the same superscript are not significantly different by Student's t-test at $p < 0.05$.

[A,B] Means within the same column and having the same superscript are not significantly different by Student's t-test at $p < 0.05$.

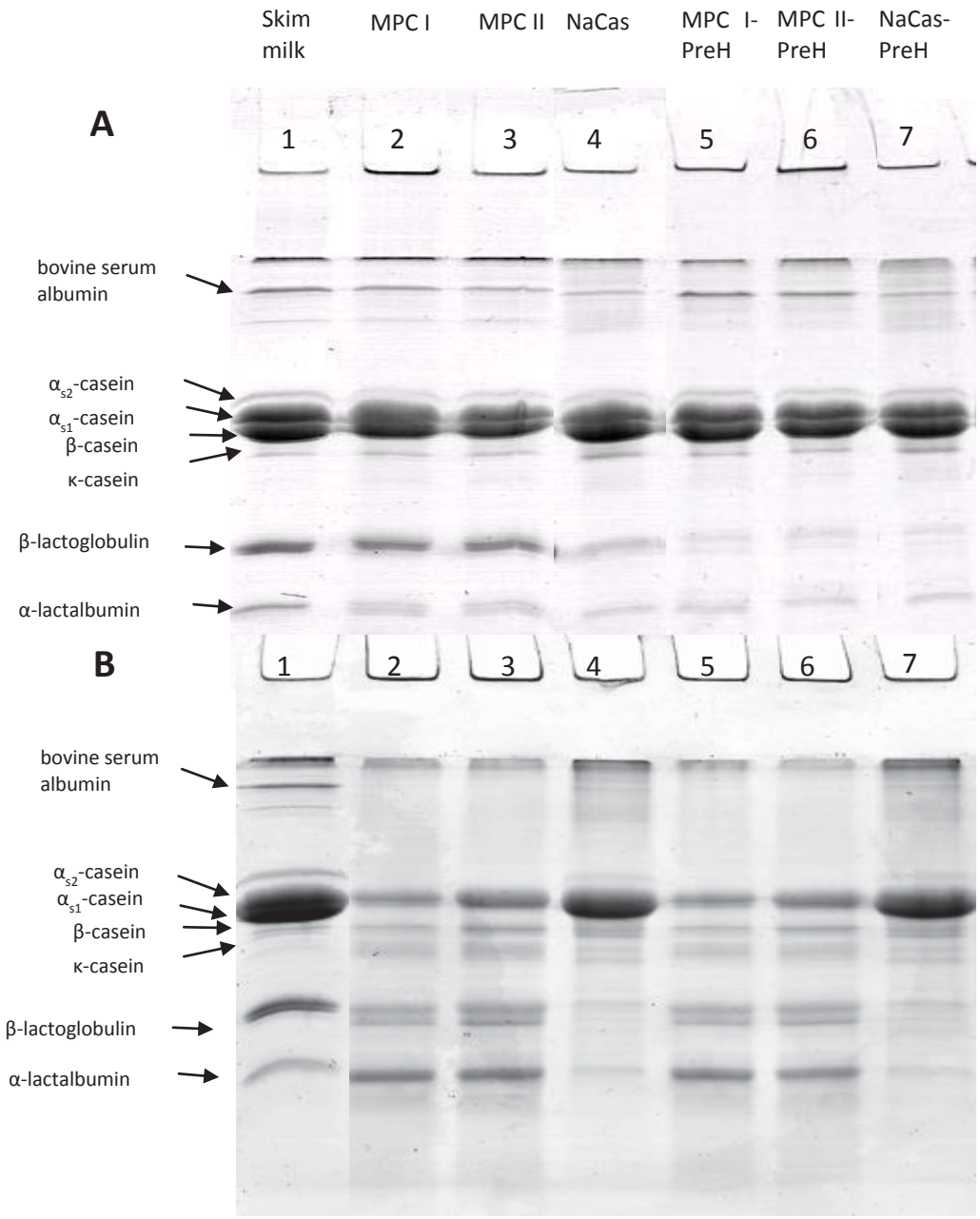

Figure 8.3. SDS-PAGE patterns of proteins adsorbed at the oil−water interface of (A) unheated and (B) heated 30% w/w oil-in-water emulsions formed with 3% w/w unheated and preheated protein dispersions. Lane 1, skim milk standard; lane 2, MPC I emulsion; lane 3, MPC II emulsion; lane 4, NaCas emulsion; lane 5, MPC I emulsion formed with preheated protein; lane 6, MPC II emulsion formed with preheated protein; lane 7, NaCas emulsion formed with preheated protein.

8.4.4 Heat stability of the model emulsions

The HCT is considered to be a quantitative measure of the susceptibility of an emulsion towards heat-induced aggregation. Preheating the protein solution before emulsification lengthened the HCT of the MPC I and MPC II emulsions, from 0.54 to around 0.7 min for the MPC I emulsion and from 10.37 to 11.41 min for the MPC II emulsion (Figure 8.4). This increased HCT was attributed to the reduced interactions between the pre-denatured whey proteins, because thiol/disulfide interchanges between denatured whey proteins occur during protein preheat treatment, fewer reactive sites (free thiol groups) are available for a further heat-induced aggregations (Dissanayake & Vasiljevic, 2009). The preheat treatment does not appear to have a beneficial effect on the HCT of the NaCas emulsions under the current experimental conditions. In addition, the HCT of the MPC II emulsion was significantly longer than that of the MPC I emulsion regardless of the protein solution preheating effect. These marked differences were probably influenced by the micellar casein/non-micellar casein ratio and the calcium ion activity in the systems.

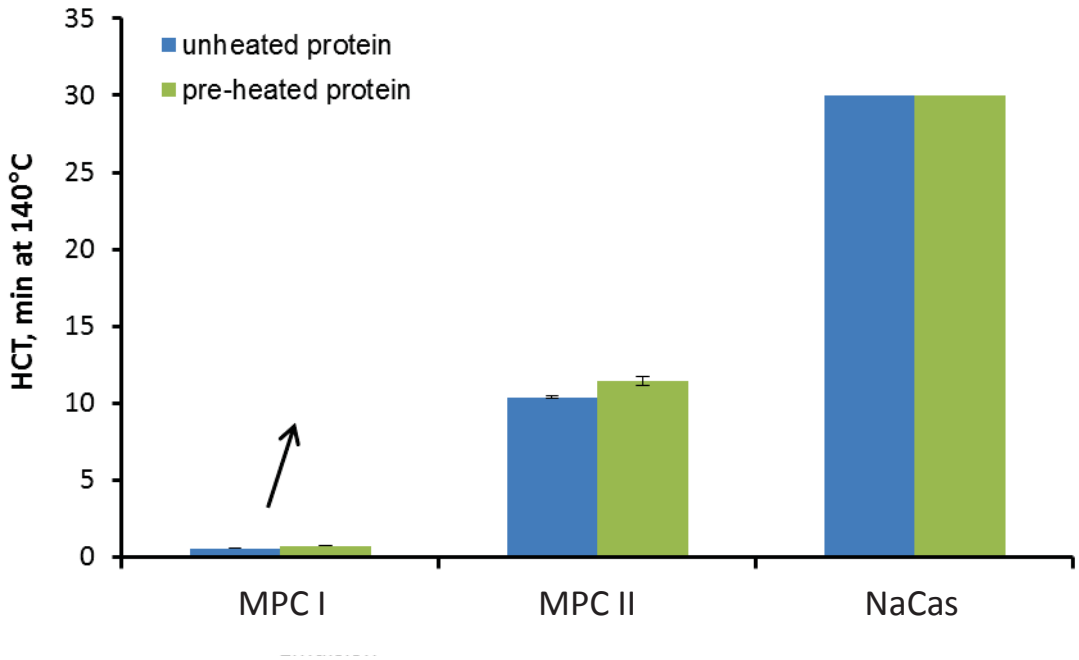

Figure 8.4. HCT profiles of 30% w/w oil-in-water emulsions stabilized by 3% w/w unheated protein and by 3% w/w preheated protein. Inset: HCT (min) of MPC I emulsion.

MPC II emulsions had longer heat stability than MPC I emulsions regardless of the protein preheating effect. This difference in stability may have resulted from the large effective droplet size of MPC I emulsion and the reduced calcium content in MPC II. The heat stability of milk-protein-stabilized emulsions has been found to be influenced by the volume fraction of casein micelles. Casein micelle coated oil droplets behave as large 'casein micelles' which increases the effective concentration of casein micelles at a fixed protein concentration, resulting in poorer heat stability (Cruijsen, 1996; Walstra et al., 2006a). Extensive bridging flocculation occurs when aggregated protein particles are adsorbed at the oil−water interface and the MPC-to-oil ratio is low. As a result, the presence of large 'casein micelles' increases the tendency to heat-induced aggregation as the κ-casein content per particle reduces (Singh & Latham, 1993).

In contrast to MPC I emulsions, the small droplet size and the low surface protein concentration (Table 8.2) in the MPC II emulsions suggested that the oil droplets were coated with some dissociated caseins, which is in agreement with Ye (2011). Parkinson and Dickinson (2007) have demonstrated that, when non-micellar caseins and whey proteins co-adsorb at the oil−water interface, the tangling tails of the caseins protrude and enhance the steric repulsion between emulsion droplets, preventing droplets from aggregation during heating and retaining low viscosity. However, it is very difficult to completely rule out the effect of calcium depletion in MPC II on the heat stability of the emulsions, since a systematic reduction in the free Ca^{2+} level by calcium chelators will change the aggregation state of the casein micelles (de Kort et al., 2011). However, the effect of Ca^{2+} activity should always be considered.

8.4.5 Microstructure of model emulsions

Confocal micrographs of unheated and heat-treated (120 ºC, 10 min) emulsions stabilized by unheated protein and preheated protein are shown in Figure 8.5. The emulsion droplets in unheated MPC I and MPC II emulsions were homogeneously distributed (Figure 8.5a). A high density of protein was observed around the surface of the oil droplets in the heated MPC I emulsions stabilized by unheated protein and preheated protein respectively (Figure 8.5b). For the heated MPC I emulsions, there are obvious droplet/droplet cluster size differences between emulsion stabilized by unheated protein and that stabilized by preheated protein (Figure 8.5 and

Table 8.2). The results indicate that the MPC I emulsion (unheated protein) may have generated irreversible aggregates while MPC I emulsion (preheated protein) may have generated weak reversible flocs. Previous studies (Cruijsen, 1996) suggest disulfide bond formation between α_{s2}- and κ-caseins during high temperature heating is partly responsible for intermolecular reactions between casein molecules, which in turn results in aggregation of the droplets. Typically, for aggregation to be irreversible the energy needed for separation must exceed ~10 k_BT, such as ~200 k_BT for covalent bonds (Walstra, 2003). Likewise, reversible flocs like those associated with each other by hydrophobic interactions tend to be held together by a few k_BT. The MPC II emulsions stabilized by unheated and preheated protein remained evenly distributed in their droplet size after heating (Figure 8.5b), although there did appear to be a small apparent increase in droplet size for the preheated protein sample. This increase in droplet size may be attributed to some extent of heat-induced coalescence, however, the exact mechanism is not known yet. Extensive droplet−droplet flocculation was observed in the NaCas emulsions regardless of the preheat treatment of the protein solution prior to emulsification (Figure 8.5a & 5b). This droplet flocculation has previously been reported in caseinate-stabilized emulsions (Seta, Baldino, Gabriele, Lupi, & de Cindio, 2013; Srinivasan et al., 2000); Chapter 5 demonstrates the phenomenon is sensitive to the protein concentration and can be accounted for by a depletion mechanism arising from the presence of excess of non-adsorbed casein nano-particles.

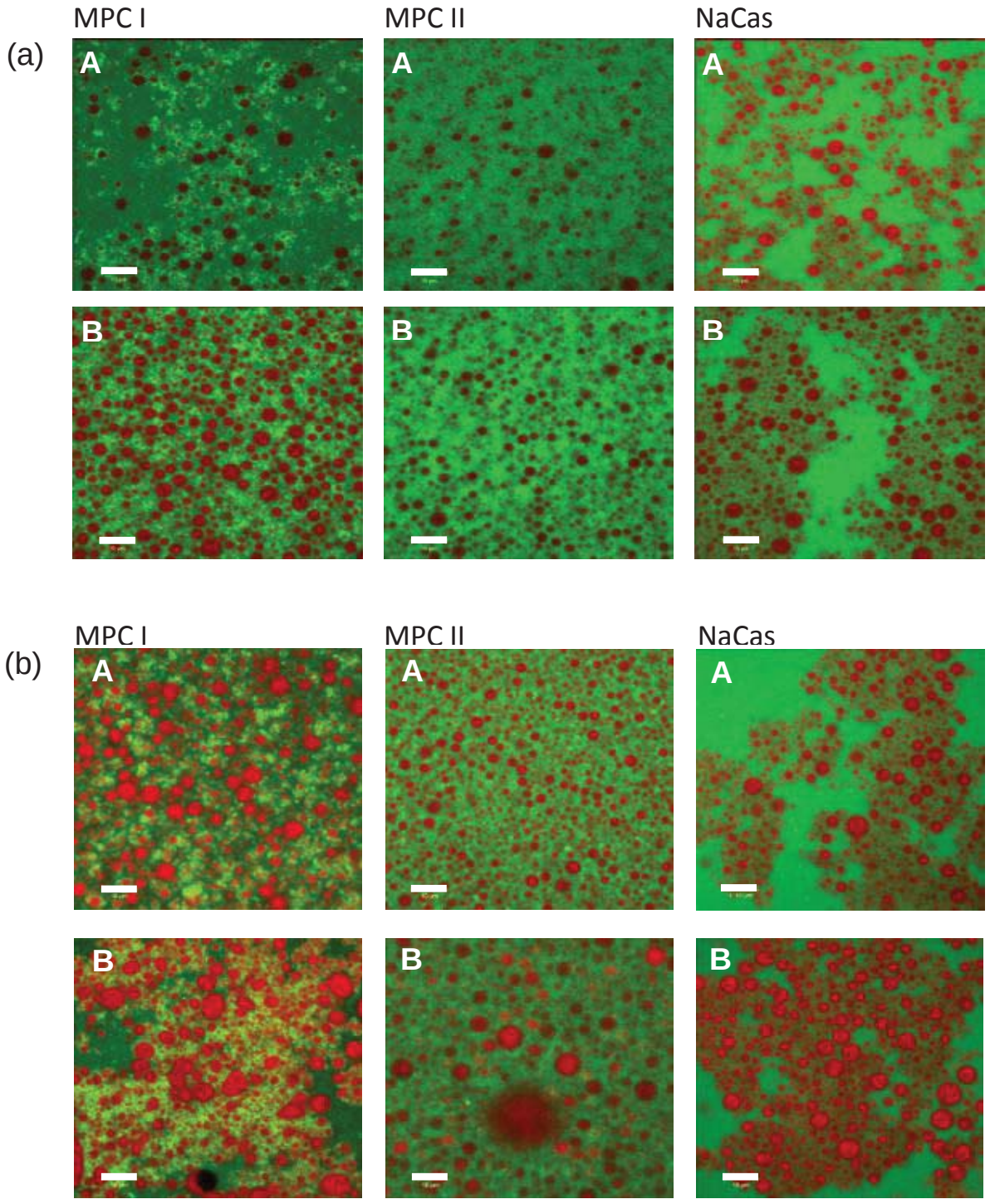

Figure 8.5. Confocal laser scanning micrographs of 3% w/w (a) unheated and (b) heated (120 °C, 10 min) milk-protein-stabilized emulsions in a 63x objective. (A) 30% w/w oil-in-water emulsions stabilized by 3% w/w unheated protein; (B) 30% w/w oil-in-water emulsions stabilized by 3% w/w preheated protein. The scale bars in A and B represent 10 μm.

8.4.6 Rheological properties of model emulsions

Emulsion viscosity is an indicator of volume and interactions of oil droplets. Increase in low-shear viscosities of milk-protein-stabilized emulsions has been attributed to heat-induced aggregations/coagulations between emulsion droplets (Dickinson & Parkinson, 2004; Euston et al., 2000; Sliwinski e al., 2003). In general, the viscosity investigated against shear rate shared similar behaviors like those discussed in Chapter 7, but not following aggregation with a viscosity index because some unheated emulsions showed different signs of aggregation.

Preheating MPC I resulted in emulsions with a lower viscosity than unheated proteins. This decrease in viscosity was observed over the entire range of shear rates as shown in Figure 8.6A. Dybowska (2008) observed an increase in viscosity when preheated MPC was used to form emulsions at the same oil volume. Heating MPC I stabilized emulsions at 120 °C for 10 min, the apparent viscosity of the emulsions increased markedly. After the secondary heat treatment, the effect of preheating MPC I was much more marginal (Figure 8.6B). The low-shear-rate viscosities measured at shear rate of 0.001 s^{-1} are 8700 Pa.s for unheated protein and 7070 Pa.s for preheated protein. The heat-induced emulsion aggregation was investigated further (Figure 8.7). It appeared that severe heat-induced aggregation had already occurred during the initial heating period (~ 2 min) in the MPC I emulsions. Figure 8.7A shows that the apparent viscosities increased significantly even after 1 min of heating at 120 °C. The extent of the change in viscosity was greater in MPC I emulsions stabilized by preheated protein than in those stabilized by unheated protein as the heating time increased (Figure 8.7B). Like the phenomenon described in Chapter 7, aggregation of aggregates was responsible for the marked increase in viscosity when emulsions were approaching to their HCT.

In contrast to the MPC I emulsions, the MPC II and NaCas emulsions had much lower initial viscosities at low shear rates and there was little difference between the emulsions formed with unheated and preheated proteins (Figure 8.6A and 8.6B). The viscosities of the MPC II emulsions were consistently lower than those of the NaCas emulsions over the whole shear rate range. The NaCas emulsions displayed shearing-thinning behavior, suggesting the formation of some droplet clusters that were disrupted at higher shear rates. This phenomenon was due to the depletion effects, which promoted emulsion flocculation.

The apparent viscosities of the heated model emulsions at a shear rate of 100 s^{-1} are shown in Figure 8.8. This shear rate (~100 s^{-1}) is used for rheological tests because it is a useful representative shear for food processes under flow, e.g. pumping through a pipe, stirring or mastication (McClements, 2005). Preheating the protein solution prior to emulsification had an impact on the viscosity of MPC I stabilized emulsion whereas it appeared to affect the viscosity of MPC II and NaCas stabilized emulsions to a lesser extent. The MPC I emulsion stabilized by preheated protein exhibited significantly ($p < 0.05$) lower viscosity (0.084 Pa.s) than the MPC I emulsion stabilized by unheated protein (0.222 Pa.s) at a shear rate of 100 s^{-1}. The difference indicates that the denaturation conditions greatly impact on the final functionality of MPC I. This effect may be associated with the decreased protein−protein interactions after the initial denaturation. The viscosity of the heated MPC II emulsion formed with unheated protein at a shear rate of 100 s^{-1} was 0.009 Pa.s, i.e. more than a 20-fold reduction compared with the viscosity measured in the heated MPC I emulsion formed with unheated protein.

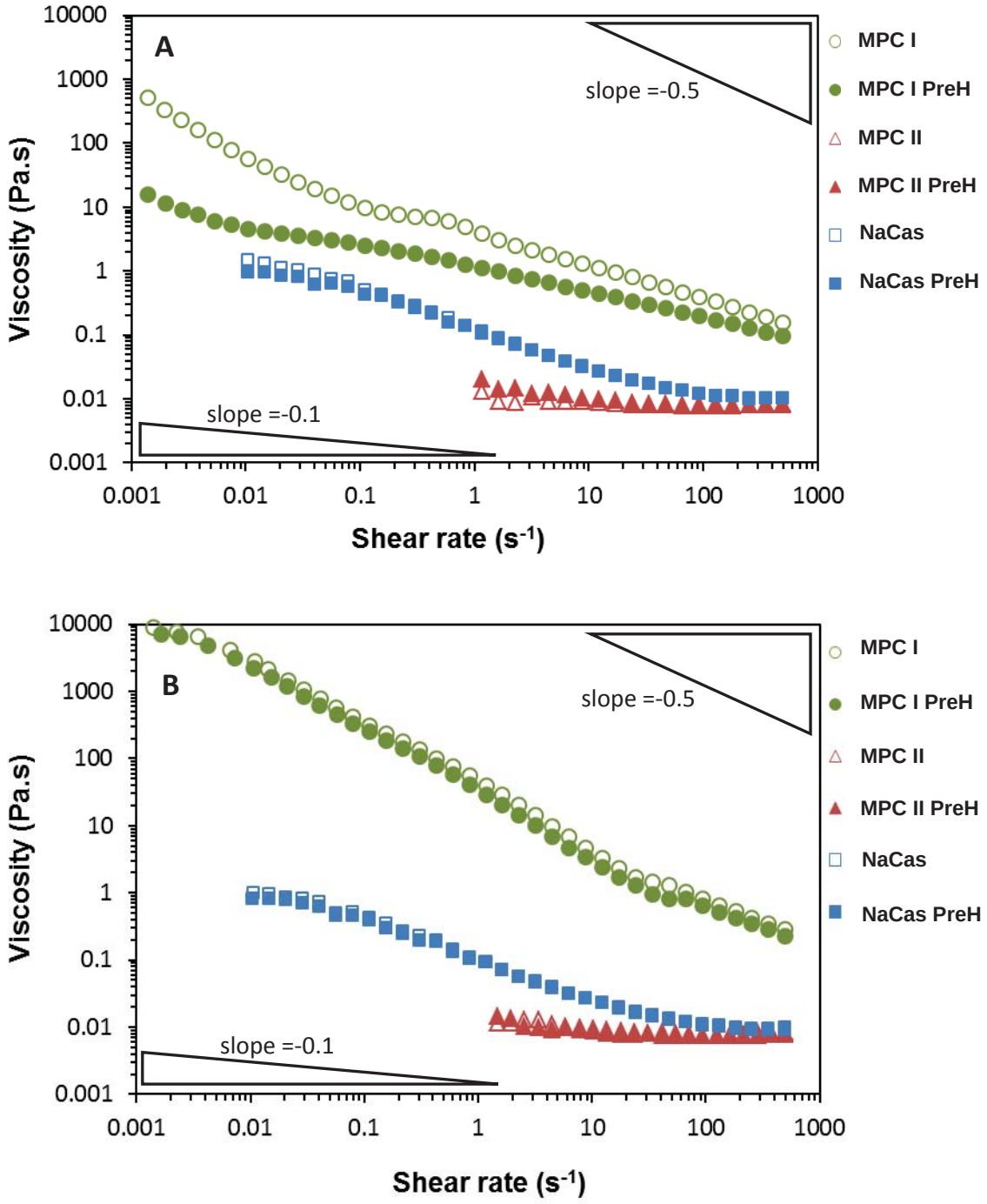

Figure 8.6. Apparent viscosities of (A) unheated and (B) heated (120 °C, 10 min) 30% w/w oil-in-water emulsions stabilized by 3% w/w unheated protein and by 3% w/w preheated protein measured at 20 °C. PreH = preheated protein solution.

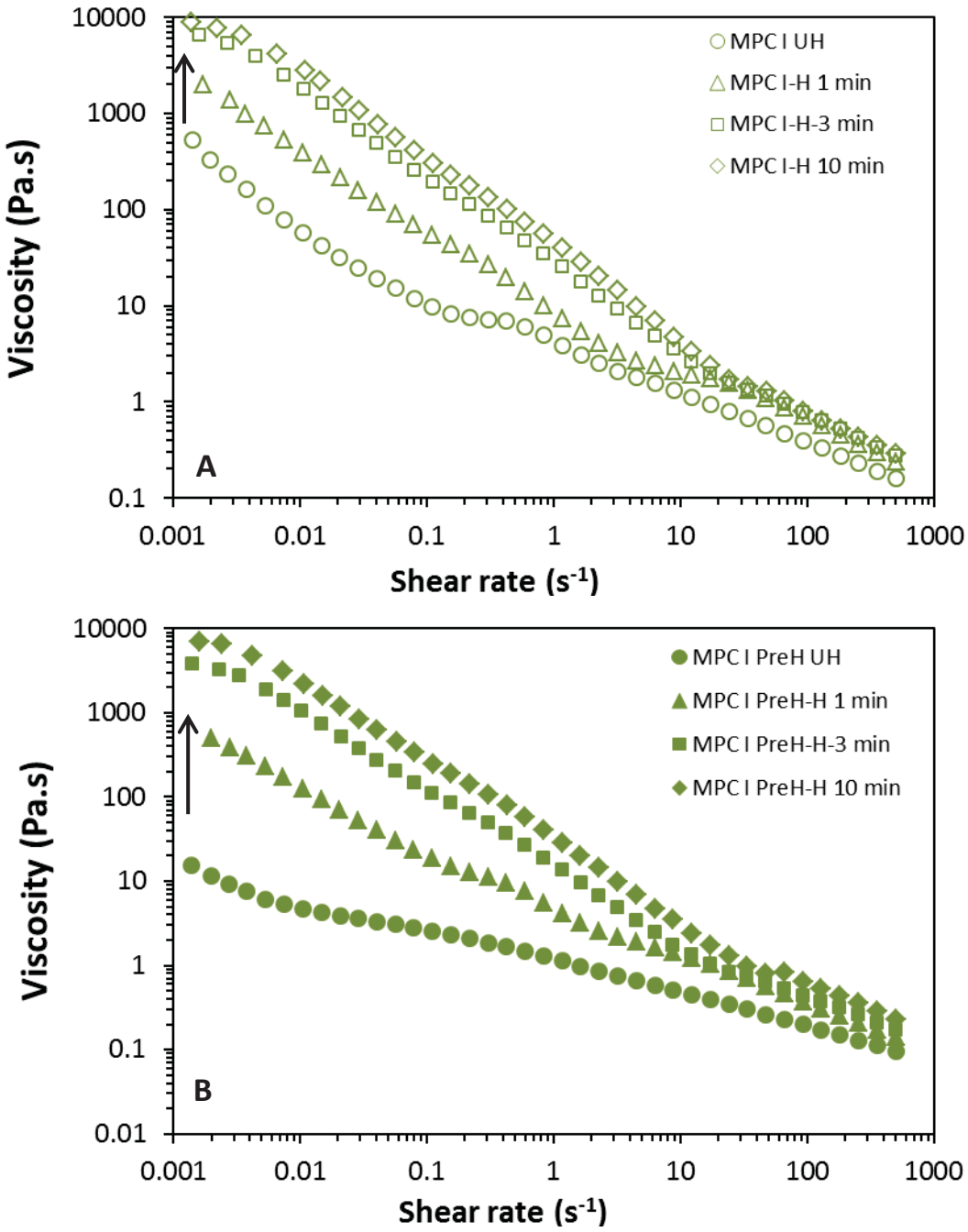

Figure 8.7. Apparent viscosities of 30% w/w oil-in-water emulsions stabilized by (A) MPC I unheated solution and (B) MPC I preheated solution before and after heating at 120 °C for 1, 3 and 10 min measured at 20 °C. PreH = preheated protein solution.

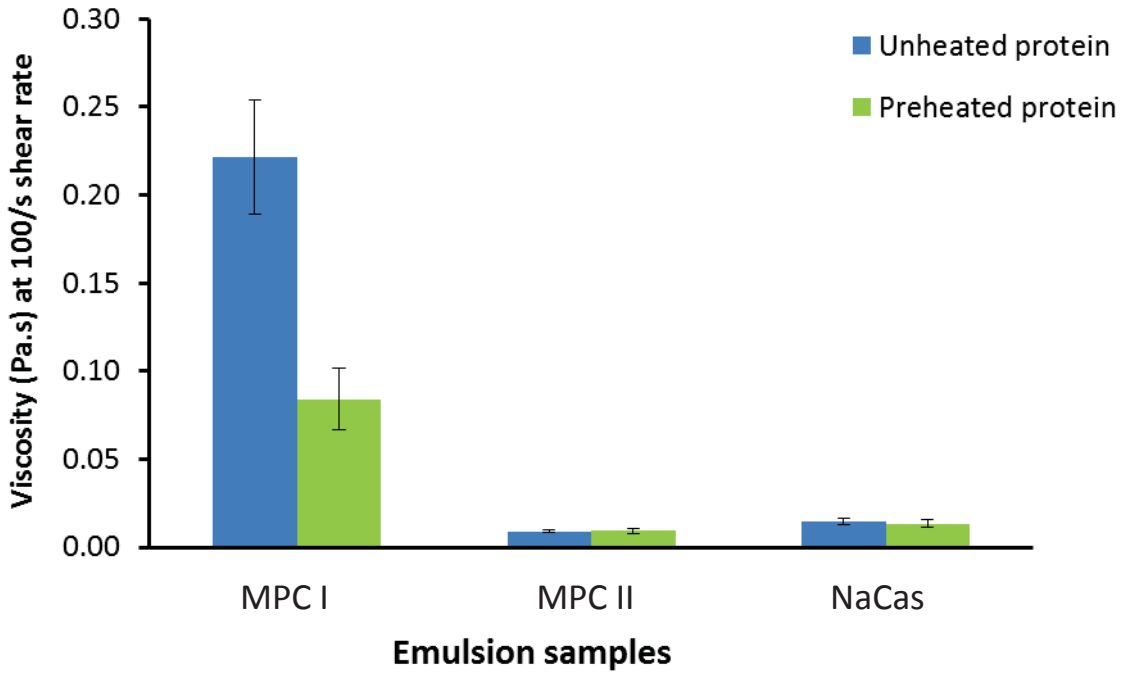

Figure 8.8. Apparent viscosities of heated 30% w/w oil-in-water model emulsions stabilized by 3% w/w unheated protein and by 3% w/w preheated protein, determined at a shear rate of $100s^{-1}$.

8.4.7 Creaming stability of model emulsions

The heated emulsions stabilized by MPC I, MPC II and NaCas were monitored both visually and with a Turbiscan over 5 days of storage at ambient temperature (20 °C) (Figure 8.9). Creaming was the main destabilization mechanism for the heated MPC I emulsions as the classified layer thickness increased gradually over time. A modified Stokes' law equation (McClements, 2005),

$$V = V_{stokes}\left(1 - \frac{\emptyset}{\emptyset_c}\right)^{k\emptyset_c}$$

suggests emulsions with micron sized oil droplets should show a steady increasing clarified layer about a week. In general, the clarified layer of heated model emulsions grew at a steady pace but was faster than that predicted from McClements' equation during 120 h of storage (2005). The clarified layer developed slower in the heated MPC I emulsion stabilized by unheated protein than that stabilized by preheated protein. This change was attributed to the higher low-shear viscosity.

Turbiscan of MPC II emulsions showed clarified and creaming layers. The amount of particles in the clarified layer was so high that it was almost impossible to detect by naked eyes. The creaming profile of MPC II emulsions generally resembles those observed in Figure 5.3 (Chapter 5) with an initial fast growth and then a plateau after 96 h (Figure 8.9). The phase separation in the MPC II emulsions was reversible, because it disappeared when the emulsion sample was gently inverted. Preheating MPC II before homogenization resulted in slight faster separation than unheated protein. The droplet size of the cream layer was very similar to that of the whole emulsion, which correlated with the reported phase separation behavior of caseinate emulsion systems, in which the presence of excess non-adsorbed caseinate can induce depletion flocculation of oil droplets, leading to rapid creaming (Dickinson & Golding, 1997b). Some phase separation was observed visually in the NaCas emulsions, regardless of the preheat treatment of the protein solution prior to emulsification. A dramatic increase in classified layer thickness was seen after 24 h and reached a plateau thereafter (Figure 8.9), indicating extensive flocculation, which was attributed to the presence of an excess non-adsorbed caseinate in the continuous phase (Dickinson & Golding, 1997b).

It was expected that preheating the protein dispersion prior to emulsification could lead to more protein adsorption and that this increase in density at the oil−water interface would improve the stability of the emulsion (Dybowska, 2008). However, the opposite was observed in heated MPC I emulsion (Figure 8.8). The high low-shear rate viscosity of the heated MPC I emulsion formed with unheated protein (Figure 8.6) predominantly contributed to the better emulsion stability. At a protein concentration around that required to coat the oil droplet surface completely, the colloidal system is stable against creaming (Dickinson, 1999b). When the oil droplets are stabilized by NaCas, the presence of an excess of non-adsorbed caseinate or casein micelles can induce depletion flocculation (Dickinson & Golding, 1997b; Liang et al., 2013b; ten Grotenhuis et al., 2003). The rapid development of the clarified layer after 24 h in MPC II emulsions suggests that a weak attraction due to depletion effect may have occurred. Calcium-depleted MPC probably contains some dissociated caseins with a size range of 20−50 nm (Ye, 2011), which is within the optimum size range of casein particles for a depletion effect. Depletion forces observed in MPC II and NaCas emulsions are much weaker and aggregates can rearrange. The creaming mechanism is completely different from Stokes' law. Protein preheating affected the emulsion stability of the MPC II emulsions slightly, probably because the formation of casein

micelle/whey protein and/or casein/whey protein complexes during heating (protein preheating + secondary heating) slightly increased the particle size of the non-adsorbed proteins (O'Kennedy & Moussey, 2006). This change in the size may decrease the depletion interaction potential and result in a different phase separation kinetic (Radford & Dickinson, 2004).

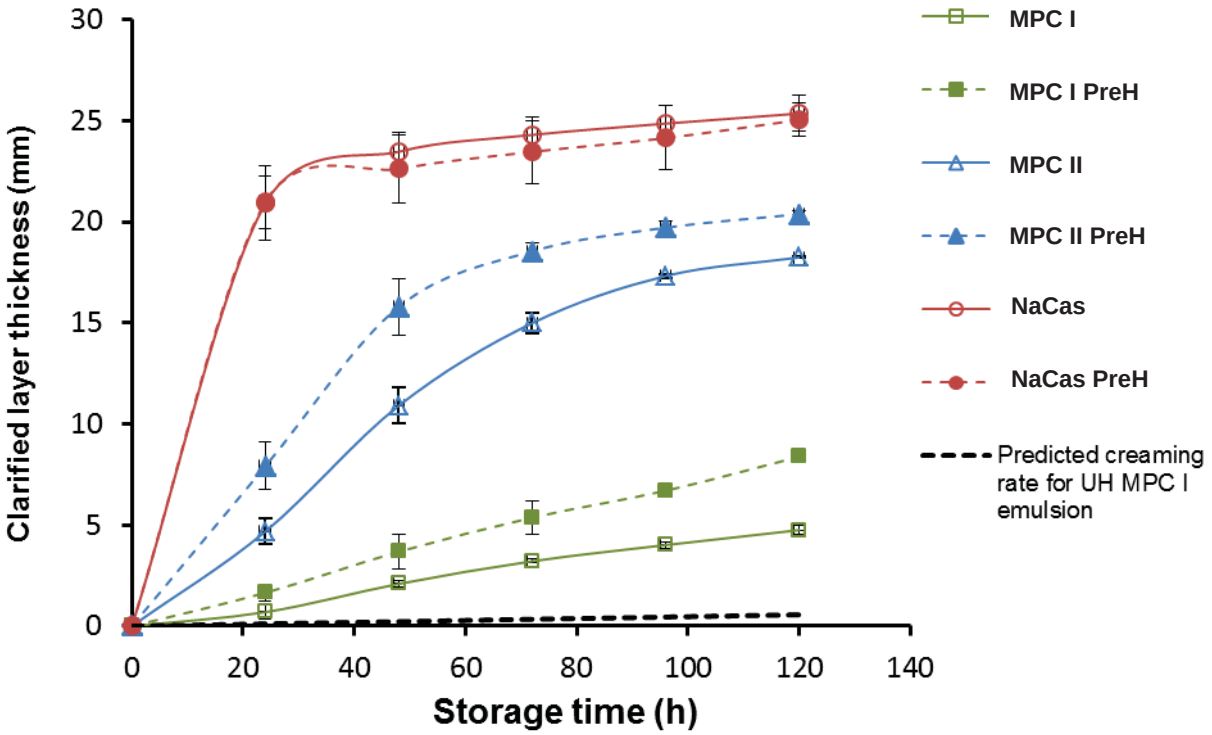

Figure 8.9. Variation in classified layer thickness as determined by Turbiscan over 120 h at 20 °C for heated 30% w/w oil-in-water emulsions stabilized by 3% w/w unheated and preheated proteins. PreH = preheated protein solution. The black dashed line shows a prediction for the creaming of concentrated emulsions with non-interacting droplets using the equation for concentrated emulsion adapted in McClements (2005), where $\emptyset_{max} \approx 0.71$ was used for a polydisperse emulsion.

8.5 Conclusions

Preheating the MPC dispersion prior to emulsification had a small beneficial effect on the heat stability of MPC-stabilized emulsions, because the pre-denaturation of the whey proteins meant that they were relatively inert during a secondary heat treatment. The aggregation state of the caseins influenced the protein adsorption behavior and the heat stability of the emulsions. In calcium-depleted MPC, the caseins dissociated from the micelles possibly had two roles. Firstly, when these dissociated casein particles adsorbed on to the emulsion droplets, they reduced the effective hydrodynamic diameter of the droplets and the volume fraction of casein particles. Secondly, the non-micellar caseins prevented extensive heat-induced flocculation of the emulsions during a secondary heat treatment. Meanwhile, the extent of depletion flocculation in the casein-stabilized emulsions was changed due to the change in the size of casein particles.

The present preliminary results provides insights about the stabilization mechanisms of milk protein ingredients with different micellar and non-micellar content and the applicability of pre-homogenization heat treatment in respect to emulsion preparation and physicochemical properties of protein-stabilized emulsion. The results will further help to understand and to optimize the manufacturing process in designing tailored viscosity, viscoelastic properties and creaming stability of food/dairy formulations with different oil contents.

Chapter 9: Physicochemical Properties and Rheological Behaviors of Whey-Protein-Stabilized Oil-in-Water Emulsions as Influenced by Pre− and Post−homogenization Heat Treatments [6]

9.1 Abstract

The effect of heat treatment on the physical stability of emulsions stabilized by whey protein concentrate (WPC), pre-denatured WPC and whey protein isolate (WPI) was investigated. Whey protein dispersions (4.5% w/w) were preheated at 90 ºC for 5 min at neutral pH prior to emulsification. The emulsion droplets stabilized by preheated WPC had fewer inter-droplet protein−protein interactions during secondary heating due to the pre-denaturation, which resulted in a reduction in subsequent heat-induced droplet−droplet and droplet−protein interactions. Protein preheating of pre-denatured WPC appeared to reactivate some reactive whey protein particles and/or aggregates that had already been formed in the production of the powders. The heat stability of whey-protein-stabilized emulsions during the secondary heat treatment (120 ºC, 10 min) was determined by protein preheating history and ionic strength. The creaming stability was influenced by the dispersed phase viscosity, particle size and interfacial layer properties. In summary, heat treatment can be used to tailor the functionalities and whey proteins and whey-protein-stabilized oil-in-water emulsions.

[6] Part of the content presented in this chapter to be submitted to *Food Structure*.

Part of the content was also presented as a graduate student poster presentation at IDF Annual Meeting, Parma, Italy, 15−19 October 2011.

9.2 Introduction

The effect of protein preheat treatment on casein-based oil-in-water emulsions has been studied in Chapter 8. It is of interest to extend the investigation to whey protein based oil-in-water emulsion system. The mechanisms, functionalities and applications of heat-induced whey protein nano-particles and/or aggregates using *β*-lactoglobulin (*β*-lg*)*, whey protein isolate (WPI) and whey protein concentrate (WPC) have recently received much attention (Bergenholtz, Poon, & Fuchs, 2003; Dissanayake & Vasiljevic, 2009; Moon & Mangino, 2004a; Puertas, Fuchs, & Cates, 2007; Purwanti et al., 2011; Spiegel & Huss, 2002). Several studies have described how thermally modified whey proteins change the final quality of whey-protein-stabilized emulsions (Bernard et al., 2011; Dybowska, 2011; Millqvist-Fureby et al., 2001; Moon & Mangino, 2004b; Sourdet, Relkin, & Cesar, 2003). Many of these studies investigated the performance of denatured whey protein aggregates in the stabilization behaviors at oil/water interface. Creaming stability of whey-protein-stabilized emulsions can be controlled by the adsorption of heat-induced whey protein nano-particles and/or aggregates and/or the increased viscosity of the continuous phase due to heat-induced effect (Dybowska, 2011). Whey protein aggregates produced from solutions of *β*-lg or WPI was also reported to affect the heat stability (Sağlam et al., 2013). However, the performance of heat-induced whey protein aggregates in terms of heat stability in an emulsion system has received little attention.

In addition, up to date, no studies have examined the effect of post-heat treatment on denatured-whey-protein-stabilized emulsions and their physicochemical properties (i.e. heat stability, creaming stability and rheological properties). The aims of this study were to evaluate the effect of the preheat treatment of protein solutions on: (1) the physicochemical properties of oil-in-water emulsions stabilized by WPC and WPI; (2) the physical stability of the emulsions against subsequent heat treatment (120 °C, 10 min).

9.3 Materials and methods

9.3.1 Materials

WPC 80, pre-denatured WPC and WPI 895 were used as model proteins and corn oil was used as oil source for the emulsion preparation (details mentioned in section 3.1.1). In the results and discussion, WPC 80 is referred to as WPC I and pre-denatured WPC is referred to as WPC II. The pre-denatured WPC was made according to the patent described in Havea (2007). The WPC I and WPI powders have almost negligible denaturation during process, ~2.5−3% soluble aggregates present in the powders (de la Fuente et al., 2002).

9.3.2 Preparation of model emulsions

The model emulsions were prepared following the procedure described in Figure 9.1. Each model emulsion was prepared at least in triplicate. The pH of the initial whey protein solutions (4.5% w/w) was adjusted to 6.8 with 1 M HCl or 1 M NaOH. The heat treatment was conducted at 90 °C for 5 min (the heating-up time was about 6 min), after which the dispersion was immediately cooled rapidly in an ice bath. The denaturation of the whey proteins in the WPC I and WPI powders was determined by native- and sodium dodecyl sulphate (SDS)-polyacrylamide gel electrophoresis (PAGE) under reducing conditions (Havea, Singh, & Creamer, 2002) and that during preheat treatment was determined by reverse phase high performance liquid chromatography (RP-HPLC) (Elgar et al., 2000). The SDS gels were scanned using an Image Scanner III (GE Healthcare Bio-Sciences AB, Uppsala, Sweden). The intensities of the protein bands were obtained using Molecular Dynamics ImageQuant software (GE Healthcare Bio-Sciences AB). For the RP-HPLC determination, 2 mL of 1% w/w protein solution was centrifuged at 13,000 g for 3 min. The supernatant of the protein solution was taken for the determination of the denaturation level of native whey proteins and the injection volume was 50 μL. The calculation of the denaturation level of whey proteins used standard WPC as the reference of native proteins.

9.3.3 Determination of effects of heat treatment on emulsions

The heat stability of the model emulsions was determined as the procedure described in Chapter 3, Section 3.2.5.

9.3.4 Determination of particle size distributions of model emulsions

The particle size and droplet size measurements were carried out using procedures described in Chapter 3, Section 3.2.3.

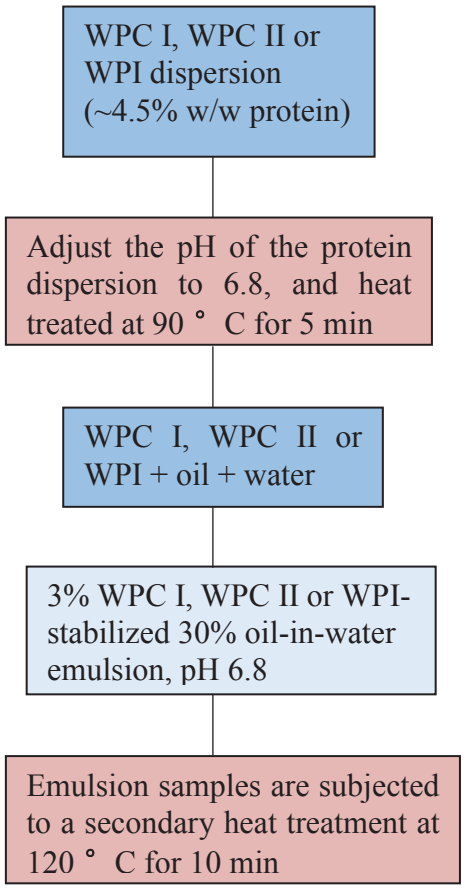

Figure 9.1. Flow chart of the preparation of model emulsions (3% w/w protein, 30% w/w oil).

9.3.5 Determination of surface protein concentration and composition

The surface protein concentration and composition were measured according to the procedures described in Chapter 3, Section 3.2.4.

9.3.6 Emulsion stability

The model emulsions were stored at ambient temperature and measured periodically for up to 5 days using a vertical scan analyser Turbiscan Classic MA 2000 (Formulaction, Toulouse, France). Details of the techniques are described in Chapter 3, Section 3.2.7.

9.3.7 Rheological properties of model emulsions

Details of the rheological measurement of emulsions have been described in Chapter 3, Section 3.2.6.

9.3.8 Statistcial analysis

All experiments were carried out at least in triplicate using freshly prepared samples and the results are reported as the mean and standard deviation of these measurements. The experimental data were analyzed by Student's t-tests using Microsoft Excel 2007 (Microsoft Corporation, Redmond, WA, USA) and significant differences among the means were determined at a 95.0% confidence level.

9.4 Results and discussion

9.4.1 Effect of preheat treatment on the denaturation of whey protein dispersions

The extent of denaturation of the whey proteins in 4.5% w/w WPC I, WPC II and WPI dispersions after the preheat treatment (90 °C, 5 min) was determined (Table 9.1). The total denaturation was ~80% for WPC I and WPC II (pre-denatured level of whey proteins is ~65%) and was slightly lower (~73%) for WPI. The extent of total denaturation in the pre-denatured WPC II powder was ~65%, and increased to a similar level to that in WPC I after the preheating process. During production of the WPC II powder, the extent of denaturation of β-lg (77.77%) was much greater than that of α-lac (32.91%).

Electrostatic interactions have been suggested to play a very important role in determining the conformation and the final aggregation state of denatured whey proteins (Dybowska, 2011; Zhai et al., 2011a). The presence of minerals (Ca, Na, K, P) influences the heat-induced aggregation behavior of whey proteins by reducing the repulsion forces, leading to more extensive formation of cross-linked protein aggregates (Purwanti et al., 2011). Therefore, it is possible that the final protein aggregate structures and denaturation rates of WPC and WPI are different under the same preheating condition. It is expected that a more compact structure will be formed in the presence of a higher level of Ca^{2+} at high heating temperature.

Table 9.1. Protein denaturation of different whey protein dispersions (4.5%, w/w) before and after preheat treatment (90 °C for 5 min), determined by RP-HPLC.

Protein sample	WPC I	WPC II	WPI	PreH WPC I	Pre H WPC II	PreH WPI
Total denaturation (%)	0	65.79 ± 0.21[a]	0	83.24 ± 2.01	79.85 ± 0.58[a]	73.10 ± 1.34
β-Lactoglobulin denaturation (%)	0	77.77 ± 0.07[a]	0	82.47 ± 2.31	79.98 ± 2.80[a]	80.19 ± 2.06
α-Lactalbumin denaturation (%)	0	32.91 ± 0.02[a]	0	85.56 ± 1.35	82.72 ± 0.41[a]	71.17 ± 1.14

PreH = preheated.
[a] Calculation of the denaturation (%) of PreH WPC I, WPC II and PreH WPC II used WPC I as a reference, and that of PreH WPI used WPI as a reference.

9.4.2 Particle size distribution of model emulsions

The surface-weighted particle size ($d_{3,2}$) values of the milk-protein-stabilized emulsions are shown in Table 9.2. There was no significant difference in the mean primary $d_{3,2}$ values among the WPC I, WPC II and WPI emulsions stabilized with unheated proteins. However, the whey-protein-stabilized emulsions stabilized with preheated protein had significantly larger primary $d_{3,2}$ values than those stabilized with the corresponding unheated protein. The larger particle size of emulsion droplets stabilized with preheated protein indicated that the whey proteins lost some emulsifying ability during emulsification after they had been preheated. Whey proteins were found to lose emulsifying ability significantly as the temperature increased because the aggregated whey proteins became less surface active and the primary particle size of emulsions stabilized with aggregated whey proteins increased (Millqvist-Fureby et al., 2001). Dybowska (2011) and Segall & Goff (2002) also observed an increase in particle size of emulsions stabilized with heated whey protein. The present result was consistent with these previous studies.

The particle size of whey-protein-stabilized oil-in-water emulsions generally increased after the secondary heat treatment. The extent of heat-induced change in particle size was controlled by the protein preheating history prior to emulsification. It is well known that larger whey protein aggregates are induced by thiol/disulfide interchange reactions and non-covalent aggregation above 75 °C (Havea et al., 2002; Wit, 2009). At high temperature, the heat-induced droplet−droplet, protein−droplet and protein−protein interactions that occurred between adsorbed proteins at the oil−water interface and in the continuous aqueous phase were responsible for the change in particle size (Euston et al., 2000; Keowmaneechai & McClements, 2006; Sliwinski et al., 2003). It was shown that the mean effective particle size of emulsions stabilized by pre-heated whey proteins including WPC II, preheated WPC I and WPC II was smaller than that formed with WPC I. In addition, the mean primary particle size of the heated WPC emulsions, regardless of protein preheat treatment, still remained larger with the addition of dissociating agents 1% SDS and an EDTA/Tween mixture (0.04 mol/kg and 5 g/kg) before the particle size measurement. This suggests that some covalently linked and calcium-bridged aggregates were formed during heating.

Table 9.2. Mean primary and effective particle sizes of 30% w/w oil-in-water emulsions formed with 3% w/w whey proteins before and after heat treatment and mean effective particle sizes after heat treatment.

Heat treatment of protein solution	Primary $d_{3,2}$ (μm)					
	Unheated WPC I	Unheated WPC II	Unheated WPI	PreH WPC I	PreH WPC II	PreH WPI
Unheated emulsion	0.64 ± 0.01 ^{aA}	0.69 ± 0.11 ^{acA}	0.63 ± 0.03 ^{aA}	1.02 ± 0.14 ^{bA}	0.89 ± 0.01 ^{bA}	0.78 ± 0.08 ^{bcA}
Heated emulsion	4.04 ± 2.33 ^{acB}	0.73 ± 0.11 ^{bA}	0.59 ± 0.09 ^{bA}	3.61 ± 0.63 ^{cB}	1.86 ± 0.24 ^{aB}	0.78 ± 0.01 ^{bA}
	Primary $d_{4,3}$ (μm)					
	Unheated WPC I	Unheated WPC II	Unheated WPI	PreH WPC I	PreH WPC II	PreH WPI
Unheated emulsion	1.31 ± 0.04 ^{aA}	1.39 ± 0.06 ^{aA}	1.32 ± 0.10 ^{aA}	2.32 ± 0.46 ^{bA}	2.42 ± 0.36 ^{bA}	1.51 ± 0.12 ^{aA}
Heated emulsion	135.4 ± 11.6 ^{aB}	3.74 ± 1.33 ^{bB}	1.52 ± 0.18 ^{cA}	25.2 ± 7.53 ^{dB}	14.1 ± 2.37 ^{eB}	3.91 ± 1.32 ^{bB}
	Effective d_{43} (μm)					
	Unheated WPC I	Unheated WPC II	Unheated WPI	PreH WPC I	PreH WPC II	PreH WPI
Unheated emulsion	0.82 ± 0.04 ^{aA}	0.74 ± 0.01 ^{bA}	0.81 ± 0.15 ^{abA}	2.85 ± 0.27 ^{cA}	1.78 ± 0.26 ^{dA}	0.76 ± 0.06 ^{abA}
Heated emulsion	188.1 ± 4.03 ^{aB}	8.15 ± 1.08 ^{bB}	3.20 ± 1.68 ^{cB}	19.9 ± 1.76 ^{dB}	16.4 ± 3.27 ^{dB}	4.09 ± 1.40 ^{cB}

^{a,b,c,d,e} Means within the same row and having the same superscript are not significantly different by Student's t-test at $p < 0.05$.

^{A,B} Means within the same column and having the same superscript are not significantly different by Student's t-test at $p < 0.05$.

9.4.3 Protein load of model emulsions

Similar amounts of protein (2.28 ± 0.90, 2.61 ± 0.06 and 2.13 ± 0.38 mg/m^2) adsorbed at the oil−water interface for the unheated WPC I, WPC II and WPI emulsions (Table 9.3). This result was in line with other studies (Tcholakova et al., 2006a), in which the minimum protein surface load for WPC-stabilized emulsions was approximately 2 mg/m^2. Preheating the whey protein solutions before emulsification slightly increased the surface protein load of the unheated model emulsions (Table 9.3). The adsorption behavior of partially denatured whey proteins has been postulated (Sliwinski et al., 2003). Mixtures of native and denatured whey proteins behave in a

complementary manner during emulsification: native whey proteins adsorb rapidly on the surface of oil droplet, whereas denatured particles form a thick layer at the oil−water interface (Dybowska, 2011; Sliwinski et al., 2003).

The amount of protein at the oil−water interface was significantly increased ($p < 0.05$) after heating for the WPC I emulsion stabilized with unheated protein (Table 9.3), however, the increase was not significant different for the WPC I emulsion stabilized with unheated and preheated proteins. This change is in line with the large standard deviation of the primary droplet size ($d_{3,2}$) in WPC I emulsion formed with unheated protein (Table 9.2).

The heated WPC II emulsion stabilized by unheated protein had a much lower surface protein load than that stabilized by preheated protein. These results suggested the formation of aggregated droplets or the formation of a multilayer at the oil−water interface. It was interesting that the preheat treatment of the WPC II solution resulted in a higher surface load when the emulsion was subjected to a subsequent heat treatment. This suggested that some reactive sites on the pre-denatured particles in WPC II may have been exposed, making them susceptible to subsequent heat-induced aggregation.

Table 9.3. Surface protein load on unheated and heated (120°C, 10 min) 30% w/w oil-in-water emulsions formed with 3% w/w unheated and preheated protein dispersions.

Heat treatment of emulsion sample	Surface protein concentration (mg/m^2) for unheated protein	Surface protein concentration (mg/m^2) for preheated protein
Unheated WPC I	2.28 ± 0.90^{aA}	8.20 ± 1.07^{aB}
Unheated WPC II	2.61 ± 0.06^{bA}	8.20 ± 0.14^{aB}
Unheated WPI	2.13 ± 0.38^{aA}	3.16 ± 0.63^{bA}
Heated WPC I	63.10 ± 27.72^{cA}	31.68 ± 6.95^{cA}
Heated WPC II	3.55 ± 0.05^{dA}	23.44 ± 6.79^{cB}
Heated WPI	2.42 ± 1.01^{abA}	4.98 ± 0.44^{dA}

[a,b,c,d] Means within the same column and having the same superscript are not significantly different by Student's t-test at $p < 0.05$.

[A,B] Means within the same row and having the same superscript are not significantly different by Student's t-test at $p < 0.05$.

9.4.4 Rheological behaviors of model emulsions

9.4.4.1 Dynamic oscillatory rheology

The evolution of the storage modulus (*G'*) during a heating and cooling cycle (20 to 90 to 20 °C) of the heat-induced whey protein emulsions is displayed in Figure 9.2, which shows that emulsions stabilized by WPC I, preheated WPC I and preheated WPC II formed gels in the heating and cooling period whereas the emulsions formed with WPC II, WPI and preheated WPI remained in liquid form. Irreversible heat-induced disulfide bridges and hydrophobic interactions are the main attractive interactions involved in the mechanisms of whey protein gelation (de la Fuente, Hemar, Tamehana, Munro, & Singh, 2002; Havea et al., 2009). As expected, a lower storage modulus was obtained when the WPC I emulsion was stabilized with preheated protein. Less whey protein aggregation occurs during the secondary heat treatment when the whey proteins are pre-denatured and subjected to high speed shearing. Because thiol/disulfide interchanges between denatured whey proteins have already occurred during protein preheat treatment, fewer reactive sites (free thiol groups) are available during a secondary heat treatment (Dissanayake & Vasiljevic, 2009). The role of high pressure shearing of pre-denatured whey proteins on heat stability has been emphasized. A synergistic effect on the pronounced improvement in heat stability was found when pre-denatured whey proteins underwent high pressure shearing or high cavitation forces generated by ultrasound (Chandrapala et al., 2011; Dissanayake & Vasiljevic, 2009). The WPC II emulsion stabilized by unheated protein also showed its good heat stability as it did not form a gel (Figure 9.2). It is worth noting that the whey protein emulsions experienced a high speed shearing during homogenization. It was found that, when the WPC II solution was homogenized twice at 20 MPa, the particle size was effectively decreased and the HCT was significantly increased and reached a plateau value above 30 MPa (Figure 9.3). Thus, the good heat stability of WPC II emulsion was partially attributed to the decreased particle size of WPC II in the continuous phase. Protein preheat treatment of WPC II seemed to generate some whey protein particles that were reactive during the secondary heat treatment and this resulted in a weak gel network. The exact mechanism for the denatured whey protein re-aggregation is still not known.

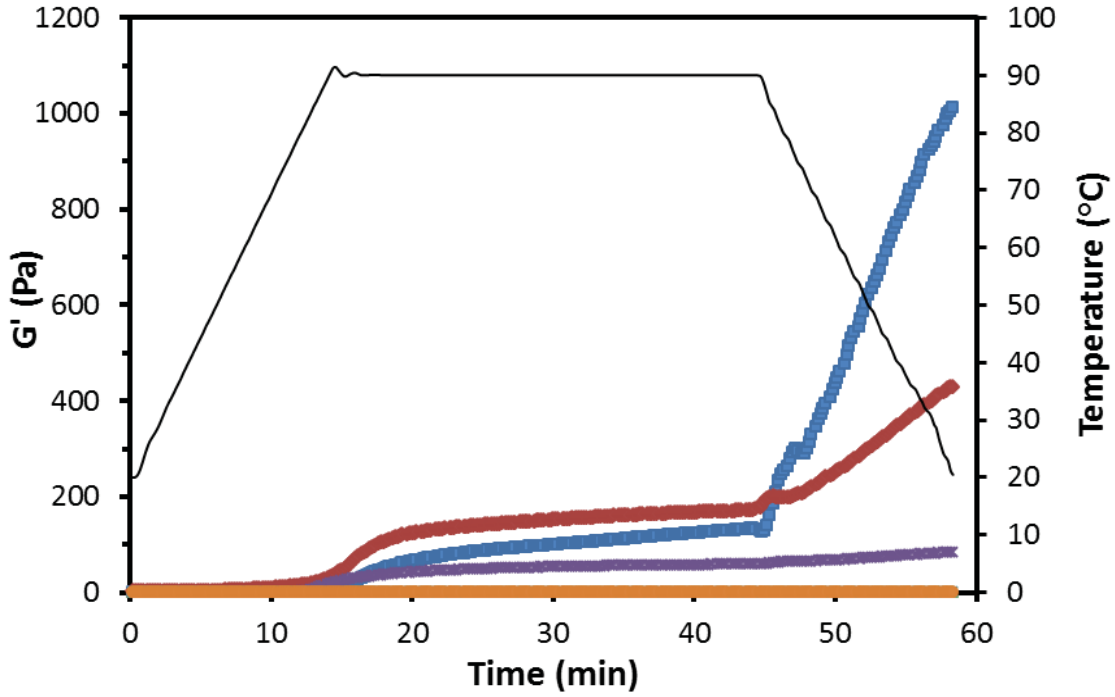

Figure 9.2. Evolution of storage modulus (G') of 30% w/w oil-in-water emulsions stabilized by 3% w/w protein as a function of time during a heating and cooling cycle (20 to 90 to 20 °C). (■) WPC I emulsion stabilized by unheated protein; (♦) WPC I emulsion stabilized by preheated protein; (▲) WPC II emulsion stabilized by unheated protein; (×) WPC II emulsion stabilized by preheated protein; (*) WPI emulsion stabilized by unheated protein; (●) WPI emulsion stabilized by preheated protein. The solid line indicates the heating and cooling cycle.

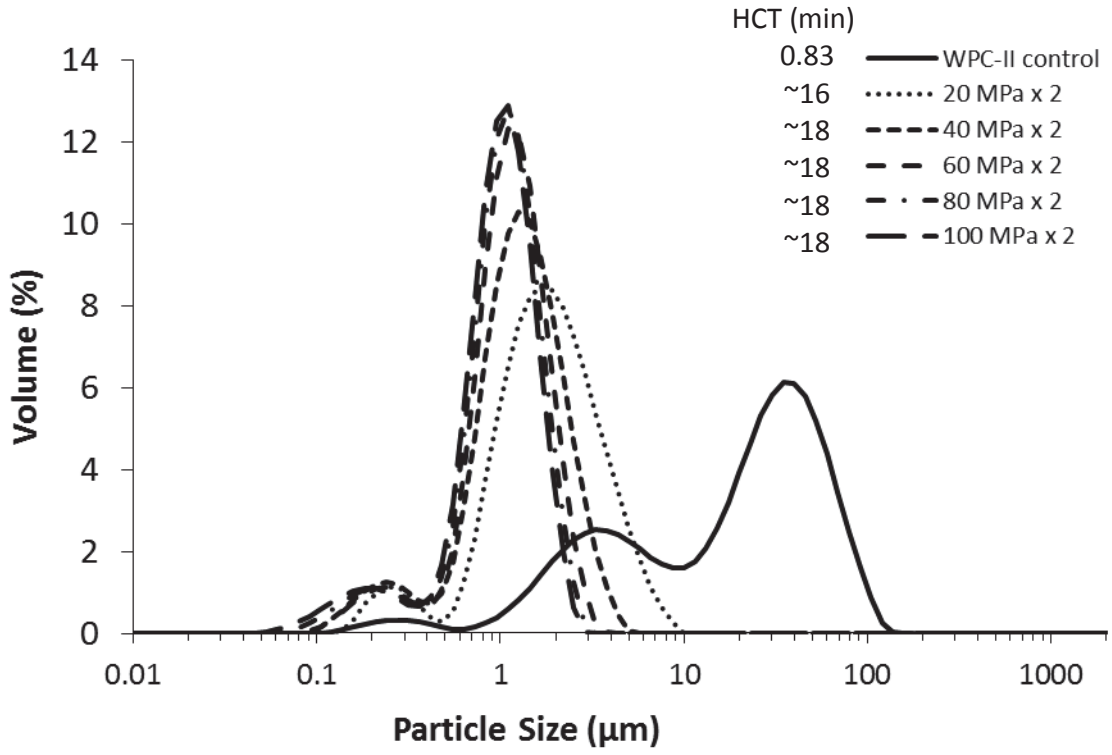

Figure 9.3. Effect of homogenization pressure on the particle size distribution of the oil-free phase of WPC II emulsions and on the HCT at 140 °C.

9.4.4.2 Shear flow behavior

Figure 9.4 shows the flow characteristics of the emulsions for the shear rate range 0.05−200 s^{-1}. Shear-thinning behavior of emulsions indicates that the flocculated droplets or aggregates break apart as the shear rate is increased (McClements, 2005). The unheated WPC I and WPI emulsions formed with preheated proteins showed significantly ($p < 0.05$) decreased n and k values, whereas those of the WPC II emulsions remained unchanged ($p > 0.05$) regardless of the protein preheat treatment. It is expected that some whey protein aggregates adsorbed at the oil−water interface and formed a thicker and more viscous surface layer (Bernard et al., 2011). Dybowska (2011) has suggested that a viscous interfacial structure formed with preheated whey proteins gives a viscous emulsion because of the increased volume fraction of the adsorbed whey protein aggregates and the formation of a thick protein layer. Enhanced droplet−droplet interactions by the presence of a small quantity of protein aggregates at the oil−water interface might also be associated with the increased emulsion viscosity (Knudsen et al., 2008).

When the whey protein emulsions were subjected to post-homogenization heat treatment (120 °C, 10 min), all the emulsions increased in viscosity and showed shear-thinning behavior ($n < 1$); however, the extent of change varied among the samples. Emulsions stabilized by WPC I, preheated WPC I and preheated WPC II showed significant increases in viscosity compared with before heat treatment. The strong shear-thinning behaviors of these emulsions can be attributed to the disruption of flocs or aggregates, which were non-covalently bonds associated. In contrast, the WPI emulsions, regardless of protein preheat treatment, displayed slight shear-thinning behaviors because WPI- and/or β-lg-stabilized emulsions are stable to heat-induced droplet flocculation in the presence of low salt concentrations (Kim et al., 2002b; Ye, 2010; Zhai et al., 2011a). Despite the increase in viscosity upon heating, the protein preheating resulted in lower viscosity for the emulsions stabilized by WPC I and WPI.

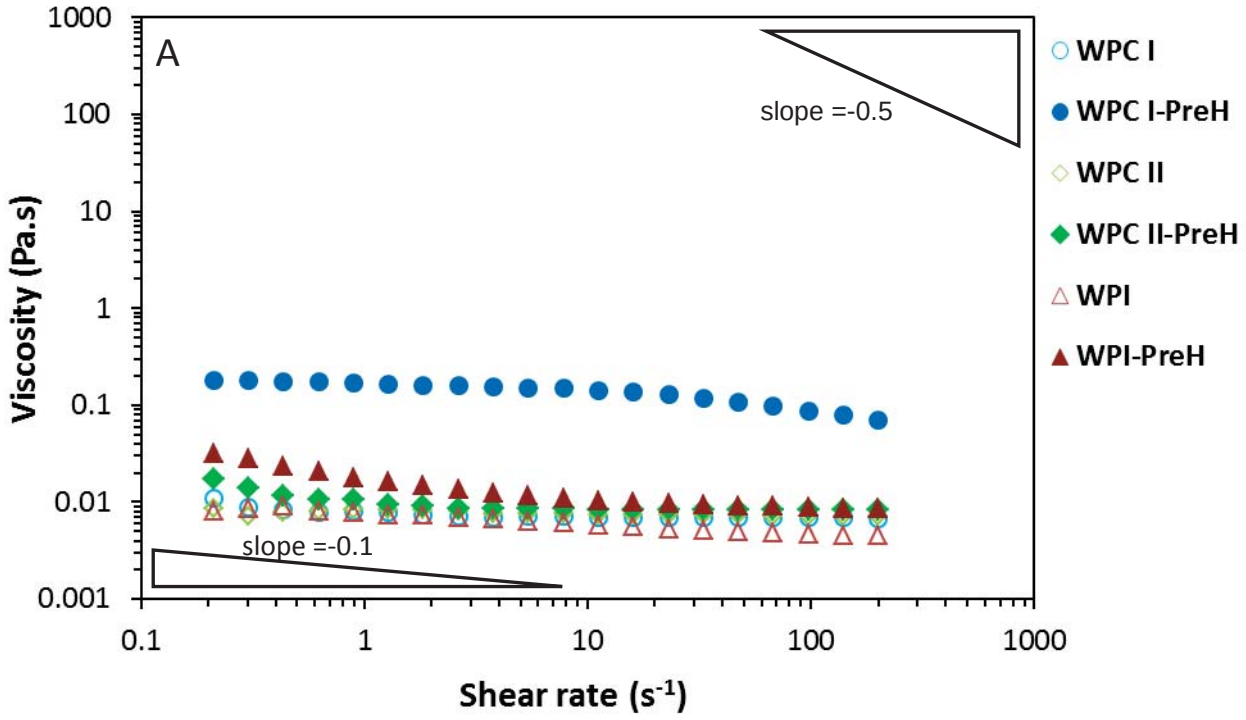

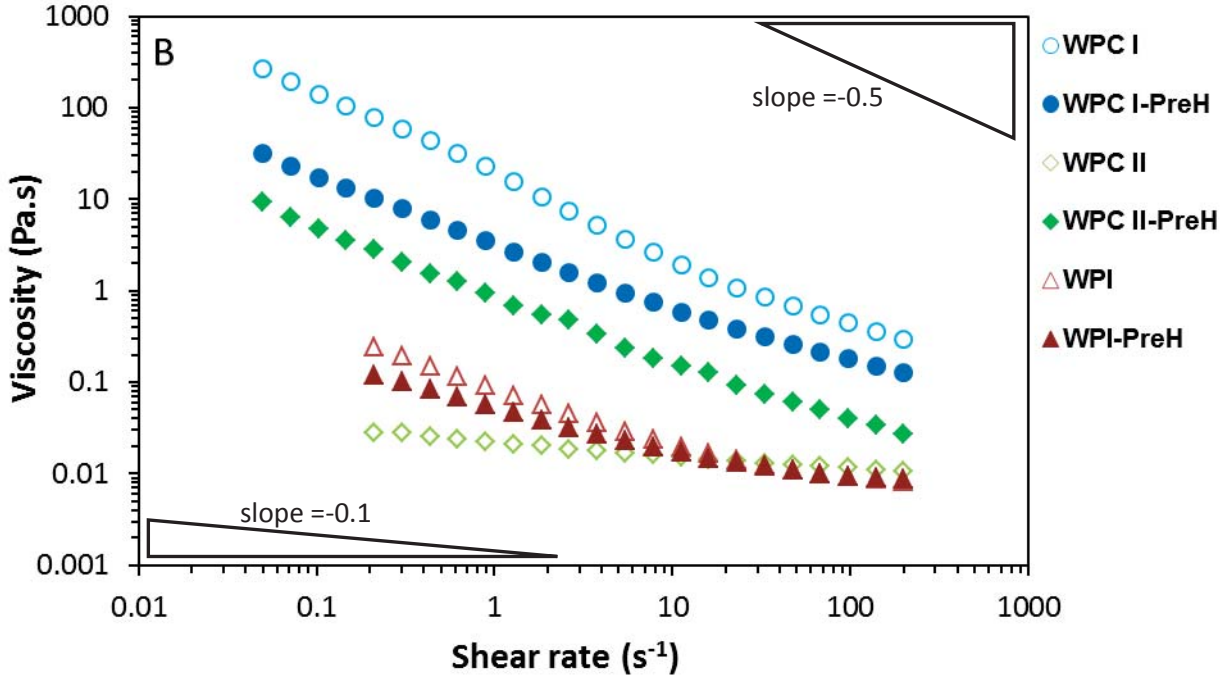

Figure 9.4. Apparent viscosity of (A) unheated and (B) heated (120°C, 10 min) 30 % w/w oil-in-water emulsions stabilized by 3% w/w unheated protein and by 3% w/w preheated protein (shear rate was increased from 0.05 to 200 s^{-1} at 20 °C). PreH = preheated protein.

9.4.5 Creaming stability of model emulsions

The unheated and heated emulsions stabilized by WPC I, WPC II and WPI were monitored both visually and with a Turbiscan over 28 days of storage at ambient temperature (20 °C) (Figure 9.5). For the unheated emulsions, the WPC I emulsion stabilized by preheated protein showed faster development of a classified layer than that stabilized by unheated protein. In contrast, the WPC II emulsion formed with preheated protein had a consistently lower classified layer thickness than that formed with unheated protein, but was not significantly different after 28 days. Interestingly, some development of sediment in the WPC II emulsion stabilized by unheated protein was detected by Turbiscan. The sedimentation disappeared when the emulsion was stabilized by preheated protein. The WPI emulsions stabilized by unheated protein and preheated protein showed very similar creaming behaviors. It was expected that a more rigid interfacial layer governed by aggregated whey protein particles will effectively stabilize the emulsion droplets against coalescence (Tcholakova et al., 2006a). Dybowska (2011) suggested

that whey protein particles rather than droplet diameters determine the stability of emulsions formed with preheated whey proteins. The whey protein particles adsorb at the oil/water interface with limited reactive sites for interaction but with sufficient electrosteric stability to improve the emulsion stability. This seemed to be the case for the WPC II emulsions but not for the WPC I emulsions. This may have been because the WPC I emulsion stabilized by preheated protein had a significantly larger primary $d_{3,2}$ value. Although preheating the protein dispersion resulted in a more viscous emulsion and a thicker interfacial layer, as a net outcome, the large mean droplet size appeared to have a greater effect on the creaming stability.

For the heated emulsions, the WPC I emulsion stabilized with unheated protein did not show any classified layer. The WPC II emulsions stabilized with unheated protein and preheated protein displayed very similar creaming behaviors and sedimentation was still observed in the emulsion stabilized by unheated protein. The WPI emulsion stabilized by preheated protein showed a slower development of a classified layer than that stabilized by unheated protein. The good physical stability of the WPC I emulsion stabilized with unheated protein can be attributed to the strong gel network formed during heating, which was sufficient to prevent any flocs and/or aggregated droplets from creaming. It was postulated that some whey protein particles and/or aggregates reactivated during the protein preheat treatment may have been involved in inter-droplet protein−protein interactions during post-homogenization heating that effectively reduced the amount of large whey protein aggregates in the continuous phase for sedimentation. This change correlated with the increased particle size and surface protein load results in the WPC II emulsion stabilized by preheated protein. The WPI emulsions stabilized by unheated protein and preheated protein showed similar primary particle size and viscosity. The discrepancy in creaming stability of the WPI emulsions might be attributed to the different conformation of whey protein particles/aggregates at the oil−water interface. Increased oil droplet interactions were proposed when heated adsorbed β-lg was used to emulsify oil droplets (Knudsen et al., 2008). The secondary heat treatment probably resulted in a less cohesive interfacial layer that had limited reactive sites for droplet−droplet interactions in the WPI emulsion stabilized by preheated protein.

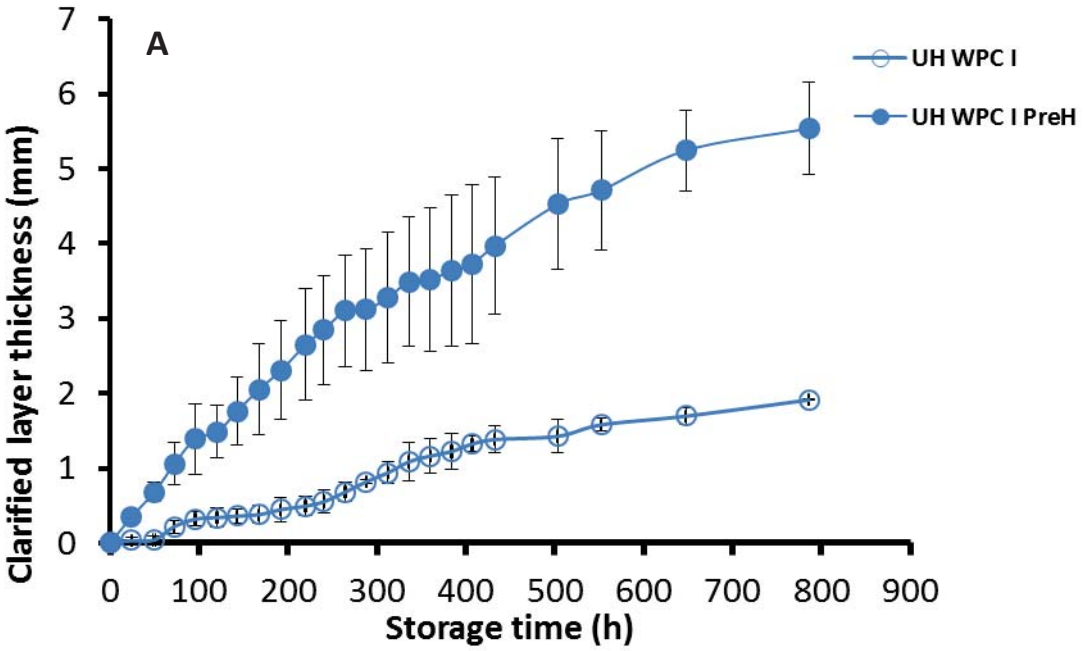
A
UH WPC I
UH WPC I PreH
Clarified layer thickness (mm)
Storage time (h)
0
1
2
3
4
5
6
7
0
100
200
300
400
500
600
700
800
900

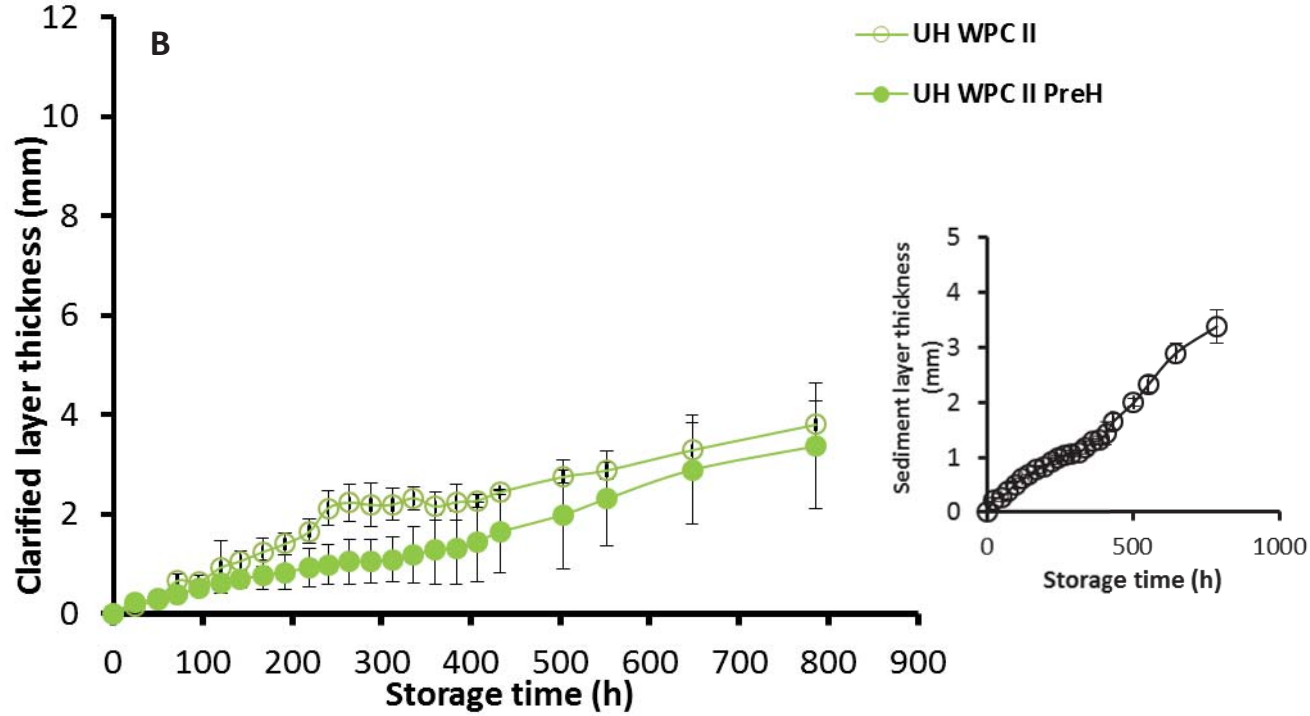
B
UH WPC II
UH WPC II PreH
Clarified layer thickness (mm)
Storage time (h)
Sediment layer thickness (mm)
Storage time (h)
0
2
4
6
8
10
12
0
100
200
300
400
500
600
700
800
900
0
1
2
3
4
5
0
500
1000

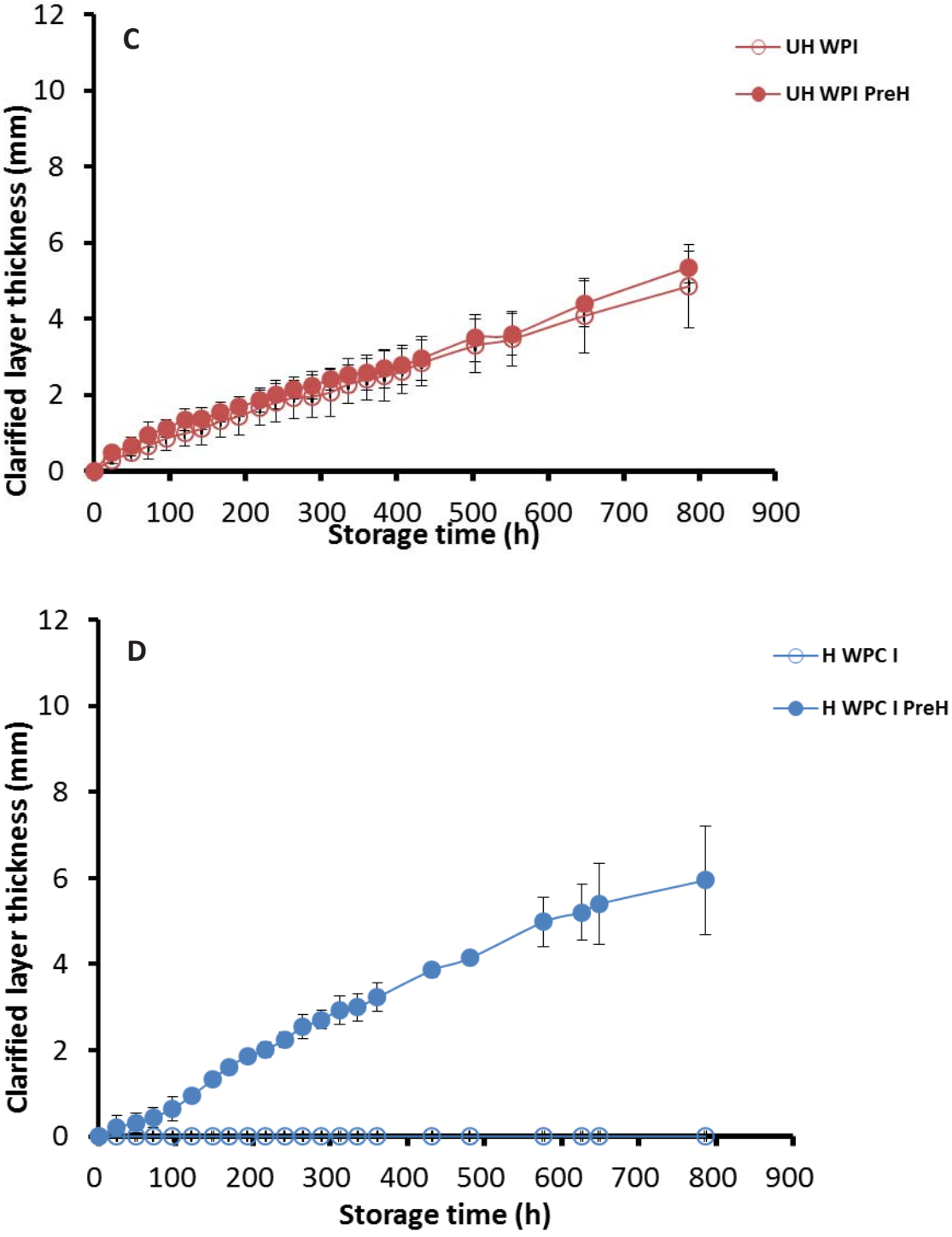
C
UH WPI
UH WPI PreH
Clarified layer thickness (mm)
Storage time (h)
0
2
4
6
8
10
12
0
100
200
300
400
500
600
700
800
900
D
H WPC I
H WPC I PreH
Clarified layer thickness (mm)
Storage time (h)

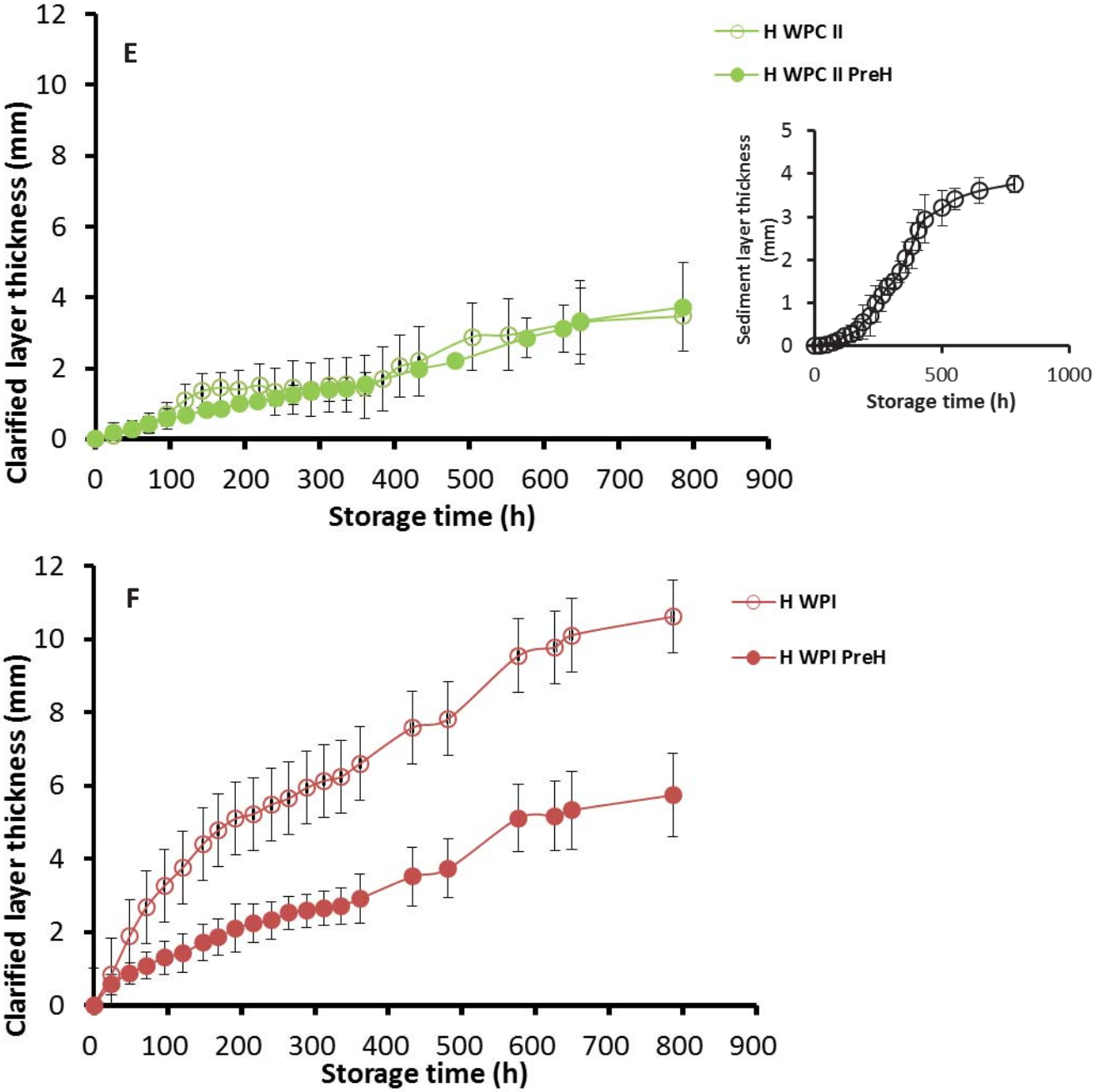

Figure 9.5. Variation in backscattering, monitored over 672 h (28 days), for unheated and heated (120 °C for 10 min) 30% w/w oil-in-water emulsions stabilized by 3% w/w unheated and preheated protein solutions expressed as classified layer thickness at room temperature: (A) unheated WPC I emulsions; (B) unheated WPC II emulsions; inset, evolution of sediment layer; (C) unheated WPI emulsions; (D) heated WPC I emulsions; (E) heated WPC II emulsions; inset, evolution of sediment layer; (F) heated WPI emulsions. PreH=preheated protein.

9.5 Conclusions

In this study, the effect of preheating whey protein on heat stability, creaming stability, microstructure and rheological properties was investigated. The heat stability of WPC and WPI emulsions is improved by denatured and/or aggregated whey proteins. The fewer free thiol groups available during post-homogenization heating are responsible for the change. Interestingly, the preheating of pre-denatured WPC seems to reactivate some reactive sites for aggregation, resulting in a viscous and weak gel-like texture during post-homogenization heating. The increased emulsion viscosity and the formation of a thicker interfacial layer are found to help to delay creaming of the emulsion. Heat-induced whey protein particles and/or aggregates and thermal processing can be used to tailor the viscosity, viscoelastic properties and sedimentation of low fat emulsions. Investigation of the interrelationships among the conformational changes of denatured whey proteins at the oil−water interface, the particle size of denatured whey protein particles and controlled emulsion destabilization is the emphasis of future study.

Chapter 10: Summary and Recommendations for Future Work

10.1 Overall conclusions

Oil-in-water emulsions are an important basis of many pharmaceutical, nutraceutical and food products such as infant formulae, parenteral emulsions and enteral medical beverages. Because of the appreciable increase in sarcopenia, weight loss and malnutrition within the population of older adults (> 65 years), there is increased interest in formulating small serve volume, high energy medical nutrition products, such as high protein-based emulsions, that can help to provide a concentrated source of energy and essential fatty acids, vitamins, minerals and bioactive compounds. Interactions between the ingredients, such as droplet−droplet, protein−droplet, protein−protein and protein−carbohydrate interactions, affect the emulsion stability and rheological properties; this is highly undesirable with respect to processing, storage and consumption. Whereas fairly harsh heat treatments (UHT or retort sterilization processes) are required to achieve high microbiological quality, they will affect the physical stability, particularly creaming and viscosity, of the product. From the point of view of an enhancement in nutritional intake, the design of a low volume and high energy density product is suggested. From the patient's point of view, low viscosity products (shear rate between 50 and 100 s^{-1}) are desired. In addition, for long term storage, high viscosity at low shear rates is required. Increasing total solids increases the overall product viscosity, which achieves the storage requirement but does not fulfil the patient's consumption requirement. It is very challenging to produce concentrated-protein-based emulsion products with high heat stability, low creaming rate and low viscosity. Therefore, the aim of this thesis was to obtain a better understanding of the influence of inter-particle and ingredient interactions on heat stability, creaming stability and rheological properties using model concentrated-protein-based oil-in-water emulsions. Overall, this thesis has shown that factors such as protein concentration, oil concentration, type of milk protein or surfactant used as emulsifier, severity of heat treatment, addition of carbohydrate and preheating of the protein prior to homogenization influence the physical stability of simple protein-stabilized oil-in-water emulsions.

Chapter 2 is a critical literature review on aspects of protein-stabilized oil-in-water emulsions as influenced by the type of adsorbed and non-adsorbed proteins, the concentrations of oil and protein, the droplet size and droplet size distribution, the addition of other emulsifiers and the addition of other food components (carbohydrates, minerals, calcium chelating agents). The recent advance in modulating steric repulsion is summarized and classified according to protein−surfactant, protein−protein and protein−polysaccharide interactions. Some of the recent findings from the PhD work with respect to depletion destabilization/restabilization mechanisms are also incorporated in the review.

Chapter 4 describes a study of the influence of the type of adsorbed material and the type of continuous phase protein on the physicochemical properties of heated concentrated-protein-based (8.5% w/w) oil-in-water emulsions. The primary goal of this study was to obtain a better understanding of the contribution of adsorbed and non-adsorbed protein/surfactant to the heat stability, creaming stability, microstructure and rheological properties and to categorize different emulsion systems using heat-stable proteins/surfactants and heat-sensitive proteins. The secondary goal was to obtain a better understanding of the role and impact of non-micellar casein in heated concentrated-protein-based oil-in-water emulsions. It was demonstrated that non-adsorbed whey proteins were involved in the heat-induced destabilization of not only whey-protein-stabilized emulsions [whey protein concentration (WPC) and whey protein isolate (WPI)], but also sodium caseinate (NaCas)-stabilized emulsions. The NaCas-stabilized droplets acted as an emulsion structure filler in the gel network, probably through heat-exchanged interfacial interactions. Replacement of the continuous phase whey protein with whey protein hydrolyzate (WPH) improved the heat stability of the emulsions with one notable exception, in which surface-active fractions from hydrolyzed whey protein were seen to promote droplet coalescence at high heating temperatures of Tween-20-stabilized emulsions. Emulsions containing high concentrations of micellar or non-micellar caseins, despite being heat stable, destabilized after a short period of storage because of depletion flocculation. The extent of depletion flocculation appeared to depend on the non-adsorbed protein concentration, the aggregation state and the polydispersity of the caseins.

Chapter 5 describes a study of the influence of the depletion interaction potential and the continuous phase viscosity on the emulsion stability of NaCas-stabilized oil-in-water emulsions.

The effect of xanthan gum and maltodextrin was also investigated, because polysaccharide is often added as a thickening agent to modulate the viscosity of the final product. A known amount of non-adsorbed NaCas, xanthan or low dextrose equivalent maltodextrin was added to the stock NaCas-stabilized emulsion to yield model emulsions and the samples were analyzed for their creaming stability, microstructure and rheology. There was a strong correlation between the depletion interaction potential and the creaming stability. With increasing non-adsorbed NaCas concentration up to 5% w/w, not only the strength of the droplet−droplet interactions but also the volume of bound droplets within the depletion-induced droplet network increased. Interestingly, it was found that the rate of formation of the droplet network reduced and the creaming stability improved at NaCas concentrations > 6% w/w. The increase in the continuous phase viscosity was partially attributed to the slow evolution of the depletion-induced droplet network. The addition of xanthan gum mimicked the change in phase separation behavior in the NaCas system. Surprisingly, the addition of maltodextrin not only slowed the creaming rate because of the increased continuous phase viscosity but also weakened the depletion interaction potential by reducing the particle size of the non-adsorbed NaCas.

In Chapter 6, the effect of heat treatment on the phase separation behavior of heated NaCas-stabilized emulsions was investigated by measuring the creaming rate and the physicochemical changes in NaCas in the continuous phase, which included amount of intact caseins, particle size and viscosity before and after heating (up to 60 min at 120 °C). It was found that the creaming stability of the NaCas-stabilized emulsions was markedly dependent on the heating duration. The heat-induced degradation of NaCas was the major cause of the reduced emulsion stability. NaCas dissociated into smaller peptides after severe heating because of heat-induced proteolysis, mainly of α_s- and β-caseins. This resulted in a decrease in the concentration of intact NaCas to the optimum for inducing depletion energy. As a consequence, the depletion interaction potential was reduced and the formation and rearrangement of the droplet network were more rapid. At high NaCas concentration (6% w/w), the marked reduction in continuous phase viscosity also played an important role in determining the rate of phase separation. Overall, the results in Chapters 5 and 6 showed that the depletion interaction potential and the continuous phase viscosity determined the delay time for the depletion-induced phase separation of the droplet network. Both factors were influenced by the concentration and particle size of the non-adsorbed

NaCas nano-particles, which in turn were affected by the presence of a third ingredient and the processing conditions.

The aim of the study in Chapter 7 was to determine to what extent different types of carbohydrate and the carbohydrate concentration affected the heat stability of milk protein concentrate (MPC)-stabilized emulsions. The effects of carbohydrates on the heat coagulation and the heat-induced changes in high protein MPC solutions and MPC-stabilized emulsions were evaluated by measuring the heat coagulation time (HCT) and changes in free calcium content, particle size, droplet size, microstructure and viscosity before and after heating. The HCTs of the MPC solutions and the MPC-stabilized emulsions were noticeably dependent on the initial heating pH and the heat stability maximum decreased on the addition of carbohydrate regardless of the carbohydrate type. Reducing carbohydrates such as glucose, maltose and maltodextrin decreased the heat stability significantly. Non-reducing carbohydrates such as sucrose and trehalose decreased the heat stability moderately; trehalose was the most effective carbohydrate in retaining the heat stability. In general, several factors, including increased volume fraction of casein micelle particles, increased free Ca^{2+} content and decreased solvent quality, may have been responsible for the reduced heat stability on the addition of carbohydrate. Interestingly, on the addition of 30% w/w maltodextrin, some non-covalent-linked large flocculates were formed even before heating. This also contributed to the decreased heat stability. The results in Chapter 7 basically confirmed that the extent of heat-induced destabilization of MPC solutions and MPC-stabilized emulsions was dependent on the type and concentration of carbohydrate and the initial heating pH.

Chapters 8 and 9 evaluated the use of pre-homogenization heat treatment and the influence of protein type on the physicochemical properties of heated protein-stabilized emulsions. The physicochemical properties, including the rheology of casein-stabilized and whey-protein-stabilized emulsions, were studied by measuring the HCT, surface protein coverage, protein particle size, droplet size, microstructure and viscosity. The emulsions stabilized by preheated proteins had slightly higher heat stability without affecting the emulsifying ability. This change was attributed to the denaturation of whey proteins during the pre-homogenization heat treatment, which resulted in a reduction in subsequent heat-induced inter-particle interactions. In addition, the presence of some non-micellar caseins gave better emulsification and had a positive

effect on inhibiting heat-induced whey protein aggregation during a secondary heat treatment by incorporating non-micellar caseins at the oil/water interface. The pre-homogenization heat treatment together with subsequent homogenization reduced the particle size and improved the heat stability of the denatured whey protein aggregates.

Summary Overview

The relationship between the attraction, emulsion structure, flow behavior and stability of concentrated-protein-based oil-in-water emulsions is summarized in Figure 10.1.

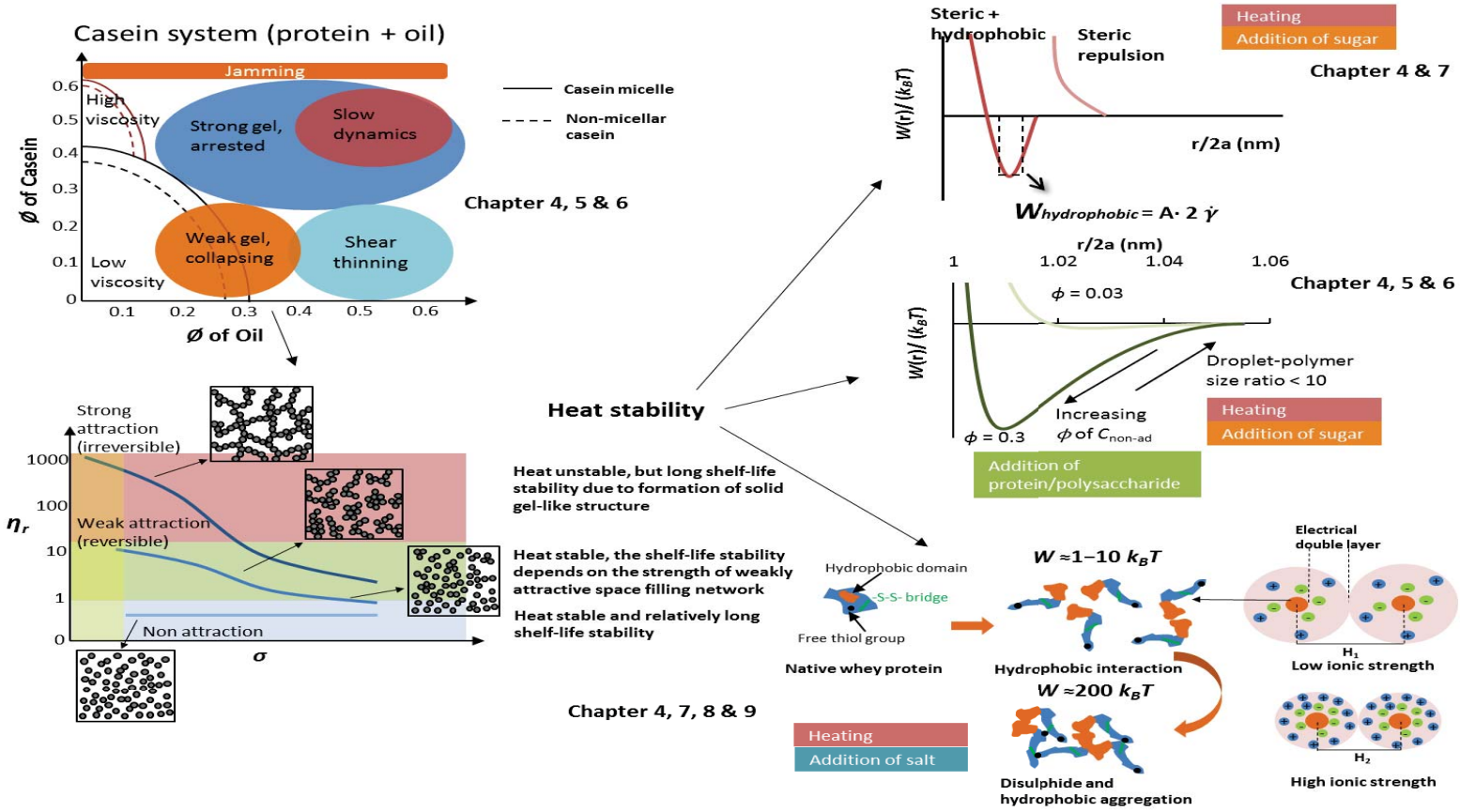

Figure 10.1. The relationship between the colloidal interactions, emulsion structure, flow behavior and physical stability of the protein-stabilized oil-in-water emulsions.

Figure 10.1 shows the schematic illustration of how the colloidal interactions and properties of proteins affect the emulsion structure, flow behavior and physical stability of protein-stabilized oil-in-water emulsions. The stability and viscosity are partially regulated by the total interaction potential which is the sum of the electrostatic interaction, steric stabilization and depletion interaction. The presence of carbohydrate (mono- or polysaccharide) and high temperature heating cause the casein micelles or non-micellar caseins (NaCas nano-particles) reduce in size due to different type of dissociation mechanism. Figure 10.1 shows that the volume fraction of protein and the dissociation of intact caseins into smaller particles affect the heat stability, creaming stability and viscosity of the high protein emulsions. The heat stability is also dependent on the extent of aggregation of whey proteins which is determined by the protein concentration, the level of ionic strength and the presence of a steric stabilizer (i.e. casein micelle or non-micellar casein). Moreover, it is impossible to cover all the factors in one diagram, the contribution of volume fraction of particle, particle size distribution and the interfacial layer thickness should be taken into account.

10.2 Industrial significance for the dairy industry

The PhD research was primarily intended to develop underpinning fundamental knowledge that would be of commercial applicability for a range of dairy emulsion-based compositions. It is difficult to quantify the specific value of the commercial developments of the PhD research. However, the findings generated by the study have significant applicability in determining best-practice approaches for the formulation and processing of dairy foods, notably in UHT and retorted beverages, where the structural and material properties of the emulsion are particularly sensitive to protein treatment. Such findings serve to provide a more iterative basis for formulating such products, ensuring a minimization of product failures and recalls, and greatly reducing development times to achieve desired product outcomes.

An important finding with regards to the heat stability of concentrated-protein-based emulsions is that non-micellar casein and Tween 20 are very heat stable emulsifiers. A heat stable high protein emulsion can be prepared by incorporating small amount of non-micellar casein or Tween 20 during the emulsification process. Another parameter can be used to tailor the heat

stability is trehalose. The heat stability of high solid emulsion containing high protein and high carbohydrate can be largely retained by replacing carbohydrates (sucrose and/or maltodextrin) that are often found in medical nutrition formulation with trehalose. In addition, the viscosity of MPC-stabilized emulsions containing up to 30% w/w trehalose had very similar viscosity profiles as those without addition of carbohydrate under sterilization condition. In addition, another important finding in this thesis is that hydrolyzed protein (WPH) is a very heat stable protein ingredient that does not induce emulsion instability driven by depletion flocculation. Essentially, the particle size of whey protein peptide is far too small comparing to the droplet size to induce depletion energy for the formation of droplet network. This effect was found similar to that of heat-induced degradation of caseins on the depletion energy. The hydrolyzed whey proteins or casein proteins can be added to formulation for manipulating the viscosity without affecting the heat stability and creaming stability. By optimizing the molecular weight profile of milk protein peptides, the functionality of concentrated-protein-based emulsions can be further enhanced.

The knowledge obtained on the protein−protein, protein−carbohydrate, and droplet−droplet interactions before and after heat treatment can facilitate the development of a novel emulsion product with gel-like texture. Texturized nutrition beverages may be useful for patients with swallowing disorders (WO2011/112087). In the combined use of calcium chelators, a novel induced viscosity product can be produced by carefully selecting the suitable type and concentration of protein, small molecular surfactant and carbohydrate.

The knowledge obtained on the phase separation behavior of NaCas emulsions as influenced by protein concentration and non-adsorbed biopolymers may give interesting opportunities for the development of novel emulsion products. For instance, the use of an arrested spinodal decomposition process to produce food colloids with solid-like properties has been demonstrated in model casein micelle/poly(ethylene oxide) systems (Gibaud, Mahmoudi, Oberdisse, Lindner, Pedersen, Oliveira, Stradner & Schurtenberger, 2012). In the development of a protein gel (containing fat) where acidification is required, the depletion flocculation process can be incorporated. For instance, the pH of the protein gel can be adjusted after the formation of a space-filling droplet network. Protein gels with different structural and mechanical properties can

be tailored made through careful control of the properties of non-adsorbing biopolymers and the solvent conditions.

10.3 Recommendations for future work

Although several aspects, including protein concentration, oil concentration, type of milk protein or surfactant used as emulsifier, severity of heat treatment, addition of carbohydrate and preheating of the protein prior to homogenization, have been investigated, some important knowledge gaps derived from this PhD work deserve further investigation.

- The impact of the interfacial material and non-adsorbed proteins on the physicochemical properties of concentrated-protein-based emulsions was successfully demonstrated using food-grade heat-stable proteins/surfactants and heat-sensitive proteins. An investigation of the interfacial properties, including interfacial tension, interfacial composition and rheology, of Tween-20-stabilized emulsions containing WPH would provide useful insight into the exact mechanism(s) that cause coalescence during heating. For instance, the heat-induced coalescence may be dependent on the polysorbate type, and the use of other types of polysorbate surfactant such as Tweens 40, 60 and 80 may help to explain how the molecular conformation of Tween affects the affinity between the Tween molecule and whey protein peptides. Also, the use of different types of WPH may help to determine the role of the molecular weight and the hydrophobicity of whey protein peptides in heat-induced coalescence.

- Characterization and categorization of model emulsions in four emulsion systems using the stability map approach was conducted using simple emulsions (protein + oil). It would be useful to continue to characterize and categorize model emulsions containing other ingredients that are close to real formulations. For example, it would be interesting to study how the characteristics of the emulsions formed change on adding carbohydrate (protein + oil + carbohydrate), polysaccharide (protein + oil + carbohydrate + polysaccharide) and minerals (protein + oil + carbohydrate + polysaccharide + minerals). The stability map of the four emulsion systems could be further developed for casein-

based and whey-protein-based applications. Moreover, the properties of emulsion droplets stabilized by different food-grade surfactants [(i.e. lecithin, monoglyceride, Spans (sorbitan esters) and DATEM (diacetyl tartaric acid ester of mono- and diglycerides)] could be further compared based on the surface charge and molecular conformation and categorized using the stability map approach because lecithin and DATEM are commonly used as emulsifiers in liquid nutritional formulations (McSweeney, 2008).

- The correlation between non-adsorbed biopolymer concentration and depletion-induced phase separation was well illustrated using NaCas as the casein-based depletant. It would be interesting to study the effect of the non-spherical conformation of caseins on the phase separation behavior of depletion-induced networks using individual caseins such as α_{s1}-, β- and κ-caseins because they are proposed to have different micelle conformations. In this thesis, it was assumed that the conformation and the particle size of the NaCas nano-particle did not change as a function of protein concentration. Indeed, α_{s1}-casein is known as a telechelic polymer and assumes a rod-like conformation at high casein concentrations and a flower-like conformation in the presence of a low level of ionic calcium (Horne, 2002). In addition, telechelic polymers, which consist of two associative groups (hydrophobic domains), have higher viscosity at a constant concentration than polymers comprising fewer associative groups (Chassenieux et al., 2011). Hence, the importance of α_{s1}-casein for the self-assembly of the NaCas nano-particle should be taken into account in the calculation of the depletion interaction potential and the change in viscosity at high casein concentrations. Other light scattering techniques such as small-angle X-ray scattering could be incorporated to obtain a direct determination of the size of the casein nano-particle.

- Two other interesting lines of research with respect to the depletion-induced droplet network would be to further extend the network to both an MPC-stabilized emulsion system and a whey-protein-stabilized emulsion system. For the MPC system, it would be of great interest to correlate the phase separation behaviors observed in the NaCas system with those that may arise in a casein micelle system because the micelle size and the

polydispersity of the micelle are different. Furthermore, in the MPC system, the behavior of heated MPC-stabilized emulsions is influenced by the presence of heat-induced casein micelle/whey protein complexes. Both the heat treatment and the concentration affect the size, shape and voluminosity of the casein micelles (Dalgleish & Corredig, 2012). Validation of the knowledge obtained in the unheated casein-stabilized emulsion system should continue in the heated system. For the whey-protein-stabilized emulsion system, theoretically and experimentally (Rosa et al., 2006), depletion flocculation could occur in emulsions containing denatured whey protein nano-particles (50−300 nm). A systematic study of a depletion-induced emulsion network with respect to the factors (i.e. heat severity, heating pH, presence of NaCl or $CaCl_2$) that affect the phase separation kinetics should be conducted in the whey protein system.

- It was shown that adding carbohydrate at ≥ 10% w/w affected the heat stability and viscosity of MPC-stabilized emulsions by changing the free Ca^{2+} content and the effective volume fraction of casein particles. The relationship between the partial collapse of κ-casein because of poor solvent quality and the heat stability has not been fully probed. Additional work to address this issue would be to carry out light scattering measurements to determine the hydrodynamic radius of the casein micelle before and during heating. At present, there is a lack of additional information on how casein micelles interact with whey proteins during heating at different pHs in the presence of carbohydrate and how the heat-induced casein micelle/whey protein complexes affect the heat stability. A study using sodium dodecyl sulphate-polyacrylamide gel electrophoresis should be undertaken to address these questions.

- The shear flow behaviors of concentrated-protein-based emulsions before and after heat treatment have been measured. However, the impact of the polydispersity of the protein particle and the emulsion droplet on the overall rheological properties of protein-stabilized emulsions has not been systematically investigated as a function of the volume fraction. It is known that the polydispersity of particles contributes markedly to the viscosity of a dispersion or an emulsion at volume fractions $\emptyset > 0.4$. Under shear conditions, small particles can pack effectively within the gap between large particles,

providing lubrication of the flow of the large particles, and therefore decreasing the overall viscosity (Servais et al., 2002). It would be worth investigating the rheology of a mixture of casein micelles with different sizes and proportions and in the presence of emulsion droplets. This would provide a lever to manipulate and to predict the viscosity of a concentrated fluid.

- The chaperone-like behavior of caseins was investigated in Chapters 4 and 8. The stabilizing effects of non-micellar caseins on the heat-induced destabilization of whey proteins, as investigated in these chapters, have been determined only qualitatively. As such, a quantitative study of the effect of the biological-chaperone-like activity of micellar and non-micellar caseins on the aggregation of whey proteins in different environments (i.e. pH, carbohydrate, polysaccharide and mineral) during heating would be worthwhile. In contrast, trehalose and glycerol are known as chemical chaperones of aggregated globular proteins (Crowe, 2007; Ghahghaei, Bathaie, Shahraki, & Rahmany Asgarabad, 2011). It would be interesting to compare the activities of biological chaperones and chemical chaperones in concentrated-protein-based emulsion systems. This would provide an alternative lever to control the heat stability of the final products. A non-invasive technique such as surface plasmon resonance has shown the relation between β-lg−casein interactions and an understanding of their binding affinity and the refolding behavior of denatured β-lg (Grygorczyk, 2009). This method may be useful in obtaining real time information on particle−particle interactions.

- Finally, the results presented in this thesis were concerned with shelf life stability in only a short period of time (mostly within 1 month; up to 6 months was investigated only in Chapter 5) rather than for the commercial requirement (about 6−9 months). Age gelation and sedimentation could arise in casein-enriched liquid nutritional products during storage (Datta & Deeth, 2001). Both casein ingredients and non-protein components have been suggested to be involved in the age gelation of high protein products (Grygorczyk, 2009). Investigation in more detail of the individual contributions of ingredients to the age gelation in casein-enriched systems is recommended.

10.4 Concluding remarks

In conclusion, the physicochemical properties of high solids content protein-stabilized oil-in-water emulsions are a comparatively emerging area of study in terms of their protein and carbohydrate contents. The formulation of heat- and shelf-stable liquid nutrition products with high protein concentration (> 8% w/w), high carbohydrate concentration (> 10% w/w) and an acceptable viscosity is still challenging. This thesis has provided new insights into and better understanding of various aspects of the effects of non-adsorbed proteins/polysaccharides on the structure and stability of emulsions, the inter-particle interactions occurring in concentrated-protein-based emulsions during heating, the effects of the addition of carbohydrate and changes in processing conditions on the physicochemical properties of MPC-stabilized emulsions. Such knowledge facilitates food scientists to control and manipulate the physical stability and macroscopic rheology of protein-stabilized oil-in-water emulsions. Continuing research on the behavior of adsorbed and non-adsorbed proteins in the presence of additional ingredients and under different processing conditions, together with theoretical modeling and comparison studies under commercial processing conditions, may open new, innovative routes or solutions to the development of new products/ingredients with novel structures and textures that may benefit the elderly and patients with swallowing disorders or suffering from malnutrition.

Reference

Aben, S., Holtze, C., Tadros, T., & Schurtenberger, P. (2012). Rheological investigations on the creaming of depletion-flocculated emulsions. *Langmuir, 28*, 7967−7975.

Agboola, S. O., Singh, H., Munro, P. A., Dalgleish, D., & Singh, A. M. (1998a). Stability of emulsions formed using whey protein hydrolysate: Effects of lecithin addition and retorting. *Journal of Agricultural and Food Chemistry, 46*, 1814−1819.

Agboola, S. O., Singh, H., Munro, P. A., Dalgleish, D. G., & Singh, A. M. (1998b). Destabilization of oil-in-water emulsions formed using highly hydrolyzed whey proteins. *Journal of Agricultural and Food Chemistry, 46*, 84−90.

Akinshina, A., Ettelaie, R., Dickinson, E., & Smyth, G. (2008). Interactions between adsorbed layers of αs1-casein with covalently bound side chains: A self-consistent field study. *Biomacromolecules, 9*, 3188−3200.

Alexander, M., Rojas-Ochoa, L. F., Leser, M., & Schurtenberger, P. (2002). Structure, dynamics, and optical properties of concentrated milk suspensions: An analogy to hard-sphere liquids. *Journal of Colloid and Interface Science, 253*, 35−46.

Álvarez Cerimedo, M. S., Iriart, C. H., Candal, R. J., & Herrera, M. L. (2010). Stability of emulsions formulated with high concentrations of sodium caseinate and trehalose. *Food Research International, 43*, 1482−1493.

Anema, S. G. (1998). Effect of milk concentration on heat-induced, pH-dependent dissociation of casein from micelles in reconstituted skim milk at temperatures between 20 and 120 °C. *Journal of Agricultural and Food Chemistry*, *46*, 2299–2305.

Anema, S. G. (2007). Role of κ-casein in the association of denatured whey proteins with casein micelles in heated reconstituted skim milk. *Journal of Agricultural and Food Chemistry, 55*, 3635−3642.

Anema, S. G. (2008). On heating milk, the dissociation of κ-casein from the casein micelles can precede interactions with the denatured whey proteins. *Journal of Dairy Research, 75*, 415−421.

Anema, S. G. (2009). Effect of milk solids concentration on the pH, soluble calcium and soluble phosphate levels of milk during heating. *Dairy Science and Technology, 89*, 501−510.

Anema, S. G., & Li, Y. (2003). Effect of pH on the association of denatured whey proteins with casein micelles in heated reconstituted skim milk. *Journal of Agricultural and Food Chemistry, 51*, 1640−1646.

Anema, S. G., Lowe, E. K., & Li, Y. (2004). Effect of pH on the viscosity of heated reconstituted skim milk *International Dairy Journal, 14*, 541−548.

Asakura, S., & Oosawa, F. (1954). On interaction between two bodies immersed in a solution of macromolecules. *Journal of Chemical Physics, 22*, 1255−1256.

Ashoor, S. H., & Zent, J. B. (1984). Maillard browning of common amino acids and sugars. *Journal of Food Science, 49*, 1206−1207.

Audebrand, M., Ropers, M.-H., & Riaublanc, A. (2013). Disappearance of intermolecular beta-sheets upon adsorption of beta-lactoglobulin aggregates at the oil–water interfaces of emulsions. *Food Hydrocolloids, 33*, 178−185.

Augustin, M. A., Oliver, C. M., & Hemar, Y. (2011). Chapter 7: Casein, caseinates, and milk protein concentrates. In R. C. Chandan & A. Kilara (Eds.), *Dairy Ingredients for Food Processing* (pp. 161−178). Ames, Iowa, USA: Blackwell Publishing Ltd.

Augustin, M. A., Udabage, P., & Steve, L. T. (2007). Influence of processing on functionality of milk and dairy proteins. *Advances in Food and Nutrition Research, 53*, 1−38.

Balastre, M., Li, F., Schorr, P., Yang, J., Mays, J. W., & Tirrell, M. V. (2002). A study of polyelectrolyte brushes formed from adsorption of amphiphilic diblock copolymers using the surface forces apparatus. *Macromolecules, 35*, 9480−9486.

Barone, G., Del Vecchio, P., Giancola, C., & Notaro, G. (1992). Conformational stability of proteins and peptide-peptide interactions in the presence of carbohydrates. *Thermochimica Acta, 199*, 189−196.

Beliciu, C. M., & Moraru, C. I. (2011). The effect of protein concentration and heat treatment temperature on micellar casein-soy protein mixtures. *Food Hydrocolloids, 25*, 1448−1460.

Beliciu, C. M., Sauer, A., & Moraru, C. I. (2012). The effect of commercial sterilization regimens on micellar casein concentrates. *Journal of Dairy Science, 95*, 5510−5526.

Belyakova, L. E., Antipova, A. S., Semenova, M. G., Dickinson, E., Merino, L. M., & Tsapkina, E. N. (2003). Effect of sucrose on molecular and interaction parameters of sodium caseinate in aqueous solution: relationship to protein gelation *Colloids and Surfaces B: Biointerfaces, 31*, 31−46.

Bengoechea, C., Jones, O. G., Guerrero, A., & McClements, D. J. (2011). Formation and characterization of lactoferrin/pectin electrostatic complexes: Impact of composition, pH and thermal treatment. *Food Hydrocolloids, 25*, 1227−1232.

Bergenholtz, J., Poon, W. C. K., & Fuchs, M. (2003). Gelation in model colloid-polymer mixtures. *Langmuir, 19*, 4493−4503.

Berli, C. L. A., & Quemada, D. (2000). Rheological modeling of microgel suspensions involving solid−liquid transition. *Langmuir, 16*, 7968−7974.

Berli, C. L. A., Quemada, D., & Parker, A. (2002). Modelling the viscosity of depletion flocculated emulsions. *Colloids and Surfaces A: Physicochemical and Engineering Aspects, 203*, 11−20.

Bernal, V., & Jelen, P. (1985). Thermal stability of whey protein-A calorimetric study. *Journal of Dairy Science, 68*, 2847−2852.

Bernard, C., Regnault, S., Gendreau, S., Charbonneau, S., & Relkin, P. (2011). Enhancement of emulsifying properties of whey proteins by controlling spray-drying parameters. *Food Hydrocolloids, 25*, 758−763.

Biggs, S., & Healy, T. W. (1994). Electrosteric stabilisation of colloidal zirconia with low-molecular-weight polyacrylic acid. An atomic force microscopy study. *Journal of the Chemical Society, Faraday Transactions, 90*, 3415−3421.

Blijdenstein, T. B. J., van Vliet, T., van der Linden, E., & van Aken, G. A. (2003). Suppression of depletion flocculation in oil-in-water emulsions: A kinetic effect of β-lactoglobulin. *Food Hydrocolloids, 17*, 661−669.

Blijdenstein, T. B. J., Veerman, C., & van der Linden, E. (2004). Depletion−flocculation in oil-in-water emulsions using fibrillar protein assemblies. *Langmuir, 20*, 4881−4884.

Blijdenstein, T. B. J., Zoet, F. D., van Vliet, T., van der Linden, E., & van Aken, G. A. (2004). Dextran-induced depletion flocculation in oil-in-water emulsions in the presence of sucrose. *Food Hydrocolloids, 18*, 857−863.

Block, S., & Helm, C. A. (2008). Conformation of poly(styrene sulfonate) layers physisorbed from high salt solution studied by force measurements on two different length scales. *The Journal of Physical Chemistry B, 112*, 9318−9327.

Blomberg, E., Claesson, P. M., & Fröberg, J. C. (1998). Surfaces coated with protein layers: a surface force and ESCA study. *Biomaterials, 19*, 371−386.

Bouchoux, A., Debbou, B., Gésan-Guiziou, G., Famelart, M. H., Doublier, J. L., & Cabane, B. (2009). Rheology and phase behavior of dense casein micelle dispersions. *Journal of Chemical Physics, 131*, 165106.

Bouchoux, A., Gésan-Guiziou, G., Pérez, J., & Cabane, B. (2010). How to squeeze a sponge: Casein micelles under osmotic stress, a SAXS study. *Biophysical Journal, 99*, 3754−3762.

Boye, J. I., Alli, I., & Ismail, A. A. (1997). Use of differential scanning calorimetry and infrared spectroscopy in the study of thermal and structural stability of α-lactalbumin. *Journal of Agricultural and Food Chemistry, 45*, 1116−1125.

Britten, M., & Giroux, H. J. (1993). Interfacial properties of milk protein-stabilized emulsions as influenced by protein concentration. *Journal of Agricultural and Food Chemistry, 41*, 1187−1191.

Brun, J. M., & Dalgleish, D. G. (1999). Some effects of heat on the competitive adsorption of caseins and whey proteins in oil-in-water emulsions. *International Dairy Journal, 9*, 323−327.

Bryant, C. M., & McClements, D. J. (2000). Influence of xanthan gum on physical characteristics of heat-denatured whey protein solutions and gels. *Food Hydrocolloids, 14*, 383−390.

Buscall, R. (1994). An effective hard-sphere model of the non-Newtonian viscosity of stable colloidal dispersions: Comparison with further data for sterically stabilised latices and with data for microgel particles. *Colloids and Surfaces A: Physicochemical and Engineering Aspects, 83*, 33−42.

Buscall, R., Choudhury, T. H., Faers, M. A., Goodwin, J. W., Luckham, P. A., & Partridge, S. J. (2009). Towards rationalising collapse times for the delayed sedimentation of weakly-aggregated colloidal gels. *Soft Matter, 5*, 1345−1349.

Buzzaccaro, S., Rusconi, R., & Piazza, R. (2007). Sticky hard spheres: Equation of state, phase diagram, and metastable gels. *Phys. Rev. Lett., 99*, 098301.

Campbell, W. W., & Leidy, H. J. (2007). Dietary protein and resistance training effects on muscle and body composition in older persons. *Journal of the American College of Nutrition, 26*, 696S−703S.

Capron, I., Nicolai, T., & Durand, D. (1999). Heat induced aggregation and gelation of β-lactoglobulin in the presence of κ-carrageenan. *Food Hydrocolloids, 13*, 1−5.

Chanamai, R., & McClements, D. J. (2000). Impact of weighting agents and sucrose on gravitational separation of beverage emulsions. *Journal of Agricultural and Food Chemistry, 48*, 5561−5565.

Chanamai, R., & McClements, D. J. (2001). Depletion flocculation of beverage emulsions by gum arabic and modified starch. *Journal of Food Science, 66*, 457−463.

Chandrapala, J., Zisu, B., Palmer, M., Kentish, S., & Ashokkumar, M. (2011). Effects of ultrasound on the thermal and structural characteristics of proteins in reconstituted whey protein concentrate. *Ultrasonics Sonochemistry, 18*, 951−957.

Chassenieux, C., Nicolai, T., & Benyahia, L. (2011). Rheology of associative polymer solutions. *Current Opinion in Colloid & Interface Science, 16*, 18−26.

Chauvierre, C., Labarre, D., Couvreur, P., & Vauthier, C. (2004). A new approach for the characterization of insoluble amphiphilic copolymers based on their emulsifying properties. *Colloid and Polymer Science, 282*, 1097−1104.

Chen, J., & Dickinson, E. (1998). Viscoelastic properties of protein-stabilized emulsions: Effect of protein−surfactant interactions. *Journal of Agricultural and Food Chemistry, 46*, 91−97.

Chronakis, I. S. (1998). On the molecular characteristics, compositional properties, and structural-functional mechanisms of maltodextrins: A review. *Critical Reviews in Food Science and Nutrition, 38*, 599−637.

Claesson, P. M., Blomberg, E., Fröberg, J. C., Nylander, T., & Arnebrant, T. (1995). Protein interactions at solid surfaces. *Advances in Colloid and Interface Science, 57*, 161−227.

Claesson, P. M., Blomberg, E., & Poptoshev, E. (2004). Surface forces and emulsion stability. In S. E. Friberg, K. Larsson & J. Sjoblom (Eds.), *Food Emulsions* (4th ed.): Marcel Dekker, New York, NY.

Corredig, M., Ion Titapiccolo, G., Gaygadzhiev, Z., & Alexander, M. (2011). Rennet-induced aggregation of milk containing homogenized fat globules. Effect of interacting and non-interacting fat globules observed using diffusing wave spectroscopy. *International Dairy Journal, 21*, 679−684.

Creamer, L. K., & MacGibbon, A. K. H. (1996). Some recent advances in the basic chemistry of milk proteins and lipids *International Dairy Journal, 6*, 539−568.

Creamer, L. K., Plowman, J. E., Liddell, M. J., Smith, M. H., & Hill, J. P. (1998). Micelle stability: κ-casein structure and function. *Journal of Dairy Science, 81*, 3004−3012.

Creamer, L. K., & Sawyer, L. (2003). β-Lactoglobulin. In H. Roginski, J. W. Fuquay & P. F. Fox (Eds.), *Encyclopedia of Dairy Sciences* (Vol. 3, pp. 1932−1939). Academic Press, London.

Crowe, J. (2007). Trehalose as a "Chemical chaperone". In P. Csermely & L. Vígh (Eds.), *Molecular Aspects of the Stress Response: Chaperones, Membranes and Networks* (Vol. 594, pp. 143−158). Springer, New York, NY.

Crowley, S. V., Megemont, M., Gazi, I., Kelly, A. L., Huppertz, T., & O'Mahony, J. A. (2014). Heat stability of reconstituted milk protein concentrate powders. *International Dairy Journal, 37*, 104−110.

Cruijsen, J. M. M. (1996). Physical stability of caseinate-stabilized emulsions during heating. Agricultural University of Wageningen, Wageningen.

Dahbi, L., Alexander, M., Trappe, V., Dhont, J. K. G., & Schurtenberger, P. (2010). Rheology and structural arrest of casein suspensions. *Journal of Colloid and Interface Science, 342*, 564−570.

Dalgleish, D. G. (1993). The sizes and conformations of the proteins in adsorbed layers of individual caseins on latices and in oil-in-water emulsions. *Colloids and Surfaces B: Biointerfaces, 1*, 1−8.

Dalgleish, D. G. (1996). Conformations and structures of milk proteins adsorbed to oil-water interfaces. *Food Research International, 29*, 541−547.

Dalgleish, D. G. (1997). Adsorption of protein and the stability of emulsions. *Trends in Food Science & Technology, 8*, 1−6.

Dalgleish, D. G. (1998). Casein micelles as colloids: surface structures and stabilities. *Journal of Dairy Science, 81*, 3013−3018.

Dalgleish, D. G. (2006). Food emulsions - their structures and structure-forming properties. *Food Hydrocolloids, 20*, 415−422.

Dalgleish, D. G. (2011). On the structural models of bovine casein micelles - review and possible improvements. *Soft Matter, 7*, 2265−2272.

Dalgleish, D. G., & Corredig, M. (2012). The structure of the casein micelle of milk and its changes during processing. *Annual Review of Food Science and Technology, 3*, 449−467.

Dalgleish, D. G., Goff, H. D., Brun, J. M., & Luan, B. (2002a). Exchange reactions between whey proteins and caseins in heated soya oil-in-water emulsion systems-overall aspects of the reaction. *Food Hydrocolloids, 16*, 303−311.

Dalgleish, D. G., Goff, H. D., & Luan, B. (2002b). Exchange reactions between whey proteins and caseins in heated soya oil-in-water emulsion systems-behavior of individual proteins. *Food Hydrocolloids, 16*, 295−302.

Damodaran, S. (2004). Adsorbed layers formed from mixtures of proteins. *Current Opinion in Colloid and Interface Science, 9*, 328−339.

Darling, D. F., & Butcher, D. W. (1978). Milk-fat globule membrane in homogenized cream. *Journal of Dairy Research, 45*, 197−208.

Datta, N., & Deeth, H. C. (2001). Age gelation of UHT milk - A review. *Food and Bioproducts Processing, 79*, 197−210.

Davies, D. T., & White, J. C. D. (1966). The stability of milk protein to heat: I. Subjective measurement of heat stability of milk. *Journal of Dairy Research, 33*, 67−81.

de Kort, E. (2012). Influence of calcium chelators on concentrated micellar casein solutions: from micellar structure to viscosity and heat stability. Agricultural University of Wageningen, The Netherlands.

de Kort, E., Minor, M., Snoeren, T., van Hooijdonk, T., & van der Linden, E. (2011). Effect of calcium chelators on physical changes in casein micelles in concentrated micellar casein solutions. *International Dairy Journal, 21*, 907−913.

de Kort, E., Minor, M., Snoeren, T., van Hooijdonk, T., & van der Linden, E. (2012). Effect of calcium chelators on heat coagulation and heat-induced changes of concentrated micellar casein solutions: The role of calcium-ion activity and micellar integrity. *International Dairy Journal, 26*, 112−119.

de Kruif, C. G. (1992). Casein micelles: Diffusivity as a function of renneting time. *Langmuir, 8*, 2932−2937.

de Kruif, C. G. (1998). Supra-aggregates of casein micelles as a prelude to coagulation. *Journal of Dairy Science, 81*, 3019−3028.

de Kruif, C. G., & Holt, C. (2003). Casein micelle structure, functions, and interactions. In P. F. Fox & P. L. H. McSweeney (Eds.), *Advanced Dairy Chemistry-1. Proteins. Part A.* (pp. 233−270). Kluwer Academic/Plenum Publishers, New York, NY.

de Kruif, C. G., Huppertz, T., Urban, V. S., & Petukhov, A. V. (2012). Casein micelles and their internal structure. *Advances in Colloid and Interface Science, 171-172*, 36−52.

de Kruif, C. G., van Iersel, E. M. F., Vrij, A., & Russel, W. B. (1985). Hard sphere colloidal dispersions: Viscosity as a function of shear rate and volume fraction. *Journal of Chemical Physics, 83*, 4717−4725.

de Kruif, C. G., & Zhulina, E. B. (1996). κ-casein as a polyelectrolyte brush on the surface of casein micelles. *Colloids and Surfaces A: Physicochemical and Engineering Aspects, 117*, 151−159.

de la Fuente, M. A., Hemar, Y., Tamehana, M., Munro, P. A., & Singh, H. (2002). Process-induced changes in whey proteins during the manufacture of whey protein concentrates. *International Dairy Journal, 12*, 361−369.

Decher, G. (1997). Fuzzy nanoassemblies: Toward layered polymeric multicomposites. *Science, 277*, 1232−1237.

Demetriades, K., Coupland, J. N., & McClements, D. J. (1997). Physical properties of whey protein stabilized emulsions as related to pH and NaCl. *Journal of Food Science, 62*, 342−347.

Demetriades, K., & McClements, D. J. (1998). Influence of pH and heating on physicochemical properties of whey protein-stabilized emulsions containing a nonionic surfactant. *Journal of Agricultural and Food Chemistry, 46*, 3936−3942.

Dickinson, E. (1992). *An Introduction to Food Colloids*. Oxford Science Publishers, Oxford.

Dickinson, E. (1997). Properties of emulsions stabilized with milk proteins: Overview of some recent developments. *Journal of Dairy Science, 80*, 2607−2619.

Dickinson, E. (1998). Proteins at interfaces and in emulsions Stability, rheology and interactions. *Journal of the Chemical Society-Faraday Transsactions, 94*, 1657−1669.

Dickinson, E. (1999a). Adsorbed protein layers at fluid interfaces: interactions, structure and surface rheology. *Colloids and Surfaces B: Biointerfaces, 15*, 161−176.

Dickinson, E. (1999b). Caseins in emulsions: Interfacial properties and interactions. *International Dairy Journal, 9*, 305−312.

Dickinson, E. (2001). Milk protein interfacial layers and the relationship to emulsion stability and rheology. *Colloids and Surfaces B: Biointerfaces, 20*, 197−210.

Dickinson, E. (2003). Hydrocolloids at interfaces and the influence on the properties of dispersed systems. *Food Hydrocolloids, 17*, 25−39.

Dickinson, E. (2006). Colloid science of mixed ingredients. *Soft Matter, 2*, 642−652.

Dickinson, E. (2008). Interfacial structure and stability of food emulsions as affected by protein-polysaccharide interactions. *Soft Matter, 4*, 932−942.

Dickinson, E. (2009). Hydrocolloids as emulsifiers and emulsion stabilizers. *Food Hydrocolloids, 23*, 1473−1482.

Dickinson, E. (2010). Flocculation of protein-stabilized oil-in-water emulsions. *Colloids and Surfaces B: Biointerfaces, 81*, 130−140.

Dickinson, E. (2012). Emulsion gels: The structuring of soft solids with protein-stabilized oil droplets. *Food Hydrocolloids, 28*, 224−241.

Dickinson, E. (2013). Stabilising emulsion-based colloidal structures with mixed food ingredients. *Journal of the Science of Food and Agriculture, 93*, 710−721.

Dickinson, E., & Golding, M. (1997a). Depletion flocculation of emulsions containing unadsorbed sodium caseinate. *Food Hydrocolloids, 11*, 13−18.

Dickinson, E., & Golding, M. (1997b). Rheology of sodium caseinate stabilized oil-in-water emulsions. *Journal of Colloid and Interface Science, 191*, 166−176.

Dickinson, E., Golding, M., & Povey, M. J. W. (1997c). Creaming and flocculation of oil-in-water emulsions containing sodium caseinate. *Journal of Colloid and Interface Science, 185*, 515−529.

Dickinson, E., & Matia Merino, L. (2002). Effect of sugars on the rheological properties of acid caseinate-stabilized emulsion gels. *Food Hydrocolloids, 16*, 321−331.

Dickinson, E., & Matsumura, Y. (1991). Time-dependent polymerization of β-lactoglobulin through disulfide bonds at the oil-water interface in emulsions. *International Journal of Biological Macromolecules, 13*, 26−30.

Dickinson, E., & Parkinson, E. L. (2004). Heat-induced aggregation of milk protein-stabilized emulsions: sensitivity to processing and composition. *International Dairy Journal, 14*, 635−645.

Dickinson, E., & Ritzoulis, C. (2000). Creaming and rheology of oil-in-water emulsions containing sodium dodecyl sulfate and sodium caseinate. *Journal of Colloid and Interface Science, 224*, 148−154.

Dickinson, E., Ritzoulis, C., & Povey, M. J. W. (1999). Stability of emulsions containing both sodium caseinate and Tween 20. *Journal of Colloid and Interface Science, 212*, 466−473.

Dickinson, E., Semenova, M. G., & Antipova, A. S. (1998). Salt stability of casein emulsions. *Food Hydrocolloids, 12*, 227−235.

Dickinson, E., & Stainsby, G. (1982). *Colloids in Food*. London: Applied Science Publishers.

Diftis, N., & Kiosseoglou, V. (2006). Stability against heat-induced aggregation of emulsions prepared with a dry-heated soy protein isolate–dextran mixture. *Food Hydrocolloids, 20*, 787−792.

Dissanayake, M., & Vasiljevic, T. (2009). Functional properties of whey proteins affected by heat treatment and hydrodynamic high-pressure shearing. *Journal of Dairy Science, 92*, 1387−1397.

Dokic-Baucal, L., Dokic, P., & Jakovljevic, J. (2004). Influence of different maltodextrins on properties of O/W emulsions. *Food Hydrocolloids, 18*, 233−239.

Donato, L., & Dalgleish, D. G. (2006). Effect of the pH of heating on the qualitative and quantitative compositions of the sera of reconstituted skim milks and on the mechanisms of formation of soluble aggregates. *Journal of Agricultural and Food Chemistry, 54*, 7804−7811.

Dumay, E., Chevalier-Lucia, D., Picart-Palmade, L., Benzaria, A., Gràcia-Julià, A., & Blayo, C. (2013). Technological aspects and potential applications of (ultra) high-pressure homogenisation. *Trends in Food Science & Technology, 31*, 13−26.

Dybowska, B. E. (2007). Influence of protein concentration and heating conditions on milk protein-stabilized oil-in-water emulsions. *Milchwissenschaft, 62*, 139v142.

Dybowska, B. E. (2008). Properties of milk protein concentrate stabilized oil-in-water emulsions. *Journal of Food Engineering, 88*, 507−513.

Dybowska, B. E. (2011). Whey protein-stabilized emulsion properties in relation to thermal modification of the continuous phase. *Journal of Food Engineering, 104*, 81−88.

Eastman, J. (2005). Colloid Stability. In T. Cosgrove (Ed.), *Colloid Science: Principles, Methods and Applications* (pp. 36−49). Blackwell Publishing Ltd, Oxford.

Edwards, P. B., Creamer, L. K., & Jameson, G. B. (2008). Structure and stability of whey proteins. In A. Thompson, M. Boland & H. Singh (Eds.), *Milk Proteins* (Chapter 6, pp. 321−345). Academic Press, San Diego, CA.

Elgar, D. F., Norris, C. S., Ayers, J. S., Pritchard, M., Otter, D. E., & Palmano, K. P. (2000). Simultaneous separation and quantitation of the major bovine whey proteins including proteose peptone and caseinomacropeptide by reversed-phase high-performance liquid chromatography on polystyrene-divinylbenzene. *Journal of Chromatography A, 878*, 183−196.

Ettelaie, R., Khandelwal, N., & Wilkinson, R. (2014). Interactions between casein layers adsorbed on hydrophobic surfaces from self consistent field theory: κ-casein versus para-κ-casein. *Food Hydrocolloids, 34*, 236−246.

Euston, S. R. (2004). Computer simulation of proteins: adsorption, gelation and self-association. *Current Opinion in Colloid & Interface Science, 9*, 321−327.

Euston, S. R., Al-Bakkush, A.-A., & Campbell, L. (2009). Comparing the heat stability of soya protein and milk whey protein emulsions. *Food Hydrocolloids, 23*, 2485−2492.

Euston, S. R., Finnigan, S. R., & Hirst, R. L. (2000). Aggregation kinetics of heated whey protein-stabilized emulsions. *Food Hydrocolloids, 14*, 155−161.

Euston, S. R., Finnigan, S. R., & Hirst, R. L. (2001a). Aggregation kinetics of heated whey protein-stabilised emulsions: Effect of low-molecular weight emulsifiers. *Food Hydrocolloids, 15*, 253−262.

Euston, S. R., Finnigan, S. R., & Hirst, R. L. (2001b). Heat-induced destabilization of oil-in-water emulsions formed from hydrolyzed whey protein. *Journal of Agricultural and Food Chemistry, 49*, 5576−5583.

Euston, S. R., Finnigan, S. R., & Hirst, R. L. (2002). Kinetics of droplet aggregation in heated whey protein-stabilized emulsions: effect of polysaccharides. *Food Hydrocolloids, 16*, 499−505.

Euston, S. R., & Hirst, R. L. (1999). Comparison of the concentration-dependent emulsifying properties of protein products containing aggregated and non-aggregated milk protein. *International Dairy Journal, 9*, 693−701.

Evans, M., Ratcliffe, I., & Williams, P. A. (2013). Emulsion stabilisation using polysaccharide–protein complexes. *Current Opinion in Colloid & Interface Science, 18*, 272−282.

Faka, M., Lewis, M. J., Grandison, A. S., & Deeth, H. (2009). The effect of free Ca^{2+} on the heat stability and other characteristics of low-heat skim milk powder. *International Dairy Journal, 19*, 386−392.

Farrer, D., & Lips, A. (1999). On the self-assembly of sodium caseinate. *International Dairy Journal, 9*, 281−286.

Farrell Jr., H. M., Jimenez-Flores, R., Bleck, G. T., Brown, E. M., Butler, J. E., Creamer, L. K., Hicks, C. L., Hollar, C. M., Ng-Kwai-Hang, K. F., & Swaisgood, H. E. (2004). Nomenclature of the proteins of cow's milk-Sixth revision. *Journal of Dairy Science, 87*, 1641−1674.

Farris, R. J. (1968). Prediction of the viscosity of multimodal suspensions from unimodal viscosity data. *Transactions of the Society of Rheology (1957-1977), 12*, 281−301.

Floury, J., Desrumaux, A., & Lardières, J. (2000). Effect of high-pressure homogenization on droplet size distributions and rheological properties of model oil-in-water emulsions. *Innovative Food Science and Emerging Technologies, 1*, 127−134.

Foegeding, E. A., Luck, P., & Vardhanabhuti, B. (2011). Whey protein products. In W. F. John (Ed.), *Encyclopedia of Dairy Sciences* (pp. 873−878). Academic Press, San Diego, CA.

Ford, L. D., Borwankar, R. P., Pechak, D., & Schwimmer, B. (2004). Dressings and sauces. In S. E. Friberg, K. Larsson & J. Sjoblom (Eds.), *Food Emulsions* (4th ed., Chapter 13). Marcel Dekker, Inc., New York, NY.

Fox, P. F., & McSweeney, P. L. H. (1998). Milk proteins. In *Dairy Chemistry and Biochemistry* (pp. 146−237). Thomson Science, Weinheim.

Fredrick, E., Walstra, P., & Dewettinck, K. (2010). Factors governing partial coalescence in oil-in-water emulsions. *Advances in Colloid and Interface Science, 153*, 30−42.

Fritz, G., Schädler, V., Willenbacher, N., & Wagner, N. J. (2002). Electrosteric stabilization of colloidal dispersions. *Langmuir, 18*, 6381−6390.

Gao, R., van Leeuwen, H. P., Temminghoff, E. J., van Valenberg, H. J., Eisner, M. D., & van Boekel, M. A. (2010). Effect of disaccharides on ion properties in milk-based systems. *Journal of Agricultural and Food Chemistry, 58*, 6449−6457.

Gaucheron, F., Mollé, D., & Pannetier, R. (2001). Influence of pH on the heat-induced proteolysis of casein molecules. *Journal of Dairy Research, 68*, 71−80.

Genovese, D. B. (2012). Shear rheology of hard-sphere, dispersed, and aggregated suspensions, and filler-matrix composites. *Advances in Colloid and Interface Science, 171–172*, 1−16.

Ghahghaei, A., Bathaie, S. Z., Shahraki, A., & Rahmany Asgarabad, F. (2011). Comparison of the chaperoning action of glycerol and β-casein on aggregation of proteins in the presence of crowding agent. *International Journal of Peptide Research and Therapeutics, 17*, 101−111.

Ghosh, S., Cramp, G. L., & Coupland, J. N. (2006). Effect of aqueous composition on the freeze-thaw stability of emulsions. *Colloids and Surfaces A: Physicochemical and Engineering Aspects, 272*, 82−88.

Gibaud, T., Mahmoudi, N., Oberdisse, J., Lindner, P., Pedersen, J. S., Oliveira, C. L. P., Stradner, A., & Schurtenberger, P. (2012). New routes to food gels and glasses. *Faraday Discussions, 158*, 267−284.

Giroux, H. J., & Britten, M. (2004). Heat treatment of whey proteins in the presence of anionic surfactants. *Food Hydrocolloids, 18*, 685−692.

Goff, H. D. (1997). Instability and partial coalescence in whippable dairy emulsions. *Journal of Dairy Science, 80*, 2620−2630.

Grácia-Juliá, A., René, M., Cortés-Muñoz, M., Picart, L., López-Pedemonte, T., Chevalier, D., & Dumay, E. (2008). Effect of dynamic high pressure on whey protein aggregation: A comparison with the effect of continuous short-time thermal treatments. *Food Hydrocolloids, 22*, 1014−1032.

Grandjean, A. C., Reimers, K. J., & Buyckx, M. E. (2003). Hydration: Issues for the 21st century. *Nutrition Reviews, 61*, 261−271.

Griffin, M. C. A., Lyster, R. L. J., & Price, J. C. (1988). The disaggregation of calcium-depleted casein micelles. *European Journal of Biochemistry, 174*, 339−343.

Grimley, H. J., Grandison, A. S., & Lewis, M. J. (2010). The effect of calcium removal from milk on casein micelle stability and structure *Milchwissenschaft, 65*, 151−154.

Grygorczyk, A. (2009). Biophysical studies of milk protein interactions in relation to storage defects in high protein beverages. McGill University, Canada.

Guggisberg, D., Chollet, M., Schreier, K., Portmann, R., & Egger, L. (2012). Effects of heat treatment of cream on the physical–chemical properties of model oil-in-buttermilk emulsions. *International Dairy Journal, 26*, 88−93.

Guinee, T. P., O'Kennedy, B. T., & Kelly, P. M. (2006). Effect of milk protein standardization using different methods on the composition and yields of cheddar cheese. *Journal of Dairy Science, 89*, 468−482.

Guo, M. R., Fox, P. F., Flynn, A., & Kindstedt, P. S. (1996). Heat-induced modifications of the functional properties of sodium caseinate. *International Dairy Journal, 6*, 473−483.

Guo, M. R., Fox, P. F., Flynn, A., & Mahammad, K. S. (1989). Heat-induced changes in sodium caseinate. *Journal of Dairy Research, 56*, 503−512.

Guyomarc'h, F., Nono, M., Nicolai, T., & Durand, D. (2009). Heat-induced aggregation of whey proteins in the presence of κ-casein or sodium caseinate. *Food Hydrocolloids, 23*, 1103−1110.

Guzey, D., & McClements, D. J. (2006). Formation, stability and properties of multilayer emulsions for application in the food industry. *Advances in Colloid and Interface Science, 128-130*, 227−248.

HadjSadok, A., Pitkowski, A., Nicolai, T., Benyahia, L., & Moulai-Mostefa, N. (2008). Characterisation of sodium caseinate as a function of ionic strength, pH and temperature using static and dynamic light scattering. *Food Hydrocolloids, 22*, 1460−1466.

Haggarty, N. W. (2003). Minor proteins, bovine serum albumin and vitamin-binding proteins. In H. Roginski, J. W. Fuquay & P. F. Fox (Eds.), *Encyclopedia of Dairy Sciences* (Vol. 3, pp. 1939−1946). Academic Press, London.

Hansted, J. G., Wejse, P. L., Bertelsen, H., & Otzen, D. E. (2011). Effect of protein–surfactant interactions on aggregation of β-lactoglobulin. *Biochimica et Biophysica Acta (BBA) - Proteins and Proteomics, 1814*, 713−723.

Havea, P. (2007). Method for preparing a dried modified whey protein. In Vol. WO/2007/108709.

Havea, P., Singh, H., & Creamer, L. K. (2002). Heat-induced aggregation of whey proteins: Comparison of cheese WPC with acid WPC and relevance of mineral composition. *Journal of Agricultural and Food Chemistry, 50*, 4674−4681.

Havea, P., Singh, H., & Creamer, L. K. (2002). Heat-induced aggregation of whey proteins: Comparison of cheese WPC with acid WPC and relevance of mineral composition. *Journal of Agricultural and Food Chemistry, 50*, 4674−4681.

Havea, P., Singh, H., Creamer, L. K., & Campanella, O. H. (1998). Electrophoretic characterization of the protein products formed during heat treatment of whey protein concentrate solutions. *Journal of Dairy Research, 65*, 79−91.

Havea, P., Watkinson, P., & Kuhn-Sherlock, B. (2009). Heat-induced whey protein gels: Protein−protein interactions and functional properties. *Journal of Agricultural and Food Chemistry, 57*, 1506−1512.

Hemar, Y., Hall, C. E., & Singh, H. (2005). Rheological properties of oil-in-water emulsions formed with milk protein concentrate. *Journal of Texture Studies, 36*, 289−302.

Hemar, Y., & Horne, D. S. (1998). Electrostatic interactions in adsorbed protein layers probed by a sedimentation technique. *Journal of Colloid and Interface Science, 206*, 138−145.

Hemar, Y., Tamehana, M., Munro, P. A., & Singh, H. (2001). Influence of xanthan gum on the formation and stability of sodium caseinate oil-in-water emulsions. *Food Hydrocolloids, 15*, 513−519.

Hernandez, G. P. (2005). Use of ingredients and processing to control the stability of high whey protein concentration retort sterilized beverages. Texas A&M University, Houston, TX.

Hiemenz, P. C., & Rajagopalan, R. (1997). *Principles of Colloid and Surface Chemistry, 3rd Edition* (3rd ed.). New York: Marcel Dekker.

Holladn, J. W., Gupta, R., Deeth, H. C., & Alewood, P. F. (2011). Proteomic analysis of temperature-dependent changes in stored UHT milk. *Journal of Agricultural and Food Chemistry, 59*, 1837−1846.

Holt, C. (1992). Structure and stability of bovine casein micelles. *Advances in Protein Chemistry, 43*, 63−153.

Holt, C., Muir, D. D., & Sweetsur, A. W. M. (1978). The heat stability of milk and concentrated milk containing added aldehydes and sugars. *Journal of Dairy Research, 45*, 47−52.

Holt, C., & Sawyer, L. (1993). Caseins as rheomorphic proteins: Interpretation of primary and secondary structures of the αS1-, β- and κ-caseins. *Journal of the Chemical Society, Faraday Transactions, 89*, 2683−2692.

Horne, D. S. (2002). Casein structure, self-assembly and gelation. *Current Opinion in Colloid and Interface Science, 7*, 456−461.

Howe, A. M., Clarke, A., & Whitesides, T. H. (1997). Viscosity of emulsions of polydisperse droplets with a thick adsorbed layer. *Langmuir, 13*, 2617−2626.

Huck-Iriart, C., Álvarez-Cerimedo, M. S., Candal, R. J., & Herrera, M. L. (2011). Structures and stability of lipid emulsions formulated with sodium caseinate. *Current Opinion in Colloid & Interface Science, 16*, 412−420.

Hunt, J. A., & Dalgleish, D. G. (1994). Adsorption behavior of whey protein isolate and caseinate in soya oil-in-water emulsions. *Food Hydrocolloids, 8*, 175−187.

Hunt, J. A., & Dalgleish, D. G. (1995). Heat stability of oil-in-water emulsions containing milk proteins: effect of ionic strength and pH. *Journal of Food Science, 60*, 1120−1123.

Hunter, R. J. (1986). *Fundations of Colloid Science1*(Vol. 1). Oxford University Press, Oxford.

Huppertz, T. (2013). Chemistry of the caseins. In P. L. H. McSweeney & P. F. Fox (Eds.), *Advanced Dairy Chemistry Volume 1A: Proteins: Basic Aspects,* (4th ed., Vol. 1, Chapter4, pp. 135−160). Springer Science+Business Media, New York, NY.

Huppertz, T., & Fox, P. F. (2006a). Effect of NaCl on some physico-chemical properties of concentrated bovine milk. *International Dairy Journal, 16*, 1142−1148.

Huppertz, T., & Fox, P. F. (2006b). Influence of added lyophilized butter serum on the heat stability of unconcentrated and concentrated bovine milk. *International Journal of Dairy Technology, 59*, 18−21.

Huppertz, T., Tan-Kintia, R. H., Arriaga, T., & Fox, P. F. (2012). Sterically-stabilized association colloids at unfavourable solvent conditions: heat-induced coagulation of casein micelles in high-carbohydrate media. In *Food Colloids 2012: Creation and Breakdown of Structure*. Copenhagen, Denmark.

Hustinx, J. C. A., Singh, T. K., & Fox, P. F. (1997). Heat-induced hydrolysis of sodium caseinate. *International Dairy Journal, 7*, 207−212.

Ibanoglu, E. (2005). Effect of hydrocolloids on the thermal denaturation of proteins. *Food Chemistry, 90*, 621−626.

Israelachvili, J., & Wennerström, H. (1996). Role of hydration and water structure in biological and colloidal interactions. *Nature, 379*, 219−225.

Jafari, S. M., Assadpoor, E., He, Y., & Bhandari, B. (2008). Re-coalescence of emulsion droplets during high-energy emulsification. *Food Hydrocolloids, 22*, 1191−1202.

Jafari, S. M., He, Y., & Bhandari, B. (2006). Nano-emulsion production by sonication and microfluidization-A comparison. *International Journal of Food Properties, 9*, 475−485.

Jafari, S. M., He, Y., & Bhandari, B. (2007a). Optimization of nano-emulsions production by microfluidization. *European Food Research and Technology, 225*, 733−741.

Jafari, S. M., He, Y., & Bhandari, B. (2007b). Production of sub-micron emulsions by ultrasound and microfluidization techniques. *Journal of Food Engineering, 82*, 478−488.

Jahaniaval, F., Kakuda, Y., Abraham, V., & Marcone, M. F. (2000). Soluble protein fractions from pH and heat treated sodium caseinate: Physicochemical and functional properties *Food Research International, 33*, 637−647.

Jain, N. K., & Roy, I. (2009). Effect of trehalose on protein structure. *Protein Science, 18*, 24−36.

Jeurnink, T. J. M., & de Kruif, C. G. (1995). Calcium concentration in milk in relation to heat stability and fouling. *Netherlands Milk and Dairy Journal, 49*, 151−165.

Jimenez-Flores, R., Ye, A., & Singh, H. (2005). Interactions of whey proteins during heat treatment of oil-in-water emulsions formed with whey protein isolate and hydroxylated lecithin. *Journal of Agricultural and Food Chemistry, 53*, 4213−4219.

Ju, Z. Y., Hettiarachchy, N., & Kilara, A. (1999). Thermal properties of whey protein aggregates. *Journal of Dairy Science, 82*, 1882−1889.

Kasinos, M., Tran Le, T., & van der Meeren, P. (2014). Improved heat stability of recombined evaporated milk emulsions upon addition of phospholipid enriched dairy by-products. *Food Hydrocolloids, 34*, 112−118.

Keenan, T. W., & Dylewski, D. P. (1995). Intracellular orgin of milk lipid globules and the nature and structure of the milk lipid globule membrane. In P. F. Fox (Ed.), *Intracellular Origin of Milk Lipid Globules and the Nature and Structure of the Milk Lipid Globule Membrane*. Chapman & Hall, London.

Keerati-u-rai, M., & Corredig, M. (2009). Heat-induced changes in oil-in-water emulsions stabilized with soy protein isolate. *Food Hydrocolloids, 23*, 2141−2148.

Kehoe, J. J., & Foegeding, E. A. (2011). Interaction between β-casein and whey proteins as a function of pH and salt concentration. *Journal of Agricultural and Food Chemistry, 59*, 349−355.

Kelley, D., & McClements, D. J. (2003). Influence of sodium dodecyl sulfate on the thermal stability of bovine serum albumin stabilized oil-in-water emulsions. *Food Hydrocolloids, 17*, 87−93.

Kelly, P. M., Kelly, J., Mehra, R., Oldfield, D. J., Raggett, E., & O'Kennedy, B. T. (2000). Implementation of integrated membrane processed for pilot scale development of fractionated milk components *Lait 80*, 139−153.

Keowmaneechai, E., & McClements, D. J. (2002). Effect of $CaCl_2$ and KCl on physiochemical properties of model nutritional beverages based on whey protein stabilized oil-in-water emulsions *Journal of Food Science, 67*, 665−671.

Keowmaneechai, E., & McClements, D. J. (2006). Influence of EDTA and citrate on thermal stability of whey protein stabilized oil-in-water emulsions containing calcium chloride. *Food Research International, 39*, 230−239.

Kilara, A., & Vaghela, M. N. (2004). Whey proteins. In R. Y. Yada (Ed.), *Proteins in Food Processing* (pp. 72−94). Woodhead Publishing Limited, Cambridge.

Kim, D. A., Cornec, M., & Narsimhan, G. (2005). Effect of thermal treatment on interfacial properties of β-lactoglobulin. *Journal of Colloid and Interface Science, 285*, 100−109.

Kim, H. J., Decker, E. A., & McClements, D. J. (2002a). Impact of protein surface denaturation on droplet flocculation in hexadecane oil-in-water emulsions stabilized by β-lactoglobulin. *Journal of Agricultural and Food Chemistry, 50*, 7131−7137.

Kim, H. J., Decker, E. A., & McClements, D. J. (2002b). Role of postadsorption conformation changes of β-lactoglobulin on its ability to stabilize oil droplets against flocculation during heating at neutral pH. *Langmuir, 18*, 7577−7583.

Kim, H. J., Decker, E. A., & McClements, D. J. (2003). Influence of sucrose on droplet flocculation in hexadecane oil-in-water emulsions stabilized by β-lactoglobulin. *Journal of Agricultural and Food Chemistry, 51*, 766−772.

Kimura, A., Fukuda, T., Zhang, M., Motoyama, S., Maruyama, N., & Utsumi, S. (2008). Comparison of physicochemical properties of 7s and 11s globulins from pea, fava bean, cowpea, and French bean with those of soybean-french bean 7s globulin exhibits excellent properties. *Journal of Agricultural and Food Chemistry, 56*, 10273−10279.

Knudsen, J. C., Ogendal, L. H., & Skibsted, L. H. (2008). Droplet surface properties and rheology of concentrated oil in water emulsions stabilized by heat-modified β-lactoglobulin B. *Langmuir, 24*, 2603−2610.

Kocak, H. R., & Zadow, J. G. (1985). Controlling age gelation of UHT milk with additives. *Australian Journal of Dairy Technology, 40*, 58−64.

Kramers, H. A. (1940). Brownian motion in a field of force and the diffusion model of chemical reactions. *Physica, 7*, 284−304.

Kuhn, K. R., & Cunha, R. L. (2012). Flaxseed oil–whey protein isolate emulsions: Effect of high pressure homogenization. *Journal of Food Engineering, 111*, 449−457.

Kulmyrzaev, A., Bryant, C., & McClements, D. J. (2000). Influence of sucrose on the thermal denaturation, gelation, and emulsion stabilization of whey proteins. *Journal of Agricultural and Food Chemistry, 48*, 1593−1597.

Langton, M., & Hermansson, A. M. (1996). Image analysis of particulate whey protein gels. *Food Hydrocolloids, 10*, 179−191.

Lee, L., Niknafs, N., Hancocks, R. D., & Norton, I. T. (2013). Emulsification: Mechanistic understanding. *Trends in Food Science & Technology, 31*, 72−78.

Lee, L., & Norton, I. T. (2013). Comparing droplet breakup for a high-pressure valve homogeniser and a Microfluidizer for the potential production of food-grade nanoemulsions. *Journal of Food Engineering, 114*, 158−163.

Lefèvre, T., & Subirade, M. (2003). Formation of intermolecular β-sheet structures: a phenomenon relevant to protein film structure at oil–water interfaces of emulsions. *Journal of Colloid and Interface Science, 263*, 59−67.

Leman, J., & Kinsella, J. E. (1989). Surface activity, film formation, and emulsifying properties of milk proteins. *Critical Reviews in Food Science and Nutrition, 28*, 115−138.

Lewis, M. J. (2011). The measurement and significance of ionic calcium in milk – A review. *International Journal of Dairy Technology, 64*, 1−13.

Li, C., Fu, X., Luo, F., & Huang, Q. (2013). Effects of maltose on stability and rheological properties of orange oil-in-water emulsion formed by OSA modified starch. *Food Hydrocolloids, 32*, 79−86.

Liang, Y., Gillies, G., Patel, H., Matia-Merino, L., Ye, A., & Golding, M. (2014). Physical stability, microstructure and rheology of sodium-caseinate-stabilized emulsions as influenced by protein concentration and non-adsorbing polysaccharides. *Food Hydrocolloids, 36*, 245–255.

Liang, Y., Matia-Merino, L., Patel, H., Ye, A., Gillies, G., & Golding, M. (2014). Effect of sugar type and concentration on the heat coagulation of oil-in-water emulsions stabilized by milk-protein-concentrate. *Food Hydrocolloids*, *41*, 332–342.

Liang, Y., Patel, H., Matia-Merino, L., Ye, A., & Golding, M. (2013a). Effect of pre- and post-heat treatments on the physicochemical, microstructural and rheological properties of milk protein concentrate-stabilised oil-in-water emulsions. *International Dairy Journal, 32*, 184−191.

Liang, Y., Patel, H., Matia-Merino, L., Ye, A., & Golding, M. (2013b). Structure and stability of heat-treated concentrated dairy-protein-stabilised oil-in-water emulsions: A stability map characterisation approach. *Food Hydrocolloids, 33*, 297−308.

Liu, F., & Tang, C.-H. (2013). Soy protein nanoparticle aggregates as pickering stabilizers for oil-in-water emulsions. *Journal of Agricultural and Food Chemistry, 61*, 8888−8898.

Liu, T. X., Relkin, P., & Launay, B. (1994). Thermal denaturation and heat-induced gelation properties of β-lactoglobulin. Effects of some chemical parameters. *Thermochimica Acta, 246*, 387−403.

Livney, Y. D., Corredig, M., & Dalgleish, D. G. (2003). Influence of thermal processing on the properties of dairy colloids. *Current Opinion in Colloid & Interface Science, 8*, 359−364.

Long, Z., Zhao, Q., Liu, T., Kuang, W., Xu, J., & Zhao, M. (2013). Influence of xanthan gum on physical characteristics of sodium caseinate solutions and emulsions. *Food Hydrocolloids, 32*, 123−129.

Lopez, C. (2005). Focus on the supramolecular structure of milk fat in dairy products. *Reproduction Nutrition. Development, 45*, 497−511.

Loren, N., Langton, M., & Hermansson, A. M. (2007). Chapter 9: Confocal flurescence microscopy (CLSM) for food structure characterisation. In D. J. McClements (Ed.), *Understanding and controlling the microstructure of complex foods* (pp. 232−258). Cambridge, England: Woodhead Publishing Limited.

Lu, P. J., Zaccarelli, E., Ciulla, F., Schofield, A. B., Sciortino, F., & Weitz, D. A. (2008). Gelation of particles with short-range attraction. *Nature, 453*, 499−503.

Lucey, J. A., Srinivasan, M., Singh, H., & Munro, P. A. (2000). Characterization of commercial and experimental sodium caseinates by multiangle laser light scattering and size-exclusion chromatography. *Journal of Agricultural and Food Chemistry, 48*, 1610−1616.

Malvern Instruments Ltd. (2004). *Zetasizer nano series user manual*.

Manley, S., Skotheim, J. M., Mahadevan, L., & Weitz, D. A. (2005). Gravitational collapse of colloidal gels. *Physical Review Letters, 94*, 218−302.

Manoj, P., Watson, A. D., Hibberd, D. J., Fillery-Travis, A. J., & Robins, M. M. (1998). Characterization of a depletion-flocculated polydisperse emulsion.II. Steady-State Rheological Investigations. *Journal of Colloid and Interface Science, 207*, 294−302.

Margetts, B. M., Thompson, R. L., Elia, M., & Jackson, A. A. (2003). Prevalence of risk of undernutrition is associated with poor health status in older people in the UK. *European Journal of Clinical Nutrition, 57*, 69−74.

Mason, T. G., Bibette, J., & Weitz, D. A. (1995). Elasticity of compressed emulsions. *Physical Review Letters, 75*, 2051−2054.

McCarthy, N. A., Kelly, A. L., O'Mahony, J. A., & Fenelon, M. A. (2014). Sensitivity of emulsions stabilised by bovine β-casein and lactoferrin to heat and $CaCl_2$. *Food Hydrocolloids, 35*, 420−428.

McCarthy, N. A., Kelly, A. L., O'Mahony, J. A., & Fenelon, M. A. (2013). The physical characteristics and emulsification properties of partially dephosphorylated bovine β-casein. *Food Chemistry, 138*, 1304−1311.

McClements, D. J. (2002). Modulation of globular protein functionality by weakly interacting cosolvents. *Critical Reviews in Food Science and Nutrition, 42*, 417−471.

McClements, D. J. (2004). Protein-stabilized emulsions. *Current Opinion in Colloid & Interface Science, 9*, 305−313.

McClements, D. J. (2005). *Food Emulsions: Principles, Practices, and Techniques* (2nd ed.). CRC Press, Boca Raton, FL.

McCrae, C. H. (1999). Heat stability of milk emulsions: phospholipid–protein interactions. *International Dairy Journal, 9*, 227−231.

McCrae, C. H., & Muir, D. D. (1991). Effect of surface protein concentration on the heat stability of systems containing homogenized fat globules from recombined milk. *International Dairy Journal, 1*, 89−100.

McCrae, C. H., & Muir, D. D. (1992). Heat stability of recombined milk: influence of lecithins on the heat coagulation time-pH profile. *Journal of Dairy Research, 59*, 177−185.

McMahon, D. J., & Oommen, B. S. (2008). Supramolecular structure of the casein micelle. *Journal of Dairy Science, 91*, 1709−1721.

McSweeney, S. L. (2008). Emulsifiers in infant nutritional products. In G. L. Hasenhuettl & R. W. Hartel (Eds.), *Food emulsifiers and their applications, 2nd Edition* (2nd ed., Chapter 8, pp. 233−255). Springer Science + Business Media, LLC, New York, NY.

McSweeney, S. L., Healy, R., & Mulvihill, D. M. (2008). Effect of lecithin and monoglycerides on the heat stability of a model infant formula emulsion. *Food Hydrocolloids, 22*, 888−898.

McSweeney, S. L., Mulvihill, D. M., & O'Callaghan, D. M. (2004). The influence of pH on the heat-induced aggregation of model milk protein ingredient systems and model infant formula emulsions stabilized by milk protein ingredients *Food Hydrocolloids, 18*, 109−125.

Meeker, S. P., Poon, W. C. K., & Pusey, P. N. (1997). Concentration dependence of the low-shear viscosity of suspensions of hard-sphere colloids. *Physical Review E, 55*, 5718−5722.

Mengual, O., Meunier, G., Cayré, I., Puech, K., & Snabre, P. (1999). TURBISCAN MA 2000: multiple light scattering measurement for concentrated emulsion and suspension instability analysis. *Talanta, 50*, 445−456.

Metwalli, A. A. M., & van Boekel, M. A. J. S. (1998). On the kinetics of heat-induced deamidation and breakdown of caseinate. *Food Chemistry, 61*, 53−61.

Mezzenga, R., Schurtenberger, P., Burbidge, A., & Michel, M. (2005). Understanding foods as soft materials. *Nature Materials, 4*, 729−740.

Michalski, M.-C., & Januel, C. (2006). Does homogenization affect the human health properties of cow's milk? *Trends in Food Science & Technology, 17*, 423−437.

Millqvist-Fureby, A., Elofsson, U., & Bergenstahl, B. (2001). Surface composition of spray-dried milk protein-stabilised emulsions in relation to pre-heat treatment of proteins. *Colloids and Surfaces B: Biointerfaces, 21*, 47−58.

Mizuno, R., & Lucey, J. A. (2005). Effects of emulsifying salts on the turbidity and calcium phosphate-protein interactions in casein micelles. *Journal of Dairy Science, 88*, 3070−3078.

Monahan, F. J., McClements, D. J., & German, J. B. (1996). Disulfide-mediated polymerization reactions and physical properties of heated WPI-stabilized emulsions *Journal of Food Science, 61*, 504−509.

Moon, B., & Mangino, M. E. (2004a). The effect of preheating on functionality of whey protein concentrates. *Milchwissenschaft, 59*, 294−297.

Moon, B., & Mangino, M. E. (2004b). The effect of preheating on solubility and emulsion stability of whey protein concentrates. *Milchwissenschaft, 59*, 165−169.

Morgan, P. E., Treweek, T. M., Lindner, R. A., Price, W. E., & Carver, J. A. (2005). Casein proteins as molecular chaperones. *Journal of Agricultural and Food Chemistry, 53*, 2670−2683.

Moro, A., Báez, G. D., Ballerini, G. A., Busti, P. A., & Delorenzi, N. J. (2013). Emulsifying and foaming properties of β-lactoglobulin modified by heat treatment. *Food Research International, 51*, 1−7.

Moro, A., Gatti, C., & Delorenzi, N. (2001). Hydrophobicity of whey protein concentrates measured by fluorescence quenching and its relation with surface functional properties. *Journal of Agricultural and Food Chemistry, 49*, 4784−4789.

Morr, C. V., & Ha, E. Y. W. (1993). Whey protein concentrates and isolates: Processing and functional properties. *Critical Reviews in Food Science and Nutrition, 33*, 431−476.

Moschakis, T., Murray, B. S., & Dickinson, E. (2005). Microstructural evolution of viscoelastic emulsions stabilised by sodium caseinate and xanthan gum. *Journal of Colloid and Interface Science, 284*, 714−728.

Mozersky, S. M., Farrell Jr, H. M., & Barford, R. A. (1991). The effects of sucrose and lactose on the sizes of casein micelles reconstituted from bovine caseins. *Journal of Dairy Science, 74*, 2382−2393.

Mulvihill, D. M., & Murphy, P. C. (1991). Surface active and emulsifying properties of caseins/caseinates as influenced by state of aggregation *International Dairy Journal, 1*, 13−37.

Munro, P. A. (2002). Caseins, functional properties and food uses. In H. Roginski, J. W. Fuquay & P. F. Fox (Eds.), *Encyclopedia of Dairy Sciences* (Vol. 3, pp. 1909−1915). London: Elsevier Science.

Nair, P. K., Alexander, M., Dalgleish, D., & Corredig, M. (2014). Physico-chemical properties of casein micelles in unheated skim milk concentrated by osmotic stressing: Interactions and changes in the composition of the serum phase. *Food Hydrocolloids, 34*, 46−53.

Nair, P. K., Dalgleish, D. G., & Corredig, M. (2013). Colloidal properties of concentrated heated milk. *Soft Matter, 9*, 3815−3824.

Napper, D. H. (1983). *Polymeric Stabilization of Colloidal Dispersions*: Academic Press, London.

Neirynck, N., Dewettinck, K., & van Der Meeren, P. (2009). Influence of protein concentration and homogenisation pressure on O/W emulsifying and emulsion-stabilising properties of sodium caseinate and whey protein isolate. *Milchwissenschaft, 64*, 36−40.

Nguyen, N. H. A., & Anema, S. G. (2010). Effect of ultrasonication on the properties of skim milk used in the formation of acid gels. *Innovative Food Science and Emerging Technologies, 11*, 616−622.

Nicolai, T., Britten, M., & Schmitt, C. (2011). β-Lactoglobulin and WPI aggregates: Formation, structure and applications. *Food Hydrocolloids, 25*, 1945–1962.

Nicolai, T., & Durand, D. (2013). Controlled food protein aggregation for new functionality. *Current Opinion in Colloid & Interface Science, 18*, 249–256.

Nieuwenhuizen, W. F., Weenen, H., Rigby, P., & Hetherington, M. M. (2010). Older adults and patients in need of nutritional support: Review of current treatment options and factors influencing nutritional intake. *Clinical Nutrition, 29*, 160−169.

Nikiforidis, C. V., & Kiosseoglou, V. (2007). The role of Tween in inhibiting heat-induced destabilization of yolk-based emulsions. *Food Hydrocolloids, 21*, 1310−1318.

Nikiforidis, C. V., & Kiosseoglou, V. (2008). Factors affecting the heat-induced physicochemical destabilization of food oil-in-water emulsions. In K. N. Papadopoulos (Ed.), *Food Chemistry Research Developments* (pp. 223−241). Nova Science Publishers, New York, NY.

Njeuwenhuijse, J. A., van Vliet, T., & Walstra, P. (1992). Kinetic aspects of heat-induced coagulation of concentrated skim milk. *Netherlands Milk and Dairy Journal, 46*, 45−68.

Nylander, T., & Wahlgren, N. M. (1994). Competitive and sequential adsorption of β-casein and β-lactoglobulin on hydrophobic surfaces and the interfacial structure of β-casein. *Journal of Colloid and Interface Science, 162*, 151−162.

Nylander, T., & Wahlgren, N. M. (1997). Forces between adsorbed layers of β-casein. *Langmuir, 13*, 6219−6225.

O'Brien, J. (1996). Stability of trehalose, sucrose and glucose to nonenzymatic browning in model systems. *Journal of Food Science, 61*, 679−682.

O'Connell, J. E., & Fox, P. F. (2000). The two-stage coagulation of milk proteins in the minimum of the heat coagulation time-ph profile of milk: Effect of casein micelle size. *Journal of Dairy Science, 83*, 378−386.

O'Kennedy, B. T., & Mounsey, J. S. (2006). Control of heat-induced aggregation of whey proteins using casein. *Journal of Agricultural and Food Chemistry, 54*, 5637−5642.

Onwulata, C. I., Konstance, R. P., & Tomasula, P. M. (2002). Viscous properties oftable microparticulated dairy proteins and sucrose. *Journal of Dairy Science*, *85, 1677−1683*.

O'Regan, J., Ennis, M. P., & Mulvihill, D. M. (2009). Milk proteins. In G. O. Philips & P. A. Williams (Eds.), *Handbook of Hydrocolloids* (2nd ed., pp. 299−358), CRC Press, Boca Raton, FL.

O'Regan, J., & Mulvihill, D. M. (2010). Heat stability and freeze-thaw stability of oil-in-water emulsions stabilised by sodium caseinate-maltodextrin conjugates. *Food Chemistry, 119*, 182−190.

Ortega-Vinuesa, J. L., Martín-Rodríguez, A., & Hidalgo-Álvarez, R. (1996). Colloidal stability of polymer colloids with different interfacial properties: Mechanisms. *Journal of Colloid and Interface Science, 184*, 259−267.

Pal, R. (1996). Effect of droplet size on the rheology of emulsions. *AIChE Journal, 42*, 3181−3190.

Pal, R. (2000). Shear viscosity behavior of emulsions of two immiscible liquids. *Journal of Colloid and Interface Science, 225*, 359−366.

Panouillé, M., Benyahia, L., Durand, D., & Nicolai, T. (2005). Dynamic mechanical properties of suspensions of micellar casein particles. *Journal of Colloid and Interface Science, 287*, 468−475.

Panzica, M., Emanuele, A., & Cordone, L. (2012). Thermal aggregation of bovine serum albumin in trehalose and sucrose aqueous solutions. *The Journal of Physical Chemistry B, 116*, 11829−11836.

Parker, A. (2009). Time dependence in jamming and unjamming. Agricultural University of Wageningen, Wageningen.

Parker, A., Gunning, P. A., Ng, K., & Robins, M. M. (1995). How does xanthan stabilise salad dressing? *Food Hydrocolloids, 9*, 333−342.

Parker, E. A., Donato, L., & Dalgleish, D. G. (2005). Effects of added sodium caseinate on the formation of particles in heated milk. *Journal of Agricultural and Food Chemistry, 53*, 8265−8272.

Parkinson, E. L., & Dickinson, E. (2004). Inhibition of heat-induced aggregation of a β-lactoglobulin-stabilized emulsion by very small additions of casein. *Colloids and Surfaces B: Biointerfaces, 39*, 23−30.

Parkinson, E. L., & Dickinson, E. (2007). Synergistic stabilization of heat-treated emulsions containing mixtures of milk proteins. *International Dairy Journal, 17*, 95−103.

Parkinson, E. L., Ettelaie, R., & Dickinson, E. (2005). Using self-consistent-field theory to understand enhanced steric stabilization by casein-like copolymers at low surface coverage in mixed protein layers. *Biomacromolecules, 6*, 3018−3029.

Pawar, A. B., Caggioni, M., Ergun, R., Hartel, R. W., & Spicer, P. T. (2011). Arrested coalescence in Pickering emulsions. *Soft Matter, 7*, 7710−7716.

Pawar, A. B., Caggioni, M., Hartel, R. W., & Spicer, P. T. (2012). Arrested coalescence of viscoelastic droplets with internal microstructure. *Faraday Discussions, 158*, 341−350.

Perrechil, F. A., & Cunha, R. L. (2010). Oil-in-water emulsions stabilized by sodium caseinate: Influence of pH, high-pressure homogenization and locust bean gum addition. *Journal of Food Engineering, 97*, 441−448.

Picone, C., Takeuchi, K., & Cunha, R. (2011). Heat-induced whey protein gels: Effects of pH and the addition of sodium caseinate. *Food Biophysics, 6*, 77−83.

Pincus, P. (1991). Colloid stabilization with grafted polyelectrolytes. *Macromolecules, 24*, 2912−2919.

Piorkowski, D. T., & McClements, D. J. (2014). Beverage emulsions: Recent developments in formulation, production, and applications. *Food Hydrocolloids*, in press. http://dx.doi.org/10.1016/j.foodhyd.2013.07.009.

Pitkowski, A., Durand, D., & Nicolai, T. (2008). Structure and dynamical mechanical properties of suspensions of sodium caseinate. *Journal of Colloid and Interface Science, 326*, 96−102.

Popa, I., Gillies, G., Papastavrou, G., & Borkovec, M. (2009). Attractive electrostatic forces between identical colloidal particles induced by adsorbed polyelectrolytes. *The Journal of Physical Chemistry B, 113*, 8458−8461.

Popa, I., Gillies, G., Papastavrou, G., & Borkovec, M. (2010). Attractive and repulsive electrostatic forces between positively charged latex particles in the presence of anionic linear polyelectrolytes. *The Journal of Physical Chemistry B, 114*, 3170−3177.

Puertas, A. M., Fuchs, M., & Cates, M. E. (2007). Competition between glass transition and liquid-gas phase separation in attracting colloids. *J. Phys. Condens. Matter, 19*, 205140.

Purwanti, N., Moerkens, A., van der Goot, A. J., & Boom, R. (2012). Reducing the stiffness of concentrated whey protein isolate (WPI) gels by using WPI microparticles. *Food Hydrocolloids, 26*, 240−248.

Purwanti, N., Smiddy, M., Jan van der Goot, A., de Vries, R., Alting, A., & Boom, R. (2011). Modulation of rheological properties by heat-induced aggregation of whey protein solution. *Food Hydrocolloids, 25*, 1482−1489.

Qian, C., & McClements, D. J. (2011). Formation of nanoemulsions stabilized by model food-grade emulsifiers using high-pressure homogenization: Factors affecting particle size. *Food Hydrocolloids, 25*, 1000−1008.

Radford, S. J., & Dickinson, E. (2004). Depletion flocculation of caseinate-stabilised emulsions: what is the optimum size of the non-adsorbed protein nano-particles? *Colloids and Surfaces A: Physicochemical and Engineering Aspects, 238*, 71−81.

Raikos, V. (2010). Effect of heat treatment on milk protein functionality at emulsion interfaces. A review. *Food Hydrocolloids, 24*, 259−265.

Rao, J., & McClements, D. J. (2011). Food-grade microemulsions, nanoemulsions and emulsions: Fabrication from sucrose monopalmitate & lemon oil. *Food Hydrocolloids, 25*, 1413−1423.

Rao, M. A. (2007a). Chapter 1-Introduction: Food Rheology and Structure. In M. A. Rao (Ed.), *Rheology of fluid and semisolid foods: Principles and applications* (2nd ed., pp. 1−24). New York, NY: Springer Science+Business Media, LLC.

Rao, M. A. (2007b). *Rheology of fluid and semisolid foods: Principles and applications* (2nd ed.). New York, NY: Springer Science+Business Media, LLC.

Rattray, W., & Jelen, P. (1997). Thermal stability of skim milk/whey protein solution blends. *Food Research International, 30*, 327−334.

Reh, C. T., & Gerber, A. (2003). Total solids determination in dairy products by microwave oven technique. *Food Chemistry, 82*, 125−131.

Relkin, P. (1996). Thermal unfolding of β-lactoglobulin, α-lactalbumin, and bovine serum albumin. A thermodynamic approach. *Critical Reviews in Food Science and Nutrition, 36*, 565−601.

Relkin, P., & Sourdet, S. (2005). Factors affecting fat droplet aggregation in whipped frozen protein-stabilized emulsions. *Food Hydrocolloids, 19*, 503−511.

Rosa, P., Sala, G., van Vliet, T. O. N., & van de Velde, F. (2006). Cold gelation of whey protein emulsions. *Journal of Texture Studies, 37*, 516−537.

Rossetti, F. C., Depieri, L. V., & Bentley, M. V. L. B. (2013). Chapter 6: Confocal laser scanning microscopy as a tool for the investigation of skin druy delivery systems and diagnosis of skin disorders. In N. Lagali (Ed.), *Confocal Laser Microscopy. Principles and Applications in Medicine, Biology, and the Food Sciences.* Croatia: InTech.

Rullier, B., Novales, B., & Axelos, M. A. V. (2008). Effect of protein aggregates on foaming properties of β-lactoglobulin. *Colloids and Surfaces A: Physicochemical and Engineering Aspects, 330*, 96−102.

Rulliere, C., Perenes, L., Senocq, D., Dodi, A., & Marchesseau, S. (2012). Heat treatment effect on polyphosphate chain length in aqueous and calcium solutions. *Food Chemistry, 134*, 712−716.

Ryan, A. S., Benson, J. D., & Flammang, A. M. (2000). Infant formulas and medical foods. In M. K. Schmidl & T. P. Labuza (Eds.), *Essentials of Functional Foods* (Chapter 6, pp. 137−163). Aspen Publishers, Inc., Gaithersburg, MD.

Ryan, K. N., Vardhanabhuti, B., Jaramillo, D. P., van Zanten, J. H., Coupland, J. N., & Foegeding, E. A. (2012). Stability and mechanism of whey protein soluble aggregates thermally treated with salts. *Food Hydrocolloids, 27*, 411−420.

Ryan, K. N., Zhong, Q., & Foegeding, E. A. (2013). Use of whey protein soluble aggregates for thermal stability—A hpothesis paper. *Journal of Food Science, 78*, R1105−R1115.

Sağlam, D., Venema, P., de Vries, R., Shi, J., & van der Linden, E. (2013). Concentrated whey protein particle dispersions: Heat stability and rheological properties. *Food Hydrocolloids, 30*, 100−109.

Sağlam, D., Venema, P., de Vries, R., & van der Linden, E. (2014). Exceptional heat stability of high protein content dispersions containing whey protein particles. *Food Hydrocolloids, 34*, 68−77.

Sakono, M., Motomura, K., Maruyama, T., Kamiya, N., & Goto, M. (2011). Alpha casein micelles show not only molecular chaperone-like aggregation inhibition properties but also protein refolding activity from the denatured state. *Biochemical and Biophysical Research Communications, 404*, 494−497.

San Martin-González, M. F., Roach, A., & Harte, F. (2009). Rheological properties of corn oil emulsions stabilized by commercial micellar casein and high pressure homogenization. *LWT - Food Science and Technology, 42*, 307−311.

Sandra, S., & Dalgleish, D. G. (2005). Effects of ultra-high-pressure homogenization and heating on structural properties of casein micelles in reconstituted skim milk powder. *International Dairy Journal, 15*, 1095−1104.

Sauer, A., & Moraru, C. I. (2012). Heat stability of micellar casein concentrates as affected by temperature and pH. *Journal of Dairy Science, 95*, 6339−6350.

Schaertl, W., & Sillescu, H. (1994). Brownian dynamics of polydisperse colloidal hard spheres: Equilibrium structures and random close packings. *Journal of Statistical Physics, 77*, 1007−1025.

Scherze, I., & Muschiolik, G. (2001). Effects of various whey protein hydrolysates on the emulsifying and surface properties of hydrolysed lecithin. *Colloids and Surfaces B: Biointerfaces, 21*, 107−117.

Schmelz, T., Lesmes, U., Weiss, J., & McClements, D. J. (2011). Modulation of physicochemical properties of lipid droplets using β-lactoglobulin and/or lactoferrin interfacial coatings. *Food Hydrocolloids, 25*, 1181−1189.

Schmitt, C., Bovay, C., Rouvet, M., Shojaei-Rami, S., & Kolodziejczyk, E. (2007). Whey protein soluble aggregates from heating with NaCl: physicochemical, interfacial and foaming properties. *Langmuir, 23*, 4155−4166.

Schorsch, C., Jones, M. G., & Norton, I. T. (2002). Micellar casein gelation at high sucrose content. *Journal of Dairy Science, 85*, 3155−3163.

Schultz, S., Wagner, G., Urban, K., & Ulrich, J. (2004). High-pressure homogenization as a process for emulsion formation. *Chemical Engineering & Technology, 27*, 361−368.

Seebergh, J. E., & Berg, J. C. (1994). Depletion flocculation of aqueous, electrosterically-stabilized latex dispersions. *Langmuir, 10*, 454−463.

Segall, K. I., & Goff, H. D. (2002). Secondary adsorption of milk proteins from the continuous phase to the oil-water interface in dairy emulsions. *International Dairy Journal, 12*, 889−897.

Semenova, M. G., Antipova, A. S., & Belyakova, L. E. (2002). Food protein interactions in sugar solutions. *Current Opinion in Colloid and Interface Science, 7*, 438−444.

Semenova, M. G., Belyakova, L. E., Polikarpov, Y. N., Antipova, A. S., & Dickinson, E. (2009). Light scattering study of sodium caseinate + dextran sulfate in aqueous solution: Relationship to emulsion stability. *Food Hydrocolloids, 23*, 629−639.

Servais, C., Jones, R., & Roberts, I. (2002). The influence of particle size distribution on the processing of food. *Journal of Food Engineering, 51*, 201−208.

Seta, L., Baldino, N., Gabriele, D., Lupi, F. R., & de Cindio, B. (2013). The influence of carrageenan on interfacial properties and short-term stability of milk whey proteins emulsions. *Food Hydrocolloids, 32*, 373−382.

Sharma, R., & Singh, H. (1999). Heat stability of recombined milk systems as influenced by the composition of fat globule surface layers. *Milchwissenschaft, 54*, 193−196.

Sievanen, K., Huppertz, T., Kelly, A. L., & Fox, P. F. (2008). Influence of added calcium chloride on the heat stability of unconcentrated and concentrated bovine milk *International Journal of Dairy Technology, 61*, 151−155.

Singh, A. M., & Dalgleish, D. G. (1998). The emulsifying properties of hydrolyzates of whey proteins. *Journal of Dairy Science, 81*, 918−924.

Singh, H. (2004). Heat stability of milk. *International Journal of Dairy Technology, 57*, 111−119.

Singh, H., & Fox, P. F. (1985). Heat stability of milk: pH-dependent dissociation of micellar κ-casein on heating milk at ultra high temperatures. *Journal of Dairy Research, 52*, 529−538.

Singh, H., Fox, P. F., & Cuddigan, M. (1993). Emulsifying properties of protein fractions prepared from heated milk. *Food Chemistry, 47*, 1−6.

Singh, H., & Latham, J. M. (1993). Heat stability of milk: Aggregation and dissociation of protein at ultra-high temperatures. *International Dairy Journal, 3*, 225−237.

Singh, H., Sharma, R., Taylor, M. W., & Creamer, L. K. (1996). Heat-induced aggregation and dissociation of protein and fat particles in recombined milk. *Netherlands Milk and Dairy Journal, 50*, 149−166.

Singh, H., Sharma, R., & Tokley, R. P. (1992). Influence of incorporation of soya lecithin into skim milk powder on the heat stability of recombined evaporated milk. *Australian Journal of Dairy Technology, 47*, 33−37.

Sliwinski, E. L., Roubos, P. J., Zoet, F. D., van Boekel, M. A. J. S., & Wouters, J. T. M. (2003). Effects of heat on physicochemical properties of whey protein-stabilised emulsions. *Colloids and Surfaces B: Biointerfaces, 31*, 231−242.

Sourdet, S., Relkin, P., & Cesar, B. (2003). Effects of milk protein type and pre-heating on physical stability of whipped and frozen emulsions *Colloids and Surfaces B: Biointerfaces, 31*, 55−64.

Spiegel, T., & Huss, M. (2002). Whey protein aggregation under shear conditions – effects of pH-value and removal of calcium. *International Journal of Food Science & Technology, 37*, 559−568.

Srinivasan, M., Singh, H., & Munro, P. A. (1996). Sodium caseinate-stabilized emulsions: factors affecting coverage and composition of surface proteins. *Journal of Agricultural and Food Chemistry, 44*, 3807−3811.

Srinivasan, M., Singh, H., & Munro, P. A. (1999). Adsorption behavior of sodium and calcium caseinates in oil-in-water emulsions. *International Dairy Journal, 9*, 337−341.

Srinivasan, M., Singh, H., & Munro, P. A. (2000). The effect of sodium chloride on the formation and stability of sodium caseinate emulsions *Food Hydrocolloids, 14*, 497−507.

Srinivasan, M., Singh, H., & Munro, P. A. (2001). Creaming stability of oil-in-water emulsions formed with sodium and calcium caseinates. *Journal of Food Science, 66*, 441−446.

Srinivasan, M., Singh, H., & Munro, P. A. (2002). Formation and stability of sodium caseinate emulsions: influence of retorting (121°C for 15 min) before or after emulsification. *Food Hydrocolloids, 16*, 153−160.

Srinivasan, M., Singh, H., & Munro, P. A. (2003). Influence of retorting (121 °C for 15 min), before or after emulsification, on the properties of calcium caseinate oil-in-water emulsions. *Food Chemistry, 80*, 61−69.

Starrs, L., Poon, W. C. K., Hibberd, D. J., & Robins, M. M. (2002). Collapse of transient gels in colloid-polymer mixtures. *Journal of Physics: Condensed Matter, 14*, 2485−2505.

Steffe, J. F., & Daubert, C. R. (2006). *Bioprocessing Pipelines: Rheology and Analysis*. East Lansing, MI: Freeman Press.

Sun, C., Gunasekaran, S., & Richards, M. P. (2007). Effect of xanthan gum on physicochemical properties of whey protein isolate stabilized oil-in-water emulsions. *Food Hydrocolloids, 21*, 555−564.

Surel, C., Foucquier, J., Perrot, N., Mackie, A., Garnier, C., Riaublanc, A., & Anton, M. (2014). Composition and structure of interface impacts texture of O/W emulsions. *Food Hydrocolloids, 34*, 3−9.

Surh, J. H. (2009). Comparison of emulsion-stabilizing property between sodicum caeinate and whey protein concentrate: susceptibility to changes in protein concentration and pH. *Food Science and Biotechnology, 18*, 610−617.

Surh, J. H., Decker, E. A., & McClements, D. J. (2006a). Influence of pH and pectin type on properties and stability of sodium-caseinate stabilized oil-in-water emulsions. *Food Hydrocolloids, 20*, 607−618.

Surh, J. H., Ward, L. S., & McClements, D. J. (2006b). Ability of conventional and nutritionally-modified whey protein concentrates to stabilize oil-in-water emulsions. *Food Research International, 39*, 761−771.

Swaisgood, H. E. (2003). Chemistry of the caseins. In P. F. Fox & P. L. H. McSweeney (Eds.), *Advanced Dairy Chemistry 1. Proteins* (3rd ed., pp. 139−201). Elsevier Applied Science, London.

Sweetsur, A. W. M., & Muir, D. D. (1983). Effect of homogenization on the heat stability of milk. *Journal of Dairy Research, 50*, 291−300.

Tadros, T. (2004). Application of rheology for assessment and prediction of the long-term physical stability of emulsions. *Advances in Colloid and Interface Science, 108–109*, 227−258.

Tadros, T., Izquierdo, P., Esquena, J., & Solans, C. (2004). Formation and stability of nano-emulsions. *Advances in Colloid and Interface Science, 108–109*, 303−318.

Tan-Kintia, R. H., & Fox, P. F. (1996). Effect of enzymic hydrolysis of lactose on the heat stability of milk or concentrated milk. *Netherlands Milk and Dairy Journal, 50*, 267−277.

Tan, C.-T. (2004). Beverage emulsions. In S. E. Friberg, K. Larsson & J. Sjoblom (Eds.), *Food Emulsions* (4th ed., Chapter 12). Marcel Dekker, Inc., New York, NY.

Tan, H. L. (2010). The microstructure and rheology of complex fluids containing Na-caseinate. Victoria University of Wellington. New Zealand.

Tanaka, H., Nishikawa, Y., & Koyama, T. (2005). Network-forming phase separation of colloidal suspensions. *Journal of Physics Condensed Matter, 17*, L143−L153.

Tang, X., & Pikal, M. (2005). The effect of stabilizers and denaturants on the cold denaturation temperatures of proteins and implications for freeze-drying. *Pharmaceutical Research, 22*, 1167−1175.

Tangsuphoom, N., & Coupland, J. N. (2009). Effect of thermal treatments on the properties of coconut milk emulsions prepared with surface-active stabilizers. *Food Hydrocolloids, 23*, 1792−1800.

Tcholakova, S., Denkov, N. D., & Danner, T. (2004). Role of surfactant type and concentration for the mean drop size during emulsification in turbulent flow. *Langmuir, 20*, 7444−7458.

Tcholakova, S., Denkov, N. D., Ivanov, I. B., & Campbell, B. (2002). Coalescence in β-lactoglobulin-stabilized emulsions: Effects of protein adsorption and drop size. *Langmuir, 18*, 8960−8971.

Tcholakova, S., Denkov, N. D., Ivanov, I. B., & Campbell, B. (2006a). Coalescence stability of emulsions containing globular milk proteins. *Advances in Colloid and Interface Science, 123-126*, 259−293.

Tcholakova, S., Denkov, N. D., Sidzhakova, D., & Campbell, B. (2006b). Effect of thermal treatment, ionic strength, and pH on the short-term and long-term coalescence stability of β-lactoglobulin emulsions. *Langmuir, 22*, 6042−6052.

Teece, L. J., Faers, M. A., & Bartlett, P. (2011). Ageing and collapse in gels with long-range attractions. *Soft Matter, 7*, 1341−1351.

ten Grotenhuis, E., Tuinier, R., & de Kruif, C. G. (2003). Phase stability of concentrated dairy products. *Journal of Dairy Science, 86*, 764−769.

Thomar, P., Durand, D., Benyahia, L., & Nicolai, T. (2012). Slow dynamics and structure in jammed milk protein suspensions. *Faraday Discussions, 158*, 325−339.

Thomar, P., Nicolai, T., Benyahia, L., & Durand, D. (2013). Comparative study of the rheology and the structure of sodium and calcium caseinate solutions. *International Dairy Journal, 31*, 100−106.

Thorn, D. C., Ecroyd, h., & Carver, J. A. (2009). The two-faced nature of milk casein proteins: amyloid fibril formation and chaperone-like activity. *Australian Journal of Dairy Technology, 64*, 34−40.

Thorn, D. C., Meehan, S., Sunde, M., Rekas, A., Gras, S. L., MacPhee, C. E., Dobson, C. M., Wilson, M. R., & Carver, J. A. (2005). Amyloid fibril formation by bovine milk κ-casein and its inhibition by the molecular chaperones α_S- and β-casein. *Biochemistry, 44*, 17027−17036.

Thurn, A., Burchard, W., & Niki, R. (1987a). Structure of casein micelles I. Small angle neutron scattering and light scattering from β- and κ-casein. *Colloid and Polymer Science, 265*, 653−666.

Thurn, A., Burchard, W., & Niki, R. (1987b). Structure of casein micelles II. α_{S1}-Casein. *Colloid and Polymer Science, 265*, 897−902.

Timasheff, S. N. (1993). The control of protein stability and association by weak interactions with water: How do solvents affect these processes? *Annual Review of Biophysics and Biomolecular Structure, 22*, 67−97.

Tokle, T., Lesmes, U., & McClements, D. J. (2010). Impact of electrostatic deposition of anionic polysaccharides on the stability of oil droplets coated by lactoferrin. *Journal of Agricultural and Food Chemistry, 58*, 9825−9832.

Tran, T., & Rousseau, D. (2013). Stabilization of acidic soy protein-based dispersions and emulsions by soy soluble polysaccharides. *Food Hydrocolloids, 30*, 382−392.

Tran Le, T., El-Bakry, M., Neirynck, N., Bogus, M., Hoa, H. D., & van der Meeren, P. (2007). Hydrophilic lecithins protect milk proteins against heat-induced aggregation. *Colloids and Surfaces B: Biointerfaces, 60*, 167−173.

Tran Le, T., Sabatino, P., Heyman, B., Kasinos, M., Dinh, H. H., Dewettinck, K., Martins, J., & van der Meeren, P. (2011). Improved heat stability by whey protein-surfactant interaction. *Food Hydrocolloids, 25*, 594−603.

Trappe, V., Prasad, V., Cipelletti, L., Segre, P. N., & Weitz, D. A. (2001). Jamming phase diagram for attractive particles. *Nature, 411*, 772−775.

Trejo, R., Dokland, T., Jurat-Fuentes, J., & Harte, F. (2011). Cryo-transmission electron tomography of native casein micelles from bovine milk. *Journal of Dairy Science, 94*, 5770−5775.

Treweek, T. M., Thorn, D. C., Price, W. E., & Carver, J. A. (2011). The chaperone action of bovine milk αS1- and αS2-caseins and their associated form αS-casein. *Archives of Biochemistry and Biophysics, 510*, 42−52.

Tsioulpas, A., Koliandris, A., Grandison, A. S., & Lewis, M. J. (2010). Effects of stabiliser addition and in-container sterilisation on selected properties of milk related to casein micelle stability. *Food Chemistry, 122*, 1027−1034.

Tsioulpas, A., Lewis, M. J., & Grandison, A. S. (2007). Effect of minerals on casein micelle stability of cows' milk. *Journal of Dairy Research, 74*, 167−173.

Tuinier, R., & de Kruif, C. G. (1999). Phase separation, creaming, and network formation of oil-in-water emulsions induced by an exocellular polysaccharide. *Journal of Colloid and Interface Science, 218*, 201−210.

Tuinier, R., & de Kruif, C. G. (2002). Stability of casein micelles in milk. *Journal of Chemical Physics, 117*, 1290−1295.

Udomrati, S., Ikeda, S., & Gohtani, S. (2013). Rheological properties and stability of oil-in-water emulsions containing tapioca maltodextrin in the aqueous phase. *Journal of Food Engineering, 116*, 170−175.

van Boekel, M. A. J. S. (1999). Heat-induced deamidation, dephosphorylation and breakdown of caseinate. *International Dairy Journal, 9*, 237−241.

van Boekel, M. A. J. S., Nieuwenhuijse, J. A., & Walstra, P. (1989a). The heat coagulation of milk. 1. Mechanisms. *Netherlands Milk and Dairy Journal, 43*, 97−127.

van Boekel, M. A. J. S., Nieuwenhuijse, J. A., & Walstra, P. (1989b). The heat coagulation of milk. 2. Kinetic studies. . *Netherlands Milk and Dairy Journal, 43*, 129−146.

van Boekel, M. A. J. S., Nieuwenhuijse, J. A., & Walstra, P. (1989c). The heat coagulation of milk. 3. Comparison of theory and experiment. *Netherlands Milk and Dairy Journal, 43*, 147−162.

van der Meeren, P., El-Bakry, M., Neirynck, N., & Noppe, P. (2005). Influence of hydrolysed lecithin addition on protein adsorption and heat stability of a sterilised coffee cream simulant. *International Dairy Journal, 15*, 1235−1243.

van der Werff, J. C., & de Kruif, C. G. (1989). Hard sphere colloidal dispersions: The scaling of rheological properties with particle size, volume fraction, and shear rate. *Journal of Rheology, 33*, 421−454.

van Gruijthuijsen, K., Herle, V., Tuinier, R., Schurtenberger, P., & Stradner, A. (2012). Origin of suppressed demixing in casein/xanthan mixtures. *Soft Matter, 8*, 1547−1555.

Vasbinder, A. J., & de Kruif, C. G. (2003). Casein–whey protein interactions in heated milk: the influence of pH. *International Dairy Journal, 13*, 669−677.

Vasbinder, A. J., van de Velde, F., & de Kruif, C. G. (2004). Gelation of casein-whey protein mixtures. *Journal of Dairy Science, 87*, 1167−1176.

Vega, C., Goff, D. H., & Roos, Y. H. (2007). Casein molecular assembly affects the properties of milk fat emulsions encapsulated in lactose or trehalose matrices. *International Dairy Journal, 17*, 683−695.

Vélez, G., Fernández, M. A., Muñoz, J., Williams, P. A., & English, R. J. (2003). Role of hydrocolloids in the creaming of oil in water emulsions. *Journal of Agricultural and Food Chemistry, 51*, 265−269.

Vincent, B. (1990). The calculation of depletion layer thickness as a function of bulk polymer concentration. *Colloids and Surfaces, 50*, 241−249.

Vold, M. J. (1961). The effect of adsorption on the van der waals interaction of spherical colloidal particles. *Journal of Colloid Science, 16*, 1−12.

Vrij, A. (1976). Polymers at interfaces and the interactions in colloidal dispersions. *Pure and Applied Chemistry, 48*, 471−483.

Walstra, P. (2003). *Physical Chemistry of Foods*. Marcel Dekker, New York, NY.

Walstra, P. (2005). Emulsions. In J. Lyklema (Ed.), *Fundamentals of Interface and Colloid Science* (Vol. 5, pp. 1−94). Elsevier, Amsterdam.

Walstra, P., Wouters, J. T. M., & Geurts, T. J. (2006a). Heat treatment. In P. Walstra, J. T. M. Wouters & T. J. Geurts (Eds.), *Dairy Science and Technology* (2nd ed., pp. 225−272) CRC Press, Boca Raton, FL.

Walstra, P., Wouters, J. T. M., & Geurts, T. J. (2006b). Milk components. In P. Walstra, J. T. M. Wouters & T. J. Geurts (Eds.), *Dairy Science and Technology* (2nd ed., pp. 17−108) CRC Press, Boca Raton, FL.

Walstra, P., Wouters, J. T. M., & Geurts, T. J. (2006c). Milk: Main characteristics. In P. Walstra, J. T. M. Wouters & T. J. Geurts (Eds.), *Dairy Science and Technology* (2nd ed., pp. 3−16) CRC Press, Boca Raton, FL.

Weaver, C. M. (2010). Role of dairy beverages in the diet. *Physiology & Behavior, 100*, 63−66.

Wit, J. N. d. (2009). Thermal behavior of bovine β-lactoglobulin at temperatures up to 150 °C. a review *Trends in Food Science & Technology, 20*, 27−34.

Wooster, T. J., & Augustin, M. A. (2006). β-Lactoglobulin-dextran Maillard conjugates: Their effect on interfacial thickness and emulsion stability. *Journal of Colloid and Interface Science, 303*, 564−572.

Wooster, T. J., Golding, M., & Sanguansri, P. (2008). Impact of oil type on nanoemulsion formation and ostwald ripening stability. *Langmuir, 24*, 12758−12765.

Wulff-Pérez, M., Torcello-Gómez, A., Gálvez-Ruíz, M. J., & Martín-Rodríguez, A. (2009). Stability of emulsions for parenteral feeding: Preparation and characterization of o/w nanoemulsions with natural oils and Pluronic f68 as surfactant. *Food Hydrocolloids, 23*, 1096−1102.

Xiong, Y. (1997). Protein denaturation and functionality losses. In M. Erickson & Y.-C. Hung (Eds.), *Quality in Frozen Food* (pp. 111−140). Springer, US.

Xu, K., & Yao, P. (2009). Stable oil-in-water emulsions prepared from soy protein−dextran conjugates. *Langmuir, 25*, 9714−9720.

Yang, Y., Leser, M. E., Sher, A. A., & McClements, D. J. (2013). Formation and stability of emulsions using a natural small molecule surfactant: Quillaja saponin (Q-Naturale®). *Food Hydrocolloids, 30*, 589−596.

Ye, A. (2003). Behavior of fat globules and membrane proteins under different processing environments as related to milk powder manufacture. Massey University, Palmerston North.

Ye, A. (2008). Interfacial composition and stability of emulsions made with mixtures of commercial sodium caseinate and whey protein concentrate. *Food Chemistry, 110*, 946−952.

Ye, A. (2010). Surface protein composition and concentration of whey protein isolate-stabilized oil-in-water emulsions: Effect of heat treatment. *Colloids and Surfaces B: Biointerfaces, 78*, 24−29.

Ye, A. (2011). Functional properties of milk protein concentrates: Emulsifying properties, adsorption and stability of emulsions. *International Dairy Journal, 21*, 14−20.

Ye, A., Hemar, Y., & Singh, H. (2004). Influence of polysaccharides on the rate of coalescence in oil-in-water emulsions formed with highly hydrolyzed whey proteins. *Journal of Agricultural and Food Chemistry, 52*, 5491−5498.

Ye, A., Lo, J., & Singh, H. (2012). Formation of interfacial milk protein complexation to stabilize oil-in-water emulsions against calcium. *Journal of Colloid and Interface Science, 378*, 184−190.

Ye, A., & Singh, H. (2000). Influence of calcium chloride addition on the properties of emulsions stabilized by whey protein concentrate. *Food Hydrocolloids, 14*, 337−346.

Ye, A., & Singh, H. (2001). Interfacial composition and stability of sodium caseinate emulsions as influenced by calcium ions. *Food Hydrocolloids, 15*, 195−207.

Ye, A., & Singh, H. (2006). Heat stability of oil-in-water emulsions formed with intact or hydrolysed whey proteins: Influence of polysaccharides. *Food Hydrocolloids, 20*, 269−276.

Ye, A., Srinivasan, M., & Singh, H. (2000). Influence of NaCl addition on the properties of emulsions formed with commercial calcium caseinate. *Food Chemistry, 69*, 237−244.

Ye, A., Zhu, X., & Singh, H. (2013). Oil-in-water emulsion system stabilized by protein-coated nanoemulsion droplets. *Langmuir, 29*, 14403−14410.

Yong, Y. H., & Foegeding, E. A. (2010). Caseins: Utilizing molecular chaperone properties to control protein aggregation in foods. *Journal of Agricultural and Food Chemistry, 58*, 685−693.

Zhai, J., Hoffmann, S. V., Day, L., Lee, T.-H., Augustin, M. A., Aguilar, M.-I., & Wooster, T. J. (2011a). Conformational changes of α-lactalbumin adsorbed at oil–water interfaces: Interplay between protein structure and emulsion stability. *Langmuir, 28*, 2357−2367.

Zhai, J., Wooster, T. J., Hoffmann, S. V., Lee, T.-H., Augustin, M. A., & Aguilar, M.-I. (2011b). Structural rearrangement of β-lactoglobulin at different oil–water interfaces and its effect on emulsion stability. *Langmuir, 27*, 9227−9236.

Zhang, W., & Zhong, Q. (2010). Microemulsions as nanoreactors to produce whey protein nanoparticles with enhanced heat stability by thermal pretreatment *Food Chemistry, 119*, 1318−1325.

Zhang, Y., & Brew, K. (2003). α-Lactalbumin. In H. Roginski, J. W. Fuquay & P. F. Fox (Eds.), *Encyclopedia of Dairy Sciences* (Vol. 3, pp. 1924−1932). Academic Press, London.

Zittle, C. A. (1969). Influence of heat on κ-casein. *Journal of Dairy Science, 52*, 12−16.

Appendix: Publications

Paper One

(This published work is from Chapter 4)

Appendix

Food Hydrocolloids 33 (2013) 297–308

Contents lists available at SciVerse ScienceDirect

Food Hydrocolloids

journal homepage: www.elsevier.com/locate/foodhyd

Structure and stability of heat-treated concentrated dairy-protein-stabilised oil-in-water emulsions: A stability map characterisation approach

Yichao Liang [a,b,*], Hasmukh Patel [c], Lara Matia-Merino [b], Aiqian Ye [d], Matt Golding [b,d,**]

[a] Fonterra Research and Development Centre, Private Bag 11 029, Palmerston North 4442, New Zealand
[b] Institute of Food, Nutrition and Human Health, Massey University, Private Bag 11 222, Palmerston North, New Zealand
[c] Dairy Science Department, Box 2104, South Dakota State University, Brookings, SD, USA
[d] Riddet Institute, Massey University, Private Bag 11 222, Palmerston North, New Zealand

ARTICLE INFO

Article history:
Received 18 December 2012
Accepted 23 March 2013

Keywords:
Milk protein
Heat treatment
Microstructure
Flocculation
Emulsion stability
Emulsion rheology

ABSTRACT

Emulsion instabilities such as depletion flocculation, coalescence, aggregation and heat-induced protein aggregation may be detrimental to the production of sterilised food emulsions. The type and the amount of protein present in the continuous phase and at the oil–water interface are crucial in the design of emulsions with appropriate stability. In this study, four oil-in-water model emulsion systems (pH 6.8–7.0) were formulated, characterised and categorised according to the potential interactions between protein-coated or surfactant-coated emulsion droplets and non-adsorbed proteins present in the continuous phase. The heat stability, the creaming behaviour and the flow behaviour of the model emulsions were influenced by both the emulsifier type and the type of protein in the continuous phase. The results suggest that this stability map approach of predicting droplet–droplet, droplet–protein and protein–protein interactions will be useful for the future design of heat-stable emulsion-based beverages with good creaming stability at high protein concentrations.

1. Introduction

Dairy beverages are generally oil-in-water emulsions that contain oil-soluble (e.g. vitamins) and water-soluble (milk proteins, carbohydrates, minerals etc.) nutrients (Keowmaneechai & McClements, 2006). Proteins are often used to emulsify and to stabilise oil droplets in an aqueous medium (Dickinson, 1997). The challenges in developing oil-in-water emulsions with long shelf life stability increase when these emulsions are formulated with high protein content and when they are subjected to harsh heat treatment (e.g. retort-, and ultra-high-temperature processes). The severity and the duration of heat processing may result in destabilisation of the emulsion, with the extent and the type of breakdown depending on several factors, such as protein molecular flexibility, type and concentration of emulsifier and ionic strength in the aqueous phase (McClements, 2005). Emulsions with good stability against heating during production and with good creaming stability during storage are therefore highly desired, but can be challenging to formulate.

The heat stability of an emulsion is determined by the properties of droplet–droplet, protein–droplet and protein–protein interactions (Agboola, Singh, Munro, Dalgleish, & Singh, 1998; Nikiforidis & Kiosseoglou, 2007; Raikos, 2010). It has been extensively illustrated that heating above the thermal denaturation temperature of whey proteins in an emulsion and/or in solution can promote instability, such as aggregation and gelation (Havea, Singh, & Creamer, 2002; de Kort, Minor, Snoeren, van Hooijdonk, & van der Linden, 2012; Sliwinski, Roubos, Zoet, Boekel, & Wouters, 2003). However, sodium caseinate (Na–CN) has been reported to increase the heat stability of dairy emulsion if it is predominantly adsorbed on the surface of the oil droplets (Sharma & Singh, 1999). Systematic studies on the influence of the structure at the oil–water interface on the heat stability of protein-based emulsions have been carried out by a number of workers (Dickinson & Parkinson, 2004; McSweeney, Healy, & Mulvihill, 2008; Nikiforidis & Kiosseoglou, 2007). Dickinson and Parkinson (2004) reported that the heat stability of whey protein emulsions increased with the

* Corresponding author. Institute of Food, Nutrition and Human Health, Massey University, Private Bag 11 222, Palmerston North 4442, New Zealand. Tel.: +64 06 356 9099x81428; fax: +64 06 350 5618.
** Corresponding author. Institute of Food, Nutrition and Human Health, Massey University, Private Bag 11 222, Palmerston North 4442, New Zealand. Tel.: +64 06 356 9099x81428; fax: +64 06 350 5618.
E-mail addresses: 08009139@uni.massey.ac.nz, kendison.liang@fonterra.com (Y. Liang), M.Golding@massey.ac.nz (M. Golding).

0268-005X/$ – see front matter © 2013 Elsevier Ltd. All rights reserved.
http://dx.doi.org/10.1016/j.foodhyd.2013.03.012

Appendix

addition of small amounts of casein. The improvement was attributed to the co-adsorption of casein at the oil–water interface. The dangling tails of the casein protruded and prevented whey-protein-stabilised droplets from aggregation (Parkinson & Dickinson, 2007).

Non-ionic surfactants such as Tween can also be used to stabilise heat-sensitive globular protein emulsions (Nikiforidis & Kiosseoglou, 2007). It has been postulated that Tween inhibits heat-induced droplet aggregation by competitively displacing adsorbed globular proteins from the interface and interacting with the reactive groups of the adsorbed protein molecules and those of non-adsorbed proteins in the continuous phase, diminishing their hydrophobic area. In this manner, the probability of hydrophobic bond formation is reduced and droplet flocculation is inhibited (Nikiforidis & Kiosseoglou, 2007). McSweeney et al. (2008) reported that the addition of lecithin improved the heat stability of infant formula emulsions. The proposed stabilizing mechanism was similar to that of Tween and was attributed to lecithin's ability to limit the hydrophobic reactive sites of protein molecules by interacting with interfacial protein and/or non-adsorbed protein. A number of previous studies on heat-induced emulsion instability emphasized the interactions between adsorbed proteins and their contribution to the heat stability of emulsions. In an emulsion system that has a high protein-to-oil ratio (e.g. 0.8), the non-adsorbed protein–protein interactions may also play an important role in emulsion instability in association with heating (Kiosseoglou & Nikiforidis, 2008).

The fundamental principles of emulsion stability and heat-induced interactions in milk-protein-based emulsions have been established. They cover a range of protein ingredients, i.e. whey protein concentrate (WPC) (Euston, Al-Bakkush, & Campbell, 2009; Euston, Finnigan, & Hirst, 2000), whey protein isolate (WPI) (Demetriades, Coupland, & McClements, 1997), whey protein hydrolysate (WPH) (Euston, Finnigan, & Hirst, 2001), milk protein concentrate (MPC) (Dybowska, 2008; Ye, 2011), skim milk powder (SMP) (McSweeney, Mulvihill, & O'Callaghan, 2004), Na–CN (Srinivasan, Singh, & Munro, 2002), calcium caseinate (Segall & Goff, 1999) and mixed whey proteins and caseins (Dickinson & Parkinson, 2004; Ye, 2008). However, the interactions of proteins between the interface and the continuous phase, with different compositions, in a high protein system are less well understood in milk-protein-based beverages. One of the main objectives of the present study was to probe the possible destabilising mechanism(s) in a high protein system by investigating the influence of the continuous phase component in a model emulsion containing heat-stable droplets.

Emulsions can, of course, be destabilised by a number of mechanisms and it is important to note that non-adsorbed protein may cause the instability of oil-in-water emulsions regardless of the heat treatment. The relationship between emulsion stability and Na–CN concentration has been studied (Huck-Iriart, Álvarez-Cerimedo, Candal, & Herrera, 2011). It has been suggested that Na–CN, at relatively low concentration, will result in bridging flocculation. At protein concentrations that are close to the saturation surface coverage value, the emulsion is stable and the creaming rate follows Stokes' law. In the presence of a considerable excess of non-adsorbed protein in the continuous phase, the emulsion droplets will undergo droplet flocculation, resulting in rapid phase separation. At higher protein concentrations, the flocculated droplets are partially stabilised by a strong particle gel network (Dickinson, 1999; Dickinson & Golding, 1997a). At a fixed casein concentration, the strength of the depletion attraction depends on the effective size of the non-adsorbed polymers and the size of the oil droplets (Radford, Dickinson, & Golding, 2004).

To our knowledge, few studies have investigated the impact of various milk protein types in the dispersed and continuous phases and the influence of high temperature treatment on the macroscopic and microscopic stabilities of emulsions fortified with high amounts of protein. The objective of this study was to design a simple model system to understand the emulsion interactions at high temperatures that determine stability or instability, to characterize the roles of the proteins and surfactants present at the interface and/or in solution of an emulsion, to address heat destabilisation at high temperatures in mixed protein systems and to predict emulsion stability.

In this study, we formulated, characterised and categorised the heat-treated model emulsions into four proposed model systems in terms of their continuous and dispersed phase interactions. A schematic presentation of four model droplet–droplet, droplet–protein and protein–protein interaction diagrams with respect to the role of the type of adsorbed and non-adsorbed protein is shown in Fig. 1. In order to achieve the proposed model systems, we used commercial milk proteins – heat-sensitive proteins (WPC) and heat-insensitive proteins (MPC-I, MPC-II, Na–CN and WPH) – and surfactant (Tween 20).

2. Materials and methods

2.1. Materials

Milk protein concentrate 485 (MPC-I), low calcium MPC (MPC-II), sodium caseinate 180 (Na–CN), whey protein concentrate 80 (WPC) and whey protein hydrolysate (WPH) were obtained from Fonterra Co-operative Group Ltd, Auckland, New Zealand. The compositions of the milk protein powders are shown in Table 1. The low calcium MPC was a spray-dried ingredient and has been described in a previous study (Ye, 2011). Polysorbate 20 (Tween 20) was acquired from Merck Chemicals, Darmstadt, Germany. Bulk corn oil was purchased from Davis Trading Co., Palmerston North, New Zealand. All of the chemicals used were of analytical grade, obtained from either BDH Chemicals (BDH Ltd, Poole, England) or Sigma Chemical Co. (St Louis, MO, USA) unless otherwise specified.

2.2. Preparation of model emulsion systems

Two primary stock emulsions stabilised with edible Na–CN or Tween 20 were prepared. Na–CN was selected as an emulsifier because of its excellent heat stability and good emulsifying properties. From preliminary experiments, an oil-in-water emulsion stabilised with Tween 20 (10% w/w oil) was also found to be very heat stable, with no coagulation being observed on heating at 120 °C for at least 40 min.

Na–CN (1.0% w/w) was reconstituted in reverse osmosis water at 50 °C for 60 min; 1.0% (w/w) Tween 20 was used as a non-protein emulsifier. Corn oil (20% w/w) was mixed with emulsifier and was then pre-homogenized at 13 500 rev min^{-1} for 2 min using an Ultra-Turrax T25 (IKA®-Werke GmbH & Co. KG, Staufen, Germany) to form a coarse emulsion. The coarse emulsion was heated to 60 °C and homogenized using a two-stage homogenizer (type Panda, Niro Soavi, Parma, Italy) at 20 MPa (first stage) and 4 MPa (second stage) to form a stock emulsion.

The model emulsions were prepared following the procedure described in Fig. 2. The stock emulsion (20% w/w oil) stabilised by either 0.5% (w/w) Na–CN or 0.5% (w/w) Tween 20 was mixed with stock protein solutions – MPC-I, MPC-II, WPC and WPH respectively in a 1:1 weight ratio to yield final dispersions containing 8.5% (w/w) protein and 10% (w/w) oil. Model emulsions (8.5% protein, 10% oil) stabilised by sole protein ingredients were also prepared for comparison. WPC was used as a heat-sensitive control while

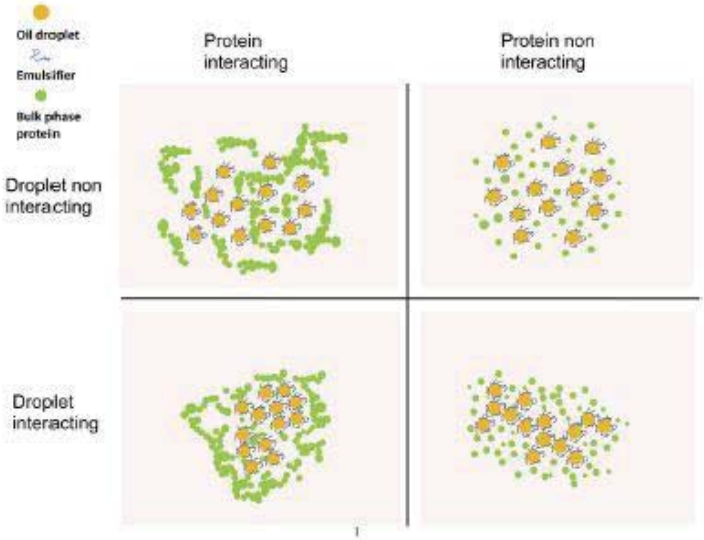

Fig. 1. Schematic diagrams of the proposed model systems: top left system, no interactions between droplets but non-adsorbed proteins interact with each other (i.e. an unstable system with a partly liquid and a partly gel-like structure); top right system, no droplet–droplet interactions and no protein–protein interactions at the oil–water interface and in the continuous phase (i.e. a stable system with no coagulation and no phase separation); bottom left system, interactions between adsorbed proteins, between non-adsorbed proteins and between adsorbed and non-adsorbed proteins (i.e. a whey protein emulsion gel); bottom right system, interactions between droplets but no protein–protein interactions at the oil–water interface and in the continuous phase (i.e. a phase separation induced by depletion flocculation).

Na–CN and MPC were used as heat-stable controls containing non-micellar casein and micellar casein respectively. The approximate total casein and whey protein contents are shown in Table 2. Reverse-phase high-performance liquid chromatography (RP-HPLC) was used to determine whey protein composition (Elgar et al., 2000). Sodium azide (0.02% w/w) was added to the emulsion samples as an anti-microbial agent. All emulsions were stored at 4 °C overnight until further use. The pH at 20 °C was measured to be approximately 6.8 ± 0.04 for all model emulsions. Each model emulsion was prepared at least in duplicate.

2.3. Characterisation of heat stability of model emulsions

In order to evaluate the effect of heat treatments that are close to commercial processing (sterilisation) at laboratory scale, 5 mL aliquots of milk-protein-stabilised emulsion samples were transferred into 8 mL glass tubes with rubber-lined caps (Wheaton, Millville, NJ, USA) and were immersed in a silicone oil bath that was thermostatically controlled at 120 ± 1 °C, with a constant rocking speed (8 rev min^{-1}). All samples were removed after 10 min and immediately cooled under running tap water. The heat-treated emulsions were allowed to equilibrate to room temperature and were held for at least 1 h before further analysis (i.e. particle size and rheological measurements) was carried out. The gelled or coagulated samples were not included in particle size, creaming stability and rheological measurements.

Table 1
Compositions of commercial milk protein ingredients.

	Protein [g/(100 g)$^{-1}$]	Sodium [mg/(100 g)$^{-1}$]	Calcium [mg/(100 g)$^{-1}$]
Milk protein concentrate (MPC) 485 (MPC-I)	81.5	70	2230
Low calcium MPC (MPC-II)	82.2	1150	1340
Sodium caseinate (Na–CN)	92.7	1120	30
Whey protein concentrate (WPC)	80.3	340	400
Whey protein isolate (WPI)	93.5	600	64
Whey protein hydrolysate (WPH)[a]	91.9	585	198

[a] The degree of hydrolysis was 18.1%.

2.4. Determination of surface protein composition

In order to verify whether surface protein exchange interactions are associated with the heat-induced destabilisation observed in

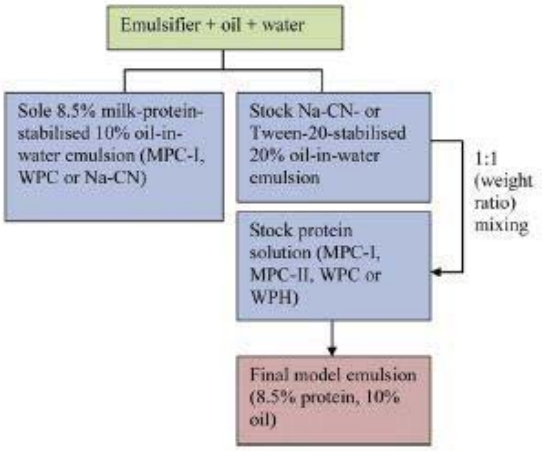

Fig. 2. Flow chart of the preparation of model emulsions (8.5% w/w protein, 10% w/w oil).

Appendix

Table 2
Distributions of casein and whey protein in the protein- and surfactant-stabilised model emulsions (8.5% w/w protein, 10% w/w oil).

Compositions of model emulsions (% w/w)		Micellar casein (% w/w)	Non-micellar casein (% w/w)	Whey protein (% w/w)
Continuous phase	Dispersed phase			
MPC-I	MPC-I	~6.8	trace	~1.7
Na–CN	Na–CN	–	8.5	–
WPC	WPC	–	–	8.5
8.0% MPC-I	0.5% Na–CN	~6.4	0.5	~1.6
8.0% MPC-II	0.5% Na–CN	~3.84	~3.06	~1.6
8.0% WPC	0.5% Na–CN	–	0.5	8.0
8.0% WPH	0.5% Na–CN	–	0.5	8.0
8.5% MPC-I	0.5% Tween 20	~6.8	trace	~1.7
8.5% MPC-II	0.5% Tween 20	~4.08	~2.72	~1.7
8.5% WPC	0.5% Tween 20	–	–	8.5
8.5% WPH	0.5% Tween 20	–	–	8.5

Na–CN-stabilised WPC emulsions, the composition of the protein adsorbed at the surface of the emulsion droplets was evaluated using sodium dodecyl sulphate polyacrylamide gel electrophoresis (SDS-PAGE) according to the method of Dalgleish, Goff, and Luan (2002).

2.5. Particle size determination

The particle size distribution of the model emulsions was measured by static light scattering using a Malvern Mastersizer Hydro 2000S (Malvern Instruments Ltd, Malvern, Worcestershire, UK). The measurements were carried out using procedures described previously (Ye, 2011). The average droplet size was expressed as the surface-weighted diameter $d_{3,2}$ (μm) and the volume-weighted mean diameter $d_{4,3}$ (μm).

2.6. Emulsion stability

The model emulsions were transferred into flat-bottom screw-top tubes (15 mm × 140 mm). They were stored at room temperature and measured periodically using a vertical scan analyser Turbiscan Classic MA 2000 (Formulaction, Toulouse, France). The transmission (T) and backscattering (BS) profiles as a function of the sample height (total height = 60 mm) were collected at room temperature. Transmission is useful for analysing non-opaque samples whereas backscattering is useful for analysing opaque samples (Chauvierre, Labarre, Couvreur, & Vauthier, 2004; Mengual, Meunier, Cayré, Puech, & Snabre, 1999). Measurements were carried out after preparation of the emulsions and at different times for 7 days.

The creaming curves were obtained by subtracting the BS profiles measured at 0 h (BS_0) from those measured at time t (BS_t), $\Delta BS = BS_t - BS_0$. The shape of the creaming curve gives a good indication of creaming, flocculation and other destabilisation processes. BS mean values (BS_{av}) in the selected zone of the tube were measured as a function of storage time to determine flocculation kinetics because BS_{av} varies with the change in particle size (Chauvierre et al., 2004). The zone 15–30 mm was chosen for analysis of the model emulsions through the whole storage period and the aim was to avoid the area affected by creaming. Visual determination of the serum layer thickness of the model emulsions was also carried out.

2.7. Rheological properties of model emulsions

The rheological properties of the model emulsions were determined by a controlled-stress rheometer (Physica MCR301, Anton Paar, Graz, Austria) at 20 °C using a cone and plate geometry (cone diameter = 50 mm, angle = 2.009°, gap = 0.047 mm). The flow curves were recorded at room temperature, using 24 measuring data points at shear rates ranging from 0.05 to 200 s^{-1}. The apparent viscosity was recorded as a function of shear rate. Analysis of the flow behaviour was conducted using the Rheoplus 32 V3.21 software (Anton Paar). The power law model was fitted to the data:

$$\tau = K\dot{\gamma}^n$$

where τ is shear stress (pa), $\dot{\gamma}$ is shear rate (s^{-1}), K is the consistency coefficient (Pa.s^n) and n is the flow behaviour index. The apparent viscosity at a shear rate of 100 s^{-1} was analysed because it is a useful representation of food processes under flow, for instance pumping through a pipe, stirring or mastication (McClements, 2005). Measurements were carried out twice on each sample and the mean values of viscosity were obtained from duplicate samples.

2.8. Microstructure of model emulsions

2.8.1. Confocal laser scanning microscopy

Images of the emulsions were captured using a Leica SP5 DM6000B (Heidelberg, Germany) confocal laser scanning microscope. A 0.5 mL aliquot of each emulsion sample was transferred into a 2 mL centrifuge tube before adding Nile Red and Fast Green (approximately 0.1% w/w). After thorough mixing, a drop of each sample was placed on a microscope slide (Sail, Sailing Medical-Lab Industries Co. Ltd, China). Samples were examined at $\lambda = 543$ nm for Nile Red and $\lambda = 488$ nm for Fast Green. Images were scanned at a constant 7 μm below the level of the coverslip.

2.8.2. Transmission electron microscopy (TEM)

TEM images of the emulsion samples before and after heat treatment (120 °C for 10 min) were captured using a Philips CM10 transmission electron microscope. Emulsion samples were fixed, stained and processed as described by Langton and Hermansson (1996).

2.9. Statistical analysis

The experimental data were analysed by Student's t-tests and the significant differences among the means were determined at a 95.0% confidence level. Treatment means were considered to be significantly different at $p < 0.05$.

3. Results and discussion

3.1. Model emulsions with interactions between adsorbed proteins, interactions between non-adsorbed proteins and cross-interactions between adsorbed and non-adsorbed proteins

The 8.5% (w/w) WPC-stabilised emulsion formed a paste-like texture upon heating indicating a high degree of structure. The droplets interact with each other to form clusters and the droplet clusters appeared to interact with whey proteins in the continuous phase to form a gel matrix (Fig. 3A). It was calculated that the interfacial whey protein concentration was approximately 0.4% (w/w) and that the rest of the whey proteins remained non-adsorbed (~8.1% w/w) in the continuous phase. In the case of an emulsion with a high protein to oil ratio, the extent of destabilisation of the emulsion will be influenced by the concentration of non-adsorbed protein in the continuous phase. The extent of heat-induced droplet–droplet and droplet–protein aggregations would be strengthened if non-adsorbed whey proteins were present (Euston et al., 2000). Previous studies have also shown that calcium ions

promote protein aggregation/coagulation in emulsion and solution systems (Keowmaneechai & McClements, 2006; Riou, Havea, McCarthy, Watkinson, & Singh, 2011). WPC at 8.5% (w/w) has a reasonably high calcium content (~8.5 mM/L), which may contribute to the extent of heat-induced whey protein aggregation. To determine the phase transition of whey protein emulsions in the initial heat-induced aggregation/gelation process, a heat stability map (90 °C for 10 min) of whey protein concentration against calcium content in a 10% oil-in-water emulsion was obtained using WPI as a whey protein source of low ionic strength (Fig. 4). It was found the WPI emulsions at high protein contents [4.5 and 6.5% (w/w)] formed a precipitate or a gel-like texture in the presence of 4 and 5 mM $CaCl_2$ respectively during heating. β-Lactoglobulin (β-lg) is a major component of whey proteins and has two internal disulphide bonds and one free thiol group (Havea et al., 2002). The β-lg content of WPI can be almost twice that of WPC (Morr & Ha, 1993). Our RP-HPLC results showed WPI contained about 70.2% ± 1.5% β-lg while WPC contained about 35.7% ± 2.8% β-lg. Therefore 4.5% (w/w) WPI is approximately equivalent to 8.5% (w/w) WPC in terms of β-lg content. Additionally, as the WPC content in the model emulsion is within the range of gelation concentration, it has a strong tendency to gel upon heating (Havea et al., 2002). The results confirmed the role of calcium in the heat stability of whey protein emulsions of high protein content. The gel-like texture observed in the heated 8.5% (w/w) whey-protein-stabilised emulsion fitted with a model in which interactions occur between all adsorbed and non-adsorbed proteins.

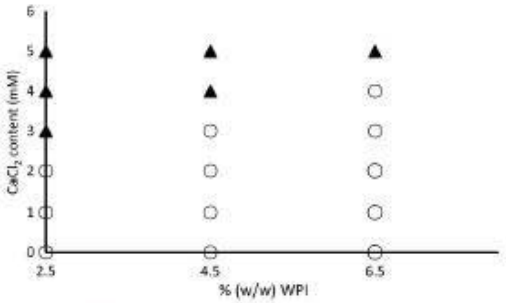

Fig. 4. Heat stability map of WPI-stabilised 10% (w/w) oil-in-water emulsions (pH 6.8–7.0) with different $CaCl_2$ contents after heating for 10 min at 90 °C. Depending on the visual appearance and measured viscosity after heating, samples may be assigned to different categories: ○, stable; ▲, unstable (formed precipitate or gel-like paste).

3.2. Model emulsions with no interactions between adsorbed proteins but with protein–protein interactions in the continuous phase

Na–CN-stabilised and Tween-20-stabilised droplets were considered not to be susceptible to heat treatment. It has been shown that Na–CN-stabilised emulsion droplets are very heat stable (Srinivasan et al., 2002). A number of studies have

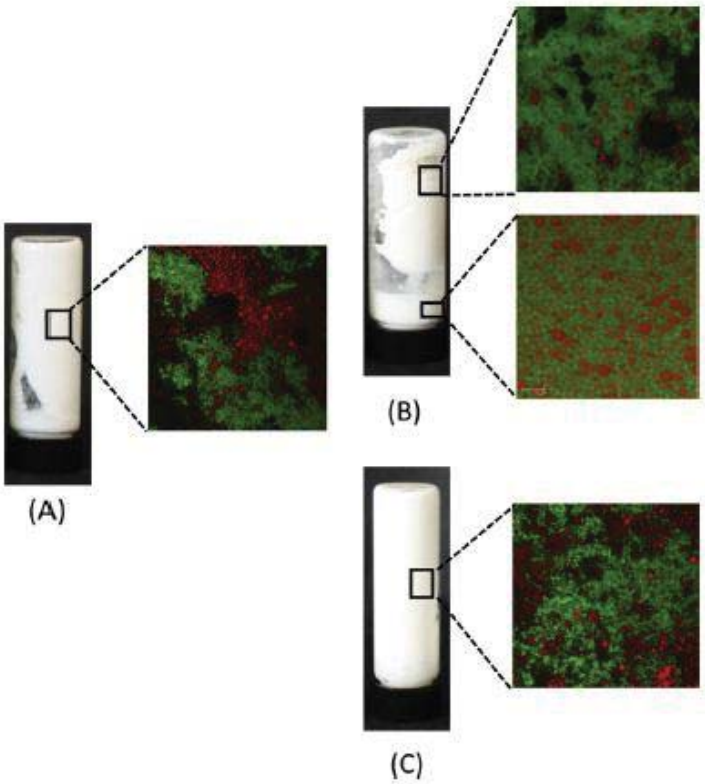

Fig. 3. Visual appearance and microstructure of heated (120 °C, 10 min) model emulsions (8.5% w/w protein, 10% w/w oil): (A) sole WPC-stabilised emulsion; (B) Tween-20-stabilised emulsion containing WPC, with the top image showing the gelled phase and the bottom image showing the serum layer expelled from the gel; (C) Na–CN-stabilised emulsion containing WPC.

Appendix

indicated that caseins, either in their individual form or in their self-assembled form (such as Na–CN), have a stabilizing effect, a so-called chaperone-like activity, against heat-induced whey protein aggregation at neutral pH when present in small amounts (Guyomarc'h, Nono, Nicolai, & Durand, 2009; O'Kennedy & Mounsey, 2006; Yong & Foegeding, 2010). It has been shown that a small amount of low molecular weight surfactant (e.g. Tween 20) would effectively shield the hydrophobic areas of heat-induced globular proteins from interactions (Nikiforidis & Kiosseoglou, 2007). For the model emulsions containing Na–CN-stabilised or Tween-20-stabilised oil droplets, it was estimated that the non-adsorbed Na–CN and Tween 20 were within 0.2–0.3% (w/w). It was expected that there would be little heat-induced flocculation between droplets and non-adsorbed proteins upon heating because of the stabilizing ability of casein and the Tween molecule against extensive heat-induced globular protein aggregation.

The Tween-20-stabilised emulsion containing WPC partially coagulated into a paste-like material following heating and retained a reasonable amount of turbid fluid, which was expelled from the paste. A homogeneous emulsion droplet distribution can be clearly seen in the serum layer of the Tween-20-stabilised emulsion containing WPC (Fig. 3B). Protein aggregates and the gel network can be clearly seen in the gelled phase; trace amounts of droplets can also be seen because they may have been trapped within the whey protein gel network (Fig. 3B). A homogeneous droplet distribution after heating when droplets were coated with Tween 20 was in agreement with the expected results. As hypothesized, the Tween-20-stabilised droplets were not affected by heat and were not displayed by milk proteins from the oil/water interface, since Tween 20 is a non-ionic and a very surface active molecule (Dickinson, 1992). However, intensive heat-induced protein–protein aggregation still occurred in presence of Tween 20. It has been reported that Tween 20 can stabilise globular-protein-stabilised oil droplets and globular protein against heat (Nikiforidis & Kiosseoglou, 2007; Tran Le et al., 2011). The high heating temperature or high protein concentration may play a critical role in the aggregation mechanism(s).

The particle size distribution of the turbid liquid layer from the Tween-20-stabilised emulsion containing WPC showed little difference from that of the Tween 20 stock emulsion (Fig. 5) suggesting there were no heat-induced droplet–droplet interaction occurred. The microstructure and particle size results suggest that

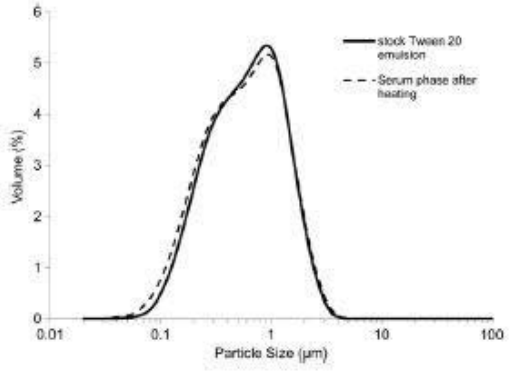

Fig. 5. Droplet size distribution of the serum phase that was expelled from the gel phase in a heated (120 °C, 10 min) Tween-20-stabilised emulsion containing 8.5% (w/w) WPC.

the proposed phenomenon (an emulsion with no droplet–droplet interactions but with protein–protein interactions in the continuous phase) may have occurred in the heated Tween-20-stabilised emulsion containing WPC. These results also agree with those of Chen and Dickinson (1998), who found that Tween-20-coated oil droplets neither were trapped within the three-dimensional whey-protein-stabilised emulsion gel matrix nor contributed to the gel strength of the emulsion. The Tween-20-coated droplets can be considered as "inactive" fillers in protein gel network (Corredig, Ion Titapiccolo, Gaygadzhiev, & Alexander, 2011).

The Na–CN-stabilised emulsion containing WPC formed a paste-like texture during heating, with the confocal micrographs showing a similar microstructure to that of the sole WPC-stabilised emulsion (Fig. 3A and C). This result was contrary to the expectation that the Na–CN would have governed the steric-stabilizing effect on heat-induced droplet–droplet and droplet–protein interactions. The interaction of Na–CN-stabilised droplets with the gel network may have been due to the high mineral content of the WPC powder, especially the presence of excess free ionic calcium (Ca^{2+}) [~8 mM in 8.0% (w/w) WPC]. The binding of Ca^{2+} to caseins will reduce the thickness of the adsorbed casein at the interface and will diminish steric repulsion by causing partial collapse of the casein tails (Hemar & Horne, 1998; Parkinson & Dickinson, 2007). It was shown recently that, after the addition of 10 mM $CaCl_2$ to a β-casein/β-lg dispersion at a 1:5 protein concentration ratio, β-casein lost its chaperone-like stabilizing effect against whey protein aggregation completely (Kehoe & Foegeding, 2011). Therefore, the Na–CN-stabilised droplets may interact with denatured whey proteins in the continuous phase because of the weakened steric repulsion.

Different amounts of EDTA (5, 10, 15 and 20 mM) were added to determine whether gelation still occurred in an Na–CN-stabilised emulsion containing WPC. All of the emulsions heated at 120 °C formed paste-like gels within 2 min. This was consistent with Keowmaneechai and McClements's study (2006), which suggested that heat-induced coagulation/gelation occurred in whey protein emulsions regardless of the addition of EDTA at high temperatures.

Exchange reactions between whey proteins and caseins at the oil–water interface could occur during heating when whey proteins are in excess (Dalgleish et al., 2002). β-Lg will preferentially displace α_{S1}- and β-caseins from the oil–water interface whereas α-lactalbumin adsorbs to the casein-stabilised droplet surface rather than displacing the other proteins (Dalgleish et al., 2002). This surface change may increase the tendency for the formation of disulphide-mediated polymers, which was expected to occur in the Na–CN-stabilised emulsion containing WPC during heating. Fig. 6 shows the SDS-PAGE patterns of the interfacial proteins of unheated and heated Na–CN-stabilised emulsions containing WPC. An increased amount of whey proteins was present at the oil–water interface even before heat treatment. Some disulphide-cross-linked whey proteins formed upon heating as the whey protein bands became denser in the presence of a dissociating agent (Fig. 6B). The emulsion droplets co-adsorbed by caseins and whey proteins may have participated as interacting particles in the presence of calcium during heating. As exchange interactions become more extensive at higher temperature, the droplets behave more like whey-protein-coated droplets. This may increase the tendency for heat-induced droplet collision and eventually the droplets become involved in the formation of the protein gel matrix. This result indicates that the exchange interactions between whey proteins and non-micellar caseins and the heating temperature are crucial in the heat-induced coagulation of an Na–CN-stabilised emulsion containing WPC.

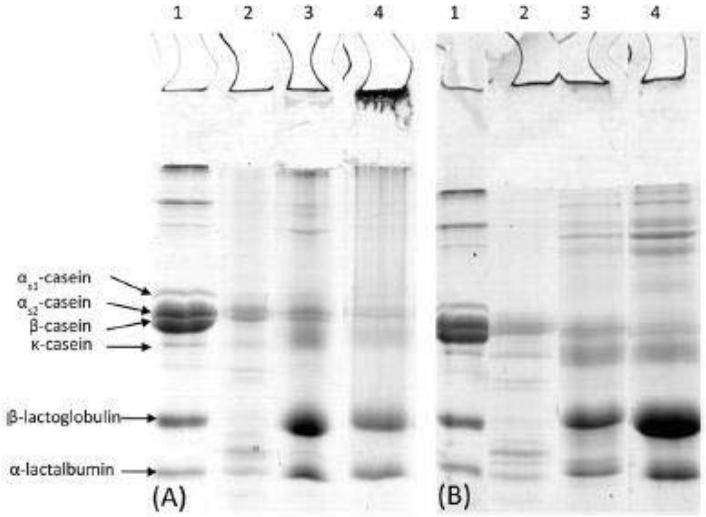

Fig. 6. SDS-PAGE patterns of the interfacial proteins (A) under non-reduced conditions and (B) under reduced conditions (β-mercaptoethanol was added). Lane 1: skim milk standard; lane 2: unheated Na–CN stock emulsion; lane 3: unheated Na–CN-stabilised WPC emulsion; lane 4: heated Na–CN-stabilised WPC emulsion. The heated emulsion was collected before extensive coagulation occurred.

3.3. *Model emulsions with no interactions between non-adsorbed proteins but with droplet–droplet interactions*

In previous studies, the creaming stability of Na–CN-stabilised emulsions has been found to be sensitive to the oil-to-protein ratio. At low oil-to-protein ratios, the creaming stability reduces because of depletion flocculation of emulsion droplets by the excess non-adsorbed caseinate particles. The creaming stability increases again at very high protein concentration, because the higher initial viscosity governed by a weak gel network helps to reduce the flocculation rate of the oil droplets (Dickinson, 1999; Dickinson & Golding, 1997a; Surh, 2009).

Emulsion separation was visually observed in the Na–CN-stabilised and Tween-20-stabilised emulsions containing MPC-I and MPC-II, regardless of heat treatment. This was probably caused by depletion flocculation because there was no change in the droplet size distribution. We confirmed the depletion phenomenon using Turbiscan, rheology and microscopy. The ΔBS (%) of the unheated and heated model emulsions over a 6-day period is shown in Fig. 7. It can be seen that the stock Na–CN emulsion showed a small change (<5%) in *BS* from time zero and displayed gravitational creaming that followed Stokes' law (Fig. 7A). The sole Na–CN-stabilised emulsion and the Na–CN-stabilised and Tween-20-stabilised emulsions containing MPC-I and MPC-II appeared to have large variations (>10%) in *BS* from time zero. These samples displayed sharp changes in *BS* (%) after 1 day and the values reached a plateau at up to 144 h (Fig. 7). The emulsions containing MPC-II showed a greater extent of separation than those containing MPC-I. The heated emulsions, which also underwent depletion flocculation, showed consistently smaller changes in ΔBS (%) than the unheated emulsions, suggesting that fewer droplets were depleted.

Fig. 8 shows confocal micrographs of model emulsions before and after heat treatment. The Na–CN-stabilised and Tween-20-stabilised emulsions containing MPC-I and MPC-II, showed a certain degree of droplet flocculation regardless of the heat treatment. The visual appearances of Na–CN-stabilised and Tween-20-stabilised emulsions containing 1–8% (w/w) MPC-I in the continuous phase are shown in Fig. 9. Gradual creaming was seen with increased protein concentration in the continuous phase. This indicates that the depletion flocculation may have been dependent on the bulk protein volume fraction. It is interesting to note that the casein micelles present in MPC-I and MPC-II appeared to be different. TEM images provided more detailed microstructure information on the dispersed and continuous phases of the model emulsions (Fig. 10). Casein micelles with more compact structure were seen in MPC-I whereas some casein micelles with more swollen structure were seen in MPC-II, suggesting that MPC-II contained more polydispersed casein micelles.

The shear flow rheology of the unheated model emulsions is shown in Fig. 11A. The sole Na–CN-stabilised emulsion exhibited slight shear-thinning behaviour, with n values close to 1. The Na–CN-stabilised and Tween-20-stabilised emulsions containing MPC-I and MPC-II, also showed shear-thinning flow behaviour. The apparent viscosity decreased with increasing shear rate, which was confirmed by the n values (<1). The flocculated droplets would occupy a greater effective volume than the sum of the individual droplet volumes; this would increase the effective volume fraction of the dispersed phase and therefore increase the low shear viscosity. At high shear rates, the breakup of flocculated droplets/clusters and the release of the trapped continuous phase resulted in Newtonian behaviour. Fig. 11B shows the marked effect of droplet–droplet interactions in Na–CN-stabilised emulsions in the presence of casein micelles at high volume fractions of oil. The droplet network induced by depletion flocculation contributes to the low shear viscosities (Dickinson & Golding, 1997b). The heat treatment of the depletion-flocculated emulsions had little effect on the viscosity and flow behaviour ($p > 0.05$).

The rate of depletion flocculation was expected to be low in an emulsion containing casein micelles, because the casein micelles in MPC and SMP have greater molecular size in the bulk phase than the optimum (Euston & Hirst, 1999). Although the optimum caseinate size to cause depletion flocculation in a casein-stabilised emulsion has been determined to be around 20 nm

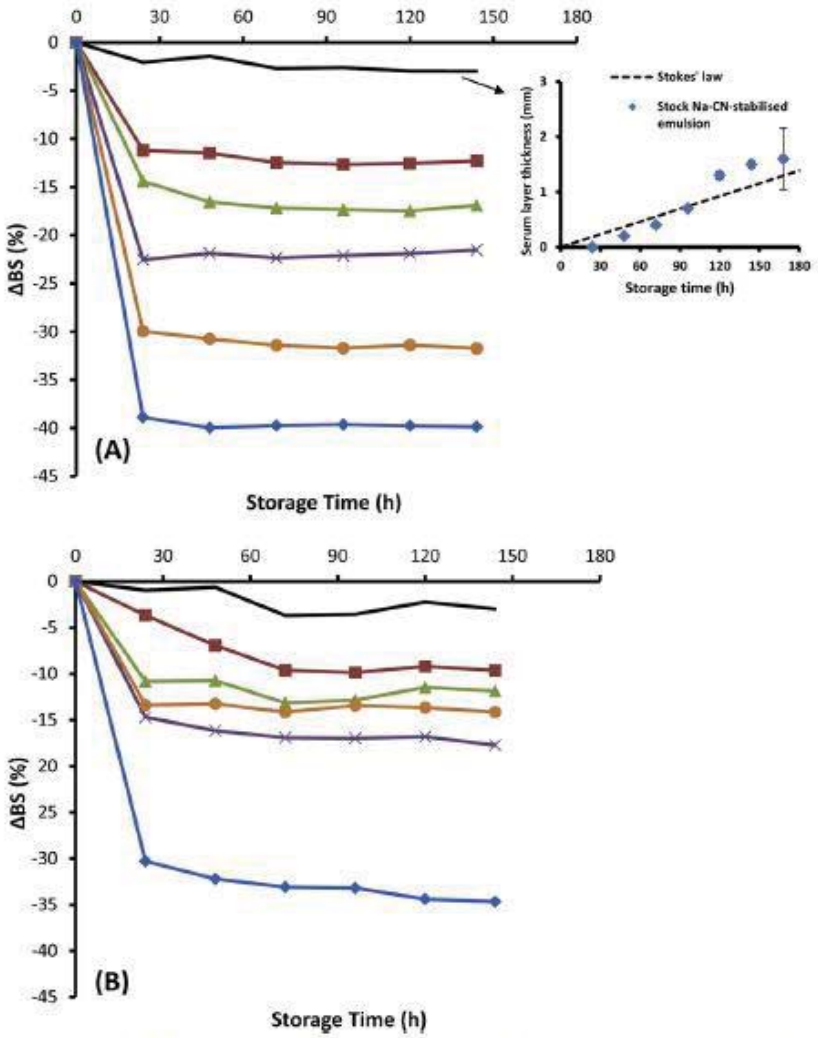

Fig. 7. Variation in backscattering expressed as ΔBS (%) of (A) unheated model emulsions. In set: Variation in serum layer thickness of stock Na–CN emulsion during storage. (B) heated (120 °C, 10 min) model emulsions (8.5% w/w protein, 10% w/w oil) monitored over 144 h at 20 °C for: a stock Na–CN emulsion (solid line); a sole Na–CN-stabilised emulsion (■); an Na–CN-stabilised emulsion containing MPC-I (▲); an Na–CN-stabilised emulsion containing MPC-II (×); a Tween-20-stabilised emulsion containing MPC-I (●); a Tween-20-stabilised emulsion containing MPC-II (♦).

in radius (Radford & Dickinson, 2004), depletion flocculation could occur in a dairy emulsion system containing Na–CN-stabilised emulsion droplets and casein micelles (ten Grotenhuis, Tuinier, & de Kruif, 2003).The polydispersity of the casein particles needs to be considered because casein nanoparticles/micelles have mean diameters in the range 40–200 nm (Lucey, Srinivasan, Singh, & Munro, 2000). Depletion flocculation occurs if the ratio between the sizes of colloidal and non-adsorbed particles exceeds 3:1 (Grotenhuis, Tuinier, & de Kruif, 2003). In the presence of a high concentration of non-adsorbed casein micelles, it is possibly that oil droplets with diameters in the range 0.4–2 μm are depleted by casein micelles. It is possible that MPC-II is more polydispersed than MPC-I because it contains more non-micellar casein particles (Ye, 2011); hence more droplets were depleted (Fig. 7).

3.4. Model emulsions with no interactions between adsorbed proteins and no interactions between non-adsorbed proteins in the continuous phase

In our hypothesis, an emulsion with good heat stability and creaming stability can be expected when there are no droplet–droplet and droplet–protein interactions. Thus MPC is used in excess to stabilise the oil droplets (i.e. no bridging flocculation) (Euston & Hirst, 1999; Sharma & Singh, 1999). We also expected the emulsion containing WPH as the continuous phase protein to be heat stable because the degree of hydrolysis of the WPH used in this study was 18.1% (Euston et al., 2001; Singh & Dalgleish, 1998). The emulsion containing WPH will not undergo depletion flocculation because hydrolysed whey proteins are too small to induce depletion interaction (Euston et al., 2001).

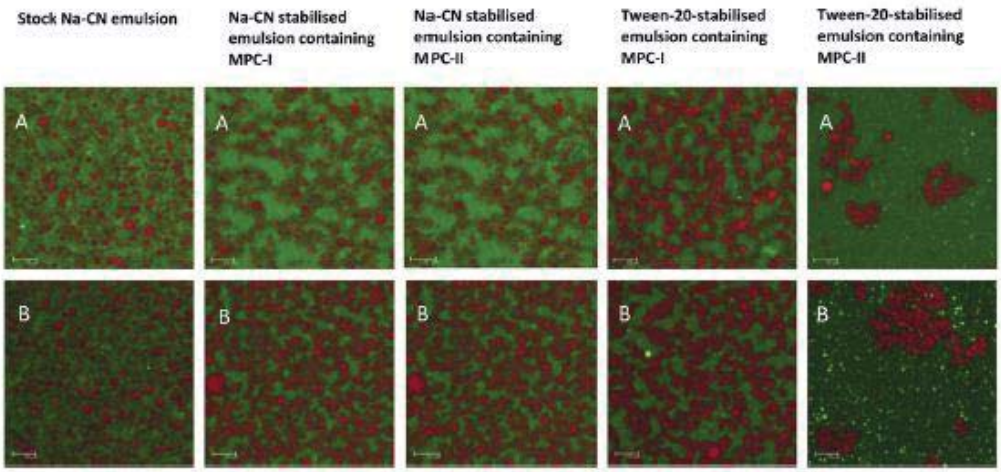

Fig. 8. Confocal micrographs of model emulsions (8.5% w/w protein, 10% w/w oil): (A) unheated emulsion; (B) heated (120 °C, 10 min) emulsion. Scale bar is 10 μm.

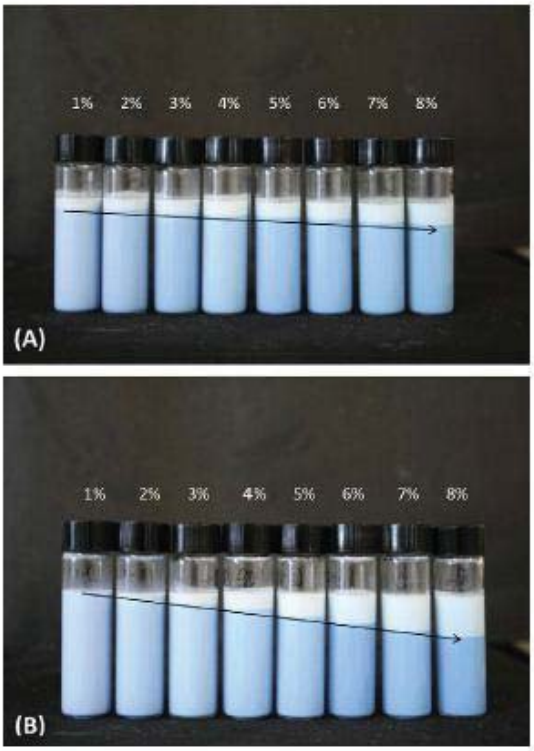

Fig. 9. Creaming profiles (after 24 h of storage at 20 °C) of unheated 10% (w/w) oil-in-water model emulsions containing 1–8% (w/w) MPC-I as the continuous phase and (A) Na–CN-stabilised oil droplets and (B) Tween-20-stabilised oil droplets. The arrow shows the creaming trend.

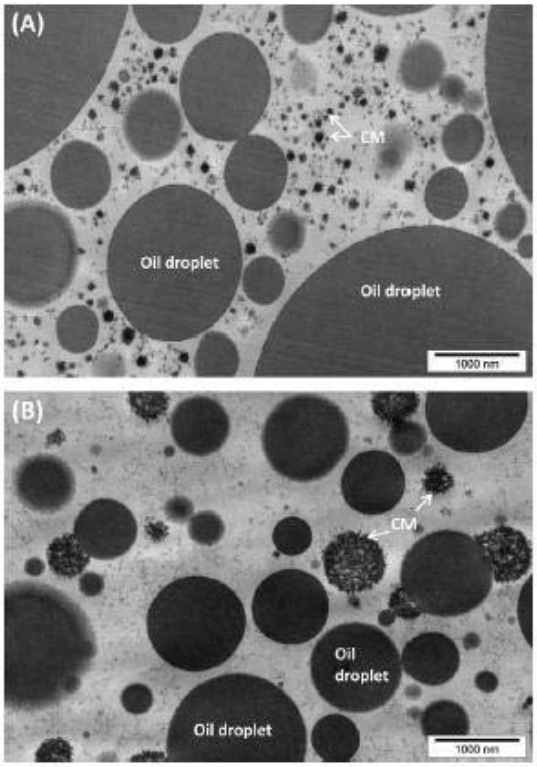

Fig. 10. TEM images of selected heated (120 °C, 10 min) model emulsions: (A) Na–CN-stabilised emulsion containing MPC-I; (B) Na–CN-stabilised emulsion containing MPC-II. The images were captured at 19 000× magnification. Scale bar is 1000 nm. CM – casein micelle.

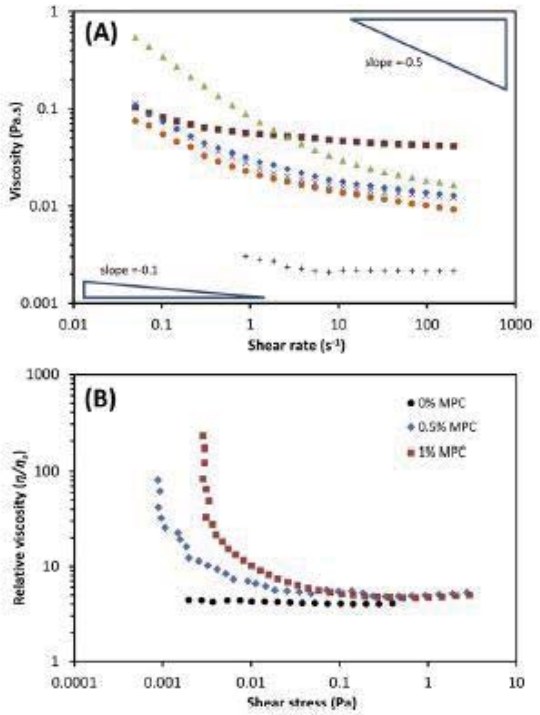

Fig. 11. (A) Flow behaviour of unheated model emulsions: stock Na–CN emulsion (+); sole Na–CN-stabilised emulsion (■); Na–CN-stabilised emulsion containing MPC-I (▲); Na–CN-stabilised emulsion containing MPC-II (×); Tween-20-stabilised emulsion containing MPC-I (●); Tween-20-stabilised emulsion containing MPC-II (♦). (B) Relative viscosity of unheated Na–CN-stabilised 30% (w/w) oil-in-water emulsions containing 0, 0.5 and 1% (w/w) MPC as a function of shear stress at 20 °C. η_0 is the corresponding viscosity of MPC in the continuous phase.

The sole MPC-I-stabilised emulsion and the Na–CN-stabilised emulsion containing WPH showed no sign of heat-induced coagulation and no rapid phase separation during ageing. This result was confirmed by the droplet size distribution, confocal microscopy, shear-flow rheology and Turbiscan data. There was no change in the primary particle size distribution between unheated and heated emulsions. The confocal micrographs showed that the emulsion droplets were homogeneously distributed in the MPC-I-stabilised emulsion and the Na–CN-stabilised emulsion containing WPH (Fig. 12). Interestingly, some very small droplets formed clusters in the heated Na–CN-stabilised emulsion containing WPH, as shown by TEM (Fig. 13). However, the droplet clusters appeared to have little effect on the creaming stability, as studied by Turbiscan. The flow curves of the heated emulsions showed Newtonian-like flow behaviour, which was similar to their corresponding continuous phase viscosity (data not shown).

We also expected the Tween-20-stabilised emulsion containing WPH to be heat stable. Unexpectedly, the emulsion was susceptible to heat-induced droplet coalescence, which eventually led to complete oil and serum separation. We found that as little as 1% (w/w) WPH was able to cause the droplet coalescence. Additionally, this heat-induced droplet coalescence appeared to be temperature dependent. Little change in particle size of Tween-20-stabilised emulsions containing 1% WPH was found after heating for 10 min at 80–110 °C. However, large droplets were formed as a function of time when the emulsion was heated

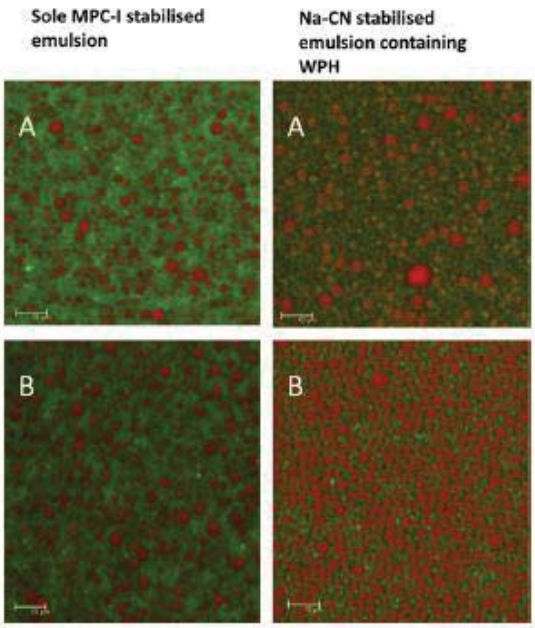

Fig. 12. Confocal micrographs of model emulsions (8.5% w/w protein, 10% w/w oil): (A) unheated emulsion; (B) heated (120 °C, 10 min) emulsion. Scale bar is 10 μm.

at 120 °C, as shown in Fig. 14. When heated beyond the critical heating time, the droplet size increased significantly. Rapid coalescence and oiling-off were observed in lecithin-stabilised emulsions containing WPH (degree of hydrolysis = 27%); the destabilisation was attributed to interfacial competition between surface active peptides of the WPH and the lecithin (Scherze & Muschiolik, 2001). A recent study also reported destabilisation in a Tween-20-stabilised coconut milk oil-in-water emulsion on heating (120 °C, 1 h). The destabilisation was attributed to the prolonged autoclave treatment (Tangsuphoom & Coupland, 2009). In our case, it is possible that some small protein peptides, formed upon heating, with very high surface hydrophobicity could displace a small molecule surfactant such as Tween 20 from the oil surface; however, they are not able to stabilise the emulsion droplets, probably because of poor steric and electrostatic repulsion governed by low molecular weight peptides, and cause destabilisation of the emulsion during heat treatment. This might

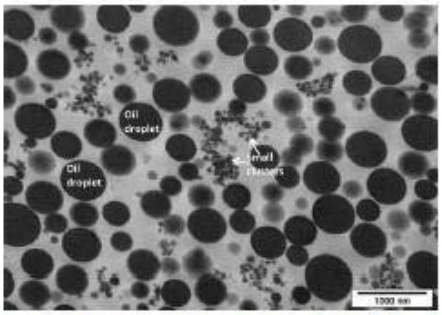

Fig. 13. TEM image of heated (120 °C, 10 min) Na–CN-stabilised emulsion containing WPH. The image was captured at 19 000× magnification. Scale bar is 1000 nm.

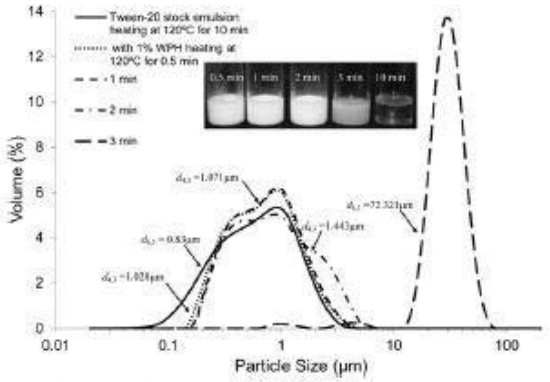

Fig. 14. Particle size distributions of Tween-20-stabilised emulsions (10% w/w oil); control heated at 120 °C for 10 min (solid line); containing 1% (w/w) WPH heated at 120 °C for 0.5 min (dotted line), for 1 min (dashed line), for 2 min (dashed dotted line) and for 3 min (long dashed line).

correspond to the collapse of the Tween-20-stabilised emulsion. A further study of the interaction between WPH and various types of surfactant at the oil–water interface is in progress to probe the destabilisation mechanism.

4. Conclusions

The heat-induced destabilisation of milk-protein-stabilised emulsion systems is influenced by the emulsifier type and the type of protein in the continuous phase. Emulsions stabilised by whey proteins or containing high whey protein concentrations are highly sensitive to calcium content and heat treatment. Non-adsorbed whey proteins are involved not only in the heat-induced destabilisation of whey-protein-rich emulsions, but also in the incorporation of Na–CN-stabilised droplets in the gel network, through heat-exchanged interfacial interaction. In contrast, whey protein peptides are heat stable. However, some active components from hydrolysed whey proteins may have been involved in droplet coalescence at high heating temperatures, depending on the interfacial composition (e.g. Tween 20).

Model emulsions containing relatively high concentrations of micellar or non-micellar caseins were found to be heat stable. However, rapid enhanced creaming, which is associated with the depletion flocculation mechanism, arises in these emulsions. The non-adsorbed protein concentration, the aggregation state and the polydispersity of protein determine the extent of depletion flocculation.

The model systems describe the potential droplet–droplet, protein–protein and droplet–protein interactions using food-grade surfactants and commercial milk protein ingredients. The destabilisation behaviours reported and addressed here have implications for the heat and creaming stabilities of real whey-protein-based and casein-based food emulsion formulations containing high protein content. Although most real food systems contain hydrocolloids and sugars in the continuous phase which can have considerable separate effects on the dispersed and continuous phases, the stability map characterisation approach could be useful for the future design of heat-stable emulsion-based beverages with good creaming stability.

Acknowledgements

The authors gratefully thank the Fonterra Research and Development Centre and the Foundation for Research, Science and Technology for financial support. Graeme Gillies and Sheelagh Hewitt are thanked for their helpful discussions. Michael Loh and Abraham Chawanji are thanked for their assistance with the microscopy work. Claire Woodhall for proofreading the manuscript.

References

Agboola, S. O., Singh, H., Munro, P. A., Dalgleish, D. G., & Singh, A. M. (1998). Stability of emulsions formed using whey protein hydrolysate: effects of lecithin addition and retorting. *Journal of Agricultural and Food Chemistry, 46*, 1814–1819.

Chauvierre, C., Labarre, D., Couvreur, P., & Vauthier, C. (2004). A new approach for the characterization of insoluble amphiphilic copolymers based on their emulsifying properties. *Colloid and Polymer Science, 282*, 1097–1104.

Chen, J., & Dickinson, E. (1998). Viscoelastic properties of protein-stabilized emulsions: effect of protein–surfactant interactions. *Journal of Agricultural and Food Chemistry, 46*, 91–97.

Corredig, M., Ion Titapiccolo, G., Gaygadzhiev, Z., & Alexander, M. (2011). Rennet-induced aggregation of milk containing homogenized fat globules. Effect of interacting and non-interacting fat globules observed using diffusing wave spectroscopy. *International Dairy Journal, 21*, 679–684.

Dalgleish, D. G., Goff, H. D., & Luan, B. (2002). Exchange reactions between whey proteins and caseins in heated soya oil-in-water emulsion systems-behavior of individual proteins. *Food Hydrocolloids, 16*, 295–302.

Demetriades, K., Coupland, J. N., & McClements, D. J. (1997). Physical properties of whey protein stabilized emulsions as related to pH and NaCl. *Journal of Food Science, 62*, 342–347.

Dickinson, E. (1992). *An introduction to food colloids*. Oxford: Oxford University Press.

Dickinson, E. (1997). Properties of emulsions stabilized with milk proteins: overview of some recent developments. *Journal of Dairy Science, 80*, 2607–2619.

Dickinson, E. (1999). Adsorbed protein layers at fluid interfaces: interactions, structure and surface rheology. *Colloids and Surfaces B: Biointerfaces, 15*, 161–176.

Dickinson, E., & Golding, M. (1997a). Depletion flocculation of emulsions containing unadsorbed sodium caseinate. *Food Hydrocolloids, 11*, 13–18.

Dickinson, E., & Golding, M. (1997b). Rheology of sodium caseinate stabilized oil-in-water emulsions. *Journal of Colloid and Interface Science, 191*, 166–176.

Dickinson, E., & Parkinson, E. L. (2004). Heat-induced aggregation of milk protein-stabilized emulsions: sensitivity to processing and composition. *International Dairy Journal, 14*, 635–645.

Dybowska, B. E. (2008). Properties of milk protein concentrate stabilized oil-in-water emulsions. *Journal of Food Engineering, 88*, 507–513.

Elgar, D. F., Norris, C. S., Ayers, J. S., Pritchard, M., Otter, D. E., & Palmano, K. P. (2000). Simultaneous separation and quantitation of the major bovine whey proteins including proteose peptone and caseinomacropeptide by reversed-phase high-performance liquid chromatography on polystyrene–divinylbenzene. *Journal of Chromatography A, 878*, 183–196.

Euston, S. R., Al-Bakkush, A.-A., & Campbell, L. (2009). Comparing the heat stability of soya protein and milk whey protein emulsions. *Food Hydrocolloids, 23*, 2485–2492.

Euston, S. R., Finnigan, S. R., & Hirst, R. L. (2000). Aggregation kinetics of heated whey protein-stabilized emulsions. *Food Hydrocolloids, 14*, 155–161.

Euston, S. R., Finnigan, S. R., & Hirst, R. L. (2001). Heat-induced destabilization of oil-in-water emulsions formed from hydrolyzed whey protein. *Journal of Agricultural and Food Chemistry, 49*, 5576–5583.

Euston, S. R., & Hirst, R. L. (1999). Comparison of the concentration-dependent emulsifying properties of protein products containing aggregated and non-aggregated milk protein. *International Dairy Journal, 9*, 693–701.

Guyomarc'h, F., Nono, M., Nicolai, T., & Durand, D. (2009). Heat-induced aggregation of whey proteins in the presence of κ-casein or sodium caseinate. *Food Hydrocolloids, 23*, 1103–1110.

Havea, P., Singh, H., & Creamer, L. K. (2002). Heat-induced aggregation of whey proteins: comparison of cheese WPC with acid WPC and relevance of mineral composition. *Journal of Agricultural and Food Chemistry, 50*, 4674–4681.

Hemar, Y., & Horne, D. S. (1998). Electrostatic interactions in adsorbed protein layers probed by a sedimentation technique. *Journal of Colloid and Interface Science, 206*, 138–145.

Huck-Iriart, C., Álvarez-Cerimedo, M. S., Candal, R. J., & Herrera, M. L. (2011). Structures and stability of lipid emulsions formulated with sodium caseinate. *Current Opinion in Colloid & Interface Science, 16*, 412–420.

Kehoe, J. J., & Foegeding, E. A. (2011). Interaction between β-casein and whey proteins as a function of pH and salt concentration. *Journal of Agricultural and Food Chemistry, 59*, 349–355.

Keowmaneechai, E., & McClements, D. J. (2006). Influence of EDTA and citrate on thermal stability of whey protein stabilized oil-in-water emulsions containing calcium chloride. *Food Research International, 39*, 230–239.

Kiosseoglou, V., & Nikiforidis, C. V. (2008). Factors affecting the heat-induced physicochemical destabilization of food oil-in-water emulsions. In K. N. Papadopoulos (Ed.), *Food chemistry research developments* (pp. 223–241). New York: Nova Science Publishers.

de Kort, E., Minor, M., Snoeren, T., van Hooijdonk, T., & van der Linden, E. (2012). Effect of calcium chelators on heat coagulation and heat-induced changes of concentrated micellar casein solutions: the role of calcium-ion activity and micellar integrity. *International Dairy Journal, 26*, 112–119.

Appendix

Langton, M., & Hermansson, A. M. (1996). Image analysis of particulate whey protein gels. *Food Hydrocolloids, 10*, 179–191.
Lucey, J. A., Srinivasan, M., Singh, H., & Munro, P. A. (2000). Characterization of commercial and experimental sodium caseinates by multiangle laser light scattering and size-exclusion chromatography. *Journal of Agricultural and Food Chemistry, 48*, 1610–1616.
McClements, D. J. (2005). *Food emulsions: Principles, practices, and techniques* (2nd ed.). Boca Raton, FL: CRC Press.
McSweeney, S. L., Healy, R., & Mulvihill, D. M. (2008). Effect of lecithin and monoglycerides on the heat stability of a model infant formula emulsion. *Food Hydrocolloids, 22*, 888–898.
McSweeney, S. L., Mulvihill, D. M., & O'Callaghan, D. M. (2004). The influence of pH on the heat-induced aggregation of model milk protein ingredient systems and model infant formula emulsions stabilized by milk protein ingredients. *Food Hydrocolloids, 18*, 109–125.
Mengual, O., Meunier, G., Cayré, I., Puech, K., & Snabre, P. (1999). TURBISCAN MA 2000: multiple light scattering measurement for concentrated emulsion and suspension instability analysis. *Talanta, 50*, 445–456.
Morr, C. V., & Ha, E. Y. W. (1993). Whey protein concentrates and isolates: processing and functional properties. *Critical Reviews in Food Science and Nutrition, 33*, 431–476.
Nikiforidis, C. V., & Kiosseoglou, V. (2007). The role of Tween in inhibiting heat-induced destabilization of yolk-based emulsions. *Food Hydrocolloids, 21*, 1310–1318.
O'Kennedy, B. T., & Mounsey, J. S. (2006). Control of heat-induced aggregation of whey proteins using casein. *Journal of Agricultural and Food Chemistry, 54*, 5637–5642.
Parkinson, E. L., & Dickinson, E. (2007). Synergistic stabilization of heat-treated emulsions containing mixtures of milk proteins. *International Dairy Journal, 17*, 95–103.
Radford, S. J., & Dickinson, E. (2004). Depletion flocculation of caseinate-stabilised emulsions: what is the optimum size of the non-adsorbed protein nano-particles? *Colloids and Surfaces A: Physicochemical and Engineering Aspects, 238*, 71–81.
Radford, S. J., Dickinson, E., & Golding, M. (2004). Stability and rheology of emulsions containing sodium caseinate: combined effects of ionic calcium and alcohol. *Journal of Colloid and Interface Science, 274*, 673–686.
Raikos, V. (2010). Effect of heat treatment on milk protein functionality at emulsion interfaces. A review. *Food Hydrocolloids, 24*, 259–265.
Riou, E., Havea, P., McCarthy, O., Watkinson, P., & Singh, H. (2011). Behavior of protein in the presence of calcium during heating of whey protein concentrate solutions. *Journal of Agricultural and Food Chemistry, 59*, 13156–13164.
Scherze, I., & Muschiolik, G. (2001). Effects of various whey protein hydrolysates on the emulsifying and surface properties of hydrolysed lecithin. *Colloids and Surfaces B: Biointerfaces, 21*, 107–117.
Segall, K. I., & Goff, H. D. (1999). Influence of adsorbed milk protein type and surface concentration on the quiescent and shear stability of butteroil emulsions. *International Dairy Journal, 9*, 683–691.
Sharma, R., & Singh, H. (1999). Heat stability of recombined milk system as influenced by the composition of fat globule surface layers. *Milchwissenschaft, 54*, 193–196.
Singh, A. M., & Dalgleish, D. G. (1998). The emulsifying properties of hydrolyzates of whey proteins. *Journal of Dairy Science, 81*, 918–924.
Sliwinski, E. L., Roubos, P. J., Zoet, F. D., Boekel, M. A. J. S. v., & Wouters, J. T. M. (2003). Effects of heat on physicochemical properties of whey protein-stabilised emulsions. *Colloids and Surfaces B: Biointerfaces, 31*, 231–242.
Srinivasan, M., Singh, H., & Munro, P. A. (2002). Formation and stability of sodium caseinate emulsions: influence of retorting (121 °C for 15 min) before or after emulsification. *Food Hydrocolloids, 16*, 153–160.
Surh, J. H. (2009). Comparison of emulsion-stabilizing property between sodicum caeinate and whey protein concentrate: susceptibility to changes in protein concentration and pH. *Food Science and Biotechnology, 18*, 610–617.
Tangsuphoom, N., & Coupland, J. N. (2009). Effect of thermal treatments on the properties of coconut milk emulsions prepared with surface-active stabilizers. *Food Hydrocolloids, 23*, 1792–1800.
ten Grotenhuis, E., Tuinier, R., & de Kruif, C. G. (2003). Phase stability of concentrated dairy products. *Journal of Dairy Science, 86*, 764–769.
Tran Le, T., Sabatino, P., Heyman, B., Kasinos, M., Dinh, H. H., Dewettinck, K., et al. (2011). Improved heat stability by whey protein-surfactant interaction. *Food Hydrocolloids, 25*, 594–603.
Ye, A. (2008). Interfacial composition and stability of emulsions made with mixtures of commercial sodium caseinate and whey protein concentrate. *Food Chemistry, 110*, 946–952.
Ye, A. (2011). Functional properties of milk protein concentrates: emulsifying properties, adsorption and stability of emulsions. *International Dairy Journal, 21*, 14–20.
Yong, Y. H., & Foegeding, E. A. (2010). Caseins: utilizing molecular chaperone properties to control protein aggregation in foods. *Journal of Agricultural and Food Chemistry, 58*, 685–693.

Paper Two

(This published work is from Chapter 5)

Appendix

Food Hydrocolloids 36 (2014) 245–255

Contents lists available at ScienceDirect

Food Hydrocolloids

journal homepage: www.elsevier.com/locate/foodhyd

Physical stability, microstructure and rheology of sodium-caseinate-stabilized emulsions as influenced by protein concentration and non-adsorbing polysaccharides

Yichao Liang [a,b], Graeme Gillies [a,*], Hasmukh Patel [c], Lara Matia-Merino [b], Aiqian Ye [d], Matt Golding [b,d]

[a] Fonterra Research and Development Centre, Private Bag 11 029, Palmerston North 4442, New Zealand
[b] Institute of Food, Nutrition and Human Health, Massey University, Private Bag 11 222, Palmerston North 4442, New Zealand
[c] Dairy Science Department, South Dakota State University, Box 2104, Brookings, SD 57007, USA
[d] Riddet Institute, Massey University, Private Bag 11 222, Palmerston North 4442, New Zealand

ARTICLE INFO

Article history:
Received 3 April 2013
Accepted 11 October 2013

Keywords:
Sodium caseinate
Xanthan gum
Maltodextrin
Depletion flocculation
Stability
Rheology

ABSTRACT

We explored the stability and rheological properties of 30% oil-in-water emulsions stabilized with sodium caseinate (1–10% w/w). The dynamics of the formation of a transient droplet network were investigated using microstructure, rheology and creaming. The behaviour was classified into two types of depletion-flocculated caseinate emulsions: (1) emulsions with intermediate caseinate concentrations (1.5–4%) displayed rapid phase separation because of compaction of the flocculated networks; (2) emulsions with high caseinate concentrations (5–10%) displayed increased creaming stability, because the higher continuous phase concentration contributed to retarded formation of the viscous transient droplet network with stronger attractions. Small deformation rheology showed that the development of a transient droplet network depended markedly on the caseinate concentration. We distinguished between the contributions of the continuous phase viscosity and the depletion force by investigating the influence of maltodextrin and xanthan gum on the stability and rheology of 1.5% caseinate emulsions. Surprisingly, the droplet–droplet interactions were weakened by the addition of maltodextrin, and the stabilizing mechanism differed from the prediction that high zero shear viscosity is the dominant factor in preventing phase separation of a depletion-flocculated emulsion. We attributed the change in the depletion force to the change in caseinate particle size; a small change in caseinate size could have changed the depletion interaction potential moderately. Furthermore, the droplet rearrangements within the flocculated network played an important role in the stability of the emulsions, and were possibly influenced by both the strength of the depletion force and the continuous phase viscosity at high caseinate concentrations. Both depletion force and continuous phase viscosity increased with the addition of xanthan gum. The phase separation kinetics and the restabilization mechanisms were analogous to those of the caseinate system.

1. Introduction

Oil-in-water emulsions are an important basis of many food, cosmetic and nutraceutical products. For most food emulsions, long term physical stability is critical, with coalescence, flocculation and creaming being the main reasons for instability. Creaming has a detrimental effect on the quality of food emulsions as an emulsion tends to separate into a droplet-rich cream layer and a clarified layer over time, reducing its visual appearance and mouthfeel (McClements, 2005). Creaming occurs when gravitational separation outweighs the diffusion of droplets. For a typical oil with a density around 0.9 g/mL, creaming can be expected when the droplet diameter exceeds 1 μm (Dickinson, 1992). The creaming rate may be changed by the density of the dispersed phase and the viscosity of the continuous phase, but in the latter case the propensity to separate gravitationally will always remain (Dickinson, 1992). Creaming rates of isolated droplets are calculable from by combining Stokes' law with the gravitational or buoyancy force. In more concentrated systems the upward flow of droplets is hindered by the consequent downward flow of the continuous phase. There

* Corresponding author. Tel.: +64 6 350 4649x64573; fax: +64 6 356 1476.
E-mail address: graeme.gillies@fonterra.com (G. Gillies).

0268-005X/$ – see front matter © 2013 Elsevier Ltd. All rights reserved.
http://dx.doi.org/10.1016/j.foodhyd.2013.10.006

Appendix

are several approaches for predicting sedimentation under such conditions, in this article we use the following equation from McClements (2005),

$$v = \frac{2a^2\Delta\rho g}{9\eta_s}(1-\phi/\phi_{max})^{6.6\phi_{max}} \quad (1)$$

Where v is the velocity, a is the droplet radius, $\Delta\rho$ is difference in density between the two phases, g is acceleration by gravity, η_s is the viscosity of the continuous phase ϕ is the volume fraction of the dispersed phase, while $\phi_{max} \approx 0.71$ is the maximum packing density for a polydisperse emulsion. Droplet flocculation can also influence coalescence and creaming. Aggregated or flocculated droplets tend to cream faster because flocs have a larger effective size than individual droplets. Flocculation occurs when there is insufficient kinetic boundary to prevent the close approach of droplets (Dickinson, 2010). Nevertheless, creaming may be prevented when a firm, percolating droplet network is formed. Such networks are formed when the positions of the droplets are fixed by a strong force (McClements, 2005).

Many food emulsions contain mixtures of proteins and polysaccharides, which have marked impacts on the emulsion structure and stability. Sodium caseinate is a well-known emulsifier that is used for its excellent heat stability and emulsifying properties (Dickinson, 1999; Srinivasan, Singh, & Munro, 2002). Sodium caseinate consists of phosphorylated proteins (α_{s1}-, α_{s2}-, β- and κ-caseins), which stabilize oil droplets against coalescence through electrostatic and steric repulsion (Dickinson, 1999; Leman & Kinsella, 1989). The stability of oil-in-water emulsions stabilized by caseinate at neutral pH has been investigated extensively (Álvarez Cerimedo, Iriart, Candal, & Herrera, 2010; Dickinson & Golding, 1997a, 1997b; Dickinson, Golding, & Povey, 1997; ten Grotenhuis, Tuinier, & de Kruif, 2003; Radford & Dickinson, 2004; Srinivasan et al., 2002). Caseinate adsorbs at the oil/water interface with a maximum surface coverage of ~3 mg/m^2 (Srinivasan et al., 2002). In addition, caseinate self-assembles into small aggregates (~10 nm in radius) that have a small weight fraction of large particles with a hydrodynamic radius of ~65 nm (HadjSadok, Pitkowski, Nicolai, Benyahia, & Moulai-Mostefa, 2008). These self-assemblies are now referred to as casein sub-micelles or alternatively nano-particles; they induce depletion flocculation of oil droplets depending on the droplet and protein diameters and the non-adsorbed caseinate concentration.

Many hydrocolloids are used to stabilize the structure of food emulsions; their thickening/gelling abilities mean that they will form weak gel-like entangled biopolymer networks at low concentrations (Dickinson, 2009). Polysaccharides such as xanthan gum and maltodextrin are frequently used in emulsions to inhibit gravity-induced creaming and/or phase separation by increasing the low shear viscosity. Unfortunately, above a certain critical polysaccharide concentration, phase separation occurs because of a depletion effect (Aben, Holtze, Tadros, & Schurtenberger, 2012; Dickinson, Semenova, Antipova, & Pelan, 1998; Hemar, Tamehana, Munro, & Singh, 2001; Parker, Gunning, Ng, & Robins, 1995; Sun, Gunasekaran, & Richards, 2007; Tuinier & de Kruif, 1999).

Depletion flocculation tends to occur in droplet/polymer mixtures with a marked size difference between the populations and at above a critical non-adsorbed polymer concentration. The smaller population is typically a non-adsorbing polymer, but in this study is sodium caseinate nano-particles, and the larger population is oil droplets. Depletion interaction between two oil droplets occurs when the gap between the two surfaces becomes smaller than the diameter of the caseinate nano-particles; the nano-particles are sterically excluded from the interstitial space, increasing the concentration of smaller particles in the bulk solution. This imbalance inosmotic pressure results in an effective attraction between larger particles (Asakura & Oosawa, 1954; Vrij, 1976). At sufficiently high concentrations of oil, the depletion attraction will create a droplet network that spans the entire sample volume; this network can result in partial restabilization of the emulsion (Aben et al., 2012; Dickinson, 1999). When the strength of the depletion interaction is comparable with the thermal energy, droplets fluctuate in and out of the attractive zone of other droplets allowing the microstructural network to rearrange (Starrs, Poon, Hibberd, & Robins, 2002) and eventually collapses under the influence of gravity (Aben et al., 2012; Dickinson & Golding, 1997b; Hemar et al., 2001; Lu et al., 2008; Moschakis, Murray, & Dickinson, 2005; Teece, Faers, & Bartlett, 2011). The actual rate at a network evolves should depend on the time for a droplet to escape from the attractive zone of neighbouring particles. The concept of the escape time was put forward by Kramers (1940), and while an analytical solution to the escape time for depletion interactions is not known to the authors, the escape time for triangle shaped interaction – distance profiles suggest a following form could apply (Buscall et al., 2009):

$$\tau = \tau_0/e^{\frac{-W}{kT}} = \frac{\pi\eta_s a\Delta^2}{k_B T}e^{\frac{zW}{k_B T}} \quad (2)$$

Here τ is a time that should scale with the escape time, τ_0 is the time required for droplets to freely diffuse across $\langle\Delta^2\rangle$, where Δ is the range of the depletion potential. The triangle brackets remind the reader that displacement by diffusion is always the mean-squared displacement. W is the interaction potential, z is the number of neighbours the particle is attached to and k_BT is the thermal energy. Examining equation (2) reveals that judicious choice of three key parameters, range of the interaction, viscosity of the continuous phase and interaction potential can change a shelf life of a product from hours to months.

The effect of the continuous phase viscosity on the stability of caseinate-stabilized emulsions at higher protein concentration has received little attention. Immediate depletion flocculation can be prevented by either the apparent yield stress or the high viscosity of solutions of polysaccharide (van Gruijthuijsen, Herle, Tuinier, Schurtenberger, & Stradner, 2012; Vélez, Fernández, Muñoz, Williams, & English, 2002; Ye, Hemar, & Singh, 2004). A similar viscosity effect is observed in emulsions containing high concentrations of β-lactoglobulin (Blijdenstein, van Vliet, van der Linden, & van Aken, 2003). Thus, increasing the non-adsorbed caseinate concentration in an emulsion is expected to have two effects. (1) The depletion energy increases, which may lead to a firmer droplet network. (2) The continuous phase viscosity increases (Carr, Munro, & Campanella, 2002; Thomar, Durand, Benyahia, & Nicolai, 2012), with the increase being more pronounced above a critical concentration (~10% w/w) because of close packing of the caseinate particles (Pitkowski, Durand, & Nicolai, 2008). Furthermore, an increased concentration of caseinate may change its molecular conformation towards a more elongated rod-like shape (Farrer & Lips, 1999). It is possible that the properties of the continuous phase at high caseinate concentrations influence the dynamics of the formation of a transient emulsion network and its subsequent rearrangement rate. Therefore, it is important to understand the non-equilibrium behaviour of caseinate emulsion systems over a wider range of protein concentrations.

It is hypothesized that the inhibition of phase separation at elevated caseinate concentrations may be due to either a retardation of the dynamics of droplet–droplet interactions (because of viscous effects) or an increase in the depletion interaction potential, thereby strengthening the droplet network. To test the validity of the hypothesis, we used two highly contrasting viscosity-controlling hydrocolloids, xanthan gum and maltodextrin, to

Appendix

assess the stabilizing mechanisms. Xanthan gum induces depletion flocculation and confers high viscosity at low concentration (Moschakis et al., 2005). This investigation was based on co-soluble concentrations identified by HadjSadok, Moulai-Mostefa, and Rebiha (2010), namely sodium caseinate concentrations below 1.27% and xanthan gum concentration below 0.5%. Maltodextrin [dextrose equivalent (DE) ~ 2] levels were also adapted from previously published co-soluble concentrations that would confer high continuous phase viscosities (Akhtar, Murray, & Dickinson, 2006). In a number of studies, mixtures of polymers have been homogenized to yield model emulsions (Álvarez Cerimedo et al., 2010; Dokic-Baucal, Dokic, & Jakovljevic, 2004; Hemar et al., 2001; Long et al., 2012, 2013; Perrechil & Cunha, 2010). For the experiments reported in this study, we made a stock caseinate emulsion and diluted it to achieve different compositions while maintaining the same droplet size, surface area and surface load. The interrelations among the extent of depletion flocculation, the formation of the droplet network and its structural rearrangement and the caseinate concentration are discussed in this study.

2. Materials and methods

2.1. Materials

Sodium caseinate 180 (Na-CN) was obtained from Fonterra Co-operative Group Ltd, Auckland, New Zealand. Maltodextrin (Glucidex® 2) was purchased from Roquette, France. Xanthan gum (Grindsted® Xanthan 80) was obtained from DuPont-Danisco (Vernon, TX, USA). Bulk corn oil was purchased from Davis Trading Co., Palmerston North, New Zealand. All chemicals used were of analytical grade, obtained from either BDH Chemicals (BDH Ltd, Poole, England) or Sigma Chemical Co. (St Louis, MO, USA) unless otherwise specified. Milli-Q water (deionized water from a Milli-Q plus R system, Millipore, Bedford, MA, USA) was used for the preparation of the dispersions.

2.2. Preparation of model emulsions

Na-CN (3.0% w/w) was reconstituted in Milli-Q water at 50 °C for 60 min. Corn oil (60% w/w) was mixed with the protein solution. The mixture was then pre-homogenized at 24 000 rev/min for 2 min using an Ultra-Turrax T25 (IKA®-Werke GmbH & Co. KG, Staufen, Germany) to form a coarse emulsion, which was heated to 70 °C and homogenized by three passes through a high pressure homogenizer (type Panda, Niro Soavi, Parma, Italy) at 20 MPa (first stage) and 4 MPa (second stage). The caseinate in the stock emulsion (3% Na-CN and 60% oil) was distributed at the oil/water interface and in the solution. Stock solutions of 2% xanthan gum (xanthan) and 40% maltodextrin were prepared. Xanthan powder was dissolved in Milli-Q water at 70 °C for 2 h while stirring at 500 rev/min. Known amounts of xanthan or maltodextrin were mixed with the stock Na-CN emulsion at a 1:1 mass ratio to yield 30% oil-in-water emulsions containing 0.01–0.2% (w/w) xanthan or 5–20% (w/w) maltodextrin. The maltodextrin concentrations were outside the range for inducing depletion flocculation (Akhtar et al., 2006) and maltodextrin did not result in destabilization of the emulsions under the conditions used in this study. Sodium azide (0.02% w/w) was added to the emulsion samples as an antimicrobial agent. All emulsions were stored at 4 °C overnight until further use. The emulsion pH was 6.8 ± 0.04 and was regulated with occasional addition of 1 M NaOH. This variation in pH due to protein concentration effect is not expected to impact on the stability of the caseinate emulsions. Each model emulsion was prepared at least in triplicate. Throughout the colour version of this article, blue is used to represent caseinate emulsions without polysaccharides, red indicates the addition of xanthan and green indicates the addition of maltodextrin. In this article the concentration of polysaccharide and caseinate is reported on a mass basis relative to the entire emulsion and not the concentration in the aqueous phase. Aqueous concentrations are given in Tables 1 and 2.

2.3. Particle size determination

The volume weighted size distribution of the model emulsions was measured by static light scattering using a Malvern Mastersizer Hydro 2000S (Malvern Instruments Ltd, Malvern, Worcestershire, UK). The measurements were carried out using procedures described previously (Liang, Patel, Matia-Merino, Ye, & Golding, 2013). This approach measures the primary droplet size since the model emulsions are stable against coalescence and the procedure involves a dilution step that eliminates any depletion forces that may hold aggregates together.

2.4. Calculation and application of depletion interaction potential

We used a radius-dependent depletion interaction combined with a Boltzmann partition as an ad-hoc estimate for the fraction of freely dispersed droplets with respect to the droplets in the collapsing network. Using data from a histogram of droplet diameters, we calculated a surface area of 7.45 m^2/mL oil. Then, using an adsorption density of 3 mg/m^2, the concentration of caseinate remaining in the continuous phase, $C_{non\text{-}ad}$, was established (Table 1). The depletion interaction, W, was calculated from $W = -\Pi V$, where Π is the osmotic pressure and V is the volume of overlapping depleted layers; this attractive force is conventionally negative. The osmotic pressure was calculated from an expansion of van't Hoff's law, which accounts for the size of the caseinate nanoparticle (Radford & Dickinson, 2004).

$$\Pi = \frac{C_{non-ad} N_A}{M} k_B T \left(1 + \frac{C_{non-ad}}{\rho}\right) \quad (3)$$

N_A is the Avogadro number, M is the molecular weight of the caseinate nano-particle (2650 kDa was calculated from a radius of 10 nm according to: $M = 1.33\pi r_{cn}^3 \rho N_A$) ρ is the density of caseinate (~ 1050 kg/m^3) and k_BT is the thermal energy.

For simplicity, it is convenient to refer to the maximum depletion interaction rather than the dependence of the depletion interaction on droplet separation. The depletion effect between two droplets is greatest when the two droplet surfaces touch. The excluded volume V can be calculated from two sphere caps. Each sphere cap has a radius of $a + r_{cn}$ and a height of r_{cn}, where a is the radius of the droplet and $r_{cn} = 10$ nm is the radius of a caseinate nano-particle. The volume of each sphere cap is

Table 1
The concentration of non-adsorbed caseinate particles as a function of the overall fraction of caseinate in the entire emulsion.

Overall mass fraction C (g/kg)	Aqueous phase concentration $C_{non\text{-}ad}$ (g/kg)	Osmotic pressure (Pa)	Depletion interaction potential $(W_{dep})/k_BT$	Continuous phase viscosity (mPa s)
15	10.8	10.13	−1.0	1.68
20	17.9	17.06	−1.7	2.09
30	32.2	31.46	−3.2	3.25
40	46.5	46.57	−4.8	5.06
50	60.8	62.40	−6.4	7.87
60	75.1	78.94	−8.1	12.25
80	103.6	114.18	−11.7	60.86
100	132.2	152.27	−15.6	816.84

Appendix

Table 2
The concentration of added polysaccharide and the viscosity when mixed with a 1.5% caseinate solution.

Overall mass fraction C (g/kg)	Aqueous phase concentration $C_{non\text{-}ad}$ (g/kg)	Continuous phase viscosity (mPa)
0.1 xanthan	0.143	1.8
0.25	0.357	3.1
0.5	0.714	13.1
0.75	1.07	76.6
1.0	1.43	476
25 maltodextrin	35.7	2.9
50	71.4	4.1
75	107	7.2
100	143	12.4
150	214	40.6
200	286	140

$$V_{sc}(a) = \frac{\pi r_{cn}^2}{3}(3a + 2r_{cn}) = \pi a r_{cn}^2\left(1 + \frac{2r_{cn}}{3a}\right) \quad (4)$$

When $a > 15r_{cn}$, the approximation $V_{sc}(a) \approx \pi a r_{cn}^2$ has less than 5% error. An average sphere cap volume $\overline{V_{SC}} = 5.6 \times 10^{-23}$ m^3 can then be established from the droplet distribution, and the radius-dependent depletion interaction potential can be calculated without assuming symmetrical interactions via

$$W(a) = -\Pi \times \left(V_{sc}(a) + \overline{V_{SC}}\right) \quad (5)$$

Similarly, the average depletion interaction potential is $\overline{W} = -2\Pi\overline{V_{SC}}$. It should be noted that these averages are number averages and we did not find $\overline{W}$ particularly informative; rather, it was the distribution of interaction potentials using equation (3) that best described the data. To facilitate the reader's comparisons with previously published data, we present $W_{4,3}$, the interaction potential calculated from $d_{4,3}$ (1.234 μm) which in this article $W_{4,3} = 3.3\overline{W}$

An approximation of the droplet network population can now be established by applying a Boltzmann partition function to the histogram of droplet diameters via:

$$\frac{n_i}{N_i - n_i} = e^{-W(a_i)/k_BT} \quad (6)$$

Here, N is the total number of droplets in the sample, n is the number of freely dispersed droplets and $N - n$ is the number of droplets in the collapsing network. The subscript i indicates droplets from a particular histogram bin. When equation (6) is applied to the entire histogram of droplet diameters, the volumes of freely dispersed and network droplets can be established for a given osmotic pressure. In the case of a collapsing network forming a cream layer and a clarified layer, the osmotic pressure can be fitted to experimental data for the clarified layer and assuming that the concentration of freely dispersed droplets in the cream layer is the same as that in the clarified layer. This approach is only approximate and does not consider complexities such as: multiple droplet interactions, possible re-equilibration of freely dispersed and network droplet populations as the network collapses, or how the collapsing layer may expel freely dispersed droplets with the necessary back flow of serum.

2.5. Emulsion stability

Freshly prepared emulsions were placed into flat-bottomed screw-top tubes (15 mm × 140 mm), stored at room temperature and measured periodically using a vertical scan analyser Turbiscan Classic MA 2000 (Formulaction, Toulouse, France). The transmitted light and the backscattered light as a function of the sample height (total height = 60 mm) were collected at room temperature. Transmission is useful for analysing non-opaque samples whereas backscattering is useful for analysing opaque samples (Chauvierre, Labarre, Couvreur, & Vauthier, 2004; Mengual, Meunier, Cayré, Puech, & Snabre, 1999). Measurements were carried out after preparation of the emulsions and at different times for 7 days. Visual observation was carried out up to 6 months.

2.6. Rheology measurements

2.6.1. Rheological properties of model solutions

Throughout this publication, the viscosity of emulsions is reported relative to the zero shear viscosity of the continuous phase. The viscosity of the continuous phase was determined by preparing the relevant solutions that accounted for the excluded volume of the oil and the adsorption of sodium caseinate at 3 mg/m^2 where the surface area was determined from droplet size histograms. Xanthan and maltodextrin were assumed to not adsorb to the surface. Shear-rate-dependent flow curves of these solutions were obtained by first pre-shearing at 500 s^{-1} to eliminate any shear history and subsequently decreasing the shear rate from 500 s^{-1} to lower shear rates and then increasing it again to 500 s^{-1}. The flow curves showed no hysteresis within experimental error (5%).

2.6.2. Rheological properties of model emulsions

The shear flow properties of the model emulsions were determined with a stress-controlled rheometer (Physica MCR301, Anton Paar, Graz, Austria) at 20 °C using a cup and bob geometry. Samples were pre-sheared at shear rate of 300 s^{-1} for 1 min to erase any shear history. Flow curves at shear rates from 0.001 to 500 s^{-1} were obtained. To ensure that wall slip was not significant, we investigated a few Na-CN concentrations using vane and cone–plate geometries; the results obtained were essentially the same as those obtained using the cup and bob geometry, suggesting that wall slip was negligible in our measurements. The dynamic viscoelastic properties of the emulsions were assessed as function of time at 20 °C. Emulsion samples were gently poured into the cup and a layer of mineral oil was applied to prevent water evaporation during the measurement. The emulsions were pre-sheared at 300 s^{-1} for 1 min to disrupt any flocculated or phase-separated regions, and then a constant small strain, 0.5%, which was determined from the linear viscoelastic region, was applied at 1 Hz for 6 h. After 6 h, shear flow rheological measurements at shear rates from 0.001 to 500 s^{-1} were made. In order to elucidate droplet interactions we refer to viscosity of the emulsion relative to the viscosity of the continuous phase viscosity unless otherwise stated.

2.7. Microstructure of model emulsions

Images of the emulsions were captured using a Zeiss LSM 510 (Jena, Germany) confocal laser scanning microscope. A 0.5 mL aliquot of each emulsion sample was transferred into a 2 mL centrifuge tube before adding Nile Red and Fast Green (approximately 0.1% w/w). After thorough mixing, a drop of each sample was placed on a microscope slide (Sail, Sailing Medical-Lab Industries Co. Ltd, China). Samples were examined at λ = 543 nm for Nile Red and λ = 488 nm for Fast Green. Images were scanned at a constant 7 μm below the level of the coverslip. For the time-dependent image capturing, the coverslip was sealed by glue to prevent evaporation. Images were converted to grey scale to improve clarity; oil droplets are represented by grey, while the continuous phase is shown as black.

Appendix

2.8. Statistical analysis

All experiments were carried out at least in triplicate using freshly prepared samples and the results are reported as the mean and standard deviation of these measurements.

3. Results and discussion

3.1. Influence of non-adsorbing polymers on the phase separation of caseinate-stabilized emulsions

The volume weighted size distribution of the stock Na-CN-stabilized emulsion droplets is shown in Fig. 1. The volume/surface weighted average diameter ($d_{3,2}$) of the droplets was 0.73 ± 0.02 μm and the volume-weighted mean diameter ($d_{4,3}$) was 1.234 ± 0.11 μm. Na-CN emulsions showed gravimetric separation with a clear meniscus within a few days of preparation (Fig. 2). The experimental creaming profile of the 1% Na-CN emulsion was well fitted with equation (1) using a droplet radius of >1 μm for a concentrated emulsion. At Na-CN concentrations between 1.5 and 4%, the height of the meniscus rose faster than the rate predicted from the gravitational force of isolated droplets using Stokes' law after an initial delay. The significant changes in creaming behaviour from low to moderate Na-CN concentration were in good agreement with previous findings (Dickinson & Golding, 1997b; Huck-Iriart, Álvarez-Cerimedo, Candal, & Herrera, 2011). Fitting effective droplet radii via equation (1) to the maximum creaming rates results in radii of ~45 μm in the 1.5% samples and ~5 μm in the 4% sample. Alternatively, using the Boltzmann distribution and the range of droplet sizes, see Section 2.4, we estimate the volume fraction of droplets bound to another varies from 13.2% at 1% caseinate to 27.6% at 4% caseinate. These volume fractions are sufficient to create a sample spanning network, however, bonds in the network are expected to be short lived. A significant volume fraction (10%) of droplets with long lived network junctions only occurs above concentrations of 3% caseinate based on a $4k_BT$ threshold. The lifetime of network bonds is naturally further influenced by the continuous phase viscosity as droplets are less able to diffuse out of the attractive well.

Further increasing the Na-CN concentration reduced the creaming rate, with 6% Na-CN emulsions showing no visible creaming after a week. Nonetheless, 5 and 6% Na-CN emulsions eventually phase separated, with a visible clarified layer at the bottom of the tube, after 2 months of storage. At concentrations above 8% Na-CN, there was no sign of phase separation even after 6 months. A "delay" in the first appearance of a clarified layer has been observed in collapsing attractive networks (Buscall, 1994; Munoz, 2003; Manley, Skotheim, Mahadevan, & Weitz, 2005; Moschakis et al., 2005; Parker et al., 1995; Vélez, Fernández, Muñoz, Williams, & English, 2003). The meniscus height profile during ageing has a form that can be fitted by a model reported for collapsing particle networks, in which phase separation is driven by coarsening of the network and its subsequent viscous compression is due to gravity rather than the rapid creaming of larger aggregates (Manley et al., 2005). Emulsions containing less than 4% Na-CN showed some residual turbidity below the rising meniscus. This turbidity was particularly noticeable in emulsions containing 1.5 and 2% Na-CN. At these low concentrations, our calculations predict the volume fraction of freely dispersed is 10% and 7.5% which compares well with the experimental values of 4.3 and 1.2% given that three or more body interactions have been ignored. Better fits could be achieved by reducing the size of the casein nano-particles, which we have not attempted.

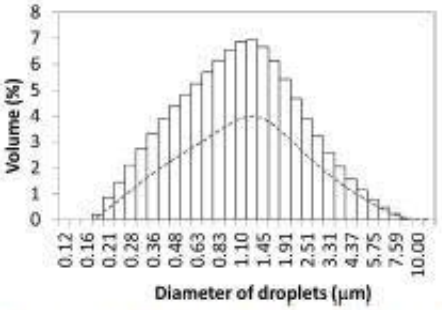

Fig. 1. Droplet size distribution in a 60% (w/w) oil-in-water stock emulsion stabilized by 3% (w/w) Na-CN. Dashed line represents the droplet population in a network based Section 2.4 using an osmotic pressure of 5 Pa, note below diameters of 0.5 micron only ~50% of the droplets participate in the network above diameters of 3 microns ~ 80% of the droplets participate in the network.

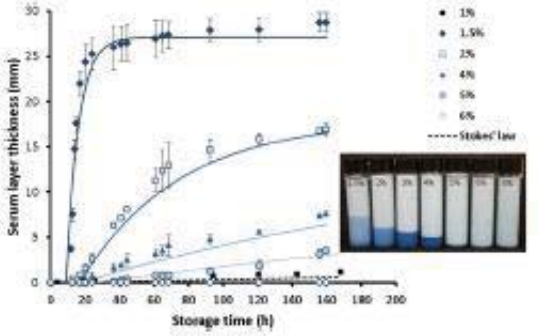

Fig. 2. Variation in clarified layer thickness as monitored by Turbiscan over 160 h at 20 °C for 30% (w/w) oil-in-water emulsions containing 1, 1.5, 2, 4, 5 and 6% (w/w) Na-CN. The black dashed line shows a prediction for the creaming of concentrated emulsions with non-interacting droplets equation (1). Inset: visual appearance of Na-CN-stabilized oil-in-water emulsions after storage for 2 weeks at 20 °C. A small amount of 2% methylene blue stain was added for better observation of the movement of the creaming boundaries. The solid lines show the form $h_0 - h(t) = \Delta h(1 - e^{-t/\tau})$ as predicted by Manley et al. (2005), giving, where h_0 is the initial height, Δh is the total change in height, t is time and τ is the time scale for the collapse, not related to τ in equation (2).

The addition of xanthan to 1.5% Na-CN-stabilized emulsions resulted in a distinct meniscus that rose with time and could be observed in samples with 0.01–0.075% xanthan (Fig. 3a). Although the theoretical fit for the creaming profiles of Na-CN emulsions with xanthan was different (data not shown), the creaming behaviour was qualitatively similar to that observed in Na-CN emulsions without added polysaccharides. At concentrations above 0.075% xanthan, phase separation was delayed beyond 2 weeks and even the 1.5% Na-CN-stabilized emulsion containing 0.1% xanthan creamed and a clear clarified layer could be seen after 2 months (data not shown). At a concentration of 0.2% xanthan, no visible separation was observed over 6 months. The addition of 0.025 and 0.05% xanthan resulted in transparent cracks throughout the sample. These cracks were tentatively attributed to a local fracture driven by phase separation; round holes would be expected when phase separation deforms the network without fracture.

The addition of maltodextrin to the 1.5% Na-CN-stabilized emulsions inhibited gravity separation (Fig. 3b). Rapid creaming still occurred at low concentrations of maltodextrin because a

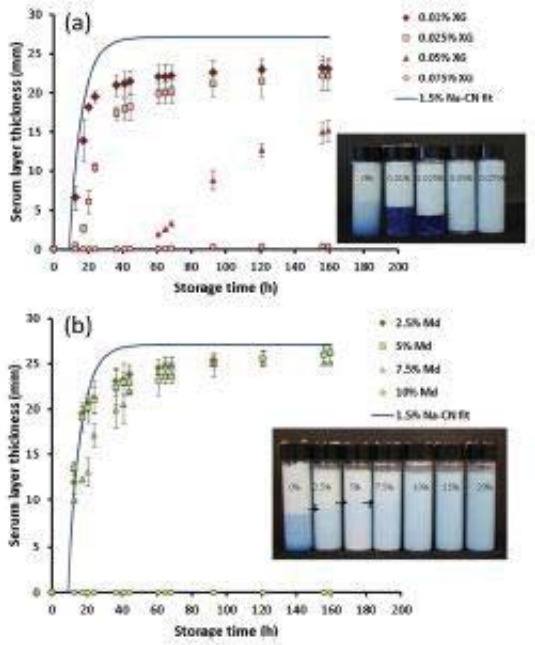

Fig. 3. (a) Variation in clarified layer thickness as determined by Turbiscan over 160 h at 20 °C for 1.5% (w/w) Na-CN-stabilized 30% (w/w) oil-in-water emulsions containing 0.01, 0.025, 0.05 and 0.075% (w/w) xanthan. Solid line in dark blue is the fit to 1.5% Na-CN emulsion from Fig. 2 to aid comparison. Inset: visual appearance of 1.5% Na-CN-stabilized emulsions containing xanthan after 2 weeks of storage at 20 °C. (b) Variation in clarified layer thickness as determined by Turbiscan over 160 h at 20 °C for 1.5% (w/w) Na-CN-stabilized 30% (w/w) oil-in-water emulsions containing 2.5, 5, 7.5 and 10% (w/w) maltodextrin. Solid line in dark blue is the fit to 1.5% Na-CN emulsion to aid comparison. Inset: visual appearance of 1.5% Na-CN-stabilized emulsions containing maltodextrin after 2 weeks of storage at 20 °C. Arrows indicate the barely visible boundary between the cream phase and the stationary phase. (For interpretation of the references to colour in this figure legend, the reader is referred to the web version of this article.)

rising meniscus was visible; however, compared with the emulsion without maltodextrin, a larger fraction of the emulsion remained stable against creaming. The creaming behaviour of Na-CN emulsions containing 2.5–7.5% maltodextrin showed good correlation with the calculated creaming rate of the control emulsion (1.5% Na-CN). The difference in turbidity between the cream layer and the clarified layer in emulsions with maltodextrin became less noticeable as the maltodextrin concentration increased. The collapsing network phenomenon was not obvious at high concentrations of maltodextrin (10%). The effect of maltodextrin was further investigated using a Turbiscan to monitor the variation in backscattered light with sample height (%) (Fig. 4). The volume fraction of the freely dispersed droplets was estimated from a calibration curve of the backscattered intensity of the stock emulsion with various dilutions. Volume fraction were of dispersed droplets were 4.3, 7.9, 9.5, 10.3, and 10.7% for 0, 2.5, 5, 7.5, and 10% maltodextrin respectively. Fitting an osmotic pressure to these values using a 10 nm sphere cap results in a W_{43} between ~$3k_BT$ and ~$1k_BT$ which seems too large for the phenomena observed, likely values would be a factor of 3 times smaller. Nonetheless, the predicted trends are plausible. The droplet diameters measured in the cream layer for the emulsions containing 0, 2.5, 5, 7.5, 10 and 15% maltodextrin were 0.78, 0.85, 0.96, 1.102, 0.75 and 0.69 μm respectively, after 7 days of storage. The increasing diameter with up to 7.5% maltodextrin further suggests increasingly weaker attractions. The increase in diameter is a consequence of the radius dependent attraction with the larger droplets more likely bound in the network, equations (4)–(6), see Fig. 1 as an example. At maltodextrin concentrations of 10% and above, the mean diameter returned to the value measured in the stock emulsion; this finding, together with the lack of a collapsing network, indicated that the attraction was effectively zero.

The decreasing droplet–droplet attraction with increasing maltodextrin concentration has been attributed to the change in caseinate particle size (Huck-Iriart et al., 2011). The depletion energy is sensitive to the polymer-to-droplet size ratio. A small change in caseinate size could have changed the depletion interaction potential moderately (Radford & Dickinson, 2004). Consequently, the change will influence the extent of the associated droplets in the transient droplet network and the creaming behaviour. It has been reported that the presence of sucrose dissociates casein particles (Belyakova et al., 2003; Mozersky, Farrell Jr., & Barford, 1991). In our case, it is possible that the casein particles became smaller in the presence of maltodextrin, hence changing the depletion interaction potential.

3.2. Influence of non-adsorbing polymers on the microstructure of caseinate-stabilized emulsions

The structural evolution of the transient droplet network during ageing of the emulsions as a function of Na-CN concentration is shown in Fig. 5. The 2% and 4% Na-CN emulsions are open networks with small voids that compact with time with no sign of the individual 3–20 μm aggregates required to fit Stokes' law to creaming profiles. The 5% Na-CN emulsion initially showed a more open network with larger voids than observed at lower concentrations of Na-CN. This network also showed compaction during ageing. However, after 6 h, the network formed in the 5% Na-CN emulsion seemed to compact at a slower rate and appeared to retain a more open structure than the network formed in the 4% Na-CN emulsion. The 6% Na-CN emulsion showed some flocculated clusters initially and an open network with large voids became more visible after 4 and 6 h. It was difficult to see structural changes in the 8% Na-CN emulsion and there were no signs of the appearance of a macroscopic droplet network during the first 6 h. The large depletion

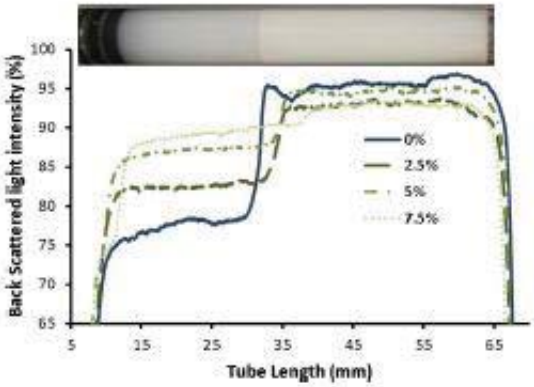

Fig. 4. Variation in the backscattered light intensity (%) of 1.5% Na-CN-stabilized 30% (w/w) oil-in-water emulsions as a function of maltodextrin concentration after 2 weeks of storage at 20 °C. The visual appearance of the 1.5% Na-CN emulsion is added to distinguish the cream layer from the clarified layer.

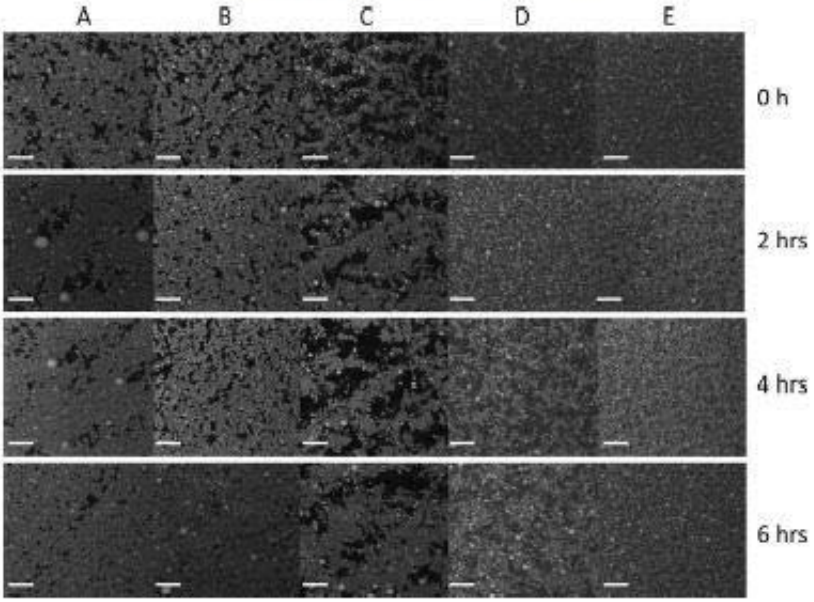

Fig. 5. Representative confocal micrographs of Na-CN-stabilized 30% (w/w) oil-in-water emulsions containing (A) 2%, (B) 4%, (C) 5%, (D) 6% and (E) 8% Na-CN as a function of time. Scale bar = 20 μm.

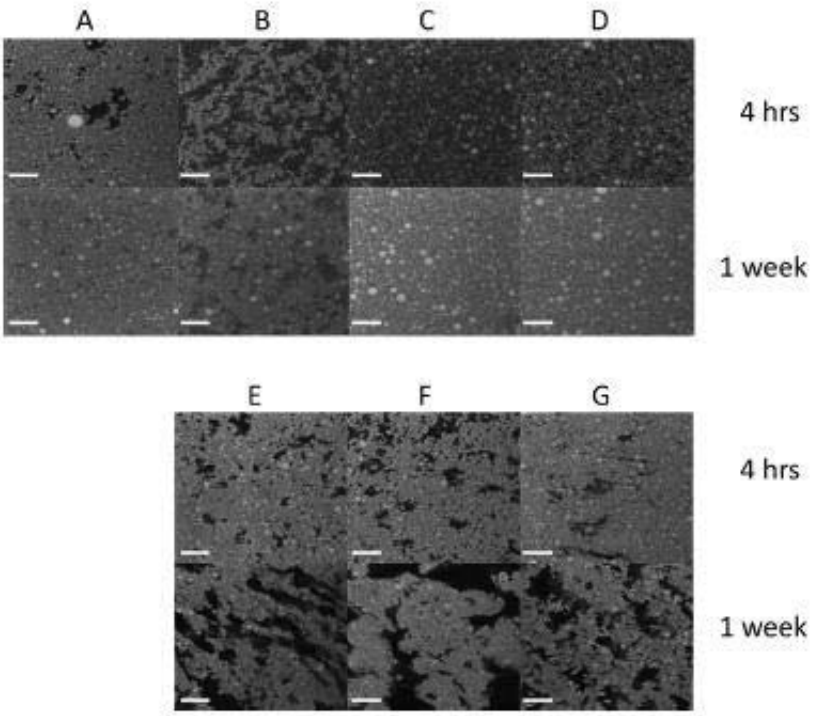

Fig. 6. Confocal micrographs of 1.5% Na-CN stabilized 30% (w/w) oil-in-water emulsions containing (A) 0% polysaccharide, (B) 5% maltodextrin, (C) 10% maltodextrin, (D) 15% maltodextrin, (E) 0.05% xanthan, (F) 0.075% xanthan and (G) 0.1% xanthan after 4 h and 1 week. Scale bar = 20 μm.

attraction in the 8% Na-CN emulsion was expected to lead to substantial dynamically arrested phase separation through a strengthening of the bonds between interconnected clusters; however, the development of a network was compromised by slow viscous rearrangement of these clusters.

Fig. 6A–D show the microstructures of 1.5% Na-CN-stabilized emulsions containing various concentrations of maltodextrin. The emulsion with 5% maltodextrin was qualitatively similar to the analogous emulsion without maltodextrin, but was not similar to Na-CN emulsions with high continuous phase viscosity. After 4 h, the 5% maltodextrin emulsion had an open droplet network with voids that eventually compacted. Further increasing the concentration of maltodextrin reduced the network formation as flocculated clusters or network-like structures were not visible after 4 h and even after 1 week. Fig. 6E–G show the effect of xanthan addition on 1.5% Na-CN-stabilized emulsions. It can be seen that the emulsion droplets associated with each other, forming a flocculated microstructure. All Na-CN emulsions containing xanthan had a compact structure at 4 h and were clearly different from those containing maltodextrin. The formation of a compact structure was possibly due to the increasing degree of viscoelasticity of the continuous phase provided by the xanthan (Moschakis et al., 2005). The contrast between droplet-rich and xanthan-rich phases on the confocal micrograph became more distinct after 1 week. It appeared that the excess Na-CN in the continuous phase may have formed part of the droplet network, leading to localized depletion effects within the network itself. The interrelationship between a droplet network containing a mixture of caseinate–xanthan and the network elasticity will be of interest in future work.

3.3. *Influence of non-adsorbing polymers on the mechanical properties of caseinate-stabilized emulsions*

The relative viscosity–shear stress curves for emulsions containing 1–10% Na-CN are shown in Fig. 7. In this section, all viscosity

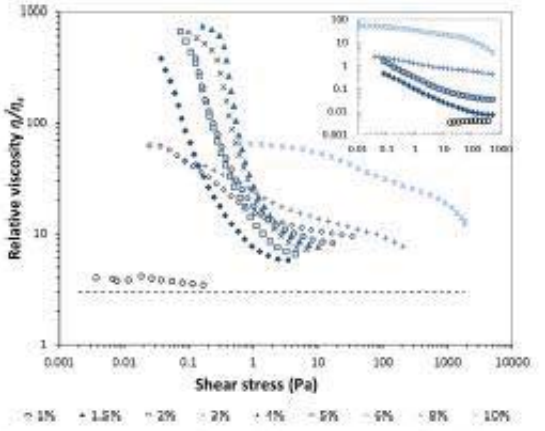

Fig. 7. Relative viscosities as a function of shear stress at 20 °C of 30% (w/w) oil-in-water emulsions containing increasing concentrations of Na-CN. Concentrations of Na-CN are given in the legend. Viscosities are relative to their low shear rate viscosity (η_0) of the continuous phase as a function of shear stress at 20 °C. The dashed line is the prediction of the zero shear relative viscosity of a hard sphere calculated using the Krieger–Dougherty equation with a volume fraction of 0.32, and a maximum packing of 0.71 (for a polydisperse system (Schaertl & Sillescu, 1994)). Inset shows the same data as emulsion viscosity in Pa s against shear rate, s^{-1}. For clarity not all data sets are shown, omitted data sets lay between data sets those of larger and smaller caseinate concentrations.

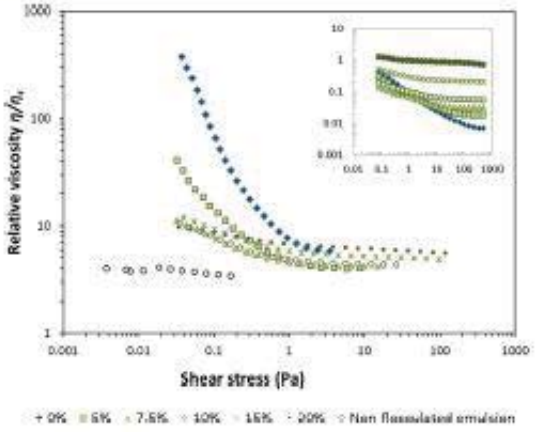

Fig. 8. Relative viscosities as a function of shear stress at 20 °C of 1.5% Na-CN-stabilized 30% (w/w) oil-in-water emulsions containing various concentrations of maltodextrin. Concentration of maltodextrin is given in the legend. Viscosities are relative to the low shear viscosity of the continuous phase (η_0). Inset: the same data represented as emulsion viscosity in Pa s against shear rate s^{-1}.

data are reported relative to the continuous phase and differences are interpreted as differences in droplet behaviour only. The 1% Na-CN emulsion contained a relative low concentration of non-adsorbed protein (<0.1%) and the viscosity of the emulsion showed a lack of shear rate dependence. The shear flow curve shared the similarity to the prediction from the Krieger–Dougherty equation further suggested that this emulsion was essentially non-interacting. From 1.5 to 4% Na-CN, the emulsions showed shear-thinning behaviour. At above critical shear stresses, the relative viscosities of the emulsions markedly decreased, indicating the breakdown of a microstructural network. The low shear viscosity increased as the Na-CN concentration increased and reflected the stronger and more numerous droplet–droplet interactions in the transient network induced by depletion flocculation (Manoj, Watson, Hibberd, Fillery-Travis, & Robins, 1998). The higher viscosity created by the depletion-induced network has been reported to transiently stabilize the emulsion against phase separation (Aben et al., 2012; Dickinson & Golding, 1997b). The high shear viscosity increased with increasing Na-CN concentration, with much larger values than those predicted by the Krieger–Doughty equation, suggesting that some shear-stable aggregates remained and that the emulsion microstructure was still sensitive to the Na-CN concentration.

The flow curves for emulsions containing ≥5% Na-CN exhibited were distinctly different from those for emulsions containing lower Na-CN concentrations. Beyond 5% Na-CN emulsions exhibited less pronounced shear-thinning behaviour as the Na-CN concentration increased. Furthermore, these emulsions showed, initially, a smaller low-shear viscosity than their counterparts with lower Na-CN concentration. However, the low-shear viscosity of the 5% Na-CN emulsion increased almost fivefold to a plateau value after 6 h of storage at 20 °C (data not shown), indicating network formation in these emulsions is more gradual. The high-shear viscosities of 5 and 6% Na-CN emulsions still increased linearly with Na-CN concentration. For 8 and 10% Na-CN emulsions, the slight shear-thinning behaviour indicated the presence of some flocculated droplets/clusters but again a strong network was not formed. The increased resistance of Na-CN emulsions against phase separation at high caseinate concentrations probably involve the slow

aggregate movement in a higher continuous phase viscosity only the emulsion viscosity is so high, creaming rates are particularly small. We estimate from equation (1), where the denominator is nine times the viscosity of the emulsion that even droplets as large as ten microns only cream about ten microns per day.

The relative viscosity–shear stress curves for emulsions containing 0–20% maltodextrin are shown in Fig. 8. It should be noted that adding maltodextrin to a 1.5% Na-CN emulsion resulted in a significant decrease in the low shear viscosity, with almost a tenfold reduction at 5% maltodextrin and a further fourfold decrease at 7.5% maltodextrin. After 6 h, the viscosity of the emulsions containing 5 and 7.5% maltodextrin decreased rather than increased, suggesting that this level of maltodextrin weakened the droplet network rather than delaying network formation. This weakening was further supported by the lower high-shear relative viscosities with increasing maltodextrin concentration. Increasing the maltodextrin concentration above 10% resulted in little change in the low shear behaviour but did increase the high shear viscosity.

To further verify the effect of the continuous phase viscosity on the structural changes during the development of the droplet network, the relative viscosity was monitored over time under a small amplitude oscillatory strain within the linear response region (Fig. 9a–c). In each figure, the time axis is normalised by the continuous phase viscosity to determine whether any differences were merely a result of increased viscosity or were caused by an alternative phenomenon. Fig. 9a shows the dynamic structural change in emulsions as a function of Na-CN concentration. The structural changes were characterized into three distinct time periods. Initially, the increase in relative viscosity reflected the formation of a transient non-equilibrium network structure. Once the relative viscosity reached a peak value, it gradually decreased. This decrease in peak viscosity suggested that the droplet network underwent thermally driven reorganization and restructuring. The transient droplet network coarsened and became more close packed (Dickinson & Golding, 1997b). Subsequently, the locally trapped continuous phase within the droplet network began to release into the clarified layer. This change led to a decrease in viscosity because the "effective" dispersed phase volume fraction decreased. During this period, the mixture of oil droplets and continuous phase began to form an interface between two different bulk phases (droplet-rich + droplet-poor). Finally, the droplet network collapsed and underwent consolidation of the cream phase once it could not withstand the gravitational stress.

The peak in relative viscosity observed in all emulsions and was markedly dependent on the Na-CN concentration. There was a clear rapid increase in the initial viscosity with an increase in the Na-CN concentration from 1.5 to 3%. The peak relative viscosity occurred slightly earlier for the 2% and 3% Na-CN emulsions than for the 1.5% Na-CN emulsion. The reorganization and rearrangement of the droplet network was still detectable within the measurement timeframe for these emulsions. The slow dynamics of the formation of the droplet network became obvious for the 4% and 5% Na-CN emulsions. It was estimated that the formation of the transient droplet network was about 100 times slower for 5% Na-CN than for 2% Na-CN, despite only a 4 fold change in continuous phase viscosity. For higher Na-CN concentrations (≥6%), the dynamics of the formation of a transient droplet network became significantly slower. It was estimated that it took the 6% Na-CN emulsion about 420 h to reach the peak in relative viscosity, based on the convergence of the slopes, this approximation was in fairly good agreement with the creaming behaviours determined by Turbiscan. Some weak polysaccharide gel network could possibly have formed in the continuous phase at the critical polymer concentration (Thomar et al., 2012), which may have strongly hindered the formation of the transient droplet network and its corresponding

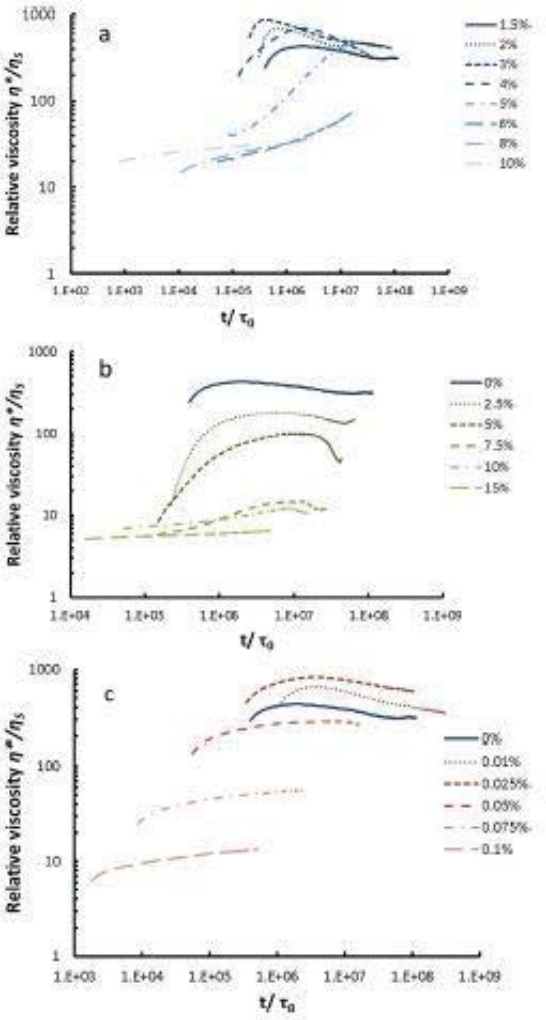

Fig. 9. Complex viscosity as a function of time for various emulsions normalised by the time taken for a droplet to diffuse an arbitrary distance, in this case 20 nm to give τ_0 from equation (2) (performed at 1 Hz, 0.5% strain, 20 °C) (a) varying concentrations of Na-CN: concentration of caseinate (w/w) is given in the legend. (b) Emulsion contains 1.5% (w/w) Na-CN and various concentrations of maltodextrin: concentration of the maltodextrin (w/w) is given in the legend. (c) Emulsion contains 1.5% (w/w) Na-CN and various concentrations of xanthan: concentration of the xanthan (w/w) is given in the legend.

structural rearrangement; subsequently, the gel network may have prevented creaming by preventing gel collapse.

The effect of maltodextrin concentration on the dynamics of structural change in 1.5% Na-CN emulsions is shown in Fig. 9b. The droplet network developed at a slower rate as the maltodextrin concentration was increased up to 10%. Furthermore, across the maltodextrin concentrations investigated, increasing the concentration also decreased the maximum viscosity by 1–2 orders of magnitude. A slower network formation with increased maltodextrin concentration is consistent with previous findings on the effect of carbohydrate on creaming stability (Blijdenstein, Zoet, van

Appendix

Vliet, van der Linden, & van Aken, 2004; Dokic-Baucal et al., 2004; Thomar et al., 2012; Udomrati, Ikeda, & Gohtani, 2013). The decrease in maximum viscosity suggested that the attractions that supported network formation were weakened with the addition of maltodextrin. It should be noted that, apart from simply increasing the continuous phase viscosity, a maltodextrin with high molecular weight fractions (i.e. low DE value) forms firmly packed segments or arranges like "fringes" to form a network structure in solution because of self-association as branched molecules are added to amylase (Chronakis, 1998). This structural change cannot be ruled out as an additional factor involved in the slowed dynamic effect.

The effect of xanthan concentration on the dynamics of structural change in 1.5% Na-CN emulsions is shown in Fig. 9c. The trend in shear rate dependence and structural evolution in the xanthan-containing Na-CN emulsions was similar to that in the Na-CN-stabilized emulsions fortified with different amounts of non-adsorbed Na-CN. The addition of xanthan up to 0.025% led to a stronger droplet network as the relative viscosity increased. The emulsions containing 0.01% and 0.025% xanthan displayed a trend such that the relative viscosity increased initially and then there was an onset rearrangement of the droplet network that eventually resulted in a decrease in relative viscosity as the network was no longer self-supporting. Further increasing the xanthan concentration led to a slower network formation as the relative viscosity of the emulsions decreased considerably. This change suggested that the viscosity of the non-adsorbed xanthan slowed down the dynamics of droplet network formation.

4. Conclusions

We investigated the creaming behaviour of emulsions (30% oil), induced by a depletion effect, over a wide range of Na-CN concentration (1–10%). At 1.5–5% Na-CN, the low shear relative viscosities were 100–1000 times greater than expected for non-interacting droplets. Creaming profiles and microscopy further indicated the formation of interconnected droplet networks that coarsened and eventually collapsed under gravity. By considering the entire population of droplet sizes, we were able to account for both the weak network formation and the portion of droplets that remained freely dispersed after the network collapse. For intermediate Na-CN concentrations (3–5%), the increase in the concentration of non-adsorbed Na-CN increased the number of droplets participating in the network, which in turn kinetically stabilized the emulsion structure against creaming. Diffusion limited aggregation is characterized with a rate constant of $8k_BT/3\eta_{ss}$, and suggests that droplets and small aggregates would be consumed into multi-droplet aggregates in an instant, yet at higher Na-CN concentrations (≥6%), the significant delay in network formation could not be accounted for by simply renormalizing time scales against the rate diffusion of single droplets. It is thought that these emulsions consist of large aggregates in a pre-network state. These large aggregates do not evolve into a network in an accessible timeframe due to the particularly small diffusive motion and their inability to redisperse. Presumably in these systems the rate of creaming in these aggregate samples would begin to resemble that creaming rates determined by aggregate size, gravity and Stokes' law.

Adding maltodextrin or xanthan influenced the creaming behaviour, but neither could be considered to be an inert viscosifying agent. The reduced network formation caused by adding maltodextrin was not an effect of viscosity, but rather a breakdown of the caseinate nano-particles that induce network formation. Once the maltodextrin concentration exceeded 15%, the droplets were entirely non-interacting and would presumably cream at a rate predicted by Stokes' law. Adding xanthan to the Na-CN emulsions resulted in local domains rich in either xanthan or Na-CN and emulsion. The effect of these local domains was that the droplets experienced a larger depletion interaction potential and the high viscosity of the combined xanthan and emulsion phases resulted in uniform phase separation across the emulsion rather than gravimetric separation.

Acknowledgements

The authors gratefully thank the Fonterra Research and Development Centre and the Ministry of Science and Innovation for financial support and Claire Woodhall for her assistance in proof reading.

References

Aken, S., Holtze, C., Tadros, T., & Schurtenberger, P. (2012). Rheological investigations on the creaming of depletion-flocculated emulsions. *Langmuir, 28*, 7967–7975.
Akhtar, M., Murray, B. S., & Dickinson, E. (2006). Perception of creaminess of model oil-in-water dairy emulsions: influence of the shear-thinning nature of a viscosity-controlling hydrocolloid. *Food Hydrocolloids, 20*, 839–847.
Álvarez Cerimedo, M. S., Iñiart, C. H., Candal, R. J., & Herrera, M. L. (2010). Stability of emulsions formulated with high concentrations of sodium caseinate and trehalose. *Food Research International, 43*, 1482–1493.
Asakura, S., & Oosawa, F. (1954). On interaction between two bodies immersed in a solution of macromolecules. *Journal of Chemical Physics, 22*, 1255–1256.
Behjakova, L. E., Antipova, A. S., Semenova, M. G., Dickinson, E., Merino, L. M., & Tsapkina, E. N. (2003). Effect of sucrose on molecular and interaction parameters of sodium caseinate in aqueous solution: relationship to protein gelation. *Colloids and Surfaces B: Biointerfaces, 31*, 31–46.
Blijdenstein, T. B. J., van Vliet, T., van der Linden, E., & van Aken, G. A. (2003). Suppression of depletion flocculation in oil-in-water emulsions: a kinetic effect of β-lactoglobulin. *Food Hydrocolloids, 17*, 661–669.
Blijdenstein, T. B. J., Zoet, F. D., van Vliet, T., van der Linden, E., & van Aken, G. A. (2004). Dextran-induced depletion flocculation in oil-in-water emulsions in the presence of sucrose. *Food Hydrocolloids, 18*, 857–863.
Buscall, R. (1994). An effective hard-sphere model of the non-Newtonian viscosity of stable colloidal dispersions: comparison with further data for sterically stabilised latices and with data for microgel particles. *Colloids and Surfaces A: Physicochemical and Engineering Aspects, 83*, 33–42.
Buscall, R., Choudhury, T. H., Faers, M. A., Goodwin, J. W., Luckham, P. A., & Partridge, S. J. (2009). Towards rationalising collapse times for the delayed sedimentation of weakly-aggregated colloidal gels. *Soft Matter, 5*, 1345–1349.
Carr, A. J., Munro, P. A., & Campanella, O. H. (2002). Effect of added monovalent or divalent cations on the rheology of sodium caseinate solutions. *International Dairy Journal, 12*, 487–492.
Chauvierre, C., Labarre, D., Couvreur, P., & Vauthier, C. (2004). A new approach for the characterization of insoluble amphiphilic copolymers based on their emulsifying properties. *Colloid and Polymer Science, 282*, 1097–1104.
Chronakis, I. S. (1998). On the molecular characteristics, compositional properties, and structural-functional mechanisms of maltodextrins: a review. *Critical Reviews in Food Science and Nutrition, 38*, 599–637.
Dickinson, E. (1992). *An introduction to food colloids*. Oxford: Oxford Science Publishers.
Dickinson, E. (1999). Caseins in emulsions: interfacial properties and interactions. *International Dairy Journal, 9*, 305–312.
Dickinson, E. (2009). Hydrocolloids as emulsifiers and emulsion stabilizers. *Food Hydrocolloids, 23*, 1473–1482.
Dickinson, E. (2010). Flocculation of protein-stabilized oil-in-water emulsions. *Colloids and Surfaces B: Biointerfaces, 81*, 130–140.
Dickinson, E., & Golding, M. (1997a). Depletion flocculation of emulsions containing unadsorbed sodium caseinate. *Food Hydrocolloids, 11*, 13–18.
Dickinson, E., & Golding, M. (1997b). Rheology of sodium caseinate stabilized oil-in-water emulsions. *Journal of Colloid and Interface Science, 191*, 166–176.
Dickinson, E., Golding, M., & Povey, M. J. W. (1997). Creaming and flocculation of oil-in-water emulsions containing sodium caseinate. *Journal of Colloid and Interface Science, 185*, 515–529.
Dickinson, E., Semenova, M. G., Antipova, A. S., & Pelan, E. G. (1998). Effect of high-methoxy pectin on properties of casein-stabilized emulsions. *Food Hydrocolloids, 12*, 425–432.
Dokic-Baucal, L., Dokic, P., & Jakovljevic, J. (2004). Influence of different maltodextrins on properties of O/W emulsions. *Food Hydrocolloids, 18*, 233–239.
Farrer, D., & Lips, A. (1999). On the self-assembly of sodium caseinate. *International Dairy Journal, 9*, 281–286.
ten Grotenhuis, E., Tuinier, R., & de Kruif, C. G. (2003). Phase stability of concentrated dairy products. *Journal of Dairy Science, 86*, 764–769.
van Gruijthuijsen, K., Herle, V., Tuinier, R., Schurtenberger, P., & Stradner, A. (2012). Origin of suppressed demixing in casein/xanthan mixtures. *Soft Matter, 8*, 1547–1555.

HadjSadok, A., Moulai-Mostefa, N., & Rebiha, M. (2010). Rheological properties and phase separation of xanthan–sodium caseinate mixtures analyzed by a response surface method. *International Journal of Food Properties, 13*, 369–380.
HadjSadok, A., Pitkowski, A., Nicolai, T., Benyahia, L., & Moulai-Mostefa, N. (2008). Characterisation of sodium caseinate as a function of ionic strength, pH and temperature using static and dynamic light scattering. *Food Hydrocolloids, 22*, 1460–1466.
Hemar, Y., Tamehana, M., Munro, P. A., & Singh, H. (2001). Influence of xanthan gum on the formation and stability of sodium caseinate oil-in-water emulsions. *Food Hydrocolloids, 15*, 513–519.
Huck-Iriart, C., Álvarez-Cerimedo, M. S., Candal, R. J., & Herrera, M. L. (2011). Structures and stability of lipid emulsions formulated with sodium caseinate. *Current Opinion in Colloid & Interface Science, 16*, 412–420.
Kramers, H. A. (1940). Brownian motion in a field of force and the diffusion model of chemical reactions. *Physica, 7*, 284–304.
Leman, J., & Kinsella, J. E. (1989). Surface activity, film formation, and emulsifying properties of milk proteins. *Critical Reviews in Food Science and Nutrition, 28*, 115–138.
Liang, Y., Patel, H., Matia-Merino, L., Ye, A., & Golding, M. (2013). Structure and stability of heat-treated concentrated dairy-protein-stabilised oil-in-water emulsions; a stability map characterisation approach. *Food Hydrocolloids, 33*, 297–308.
Long, Z., Zhao, Q., Liu, T., Kuang, W., Xu, J., & Zhao, M. (2012). Role and properties of guar gum in sodium caseinate solution and sodium caseinate stabilized emulsion. *Food Research International, 49*, 545–552.
Long, Z., Zhao, Q., Liu, T., Kuang, W., Xu, J., & Zhao, M. (2013). Influence of xanthan gum on physical characteristics of sodium caseinate solutions and emulsions. *Food Hydrocolloids, 32*, 123–129.
Lu, P. J., Zaccarelli, E., Ciulla, F., Schofield, A. B., Sciortino, F., & Weitz, D. A. (2008). Gelation of particles with short-range attraction. *Nature, 453*, 499–503.
Manley, S., Skotheim, J. M., Mahadevan, L., & Weitz, D. A. (2005). Gravitational collapse of colloidal gels. *Physical Review Letters, 94*, 218302.
Manoj, P., Watson, A. D., Hibberd, D. J., Fililey-Travis, A. J., & Robins, M. M. (1998). Characterization of a depletion-flocculated polydisperse emulsion. II. Steady-state rheological investigations. *Journal of Colloid and Interface Science, 207*, 294–302.
McClements, D. J. (2005). *Food emulsions: Principles, practices, and techniques* (2nd ed.). Boca Raton, FL: CRC Press.
Mengual, O., Meunier, G., Cayré, I., Puech, K., & Snabre, P. (1999). TURBISCAN MA 2000: multiple light scattering measurement for concentrated emulsion and suspension instability analysis. *Talanta, 50*, 445–456.
Moschakis, T., Murray, B. S., & Dickinson, E. (2005). Microstructural evolution of viscoelastic emulsions stabilised by sodium caseinate and xanthan gum. *Journal of Colloid and Interface Science, 284*, 714–728.
Mozersky, S. M., Farrell, H. M., Jr., & Barford, R. A. (1991). The effects of sucrose and lactose on the sizes of casein micelles reconstituted from bovine caseins. *Journal of Dairy Science, 74*, 2382–2393.
Parker, A., Gunning, P. A., Ng, K., & Robins, M. M. (1995). How does xanthan stabilise salad dressing? *Food Hydrocolloids, 9*, 333–342.
Perrechil, F. A., & Cunha, R. L. (2010). Oil-in-water emulsions stabilized by sodium caseinate: influence of pH, high-pressure homogenization and locust bean gum addition. *Journal of Food Engineering, 97*, 441–448.
Pitkowski, A., Durand, D., & Nicolai, T. (2008). Structure and dynamical mechanical properties of suspensions of sodium caseinate. *Journal of Colloid and Interface Science, 326*, 96–102.
Radford, S. J., & Dickinson, E. (2004). Depletion flocculation of caseinate-stabilised emulsions: what is the optimum size of the non-adsorbed protein nano-particles? *Colloids and Surfaces A: Physicochemical and Engineering Aspects, 238*, 71–81.
Schaertl, W., & Sillescu, H. (1994). Brownian dynamics of polydisperse colloidal hard spheres: Equilibrium structures and random close packings. *Journal of Statistical Physics, 77*, 1007–1025.
Srinivasan, M., Singh, H., & Munro, P. A. (2002). Formation and stability of sodium caseinate emulsions: influence of retorting (121 °C for 15 min) before or after emulsification. *Food Hydrocolloids, 16*, 153–160.
Starrs, L., Poon, W. C. K., Hibberd, D. J., & Robins, M. M. (2002). Collapse of transient gels in colloid-polymer mixtures. *Journal of Physics: Condensed Matter, 14*, 2485–2505.
Sun, C., Gunasekaran, S., & Richards, M. P. (2007). Effect of xanthan gum on physicochemical properties of whey protein isolate stabilized oil-in-water emulsions. *Food Hydrocolloids, 21*, 555–564.
Teece, L. J., Faers, M. A., & Bartlett, P. (2011). Ageing and collapse in gels with long-range attractions. *Soft Matter, 7*, 1341–1351.
Thomar, P., Durand, D., Benyahia, L., & Nicolai, T. (2012). Slow dynamics and structure in jammed milk protein suspensions. *Faraday Discussions, 158*, 325–339.
Tuinier, R., & de Kruif, C. G. (1999). Phase separation, creaming, and network formation of oil-in-water emulsions induced by an exocellular polysaccharide. *Journal of Colloid and Interface Science, 218*, 201–210.
Udomrati, S., Ikeda, S., & Gohtani, S. (2013). Rheological properties and stability of oil-in-water emulsions containing tapioca maltodextrin in the aqueous phase. *Journal of Food Engineering, 116*, 170–175.
Vélez, G., Fernández, M. A., Muñoz, J., Williams, P. A., & English, R. J. (2002). Role of hydrocolloids in the creaming of oil in water emulsions. *Journal of Agricultural and Food Chemistry, 51*, 265–269.
Vélez, G., Fernández, M. A., Muñoz, J., Williams, P. A., & English, R. J. (2003). Role of hydrocolloids in the creaming of oil in water emulsions. *Journal of Agricultural and Food Chemistry, 51*, 265–269.
Vrij, A. (1976). Polymers at interfaces and the interactions in colloidal dispersions. *Pure and Applied Chemistry, 48*, 471–483.
Ye, A., Hemar, Y., & Singh, H. (2004). Influence of polysaccharides on the rate of coalescence in oil-in-water emulsions formed with highly hydrolyzed whey proteins. *Journal of Agricultural and Food Chemistry, 52*, 5491–5498.

Paper Three

(This published work is from Chapter 7)

Appendix

Food Hydrocolloids 41 (2014) 332–342

Contents lists available at ScienceDirect

Food Hydrocolloids

journal homepage: www.elsevier.com/locate/foodhyd

Effect of sugar type and concentration on the heat coagulation of oil-in-water emulsions stabilized by milk-protein-concentrate

Yichao Liang [a,b,*], Lara Matia-Merino [b], Hasmukh Patel [c], Aiqian Ye [d], Graeme Gillies [a], Matt Golding [b,d,**]

[a] Fonterra Research and Development Centre, Private Bag 11 029, Palmerston North, New Zealand
[b] Institute of Food, Nutrition and Human Health, Massey University, Private Bag 11 222, Palmerston North, New Zealand
[c] Dairy Science Department, Box 2104, South Dakota State University, Brookings, SD 57002, USA
[d] Riddet Institute, Massey University, Private Bag 11 222, Palmerston North, New Zealand

ARTICLE INFO

Article history:
Received 15 February 2014
Accepted 17 April 2014
Available online 26 April 2014

Keywords:
Milk protein concentrate
Sugar
Emulsion
Droplet formation
Heat stability

ABSTRACT

The influence of various sugars, on the heat stability of a milk-protein-concentrate (MPC)-stabilized emulsion (10% w/w protein, 10% w/w oil) was studied. Regardless of concentration, the addition of sugars during emulsification slightly increased the droplet diameter except the addition of 20–30% w/w maltodextrin significantly ($p < 0.05$) decreased the droplet diameter and was attributed to the larger change in disperse/continuous phase viscosity ratio. Generally, the addition of sugar reduced the heat coagulation time (HCT) determined at 140 °C. The increased concentration of glucose, maltose, sucrose, trehalose shifted the pH at heat stability maximum towards more acidic values whereas the increased concentration of maltodextrin shifted the pH at heat stability maximum towards more alkaline values. The extent of destabilization also varied between sugars, with trehalose being particularly effective in retaining the original heat stability of the MPC-stabilized emulsions. Reducing sugars (glucose, maltose, maltodextrin) decreased the heat stability maximum more significantly than non-reducing sugars (sucrose and trehalose). Particle size, microstructure, and rheological measurements showed good correlations with the heat stability. Several factors, including free calcium ion level, volume fraction of the continuous phase protein and solvent quality, will also affect the heat stability of MPC-stabilized emulsions with added sugars.

1. Introduction

Dairy beverages for dietetic purposes usually include proteins, emulsifiers, minerals, oil, and sugars (Keowmaneechai & McClements, 2006). In the processing of these dairy beverages, emulsifiers and some milk proteins adsorb at the oil/water interface during homogenization to produce small oil droplets. The emulsion-based liquid slurry (pH ~ 6.8) is often heat sterilized (i.e., retort or ultrahigh-temperature processes) for long term shelf-life stability (Liang, Patel, Matia-Merino, Ye, & Golding, 2013a). Milk proteins, especially casein and caseinate, are often fortified into dairy beverages because of their excellent nutritional value and heat stability (Beliciu, Sauer, & Moraru, 2012; de Kort, Minor, Snoeren, van Hooijdonk, & van der Linden, 2012; Srinivasan, Singh, & Munro, 2002, 2003). Despite the remarkable heat stability of casein, under certain circumstances, such as high heating temperature and long heating duration, casein and caseinate may flocculate, coagulate or gel (Cruijsen, 1996; Sauer & Moraru, 2012). Recently, protein–protein and protein–ingredient interactions in dairy colloids have attracted increased attention in food industries and food institutes (de Kort, Minor, Snoeren, van Hooijdonk, & van der Linden, 2011; McSweeney, Healy, & Mulvihill, 2008; Sağlam, Venema, de Vries, Shi, & van der Linden, 2013; Sauer & Moraru, 2012). In some dairy products such as Dulce de leche, heat-induced coagulation of concentrated milk and sucrose is favourable (Pauletti, Castelao, & Seguro, 1996). Therefore, it is of great practical importance to gain more understanding of the heat-induced physicochemical changes on casein-stabilized oil-in-water emulsion systems containing ternary ingredients.

* Corresponding author. Fonterra Research and Development Centre, Private Bag 11 029, Palmerston North, New Zealand. Tel.: +64 06 350 4649x64754; fax: +64 06 356 1476.
** Corresponding author. Institute of Food, Nutrition and Human Health, Massey University Manawatu, Private Bag 11 222, Palmerston North 4442, New Zealand. Tel.: +64 06 356 9099x81428.
E-mail address: kendison@gmail.com (Y. Liang).

http://dx.doi.org/10.1016/j.foodhyd.2014.04.022
0268-005X/

Appendix

In previous work, the heat-induced instabilities of casein micelles and caseinates have been evaluated in milk, concentrated milk, whey-protein-free casein micelle systems, and casein-micelle-stabilized and sodium caseinate-stabilized oil-in-water emulsions (Cruijsen, 1996; de Kort et al., 2012; McSweeney et al., 2008; Sauer & Moraru, 2012). Those systems share a number of parameters that affect their heat stability. These include compositional factors such as the initial heating pH (O'Connell & Fox, 2003; Singh, 2004; van Boekel, Nieuwenhuijse, & Walstra, 1989a, 1989b, 1989c), the protein concentration (Walstra, Wouters, & Geurts, 2006), the oil volume (Cruijsen, 1996), the aggregation state of casein (Liang et al., 2013a), the calcium ion activity (de Kort et al., 2012), the addition of polyphosphate (Tsioulpas, Koliandris, Grandison, & Lewis, 2010), the addition of lecithin (Kasinos, Tran Le, & Van der Meeren, 2014; McSweeney et al., 2008), and the type of sugar (Cruijsen, 1996; Tan-Kintia & Fox, 1996).

It has been reported the addition of sugar can be used to control the heat-induced denaturation and aggregation behaviour of globular proteins in solution (Panzica, Emanuele, & Cordone, 2012) and in emulsion (Kim, Decker, & McClements, 2003; Kulmyrzaev, Bryant, & McClements, 2000), to improve heat stability of milk and concentrated milk (Holt, Muir, & Sweetsur, 1978; Tan-Kintia & Fox, 1996), to prevent cold protein denaturation (Xiong, 1997), to improve freeze–thaw stability (Ghosh, Cramp, & Coupland, 2006), to control the texture (Chanamai & McClements, 2000; Li, Fu, Luo, & Huang, 2013) and creaming stability of food emulsions (Álvarez-Cerimedo, Iriart, Candal, & Herrera, 2010). Semenova, Antipova, and Belyakova (2002) concluded that the addition of sugars affects the thermodynamic properties of proteins, including heat stability, preferential hydration, self-assembly, conformational stability, gelation, and surface activity. A more recent study suggested that the addition of sugar causes a decrease in pH and an increase in calcium ion activity of milk because of a combination of volume exclusion effects and hydration effects (Gao et al., 2010). Over the past few years, considerable effort has been spent on understanding the protective effect of sugars against the unfolding of globular proteins and their gelation (Semenova et al., 2002). The generally accepted heat-induced physicochemical changes on globular proteins involve: (1) the presence of sugar (up to 40% w/w sucrose) increases the denaturation temperature of globular proteins; (2) the presence of sugar effectively increases the viscosity of the continuous phase, leading to reduced protein–protein interactions in continuous phase and between the oil/water interfaces (Baier & McClements, 2001; Kulmyrzaev et al., 2000).

The effect of sugars on the heat stability of casein micelles has also been studied. When added at low concentration, sugars react like aldehydes, stabilizing concentrated milk against prolonged heating at high temperatures (Holt et al., 1978). Non-reducing sugars, such as sucrose and trehalose, and the sugar alcohols have little effect on the heat stability of milk whereas reducing sugars, such as glucose, galactose, maltose, and fructose, and the thermal degradation products of lactose enhance the heat stability of milk (Tan-Kintia & Fox, 1996). In contrast, on the emulsion system containing sodium caseinate, the presence of sucrose has little effect on the heat stability whereas lactose and glucose decrease the heat stability (Cruijsen, 1996). It is of interest to further characterize emulsions with high concentrations of sugar, especially trehalose, which has been shown to impart exceptional stability to the protein structure (Crowe, 2007; Jain & Roy, 2009).

The heat stability of protein solutions or protein-based emulsions is often studied as a function of the initial pH (van Boekel et al., 1989b, 1989c; McSweeney, Mulvihill, & O'Callaghan, 2004; Rattray & Jelen, 1997; Singh, 2004). The heat coagulation time (HCT) is the time required for a heat-induced coagulum to become visible during heating in an oil bath. It indirectly measures the resistance of milk proteins against heat-induced coagulation (Singh, 2004; Walstra et al., 2006). Milk protein concentrate (MPC) is a spray-dried ingredient that is produced by ultrafiltration/diafiltration. It contains more than 10 times less lactose than skim milk and the forms of the casein micelles and whey proteins are similar to those found in milk (Ye, 2011). However, to our best knowledge, the heat stability of MPC-stabilized oil-in-water emulsions containing high protein (i.e., >6% w/w) and high sugar (i.e., ≥10% w/w) concentrations has not been studied yet. The objectives of this research were to study the effect of sugar type and concentration on the droplet size reduction, to study the impact of pH on the heat stability characteristics of MPC containing system and to obtain qualitative information on the heat-induced behaviour of oil droplets and proteins in the continuous phase in high protein and sugar conditions.

2. Materials and methods

2.1. Materials

MPC 485 (81.5% w/w protein, 0.07% w/w sodium, 2.23% w/w calcium) was obtained from Fonterra Co-operative Group Ltd, Auckland, New Zealand. Bulk corn oil and sucrose were purchased from Davis Trading Co., Palmerston North, New Zealand. Glucose, maltose hydrate, and trehalose dihydrate were obtained from Sigma Chemical Co. (St. Louis, MO, USA). Maltodextrin (Md 180) with a dextrose equivalent (DE) value of 18 was obtained from Grain Processing Corporation (Muscatine, IA, USA). All of the chemicals used were of analytical grade, and were obtained from either BDH Chemicals (BDH Ltd., Poole, England) or Sigma Chemical Co. unless otherwise specified.

2.2. Preparation of model emulsions

MPC (10% w/w) was reconstituted in Milli-Q water at 50 °C for 60 min. Glucose, maltose, sucrose, trehalose, and maltodextrin (0–30% w/w) were added as required to MPC solutions. Corn oil (10% w/w) was mixed with the mixture of MPC and sugar and was then pre-homogenized at 24,000 rev/min for 1 min using an Ultra-Turrax T25 (IKA®-Werke GmbH & Co. KG, Staufen, Germany) to form a coarse emulsion. The coarse emulsion was heated to 60 °C and homogenized by passing it through a two-stage homogenizer (type Panda, Niro Soavi, Parma, Italy) for three passes at 20 MPa (first stage) and 4 MPa (second stage) to form the final emulsions, containing constant protein and oil concentrations (10% w/w protein, 10% w/w oil) and varied concentrations of sugar (from 0 to 30% w/w). The molar concentrations of the different sugars are shown Table 1. The amount of adsorbed proteins at oil/water interface was calculated to be 1.24 ± 0.13 g/100 g of emulsion (10% w/w oil) following the equation (McClements, 2005):

$$C_{ad} = C_{total} - C_{non-ad}, C_{non-ad} = \frac{6 \cdot \Gamma \cdot \varnothing}{d_{32}}.$$

Table 1
Molar concentration for different sugar types at concentrations used in this study.

		Weight (g/kg)		
		100	200	300
Sugar type	Molecular weight (g/mol)	Molar concentration (M)		
Glucose	180.2	0.6	1.1	1.7
Maltose	342.3	0.29	0.58	0.88
Sucrose	342.3	0.29	0.58	0.88
Trehalose	342.3	0.29	0.58	0.88
Maltodextrin (DE 18)	1000	0.10	0.20	0.30

Appendix

Here, Γ is the surface load (in kg m^{-2}), $\varnothing$ is the disperse phase volume fraction (0.1 is used in calculation), C_{non-ad} is the concentration of emulsifier in the continuous phase (in kg m^{-3}). The reported surface coverage of MPC, 12–14 mg m^{-2} (Euston & Hirst, 1999; Ye, 2011). The non-adsorbed protein concentration was estimated to be ~9.75% w/w in a 10% oil-in-water emulsion containing 10% w/w MPC. In this study, a 10% w/w MPC solution was prepared for the evaluation of the heat stability for the corresponding continuous phase of the emulsion. Sodium azide (0.02% w/w) was added to the emulsion samples as an antimicrobial agent. All emulsions were stored at 4 °C for 1–7 days until further use. Each emulsion was prepared at least in triplicate.

2.3. Characterization of heat stability of model emulsions and solutions

2.3.1. Determination of heat coagulation time (HCT)

The HCTs of the MPC-stabilized emulsions and MPC solutions were determined according to the procedure described by McSweeney et al. (2008). Subsamples of emulsions and solutions were adjusted to pH values between 6.4 and 7.4 using 1 M HCl or 1 M NaOH. The samples were allowed to equilibrate for 2 h; then the pH was re-measured and adjusted if necessary. Aliquots (2 mL) of MPC-stabilized emulsion samples were transferred into 8 mL glass tubes with rubber-lined caps (Wheaton, Millville, NJ, USA) and were immersed in a silicone oil bath that was thermostatically controlled at 140 ± 1 °C, with a constant rocking speed (8 rev/min). The time required for coagulation of the sample or for a precipitate to become visible throughout the sample was recorded as the HCT. The time, as reported in this study, excluded the heating-up period, which was estimated to be about 1 min. The coagulated samples were removed immediately and were cooled under running cold water. The pH of the coagulum was then measured.

2.3.2. Determination of heat stability (objective test)

Aliquots (5 mL) of MPC-stabilized emulsions without and with added sugar (30% w/w) at pH 6.8 were transferred into 8 mL glass tubes with rubber-lined caps (Wheaton) and were immersed in a silicone oil bath that was thermostatically controlled at 120 ± 1 °C, with a constant rocking speed (8 rev/min). The heating-up time was about 2 min and it was not included in the heating time. All samples were removed at between 1 and 20 min and were immediately cooled under running cold water. The heat-treated emulsions were allowed to equilibrate to room temperature and were held for at least 1 h before further analysis (i.e., particle size and viscosity measurements) was carried out.

2.4. Determination of the particle size distribution of the emulsions and the particle size in the MPC solutions

The particle size distribution of the model emulsions was measured by static light scattering using a Malvern Mastersizer Hydro 2000S (Malvern Instruments Ltd., Malvern, Worcestershire, UK). The measurements were carried out using procedures described previously (Liang, Patel, Matia-Merino, Ye, & Golding, 2013b). The average droplet size was expressed as the surface-weighted mean diameter $d_{3,2}$ (μm) and the volume-weighted mean diameter $d_{4,3}$ (μm). To differentiate between the particle sizes measured with and without dissociating buffer (EDTA/Tween mixture, 0.04 mol/kg and 5 g/kg), in this work, the particle size measured in dissociating solution was referred to as the "primary" particle size and that measured in water was referred to as the "effective" particle size.

2.5. Calcium-ion activity measurement

The calcium ion activity of MPC emulsions and MPC dispersions was measured with a pH meter (PHM220, Radiometer Pacific Ltd., Auckland, New Zealand) with a mV reading to one decimal place using a calcium ion electrode (ISE25Ca, Radiometer Pacific Ltd.) and a double junction reference electrode (REF251, Radiometer Pacific Ltd.). Calibration was conducted at 20 °C with standard solutions containing 0.5, 1, 2, 3, 4, 5, and 10 mM calcium/L (as $CaCl_2$) and 8 mM potassium chloride/L. The calcium electrode was held in a stock solution of 1 mM $CaCl_2$/L and the reference electrode was held in a stock solution of 8 mM potassium chloride/L for at least 60 min before the calibration was performed.

2.6. Emulsion rheology

The rheological properties of the emulsions were measured by a stress-controlled rheometer, Physica MCR 301 (Anton Paar, Graz, Austria), at 20 °C using a cone and plate geometry. Steady-state flow measurements were conducted at 20 ± 0.1 °C in the shear rate range 0.1–500 s^{-1} over 6 min. The apparent viscosity was recorded as a function of shear rate. To study the effect of viscosity ratio (dispersed/continuous) on the droplet size break-up, the viscosities of dispersed and continuous phases were determined within the Newtonian region between shear rate 1 to 1000 s^{-1}. To describe and to compare the extent of aggregation from one sample to another, a viscosity index determined at shear rate (1 s^{-1}) was used to indicate the attractiveness between unheated and heated samples. η_t/η_0 = viscosity determined after a heat treatment/viscosity before a heat treatment. Each sample was measured twice and mean values of viscosity were determined from duplicate samples.

2.7. Microstructure of model emulsions

Images of the emulsions were captured using a Zeiss LSM 510 (Jena, Germany) confocal laser scanning microscope. A 0.5 mL aliquot of each emulsion sample was transferred into a 2 mL centrifuge tube before adding Nile Red and Fast Green (approximately 0.1% w/w). After thorough mixing, a drop of each sample was placed on a microscope slide (Sail, Sailing Medical-Lab Industries Co. Ltd., China). Samples were examined at $\lambda = 543$ nm for Nile Red and $\lambda = 488$ nm for Fast Green. Images were scanned at a constant 7 μm below the level of the coverslip.

2.8. Statistical analysis

All experiments were carried out at least in triplicate using freshly prepared samples. The experimental data were analysed by Student's *t*-tests using Microsoft Excel 2007 (Microsoft Corporation, Redmond, WA, USA) and significant differences among the means were determined at a 95.0% confidence level.

3. Results and discussion

3.1. Effect of sugar type and concentration on the droplet size formation of model MPC emulsions

The primary droplet diameters of the MPC-stabilized emulsions with and without added sugar are shown in Table 2. The primary volume-weighted mean diameter ($d_{4,3}$) of the droplets in the control MPC-stabilized emulsion was 1.03 (±0.03) μm. Regardless of the sugar concentration, emulsions containing glucose, maltose, sucrose, and trehalose formed slightly larger droplets than the control emulsion. At a similar volume fraction of oil, Álvarez-Cerimedo et al. (2010) found that the addition of trehalose caused

Appendix

Table 2
Primary droplet diameters, $d_{4,3}$ (μm), of MPC-stabilized oil-in-water emulsions (10% w/w protein, 10% oil w/w) with and without the addition of different types of sugar.

Sugar type	Sugar concentration (w/w)	Droplet size, $d_{4,3}$ (μm)
Control (without sugar)		1.03 ± 0.03^{a}
Glucose	10%	1.28 ± 0.14^{b}
	20%	1.24 ± 0.16^{b}
	30%	1.19 ± 0.11^{b}
Maltose	10%	1.26 ± 0.08^{b}
	20%	1.19 ± 0.12^{b}
	30%	1.17 ± 0.12^{b}
Sucrose	10%	1.31 ± 0.13^{b}
	20%	1.30 ± 0.05^{b}
	30%	1.13 ± 0.11^{b}
Trehalose	10%	1.23 ± 0.11^{b}
	20%	1.19 ± 0.16^{a}
	30%	1.04 ± 0.06^{a}
Maltodextrin	10%	1.12 ± 0.05^{a}
	20%	0.96 ± 0.02^{a}
	30%	0.58 ± 0.13^{c}

[a,b,c] Means within the same column and having the same superscript are not significantly different from the control by Student's *t*-test at $p < 0.05$.

a reduction in the droplet diameter of sodium-caseinate-stabilized emulsions because of strong protein–sugar interactions. In our case, the addition of trehalose did not result in a reduction in the mean droplet diameter of the MPC-stabilized emulsion. However, the addition of maltodextrin resulted in a slight increase and then a significant decrease ($p < 0.05$) in the mean droplet diameter. At a maltodextrin level of 30% w/w, the $d_{4,3}$ value of the emulsion was reduced significantly to 0.57 (±0.09) μm.

It has been reported that the droplet size depends on the viscosity ratio (dispersed/continuous) of an emulsion; the lower the ratio, the smaller the droplet size that can be achieved (Lee & Norton, 2013; Qian & McClements, 2011; Wooster, Golding, & Sanguansri, 2008). In order to test this hypothesis, the influence of the ratio of the viscosities of dispersed and continuous phases (η_D/η_C) on the droplet break-up was tested further by adding maltodextrin in a narrower concentration between 20 and 30% (w/w). Fig. 1A shows the effect of maltodextrin content on the droplet size ($d_{4,3}$) and η_D/η_C ratio. The continuous phase viscosity was increased through addition of maltodextrin to each emulsion and the η_D/η_C ratio followed a linearly decreasing trend ($R^2 = 0.978$). The droplet size was independent of the η_D/η_C ratio from 10 to 20% maltodextrin. The droplet size showed a gradual decreasing trend with addition of maltodextrin between 20 and 25% and it followed a sharp decreasing trend between 25 and 30% maltodextrin. This result was in a good agreement with the literature which observed a minimum droplet size within the optimum viscosity ratio range ($\eta_D/\eta_C = 0.5–5$) for droplet break-up under simple shear flow condition (Lee & Norton, 2013; Wooster et al., 2008).

The difference between sugar types on the droplet size break-up was also compared using sucrose (See Fig. 1B). Similar to the effect of maltodextrin, addition of sucrose resulted in a linear relationship ($R^2 = 0.977$) between sugar content and η_D/η_C ratio. Generally, the effect of sucrose represented the other sugar type like glucose, maltose and trehalose because of their impact on the viscosity of continuous phase was found very similar, with η_D/η_C ratio above 2 at 30% (w/w) sugar content. It was found that the contribution of 30% sucrose on viscosity was roughly equivalent to that of 20% maltodextrin. The η_D/η_C ratio dependency on droplet size break-up upon addition of maltodextrin between 20 and 30% was not shown in emulsions containing sucrose at the same sugar concentration probably because the η_D/η_C ratio did not reach the critical point (<2). The present results suggest that not only the protein–sugar interaction but also the viscosity ratio (dispersed/continuous) influences the emulsification process.

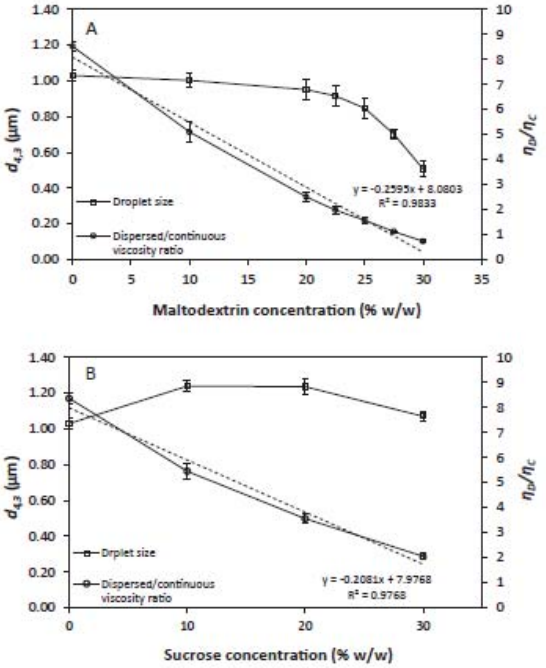

Fig. 1. Effect of sugar content (A) maltodextrin, (B) sucrose on the volume-weighted droplet size ($d_{4,3}$) (square symbol) and η_D/η_C ratio (viscosity of dispersed phase/viscosity of continuous phase which was determined within the Newtonian region between shear rate 1 to 1000 s^{-1}) (round symbol) of 10% MPC-stabilized oil-in-water emulsions (10% w/w oil).

3.2. Heat stability of MPC solutions with added sugar

The heat-induced casein micelle/whey protein interactions occurred in milk was expected to take place in a similar manner in a MPC solution since MPC contains similar components to that found in milk, caseins and whey proteins, in their native forms and also colloidal ash, calcium phosphate (O'Regan, Ennis, & Mulvihill, 2009). The HCT-pH profiles of 10% MPC solutions containing different types of sugar added at 0–30% w/w are compared in Fig. 2. They had similar shapes to that of the control 10% MPC solution but different heat stability maximum values. With the addition of 10% sugar, the heat stability maximum of the MPC solution shifted from pH 7.0 to pH 6.8 for glucose, maltose, sucrose, and trehalose but was unaffected for maltodextrin. In the presence of 20% sugar, the shape of the HCT-pH profile and the heat stability maximum of the MPC solution containing trehalose were unaffected whereas the other MPC solutions were affected. In general, the HCT decreased with the increase in sugar concentration. The pH at the heat stability maximum of the MPC solution containing sucrose did not change; however, the addition of glucose and maltose shifted the maximum to a more acidic value (pH 6.6) whereas the addition of maltodextrin shifted the maximum to a more alkaline value (pH 7.2). When the sugar concentration was further increased to 30%, the HCT decreased for all sugar types. The addition of glucose and maltose reduced the heat stability in the region of the maximum and the HCT was less dependent on the initial heating pH in the pH region 6.6–7.4. The heat stability maximum shifted to a more acidic value (from pH 6.8 to 6.6) on the addition of sucrose. The addition of maltodextrin continued to shift the maximum to a more alkaline value (pH 7.2–7.4), but no clear maximum was observed.

Appendix

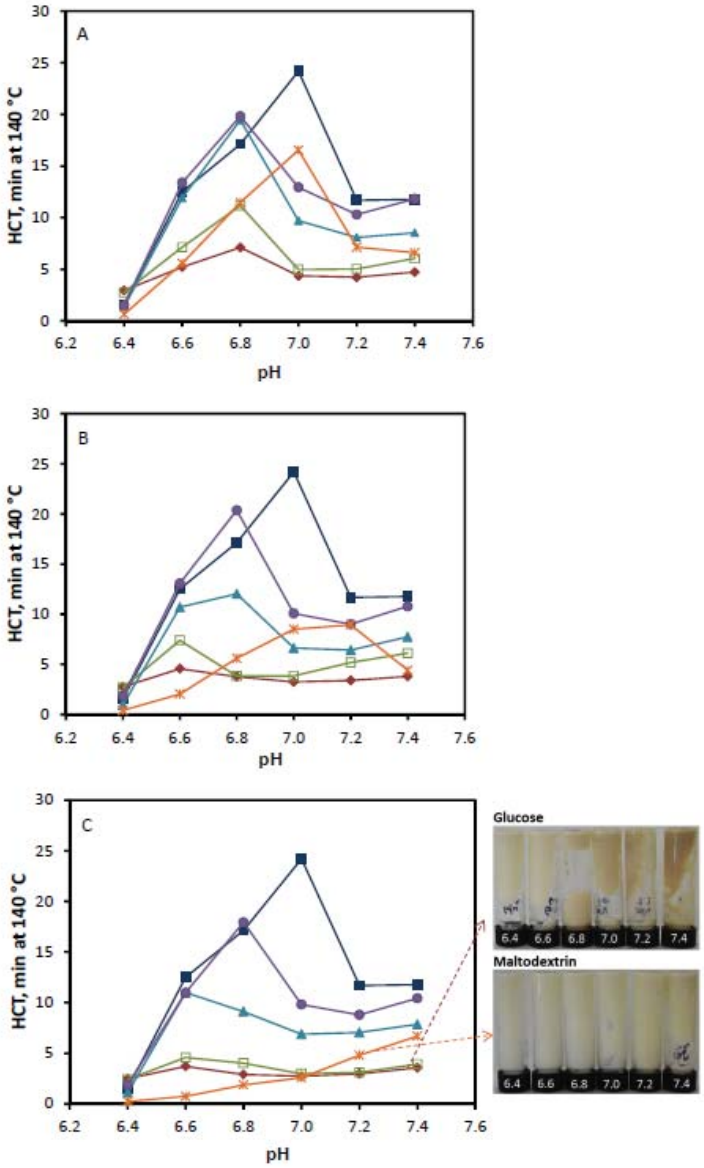

Fig. 2. HCT–pH profiles of 10% MPC solutions: with no added sugar (■) and with addition of (A) 10% w/w, (B) 20% w/w, (C) 30% w/w glucose (♦), maltose (□), sucrose (▲), trehalose (●), and maltodextrin (*). Visual images showed the colour of the heated MPC solutions containing glucose and maltodextrin as a function of pH, respectively.

The protein concentration effect in the continuous phase may partially contribute to the decrease in the HCT and the shift in the heat stability maximum to more acidic values as the sugar concentration increased. Fig. 3 shows that the HCT decreased in the region of the maximum and the heat stability maximum shifted to a more acidic pH value with increasing MPC concentration. The former phenomenon is consistent with previous results (Cruijsen, 1996; Sievanen, Huppertz, Kelly, & Fox, 2008). Fig. 4 indicates that there is a clear linear decline trend in the heat stability maximum of a MPC solution as protein concentration increases. It was assumed that the weight of the water phase of an MPC solution decreased upon addition of sugar and it will affect the HCT. The addition of sugar regardless of sugar type was shown to decrease the heat stability maximum of MPC solutions (Fig. 4).

However, the extent of change in the HCT varied among the sugar types. A shift in the pH of the heat stability maximum has also been observed in concentrated milk with the addition of sodium chloride (Huppertz & Fox, 2006a, 2006b). Reduced heat-induced dissociation of micellar κ-casein and increased micellar hydration has been attributed to the shift of the heat stability maximum to a

Appendix

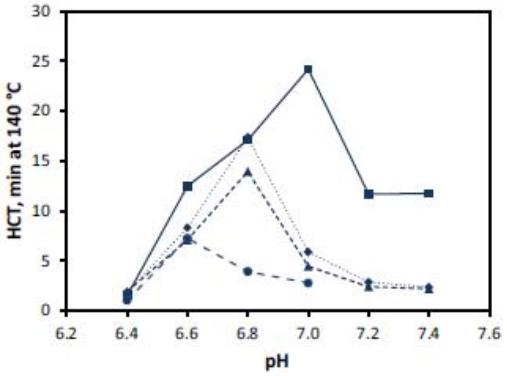

Fig. 3. HCT-pH profiles of MPC solutions at protein concentrations of 10% w/w (solid line), 12.5% w/w (round dot), 15%w/w (square dot), and 20% w/w (dash dot).

more alkaline value and the increase in the maximum HCT at a higher pH value (Huppertz & Fox, 2006a). Bridging due to the Maillard reaction has often been shown when reducing sugar is present during heating, especially at high pH values (Ashoor & Zent, 1984; Cruijsen, 1996). The heated MPC solutions containing 30% maltodextrin showed less browning than those containing 30% glucose at all pH values (maltose as well, data not shown), suggesting the Maillard reaction in maltodextrin containing samples have less contribution to the formation of covalent bonds which involve in casein–casein coagulation than the other two reducing sugars, glucose and maltose (analysis of the Maillard-induced protein aggregates will be the subject of a separate paper).

3.3. Heat stability of model MPC emulsions with added sugar

The HCT of the control 10% MPC-stabilized emulsion was lower than that of MPC solution over the entire pH range and the heat stability maximum shifted from pH 7.0 to pH 6.8 (Fig. 5). In general, across the entire pH range, adding sugars decreased the HCT of the 10% MPC-stabilized emulsions. The addition of 10% trehalose and sucrose to the emulsions slightly decreased while 10% added maltodextrin decreased the heat stability further still. The shapes of

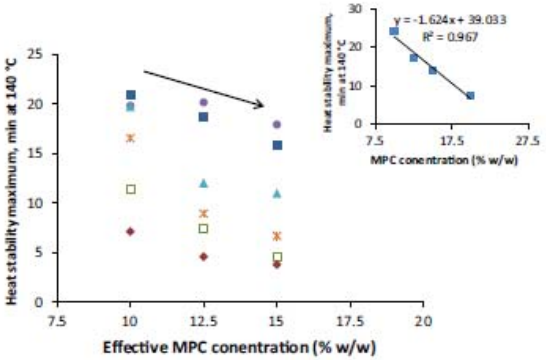

Fig. 4. The effect of protein concentration on the heat stability maximum of MPC solutions with no added sugar (■) and with the addition of 10–30% of glucose (♦), maltose (□), sucrose (▲), trehalose (●), and maltodextrin (✳). Heat stability maximum of MPC solutions containing sugar was obtained from Fig. 2. The effective protein concentration of MPC solutions was calculated based on the protein concentration in the water phase in which the weight of sugar was excluded. Inset: heat stability maximum obtained from Fig. 3 was plotted as a function of MPC concentration.

the HCT-pH profiles of trehalose and sucrose were similar while maltodextrin shifted the heat stability maximum from pH 6.8 to pH 7.0. The addition of 10% glucose and maltose decreased the heat stability markedly and shifted the heat stability maximum from pH 6.8 to pH 6.6 (Fig. 5). When trehalose and sucrose levels were increased to 20%, the heat stability of the emulsions decreased by ~8 min. However, the maximum heat stability occurred over a broader pH range for sucrose. The heat stability generally decreased slightly with the addition of 20% glucose, maltose, and maltodextrin; the HCTs of the emulsions with added glucose and maltose showed less dependence on the initial heating pH whereas the heat stability maximum of the emulsion containing maltodextrin shifted from pH 7.0 to 7.2, showing a similar trend to that of the corresponding oil-free solution. The addition of 30% sugar decreased the heat stability further. The heat stability maximum of those containing trehalose occurred over a broader pH range (6.8–7.4). The shapes of the HCT-pH profiles in MPC-stabilized emulsions containing glucose, maltose, and maltodextrin were similar to those of the oil-free MPC solutions.

The reduced HCT in MPC-stabilized emulsions compared with the solution systems resembled the heat stability change between milk and homogenized milk (Sweetsur & Muir, 1983). Upon adsorption, the adsorbed casein micelles partially spread at the oil/water interface into smaller fragments and may redistribute at the interface. Some κ-casein molecules may adsorb directly at the interface (Sharma & Singh, 1999). It can be assumed that the oil droplets are stabilized by intact casein micelles and some large micellar fragments and behave like large casein micelles as the κ-casein is still the main component governing the steric stability for the oil droplets. These large "casein micelles" may contain few κ-casein molecules per unit area at the oil/water interface. Therefore, the large oil droplets may act as κ-casein-depleted casein micelles (Sharma & Singh, 1999; Singh, Fox, & Cuddigan, 1993; Singh, Sharma, Taylor, & Creamer, 1996). It was observed that the κ-casein of adsorbed casein micelles had a greater tendency to dissociate into the continuous phase in the pH range 6.3–6.7 than the κ-casein that dissociates from bulk casein micelles upon high temperature heating (i.e., >130 °C). Even a small reduction of κ-casein content from the oil droplets that are already short of κ-casein content will have a considerable impact on the heat stability (Singh et al., 1996). Therefore, in addition to the concentration effect, those aforementioned physicochemical changes of adsorbed casein micelles are also attributed to a lower heat stability of emulsions.

3.4. Correlations between particle size, microstructure and rheological properties of heated MPC emulsions with added sugar

The effect of heat treatment at 120 °C on the physicochemical changes of MPC-stabilized emulsions containing 30% sugar was studied. Fig. 6 shows an example of particle size distribution of heated MPC-stabilized emulsions containing sugar. All the unheated MPC-stabilized emulsions showed a population of casein micelles and a second population of oil droplets. As the heating time increased, the particle size distribution of the emulsion changed from bimodal to multi-modal. The additional mode showed large particles rather than individual droplets, indicating aggregation of casein micelles, droplets and mixtures of both. The population of those aggregates generally grew in number and diameter and there was a corresponding decrease in the number of casein micelles and droplets. It has been reported that the heat-induced interparticle interactions of an oil-in-water emulsion include those between interfacial proteins, between interfacial proteins and non-adsorbed proteins and between non-adsorbed proteins (Dalgleish, 2006; Euston, Finnigan, & Hirst, 2000; Liang

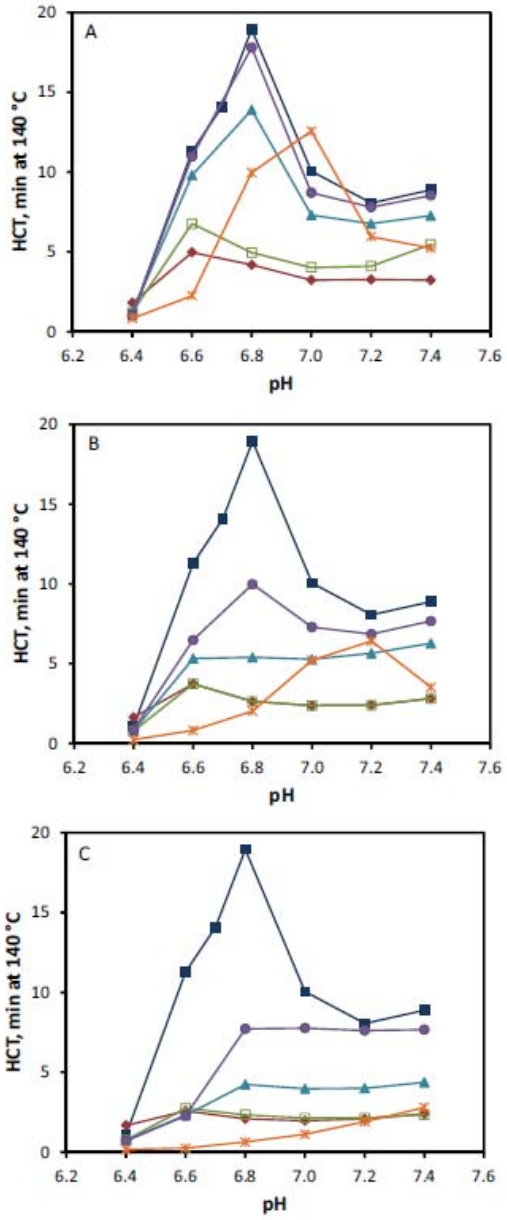

Fig. 5. HCT-pH profiles of MPC-stabilized oil-in-water emulsions (10% w/w protein, 10% w/w oil): with no added sugar (■) and with the addition of (A) 10% w/w, (B) 20% w/w, (C) 30% w/w glucose (♦), maltose (□), sucrose (▲), trehalose (●), and maltodextrin (+).

et al., 2013b). The non-adsorbed unfolded globular proteins play an important role in the formation of large aggregates during heating (Euston, Al-Bakkush, & Campbell, 2009; Euston et al., 2000; Nikiforidis & Kiosseoglou, 2007).

In general, the effect of heat treatment on the particle size of MPC-stabilized emulsions with and without added sugar was consistent with measurements on microstructure and rheology.

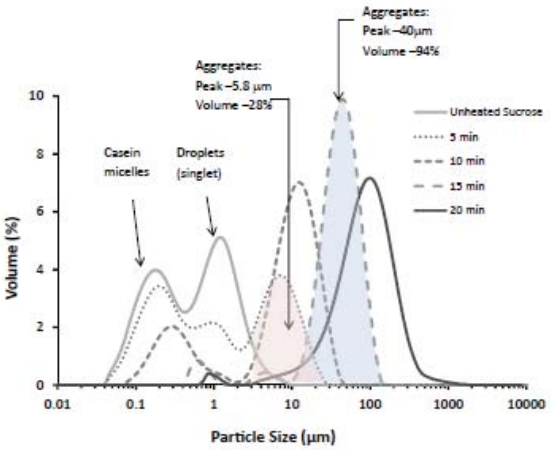

Fig. 6. Effective particle size distributions of unheated and heated (120 °C for up to 20 min at pH 6.8) MPC-stabilized oil-in-water emulsions (10% w/w protein, 10% w/w oil) with 30% w/w sucrose. Shaded region indicates how aggregates are described in other figures.

Given this consistency, only the essential features of the aggregation are presented. Aggregates are described by their relative volume in the distribution and the peak size and confocal micrographs were presented occasionally to demonstrate similarities and differences. In MPC-stabilized emulsion system, heat-induced bridging was expected, unlike the colloid system described in Liang and co-workers' earlier study (2014), where aggregates are in equilibrium with single droplets. Aggregates here do not redisperse. The adhesion of protein–protein and droplet–droplet is too strong due to the presence of covalent bridges. The lack of redispersion was evident from the particle size distribution data (Fig. 5) and the fact that large aggregates were not fully dissolved in the dissociating agent (1 mM of Tween 20 and 12.8 mM of EDTA, pH 10).

Here, the viscosity index (η_t/η_0) is used to indicate the aggregation of the samples. For the MPC emulsions containing glucose and maltose, there was little change in particle size during the initial stage of heating (Fig. 7A). The peak size of aggregates in maltose samples increased from 5 to 60 μm with a volume that increased from 4 to 91% during heating from 3 to 5 min. The corresponding viscosity index increased steadily with increased heating time. In glucose samples, the peak size of aggregates increased more rapidly from 5 μm at 4 min of heating to 158 μm after 5 min of heating. Correspondingly, the viscosity index increased markedly from 1.7 at 2 min of heating to 961 after 5 min of heating, which is more than 8 times higher than that of a weakly attractive colloid as calculated from the extracted viscosity data from Liang et al. (2014). The differences between glucose and maltose indicate a significant difference in steric stability with less steric stability in the glucose sample. From 4 to 5 min, the volume of aggregates is similar but a big increase in size occurred due to aggregation of aggregates. During the same time interval, maltose samples showed a steady loss of droplets with increasing aggregation size, no clear indication of a particular aggregation mechanism dominating. As it can be seen from the confocal micrographs, the droplets of glucose containing sample aggregated into clusters and appeared to be associated within a gel-like network. On the other hand, the maltose containing sample had more homogeneous droplet distributions at the same heating intervals than glucose, however, with further heating towards the HCT (~6.5 min), the

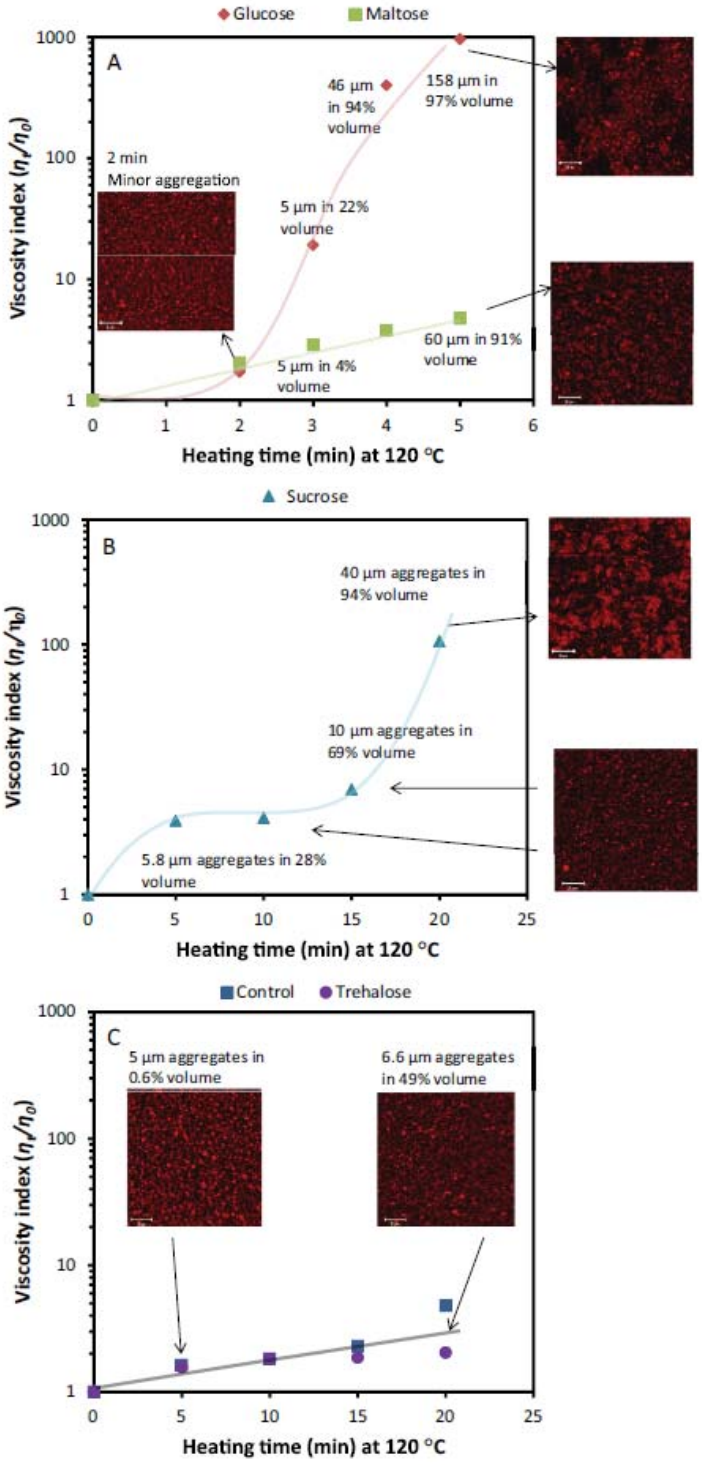

Fig. 7. Aggregation time lines of the heat-induced physicochemical changes of model MPC emulsions in terms of particle size, microstructure and viscosity. Viscosity index (η_r/η_0) of unheated and heated (120 °C, pH 6.8) MPC-stabilized oil-in-water emulsions (10% w/w protein, 10% w/w oil) with and without 30% w/w added sugar at 20 °C: (A) glucose (♦) and maltose (■); (B) sucrose (▲); (C) control (■) and trehalose (●). Confocal micrographs show the fat signal only, scale is identical in all images with 20 µm scale bars. Data labels indicate the essential features size and volume taken from particle size distributions (Fig. 5). The lines are drawn to guide the eye.

Appendix

microstructure was essentially similar to that for glucose. The sudden jump in viscosity index with a marked increase in peak size of aggregates and an open gel-like structure with increased amount of void area is a common feature in these systems. A dramatic jump in aggregation indicates steric stability has fallen below a critical level, and perhaps associates with the loss of steric stability with a rate of reaction like the sharp increase in gelation kinetic of casein micelles during acidification (Vasbinder, van de Velde, & de Kruif, 2004).

For the other reducing sugar, maltodextrin, all samples (2, 4, 6 min) formed a visible coagulum upon heating at 120 °C and no further particle size measurements were performed. It is important to note that the MPC-stabilized emulsion with added maltodextrin had a larger droplet/particle size even before heating. Fig. 8 shows that the two major peaks shifted towards larger sizes, suggesting that some large aggregates may have formed and that they were not disrupted by dilution and shear. These large aggregates also appeared in MPC-maltodextrin mixed solutions (data not shown). However, this phenomenon was not seen with the addition of 10% and 20% maltodextrin. These large aggregates were dissociated with the addition of the dissociating agent, when the primary droplet size was measured (Table 2). The particle size result suggests that a multi-layer may have formed at the oil/water interface or a bridging-type droplet/protein flocculate has formed and that it is probably linked by non-covalent bonds (Cruijsen, 1996). It has been shown that bridging-type flocculation of droplets are more susceptible to heat-induced destabilization (Liang et al., 2013a).

The emulsions containing two non-reducing sugars (sucrose and trehalose) showed less susceptibility to heat-induced aggregation than reducing sugars. For the emulsions containing sucrose, the particle size increased moderately from 0 to 15 min of heating with an appearance of 10 μm aggregates after 15 min (Fig. 7B). Further heating to 20 min, the size of aggregate changed markedly with a shifting to 40 μm and the volume increased from 69% to 94%. The confocal micrographs of sucrose containing sample showed a relatively homogeneous distribution of droplet size after heating for up to 15 min; on heating for 20 min, the droplets tended to form clusters and an interconnected droplet pattern became apparent. The emulsion containing trehalose was more resistant to heat-induced protein/oil droplet aggregation than that containing sucrose and was comparable with the control MPC-stabilized emulsion (Fig. 7C). The particle size slightly increased after 5 min of heating but there was little change in the growth of particle size between 5 and 10 min. A peak of aggregates of 6.6 μm was apparent only after 20 min of heating and the aggregate volume (49%) was nearly half of that of sucrose containing sample.

Cruijsen (1996) concluded that the heat-induced destabilization mechanisms of caseinate-stabilized emulsions containing sugar include: (1) dephosphorylation of the caseins; (2) hydrolysis of the caseins; (3) deposition of insoluble calcium phosphate on casein micelles; (4) the formation of acids, resulting in a decrease in pH to close to the isoelectric point of the caseins; (5) increase in calcium ion activity. As the calcium ion concentration has a direct correlation with the heat stability of milk, concentrated milk, and protein-stabilized emulsion systems (Cruijsen, 1996; Faka, Lewis, Grandison, & Deeth, 2009; Lewis, 2011; Sievanen et al., 2008), the effect of sugar concentration on the free calcium ions in MPC-stabilized emulsions without and with added sugars can be assessed. Fig. 9 shows the equilibrium relationship between the logarithm of the free calcium ion concentration and the pH. The logarithm of the free calcium ion concentration decreased linearly (the lowest R^2 value was 0.963) as the pH increased, regardless of the addition of sugar. The average slope value was −0.605 and the standard deviation was 0.064. The slopes of the curves were very similar among the sugar types, except for 30% maltodextrin when

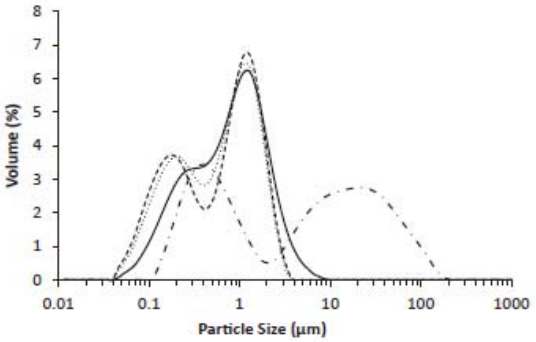

Fig. 8. Effective particle size distributions of unheated MPC-stabilized oil-in-water emulsions at pH 6.8 (10% w/w protein, 10% w/w oil): control (solid line); containing 10% w/w maltodextrin (dotted line), containing 20% w/w maltodextrin (dashed line), and containing 30% w/w maltodextrin (dashed dotted line).

the slope was −0.72. These results were in very good agreement with previous studies in milk (Tsioulpas, Lewis, & Grandison, 2007). Regardless of concentration, the addition of glucose resulted in slightly higher log free calcium ion values than for the control and the other sugar types. There was no significant difference in the log free calcium ion values for maltose, sucrose, trehalose, and maltodextrin at up to 20% addition (Fig. 9A and B). The addition of 30% sugar resulted in a marked difference in the log free calcium ion values between the control and the emulsions containing sugar. The emulsion containing 30% maltodextrin had a slightly higher log free calcium ion value from pH 6.4 to pH 6.8 than those containing the other sugar types except glucose. It has been suggested that increase in activity coefficient results in an increased Ca^{2+} activity in milk-based system (Gao et al., 2010). An increase in excluded volume effect causes ions behave far more nonideally in a single concentrated sugar solution regardless of sugar type. The presence of proteins or other type of sugar like lactose will enhance the excluded volume effect. Hence, the excluded volume accounts for the change of thermodynamic properties of ions in a sugar-concentrated milk system (Gao et al., 2010).

Several other factors may also explain the better heat stability of MPC-stabilized emulsions with added non-reducing sugars than those with added reducing sugars. Recent studies have revealed that sucrose and trehalose have stabilizing effects against heat-induced globular protein aggregation by increasing the thermal denaturation temperature of the proteins, such as bovine serum albumin (Panzica et al., 2012) and β-lactoglobulin (Tang & Pikal, 2005). Panzica et al. (2012) have indicated that the solvent quality effect governed by sucrose and trehalose is responsible for the initial stages of protein aggregation. In addition, although the Maillard type reaction between reducing sugars and proteins was not our emphasis, it is noteworthy that sucrose and trehalose are more resistant than glucose to hydrolysis of the glycosidic bonds (O'Brien, 1996).

In addition, the presence of sugar can potentially affect the solvent quality of the water phase and cause partial collapse of the κ-casein on the casein micelles and on the surface of the oil droplets, reducing the steric stabilization during heating. Schorsch, Jones, and Norton (2002) proposed that the addition of sucrose (up to 30% w/w) reduces the solvent quality and causes the collapse of the κ-casein layer of casein micelles when combined with the decreased pH during acidification based on the fact that a rennet-

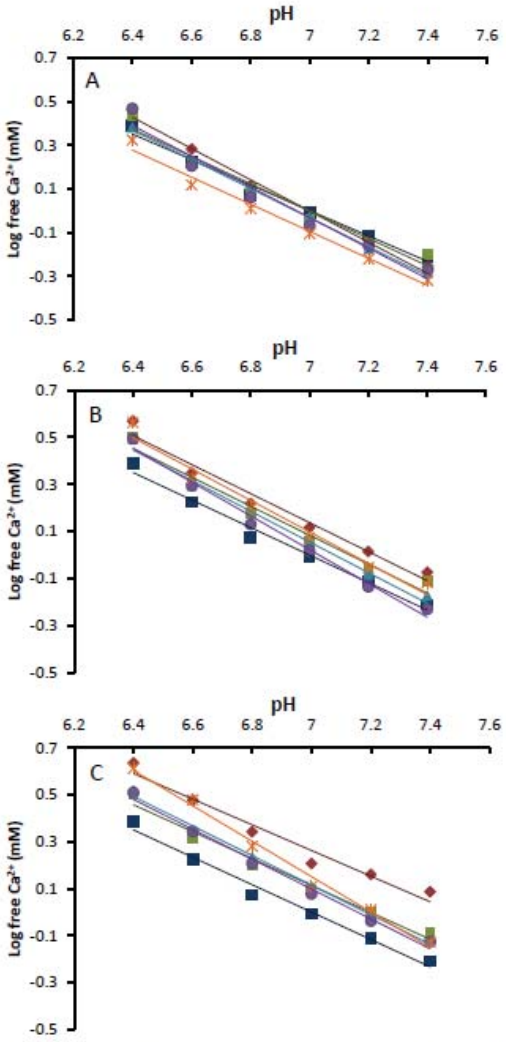

Fig. 9. Effect of pH on the logarithm of the free calcium ion concentration of MPC-stabilized emulsions with no added sugar (■) and with the addition of (a) 10% w/w, (b) 20%, w/w (c) 30% w/w glucose (♦), maltose (▩), sucrose (▲), trehalose (●), and maltodextrin (✳).

induced casein gel was weaker and had a longer gelation time. Reduced particle sizes of non-micellar caseins upon the addition of sucrose and trehalose have also been reported (Álvarez-Cerimedo et al., 2010; Belyakova et al., 2003; Dickinson & Matia Merino, 2002).

4. Conclusions

This study has demonstrated the effect of the addition of sugar on the droplet size and the heat coagulation of MPC-stabilized emulsions in high solid systems. It was found that, the addition of sugar slightly increased the droplet diameter except that the addition of 30% w/w maltodextrin significantly ($p < 0.05$) decreased the droplet diameter during emulsification. This could be attributed to the large change in disperse/continuous phase viscosity ratio. Close to the HCT, the viscosity index increased sharply corresponding to the aggregation of the aggregates and interconnected droplet clusters. Adding sugar decreases HCT of MPC solutions and emulsions suggests adding sugar generally decreases the repulsive force between protein particles and between droplets. This effect is strongly dependent on the sugar type and concentration. Heat-induced increases in aggregate size were more extensive with increasing molecular weight of the sugar. Reducing sugars showed faster coagulation and more browning suggesting the Maillard reaction accelerates the destabilization. Non-reducing sugars were more effective, especially Trehalose, in retaining the original heat stability of MPC solutions and emulsions. Several factors, including free calcium ion level, volume fraction and solvent quality of the continuous phase protein, will affect the heat stability of MPC-stabilized emulsions with added sugars.

The incorporation of other components in complex food/dairy formulations such as, low molecular weight surfactants, calcium/magnesium salts and sodium polyphosphates is known to have a large impact on the heat coagulation behaviour of concentrated milk and micellar casein solutions. The results presented in this study are useful for extending our understanding of the behaviour of casein micelles in systems containing high protein and high carbohydrate. Such insights will facilitate the formulation and stability prediction of recombined high protein beverages containing complex ingredients and can be utilized to create desirable droplet sizes and structures to maintain stability against creaming without large compromise with the heat stability.

Acknowledgements

The authors gratefully thank the Fonterra Research and Development Centre and the Foundation for Research, Science and Technology for financial support, Skelte Anema and Ran Gao for their useful discussions, and Claire Woodhall for her assistance in proof reading.

References

Álvarez-Cerimedo, M. S., Iriart, C. H., Candal, R. J., & Herrera, M. L. (2010). Stability of emulsions formulated with high concentrations of sodium caseinate and trehalose. *Food Research International, 43*, 1482–1493.
Ashoor, S. H., & Zent, J. B. (1984). Maillard browning of common amino acids and sugars. *Journal of Food Science, 49*, 1206–1207.
Baier, S., & McClements, D. J. (2001). Impact of preferential interactions on thermal stability and gelation of bovine serum albumin in aqueous sucrose solutions. *Journal of Agricultural and Food Chemistry, 49*, 2600–2608.
Beliciu, C. M., Sauer, A., & Moraru, C. I. (2012). The effect of commercial sterilization regimens on micellar casein concentrates. *Journal of Dairy Science, 95*, 5510–5526.
Belyakova, L. E., Antipova, A. S., Semenova, M. G., Dickinson, E., Merino, L. M., & Tsapkina, E. N. (2003). Effect of sucrose on molecular and interaction parameters of sodium caseinate in aqueous solution: relationship to protein gelation. *Colloids and Surfaces B: Biointerfaces, 31*, 31–46.
van Boekel, M. A. J. S., Nieuwenhuijse, J. A., & Walstra, P. (1989a). The heat coagulation of milk. 1. Mechanisms. *Netherlands Milk and Dairy Journal, 43*, 97–127.
van Boekel, M. A. J. S., Nieuwenhuijse, J. A., & Walstra, P. (1989b). The heat coagulation of milk. 2. Kinetic studies. *Netherlands Milk and Dairy Journal, 43*, 129–146.
van Boekel, M. A. J. S., Nieuwenhuijse, J. A., & Walstra, P. (1989c). The heat coagulation of milk. 3. Comparison of theory and experiment. *Netherlands Milk and Dairy Journal, 43*, 147–162.
Chanamai, R., & McClements, D. J. (2000). Impact of weighting agents and sucrose on gravitational separation of beverage emulsions. *Journal of Agricultural and Food Chemistry, 48*, 5561–5565.
Crowe, J. (2007). *Trehalose as a "chemical chaperone"*. In P. Csermely, & L. Vigh (Eds.), *Molecular aspects of the stress response: Chaperones, membranes and networks* (Vol. 594); (pp. 143–158). New York: Springer.
Cruijsen, J. M. M. (1996). *Physical stability of caseinate-stabilized emulsions during heating*. Agricultural University of Wageningen.
Dalgleish, D. G. (2006). Food emulsions–their structures and structure-forming properties. *Food Hydrocolloids, 20*, 415–422.

Appendix

Dickinson, E., & Matia Merino, L. (2002). Effect of sugars on the rheological properties of acid caseinate-stabilized emulsion gels. *Food Hydrocolloids, 16*, 321–331.
Euston, S. R., Al-Bakkush, A.-A., & Campbell, L. (2009). Comparing the heat stability of soya protein and milk whey protein emulsions. *Food Hydrocolloids, 23*, 2485–2492.
Euston, S. R., Finnigan, S. R., & Hirst, R. L. (2000). Aggregation kinetics of heated whey protein-stabilized emulsions. *Food Hydrocolloids, 14*, 155–161.
Euston, S. R., & Hirst, R. L. (1999). Comparison of the concentration-dependent emulsifying properties of protein products containing aggregated and non-aggregated milk protein. *International Dairy Journal, 9*, 693–701.
Faka, M., Lewis, M. J., Grandison, A. S., & Deeth, H. (2009). The effect of free Ca^{2+} on the heat stability and other characteristics of low-heat skim milk powder. *International Dairy Journal, 19*, 386–392.
Gao, R., van Leeuwen, H. P., Temminghoff, E. J., van Valenberg, H. J., Eisner, M. D., & van Boekel, M. A. (2010). Effect of disaccharides on ion properties in milk-based systems. *Journal of Agricultural and Food Chemistry, 58*, 6449–6457.
Ghosh, S., Cramp, G. L., & Coupland, J. N. (2006). Effect of aqueous composition on the freeze-thaw stability of emulsions. *Colloids and Surfaces A: Physicochemical and Engineering Aspects, 272*, 82–88.
Holt, C., Muir, D. D., & Sweetsur, A. W. M. (1978). The heat stability of milk and concentrated milk containing added aldehydes and sugars. *Journal of Dairy Research, 45*, 47–52.
Huppertz, T., & Fox, P. F. (2006a). Effect of NaCl on some physico-chemical properties of concentrated bovine milk. *International Dairy Journal, 16*, 1142–1148.
Huppertz, T., & Fox, P. F. (2006b). Influence of added lyophilized butter serum on the heat stability of unconcentrated and concentrated bovine milk. *International Journal of Dairy Technology, 59*, 18–21.
Jain, N. K., & Roy, I. (2009). Effect of trehalose on protein structure. *Protein Science, 18*, 24–36.
Kasinos, M., Tran Le, T., & Van der Meeren, P. (2014). Improved heat stability of recombined evaporated milk emulsions upon addition of phospholipid enriched dairy by-products. *Food Hydrocolloids, 34*, 112–118.
Keowmaneechai, E., & McClements, D. J. (2006). Influence of EDTA and citrate on thermal stability of whey protein stabilized oil-in-water emulsions containing calcium chloride. *Food Research International, 39*, 230–239.
Kim, H. J., Decker, E. A., & McClements, D. J. (2003). Influence of sucrose on droplet flocculation in hexadecane oil-in-water emulsions stabilized by β-lactoglobulin. *Journal of Agricultural and Food Chemistry, 51*, 766–772.
de Kort, E., Minor, M., Snoeren, T., van Hooijdonk, T., & van der Linden, E. (2011). Effect of calcium chelators on physical changes in casein micelles in concentrated micellar casein solutions. *International Dairy Journal, 21*, 907–913.
de Kort, E., Minor, M., Snoeren, T., van Hooijdonk, T., & van der Linden, E. (2012). Effect of calcium chelators on heat coagulation and heat-induced changes of concentrated micellar casein solutions: the role of calcium-ion activity and micellar integrity. *International Dairy Journal, 26*, 112–119.
Kulmyrzaev, A., Bryant, C., & McClements, D. J. (2000). Influence of sucrose on the thermal denaturation, gelation, and emulsion stabilization of whey proteins. *Journal of Agricultural and Food Chemistry, 48*, 1593–1597.
Lee, L., & Norton, I. T. (2013). Comparing droplet breakup for a high-pressure valve homogeniser and a microfluidizer for the potential production of food-grade nanoemulsions. *Journal of Food Engineering, 114*, 158–163.
Lewis, M. J. (2011). The measurement and significance of ionic calcium in milk – a review. *International Journal of Dairy Technology, 64*, 1–13.
Liang, Y., Gillies, G., Patel, H., Matia-Merino, L., Ye, A., & Golding, M. (2014). Physical stability, microstructure and rheology of sodium-caseinate-stabilized emulsions as influenced by protein concentration and non-adsorbing polysaccharides. *Food Hydrocolloids, 36*, 245–255.
Liang, Y., Patel, H., Matia-Merino, L., Ye, A., & Golding, M. (2013a). Effect of pre- and post-heat treatments on the physicochemical, microstructural and rheological properties of milk protein concentrate-stabilised oil-in-water emulsions. *International Dairy Journal, 32*, 184–191.
Liang, Y., Patel, H., Matia-Merino, L., Ye, A., & Golding, M. (2013b). Structure and stability of heat-treated concentrated dairy-protein-stabilised oil-in-water emulsions: a stability map characterisation approach. *Food Hydrocolloids, 33*, 297–308.
Li, C., Fu, X., Luo, F., & Huang, Q. (2013). Effects of maltose on stability and rheological properties of orange oil-in-water emulsion formed by OSA modified starch. *Food Hydrocolloids, 32*, 79–86.
McClements, D. J. (2005). Food Emulsions: Principles, Practices, and Techniques (2nd ed.). CRC Press, Boca Raton, FL.
McSweeney, S. L., Healy, R., & Mulvihill, D. M. (2008). Effect of lecithin and monoglycerides on the heat stability of a model infant formula emulsion. *Food Hydrocolloids, 22*, 888–898.
McSweeney, S. L., Mulvihill, D. M., & O'Callaghan, D. M. (2004). The influence of pH on the heat-induced aggregation of model milk protein ingredient systems and model infant formula emulsions stabilized by milk protein ingredients. *Food Hydrocolloids, 18*, 109–125.
Nikiforidis, C. V., & Kiosseoglou, V. (2007). The role of Tween in inhibiting heat-induced destabilization of yolk-based emulsions. *Food Hydrocolloids, 21*, 1310–1318.
O'Brien, J. (1996). Stability of trehalose, sucrose and glucose to nonenzymatic browning in model systems. *Journal of Food Science, 61*, 679–682.
O'Connell, J. E., & Fox, P. F. (2003). Heat-induced coagulation of milk. In P. F. Fox, & P. L. McSweeney (Eds.), *Advanced dairy chemistry 1. Proteins* (3rd ed.) (pp. 879–930). London: Elsevier Applied Science.
O'Regan, J., Ennis, M. P., & Mulvihill, D. M. (2009). Milk proteins. In G. O. Philips, & P. A. Williams (Eds.), *Handbook of hydrocolloids* (2nd ed.) (pp. 299–358). Boca Raton, FL: CRC Press.
Panzica, M., Emanuele, A., & Cordone, L. (2012). Thermal aggregation of bovine serum albumin in trehalose and sucrose aqueous solutions. *The Journal of Physical Chemistry B, 116*, 11829–11836.
Pauletti, M. S., Castelao, E. L., & Seguro, E. (1996). Kinetics of heat coagulation of concentrated milk proteins at high sucrose contents. *Journal of Food Science, 61*, 1207–1210.
Qian, C., & McClements, D. J. (2011). Formation of nanoemulsions stabilized by model food-grade emulsifiers using high-pressure homogenization: factors affecting particle size. *Food Hydrocolloids, 25*, 1000–1008.
Rattray, W., & Jelen, P. (1997). Thermal stability of skim milk/whey protein solution blends. *Food Research International, 30*, 327–334.
Sauer, A., & Moraru, C. I. (2012). Heat stability of micellar casein concentrates as affected by temperature and pH. *Journal of Dairy Science, 95*, 6339–6350.
Sağlam, D., Venema, P., de Vries, R., Shi, J., & van der Linden, E. (2013). Concentrated whey protein particle dispersions: heat stability and rheological properties. *Food Hydrocolloids, 30*, 100–109.
Schorsch, C., Jones, M. G., & Norton, I. T. (2002). Micellar casein gelation at high sucrose content. *Journal of Dairy Science, 85*, 3155–3163.
Semenova, M. G., Antipova, A. S., & Belyakova, L. E. (2002). Food protein interactions in sugar solutions. *Current Opinion in Colloid and Interface Science, 7*, 438–444.
Sharma, R., & Singh, H. (1999). Heat stability of recombined milk systems as influenced by the composition of fat globule surface layers. *Milchwissenschaft, 54*, 193–196.
Sievanen, K., Huppertz, T., Kelly, A. L., & Fox, P. F. (2008). Influence of added calcium chloride on the heat stability of unconcentrated and concentrated bovine milk. *International Journal of Dairy Technology, 61*, 151–155.
Singh, H. (2004). Heat stability of milk. *International Journal of Dairy Technology, 57*, 111–119.
Singh, H., Fox, P. F., & Cuddigan, M. (1993). Emulsifying properties of protein fractions prepared from heated milk. *Food Chemistry, 47*, 1–6.
Singh, H., Sharma, R., Taylor, M. W., & Creamer, L. K. (1996). Heat-induced aggregation and dissociation of protein and fat particles in recombined milk. *Netherlands Milk and Dairy Journal, 50*, 149–166.
Srinivasan, M., Singh, H., & Munro, P. A. (2002). Formation and stability of sodium caseinate emulsions: influence of retorting (121°C for 15 min) before or after emulsification. *Food Hydrocolloids, 16*, 153–160.
Srinivasan, M., Singh, H., & Munro, P. A. (2003). Influence of retorting (121 °C for 15 min), before or after emulsification, on the properties of calcium caseinate oil-in-water emulsions. *Food Chemistry, 80*, 61–69.
Sweetsur, A. W. M., & Muir, D. D. (1983). Effect of homogenization on the heat stability of milk. *Journal of Dairy Research, 50*, 291–300.
Tan-Kintia, R. H., & Fox, P. F. (1996). Effect of enzymic hydrolysis of lactose on the heat stability of milk or concentrated milk. *Netherlands Milk and Dairy Journal, 50*, 267–277.
Tang, X., & Pikal, M. (2005). The effect of stabilizers and denaturants on the cold denaturation temperatures of proteins and implications for freeze-drying. *Pharmaceutical Research, 22*, 1167–1175.
Tsioulpas, A., Koliandris, A., Grandison, A. S., & Lewis, M. J. (2010). Effects of stabiliser addition and in-container sterilisation on selected properties of milk related to casein micelle stability. *Food Chemistry, 122*, 1027–1034.
Tsioulpas, A., Lewis, M. J., & Grandison, A. S. (2007). Effect of minerals on casein micelle stability of cows' milk. *Journal of Dairy Research, 74*, 167–173.
Vasbinder, A. J., van de Velde, F., & de Kruif, C. G. (2004). Gelation of casein-whey protein mixtures. *Journal of Dairy Science, 87*, 1167–1176.
Walstra, P., Wouters, J. T. M., & Geurts, T. J. (2006). *Dairy science and technology* (2nd ed.). CRC Press.
Wooster, T. J., Golding, M., & Sanguansri, P. (2008). Impact of oil type on nanoemulsion formation and Ostwald ripening stability. *Langmuir, 24*, 12758–12765.
Xiong, Y. (1997). Protein denaturation and functionality losses. In M. Erickson, & Y.-C. Hung (Eds.), *Quality in frozen food* (pp. 111–140). US: Springer.
Ye, A. (2011). Functional properties of milk protein concentrates: emulsifying properties, adsorption and stability of emulsions. *International Dairy Journal, 21*, 14–20.

Paper Four

(This published work is from Chapter 8)

Appendix

International Dairy Journal 32 (2013) 184–191

Contents lists available at SciVerse ScienceDirect

International Dairy Journal

journal homepage: www.elsevier.com/locate/idairyj

Effect of pre- and post-heat treatments on the physicochemical, microstructural and rheological properties of milk protein concentrate-stabilised oil-in-water emulsions

Yichao Liang [a,b,*], Hasmukh Patel [c], Lara Matia-Merino [b], Aiqian Ye [d], Matt Golding [b,d,*]

[a] Fonterra Research and Development Centre, Private Bag 11 029, Palmerston North 4442, New Zealand
[b] Institute of Food, Nutrition and Human Health, Massey University, Private Bag 11 222, Palmerston North 4442, New Zealand
[c] Dairy Science Department, Box 2104, South Dakota State University, Brookings, SD 57007, USA
[d] Riddet Institute, Massey University, Private Bag 11 222, Palmerston North 4442, New Zealand

ARTICLE INFO

Article history:
Received 27 December 2012
Received in revised form
12 May 2013
Accepted 12 May 2013

ABSTRACT

The effect of heat treatment on the physical stability of milk protein concentrate (MPC) stabilised emulsions was investigated; 3% (w/w) MPC dispersions were preheated at 90 °C for 5 min at neutral pH prior to emulsification. Heat-treated (120 °C, 10 min) emulsions stabilised by preheated MPC had slightly fewer droplet–droplet interactions than that stabilised by unheated MPC because the whey proteins were pre-denatured (~90% denaturation of the total whey proteins), which led to a reduction in subsequent heat-induced droplet–droplet and droplet–protein interactions. Emulsions stabilised by calcium-depleted MPC were also investigated. The presence of some non-micellar casein fractions gave better emulsification and may have conferred a protective stabilising effect on whey protein aggregation, in both the dispersed phase and the continuous phase during the secondary heat treatment. It was concluded that calcium manipulation and thermal modification of MPC can be utilised to control the functionality in oil-in-water emulsions.

1. Introduction

Milk proteins are widely used to stabilise emulsion droplets. Flocculation, one of the main causes of the instability of protein-stabilised emulsions, can lead to accelerated creaming, an increase in viscosity and sedimentation, all of which greatly reduce the product quality (Dickinson, 2010; McClements, 2005). Stabilising emulsion droplets in milk-protein-based food emulsions against heat-induced flocculation is a challenge. This is particularly true for meal replacement beverages, sport drinks and infant formulae, which are usually sterilised by retort processing (i.e., 120 °C for 5–10 min) or ultra-high-temperature sterilisation (i.e., 140 °C for 3–5 s) (Keowmaneechai & McClements, 2006; McSweeney, Healy, & Mulvihill, 2008). Heat-induced flocculation can lead to rapid creaming, because the formation of protein-linked droplet clusters effectively increases the hydrodynamic diameter of the droplets, which in turn influences the rheological and creaming behaviours of emulsions (McClements, 2005).

The type of milk protein plays an important role in the physicochemical properties of an oil-in-water emulsion. Emulsions stabilised with caseinates are known to be relatively heat stable (Srinivasan, Singh, & Munro, 2002), whereas emulsions stabilised with whey proteins at the same protein concentration tend to aggregate or even gel because of interactions between droplets and with the surrounding continuous phase protein (Livney, Corredig, & Dalgleish, 2003). The incorporation of small amounts of individual casein fractions, micellar caseins or caseinates has been shown to inhibit extensive heat-induced whey protein aggregation in solutions (Guyomarc'h, Nono, Nicolai, & Durand, 2009; O'Kennedy & Mounsey, 2006) and milk-protein-stabilised oil-in-water emulsions (Parkinson & Dickinson, 2007). In the latter study, the inhibition of heat-induced destabilisation of the emulsion droplets was due to enhanced steric repulsive forces at the oil–water interface; the charged hydrophilic chains (loops and tails) of adsorbed casein molecules protruded into the continuous phase and prevented neighbouring droplets from colliding. Similar mechanisms have been reported in emulsions stabilised by protein–polysaccharide conjugates (O'Regan & Mulvihill, 2010).

Milk protein concentrate (MPC) is a spray-dried powder product that is manufactured from skim milk using ultrafiltration and diafiltration processes. Standard MPC is a high protein and low lactose

* Corresponding authors. Tel.: +64 6 350 4640x64754.
E-mail addresses: liendisonliang@fonterra.com (Y. Liang), MGolding@massey.ac.nz (M. Golding).

0958-6946/$ – see front matter © 2013 Elsevier Ltd. All rights reserved.
http://dx.doi.org/10.1016/j.idairyj.2013.05.012

Appendix

powder in which the casein is in its micellar form, similar to that found in milk, and the whey proteins are also mainly in their native form. Protein-bound minerals are retained (O'Regan, Ennis, & Mulvihill, 2009). The compositions and functionalities of different MPCs will vary and will be further affected by modifications during processing. It has been reported that the ethanol and heat stability of casein micelles increase upon the reduction of colloidal calcium content. Those changes are closely related to the aggregation state of the casein micelles and the calcium ion activity (Grimley, Grandison, & Lewis, 2010).

Skim milk solutions are heat treated not only to prevent plasmin-type proteolysis (Newstead, Paterson, Anema, Coker, & Wewala, 2006), but also to tailor the functionalities of milk proteins (Augustin & Udabage, 2007; Faka, Lewis, Grandison, & Deeth, 2009) and, in turn, to alter the physical properties of milk protein-stabilised emulsions (Raikos, 2010). Heating sodium caseinate and calcium caseinate dispersions by retort processing prior to emulsification increased the surface protein coverage and improved the creaming stability of the final emulsions, which was attributed to the increased size of the non-adsorbed protein and the increased viscosity of the continuous phase after heating (Srinivasan et al., 2002; Srinivasan, Singh, & Munro, 2003). Preheat treatment of protein dispersions prior to homogenisation has also been reported to influence the droplet size distribution, creaming stability and rheological properties of MPC-stabilised emulsions (Dybowska, 2008). The emulsion droplet size increased when the protein solution was heated before emulsification. However, the adsorption of more protein molecules at the oil–water interface increases the density of the interfacial layer, resulting in an overall enhanced stability against creaming (Dybowska, 2008, 2011).

There is extensive literature on the heat stability of milk and milk-protein-stabilised oil-in-water emulsions. However, to the best of our knowledge, few studies have examined the influence of heat on the rheological and creaming properties of MPC-stabilised emulsions under fairly harsh heating conditions (i.e., ≥120 °C for long times). The aims of this study were to evaluate: (1) the influence of protein preheat treatment on the heat stability of oil-in-water emulsions stabilised by standard MPC and calcium-depleted MPC; (2) the rheological and creaming behaviours of the emulsions after heat treatment (120 °C, 10 min). The emulsions were characterised by particle size, surface protein coverage and composition, heat coagulation time (HCT), creaming stability, rheological properties and microstructure before and after heat treatment.

2. Materials and methods

2.1. Materials

MPC 485 (MPC I: 81.5% w/w, protein; 0.07%, w/w, sodium; 2.23%, w/w, calcium), low calcium MPC (MPC II: 82%, w/w, protein; 1.15%, w/w, sodium; 1.34%, w/w, calcium) and sodium caseinate 180 (Na-CN: 92.7%, w/w, protein; 1.12%, w/w, sodium; 0.03%, w/w, calcium) were obtained from Fonterra Co-operative Group Ltd, Auckland, New Zealand. The calcium-depleted MPC was manufactured using cation exchange and ultrafiltration/diafiltration processes. Corn oil was purchased from Davis Trading Co., Palmerston North, New Zealand. All of the chemicals used were of analytical grade, obtained from either BDH Chemicals (BDH Ltd, Poole, England) or Sigma Chemical Co. (St Louis, MO, USA) unless otherwise specified.

2.2. Emulsion production

Milk protein dispersions were prepared by adding milk protein powders to Milli-Q water and then holding at 50 °C for 60 min under continuous stirring. This temperature was high enough to ensure complete dissolution of the aggregated protein products and low enough to prevent any whey protein denaturation. The pH of the final dispersions was adjusted to 6.8 with 1 M HCl or 1 M NaOH. The heat treatment was holding at 90 °C for 5 min (the heating-up time was about 6 min), after which the dispersion was immediately cooled rapidly in an ice bath. Reverse-phase high performance liquid chromatography was used to determine the amount of native whey protein after the heat treatment (Elgar et al., 2000). All the MPC solutions were mixed with sodium acetate (0.2%, w/v) at a 1:1 weight ratio to reach pH 4.6. The mixtures were then centrifuged at 17,900 × g for 6 min and the concentration of native whey protein in the supernatant was determined.

Appropriate quantities of corn oil and Milli-Q water were mixed with the protein solutions to give 30% (w/w) oil and 3% (w/w) protein in the final emulsion. A coarse emulsion pre-mix was prepared by homogenising at 8500 rpm for 3 min using an Ultra-Turrax T25 disperser (IKA®-Werke GmbH & Co. KG, Staufen, Germany). The coarse emulsion was heated to 60 °C and homogenised using a two-stage homogeniser (type Panda, Niro Soavi, Parma, Italy) at 20 MPa (first stage) and 4 MPa (second stage). At least two independent emulsion samples were prepared.

2.3. Determination of effect of heat treatment on emulsions

Aliquots (5 mL) of milk-protein-stabilised emulsion samples were transferred into 8 mL glass tubes with rubber-lined caps (Wheaton, Millville, NJ, USA) and were immersed in a silicone oil bath that was thermostatically controlled at 120 ± 1 °C and had a consistent rocking speed (8 rpm). The heating-up time was estimated to be about 1 min and was excluded from the heating time as reported in this study. MPC I samples were heated for 1, 3 and 10 min to observe the heat-induced changes. All other samples were heated for 10 min and were immediately cooled by immersing the glass vials in cold running water. The treated emulsions were allowed to equilibrate to room temperature (20 °C) and were held for at least 1 h before further analysis. The large aggregates that appeared in MPC I samples were diluted with NaOH (1 M, pH 8.0), a disodium ethylenediamine tetra-acetate (EDTA)/polysorbate 20 (Tween 20) mixture (0.04 mol kg^{-1} and 5 g kg^{-1}), urea (6 mol kg^{-1}) and sodium dodecyl sulphate (SDS) (100 g kg^{-1}). The solubility was checked visually after 24 h.

2.4. Determination of heat coagulation time of emulsions

The time required for coagulation of the sample or precipitates become visible throughout the sample was recorded as the HCT. The procedure described by McSweeney, Mulvihill, and O'Callaghan (2004) was followed with minor modifications. Aliquots (2.5 mL) of milk-protein-stabilised emulsion samples at pH 6.8 were transferred into 8 mL glass tubes with rubber-lined caps (Wheaton) and were immersed in a silicone oil bath that was thermostatically controlled at 140 ± 1 °C and had a consistent rocking speed (8 rev min^{-1}). The experiment was stopped after a heating time of 30 min. The HCT of each sample was determined three times. Mean values were determined from at least duplicate separately prepared samples.

2.5. Determination of particle size distributions of protein dispersions and emulsions

Particle size (*z*-average hydrodynamic diameter) measurements of milk protein dispersions (MPC I, MPC II and Na-CN) were performed at room temperature using the method of Ye (2011). A Malvern Zetasizer Nano ZS (Malvern Instruments Ltd, Malvern, UK) with built-in dynamic light scattering, a He/Ne laser emitting at

Appendix

633 nm and a 4.0 mW power source was used. The MPC dispersions (4.5%, w/w) were diluted 1:100 with corresponding MPC permeates, obtained by ultrafiltration (membrane of 10,000 Da cut-off) to remove the casein micelles and subsequent filtration through a 0.45 μm membrane. The Na-CN dispersion was diluted with Milli-Q water. The hydrodynamic diameter was calculated from the average diffusion coefficient, determined from five measurements with 10 sub-runs.

A Malvern Mastersizer Hydro 2000S (Malvern Instruments Ltd) was used to determine the surface-weighted mean diameters (d_{32}) and volume-weighted mean diameters (d_{43}) of the emulsion droplets. The emulsion was carefully mixed with a dissociating agent (casein-dissociating solution) that contained 3.75 g kg^{-1} EDTA and 1.25 g kg^{-1} Tween 20 at a 1:9 ratio. The mixtures were gently swirled and were measured after an equilibration time of at least 60 min. This was to dissociate the adsorbed casein micelles as much as possible and to detect the true oil droplet only ("primary" particle size). The droplet size directly measured in water is referred to as an "effective" particle size that includes the presence of any aggregates or flocculated droplets (Tangsuphoom & Coupland, 2009). The particle size of each emulsion was measured twice. Mean values were determined from at least duplicate separately prepared samples.

2.6. Determination of surface protein concentration and composition

The surface protein load and the surface protein composition in the milk-protein-stabilised emulsions were measured according to the procedure established by Ye, Srinivasan, and Singh (2000), with minor modifications. The protein content in the cream phase was determined directly using the cream phase after centrifugation and subsequent drying on a filter paper. The surface protein concentration (mg m^{-2}) was calculated from the surface area of the oil droplets, determined by Mastersizer, and the adsorbed protein (g) on the cream layer. The composition of the protein adsorbed at the surface of the emulsion droplets was evaluated using sodium dodecyl sulphate polyacrylamide gel electrophoresis (SDS-PAGE), as described by Ye, Singh, Taylor, and Anema (2004).

2.7. Emulsion rheology

The rheological properties of the emulsions were measured with a Physica MCR 301 rheometer (Anton Paar, Graz, Austria) at 20 °C using a cup and bob geometry. Steady-state flow measurements were conducted at 20 ± 0.1 °C in the shear rate range 0.001–500 s^{-1} over 6 min. The apparent viscosity was recorded as a function of shear rate. The flow behaviour was analysed using Rheoplus 32 V3.21 software (Anton Paar). The power law model was used to determine the flow behaviour:

$$\eta_{app} = K\,\dot{\gamma}^{n-1}$$

where η_{app} is apparent viscosity, $\dot{\gamma}$ is shear rate, K is the consistency coefficient (Pa s) and n is the flow behaviour index. Each sample was measured twice and mean values of viscosity were determined from duplicate samples.

2.8. Emulsion stability

Emulsion samples were transferred into flat-bottomed screw-top tubes (15 mm × 140 mm). They were stored at room temperature (20 °C) and were measured periodically using a vertical scan analyser Turbiscan Classic MA 2000 (Formulaction, Toulouse, France). The procedure has been described previously (Liang, Patel, Matia-Merino, Ye, & Golding, 2013). Measurements were taken after preparation of the emulsions and at different times during storage for 5 days.

2.9. Confocal laser scanning microscopy

A Leica (Heidelberg, Germany) confocal laser scanning microscope with the depth of focus between 40 and 100 μm was used to collect the images. Emulsion (0.5 mL) samples were transferred into test tubes and Nile Red and Fast Green (approximately 0.1%, w/w) were added. The samples were mixed thoroughly and the mixtures were placed on microscope slides (Sail, Sailing Medical-Lab Industries Co. Ltd, China) with cover slips for determination. The emulsion samples were imaged using a 63 × (depth of focus 30 μm) oil immersion objective. Observations were conducted at λ = 543 nm for Nile Red and at λ = 488 nm for Fast Green. Images in 512 × 512 pixel slices were acquired for each sample.

2.10. Statistical analysis

All experiments were carried out at least in triplicate using freshly prepared samples. The experimental data were analysed by Student's *t*-tests using Microsoft Excel 2007 (Microsoft Corporation, Redmond, WA, USA) and significant differences among the means were determined at a 95.0% confidence level.

3. Results

3.1. Particle size of milk protein dispersions and whey protein denaturation level of MPC dispersions

The mean primary particle size of each of the MPC I, MPC II and Na-CN dispersions did not change significantly ($p > 0.05$) after heat treatment at 90 °C for 5 min (Table 1). This result was in line with Dybowska (2008), who showed that the particle sizes of MPC solutions changed little after a heat treatment at 90 °C for 5 min. The present result for the MPC II dispersion, which contained both micellar and non-micellar casein, correlated well with those obtained previously (Ye, 2011). The average particle sizes of the MPC I and MPC II dispersions were very similar ($p > 0.05$) and were close to the size of casein micelles in milk (~200 nm) (Dalgleish, 1998) and in micellar casein solution (Beliciu & Moraru, 2011). The MPC I dispersion showed a monomodal size distribution. In contrast, the particle size distribution of the MPC II dispersion had one peak

Table 1
Particle sizes of milk protein concentrate (MPC) and sodium caseinate (Na-CN) dispersions before and after heating (90 °C, 5 min) and the denaturation level of whey proteins in the oil-free aqueous phase.[a]

Milk protein	Unheated (nm)	Heated (nm)	Total whey protein denaturation (%)	β-Lactoglobulin denaturation (%)	α-Lactalbumin denaturation (%)
MPC I	165.5 ± 2.8^{aA}	163.9 ± 2.7^{aA}	88.4 ± 1.2	92.8 ± 1.5	66.7 ± 2.3
MPC II	168.5 ± 3.6^{aA}	166.1 ± 4.1^{aA}	87.2 ± 1.4	89.7 ± 1.7	74.6 ± 2.2
Na-CN	94.0 ± 3.5^{aB}	99.6 ± 5.0^{aB}	n/a	n/a	n/a

[a] Each value represents the mean of two to four measurements from three independently prepared samples (n/a: not applicable); means within the same row and having the same superscript lower case letter and means within the same column and having the same superscript uppercase letter are not significantly different ($p > 0.05$).

Appendix

showing particles in the 20–70 nm size range and a second peak in the 100–600 nm size range (data not shown).

The extent of whey protein denaturation of the MPC I and MPC II dispersions after the preheat treatment (90 °C, 5 min) is shown in Table 1. The total whey protein denaturation levels for MPC I and MPC II were similar, with around 90% of the whey proteins being denatured during preheat treatment. The denaturation level of α-lactalbumin was slightly higher in the MPC II dispersion than in the MPC I dispersion.

3.2. Particle size distribution of emulsions

The primary particle size (d_{32} value) of milk-protein-stabilised emulsions is shown in Table 2. Under the same homogenisation condition, the d_{32} value indicates the emulsifying capability of the emulsifier (Euston & Hirst, 1999). There was no significant difference in the d_{32} values between the unheated emulsions stabilised by unheated protein and by preheated protein, suggesting protein preheat treatment had little impact on its emulsifying properties in terms of particle size distribution. For the unheated emulsions, the effective particle size of the emulsion stabilised by MPC I was significantly larger than that of the emulsions stabilised by MPC II and Na-CN, regardless of the preheat treatment of the protein solution prior to emulsification (Table 2).

After heat treatment at 120 °C for 10 min, the MPC II and Na-CN emulsions had similar mean particle sizes compared with that of unheated emulsions, suggesting that no heat-induced flocculation or coalescence occurred. On the other hand, the MPC I emulsion stabilised by unheated protein had a significantly larger ($p < 0.05$) particle sizes than that stabilised by preheated protein. The d_{43} value has been reported to be more sensitive to oil droplet aggregation (Relkin & Sourdet, 2005). The effective particle size (d_{43} value) of milk-protein-stabilised emulsions is shown in Table 2. Subsequent heating of the MPC I emulsions resulted in even larger droplets. To determine the solubility of the large aggregates formed in the heated MPC I emulsions, regardless of the protein preheat treatment, samples heated for 1, 3 and 10 min were diluted with various agents, as described in Section 2.3. After 24 h, the aggregates obtained from heating for 1 min could be dissolved in all dissolving agents, whereas those from heating for 3 and 10 min could not be fully dissolved. This suggested that some heat-induced droplet clusters may have been formed by extensive protein–protein interactions between adsorbed layers, with the dissolving agent being unable to dissociate the aggregates. Some covalent bonds possibly formed within the droplet clusters.

3.3. Protein load and protein composition of emulsions

Preheating the protein solution before emulsification had little effect on the surface protein load of the unheated emulsions (Table 2). The MPC II and Na-CN emulsions had similar surface protein concentrations at the oil–water interface whereas the MPC I emulsion had a significantly higher ($p < 0.05$) surface protein load. The results for the MPC I and MPC II emulsions were in good agreement with previous studies on MPC emulsions (Euston & Hirst, 1999; Ye, 2011) and that for the Na-CN emulsion correlated well with the study of Srinivasan, Singh, and Munro (2000). The protein load was not significantly different in emulsions stabilised by MPC II and Na-CN regardless of the protein preheat treatment after the subsequent heating. However, the protein load of the MPC I emulsion formed with unheated protein was significantly higher ($p < 0.05$) after the subsequent heating, suggesting heat-induced interdroplet protein–protein interactions are extensive.

SDS-PAGE patterns of the emulsions stabilised by unheated protein and preheated protein are shown in Fig. 1A (unheated) and Fig. 1B (heated). Compared with the skim milk standard (Lane 1, Fig. 1A), the proportions of the casein fractions at the surface of MPC I emulsion droplets (Lane 2) were similar to those in casein micelles but fewer whey proteins were adsorbed at the interface. For MPC II (Lane 3), more α_{S1}-casein and less β-casein were adsorbed at the oil–water interface, probably because of competitive adsorption when the aggregation state of the caseins is no longer entirely micelles, and consistent with earlier studies (Ye, 2011). The presence of whey protein bands in Fig. 1B confirmed that β-lactoglobulin/k-casein complexes formed during the preheat treatment.

3.4. Heat stability of emulsions

The HCT is considered to be a quantitative measure of the susceptibility of an emulsion towards heat-induced aggregation. Preheating the protein solution before emulsification appeared to marginally improve the HCT of the MPC I and MPC II emulsions, from 0.54 to 0.93 min for the MPC I emulsion and from 10.37 to 11.41 min for the MPC II emulsion, and was attributed to the reduced interactions between the pre-denatured whey proteins. The preheat treatment seemed to have no beneficial effect on the HCT of the Na-CN emulsions under the current experimental conditions. In addition, the HCT of the MPC II emulsion was significantly longer than that of the MPC I emulsion regardless of the protein solution preheating effect. These marked difference were probably influenced by the micellar casein:non-micellar casein ratio and the calcium ion activity in the systems.

3.5. Rheological properties of emulsions

For the unheated MPC I emulsions, protein preheat treatment resulted in reduced viscosity over the shear rate range 0.002–500 s^{-1} (Fig. 2A). This was in contrast to the study of Dybowska (2008), in which the heating of MPC solutions prior to

Table 2
Mean primary particle sizes, mean effective particle sizes and surface protein concentration of 30% (w/w) oil-in-water emulsions formed with 3% (w/w) milk protein concentrate (MPC) and sodium caseinate (Na-CN) before and after heat treatment (120 °C, 10 min).[a]

Treatment	Unheated MPC I	Unheated MPC II	Unheated Na-CN	Preheated MPC I	Preheated MPC II	Preheated Na-CN
Primary d_{32} (μm)						
Unheated	1.36 ± 0.05^{aA}	1.05 ± 0.04^{bA}	1.02 ± 0.05^{bA}	1.46 ± 0.07^{aA}	1.17 ± 0.18^{bA}	1.11 ± 0.02^{bA}
Heated	4.17 ± 1.48^{aB}	1.06 ± 0.02^{bA}	0.97 ± 0.07^{bA}	1.74 ± 0.22^{aB}	1.16 ± 0.09^{bA}	1.09 ± 0.02^{bA}
Effective d_{43} (μm)						
Unheated	13.3 ± 1.31^{aA}	2.33 ± 0.02^{bA}	2.26 ± 0.03^{bA}	10.0 ± 0.78^{aA}	2.42 ± 0.11^{bA}	2.46 ± 0.10^{bA}
Heated	228.5 ± 36.2^{aB}	2.42 ± 0.06^{bA}	2.29 ± 0.05^{bA}	189.8 ± 37.4^{aB}	2.45 ± 0.02^{bA}	2.53 ± 0.43^{bA}
Surface protein concentration (mg m^{-2})						
Unheated	13.16 ± 1.29^{aA}	4.12 ± 1.04^{aB}	2.82 ± 0.47^{aB}	60.81 ± 3.66^{aC}	4.51 ± 0.49^{aB}	2.90 ± 0.73^{aB}
Heated	13.26 ± 1.24^{aA}	3.84 ± 0.45^{aB}	3.15 ± 0.42^{aB}	13.44 ± 1.79^{bA}	4.21 ± 0.08^{aB}	3.03 ± 1.17^{aB}

[a] Each value represents the mean of two to four measurements from three independently prepared samples (n/a: not applicable); means within the same row and having the same superscript lower case letter and means within the same column and having the same superscript uppercase letter are not significantly by Student's *t*-test at $p < 0.05$.

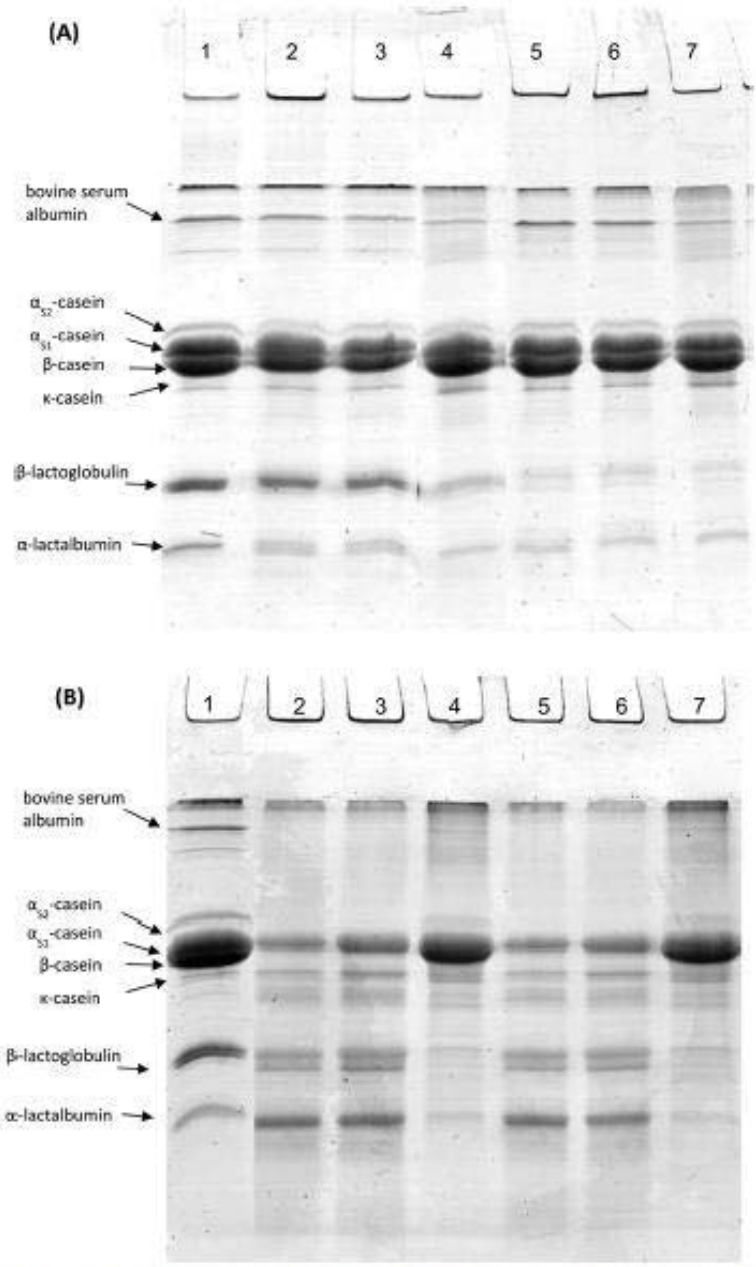

Fig. 1. SDS-PAGE patterns of proteins adsorbed at the oil–water interface of (A) unheated and (B) heated 30% (w/w) oil-in-water emulsions formed with 3% (w/w) unheated and preheated protein dispersions. Lane 1, skim milk standard; lane 2, MPC I emulsion; lane 3, MPC II emulsion; lane 4, Na-CN emulsion; lane 5, MPC I emulsion formed with preheated protein; lane 6, MPC II emulsion formed with preheated protein; lane 7, Na-CN emulsion formed with preheated protein.

emulsification resulted in increased emulsion viscosity. For the heated MPC I emulsions, the apparent viscosity of the emulsion stabilised by preheated protein was slight lower than that of the emulsion stabilised by unheated protein over the whole shear rate range (Fig. 2B). The low-shear-rate viscosities are 8700 Pa s for unheated protein and 7070 Pa s for preheated protein. It appeared that severe heat-induced aggregation had already occurred during the initial heating period (~2 min) in the MPC I emulsions. Fig. 3

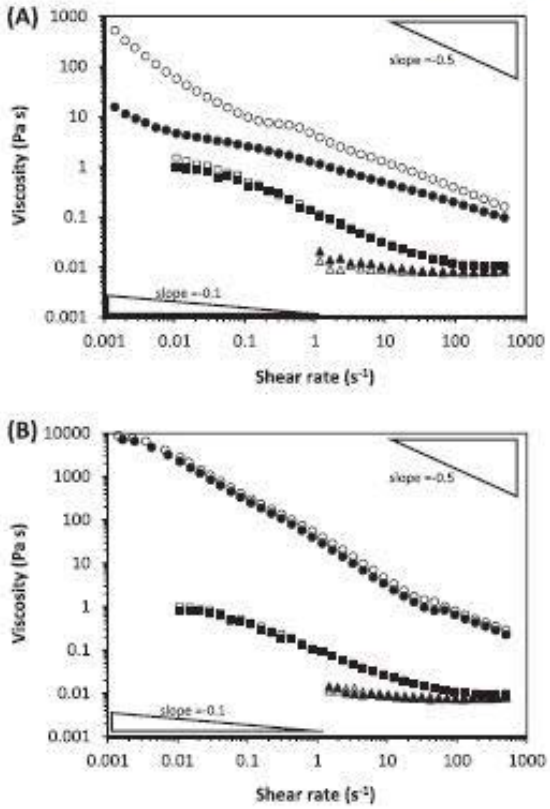

Fig. 2. Apparent viscosities of (A) unheated and (B) heated (120 °C, 10 min) 30% (w/w) oil-in-water emulsions stabilised by 3% (w/w) unheated protein (○, MPC I; △, MPC II; □, Na-CN) and by 3% (w/w) preheated protein (●, MPC I; ▲, MPC II; ■, Na-CN) at 20 °C.

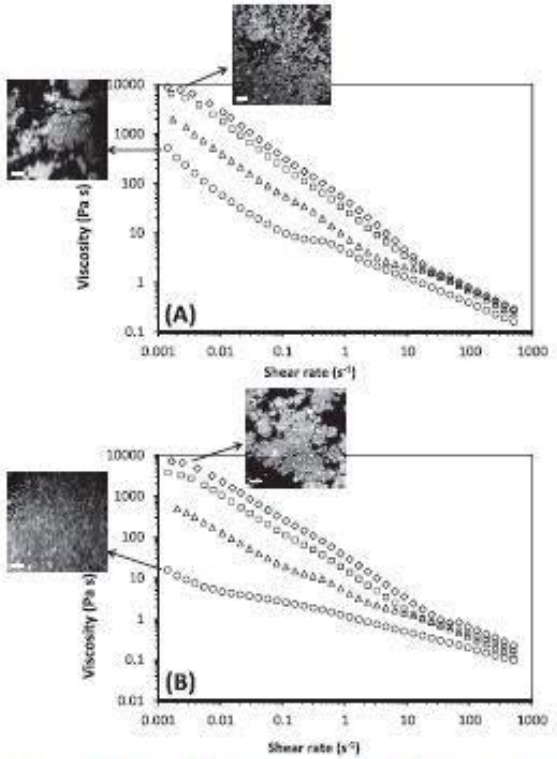

Fig. 3. Apparent viscosities of 30% (w/w) oil-in-water emulsions stabilised by (A) MPC I unheated solution and (B) MPC I preheated solution before (○) and after heating at 120 °C for 1 (△), 3 (□) and 10 (◇) min. Confocal laser scanning micrographs were captured in a 63 × objective. The scale bar represents 20 μm.

shows that the apparent viscosities increased significantly even after 1 min of heating at 120 °C. The extent of the change in viscosity was greater in MPC I emulsions stabilised by preheated protein than in those stabilised by unheated protein as the heating time increased. The initial high viscosities of the heated MPC-I-stabilised emulsions were probably due to heat-induced aggregations/interactions between protein-stabilised oil droplets and between droplets and serum proteins, forming large aggregates/flocs (Euston, Finnigan, & Hirst, 2000).

In contrast to the MPC I emulsions, the MPC II and Na-CN emulsions had much lower initial viscosities at low shear rates and there was little difference between the emulsions formed with unheated and preheated proteins (Fig. 2A and B). The viscosities of the MPC II emulsions were consistently lower than those of the Na-CN emulsions over the whole shear rate range. The Na-CN emulsions displayed shearing-thinning behaviour, suggesting the formation of some droplet clusters that were disrupted at higher shear rates. This phenomenon was due to the depletion effects, which promoted emulsion flocculation.

3.6. Creaming stability of emulsions

The heated emulsions stabilised by MPC I, MPC II and Na-CN were monitored both visually and with a Turbiscan over 5 days of storage at ambient temperature (20 °C) (Fig. 4). Creaming was the main destabilisation mechanism for the heated MPC I emulsions as the serum layer thickness increased gradually over time. It was expected, based on Stokes' Law, that emulsions containing larger droplets would be more susceptible to creaming. However, the degree of creaming was still low after 120 h for the MPC I emulsions. The serum layer developed more slowly in the heated MPC I emulsion stabilised by unheated protein, which had higher initial viscosity, than that stabilised by preheated protein.

It was almost impossible to visually detect phase separation in the MPC II emulsions at an early stage, because both the dispersed phase and the casein-micelle-rich continuous phase remained turbid during ageing. Some migration of particles at the bottom of the tubes was detected with the Turbiscan. Regardless of the preheat treatment, both heated MPC II emulsions may have phase separated. They exhibited a rapid increase in serum layer thickness after 24 h and reached a plateau value after 96 h (Fig. 4). The phase separation in the MPC II emulsions was reversible, because it disappeared when the emulsion sample was gently inverted. The droplet size of the cream layer was very similar to that of the whole emulsion. This correlated with the reported phase separation behaviour of caseinate emulsion systems, in which the presence of excess non-adsorbed caseinate can induce depletion flocculation of oil droplets, leading to rapid creaming (Dickinson & Golding, 1997). The MPC II emulsion stabilised by preheated protein had slightly faster separation than that stabilised by unheated protein.

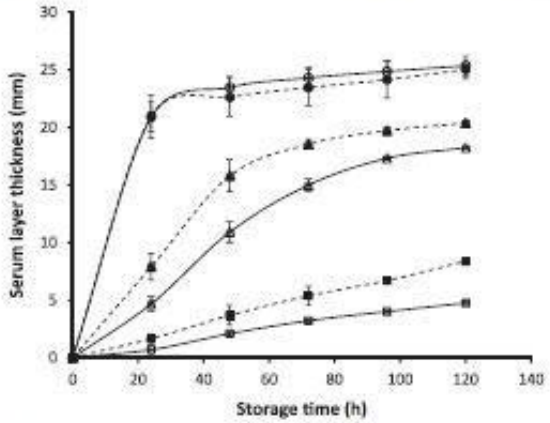

Fig. 4. Variation in serum layer thickness as determined by Turbiscan over 120 h at 20 °C for heated 30% (w/w) oil-in-water emulsions stabilised by 3% (w/w) unheated (open symbols) and preheated (closed symbols) proteins: □, ■, MPC I; △, ▲, MPC II; ○, ●, Na-CN.

Some phase separation was observed visually in the Na-CN emulsions, regardless of the preheat treatment of the protein solution prior to emulsification. A dramatic increase in serum layer thickness was seen after 24 h and reached a plateau thereafter (Fig. 4), indicating extensive flocculation, which was attributed to the presence of an excess non-adsorbed caseinate in the continuous phase (Dickinson & Golding, 1997).

4. Discussion

This work demonstrated that the emulsifying abilities of milk proteins and the corresponding emulsions are influenced by the casein aggregation state, the protein preheat treatment and the calcium content. The protein preheating prior to emulsification confers a slight beneficial effect on MPC-stabilised emulsions when they are subjected to a secondary heat treatment as it has been shown by the reduction of both droplet size and viscosity. The protein–protein interactions between pre-denatured whey proteins will be limited during the secondary heat treatment, because thiol/disulphide interchanges between denatured whey proteins or between casein micelles and denatured whey proteins have already occurred (Anema & Li, 2003b; Vasbinder & de Kruif, 2003). It has been suggested that denatured whey proteins could result in less aggregation during subsequent heat treatments because fewer free thiol groups are available (Dissanayake & Vasiljevic, 2009). As the oil-free MPC I systems were found to be heat stable after heating for 20 min at 140 °C, heat-induced droplet–droplet interactions appeared to be more important in the aggregation mechanism.

MPC II emulsions had better heat stability than MPC I emulsions regardless of the protein preheating effect, which may have been associated with the large effective droplet size of MPC I emulsion and the reduced calcium content in MPC II. The heat stability of milk-protein-stabilised emulsions has been found to be influenced by the volume fraction of casein micelles. Casein micelle coated oil droplets behave as large "casein micelles" which increases the effective concentration of casein micelles at a fixed protein concentration, resulting in poorer heat stability (Cruijsen, 1996; Walstra, Wouters, & Geurts, 2006). Extensive bridging flocculation occurs when aggregated protein particles are adsorbed at the oil–water interface and the MPC-to-oil ratio is low. As a consequence, the presence of large "casein micelles" increases the tendency to heat-induced aggregation as the κ-casein content per emulsion droplet is too low (Sharma & Singh, 1999).

In contrast to MPC I emulsions, the small droplet size and the low surface protein concentration (Table 2) in the MPC II emulsions suggested that the oil droplets were coated with some dissociated caseins, in agreement with Ye (2011). Parkinson and Dickinson (2007) have demonstrated that, when non-micellar caseins and whey proteins co-adsorb at the oil–water interface, the tangling tails of the caseins protrude and enhance the steric repulsion between emulsion droplets, preventing droplets from aggregation during heating. However, it is very difficult to completely rule out the effect of calcium depletion in MPC II on the heat stability of the emulsions, since a systematic reduction in the free Ca^{2+} level by calcium chelators will change the aggregation state of the casein micelles (de Kort, Minor, Snoeren, van Hooijdonk, & van der Linden, 2011). However, the effect of Ca^{2+} activity should always be considered.

It was expected that preheating the protein dispersion prior to emulsification could lead to more protein adsorption and that this increase in density at the oil–water interface would improve the stability of the emulsion (Dybowska, 2008). However, the opposite was observed in heated MPC I emulsions (Fig. 4). The high low-shear rate viscosity of the heated MPC I emulsion formed with unheated protein (Fig. 2) predominantly contributed to the better emulsion stability. At a protein concentration around that required to coat the oil droplet surface completely, the colloidal system is stable against creaming (Dickinson, 1999). When the oil droplets are stabilised by Na-CN, the presence of an excess of non-adsorbed caseinate or casein micelles can induce depletion flocculation (Dickinson & Golding, 1997; Liang et al., 2013; ten Grotenhuis, Tuinier, & de Kruif, 2003). The rapid development of the serum layer after 24 h in MPC II emulsions suggests that depletion flocculation may have occurred. Low calcium MPC probably contains some dissociated caseins with a size range of 20–50 nm (Ye, 2011), which is within the optimum size of casein particles for a depletion effect. Protein preheating affected the emulsion stability of the MPC II emulsions slightly, probably because the formation of casein micelle/whey protein and/or casein/whey protein complexes during heating (protein preheating + secondary heating) changed the particle size of the non-adsorbed proteins. Heat-induced whey protein–casein micelle interactions results in an increase of the effective particle size of the casein micelles (Anema & Li, 2003a). This change in the size may decrease the depletion flocculation and result in a different phase separation kinetic.

5. Conclusions

Preheating the MPC dispersion prior to emulsification had a small beneficial effect on the heat stability of MPC-stabilised emulsions, probably because the pre-denaturation of the whey proteins meant that they were relatively inert during a secondary heat treatment. The aggregation state of the caseins influenced the protein adsorption behaviour and the heat stability of the emulsions. In low calcium MPC, the caseins dissociated from the micelles possibly had two roles. First, when these dissociated casein particles adsorbed on to the emulsion droplets, they reduced the effective hydrodynamic diameter of the droplets and the volume fraction of casein particles. Second, the non-micellar caseins possibly prevented extensive heat-induced flocculation of the emulsions during a secondary heat treatment. Meanwhile, the extent of depletion flocculation in the casein-stabilised emulsions was changed due to the change in the size of casein particles.

Appendix

Acknowledgements

The authors gratefully thank the Fonterra Research and Development Centre and the Foundation for Research, Science and Technology for financial support, Skelte Anema and Graeme Gillies for their useful discussions, Michael Loh for his assistance with operation of the confocal laser scanning microscope and Claire Woodhall for proof reading the manuscript.

References

Anema, S. G., & Li, Y. (2003a). Association of denatured whey proteins with casein micelles in heated reconstituted skim milk and its effect on casein micelle size. *Journal of Dairy Research, 70*, 73–83.

Anema, S. G., & Li, Y. (2003b). Effect of pH on the association of denatured whey proteins with casein micelles in heated reconstituted skim milk. *Journal of Agricultural and Food Chemistry, 51*, 1640–1646.

Augustin, M. A., & Udabage, P. (2007). Influence of processing on functionality of milk and dairy proteins. *Advances in Food and Nutrition Research, 53*, 1–38.

Beliciu, C. M., & Moraru, C. I. (2011). The effect of protein concentration and heat treatment temperature on micellar casein-soy protein mixtures. *Food Hydrocolloids, 25*, 1448–1460.

Cruijsen, J. M. M. (1996). Physical stability of caseinate-stabilized emulsions during heating. PhD Thesis, Agricultural University of Wageningen, The Netherlands.

Dalgleish, D. G. (1998). Casein micelles as colloids: surface structures and stabilities. *Journal of Dairy Science, 81*, 3013–3018.

de Kort, E., Minor, M., Snoeren, T., van Hooijdonk, T., & van der Linden, E. (2011). Effect of calcium chelators on physical changes in casein micelles in concentrated micellar casein solutions. *International Dairy Journal, 21*, 907–913.

Dickinson, E. (1999). Caseins in emulsions: interfacial properties and interactions—An overview. *International Dairy Journal, 9*, 305–312.

Dickinson, E. (2010). Flocculation of protein-stabilized oil-in-water emulsions. *Colloids and Surfaces B: Biointerfaces, 81*, 130–140.

Dickinson, E., & Golding, M. (1997). Depletion flocculation of emulsions containing unadsorbed sodium caseinate. *Food Hydrocolloids, 11*, 13–18.

Dissanayake, M., & Vasiljevic, T. (2009). Functional properties of whey proteins affected by heat treatment and hydrodynamic high-pressure shearing. *Journal of Dairy Science, 92*, 1387–1397.

Dybowska, B. E. (2008). Properties of milk protein concentrate stabilized oil-in-water emulsions. *Journal of Food Engineering, 88*, 507–513.

Dybowska, B. E. (2011). Whey protein-stabilized emulsion properties in relation to thermal modification of the continuous phase. *Journal of Food Engineering, 104*, 81–88.

Elgar, D. F., Norris, C. S., Ayers, J. S., Pritchard, M., Otter, D. E., & Palmano, K. P. (2000). Simultaneous separation and quantitation of the major bovine whey proteins including proteose peptone and caseinomacropeptide by reversed-phase high-performance liquid chromatography on polystyrene-divinylbenzene. *Journal of Chromatography A, 878*, 183–196.

Euston, S. R., Finnigan, S. R., & Hirst, R. L. (2000). Aggregation kinetics of heated whey protein-stabilized emulsions. *Food Hydrocolloids, 14*, 155–161.

Euston, S. R., & Hirst, R. L. (1999). Comparison of the concentration-dependent emulsifying properties of protein products containing aggregated and non-aggregated milk protein. *International Dairy Journal, 9*, 603–701.

Faka, M., Lewis, M. J., Grandison, A. S., & Deeth, H. (2009). The effect of free Ca^{2+} on the heat stability and other characteristics of low-heat skim milk powder. *International Dairy Journal, 19*, 386–392.

Grimley, H. J., Grandison, A. S., & Lewis, M. J. (2010). The effect of calcium removal from milk on casein micelle stability and structure. *Milchwissenschaft, 65*, 151–154.

Guyomarc'h, F., Nono, M., Nicolai, T., & Durand, D. (2009). Heat-induced aggregation of whey proteins in the presence of κ-casein or sodium caseinate. *Food Hydrocolloids, 23*, 1103–1110.

Keowmaneechai, E., & McClements, D. J. (2006). Influence of EDTA and citrate on thermal stability of whey protein stabilized oil-in-water emulsions containing calcium chloride. *Food Research International, 39*, 230–239.

Liang, Y., Patel, H., Matia-Merino, L., Ye, A., & Golding, M. (2013). Structure and stability of heat-treated concentrated dairy-protein-stabilised oil-in-water emulsions: a stability map characterisation approach. *Food Hydrocolloids, 33*, 297–308.

Livney, Y. D., Corredig, M., & Dalgleish, D. G. (2003). Influence of thermal processing on the properties of dairy colloids. *Current Opinion in Colloid and Interface Science, 8*, 359–364.

McClements, D. J. (2005). *Food emulsions: Principles, practices, and techniques* (2nd ed.). Boca Raton, FL, USA: CRC Press.

McSweeney, S. L., Healy, R., & Mulvihill, D. M. (2008). Effect of lecithin and monoglycerides on the heat stability of a model infant formula emulsion. *Food Hydrocolloids, 22*, 888–898.

McSweeney, S. L., Mulvihill, D. M., & O'Callaghan, D. M. (2004). The influence of pH on the heat-induced aggregation of model milk protein ingredient systems and model infant formula emulsions stabilized by milk protein ingredients. *Food Hydrocolloids, 18*, 109–125.

Newstead, D. F., Paterson, G., Anema, S. G., Coker, C. J., & Wewala, A. R. (2006). Plasmin activity in direct-steam-injection UHT-processed reconstituted milk: effects of preheat treatment. *International Dairy Journal, 16*, 573–579.

O'Kennedy, B. T., & Mounsey, J. S. (2006). Control of heat-induced aggregation of whey proteins using casein. *Journal of Agricultural and Food Chemistry, 54*, 5637–5642.

O'Regan, J., Ennis, M. P., & Mulvihill, D. M. (2009). Milk proteins. In G. O. Phillips, & P. A. Williams (Eds.), *Handbook of hydrocolloids* (2nd ed.). (pp. 299–358) Cambridge, UK: Woodhead Publishing.

O'Regan, J., & Mulvihill, D. M. (2010). Heat stability and freeze–thaw stability of oil-in-water emulsions stabilised by sodium caseinate–maltodextrin conjugates. *Food Chemistry, 119*, 182–190.

Parkinson, E. L., & Dickinson, E. (2007). Synergistic stabilization of heat-treated emulsions containing mixtures of milk proteins. *International Dairy Journal, 17*, 95–103.

Rallos, V. (2010). Effect of heat treatment on milk protein functionality at emulsion interfaces. A review. *Food Hydrocolloids, 24*, 259–265.

Relkin, P., & Sourdet, S. (2005). Factors affecting fat droplet aggregation in whipped frozen protein-stabilized emulsions. *Food Hydrocolloids, 19*, 503–511.

Sharma, R., & Singh, H. (1999). Heat stability of recombined milk systems as influenced by the composition of fat globule surface layers. *Milchwissenschaft, 54*, 193–196.

Srinivasan, M., Singh, H., & Munro, P. A. (2000). The effect of sodium chloride on the formation and stability of sodium caseinate emulsions. *Food Hydrocolloids, 14*, 497–507.

Srinivasan, M., Singh, H., & Munro, P. A. (2002). Formation and stability of sodium caseinate emulsions: influence of retorting (121 °C for 15 min) before or after emulsification. *Food Hydrocolloids, 16*, 153–160.

Srinivasan, M., Singh, H., & Munro, P. A. (2003). Influence of retorting (121 °C for 15 min), before or after emulsification, on the properties of calcium caseinate oil-in-water emulsions. *Food Chemistry, 80*, 61–69.

Tangsuphoom, N., & Coupland, J. N. (2009). Effect of thermal treatments on the properties of coconut milk emulsions prepared with surface-active stabilizers. *Food Hydrocolloids, 23*, 1792–1800.

ten Grotenhuis, E., Tuinier, R., & de Kruif, C. G. (2003). Phase stability of concentrated dairy products. *Journal of Dairy Science, 86*, 764–769.

Vasbinder, A. J., & de Kruif, C. G. (2003). Casein–whey protein interactions in heated milk: the influence of pH. *International Dairy Journal, 13*, 669–677.

Walstra, P., Wouters, J. T. M., & Geurts, T. J. (2006). *Dairy science and technology* (2nd ed.). Boca Raton, FL, USA: CRC Press.

Ye, A. (2011). Functional properties of milk protein concentrates: emulsifying properties, adsorption and stability of emulsions. *International Dairy Journal, 21*, 14–20.

Ye, A., Singh, H., Taylor, M. W., & Anema, S. G. (2004). Interactions of fat globule surface proteins during concentration of whole milk in a pilot-scale multiple-effect evaporator. *Journal of Dairy Research, 71*, 471–479.

Ye, A., Srinivasan, M., & Singh, H. (2000). Influence of NaCl addition on the properties of emulsions formed with commercial calcium caseinate. *Food Chemistry, 69*, 237–244.